

# **For Reference**

---

**NOT TO BE TAKEN FROM THIS ROOM**



Ex LIBRIS  
UNIVERSITATIS  
ALBERTAENSIS

















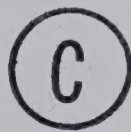




THE UNIVERSITY OF ALBERTA

GEOTECHNICAL IMPLICATIONS OF VALLEY REBOUND

by



DAVID SAMUEL MATHESON

A THESIS

SUBMITTED TO THE FACULTY OF GRADUATE STUDIES AND RESEARCH  
IN PARTIAL FULFILMENT OF THE REQUIREMENTS FOR THE DEGREE  
OF DOCTOR OF PHILOSOPHY

DEPARTMENT OF CIVIL ENGINEERING

EDMONTON, ALBERTA

SPRING, 1972





## ABSTRACT

## UNIVERSITY OF ALBERTA

## FACULTY OF GRADUATE STUDIES AND RESEARCH

The undersigned certify that they have read, and recommend to the Faculty of Graduate Studies and Research for acceptance, a thesis entitled GEOTECHNICAL IMPLICATIONS OF VALLEY REBOUND submitted by David Samuel Matheson in partial fulfilment of the requirements for the degree of Doctor of Philosophy.





## ABSTRACT

This dissertation deals with the geotechnical implications of river valley formation in the prairies of Western Canada and the Northern United States. Many of the river valleys of the area are postglacial and are characterized by extensive landslide activity where the Cretaceous bedrock of the area has been exposed.

Valley excavation is shown to result in the formation of a gentle anticlinal feature in the bedrock below the river valleys. Valley cross-sections, collected from dam site and bridge investigations, show maximum values of rebound from three to close to ten percent of the valley depth. Upward flexure of the beds in the valley wall and formation of a raised valley rim results from rebound of the valley bottom.

The cause of these features is studied and it is concluded that the major mechanism is elastic rebound due to stress relief. A finite element analysis of river valley formation indicates that drained values of Young's modulus and Poisson's ratio are required to produce the features noted in the field. Finite element results indicate that large inward movements of the valley walls will result from valley formation which, in a layered bedrock sequence with bentonite layers, will generate a concentration of high shear strains across bentonite and other layers which have a low modulus.





The formation of the valley anticlines and flexure of the valley walls will result in flexural slip along horizontal bedding planes. Field evidence is presented to show that these processes have resulted in a marked loss of strength of the bedrock along bedding planes and bentonite layers. Landslide activity in the study area is shown to be explicable in the light of these findings. The design of major civil engineering works in and along the river valleys of the study area is shown to be influenced by the processes which have accompanied valley formation.

The formation of the river valleys in the study area is shown to control the development of some landforms and tributary drainage systems in the immediate vicinity of the valley in areas where low surficial relief exists.





## ACKNOWLEDGMENTS

The author would like to express his appreciation for the guidance of Dr. S. Thomson and Dr. N. R. Morgenstern, who supervised the author during the course of this research and would like to acknowledge the major contributions that they have made to this work. Other staff members in the Department of Civil Engineering, University of Alberta, notably Dr. D. W. Murray and Dr. Z. Eisenstein, provided information and guidance to the author and their help is gratefully acknowledged.

The results of site investigations and laboratory test data have been contributed by a number of engineering organizations and the author would like to extend his sincere appreciation to:

- the Prairie Farm Rehabilitation Agency, Soil Mechanics and Materials Division and, in particular, to Mr. N. Iverson, P. Eng. and Mr. K. Lamb, P. Eng., for their assistance during the author's visit to Saskatoon.
- the U. S. Army Corps of Engineers, Missouri River Division, Omaha, Nebraska and, in particular, to Messrs. J. F. Redlinger, L. B. Underwood, Dennis Lachel and G. S. Spencer for their assistance and hospitality.
- the Water Resources Division, Alberta Department of the Environment and to Mr. I. H. Anderson, P. Eng.





and T. V. Mussivand.

- R. M. Hardy and Associates Ltd. and to Mr. M. C. Harris, P. Eng.
- E. W. Brooker and Associates Ltd. and to Dr. E. W. Brooker, P. Eng. and Mr. D. W. Hayley, P. Eng.
- International Power and Engineering Consultants Ltd. and in particular, to Mr. Alan Imrie.
- the Bridges Branch, Alberta Department of Highways and the Highways Division, Research Council of Alberta and, in particular, Mr. C. R. Neill, P. Eng. and Mr. B. P. Shields, P. Eng.

Financial assistance for this research was provided by the National Research Council of Canada, the Department of Civil Engineering, University of Alberta and the Highways Division of the Research Council of Alberta.

The author would like to acknowledge the help of Mr. E. F. Reske with the drafting and the careful typing of Mr. L. Stahl.

The author would like to express his deepest appreciation to his wife, Loretta, for her steadfast support, help and encouragement during the period of this study.





TABLE OF CONTENTS

	Page
Title Page .....	i
Approval Sheet .....	ii
Abstract .....	iii
Acknowledgments .....	v
Table of Contents .....	vii
List of Tables .....	x
List of Figures .....	xi
List of Plates .....	xx
CHAPTER I - INTRODUCTION	
1.1 Thesis Topic .....	1
1.2 Scope of the Thesis .....	2
1.3 Organization of the Thesis .....	4
CHAPTER II - THE BEDROCK OF THE WESTERN PLAINS OF NORTH AMERICA	
2.1 Introduction .....	6
2.2 Geologic Setting .....	7
2.3 Properties of the Bedrock in the Study Area .....	9
2.4 Slope Stability Experience in the Study Area .....	25
2.5 Rebound of Excavated Surfaces .....	58
2.6 Investigation Techniques .....	68
2.7 Discussion .....	81
CHAPTER III - GEOLOGIC EVIDENCE OF BEDROCK REBOUND	
3.1 Introduction .....	87
3.2 Literature Review .....	88





3.3	Case Histories Showing Rebound in the Study Area .....	104
3.4	Case Histories From Outside the Study Area .....	155
3.5	Evidence of Lateral Movement .....	173
3.6	The Raised Valley Rim .....	187
3.7	Discussion of the Geologic Evidence of Rebound .....	207

#### CHAPTER IV - FINITE ELEMENT ANALYSIS OF RIVER VALLEY FORMATION

4.1	Introduction .....	229
4.2	The Stress-Strain Behaviour of Soil and Rock .....	230
4.3	Finite Element Simulation of River Valley Excavation .....	248
4.4	Displacements Due to Valley Excavation in a Homogeneous Elastic Rock .....	261
4.5	Effect of Depth to Rigid Base .....	280
4.6	Effect of Valley Geometry and Increase in E with Depth .....	289
4.7	Discussion .....	303

#### CHAPTER V - STRESS RELIEF AND LATERAL DISPLACEMENT

5.1	Introduction .....	306
5.2	Literature Review .....	307
5.3	Flexural Slip .....	313
5.4	Finite Element Analyses of Lateral Movements Across a Weak Layer .....	325
5.5	Effect of Valley Wall Inclination and Slope Flattening on Differential Movements .....	355
5.6	Summary and Discussion .....	365



	Page
CHAPTER VI - CIVIL ENGINEERING APPLICATIONS	
6.1 Introduction .....	368
6.2 Summary of Thesis Results .....	368
6.3 Application to Slope Stability in the Study Area .....	371
6.4 Application to Design Problems .....	385
6.5 Summary .....	388
CHAPTER VII - GEOLOGICAL APPLICATIONS	
7.1 Introduction .....	390
7.2 Local Stratigraphic Correlation of Drilling Results .....	390
7.3 Application to Structural Geology .....	393
7.4 Applications to Geomorphology .....	397
LIST OF REFERENCES .....	406
APPENDIX A - MISCELLANEOUS GEOLOGIC SECTIONS .....	A-1
APPENDIX B - GEOLOGICAL OBSERVATIONS AT THE JAMES MACDONALD AND BEVERLY BRIDGES, EDMONTON, ALBERTA .....	B-1
APPENDIX C - PROFILES ADJACENT TO RIVER VALLEYS IN ALBERTA .....	C-1
APPENDIX D - STRESS AND DEFORMATION ANALYSIS OF EXCAVATIONS BY THE FINITE ELEMENT METHOD .....	D-1





## LIST OF TABLES

Table		Page
2.1	Peak and Residual Strengths of Overconsolidated Clay .....	28
2.2	Strength Results for the Edmonton Formation ...	34
2.3	Summary of the Properties of Bedrock Types, Carvel Damsite .....	35
2.4	Shear Strength of Bearpaw Shale .....	44
2.5	Direct Shear Test Results .....	51
2.6	Typical Core Recovery Using Double Wall Core Barrels .....	72
3.1	Bedrock Properties at Hairy Hill Damsite .....	114
3.2	Secant Moduli from Unconfined Compression Tests	115
3.3	Properties of the Ravenscrag Formation at Boundary Dam .....	133
3.4	Compilation of Rim Survey Results .....	195
3.5	Compilation of Maximum Values of Rebound and Reported Values of E .....	220
4.1	Values of E from Squaw Rapids .....	236
5.1	Flexural Slip Developed due to Valley Rebound for Sites in the Study Area .....	318
5.2	Differential Displacement Across Layer "B" Below the Toe of the Slope .....	353





LIST OF FIGURES

Figure		Page
2.1	Generalized Geology of Study Area .....	11
2.2	Stratigraphic Correlation Chart .....	12
2.3	Influence of a Load Reduction on a Sedimentary Rock .....	19
2.4	Relationship Between Coefficient of Earth Pressure, Overconsolidation Ratio and Angle of Shearing Resistance .....	21
2.5	Valley Cross-section and Foundation Profile with Typical Moisture Content Profile, Gardiner Dam .....	23
2.6	Typical Direct Shear Results .....	23
2.7	Profile, St. Mary River NW19-6-22-W4 .....	40
2.8	Topography Along South Saskatchewan River .....	40
2.9	Embankment Cross-section and Arrangement of Works, Gardiner (South Saskatchewan River) Dam	42
2.10	Geologic Section through Second Powerhouse, Fort Peck Dam .....	45
2.11	Geologic Profile Along Axis of Oahe Dam .....	45
2.12	Maximum Embankment Section .....	50
2.13	Section Through Right Abutment Slide .....	50
2.14	Section Through Left Abutment Slide .....	56
2.15	Shale Heave vs Time at a Typical Spillway .....	56
2.16	Centerline Vertical Movement, Fort Peck Spillway	61
2.17	Current Rate of Rebound, Fort Peck Spillway ...	62
2.18	Typical Rebound Gauge Observations, Garrison Dam .....	62
2.19	Summary of Movement, Stilling Basin and Powerhouse, Garrison Dam .....	65



Figure		Page
2.20	Schematic Cross-section through Stilling Basin Showing Theoretical Observed Rebound .....	67
2.21	Plot of Measured Vertical Movement Versus Time	67
2.22	Typical Double Walled Core Barrels .....	70
2.23	Pembina River Damsite 3 - Section, Core Recovery and Moisture Contents .....	74
2.24	Boundary Damsite 4 - Geologic Profile .....	76
3.1	Vertical Stress-Relief Joints along Valleys in the Allegheny Plateau .....	90
3.2	Stress-Relief Joints at Fontenelle Dam, Wyoming	92
3.3	Valley Bulges Documented in Europe - Attributed to Periglacial Conditions .....	93
3.4	Geologic Sections of Dam Trenches - Derwent Valley .....	96
3.5	Stauton Harold Dam, England - Cutoff Trench Section .....	98
3.6	Cross-Sections of River Valleys Showing an Anticline below the Bed of the River .....	102
3.7	Features Noted in Dam Cutoff Trenches in the Allegheny Plateau .....	105
3.8	Idealized Section Illustrating Features Resulting From Valley Formation .....	106
3.9	Displacements due to Excavation Into an Elastic Mass, for Different Values of $K_0$ .....	108
3.10	Typical Preliminary Damsite Drilling Program ..	110
3.11	Marker Bed Profiles - Hairy Hill Damsite .....	113
3.12	Carvel Damsite Geologic Section .....	117
3.13	Ardley Damsite Stratigraphy and Testholes .....	121
3.14	Ardley Damsite Stratigraphic Section from Large Diameter Testpits .....	124
3.15	James MacDonald Bridge Testhole Locations .....	126





Figure	Page
3.16 Proposed James MacDonald Bridge, Valley Bottom Profile and Testhole Logs .....	127
3.17 Capilano Bridge, Testhole Locations and Logs ..	128
3.18 Boundary Damsite 2, Geologic Profile .....	131
3.19 Boundary Damsite 2, Location Plan and Spillway Section .....	132
3.20 Centerline Stratigraphic Section - Rocky Mountain House Damsite A .....	136
3.21 St. Mary Dam Geologic Section - 700 feet Downstream of Centerline .....	138
3.22 Section of the Fort Peck Spillway .....	141
3.23 Rebound Observations and Calculations, East Abutment of Garrison Dam .....	142
3.24 Garrison Dam Geologic Section Parallel to Dam Axis .....	144
3.25 Garrison Dam, Spillway Geologic Sections Showing Major Lignite Seams .....	145
3.26 Garrison Dam, Plan of Foundation Sections .....	146
3.27 Oahe Dam Geologic Profile, Axis of Dam .....	148
3.28 Oahe Dam Geologic Sections .....	149
3.29 Oahe Dam Geologic Sections .....	150
3.30 Cross-Section of the Missouri River Valley ....	153
3.31 Bowman-Haley Damsite Plan of Borings .....	154
3.32 Bowman-Haley Damsite Geologic Section .....	156
3.33 General Geology, Portage Mountain Dam .....	158
3.34 Portage Mountain Dam Geologic Section C-C .....	161
3.35 Portage Mountain Dam Geologic Section D-D .....	162
3.36 Portage Mountain Dam - Geologic Section A-A ...	163
3.37 Three Rivers Damsite Geologic Section .....	167





Figure		Page
3.38	Beech Fork Dam Geologic Section .....	170
3.39	Smithville Dam Geologic Profile .....	172
3.40	Displacements due to Excavation at the Kimbley Open-Pit Mine, Nevada .....	176
3.41	Geologic Section, East Wall, Pier 2, Beverly Bridge .....	182
3.42	Rebound Adjacent to Utility Trenches, U. of A. Campus .....	189
3.43	Locations within the Province of Alberta Showing Evidence of Differential Rebound below River Valleys .....	191
3.44	Profiles at Redcliff .....	192
3.45	Athabasca-Oldman Damsite Profile, Line DD .....	193
3.46	Height of Raised Rim Versus Valley Width .....	196
3.47	Height of Raised Rim Versus Valley Depth .....	197
3.48	Width of Raised Rim Versus Valley Depth .....	198
3.49	Width of Raised Rim Versus Valley Width .....	199
3.50	Section of Highway 37 Cut Near Gibbons Alberta	205
3.51	Critical Stress for Buckling to Occur (Euler's Criterion) .....	213
3.52	Critical Stress for Buckling to Occur if Self Weight is Included .....	214
3.53	Normalized Maximum Values of Rebound Versus E	223
4.1	Typical Stress-Strain Relationship .....	232
4.2	Field and Laboratory Moduli .....	232
4.3	Variation of E with Depth in the Middle Chalk at Mundford, Norfolk .....	243
4.4	Data from the Buena Vista Pumping Plant .....	245
4.5	Comparison of Finite Element and Finite Difference Displacements .....	253



Figure		Page
4.6	Rebound in Valley Center Versus Depth to Rigid Base .....	255
4.7	Displacements Adjacent to Homogeneous Vertical Cut .....	256
4.8	Finite Element Representation of a Valley with Vertical Sides - Grid One .....	258
4.9	Displacements due to Valley Excavation - Grid One .....	263
4.10	Displacements due to Valley Excavation - Grid One .....	265
4.11	Vertical Displacement of the Ground Adjacent to the River Valley - Grid 1 .....	266
4.12	Vertical Displacement of the Ground Adjacent to the River Valley - Grid 1 .....	267
4.13	Vertical Displacement of the Ground Adjacent to the River Valley - Grid 1 .....	269
4.14	Variation of Vertical Displacement with E - Grid 1, $K_0 = 1.00$ .....	271
4.15	Variation of Vertical Displacement with $K_0$ - Grid 1, E = 40 KSI .....	272
4.16	Variation of Vertical Displacement with Poisson's Ratio - Grid 1, E = 40 KSI .....	273
4.17	Horizontal Movement of Valley Edge - Grid 1, E = 40 KSI .....	275
4.18	Effect of $K_0$ on Horizontal Movement of Valley Edge - Grid 1, E = 40 KSI .....	276
4.19	Variation of Horizontal Displacement with E - Grid 1 .....	277
4.20	Variation of Horizontal Displacement with $K_0$ - Grid 1 .....	277
4.21	Finite Element Grids .....	282
4.22	Comparison of Methods of Fixing Rigid Base - Grid 2 .....	284





Figure		Page
4.23	Change in Principle Stress Under a Strip Loading .....	285
4.24	Displacements Versus Depths to Rigid Base - Grid Two .....	287
4.25	Variation of Vertical Displacement with E - Grid 5 .....	288
4.26	Variation of Vertical Displacement with $\nu$ - Grid 5 .....	288
4.27	Effect of Poisson's Ratio upon Horizontal Displacements - Grid 5 .....	290
4.28	Finite Element Grids Used to Study Effect of Valley Width, Depth & Slope .....	291
4.29	Effect of Valley Wall Inclination upon Vertical Displacement of the Valley Edge - Grids 2, 2A, 2B .....	293
4.30	Effect of Valley Width upon Vertical Displacements - Grids 2, 2M, 2N, 2O .....	295
4.31	Effect of Valley Width upon Rebound .....	296
4.32	Effect of Depth of Valley upon Vertical Displacements - Grids 2, 2X, 2Y .....	297
4.33	Effect of Depth to Rigid Base on Vertical Displacements - Grid 2 .....	299
4.34	Effect of Depth to Rigid Base, Non-Homogeneous Grid .....	300
4.35	Effect of Depth to Rigid Base on Vertical Displacements Adjacent to the Valley - Grid 2 .....	302
5.1	Movements at Potrero Tunnel, San Francisco ....	309
5.2	Seattle Freeway Slide .....	309
5.3	Freeway Excavation, Minneapolis, Minnesota ....	311
5.4	Geologic Section, Minneapolis Freeway .....	311
5.5	Flexural Slip Folding .....	314





Figure		Page
5.6	Interbed Slip due to Folding .....	314
5.7	Maximum Interbed Slip due to Folding a Horizontal Stratified Sequence of Rock .....	316
5.8	Mechanism of Overthrusting due to Flexural Slip Folding .....	321
5.9	Grid 1A .....	327
5.10	Differential Displacements across Bentonite Layer ( $K_O = 0.50$ ) .....	330
5.11	Differential Displacements across Bentonite Layer ( $K_O = 1.00$ ) .....	331
5.12	Differential Displacements across Bentonite Layer ( $K_O = 2.00$ ) .....	332
5.13	Differential Displacements across Bentonite Layer ( $K_O = 3.00$ ) .....	333
5.14	Maximum Differential Displacements across Layer "A" at Toe of Slope .....	334
5.15	Maximum Differential Displacement across Layer "A" at Toe of Slope .....	335
5.16	Differential Displacement across Layer "B" ....	337
5.17	Effect of $E_L/E$ on Maximum Differential Movement - Layer "B" .....	338
5.18	Effect of $K_O$ on Maximum Differential Movement - Layer "B" .....	338
5.19	Maximum Differential Displacement across Layer "A" .....	340
5.20	Maximum Differential Displacement across Layer "B" .....	341
5.21	Effect of Variation in $\nu$ - Homogeneous Section .....	342
5.22	Effect of Variation in $\nu$ - Layer "A" .....	342
5.23	Effect of Distance to Lateral Boundary .....	344
5.24	Effect of Depth to Rigid Base on Maximum Differential Displacement .....	345



Figure		Page
5.25	Grid 8 & 8A .....	347
5.26	Effect of Thickness of Bentonite Layer .....	348
5.27	Effect of Location of Bentonite Layer in Valley Wall .....	350
5.28	Effect on Maximum Differential Displacements of Location of Bentonite Layer ..	351
5.29	Horizontal Nodal Displacement on a Section through Toe of Slope .....	352
5.30	Horizontal Nodal Displacement on a Section through Toe of Slope .....	354
5.31	Grids F & FL .....	357
5.32	Differential Displacements across Layer "B" due to a Vertical Excavation .....	358
5.33	Differential Displacements across Layer "B" due to Direct Excavation to a 2:1 Slope ...	359
5.34	Comparison of A One Stage to A Two Stage Excavation Process ( $K_o = 2.00$ ) .....	361
5.35	Differential Displacements across Layer "B" due to Flattening Slope from Vertical to 2:1 .....	362
5.36	Cumulative Differential Displacements across Layer "B" due to Vertical Excavation and Slope Flattening .....	364
6.1	Decay of Strength in Excavations in Overconsolidated Clay .....	373
7.1	Damsite Stratigraphy .....	392
7.2	Development of Tension Zones Adjacent to a Vertical Cut .....	396
7.3	Parallel Drainage Features near Redcliff, Alberta .....	399
7.4	Development of Drainage Patterns Adjacent to Postglacial River Valleys .....	401





Figure		Page
7.5	Parallel Drainage Features near Drumheller, Alberta .....	403
7.6	Formation of Backwater Swamps on Highlevel Terraces .....	405





## LIST OF PLATES

Plate		Page
2.1	View of the east abutment core trench at Boundary Dam, Saskatchewan .....	78
2.2	General view of the east abutment core trench shown in Plate 2.1 .....	78
3.1	View of the lower gouge zone on the east wall, Pier 2 excavation, Beverly Bridge	183
3.2	Closeup of the gouge zone shown in Plate 3.1	183
3.3	View of the slickensided lower shale - bentonite contact in the west abutment excavation of the Beverly bridge .....	185
3.4	View of the shale - bentonite contact cut from the block sample taken in the west abutment excavation at the Beverly Bridge	185
3.5	View of the west side of a roadcut on Highway 37 near Gibbons, Alberta .....	203
3.6	View of raised valley rim near Drumheller, Alberta with the valley of Michichi Creek to the left of the photo .....	205



## CHAPTER I

### INTRODUCTION

#### 1.1 Thesis Topic

This thesis considers the geotechnical implications of river valley formation in the prairies of Western Canada and the Northern United States. The area is underlain by heavily overconsolidated bedrock of Upper Cretaceous age which presents formidable problems to the geotechnical engineer. The bedrock of the area is extremely variable with some formations comprised primarily of clay-sized particles (termed "clay-shales") while others are more heterogeneous and contain beds of sandstone, siltstone, shale, coal and bentonite. The bedrock of the area behaves in many ways like an overconsolidated fissured clay with dominant horizontal planes of weakness along bedding.

Geotechnical engineering problems are concentrated along the river valleys due to the marked instability of many of the valley walls and the concentration of population, and hence, engineering works, in and adjacent to the river valleys of the area.

The drainage system of the area consists typically of relatively narrow valleys, many of which are postglacial, excavated several hundred feet through a relatively thin veneer of glacial deposits and bedrock. Massive slumping frequently occurs where the bedrock has been exposed by





valley downcutting and the prediction of slope stability has proved extremely difficult.

An important aspect of geotechnical engineering in the study area is the design and construction of large earth-fill dams, many of which have been erected over the last thirty years. These structures are usually founded in part on bedrock and the stability of the bedrock foundation has often been the controlling factor in the design of the dams. The large excavations required for these projects have often generated massive landslide activity and the design, and eventual cost, of these projects is usually controlled by the bedrock below and adjacent to the valley.

Most of the dam sites in the study area are situated in postglacial valleys which have been formed in the last 15,000 to 25,000 years. The valley itself and the present valley walls are thus relatively young on a geologic time-scale; it would appear likely that some of the behaviour of the bedrock of the study area can be explained on the basis of the events resulting from the formation of the river valleys.

## 1.2 Scope of the Thesis

An examination of the soil mechanics literature shows that an excavation made into an overconsolidated soil results in a large rebound of the excavation bottom. Several feet of vertical rebound has been measured below the base of deep excavations cut into the Cretaceous bedrock of



the study area at Garrison Dam (Lane and Occhipinti, 1953) Oahe Dam (Underwood et al., 1964) and the South Saskatchewan River Dam (Ringheim, 1964).

The river valleys of the study area can be regarded as large scale natural excavations. Drilling records from damsite and bridge investigations were examined and evidence of vertical rebound below the valley bottom correlated. In all cases, where reliable marker beds existed in the bedrock of the study area and sufficient drilling had been done to locate these marker beds, evidence of valley bottom rebound was noted.

The finite element method was used to simulate valley formation in a homogeneous, isotropic, linearly elastic continuum to study the effect of various input parameters upon the displacements of the bedrock due to valley formation. The implications of the bedrock behaving as a layered medium during valley formation were studied by the finite element method and from considerations of the results of flexural slip occurring between beds as a result of valley bottom rebound.

A number of landforms occur adjacent to the valleys due to valley formation and their occurrence was documented by field surveys. Field observations were made on the bedrock in-situ below and adjacent to a section of a post-glacial valley in the study area.

The results of the field data and the theoretical analyses are applied to the problems of natural slope





stability, excavated slope stability and earth dam design.

### 1.3 Organization of the Thesis

Chapter II of the thesis documents the properties of the bedrock of the study area and reviews published data on slope stability and performance of major earthfill dams in the area. A discussion of standard coring techniques and the limitations inherent in this type of investigation procedure is given.

Chapter III presents geologic sections from dam and bridge sites in the study area gathered in the course of this thesis. Geotechnical properties of the bedrock from each site are presented and literature describing rebound phenomena is reviewed. The possible mechanisms of valley bottom rebound are evaluated.

Chapter IV describes the simulation of valley formation using the finite element method assuming a homogeneous, isotropic ideal elastic rock. Data available on the laboratory and field determination of the elastic properties of soil and rock is reviewed as are published cases comparing actual excavation performance to that predicted by laboratory tests. The effect on displacement of the valley bottom and walls due to variation in Young's modulus ( $E$ ) and Poisson's ratio ( $\nu$ ) of the bedrock, the in-situ stress relieved, valley geometry and boundary conditions of the finite element grid are studied.



Chapter V considers the results of valley formation in a layered bedrock sequence. The magnitude of flexural slip due to valley bottom rebound is analyzed for the cases given in Chapter III. The differential displacement, due to valley formation, across bentonite layers is simulated by the finite element method. The effects of slope flattening in a layered bedrock sequence are considered.

Chapter VI applies the results of the previous work to slope stability problems in the study area. Implications for the design of earth dams, cofferdams and bridge piers are discussed.

Chapter VII contains a discussion of the implications of river valley formation for structural geology and geomorphology adjacent to the river valleys in the study area.





## CHAPTER II

### THE BEDROCK OF THE WESTERN PLAINS OF NORTH AMERICA

#### 2.1 Introduction

The southern portion of the three Canadian Prairie Provinces and much of the Great Plains of the Northern United States is underlain by a thick succession of relatively soft, gently dipping sedimentary strata of Cretaceous and Tertiary age. These strata are of similar origin and composition and, although classified by geologists as rock, often have properties more similar to soil. These formations often develop massive landslide activity when exposed by the valleys of postglacial rivers as described by Peterson (1958), Hardy et al. (1962), Pennell (1969) and Fleming et al. (1970).

The bedrock of the study area has proved to be an extremely difficult medium for engineering works to be constructed in. Examples of failures of dams, bridges and cuttings in the study area are numerous and a study of the literature shows that use of standard soil mechanics design procedures has in the past met with limited success (Peterson et al., 1960, Fleming et al. 1970).

In this chapter the geologic setting of the river valleys, the mode of formation and the lithology of the bedrock in the Great Plains are discussed. Engineering problems encountered during construction of a number of



major earth dams are reviewed. These problems are examined in the context of the engineering properties of the bedrock and the standard investigation and design practices in current use.

## 2.2 Geologic Setting

The Great Plains of Western Canada and the Northern United States consist generally of an area of low topographic relief through which river valleys have been incised several hundred feet deep through a thin veneer of glacial deposits and the bedrock of the area. This sedimentary bedrock is generally flat-lying and has been little disturbed by tectonic activity since deposition. The bedrock consists of a succession of marine and non-marine shales, siltstones, sandstones and clay-shale with minor amounts of bentonite and coal.

It should be noted that the terminology used in naming and classifying sedimentary rock is not settled and no satisfactory classification system for engineering purposes presently exists (Underwood, 1967). For example, in describing a fine-grained, fissile, argillaceous sedimentary rock the terms shale, clay-shale, claystone and mudstone have been used interchangeably by various authors. In this thesis the terminology used in reference material, both published papers and unpublished engineering reports, will be used for the sake of continuity. A commonly accepted definition for these descriptive terms is given by





Locker (1969):

Shale: a highly indurated readily fissile rock composed of predominantly clay and silt sized particles.

Clay-shale: an indurated readily fissile soft rock which may revert to a clay of medium to high plasticity and assume the characteristics of a highly overconsolidated clay.

Claystone: an indurated rock or soft rock which lacks fissility and is composed predominantly of clay-sized particles.

Siltstone: an indurated rock or soft rock composed predominantly of silt-sized particles.

Underwood (1967) discusses the classification and identification of shales and considers this type of rock to fall into two main categories:

1. Compaction or 'soil-like' shales which have been consolidated by the weight of overlying sediments and lack significant amounts of intergranular cement. Most compaction shales can be excavated with modern earth-moving equipment and slake rapidly when subjected to wetting and drying cycles. The fine grained argillaceous bedrock of the study area falls into this group.
2. Cemented 'rock-like' shales where the cementing material (calcareous, siliceous, ferruginous, etc.) contributes markedly to the strength of the bedrock. These shales are usually excavated by blasting, do



not slake upon wetting and drying and are generally not a troublesome material. None of the fine-grained argillaceous bedrock in the study area falls into this group.

Implicit in all discussion of the bedrock of the study area is the fact that it has been subjected to overburden loads greatly in excess of the present overburden load.

### 2.3 Properties of the Bedrock in the Study Area

Lithology: The strata of the study area consist mainly of interbedded shales, clay-shales, siltstones and sandstones. Beds of bentonite are common in many of the formations and in some formations bentonite is dispersed throughout the bedrock resulting in bentonitic shales and sandstones. Certain formations, normally those deposited in a deltaic or continental environment, have interbedded strata with little lateral continuity in the beds as the formations grade one into another. In other formations, normally those deposited in a marine environment, continuity of beds is more marked. However, usually only bentonite, limestone, marl and coal beds show uniform thickness and lateral continuity over sufficient distance to be used as marker beds.

Bentonite beds have been used as marker beds by geologists in the Bearpaw formation (Hake and Addison, 1954) for distances up to 20 miles and have been used as marker





beds in many other sedimentary formations. Bentonite beds have been traced over large distances at Fort Peck Dam in the Bearpaw formation and at Oahe Dam in the Pierre shale (Fleming et al., 1970). Bentonite layers in the Niobrara chalk are continuous over many miles and were used as marker beds at Fort Randall Dam (Underwood, 1964). Lignite beds were used as marker beds at Garrison Dam (Smith and Redlinger, 1953) and the Bowman-Haley Damsite in North Dakota (U.S.C.E., 1963b).

Figure 2.1 shows the bedrock geology of the study area with the location of the major projects discussed in this chapter. A generalized stratigraphic section of the area is given in Figure 2.2.

Origin of Bedrock: The late Cretaceous-Tertiary bedrock of the Canadian Prairies and the North-Central United States resulted from deposition of material in a subsiding basin which was flanked by highlands lying to the south and west of the study area. Erosion from the highlands provided the sediments which accumulated in the basin to the east. Volcanic activity in the highlands provided volcanic ash which was altered to form the bentonite layers and the bentonite rich strata common in the study area.

Sediments from the highlands were transported eastward in streams. The depositional environment in a particular area dictated the type of sediments which accumulated. In Western Canada, sediments deposited in the western



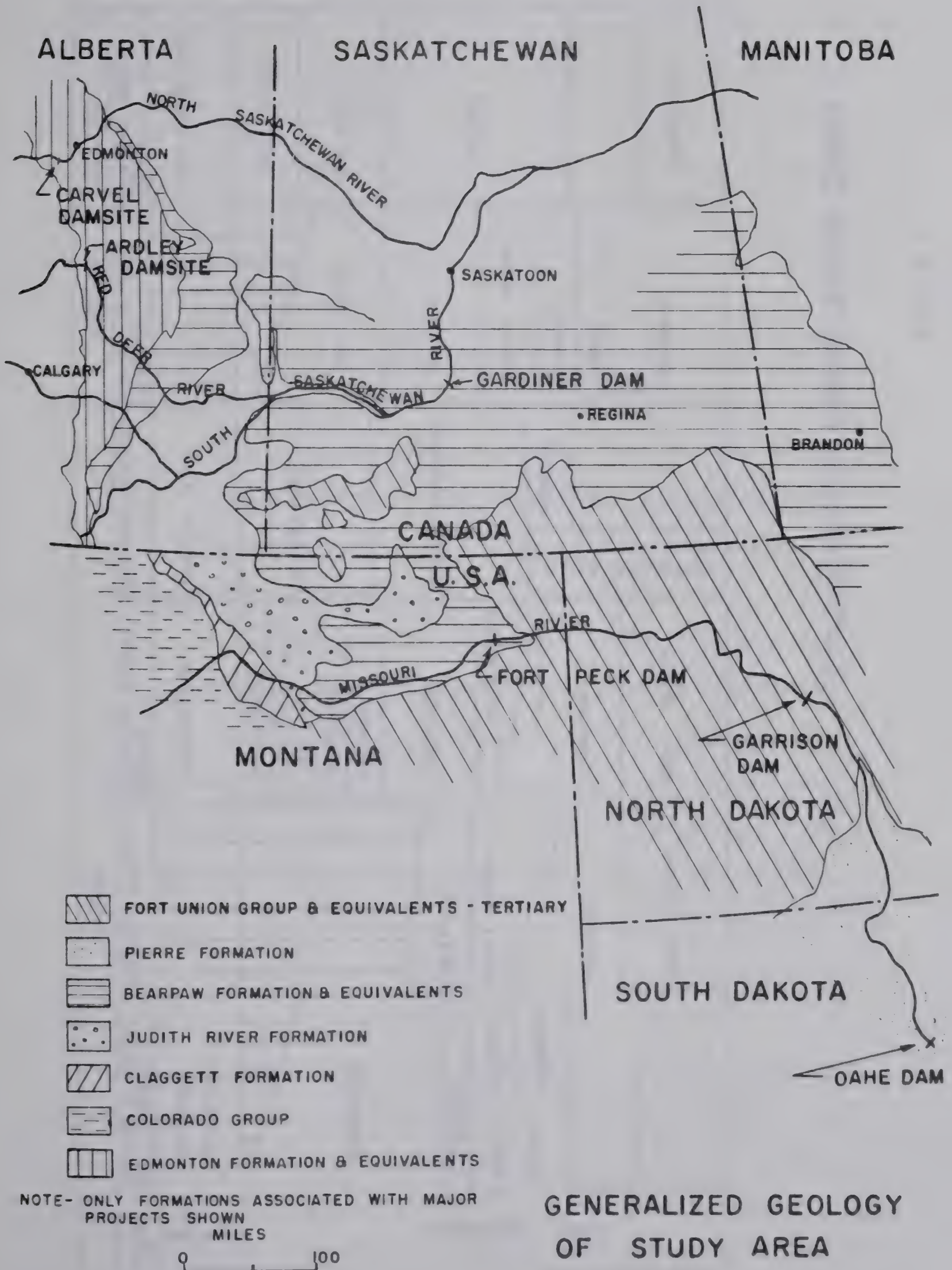


FIG. 2.1







	CANADA				UNITED STATES	
PERIOD	CENTRAL & SOUTH-ERN ALBERTA	EASTERN ALBERTA	SOUTHERN SASKAT-CHewan	SOUTHERN MANITOBA	NORTH-CENTRAL MONTANA	CENTRAL NORTH DAKOTA
TERTIARY	PASKAPOO RAVENSCRAG		RAVENSCRAG	TURTLE MTN.		FORT UNION GROUP
			FRENCHMAN			
UPPER CRETACEOUS			BATTLE	BOISSEVAIN		HELL CREEK
			WHITEMUD			
			EASTEND		FOX HILLS	FOX HILLS
	EDMONTON					
	BEARPAW	BEARPAW	BEARPAW	RIDING MOUNTAIN	BEARPAW	
	BELLY RIVER	BELLY RIVER	BELLY RIVER		JUDITH RIVER	PIERRE
	OLDMAN					
	FOREMOST			PEMBINA	CLAGGETT	
		PAKOWKI	PAKOWKI		EAGLE	
	LEA PARK	MILK RIVER	MILK RIVER	VERMILION RIVER	COLORADO	NIOBRARA

STRATIGRAPHIC CORRELATION CHART

FIG. 2.2



portion of the basin, above sea level, resulted in a complex interbedded sequence composed of sands, silts, clays and organic materials with the coarser fractions predominating. The result is typical of present day deltaic deposition and resulted in, for example, the Edmonton formation of central Alberta and the contemporaneous St. Mary formation of southern Alberta.

The eastern portion of the basin was covered by a shallow sea (termed the Pierre sea in the United States) which stretched from the Arctic to the Gulf of Mexico and in which the clay-sized particles and the finer-grained silts were deposited in a marine environment to form the Bearpaw and Pierre formations. A more uniform clay-shale resulted interspersed with bentonite layers which were formed by volcanic ash settling to the bottom of the sea.

Following this period of deposition, some 90 million years before the present, the sea retreated to the south and east. Thus, towards the end of the Cretaceous, deposition through most of the study area was in a continental environment. This continued through the Tertiary when formations such as the Paskapoo of central Alberta and the Fort Union Group of the Dakotas were deposited.

History Subsequent to Deposition: Towards the end of the Tertiary period the study area was transformed into an area of uplift due to the orogeny which transformed the western part of the basin into the present Rocky Mountains. From middle Tertiary time onwards erosion occurred





and, over a long period of time, resulted in the topographic outlines of the Western Plains as they exist today. Local topography was modified by the Pleistocene glaciation which covered most of the study area. Glacial deposits were laid down, often in great thickness, in preglacial low areas and the general effect was to produce a flat, gently rolling topographic surface.

The present drainage system of the area was formed during the retreat of the continental glaciers some 15,000 to 25,000 years ago (Scott and Brooker, 1968, Fleming et al., 1970). Large volumes of meltwater rapidly eroded wide, steep-sided channels which were often ice-marginal channels or spillways of glacial lakes. These valleys are typically one to two miles across, several hundred feet deep and are steep-sided except where landslide activity has flattened the valley sides. The Missouri River, for example, was formed some 25,000 years ago (Fleming et al., 1970) and rapid down-cutting gave the valley its depth within a few thousand years. Massive slumping along the Missouri in the Claggett, Bearpaw and Pierre formations developed a set of joints and old failure surfaces which appear to largely govern present day slope stability. The occurrence of large scale old landslide topography is not noted in the Colorado and Fort Union formations.

Landslide activity is common along many of the valleys in Alberta and can be correlated with bedrock type (Matheson 1970, Roggensack 1971). The argillaceous formations



deposited in a marine environment (the Bearpaw and Pierre formations for example) appear most susceptible to slide activity and valleys cut through these formations are characterized by continuous slide topography. These slides presently appear to be quiescent except when active river erosion is attacking the toe of the slope. Formations deposited under deltaic conditions, such as the Edmonton formation, appear much less susceptible to slide activity and the river valleys are typically steep-sided over long reaches except where active toe erosion has initiated landslides. Tertiary sediments deposited under continental conditions, such as the Paskapoo formation of western Alberta, exhibit a low propensity for landslide activity and stable near-vertical slopes of 200 feet are not uncommon.

Slide activity is common along the Missouri River in the Claggett, Bearpaw and Pierre formations and is less troublesome in the Colorado and Fort Union Group (Fleming et al., 1970).

Presence of Bentonite Beds: A useful index in assessing the potential of a given formation to cause slope stability problems is the presence of a large percentage of the clay mineral montmorillonite and the presence of beds of bentonite. Formations which contain bentonite, either as layers or dispersed as bentonitic shale or sandstone, are generally characterized by large scale landslide activity while formations which do not contain appreciable amounts of bentonite are much less troublesome. Bentonite is common in the







Edmonton, Bearpaw, and Pierre formations and is seldom found in the Tertiary Paskapoo and Ravenscrag formations and the Fort Union Group.

Bentonite may be defined as a clay composed essentially of montmorillonite formed by the decomposition of volcanic ash (Byrne, 1955). Beds of bentonite are found in many of the Cretaceous formations of the Great Plains and strata, which contain dispersed bentonite in the form of bentonitic shales and sandstone, are common.

Studies of bentonite reserves in the Province of Alberta have been conducted by the Research Council of Alberta and are reported by Byrne (1955) and Babet (1966). The greatest concentration of bentonite occurs in the upper portion of the Upper Cretaceous formations. Bentonite beds occur in the Bearpaw formation and are commonly only a few inches thick but are continuous for several miles. A persistent bed varying from 3 to 10 feet in thickness occurs in south-west Saskatchewan and south-eastern Alberta and is located about 100 feet above the base of the Bearpaw. Another bed of bentonite some 20 feet thick outcrops near the top of the Bearpaw along the Red Deer River some 20 miles downstream of Drumheller, Alberta. Major bentonite outcrops in the Bearpaw formation are noted at 17 locations in Alberta by Babet (1966).

A total of 59 known outcrops of major bentonite beds in the Edmonton formation are listed by Babet (1966).



Average bed thickness reported ranges from 2 to 10 feet but maximum thicknesses of up to 20 feet are reported.

Bentonite beds are reported as being abundant in some portions of the Bearpaw formation at Fort Peck Dam in Montana (Fleming et al., 1970) and range in thickness from a fraction of an inch to as much as 2 feet. Bentonite layers in the Pierre shale at Oahe Dam on the Missouri River range from a fraction of an inch to 18 inches (Crandell, 1958). The Degray member of the Pierre shale contains about 25 bentonite beds in its upper portion and stable outcrops of this section of the member are seldom found. Yudhbir (1969) considers the marked instability of this member to be related to the presence of these bentonite beds.

Overconsolidation of the Bedrock: The long period of erosion which occurred during the Tertiary removed a considerable depth of sediment from the present bedrock surface. Rutherford (1928) estimated that 2000 feet of material have been eroded from Central Alberta during this period. Smith and Redlinger (1953) estimate that 1200 feet of material has been eroded from the Fort Union Group at Garrison Dam in North Dakota. Melting of the continental glaciers following the Pleistocene removed several thousand feet of ice from much of the area. An estimated 4,000 feet of ice covered the Red Deer Valley near Drumheller, Alberta (Scott and Brooker, 1968). The result of unloading is an expansion or rebound which is a maximum at the bedrock



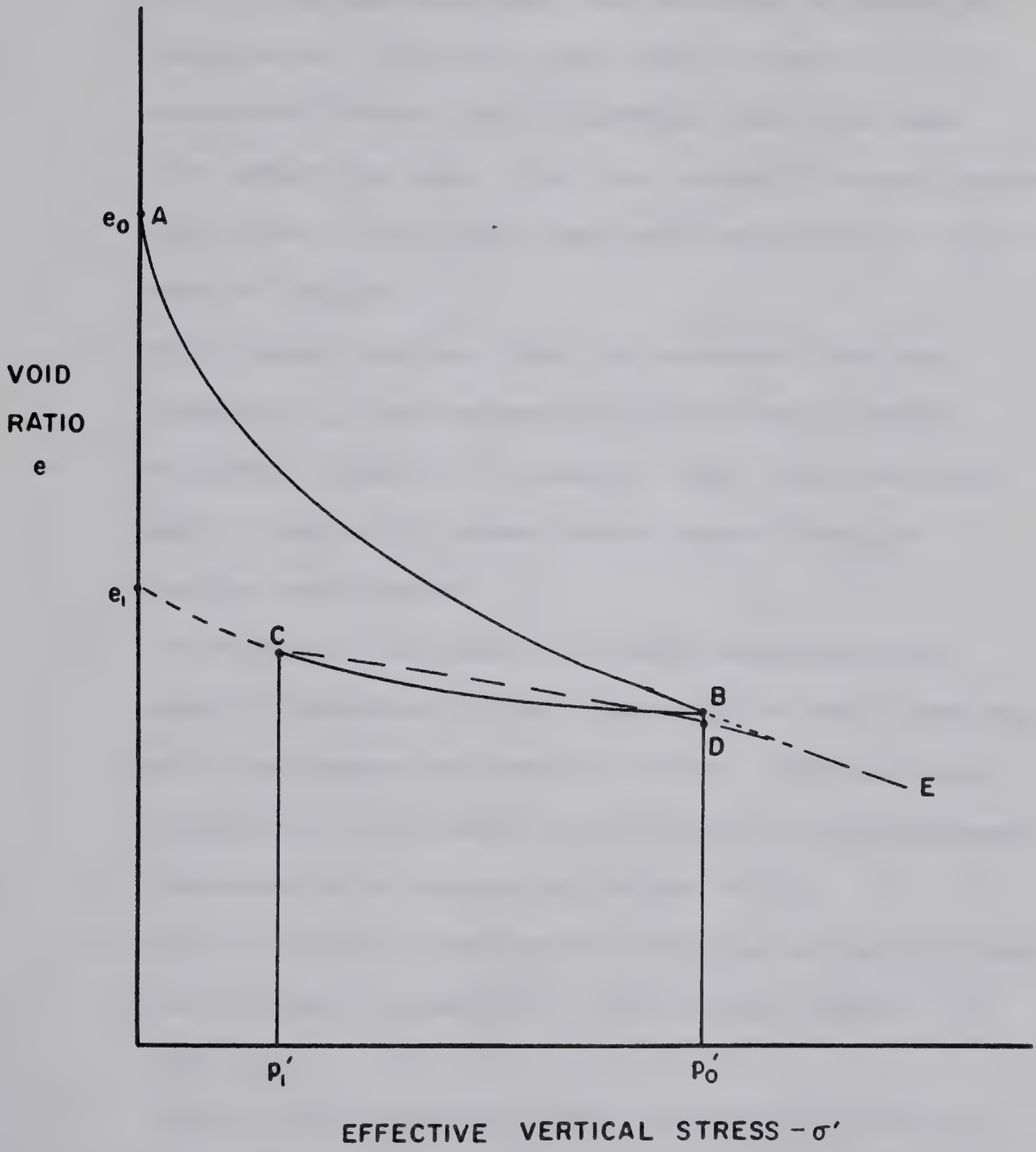


surface and decreases with depth. This rebound is considered to have two components (Peterson et al., 1960):

1. elastic rebound which is a function of the stress removed and the modulus of elasticity ( $E$ ) of the bedrock and occurs while the load is being removed. Due to the relatively short period of time during which this movement occurs, the modulus of elasticity from an undrained triaxial test must be used to give an appropriate value of  $E$ .
2. swelling or time-dependent rebound due to absorption of water which occurred at a decreasing rate as a function of the permeability of the rock mass.

The process of swelling can be modelled in an oedometer. The effect of loading and unloading a sample of sedimentary rock is shown in Figure 2.3. Initially the effective stress is increased on a sediment and consolidation occurs. As the load on the sample increases with depth of burial the void ratio  $e$  decreases and the sediment becomes denser and, in a saturated sediment, the moisture content decreases with decreasing void ratio following path AB. A reduction in effective stress on the sample from  $P'_0$  to  $P'_1$  leads to an increase in void ratio (or rebound) along path BC. Removal of all vertical stress on the sample would lead to a void ratio  $e_1$ . Reloading to the preconsolidation pressure  $P'_0$  follows path CD.





(AFTER TERZAGHI, 1955)

INFLUENCE OF A LOAD REDUCTION ON  
A SEDIMENTARY ROCK

FIG. 2.3





The effect of overconsolidation on clays is described by Terzaghi (1955) as:

1. The reduction in void ratio from  $e_0$  to less than  $e$ , which is associated with an increase in shearing resistance. Thus the peak shear strength of an overconsolidated clay is greater than the same clay under the same load in a normally consolidated state even if the clay has been weakened by a network of joints.
2. Under loads smaller than the preconsolidation pressure  $P'_0$  the compressibility of any overconsolidated sediment is smaller than the same sediment if normally consolidated under identical loading conditions.
3. The heave of the bottom of deep excavations in heavily overconsolidated clays can be very important and troublesome because the volume increase associated with the removal of the last load increments increases with increasing values of  $P'_0$ .
4. The horizontal pressure decreases less rapidly than the vertical pressure in a soil mass subject to unloading.

Brooker and Ireland (1963) found the coefficient of earth pressure at rest (the ratio of lateral to vertical effective stress) to be a function of the effective angle of shearing resistance of the soil and the stress history of the soil as shown in Figure 2.4. An increase in the



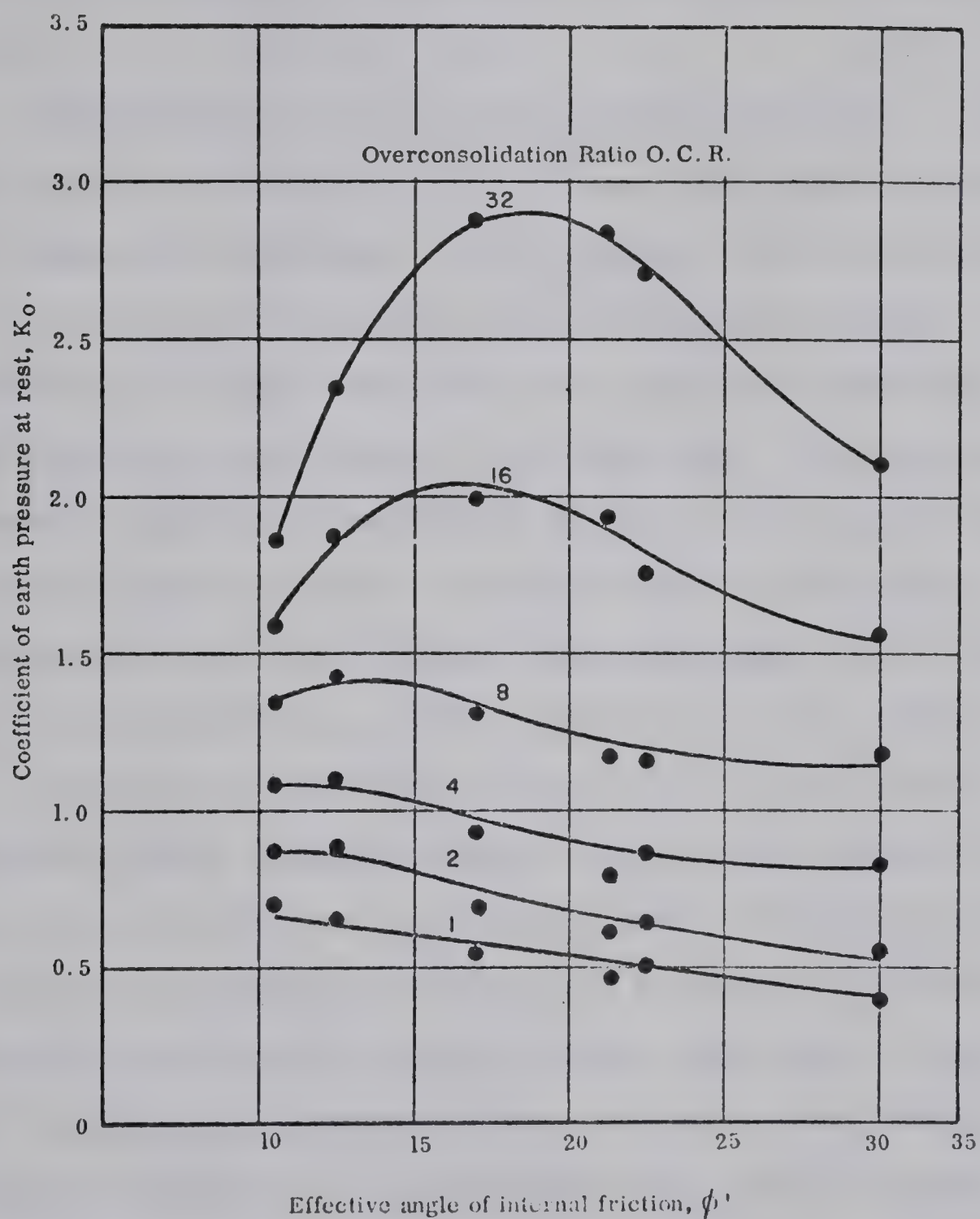


FIG. 2.4

Relationship between coefficient of earth pressure, overconsolidation ratio and angle of shearing resistance.

(BROOKER & IRELAND, 1963)



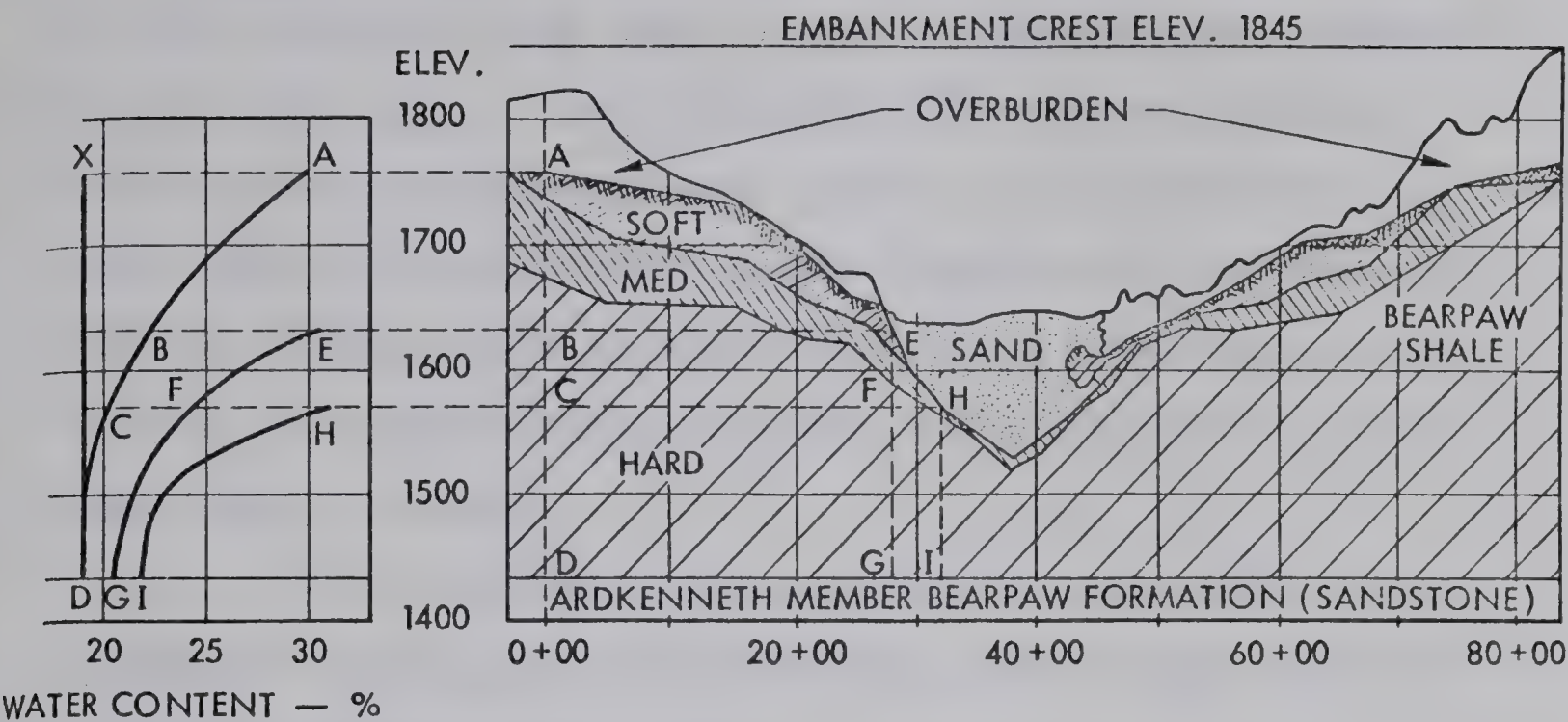


overconsolidation ratio of a soil (defined as the ratio of the present vertical effective stress to the maximum vertical effective stress the soil has had on it in its geologic past) results in an increase in magnitude of the lateral stress in the soil.

Several field observations of the behaviour of the bedrock in the study area indicate that high lateral forces exist. Smith and Redlinger, (1953) report 3 inch wide saw cuts in the bedrock at Garrison Dam (Fort Union Group) closed within 24 hours when the cuts were made below the minimum elevation the Missouri had ever cut. In-situ stress measurements made in a test drift at the South Saskatchewan River Damsite gave vertical stresses equal to the overburden pressure but gave lateral stresses equal to 1.5 the vertical stress (P.F.R.A., 1951; Peterson et al., 1960).

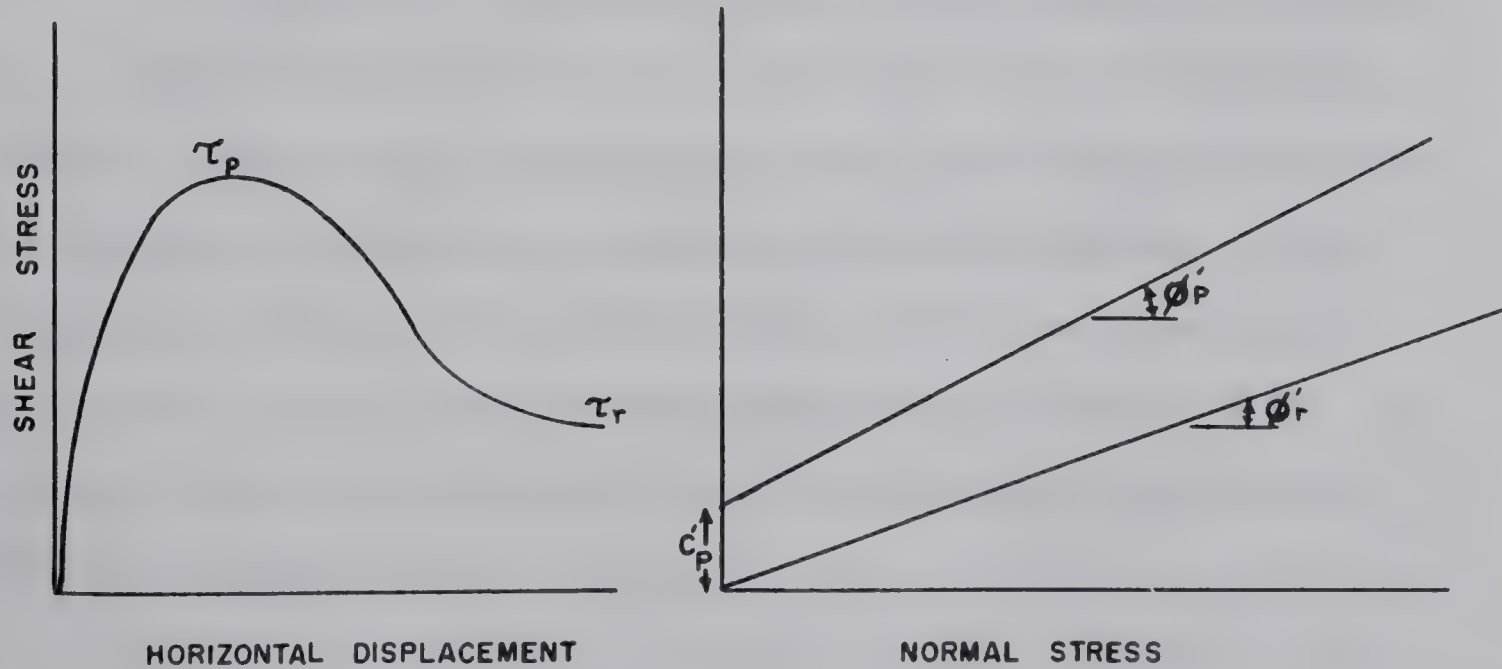
A study of water-content profiles at the South Saskatchewan River Damsite indicate that large amounts of rebound have occurred in the Bearpaw shale. Moisture content profiles are shown in Figure 2.5 for three locations - the uplands back from the river and two locations in the valley. Laboratory oedometer tests indicate that the initial moisture content of the Bearpaw shale was 14 percent under preconsolidation pressure of 150 tons per sq. ft. (Peterson, 1958). The increase in water content towards the surface of the bedrock indicates that point A has heaved or increased in elevation with respect to point D by approximately 53 feet.





Valley cross-section and foundation profile with typical moisture content profile, Gardiner Dam. (FLEMING ET. AL. 1970)

FIG. 2.5



TYPICAL DIRECT SHEAR RESULTS - FIG. 2.6





Similarly it was computed that point E had risen 36 feet and point H 26 feet. Most of this movement occurred in the upper part of the shale and differential movements should result along horizontal planes. The difference in water content between point B and E indicates a horizontal rebound between B and E of 600 feet if it is assumed all rebound is horizontal and the original water content of the shale was 14 percent.

If the original moisture content in the shale was 19 percent rather than 14 percent, the above values would be reduced by approximately half.

These rebound values assume movement to be entirely vertical or horizontal. Close to the valley, movement occurred in both directions; therefore the values should be reduced accordingly. However they clearly indicate large movements have occurred both vertically and towards the valley.

A study of the differing moisture content profiles, at a given elevation below the elevation of the river bed, shows a higher moisture content under the valley than under the uplands indicating a larger amount of rebound (or differential rebound) has occurred due to the excavation of the valley by the South Saskatchewan River due to the removal of several hundred feet of additional overburden from the floor of the valley.



## 2.4 Slope Stability Experience in the Study Area

Construction of major civil engineering works in Western Canada and the Northern United States over the last 50 years has shown that the Cretaceous bedrock of the area is an extremely troublesome material. A study of the literature reveals numerous cases where application of currently accepted soil mechanics practice met with something less than success. Prediction of the stability of slopes in the bedrock of the study area has proved especially difficult causing Hardy et al. (1962) to conclude:

"Particularly along the river valleys in the area under consideration, this deterioration of the soil seems to be actively progressing with the results that the stability of the banks is gradually decreasing and at many locations the factor of safety against failure is very close to unity. Engineering construction in these valleys, such as road and bridge work, frequently produces change in the stability conditions sufficient to precipitate major earth movements. Experience to date in the area shows that it is very difficult to determine by conventional subsoil exploration methods when such instabilities will develop. Experience has also shown that conventional methods of stability analysis are inadequate to accurately assess these slopes as they exist naturally or as they may be modified by engineering works."

Slope Stability Concepts: A pioneer study in the behaviour of landslides in clay was conducted by Collin (1846) who found:

1. many landslides in clay were deep rotational movements occurring along a cycloidal slip surface.
2. many failures in excavations made into stiff over-consolidated clays occurred some time after the







excavation was completed and was due to a progressive softening of the soil due to entry of water.

These concepts were expanded by Terzaghi (1936), Skempton (1948) and Cassel (1948) who postulated that overconsolidated fissured materials are susceptible to a decrease in strength with time due to opening of fissures, softening of the clay due to water infiltration and a decrease in strength of the mass.

The results of a typical drained direct shear test on an overconsolidated clay or soft rock is shown in Figure 2.6. Shearing resistance is mobilized as the sample is sheared across a failure plane until the peak shear strength ( $\tau'_p$ ) is reached. Further displacement results in a decrease in shearing resistance until a residual value ( $\tau'_r$ ) is reached. A series of tests under different normal stresses will yield two Mohr-Coulomb failure envelopes; one for peak and one for residual conditions. From these failure envelopes the effective angles of shearing resistance for peak and residual ( $\phi'_p$  and  $\phi'_r$ ) can be found as shown in Figure 2.6 and used in the Mohr-Coulomb failure criterion

$$\tau' = c' + (\sigma - u) \tan \phi' \quad (2.1)$$

where  $\sigma$  is the total normal stress and  $u$  is the pore water pressure.

Microscopic observations of shear induced fabrics in clays (Morgenstern and Tchalenko, 1967) show that shearing a clay to the residual strength results in a distinct slickensided surface along which particle orientation



in the direction of shear has occurred. The particle alignment is responsible for the drop in strength from peak to residual.

Numerous articles exist in the literature documenting landslides which occurred in overconsolidated fissured clays and shales at a strength well below the peak (Pope and Anderson, 1960; Gould, 1960; Peterson et al., 1960; Hardy et al., 1962). Experience has shown that stability analyses using the total stress method ( $\phi = 0$ ) or the effective stress method using peak strength parameters leads to a factor of safety higher than exists in the field. Skempton (1964) showed that residual strength parameters should be used to analyze landslides which have occurred along pre-existing failure surfaces and along which, large differential movements have occurred.

In overconsolidated clays the drop from peak to residual often leads to a marked reduction in strength as the peak strength is governed by the stress history of the soil while the residual strength is primarily a function of the mineralogical composition of the soil (Kenney, 1967; Morgenstern, 1967). The cohesion at residual decreases typically to a value very close to zero and the angle of shearing resistance decreases. Some typical values of peak and residual strength parameters reported by Skempton (1964) are shown in Table 2.1.





TABLE 2.1

## PEAK AND RESIDUAL STRENGTHS OF OVERCONSOLIDATED CLAY

(SKEMPTON 1964)

Site	Soil Type	Peak Parameters		Residual Parameters	
		$\phi_p$	$C'_p$	$\phi_r$	$C'_r$
Selset, U.K.	Unfissured boulder clay	$32^\circ$	180 p.s.f.	$30^\circ$	0
London area, U.K.	London Clay	$20^\circ$	320 p.s.f.	$16^\circ$	0
Walton's Wood, U.K.	Weathered mud-stone	$21^\circ$	320 p.s.f.	$13^\circ$	0
Jari, West Pakistan	Siwalik fm.	$22^\circ$	780 p.s.f.	$18^\circ$	0

For the cases reported at typical engineering stress levels, the peak strengths are 3 to 4 times the residual; therefore the soil parameter which should be used for design is of extreme importance in most geotechnical engineering problems.

Limit equilibrium methods can be used to analyze the stability of a slope (Bishop, 1955; Morgenstern and Price, 1967). The reliability of the results of an analysis of this type depend primarily upon the input parameters used. These are:

1. the geometry and stratigraphy of the slope.



2. the piezometric conditions.
3. geometry of the failure surface.
4. the values of  $\phi'$  and  $c'$  acting on the failure surface.

Notable progress has been made in recent years in developing inclinometers (tiltmeters) and piezometers to give information on zones of movement and piezometric conditions in the bedrock of the study area (Wilson, 1970, Brooker and Lindberg, 1965). The chief obstacle remaining in the consistent successful application of limit equilibrium methods to the analysis of valley slopes in the study area is which strength parameter to use. In certain field situations, such as the reactivation of an old landslide, stability analyses and a testing program on block samples taken from the failure plane show residual strength parameters govern the stability of the slide (Skempton and Petley, 1967). In the analysis of the stability of a normally consolidated, intact, non-fissured soil, one should use peak parameters (Skempton, 1964). However, study of the stability of slopes in the Cretaceous bedrock of the study area involves analyzing a highly overconsolidated fissured material with structural details (such as thin bentonite beds) which may control the stability of the entire slope. Use of peak parameters may lead to failure yet design on the basis of residual strengths may lead to excessively conservative and costly designs. To attempt to resolve some of these problems, the engineering experience gained in the study of landslides in the study area as well as the experience





gained in construction by a number of major earth dams in the study area will be reviewed.

(a) Slope Stability Problems in Western Canada: Landslide activity in the Cretaceous bedrock of Alberta has been an area of active research of the Department of Civil Engineering, University of Alberta for a number of years (Brooker, 1958; Hardy et al., 1962; Painter, 1965; Rennie, 1966; Hardy, 1967; Sinclair and Brooker, 1967; Hayley, 1968; Pennell, 1969; Thomson, 1970; Eigenbrod and Morgenstern, 1971). Earlier studies summarized by Hardy et al. (1962), showed that use of peak strength parameters led to factors of safety well in excess of unity when the slope was failing. Five of the larger slides were re-analyzed by Pennell (1969) in view of the development of recent theories in soil mechanics. It was concluded:

1. Residual strength parameters must be employed in the analysis of the slides to obtain a factor of safety of unity. Use of peak parameters produced factors of safety well in excess of unity. Residual angles of shearing resistance of bentonitic shale and bentonite seams in the Edmonton formation are approximately  $8.5^{\circ}$  (Sinclair and Brooker, 1967).
2. The landslides which occur in the bedrock of the area have wedge-shaped failure surfaces with a nearly horizontal bottom failure surface and a steeply-dipping back scarp.



3. The slide at Taylor, B.C. (Hardy, 1967) occurred in the Shaftesbury formation (Lower Cretaceous) when the shear strength had been reduced to the residual along the scarp and horizontal failure plane. Investigation indicated the horizontal failure surface extended some distance out from the bank about 10 feet below the bed of the river.
4. Two landslides which occurred in and near the City of Edmonton, the Lesueur and Grierson Hill slides, occurred with peak strengths developed along the scarp and near residual strengths along the bottom failure surface in the Edmonton formation (Upper Cretaceous). Both slides were believed initiated by river erosion. At the site of the Grierson Hill slide in downtown Edmonton, the North Saskatchewan River had encroached into the bank by about 50 feet between the period 1887 to 1893. Recorded movements on Grierson Hill date back to 1887.

Eigenbrod and Morgenstern (1971) studied in detail a landslide in the Edmonton formation at Devon, about 12 miles west of Edmonton, Alberta, which occurred following a highway cut along the valley of the North Saskatchewan River. The slide occurred on a horizontal bentonite layer and crossed softened mudstone in the back slope. Three perched water tables were observed in the slope but no water pressures were found along the horizontal section of the slip surface as it was in contact with a free draining coal layer.





Four boreholes drilled in the backslope of the slide in 1969 used a Pitcher Sampler to recover four inch diameter core specimens of bedrock. It was noted that dark grey mudstone was often brecciated along the interface with bentonitic sandstone. Softened material was often found where the mudstone and sandstone bands were closely spaced. Samples from two bentonite layers from testholes outside the landslide showed distinct failure zones.

A detailed examination of the general geology of the area showed the Devon slide to be located in a much larger and older slide which presumably occurred during valley formation. A borehole was drilled on the top of the valley wall in an area undisturbed by slumping. One bentonite layer was sampled which did not show failure planes. However, a very soft thin zone was found at the interface between light grey sandstone and brownish mudstone. The bedrock in this testhole appeared harder, more intact and less iron-stained than that found lower in the valley.

Stability analyses using the general non-circular limit equilibrium method (Morgenstern and Price, 1965) indicated residual parameters ( $\phi' = 8^{\circ}$ ,  $c' = 0$ ) were acting along the horizontal bentonite bed forming the base of the slide and peak parameters of  $\phi' = 33^{\circ}$  and  $c' = 190$  p.s.f. were acting on the backslope materials. Use of these laboratory results gave a factor of safety of 1.01 using measured pore-pressures.



This case is instructive in that great care must be used in sampling to define critical bentonitic layers and the locations of piezometers must be chosen with care if meaningful results are to be achieved. Mechanisms presented to account for the sheared bentonite observed outside the slide zone are:

- (1) bedding plane slip associated with anticlinal rebound in response to valley formation,
- (2) differential swelling of the bentonite constrained between adjacent non-swelling layers,
- (3) movements during the initial slide,
- (4) shear associated with ice movement during the Pleistocene.

The Cretaceous bedrock of Central Alberta (the Edmonton formation) exhibits extreme variation in composition and strength. Table 2.2 shows the results of strength tests on samples of the Edmonton formation.

Bentonitic shale samples are seen to have a high peak angle of shearing resistance, typically about  $25^{\circ}$ , yet a low residual angle of shearing resistance of about  $8.5^{\circ}$ . Bentonite samples exhibit similar residual strength parameters ( $\phi'_r = 8.5^{\circ}$ ,  $c'_r = 0$ ) as the bentonitic shale samples.

The extreme variability of properties of the different bedrock types in the Edmonton formation is shown in Table 2.3 which contains a summary of the properties of the bedrock types found at the Carvel Damsite located on the North Saskatchewan River some 26 miles southwest of Edmonton,





TABLE 2.2

## STRENGTH RESULTS FOR THE EDMONTON FORMATION

Name and Reference	Description	$W_n$	$W_l$	$W_p$	Acti- vity	Peak		Residual	
						$\phi_p$	$C'_p$ (psi)	$\phi'_r$	$C'_r$ (psi)
Lesueur (Sinclair et al., 1966)	Bentonitic Shale	20	216	59	1.7			$10^\circ$	
University of Alberta (Sinclair et al, 1966)	Bentonitic Shale	20	125	44	2.2	$27^\circ$ $8.5^\circ$	0 32	$8.5^\circ$ $8.5^\circ$	0 0
Sinclair and Brooker (1967)	Clay Shale	20	60	25	1.2	$22^\circ$	10		
	Bentonitic Shale	30	125	44	1.9	$25^\circ$ $8^\circ$	0 50		
	Bentonite	60	215	60	2.2	$14^\circ$ $9^\circ$	8 17	$8.5^\circ$ $8.5^\circ$	5 5
						$33^\circ$	0	$10.5^\circ$	9.8
Ardley Damsite (A.W.R., 1968)	Bentonitic Shale								
Carvel Damsite (P.F.R.A., 1969b)	Bentonite	34	210	39	2.5			$8^\circ-9.5^\circ$	3-8
	Bentonitic Shale	15	106	20	1.9	$39^\circ$	15	$14^\circ$	5
	Bentonitic Shale	16	109	21	2.3	$41^\circ$	29	$19.5^\circ$	4
	Shale	12	73	18	1.5	$41^\circ$	33	$20-22^\circ$	0-7



TABLE 2.3

## SUMMARY OF THE PROPERTIES OF BEDROCK TYPES

CARVEL DAMSITE ( P.F.R.A., 1969b)

Bedrock	wet p.c.f.	$W_n$ %	$W_L$ %	$W_p$ %	$Q_u$ p.s.i.	E p.s.i. $\times 10^4$	% colloidal .002 mm.
Sandstone	135 (69) 116-147	13 (102) 6-20	46 (13) 32-58	23 (13) 16-28	1052 (12) 126-2358	5.3 (12) 0.3-15	17 (9) 14-23
Bentonitic Sandstone	128 (87) 116-144	14 (173) 6-24	76 (10) 52-94	20 (10) 14-25	394 (8) 16-1450	1.5 (8) 0.1-8	21 (8) 18-26
Calcareous Sandstone	152 (14) 142-161	6 (18) 2-12	58 (1)	22 (1)	3724 (1)	20.7	18 (1)
Shale	138 (100) 111-145	13 (226) 5-38	67 (29) 42-85	21 (29) 15-27	2546 (13) 133-4984	21 (13) 3-69.4	34 (21) 24-61
Bentonitic Shale	130 (69) 110-143	19 (140) 9-49	104 (16) 76-132	26 (16) 19-43	636 (9) 63-1637	0.7 (3) 0.5-0.9	44 (11) 24-61
Bentonite	119 (12) 111-132	31 (31) 15-52	183 (17) 78-290	33 (17) 18-46	235 (2) 88-381	1.2 (2) 0.2-2.3	60 (9) 39-78

Note: (1) E is a secant modulus taken at  $1/3 - 1/2$  failure strain in an unconfined compression test.

(2) The upper figure is the average value for the number of tests conducted which is in brackets. The range of results is given immediately below.





Alberta (Figure 2.1). The site was investigated by the Prairie Farm Rehabilitation Agency during 1968 - 69 (P.F.R.A., 1969b). Bedrock consists of shales (32%), bentonitic shales (20%), sandstone (14%), bentonitic sandstone (25%) and bentonite (5%). These figures are based upon the core recovered which was 85 percent of the footage drilled. The percentage of soft erodible materials is undoubtedly higher. Most of the bedrock is weakly cemented with a bentonite binder and slakes rapidly when immersed in water.

A wide range occurs in both unconfined compressive strength (  $q_u$  ) and values of E. The average values of E from unconfined compression tests range from 210,000 p.s.i. for shale to 7,000 p.s.i. for bentonitic shale and 12,000 p.s.i. for bentonite. Variation in shear strength is given in Table 2.2.

A feature of river valleys cut through the Edmonton formation is the occurrence of stable steep slopes several hundred feet high adjacent to large retrogressive slide areas. The slides appear to be due mainly to active toe erosion of the river on the outside of meander bends as has been previously discussed.

At Carvel Damsite the stability of the natural valley slopes were studied extensively (P.F.R.A., 1969b). The natural slopes in the stretch of river extending for 5 miles either side of the site appear relatively stable at slopes of 1:1 to  $2\frac{1}{2}$ :1 for heights of between 100 and 300 feet. Upstream of this area natural slopes average  $5\frac{1}{3}$  : 1.



Stability analyses were made of the existing slopes using the wedge type of analysis (U.S.C.E., 1951) to determine the required angle of internal friction for a factor of safety of unity on an assumed horizontal failure plane along a bentonite layer at river level. Actual piezometric levels were used in the analysis from piezometers installed in the north abutment of the damsite.

The south abutment at the proposed damsite is 280 feet high with a  $2\frac{1}{4}:1$  slope. The stability analyses indicate the value of  $\phi'$  acting along the bottom failure surface for a factor of safety of unity would be  $6.3$  to  $8.6^\circ$  ( $c' = 0$ ) depending upon the strength assumed along the scarp of the potential failure surface. The north abutment is a 180 foot high slope at a slope of  $1.5:1$ . The value of  $\phi'$  which must act along the bottom failure surface for a factor of safety of unity varies from  $7$  to  $11.7$  degrees depending upon the strength assumed acting along the scarp of the potential slide.

The strength testing, previously discussed, which has been carried out on the Edmonton formation indicates the residual angle of shearing resistance of the bentonite and bentonitic shale to be about  $8.5^\circ$ . Thus residual strengths can exist along bentonite layers in the Edmonton formation and steep high river banks will remain stable provided the water table remains low. Slopes with higher water tables slump to slopes of  $5$  to  $6:1$ . If the argument that residual strengths exist along bentonite beds and weak layers in the







bedrock of the study area is accepted, then the stability of natural slopes depends primarily upon the groundwater conditions (as has been pointed out by Iverson (1970)).

A number of landslides occurring in the Cretaceous clay-shales of Western Canada were investigated in the field by Scott and Brooker (1968). A preliminary field examination of eight sites in Manitoba, Saskatchewan and Alberta were made where both stable and failed slopes in the Bearpaw formation or its stratigraphic equivalents were present.

Numerous bentonite beds were noted in the bedrock at most of the sites investigated and bentonite seams were observed in the toe area of many of the slides. It was considered that "the presence of bentonite at the base of a steep undercut slope is one of the prime geologic details contributing to slope instability" (Scott and Brooker, 1968, p. 45). The geometry of most of the failures were, in part, tangent to the horizontal and the most probable failure surface was along bentonite layers.

A zone of soft, moist, plastic shale was commonly found overlying the bentonite whereas below the bentonite seam the shale was hard, highly fractured and at a much lower water content. This phenomena was considered to be due to the bentonite seams retarding the downward movement of groundwater.

A section through a stable part of a steep undercut slope in the Bearpaw formation on the St. Mary River in



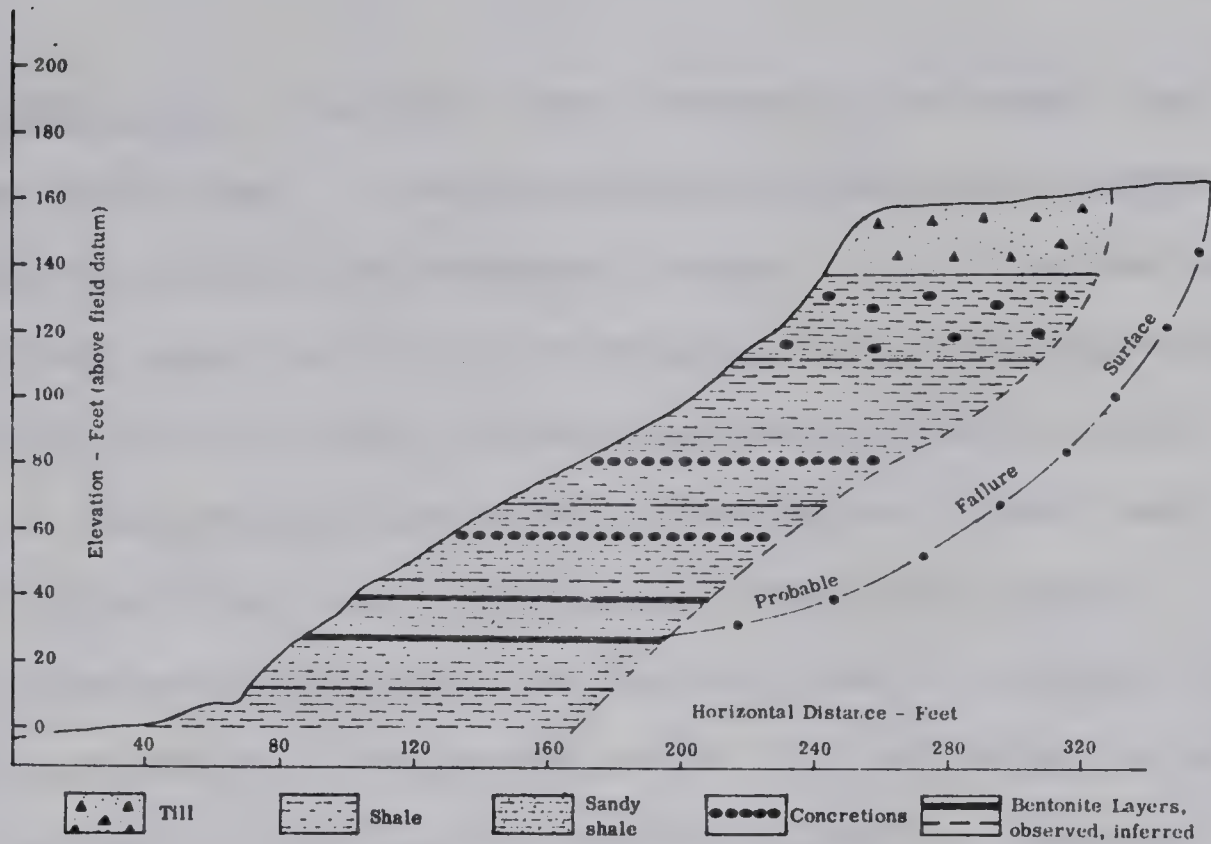
southern Alberta is shown in Figure 2.7. The shape of the probable surface in two adjacent small slides are inferred from the exposed failure surfaces of the adjoining failed slopes and illustrates the effect the presence of bentonite layers have on the geometry of landslides in the bedrock of the study area.

A study of airphotos of landslide activity along the South Saskatchewan River north of Cruikshank, Saskatchewan showed a number of fracture traces parallel to the valley edge as shown in Figure 2.8. Scott and Brooker (1968) considered these traces as possible evidence of tension fractures due to stress relief during formation of the valley. Large lateral rebound of the underlying Bearpaw shale would cause the stiff, brittle glacial till overlying bedrock to fracture parallel to the valley wall.

Typical slide zones studied by Scott and Brooker (1968) were two to three miles from scarp to toe of slide. Graben structures are common at the head region of the slide and indicate the principal surface of movement is horizontal. The slides are commonly retrogressive and have been a major agent in the widening of the river valleys in the area studied. Groundwater discharge was noted in the slide mass above the toe of several of the slides studied. The relief of residual stress was considered to be an important factor in the instability of several of the slopes studied.

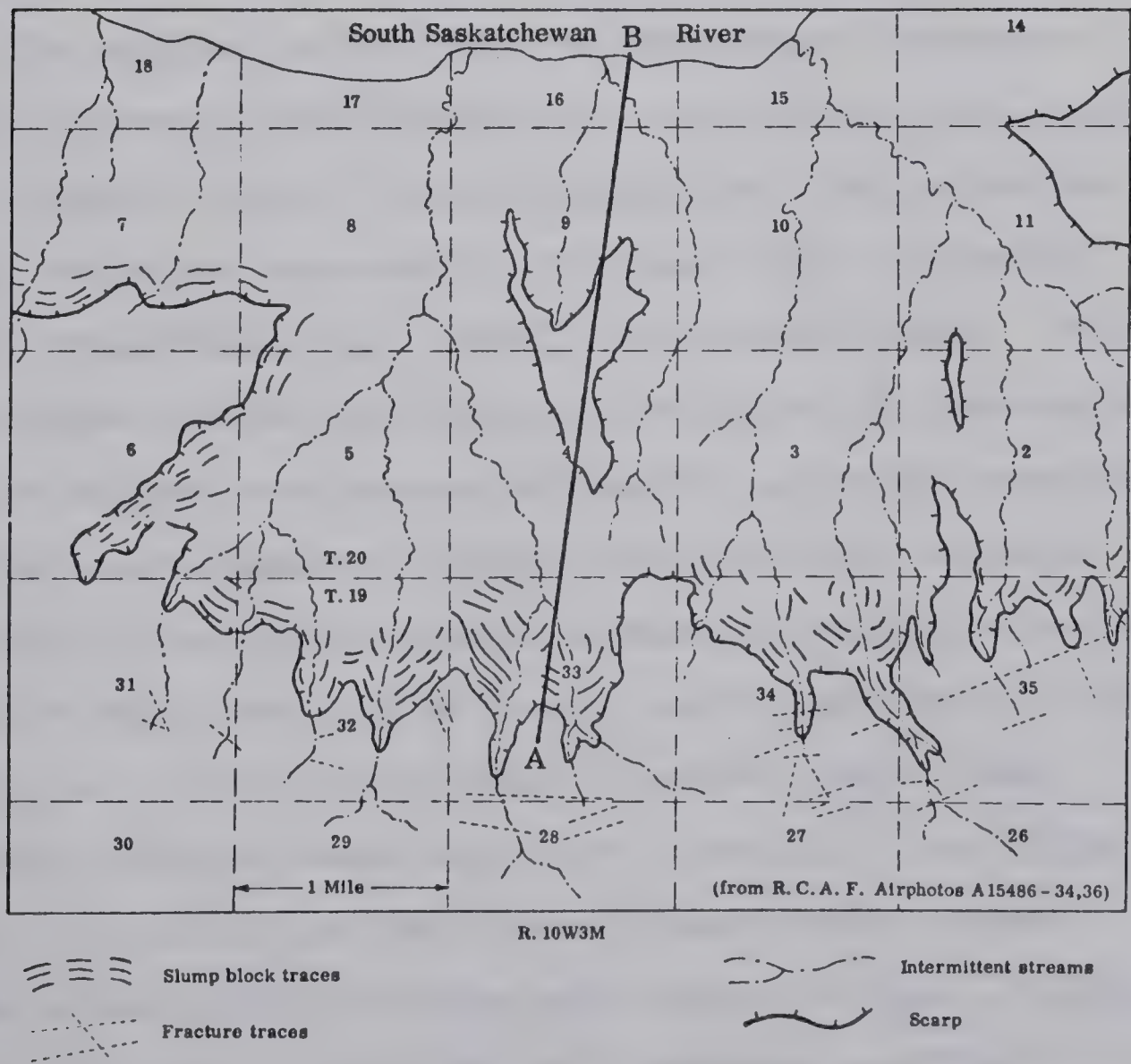






PROFILE, ST. MARY RIVER NW 19-6-22-W4 (SCOTT & BROOKER, 1968)

FIG. 2.7



TOPOGRAPHY ALONG SOUTH SASKATCHEWAN RIVER (SCOTT & BROOKER, 1968)

FIG. 2.8



(b) Gardiner Dam: Gardiner Dam (formerly the South Saskatchewan River Dam) is located on the South Saskatchewan River near Outlook, Saskatchewan (Figure 2.1). The dam was designed and constructed by the Prairie Farm Rehabilitation Agency (P.F.R.A.) of the Canada Department of Agriculture. Details of the project are given by MacKenzie (1960) and the geology of the site is discussed by Pollock (1962). A general plan and section of the dam is given in Figure 2.9. The dam consists of a compacted earth fill structure with a maximum height of 210 feet and a crest length of 16,300 feet. Construction on the dam began in 1958 and was finished in 1966.

The bedrock at the site is the Bearpaw formation (Upper Cretaceous) and consists of a relatively soft, dark, highly plastic shale. Investigations into the properties of this shale are reported by Peterson (1954), Peterson (1958), Peterson et al., (1960) and Ringheim (1964). The shale becomes harder with depth as evidenced by decreasing moisture content and increasing density and shear strength. Based on these changes in properties, the shale has been arbitrarily classified as hard, medium and soft. Unconfined strengths vary from 7 to 80 p.s.i. in the soft shale to 150 to 400 p.s.i. in the hard shale. Tangent moduli from undrained triaxial tests vary from 7,500 p.s.i. to 18,000 p.s.i. in the soft and hard zones respectively. Given access to moisture this shale will expand to form a highly plastic clay or, if confined, will generate swelling pressures up to 6 t.s.f.





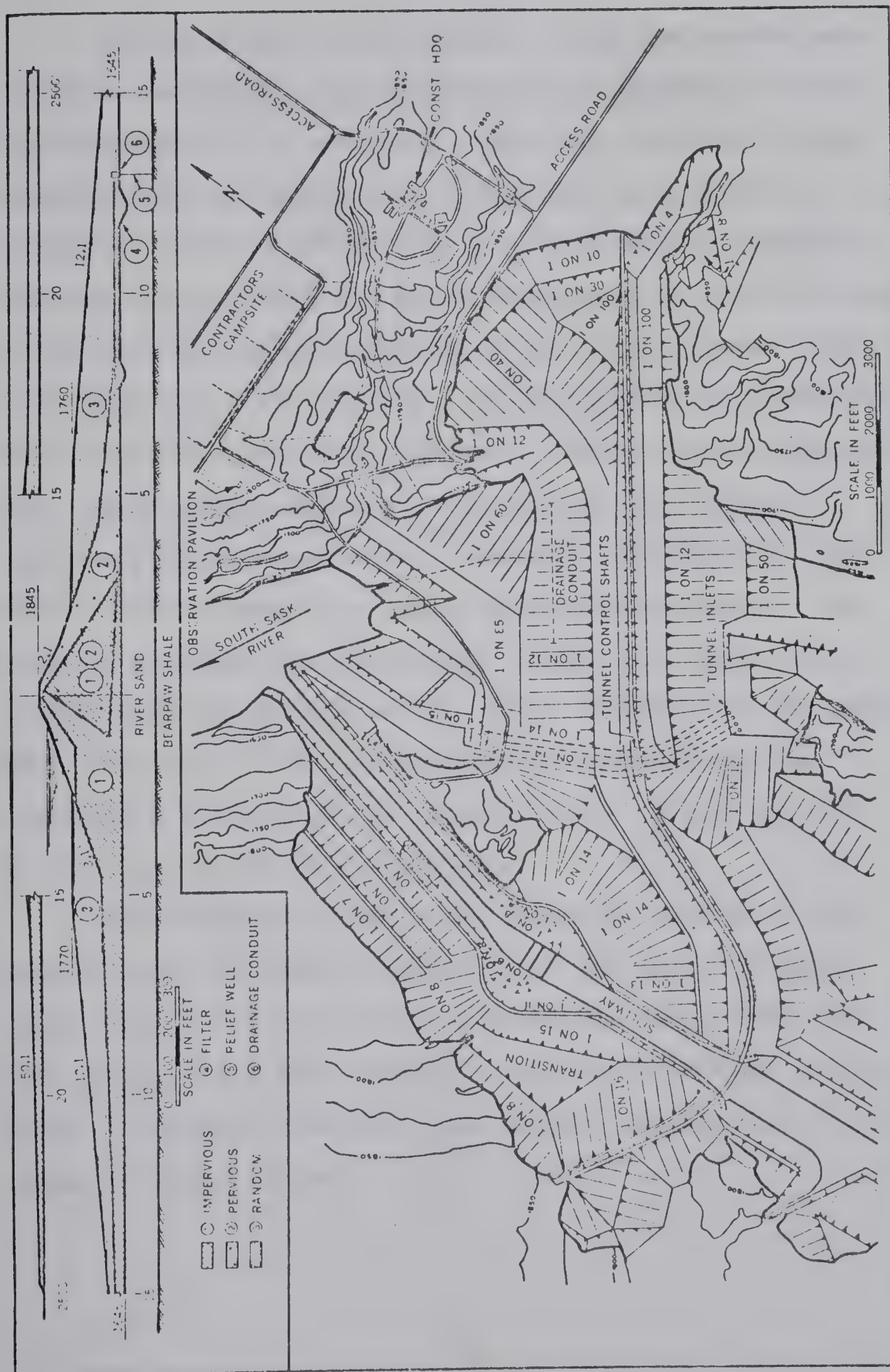


**FIG. 2.9** Embankment cross section and arrangement of works, Gardiner (South Saskatchewan River) Dam.



During construction numerous slope indicators were installed to monitor the performance of excavated slopes and embankments. A number of landslides occurred during construction; the majority of these due to excavation (Ringheim, 1964). Slides commonly began with transverse cracking at the scarp and by an overthrust at the toe caused by the mass moving horizontally over the unaffected underlying material. The vertical and horizontal displacements were generally less than 6 inches. After initial displacement the movements appeared to stabilize or reduce to a very low rate of movement. At several locations the movement at the toe was in a layer of bentonitic shale. The plane of movement was invariably in the soft shale zone, usually near the bottom of the zone. Analysis of the movements gave  $\phi' = 5^{\circ}$  to  $7^{\circ}$  assuming no cohesion and the piezometric surface at the ground level. Slopes as flat as 12:1 were found to be unstable.

The results of laboratory strength testing on the Bearpaw shale is shown in Table 2.4. The peak strength values obtained from triaxial and direct-shear tests are much greater than the strength values found acting in the field. Residual strengths from pre-cut samples were much closer to field values.







TABLE 2.4

SHEAR STRENGTH OF BEARPAW SHALE

Type of Shale	$\phi'_p$	$C'_p$ (p.s.i.)	$\phi'_r$	$C'_r$ (p.s.i.)	Source
Soft	$28^\circ$	6	- - -	- - -	Peterson et al, (1960)
Hard	$35^\circ$	10	$8.0^\circ$ - $8.4^\circ$	0.0-0.5	Weisner (1969)

(c) Fort Peck Dam: Fort Peck Dam is located on the Missouri River in northeastern Montana (Figure 2.1). The project consists of a hydraulically placed earthfill dam. The project was designed and constructed by the U.S. Army Corps of Engineers from 1934 to 1940. The bedrock is the Bearpaw formation (Upper Cretaceous). At the damsite the Missouri River is in a postglacial channel some 2 miles wide and 300 feet deep and extensive slump topography occurs along the edges of the valley.

Bentonite beds occur in the Bearpaw at this site ranging in thickness up to 2 feet (Fleming et al., 1970). Numerous faults occur in the bedrock as is illustrated in Figure 2.10 and are believed to be due to massive slumping which accompanied downcutting of the river.



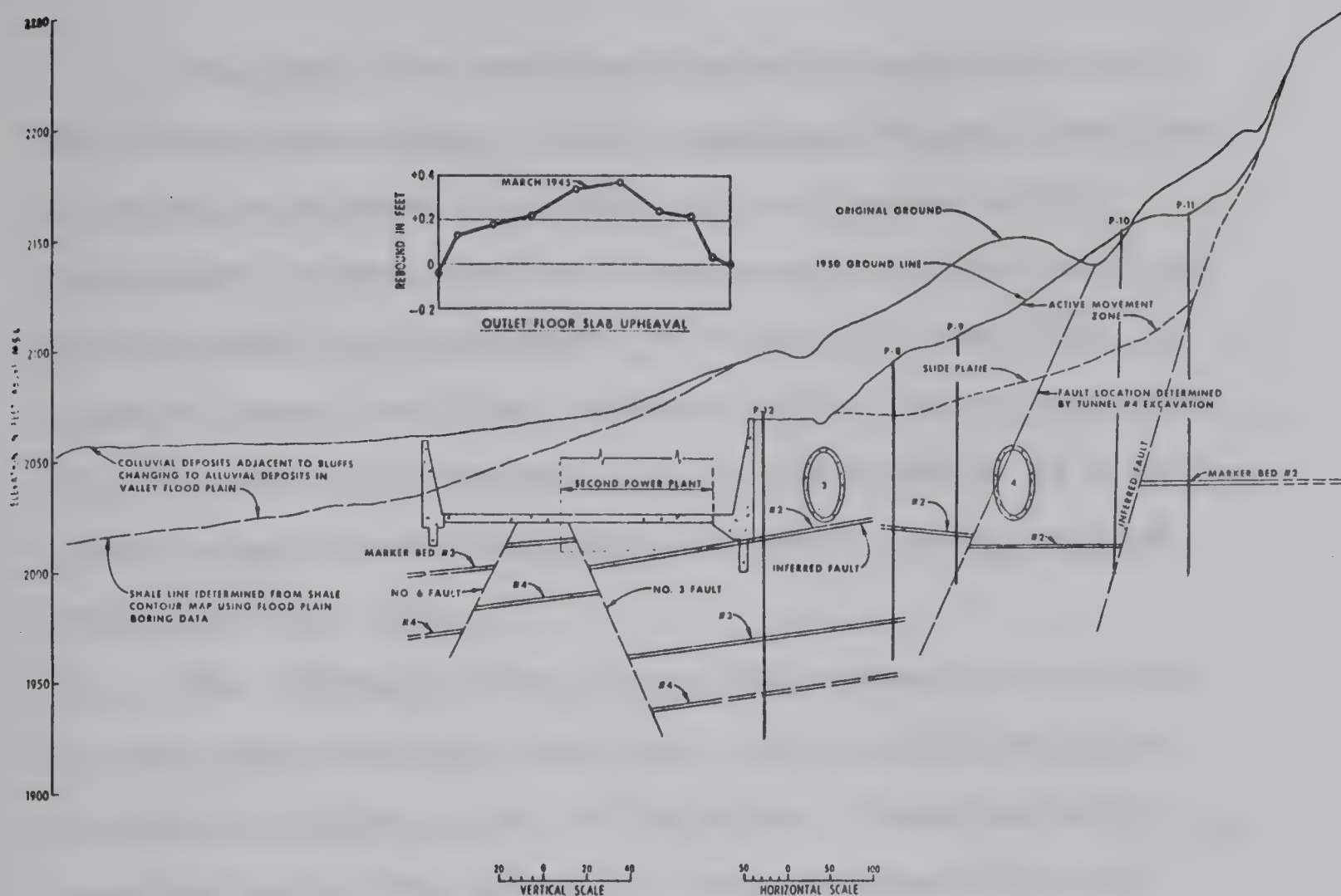


FIG. 2.10 Geologic section through second powerhouse, Fort Peck Dam.

(FLEMING ET. AL., 1970)

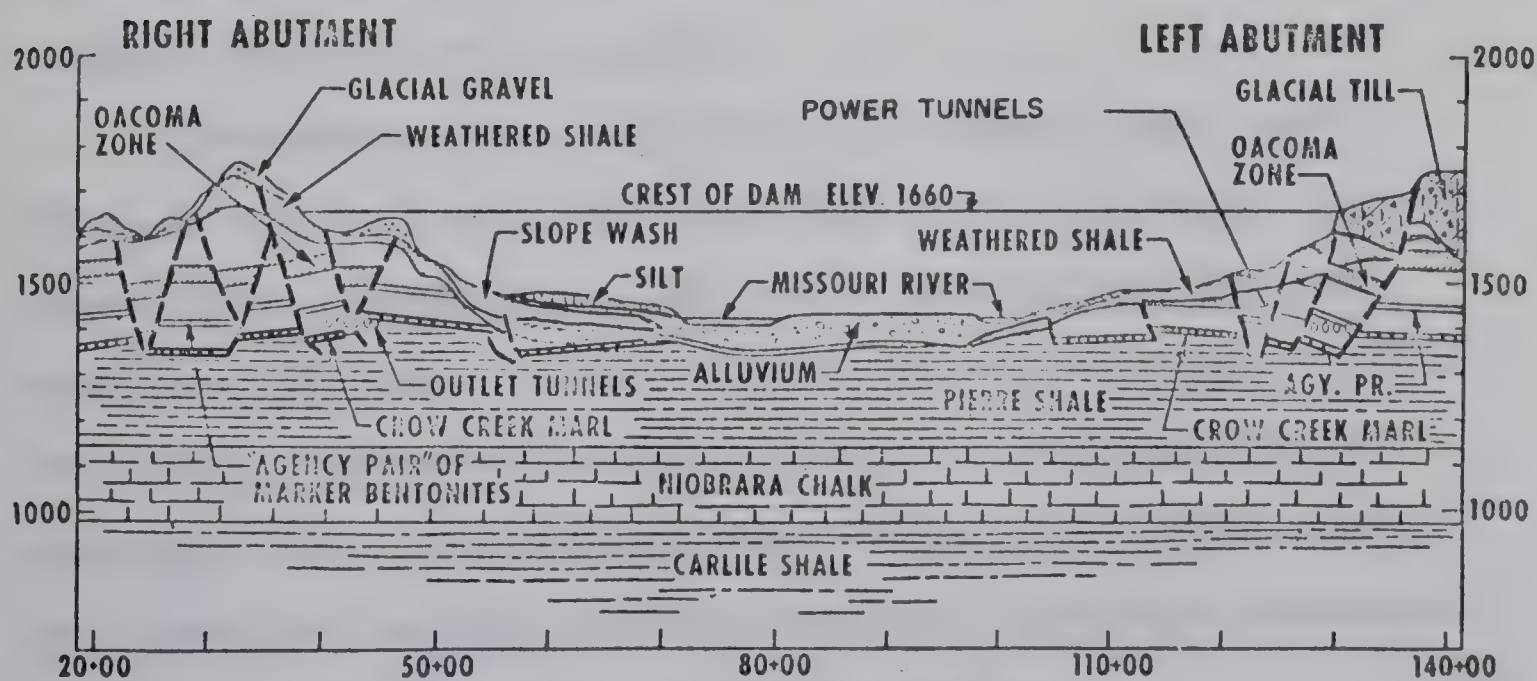


FIG. 2.11

Geologic profile along axis of Oahe Dam.

(FLEMING ET. AL., 1970)





Fort Peck was designed when soil mechanics was a relatively new science and the original design slopes were based on experience with Gatun Dam and levees on the Mississippi River. Design sideslopes of the dam were 4:1 upstream and 8:1 downstream. A failure of the fill occurred under the right abutment of the dam on September 22, 1938 and was apparently due to the presence of a weak layer in weathered shales and bentonites of the bedrock (Middlebrooks, 1942).

The adopted design slopes for excavations were 3:1 in the weathered shale and 1.5:1 in firm shale with no allowance for the height of the slope. Numerous slides occurred during the excavation for the powerhouse and spillway which continue to the present. Debris from movements on the powerhouse slope is removed each year and the slope is currently at about 2.5:1. Analysis of the slide gives a value of  $\phi'$  of about  $10^\circ$  acting along the failure surface (Fleming et al., 1970).

Movements, both vertical and lateral, have been noted in the spillway since the end of construction. Tiltmeters were installed in 1963 and a total of 12 are now being read (Fleming et al., 1970). In all of these but one, the plane of movement has been found to coincide with a bentonite bed. Rates of movement of up to 0.11 ft. per year have been measured and it is felt that major structural damage will result from continued movement.



Following the failure of the embankment in 1938, a major investigation program was begun to determine the cause of the failure (Middlebrooks, 1942). Movement apparently began on a weak zone in the upper bedrock near the right abutment of the dam. Slide planes were found in the weathered bedrock and in practically all cases bentonite was found to be "mixed with gouge material in these zones of movement" (Middlebrooks, 1942). In some cases bentonite seams were observed to be "drawn out showing considerable movement" (op. cit.). Testholes drilled near the right abutment showed high hydrostatic pressures in the shale which were considerably in excess of the maximum reservoir level.

Stability analyses following failure showed that the shear parameters acting in the bedrock for a factor of safety of unity were  $\phi = 10.4^{\circ}$  and  $C = 0.20$  t.s.f. Redesign was based on the criteria that the factor of safety of the redesigned structure should be greater than 1.50 using the derived shear parameters and no point in the foundation should be overstressed as determined from elastic theory. The upstream slopes were flattened to 7:1 and since completion of the dam have behaved satisfactorily.

(d) Garrison Dam: Garrison Dam is located about 80 miles upstream of Bismarck, North Dakota, on the Missouri River (Figure 2.1). The dam was designed and constructed by the U.S. Army Corps of Engineers and consists of a rolled earth-





fill dam with average sideslopes of 6:1. Construction began in 1946 and was completed in 1954. At the damsite, the valley is approximately 2 miles wide and 200 ft. deep. About 100 ft. of alluvium overlies bedrock below the river.

The bedrock at the site is the Fort Union Group (Tertiary) which is a flat-lying sedimentary rock composed of interbedded sands, silts and clays which have been overconsolidated by about 1000 ft. of sediments since removed by erosion. The Fort Union Group covers an area of about 120,000 square miles on either side of the Missouri River. Thick beds of lignite make excellent marker beds and can be traced for many miles. Slickensided fat (highly plastic) clays are usually found adjacent to the lignite beds which are jointed and usually water-bearing (Smith and Redlinger, 1953). The modulus of deformation for this material was taken as 27,800 p.s.i. from a series of constant stress-ratio triaxial tests. Direct shear and undrained triaxial tests gave a range in strengths which indicated  $\phi = 30$  degrees and  $c = 0.7$  t.s.f. (Fleming et al., 1970).

The Fort Union shale has a liquid limit of up to 140. The clay fraction consists of 85 to 90 percent illite and 10 to 15 percent montmorillonite. Lean clay (clay of low plasticity) is the predominant soil type but all gradations from fat (highly plastic) clays to sands occur.

Excavated slopes were designed on the basis of laboratory strength tests, field slope data and stability analyses using the Swedish Circle method. Laboratory tests



indicated strength parameters for design to be  $\phi = 30$  degrees and  $c = 0.70$  t.s.f. Field slopes, assuming a factor of safety of unity, gave a value of  $\phi$  equal to 20 degrees and a cohesion of 0.70 t.s.f. The lower field strengths were used in slope design and no slope failures have occurred since construction was finished in 1948 (Fleming et al., 1970).

(d) Oahe Dam: Oahe Dam is located on the Missouri River in central South Dakota, 6 miles northwest of Pierre (Figure 2.1). A section of the embankment is shown in Figure 2.12. The project was designed and constructed by the U.S. Army Corps of Engineers from 1950 to 1961. Major problems encountered during construction were large slides caused by excavation and rebound in deep excavations which necessitated redesign of certain hydraulic structures as is discussed by Underwood et al. (1964) and Fleming et al. (1970).

The bedrock at the site is the Pierre formation (Upper Cretaceous) which is a dark grey to black marine clay-shale interbedded with bentonite layers. Mineralogical analyses show the shale to be composed of 30 to 60 percent montmorillonite. Bentonite beds are found to contain up to 90 percent montmorillonite. The average density is 100 p.c.f. with an average water content of 25 percent. Liquid limits average 80 percent but are as high as 300 percent in the bentonite layers. Unconfined compression strengths on





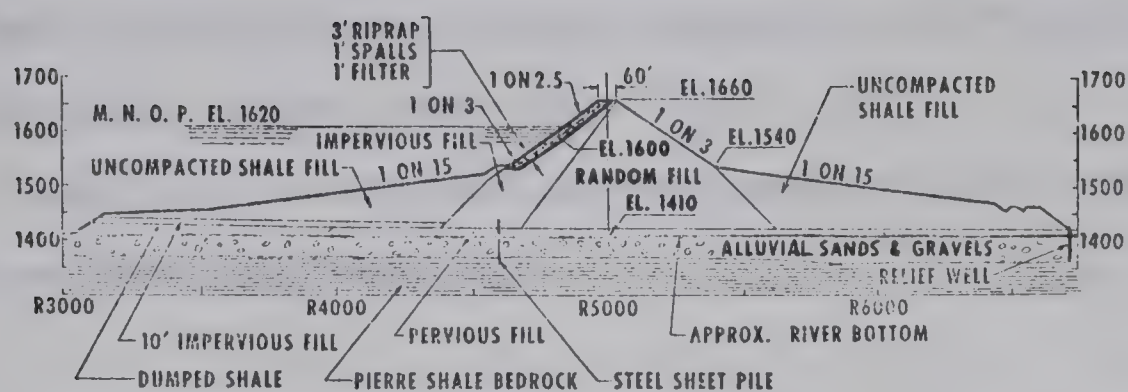


**FIG. 2.12** MAXIMUM EMBANKMENT SECTION (KNIGHT, 1963)

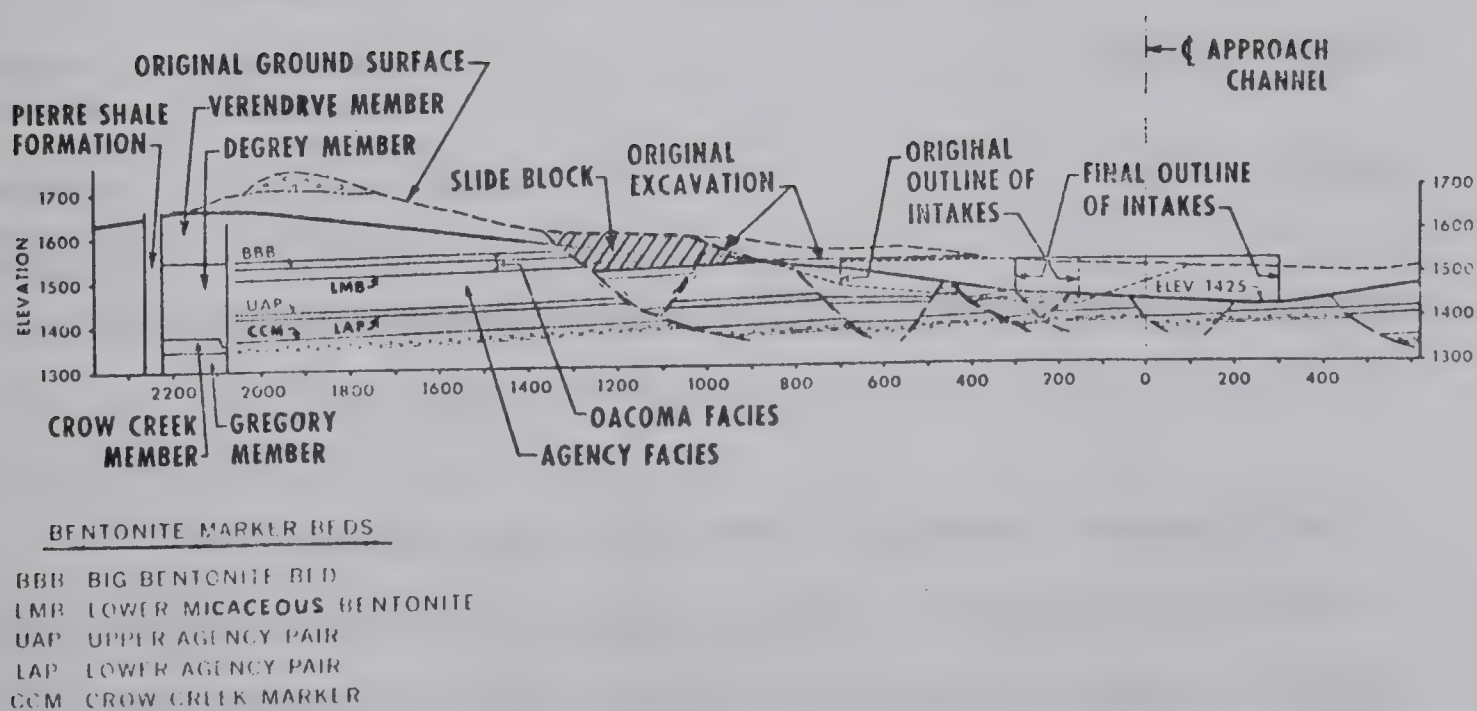


**FIG. 2.13** Section through right abutment slide.

( FLEMING ET. AL., 1970 )



5.5 inch diameter cores varied from 0 to 2550 p.s.i. Undrained triaxial tests gave an average E of 70,000 p.s.i. at a principal stress ratio of 0.75.

Results of shear testing on samples of the Pierre shale are shown in Table 2.5.

TABLE 2.5

DIRECT SHEAR TEST RESULTS ON PIERRE SHALE,  
OAHE DAM (FLEMING ET AL., 1970)

Sample	Rate of Testing	Peak Strength $\phi_p$ $C_p$ (t.s.f.)	Ultimate Strength $\phi_u$ $C_u$
Firm Shale	.008 - .007 in. /min.	32°-47° of 2.5-3.0	19.8°- 21.8° 0.6-0.9
Bent-onite	.02 in. /min.		17.2° 0.22
Weath- ered Shale	.01 in./min.		11.8° 0.26

The strength used for the 'ultimate' strength is that remaining after the peak of the stress-strain curve has been passed and the strain has reached several tenths of an inch. This is not a true residual as typically several inches of displacement in the standard shear box are required to reach residual of an intact specimen





(Skempton and Petley, 1967). The rates of strain used are much higher than those required for complete drainage of the sample to occur during shear (Gibson and Henkel, 1954). Therefore, the peak values of  $\phi$  and C shown in Table 2.5 cannot be considered as true effective strength parameters as some excess pore pressure undoubtedly occurred during testing; the ultimate strengths are probably somewhat higher than the residual strength of the Pierre shale as the samples were not sheared all the way to the residual. It is unlikely that the rate of strain used would have a significant effect upon the residual strength (Kenney, 1967).

Triaxial tests were conducted on contact planes between bentonite and shale with the contact inclined at about 45 degrees with the axis of compression. All specimens failed on the contact between the bentonite and shale, not in the bentonite itself. A considerable scatter of results occurred but at least one sample exhibited a very low shear strength and failed at 7 percent strain. Triaxial tests on slickensided surfaces showed variable results. Three of the six samples tested showed no appreciable strength along slickensided surfaces.

Large scale faulting has occurred in the Pierre shale near the surface with vertical displacements of marker beds as much as 80 feet being noted. The faults are believed to be due to movements of the valley wall towards the river valley trench at a time when the river was approaching its maximum depth of scour (Fleming et al., 1970,



p. 225-226). This theory is supported by the fact that boring logs show a greater number of slickensides near the elevation of maximum river scour. Slickensides, fault gouge and other features indicative of movement are much less numerous below depths of maximum river scour. Faults, with 60 to 80 feet of vertical displacement at the surface, show only 15 to 20 feet of vertical displacement as the elevation of maximum river scour is approached.

The excavations for the inlet and outlet works and the powerhouse at Oahe Dam approached depths of 200 feet. Early design studies (U.S.C.E., 1948) recognized that the stability of these deep excavations would depend upon a number of complex factors, namely:

1. the erratic, closely spaced pattern of joints,
2. the long term effect of reservoir seepage,
3. the zones of weakness evidenced by closely spaced slickensides,
4. variation in depth of weathering effects on the fault planes and bentonite beds,
5. the wide range of strength resulting from the effects of water on the active clay minerals in the formation.

Shear strength parameters of  $\phi = 11.8^{\circ}$  and  $c = 0.26$  t.s.f. were adopted for initial stability studies based on test data from the Fort Peck and Harlan County projects. Direct shear tests on bentonite appeared to confirm the field derived results and these values were used for





bentonite seams or fault planes. A series of undrained triaxial tests gave higher results and were not used (Fleming et al., 1970).

It was realized that the true effective strength of the bedrock was unlikely to be obtained from laboratory tests on small samples. For this reason a study of existing slopes in the Pierre shale was made and a slope chart was constructed (Knight, 1963). None of the existing slopes studied reached the height of the proposed excavations and stability analyses were done using the 'wedge' method (U.S.C.E., 1951) with  $\phi = 11.8$  degrees and  $c = 0.26$  t.s.f.

The initial design slopes for the outlet works approach channel were 3:1. A small slide occurred which was bounded in the rear by an old fault plane and had its base along bentonite seams in the Oacoma facies of the DeGrey member of the Pierre shale. The section of the failure plane was partially smeared with yellow weathered bentonite. The slide moved slowly with a rate of about 1.3 inch per day for the first ten days after failure. The effective shear strength acting along the slide was calculated at  $\phi' = 8.5$  degrees and  $c' = 0.15$  t.s.f. Results from direct shear tests on block samples from this bentonite bed agreed closely with the back-figured strengths. A section through this slide is shown in Figure 2.13.

Remedial measures consisted of stopping excavation at the toe of slope and removing some material from the top of the slide to reduce the driving force. This excavation



initiated another slow-moving slide above the first. Horizontal drains were installed and proved to have some beneficial effect upon the stability of the slide mass.

A second major slide was activated on the left abutment by the removal of some 20 feet of weathered shale at the toe of slope. Minor excavation about three-fourths of the way up the abutment had previously been done to the elevation of the dam crest and several million cubic yards of overburden had been excavated at the upstream top portion of the abutment and placed in the valley as embankment fill.

The initial displacement was an instantaneous rupture with rapid displacement some 5 feet horizontally and 22 feet vertically. The rate of movement which immediately followed the initial slump was about 4 feet per day; the rate of movement reduced in a month to less than 1 inch per day and practically ceased two months after the initial failure. A section through the slide is shown in Figure 2.14.

Attempts to excavate a portion of the slide mass led to a three-fold expansion in the area of slide activity to cover approximately 65 acres. Eventually the entire slide mass, some 6.5 million cubic yards, was removed with the final slope cut at 6:1. The effective strength parameters governing the movement were found to be roughly the same as for the first slide -  $\phi' = 8.5$  degrees and  $c' = 0.15$  t.s.f.





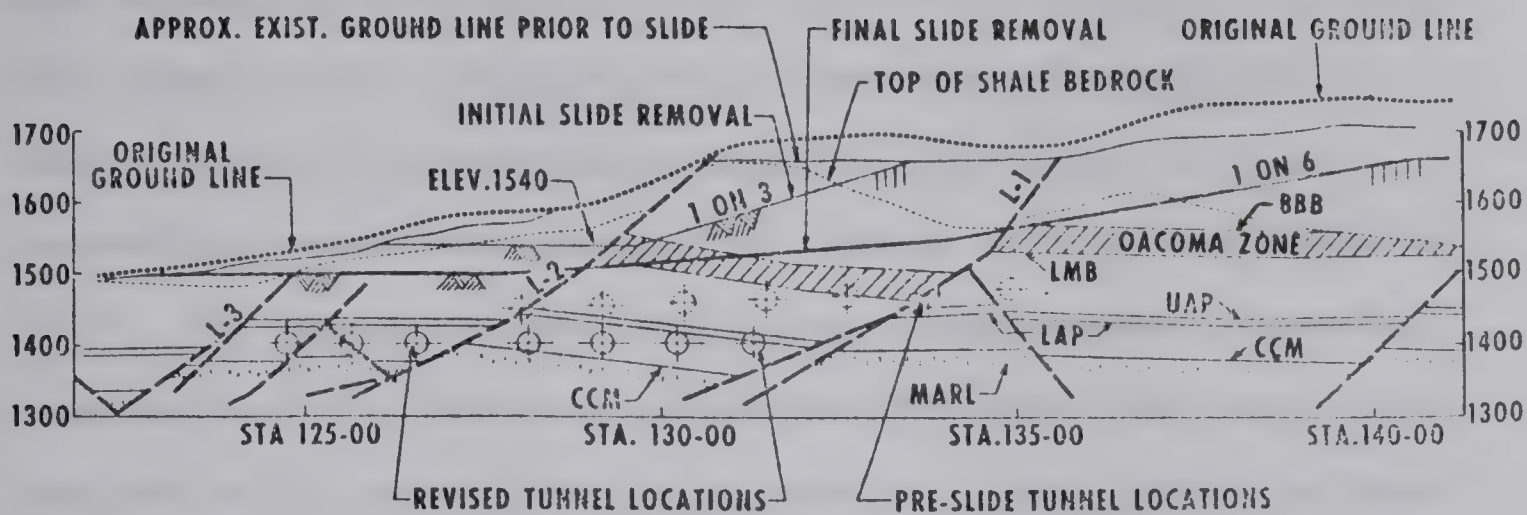


**FIG. 2.14** Section through left abutment slide.

(FLEMING ET. AL., 1970)

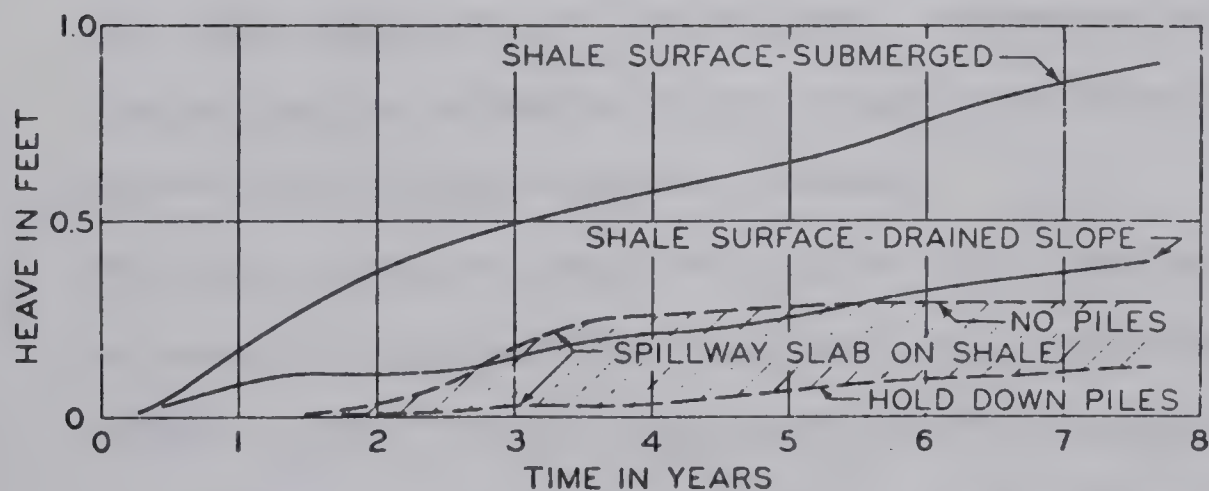


**FIG. 2.15** Shale Heave vs. Time at a Typical Spillway

(PETERSON & PETERS, 1963)



Several of the more critical slopes on the project were eventually flattened to 9:1 or 10:1. Slope indicators installed on 8:1 slopes for the powerhouse excavation showed lateral differential movements of about an inch occurring across thin bentonite layers (Wilson and Hancock, 1959). It was concluded that these displacements were not associated with landslide phenomena but were due to a concentration of strain due to release of high lateral stress.

Summary: A review of the published experience with landslide activity in the Cretaceous bedrock of the study area shows several common features:

1. The majority of landslides involved bentonite layers which acted as the bottom surface of the slide.
2. Excavation, either natural or artificial, initiated the vast majority of the slides. Attempts to flatten a failing slope were often not effective and served to initiate further slides.
3. The low values of shearing resistance (typically  $\phi'$  about 8 degrees) and the slow rate of movement noted in most cases indicates that the majority of the slides are controlled by the residual strength of the rock.

Recorded experience with bedrock stability in the study area shows the stability of natural bedrock slopes is controlled by bentonite beds or by other horizontal





planes of weakness at, or close to, their residual strength. How these beds came to exist at this low strength and why slopes should be so susceptible to failure induced by a modest excavation is a point of considerable importance.

## 2.5 Rebound of Excavated Surfaces

The removal of overburden load from a rock or soil will result in rebound or heave of the bottom of the excavation, the amount depending upon the physical properties of the soil or rock and the amount of load removed. In many instances the amount of rebound is small and of little practical significance, however in the overconsolidated Cretaceous bedrock of the study area values of rebound may be large enough to cause distress to structures placed in deep excavations.

Rebound has been considered to have two components as has been previously discussed - undrained elastic rebound and swelling due to absorption of water. Values of the undrained modulus of elasticity,  $E$ , of the rock are found from standard unconfined or undrained triaxial tests, or from field plate bearing tests and observations on the behaviour of excavations or loaded areas. This topic will be discussed in detail in Chapter IV of this thesis. The swelling index ( $C_s$ ) from the standard oedometer test shows the amount of time-dependent rebound which can be expected from a given rock type (Casagrande, 1949).



Peterson and Peters (1963) give examples of the occurrence of rebound in spillway excavations cut in the Bearpaw shale of Western Canada or its stratigraphic equivalent. Amounts of rebound of up to 0.8 feet have been reported in small spillway excavations as occurring mainly in the upper 10 to 15 feet of the shale. This phenomenon is considered to be primarily due to swelling of the shale as the heave is largely dependent upon the presence of surface water. The rate of heave is reported as being relatively uniform for 8 years as shown in Figure 2.15 for a typical case.

The swelling (or time-dependent rebound) of the Bearpaw shale has important implications on the design of spillway structures and has necessitated the placement of hold-down piles to reduce movement, and damage, in the floor of these spillways. However, undrained elastic rebound undoubtedly occurred during the excavation of these spillways and the fact it is not reported indicates that instrumentation capable of measuring it was not installed prior to the beginning of excavation.

Rebound gauges were installed in excavation areas at the South Saskatchewan River Dam prior to construction. All gauges were installed in the hard shale zone and showed elastic rebound in the shale to be in the order of 0.7 percent of the excavation depth for gauges installed 10 to 20 feet below the final grade and 0.4 percent of the excavation depth for gauges installed 100 feet below final grade (Ringheim, 1964). Laboratory tests on Bearpaw shale







gave tangent moduli from undrained triaxial tests varying from 7500 p.s.i. in the soft shale to 20,000 p.s.i. in the hard shale (Peterson, 1954).

Large amounts of excavation rebound have been noted by the U.S. Army Corps of Engineers at several of the large dams on the Missouri River. Vertical rebound has been a problem at Fort Peck Dam since prior to the end of construction. Between 1 and 2 feet of vertical rebound has occurred along the centerline of the spillway since October, 1937, as shown in Figure 2.16. The rate of movement is steady and shows no sign of decreasing and appears to correlate with slope height except where low angle faults occur. Fault planes appear to concentrate the movement in certain local zones as shown in Figure 2.17.

Smith and Redlinger (1953) compared the elevation of lignite beds in two testholes at Garrison Dam where the Fort Union Group has been overconsolidated by an estimated 80 to 100 t.s.f. One testhole was drilled on the east abutment of the dam and one on the east floodplain with a difference in elevation between them of about 200 feet over a horizontal distance of 659 feet. The testhole logs showed the lignite beds below the flood plain were 4.6 to 7.4 feet above similar beds below the valley wall. The Fort Union Group at the damsite is nearly flat-lying and this measured rebound can only be due to the cutting of the river valley. Laboratory tests gave an undrained modulus of elasticity of the bedrock of 27,800 p.s.i. and a swelling index from the



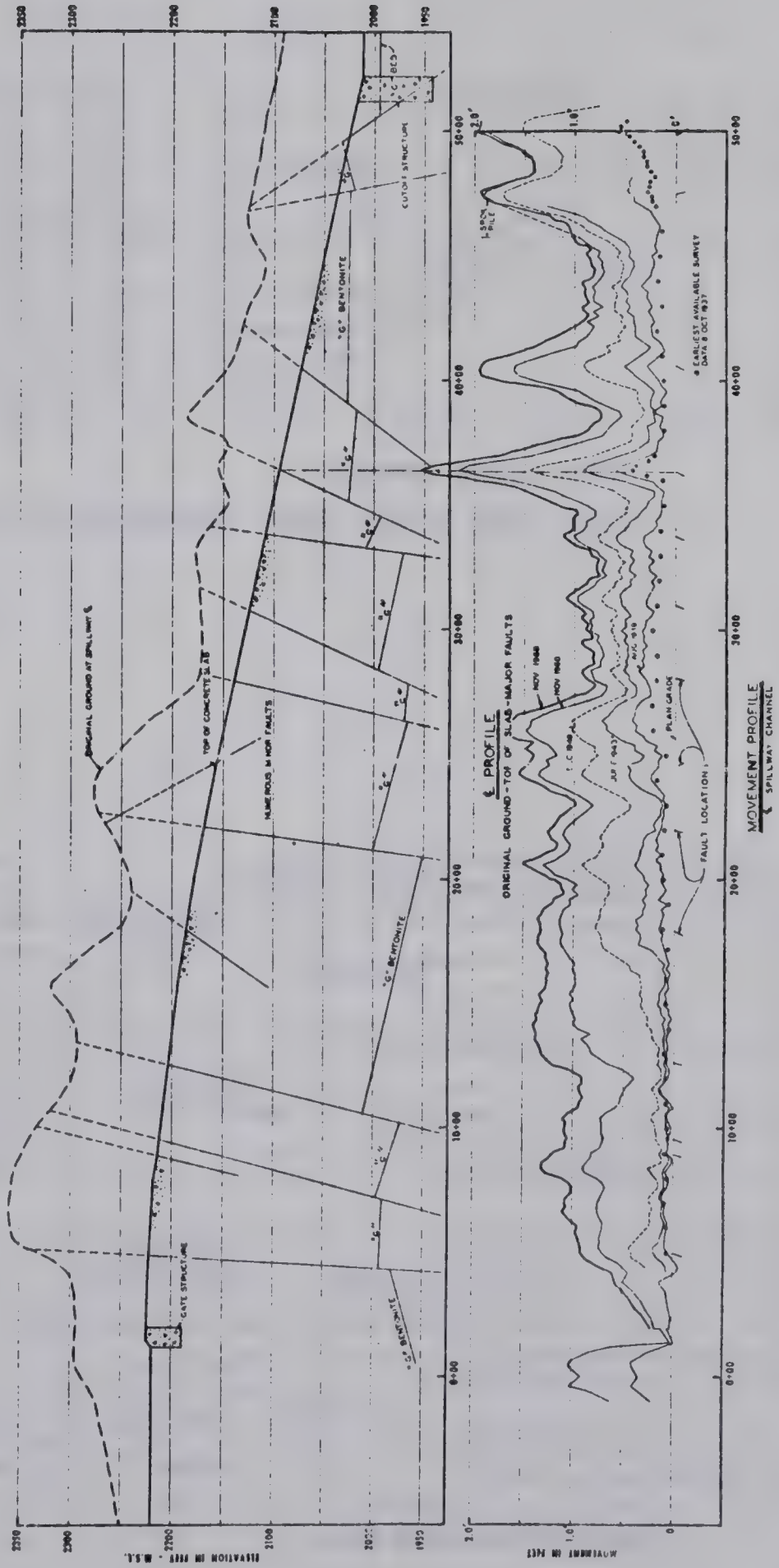
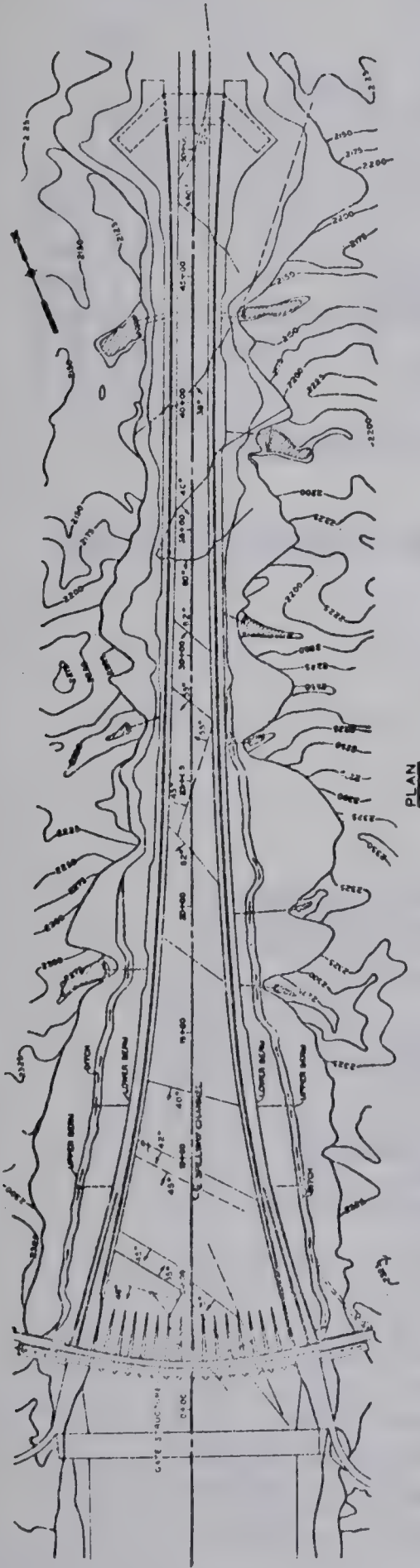


FIG. 2.16 Centerline vertical movement, Fort Peck spillway. ( FLEMING ET. AL. 1970 )





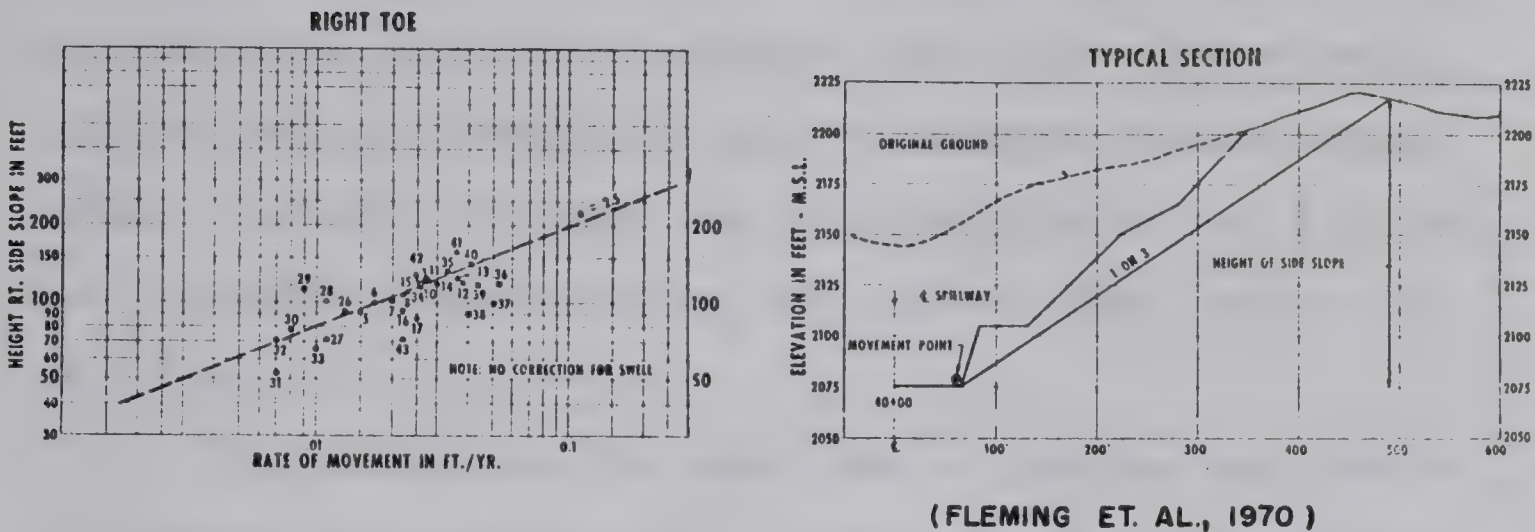


FIG. 2.17 CURRENT RATE OF REBOUND, FORT PECK SPILLWAY

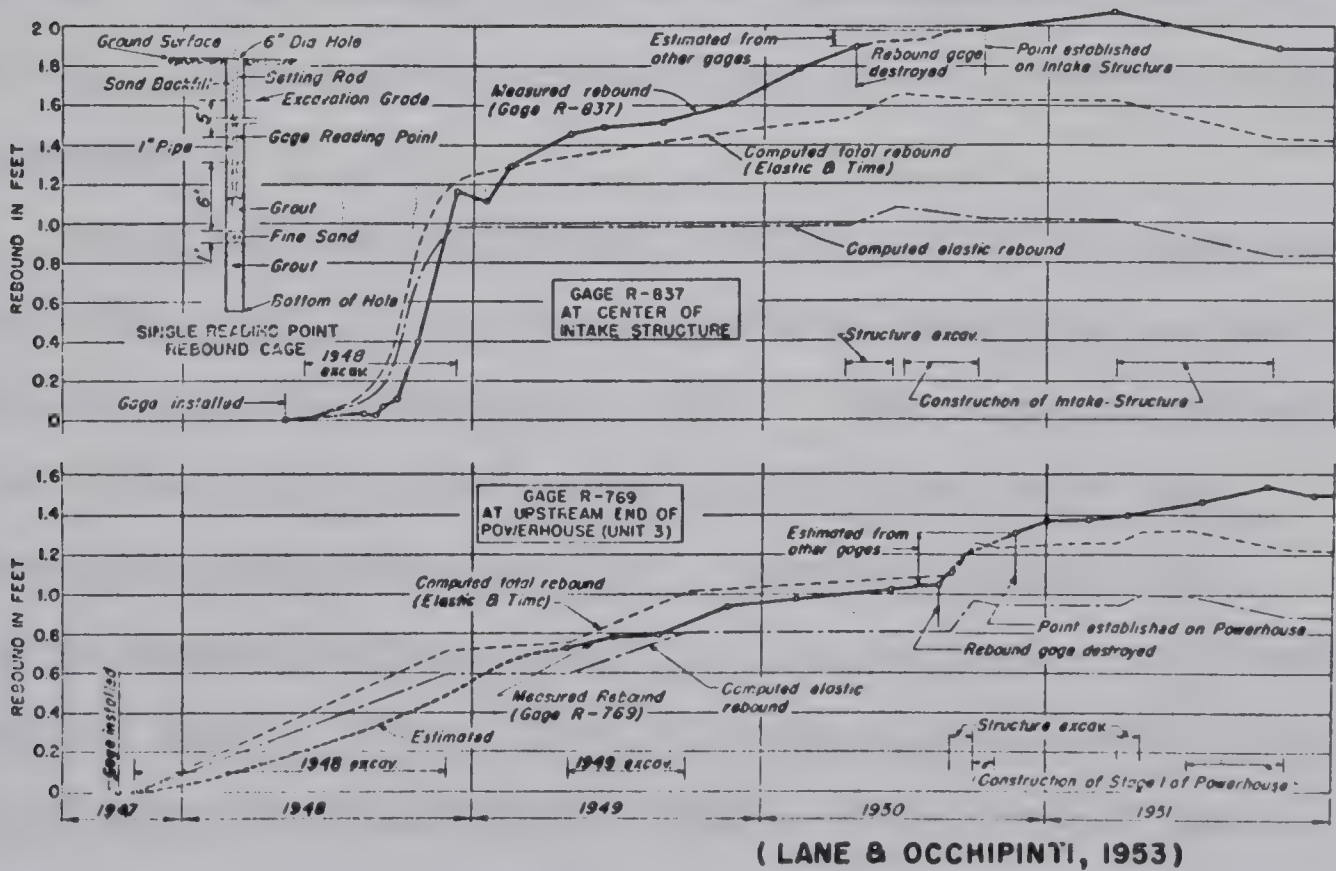


FIG. 2.18 TYPICAL REBOUND GAUGE OBSERVATIONS, GARRISON DAM



oedometer of 0.018. Computed values of rebound using these parameters are reported as 1.0 foot due to swelling and 1.6 feet due to elastic rebound, a total of 2.6 feet. Lowering of the water table in the valley walls due to cutting of the valley was thought to lower the strata in the valley walls 1.6 feet, 0.5 feet due to consolidation and 1.1 feet due to elastic compression. The sum of these effects is 4.2 feet.

These observations show that a considerable amount of differential rebound will occur below the bottom of a river valley cut through the Cretaceous bedrock of the study area. A portion of the total rebound will be elastic behaviour controlled by the undrained modulus of the bedrock and will occur as rapidly as the valley is cut. The remainder of the rebound will be a time-dependent swelling which will continue for a considerable time after the valley is excavated.

About 100 rebound gauges were installed in excavation areas at Garrison Dam to monitor rebound behaviour as described by Lane and Occhipinti (1953). The depth of excavation for the inlet, and outlet works and the powerhouse at Garrison Dam approached 200 feet. Several gauges were placed at depths varying from 5 to 150 feet below the final excavation grade. Over 2 feet of rebound was observed due to a 175 feet deep excavation. About 60 percent of the rebound occurred during excavation with the other 40 percent occurring at a decreasing rate after the end of





excavation. The amount of rebound measured in general reflected the topography of the original ground with the gauges at the deepest excavations showing the largest rebound. About half the movement occurred in the upper 100 feet of bedrock below the excavation bottom.

Lane and Occhipinti (1953) considered the movements to be composed of two main components - elastic rebound and swelling due to absorption of water. The laboratory derived moduli of  $E = 27,800$  p.s.i. and  $C_s = 0.018$  were used to predict movements assuming rebound and swelling occurred down to elevation 1265, some 350 feet below the excavation bottom. Computed values of rebound agree reasonably well with observed behaviour as shown in Figure 2.18. The calculations to relate observed to theoretical rebound below the valley floor at Garrison Dam (Smith and Redlinger, 1953) appear to use the same model.

Vertical creep-like movements have been noted at Garrison Dam since its completion (Fleming et al., 1970). The rate of movement is much smaller than at Fort Peck and averages 0.036 feet per year in the 120 feet deep spillway which has 2:1 sideslopes. Movement recorded on a section through the powerhouse and stilling basin excavation (255 feet deep) is somewhat smaller as shown in Figure 2.19. No structural damage has occurred due to the rebound but the current rate of movement could, in time, cause tilting or differential movement problems.



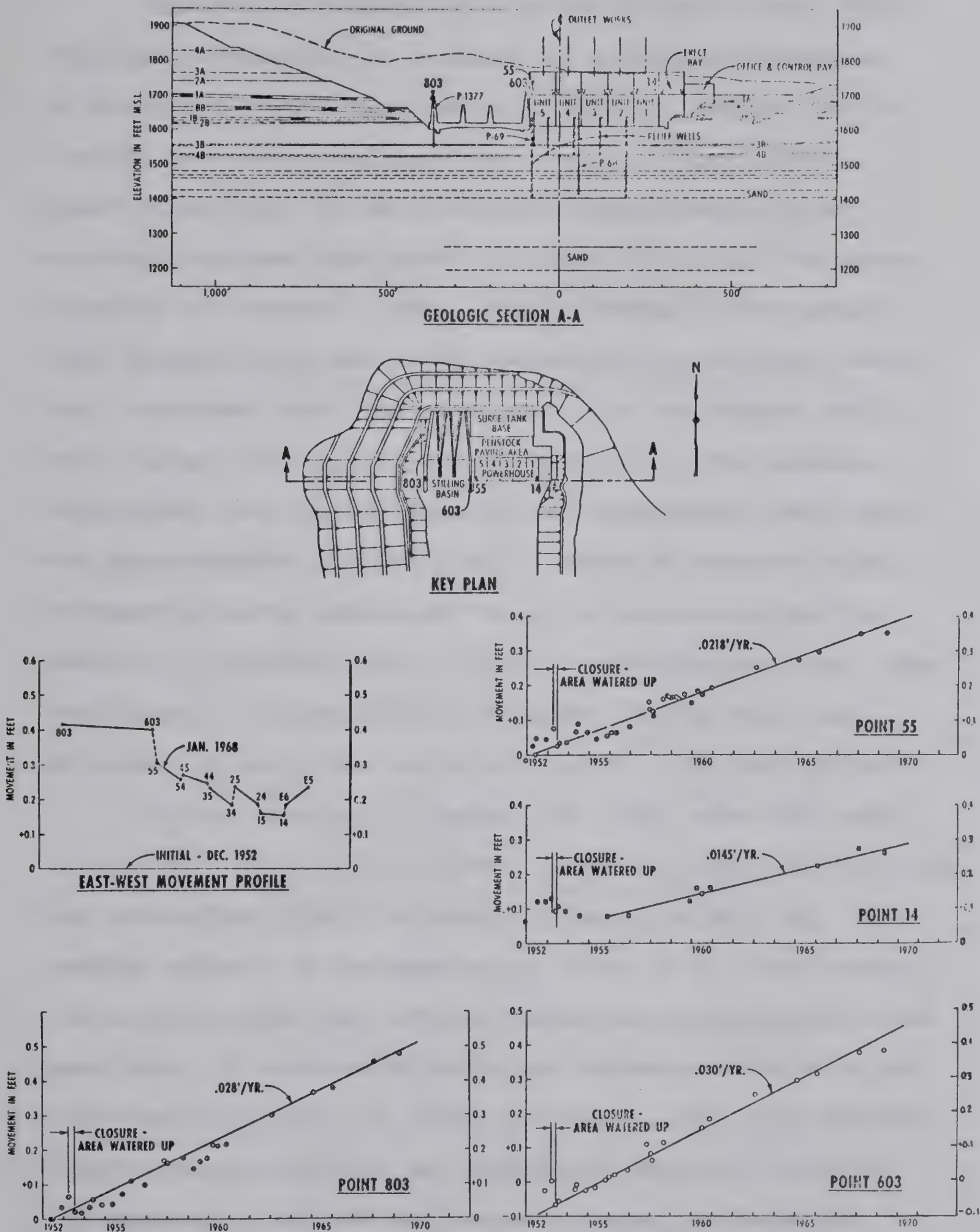


FIG. 2.19 Summary of movement, stilling basin and powerhouse, Garrison Dam.  
( FLEMING ET. AL, 1970 )





Excavation rebound at Oahe Dam in the Pierre shale resulted in redesign of a number of hydraulic structures as described by Underwood et al., (1964). Excavation for the 200 feet deep stilling basin began in April, 1952. Observations made on an underground bench mark during excavation showed that about 8 inches of rebound had taken place up to December, 1954. The behaviour of the excavation agreed fairly well with predictions based upon laboratory undrained moduli of elasticity for the Pierre shale, which ranged from 20,000 to 140,000 p.s.i. The modulus determined from the movement of the underground bench mark was approximately 100,000 p.s.i. About 90 percent of the movement occurred concurrent with the excavation and the remaining 10 percent took place at a diminishing rate. The coefficient of permeability of intact Pierre shale was estimated to be in the order of  $1 \times 10^{-10}$  cm. per second.

On the morning of January 10, 1955, when the excavation was almost to final grade, a sharp ridge was noted in the excavation floor. A survey revealed an over-all average rebound of the excavation floor of 0.3 feet which had occurred over the last few weeks when no excavation had been done. A maximum differential movement occurred along a pre-existing fault as shown in Figure 2.20. The rebound departed from predicted and previously measured behaviour and apparently rupture had occurred along pre-existing "fault" planes.



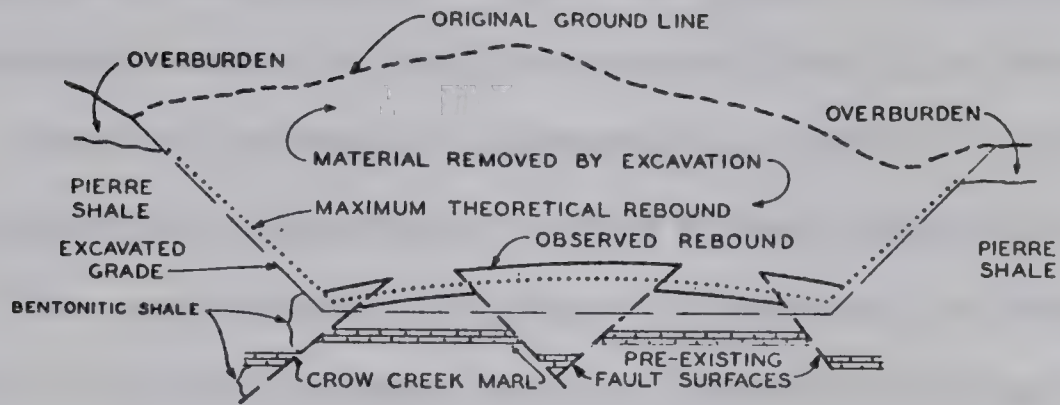
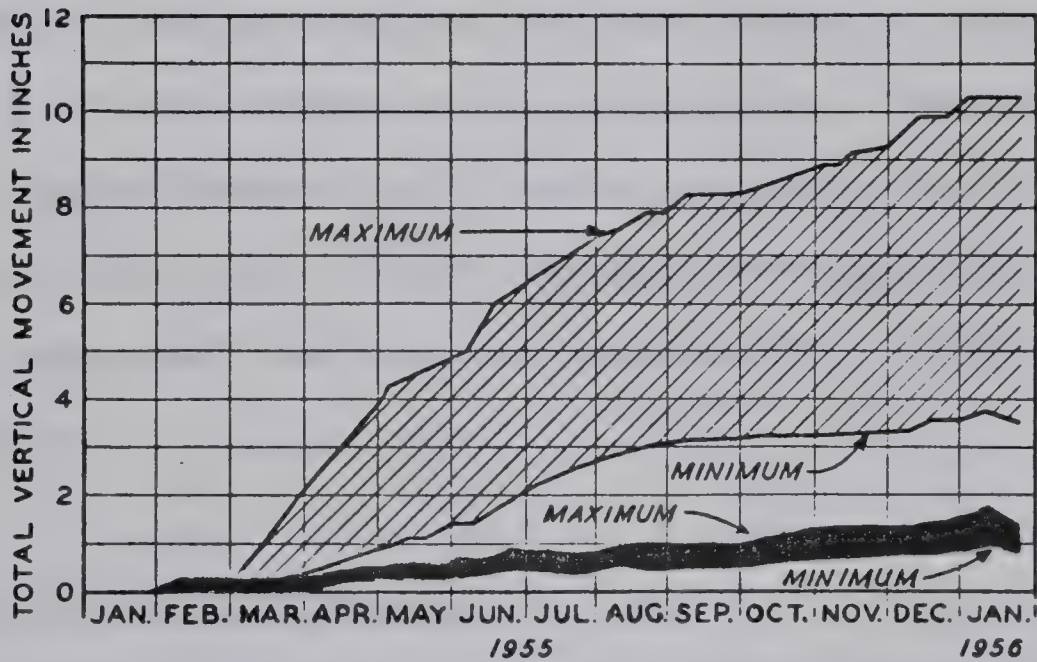




FIG.2.20—SCHEMATIC CROSS SECTION THROUGH STILLING BASIN SHOWING THEORETICAL AND OBSERVED REBOUND (UNDERWOOD ET. AL,1964)



**LEGEND**

-  INDICATES RANGE OF VERTICAL MOVEMENT RECORDED AT DEPTHS OF 0 TO 10 FEET BELOW THE SURFACE OF THE BOTTOM OF THE EXCAVATION.
-  INDICATES RANGE OF VERTICAL MOVEMENT RECORDED AT DEPTHS OF 10 TO 40 FEET BELOW THE SURFACE OF THE BOTTOM OF THE EXCAVATION.

( UNDERWOOD ET. AL., 1964)

FIG. 2.21—PLOT OF MEASURED VERTICAL MOVEMENT VERSUS TIME





Instrumentation was installed and behaviour of the excavation was observed over the next year. Upward movements observed near the surface ranged from 3 to over 10 inches. Vertical movements observed at depths of 10 to 40 feet below the excavation bottom ranged from 0.5 to 1.5 inches. The deep movements showed a tendency to decrease with time but this tendency was not as marked as near the surface as is shown in Figure 2.21.

The cause of the rebound was considered by Underwood et al., (1964) initially to be elastic rebound due to the removal of overburden. The abrupt differential movement of the base of the excavation was considered to be due to the rupture of the bottom of the excavation. Swelling of the shale due to absorption of water was not considered a significant factor due to the insignificant quantity of water available and the very low permeability of the Pierre shale.

## 2.6 Investigation Techniques

The cases presented in the previous section show that stability of bedrock slopes in the study area are controlled by minor geologic detail. Current methods of field investigation used in civil engineering practice do not always reveal these zones of weakness (i.e. bentonite beds) nor do they give samples which can be tested to provide the appropriate strengths which control the stability of the valley walls in many cases.



The standard method of investigating the bedrock in the study area consists of taking continuous cores of the bedrock which are logged to provide information on the geology of the site. Selected core samples are tested in the laboratory to determine the engineering properties of the rock. The standard reference on the subject is Hvorslev (1949). The field investigation methods and techniques used today are essentially the same as outlined by Hvorslev over two decades ago.

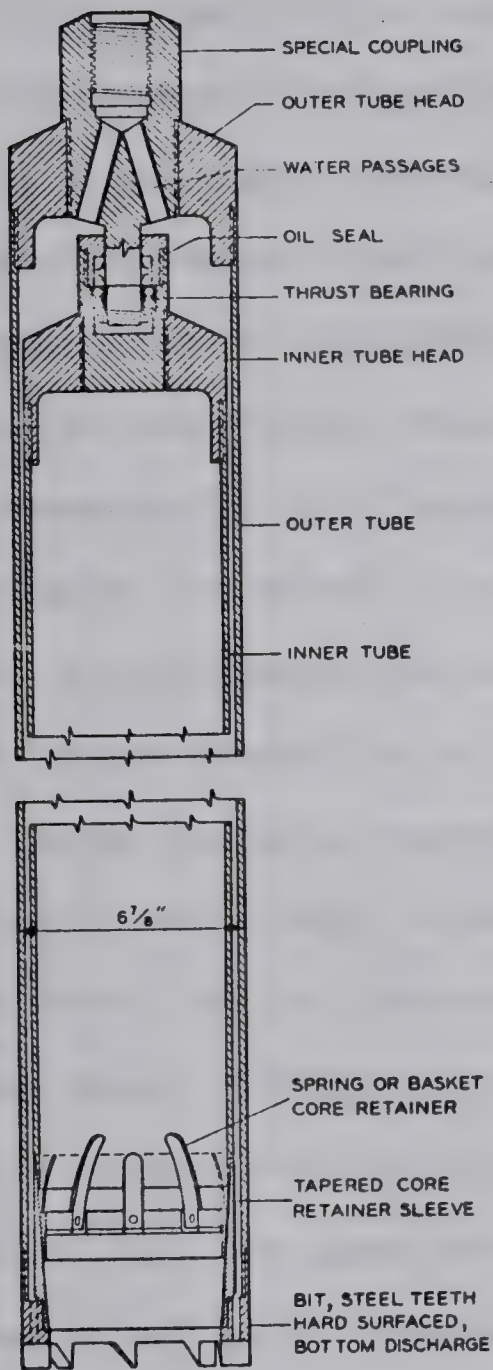
The standard method of coring in the study area consists of using a truck mounted rotary drill (Failing 1500, Mobile B-61 or equivalent) with a double-wall core barrel. The outer wall of the core barrel rotates and the rock is ground up by cutting teeth set at the bottom of the outer core barrel. This material is removed by circulating fluid (water or a water-bentonite slurry) or air which is pumped down the hollow drill-rod and passes between the inner and outer core barrel. The core is contained in the inner core barrel and is protected, to some extent, from the circulating fluid. The inner barrel has a swivel head and does not rotate during the coring operation.

A typical core barrel of this type is illustrated in Figure 2.22. Core barrels of this type (the Failing CB-19A) are currently used by such organizations as the Prairie Farm Rehabilitation Agency (P.F.R.A.) and the Water Resources Division of the Alberta Government (W.R.A.) and are standard equipment among a number of private drilling companies in the province of Alberta.



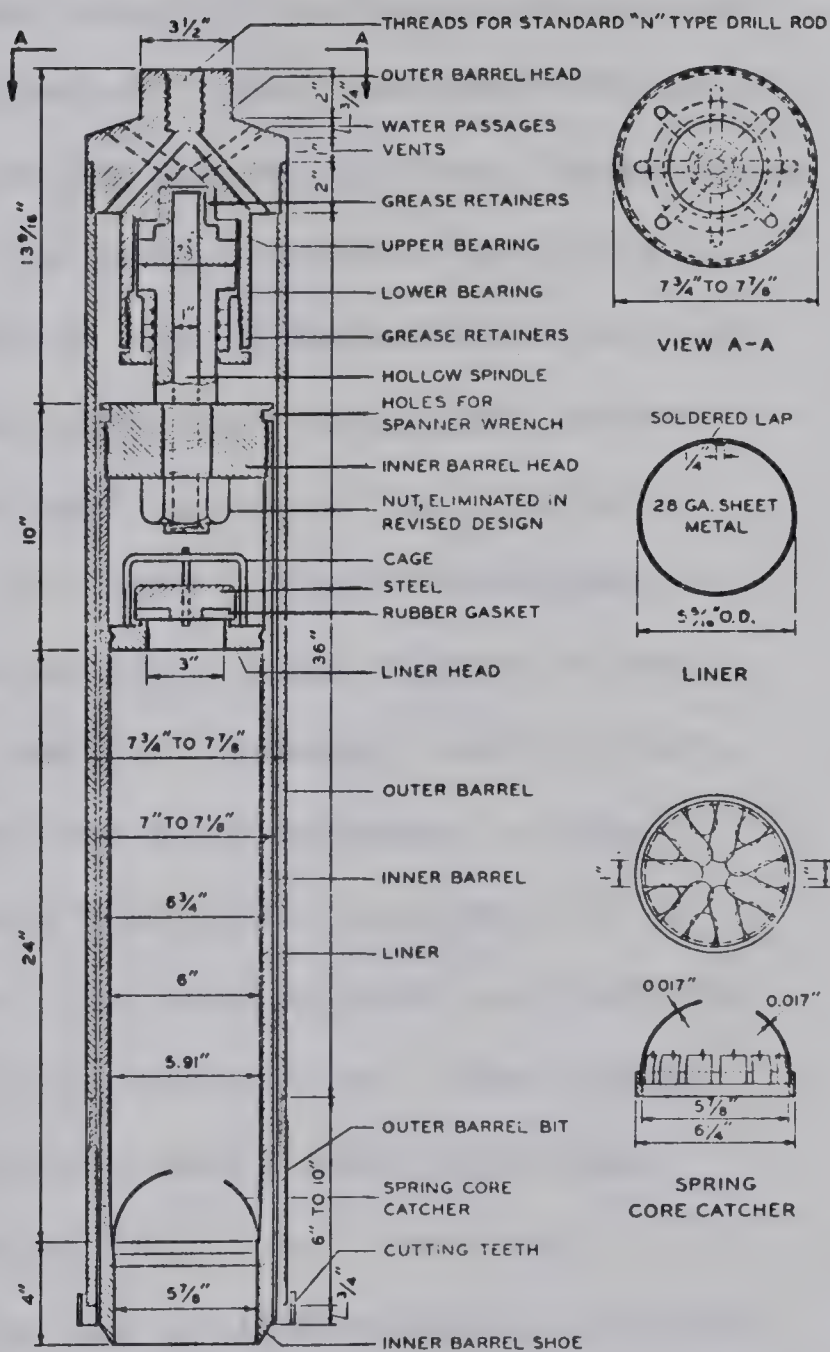






GEO. E. FAILING SUPPLY CO., ENID, OKLAHOMA

FAILING DOUBLE TUBE CORE BARREL



H. L. JOHNSON: CIVIL ENGINEERING, 1940, VOL. 10, P. 348

DENISON DOUBLE TUBE CORE BARREL

(HVORSLEV, 1948)

TYPICAL DOUBLE WALLED CORE BARRELS

FIG. 2.22



The double-walled core barrel will generally yield good results in the harder rocks of the study area but give poor recovery in the weaker, softer strata. Experience of P.F.R.A. and W.R.A. shows that seams of soft bentonite are often washed out and not recovered. Poor recovery of coal and other badly fractured rock is due to the core fragmenting and then being lost through the core catcher. A typical experience is recorded by Wilson and Hancock (1959) at Oahe Dam in the Pierre shale. Inclinoimeters indicated lateral movements in thin sharply defined zones as has been previously discussed. In hole no. 2408T, kinks developed in the inclinometer casing so that after four months it was no longer possible to lower the inclinometer past 15 feet. A large diameter auger boring was made adjacent to the casing and a man, working from this hole, was able to excavate around the casing at the trouble zone and relieve the sharp differential strain on the casing. The ground was found to be displaced along a small bentonite seam which had not been noted during drilling. The badly weathered core from this hole was re-inspected but no trace of the 3/8 inch thick layer was found as it, in all probability, had been washed away during drilling.

The aim in bedrock coring is to obtain as continuous and complete a core recovery as possible. Values of core recovery (foot of core recovered for footage drilled) for certain dams are shown in Table 2.6. Values of core recovery in the study area using a conventional double-





TABLE 2.6

## TYPICAL CORE RECOVERY USING DOUBLE WALL CORE BARRELS

Site	Bedrock	Source	Average % Recovery
Pembina Damsite Alberta	Edmonton fm. (Upper Cretaceous)	R.M. Hardy & Associates (1966)	75%
Hairy Hill Dam- site, North Saskatchewan River, Alberta	Ribstone fm. (Upper Cretaceous) Lea Park fm. (Upper Cretaceous)	P.F.R.A. (1970b)	50 - 60 %  90%
Three Rivers Damsite, Oldman River, Alberta	Porcupine Hills fm. (Tertiary) Willow Creek fm. (Upper Cretaceous)	P.F.R.A. (1965a)	70 - 80 %
Tomahawk Damsite North Saskatchewan River, Alberta	Paskapoo fm. (Tertiary) Edmonton fm. (Upper Cretaceous)	P.F.R.A. (1969c)	75%
Carvel Dansite North Saskatchewan River, Alberta	Edmonton fm. (Upper Cretaceous)	P.F.R.A. (1969b)	85%
Pomona Dam Kansas, U.S.A.	Pennsylvanian limestones and shales	U.S.C.E. (1954)	98.9%
Smithville Dam Missouri, U.S.A.	Pennsylvanian limestones and shales	U.S.C.E. (1969b)	98.4%



walled core barrel (mainly the Failing CB-19A which is 10 feet long, 3.5 inch outer diameter and 1 7/8 inch inner diameter) averaged about 80 percent. Two projects investigated by the U.S. Army Corps of Engineers in a hard shale-limestone sequence of Pennsylvanian age in Kansas and Missouri had core recoveries of 98.4 and 98.9 percent. It can be seen that only mediocre results can be obtained using the conventional double-walled core barrel in the soft Cretaceous bedrock of the study area. Excellent core recovery can be obtained, however, in harder rocks.

Poor core recovery is typically found for testholes drilled below valley bottoms in the study area. A well documented example is the Pembina River Damsite Number 3 investigated by the firm of R.M. Hardy and Associates for the Alberta Water Resources Division (R. M. Hardy and Associates, 1966). The site is located on the Pembina River about 1000 feet upstream of the Highway 16 bridge at Evansburg, Alberta. At the site, the Pembina River has carved a postglacial valley about 200 feet deep and 1300 feet wide through 20 feet of glacial drift, 50 feet of well cemented hard Tertiary sandstone of the Paskapoo formation and about 130 feet of interbedded shale, bentonitic shale and sandstone of the Edmonton formation (Upper Cretaceous).

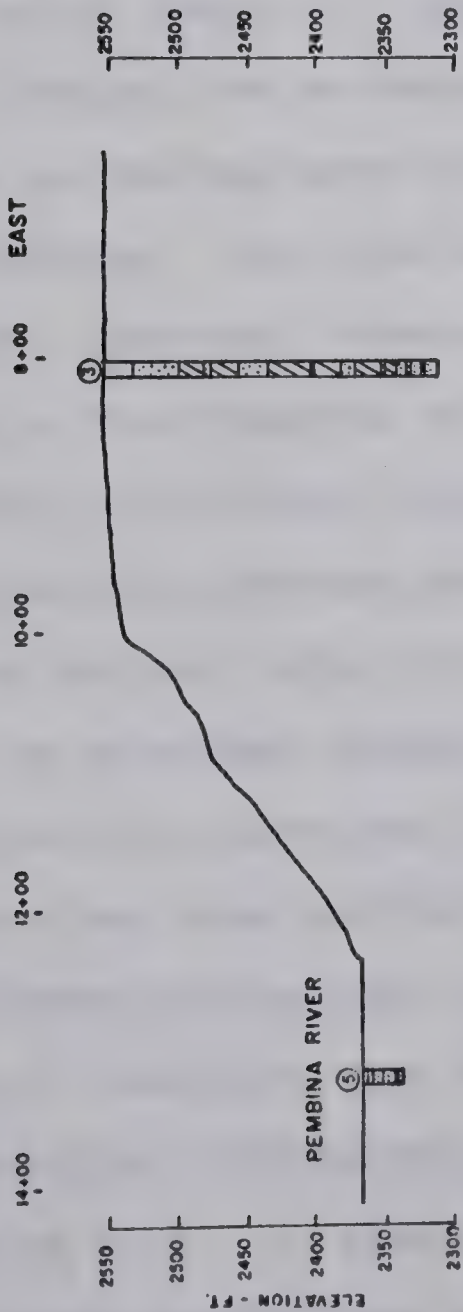
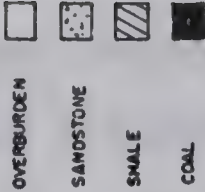
A cross-section of the valley is shown in Figure 2.23 which also shows core recovery and natural water contents at various elevations. The core barrel used on this project





WEIGHTED AVERAGE % CORE RECOVERY					
HOLE NO.	ELEV.	2550-2500	2500-2450	2450-2400	2400-2350/2350-2300
WEST ABUTMENT					
1	86.9	73.8	91.8		
2	38.0	74.3	91.2	83.9	
7	89.8	85.8	79.2		
0	89.5	91.7			
RIVER BOTTOM					
5					37.4
6					56.9
H					24.6
B					66.3
EAST ABUTMENT					
3	61.5	64.3	98.0	70.5	77.8
4	63.2	62.7	77.3	89.0	87.2

LEGEND



SUMMARY OF MEAN MOISTURE CONTENTS FOR SHALE (EDMONTON FM.)			
ELEVATION	WEST ABUTMENT	RIVER BOTTOM	EAST ABUTMENT
2550-2500	18.3		
2500-2450	13.9		14.7
2450-2400	13.8		13.9
2400-2350	9.0	15.8	9.9
2350-2300		10.8	10.8

NOTES

- LOCATION NW.17-53-7-W8
- CORED USING CB-19A CORE BARREL
- SCALE AS SHOWN
- ONLY TESTHOLES ON E SHOWN

PEMBINA RIVER DAMSITE 3 - SECTION, CORE RECOVERY AND MOISTURE CONTENTS (R.M. HARDY & ASSOC., 1966)

FIG. 2.23



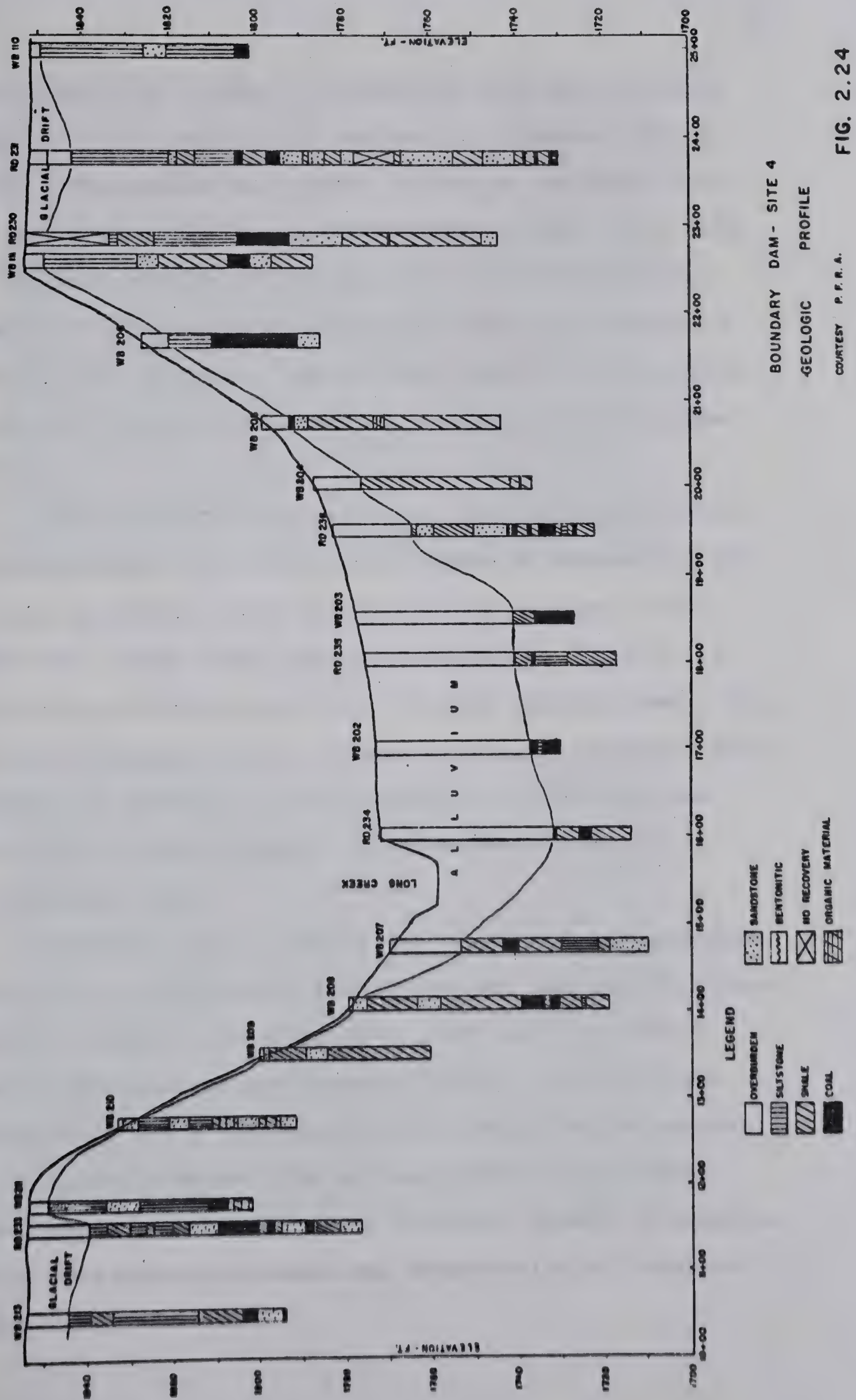
was the Failing CB-19A and core recovery of about 75 per-cent was obtained in the abutment testholes. The testholes drilled in the river valley gave a very low recovery ranging from 37.4 to 66.3 percent indicating a soft, badly fractured bedrock near the bedrock surface below the valley floor. Water contents found below the valley floor were higher than those at a similar elevation below the abutments indicating a substantial amount of rebound had occurred due to the formation of the valley, although the absence of marker beds precludes any reliable estimate as to the exact amount of rebound which has occurred.

Similar low recovery ratios were noted at Ardley Dam site on the Red Deer River about 30 miles east of Red Deer, Alberta. The site has been investigated by the Water Resources Division, Alberta Government (A.W.R., 1968). The bedrock is the Edmonton formation. Testholes drilled below the valley floor were characterized by poor recovery, a higher moisture content and a greater degree of fracturing than the bedrock below the abutments at the same elevation.

An excellent example of the limitations of present investigation techniques is given at Boundary Dam located on Long Creek near Estavan, Saskatchewan. The site was investigated during 1956 (P.F.R.A., 1956a) and a large number of testholes were drilled by wash-boring methods and double-walled core barrels. A centerline section is shown in Figure 2.24. No clear picture of the stratigraphy can be obtained despite the detailed drilling program. Two









zones containing a high proportion of coal clearly exist below the valley and in the abutments. However, one is unable to determine the precise nature of the upper coal zone and whether it is composed of one 20 feet thick coal bed (as indicated in RD 230 and WB 206) or several coal seams interbedded with sandstone and shale (as indicated in RD 231 and RD 233). The drilling results would appear to indicate little or no lateral continuity in the upper coal zone.

Core trenches were excavated into the valley walls during construction of the dam as shown in Plates 2.1 and 2.2. It is evident that three distinct, uniform, interbedded coal seams exist over an approximate depth of 20 feet which are continuous over the area investigated. Thus, it can be concluded that standard drilling techniques were incapable of providing much insight as to the detailed geology of the site despite the considerable amount of investigation done.

Somewhat better results can be obtained in the soft rock of the study area by use of the Denison sampler illustrated in Figure 2.22 (Hvorslev, 1948) and the Pitcher sampler (Morgenstern and Thomson, 1971). Both of these core barrels use a thin walled inner barrel which extends to, or slightly below, the cutting teeth of the outer barrel which has the effect of providing greater protection to the core against washing and transmission of torsional forces during drilling.







Plate 2.1 View of the east abutment core trench at Boundary Dam Saskatchewan. Note the three separate coal layers and the upwarping of the beds towards the valley. ( Courtesy of P.F.R.A. )



Plate 2.2 General view of the east abutment core trench shown in Plate 2.1. ( Courtesy of P.F.R.A. )





The Pitcher sampler has been used successfully in the softer rocks of the Edmonton formation (Pennell, 1969), in the Smoky River Group in northern Alberta (Hayley, 1968) and in the Belly River formation east of Edmonton (Locker, 1969). Two testholes were drilled at Carvel Damsite, 30 miles west of Edmonton on the North Saskatchewan River, as part of this study. Use of the Pitcher sampler gave better core recovery (typically 95%) in the softer rocks of the Edmonton formation than was obtained using the Failing CB-19A double-walled core barrel (typically 80%). However, the Pitcher sampler was unable to sample the harder shales and sandstones at Carvel. Similar observations were made by Locker (1969) who found the Pitcher sampler unable to successfully sample the highly indurated Paskapoo formation.

Thus, in summary, conventional coring techniques have not been successful in obtaining samples of the weaker members of the bedrock of the study area. A carefully conducted, comprehensive drilling program using conventional coring techniques will give a good overall picture of the geology of a site and will provide samples of the overall rock mass for testing but will not, except under exceptional circumstances, provide a complete picture of the minor geologic detail and softer zones which appear to govern the stability of the bedrock mass.

An alternative approach is the excavation of shafts and drifts which allow examination of the rock in-situ and allow block samples to be cut from selected zones. Test





pits and drifts were used at Fort Peck following the failure in 1938 to investigate zones of movement (Middlebrooks, 1942). The construction of these shafts allowed large scale field tests to be run on undisturbed weathered bentonite in the drifts driven into the weathered shale.

A test drift 365 feet long was excavated at Gardiner Dam (P.F.R.A., 1951) to provide samples and data on movement in the river valley walls and to allow insitu stress measurements. The results have been discussed previously in this chapter.

A method for determining the level of slide action in the Pierre shale at Oahe Dam consisted of drilling 30 inch diameter calyx holes. The stratigraphy exposed was inspected by lowering a man to depths of 60 feet in a specially designed light steel cage. Excellent data was obtained but the method had to be abandoned due to danger of falls in uncased holes (Knight, 1963).

The poor recovery below the Red Deer River Valley bottom at the Ardley Damsite in central Alberta has been previously discussed in this chapter. The Water Resources Division of the Alberta Government retained E. W. Brooker and Associates (Brooker and Associates, 1969) to further investigate the bedrock conditions below the river valley at the site. Three large diameter testpits were drilled to a depth of 48 feet using a truck mounted 'Williams Earth Digger' with a 48 inch diameter auger owned by Franki of Canada Ltd. The section of the pit in bedrock was lined



with a 12 gauge steel tunnel liner to provide a continuous 48 inch liner. Liner segments were removed from the wall two at a time to allow unobstructed examination of a segment of wall 3 feet square at a time. The surface exposed was cleaned of disturbance, photographed and logged in detail. Numerous samples were obtained for index properties and block samples were cut for strength testing.

The results of this investigation yielded a much better picture of the condition of the bedrock than the previous coring program which consists of 7 testholes drilled in the river bottom area and will be discussed in more detail in Chapter III.

## 2.7 Discussion

Recorded experience with the projects discussed shows that problems can be expected with slope stability and rebound of excavation bottoms when the bedrock of the area is unloaded. The formations which were deposited under marine conditions and contain a high percentage of bentonite and montmorillonite are especially troublesome.

The tendency for these formations to exhibit large scale instability and their rebound characteristics may be related. Experience at Gardiner, Garrison and Oahe Dams shows that rebound varying from about 0.5 to 1.0 percent of the excavation depth will occur while excavation is in progress. Time dependent rebound will occur at a decreasing rate following the end of excavation and will yield an





additional amount of rebound which in a few years may equal or exceed the amount of initial "elastic" rebound. Rebound will continue at a slow constant rate for a considerable period of time following the end of construction. Movements of this type at rates of up to 0.07 inch per year have been monitored at Fort Peck and Garrison Dams. The effect of continued swelling over long periods of time is evident at Garrison Dam where about 2 feet of total rebound occurred over a period of 4 years following the completion of a 200 feet excavation. The observed rebound below the valley of the Missouri River which has been in existence for about 25,000 years at the site (Fleming et al., 1970) is between 4.6 and 7.2 feet. This additional amount of rebound appears to be due to continued rebound of the bedrock over many centuries. However, both the "elastic" and "continuing swell" components of rebound are apparently a direct function of the stress removed during unloading. The presence of joints or faults, such as at Fort Peck Dam, appear to concentrate continuing "swelling" of the bedrock. This seems to be due primarily to the fact that the discontinuities in the bedrock provide a means of water access to the rock which, if intact, has such a low permeability as to be almost impermeable. The conventional interpretation of rebound behaviour, elastic rebound followed by swelling, is open to question as will be discussed in Chapter IV.

The effects of vertical rebound have been shown to be increased moisture content below the valley floor and



poor core recovery which is apparently due to a high degree of jointing and fracturing in the bedrock.

The bedrock of the study area is overconsolidated and field and laboratory evidence shows that the lateral stress is likely several times the vertical stress. Therefore, lateral rebound, both elastic and time-dependent should be greater than the vertical rebound if the bedrock is not highly anisotropic. A considerable weight of indirect evidence supports the existence of large amounts of lateral rebound having occurred due to valley formation. These are:

1. the increase in moisture content at Gardiner Dam towards the valley which led Peterson et al., (1960) to conclude several hundred feet of lateral rebound had occurred towards the river.
2. the presence of apparent tension fractures in the till parallelling the South Saskatchewan River.
3. the fact that the majority of slides documented appear to have occurred with residual strength parameters controlling the movement.

The occurrence of residual strength to govern the movement of a landslide implies that large movements have taken place along a clearly defined surface resulting in particle orientation in the direction of shear. Lateral expansion due to stress relief associated with valley formation appears to be a physically possible mechanism to produce this effect.







The fact that formations which contain a high montmorillonite content and have beds of bentonite are very prone to sliding has been discussed. Bentonite beds have been shown to be widespread in the bedrock of the area and characteristically have a strength and modulus of elasticity much lower than the surrounding rock. The majority of the well documented slides discussed occurred with the bottom of the slide moving in or along a bentonite bed.

Unloading of the bedrock, whether by artificial excavation, valley downcutting or active toe erosion on the outside of a river meander bend, has the effect of releasing lateral stress. Rebound will occur, some of which is immediate and some of which can be considered as time-dependent swelling. The presence of beds with differing moduli of elasticity will result in differential strains across weak layers and at unit contacts. Lateral displacement noted across thin bentonite beds at Oahe Dam by Wilson and Hancock (1959) has been discussed. Further evidence supporting this mechanism has been noted by the P.F.R.A. at three damsites located on the North Saskatchewan River: Carvel Damsite (Edmonton formation), Tomahawk Damsite located 10 miles downstream of Drayton Valley, Alberta (Paskapoo formation overlying Edmonton formation) and Hairy Hill Damsite located some 80 miles downstream of Edmonton, Alberta (Ribstone formation overlying Lea Park formation). At each site it was noted that "a horizontal separation along bedding planes between



different bedrock types, such as sandstone and shale, occurs repeatedly in the core, indicating the bonding between layers is weak" (P.F.R.A., 1969a, 1969b, 1970).

Therefore, the data available indicates that the presence of bedrock units which have differing moduli of elasticity can result in relatively large differential movements when high lateral stresses are relieved. Two questions must be answered before the relative importance of this mechanism can be assessed:

1. what displacement must occur in the field to shear a soil or rock mass to the peak and then to the residual strength?
2. what magnitude of displacement across weak layers and at unit contacts can occur due to stress relief associated with valley downcutting in the bedrock of the study area?

The present state of knowledge does not provide a definite answer to the first question. Laboratory direct shear tests on small samples typically require a displacement of about 0.2 inch to reach the peak in the stress-strain curve and displacements of several inches to reach the residual (Skempton, 1964). Smaller displacements (in the order of 5 mm.) are required to shear natural joints to the residual (Skempton and Petley, 1967). James (1970) showed that much larger displacements, in the order of 20 to 30 feet, were required before slides in the London Clay reached residual strength. However, the London Clay is a







relatively homogeneous material without the horizontal planes of weakness such as are provided in the Cretaceous bedrock of the study area by bentonite zones and abrupt changes in lithology. Evidence discussed in a subsequent section of this thesis indicates a much smaller relative displacement is required in a layered medium to reach the residual strength.

The magnitude of displacements due to valley down-cutting can be studied by use of the finite element method. Results giving the amount of elastic rebound due to valley formation require information on the values of the modulus of elasticity ( $E$ ), Poisson's ratio ( $\nu$ ) and coefficient of earth pressure at rest ( $K_0$ ) which act in the field. Data on these points is scanty and little knowledge of the appropriate boundary conditions exists. However, use of a realistic range of input parameters will yield considerable insight into the order of magnitude of displacements which have occurred.



## CHAPTER III

### GEOLOGIC EVIDENCE OF BEDROCK REBOUND

#### 3.1 Introduction

Chapter II discussed the bedrock of the Great Plains of Western Canada and the Northern United States. Excavation, either natural or artificial, results in a vertical rebound of the excavation bottom and inward movement of the excavation walls. A portion of the rebound has been seen to be elastic and occurs while the load is being removed. The remainder of the rebound can be considered as time-dependent rebound or swelling and can continue for many years after the load has been removed.

This chapter will review the literature available which documents valley rebound both inside and outside the study area as well as the effect this phenomena has on the physical properties of the rock below, and adjacent to, valley sections where rebound has occurred. Case histories from damsite and bridge investigations in the study area show that a rise in the bedrock below the valley bottom to form a gentle anticline is a ubiquitous feature in the study area. An upward warping of the strata adjacent to the valley occurs in many cases and is termed valley flexure. Surface expression of valley flexure is sometimes visible as a rise in the ground surface adjacent to the valley in the form of a raised valley rim.





Detailed observations are presented on the state of bedrock exposed below the North Saskatchewan River in Edmonton, Alberta in the pier excavations of two bridges. The presence of soft zones, apparently due to lateral movement between beds, and shear planes in a bentonite layer outcropping above river level are discussed.

A review of the case histories in the study area indicates the dominant mechanism which forms the valley anticlines is vertical rebound due to release of stress associated with river valley formation. Time-dependent rebound or swelling appears to contribute markedly to the rebound causing the valley anticline. Buckling of horizontally bedded strata appears a possible mechanism only if extremely high lateral stresses, which would likely be tectonic in origin, exist and the strata exist as discrete, continuous beds with no cohesion acting between them. Buckling of the bedrock may have occurred at some sites in Britain and at Portage Mountain Dam in Canada.

### 3.2 Literature Review

Western Canada and the Northern United States are not unique in having deep river valleys incised through relatively soft, sedimentary bedrock. A number of well documented cases exist, largely from dam investigations, in Europe, England and elsewhere which provide valuable geologic information on the results of river valley formation.



Features noted include stress-relief joints, valley bulging and valley cambering.

### Stress-relief joints:

The occurrence of stress-relief joints parallelling river valleys has been extensively documented in the geological literature as detailed in Chapter II. A number of similar observations have been made in connection with engineering projects.

Ferguson (1967) describes the occurrence of vertical joints which occur parallel to valleys cut through Devonian and Permian sedimentary bedrock in the Allegheny Plateau of the eastern United States. Subsurface exploration revealed these fractures to be practically non-existent below the valley bottom as shown in Figure 3.1. The base of vertical jointing in the valley walls usually ended in a horizontal gouge or mylonite zone.

A similar feature was noted by Imrie (1967) at Portage Mountain Dam in north-eastern British Columbia. Vertical sheeting occurs in the bedrock parallel to the valley walls on both abutments but the feature only extends a few tens of feet away from the canyon. The bedrock consists of interbedded sandstones, shales and coal of the Dunlevy and Gething Formations (Lower Cretaceous).

Bellport (1967) describes how leakage through stress-relief joints along the Green River in Wyoming threatened the safety of Fontenelle Dam. The system of stress-relief







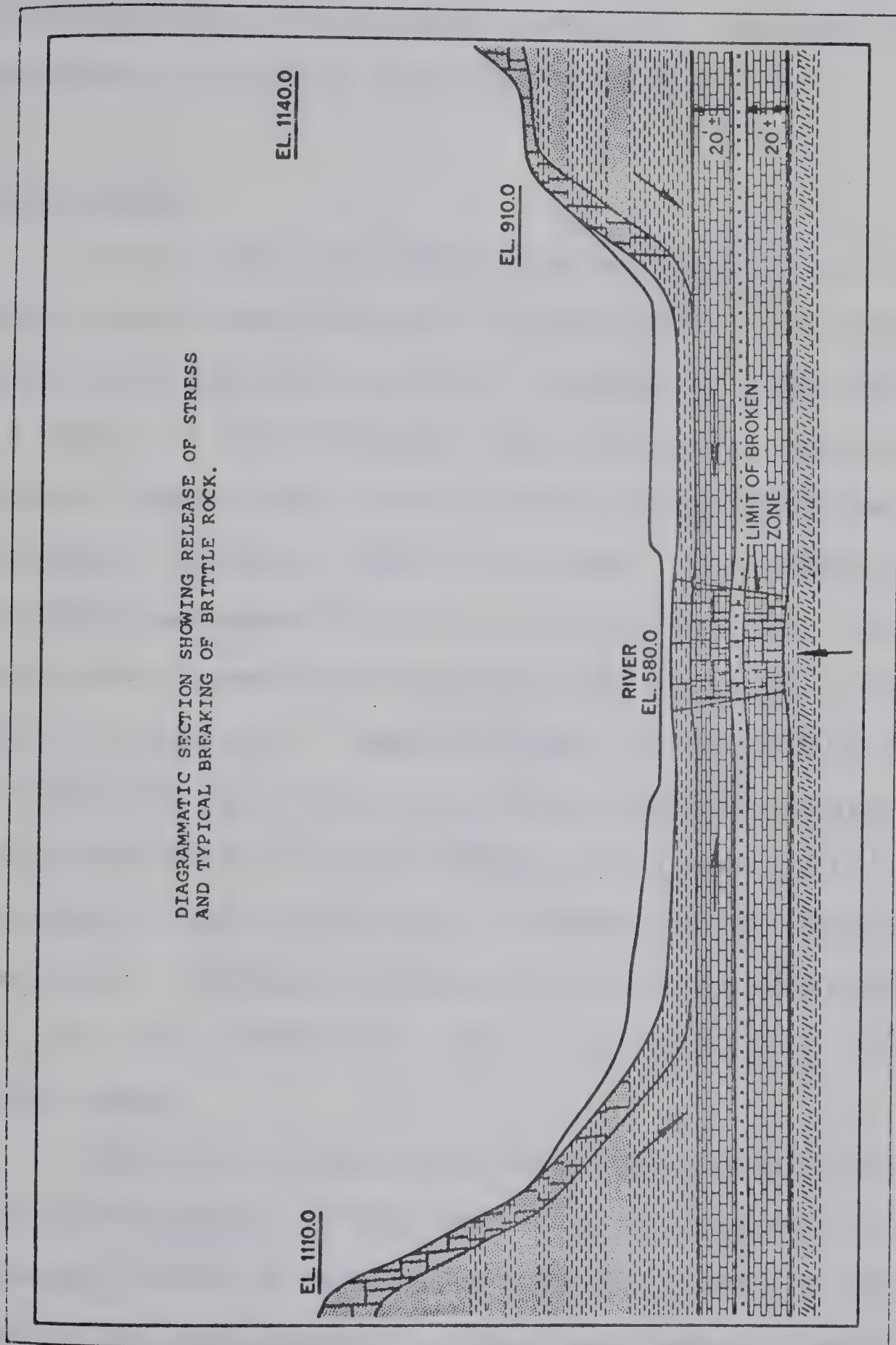


FIG-3.1 VERTICAL STRESS-RELIEF JOINTS ALONG VALLEYS IN THE ALLEGHENY PLATEAU

( FERGUSON, 1967 )



joints developed in the Green River formation, composed of alternating beds of calcareous sandstone, siltstone and carbonaceous shale, is shown in Figure 3.2.

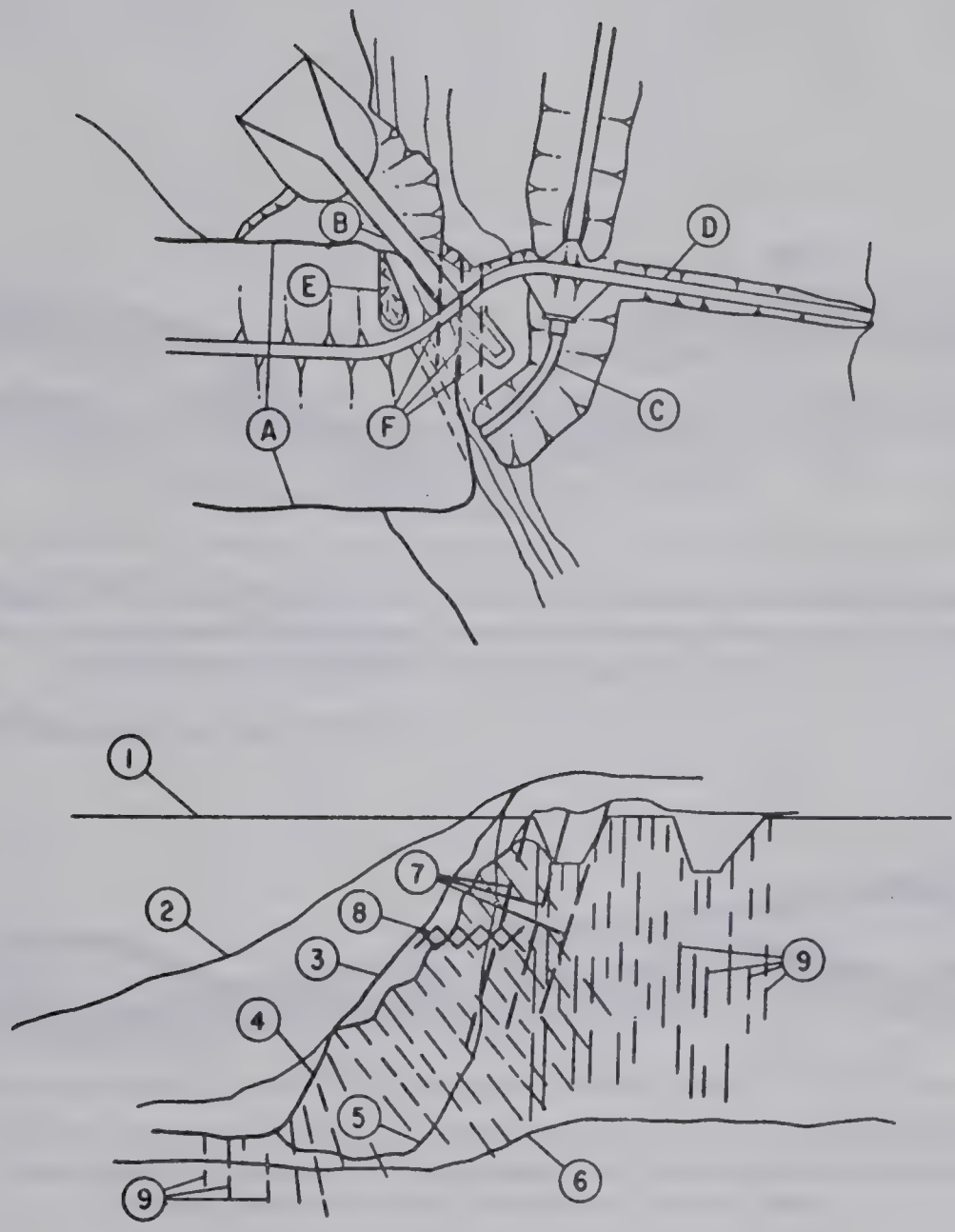
#### Valley Bulges:

Valley bulges are defined by Hollingworth et al., (1944) as anticlinal uprisings of the material comprising the valley floor and may consist of a simple or compound fold or a series of discontinuous elongated domes. The occurrence of these features was first comprehensively described in the Northampton Ironstone Field in England. The feature is best developed where the valley bottoms have cut into a weak argillaceous formation underlying more competent strata as shown in Figure 3.3. Upward movement of the valley floor has impressed high dips on the beds along the margins of these structures in the Northampton Ironstone Field and has resulted in fracturing along the margin of the bulge in some cases. Evidence of plastic flow of the underlying soft Lias clay towards the valley center has been reported in some cases.

Cambering is associated with valley bulging due to valleyward movement of the underlying argillaceous material. Competent blocks of cambered strata may become partly detached and move downhill. The fracturing related to cambering results in deep debris-filled cracks or 'gulls' parallel to the valley wall.



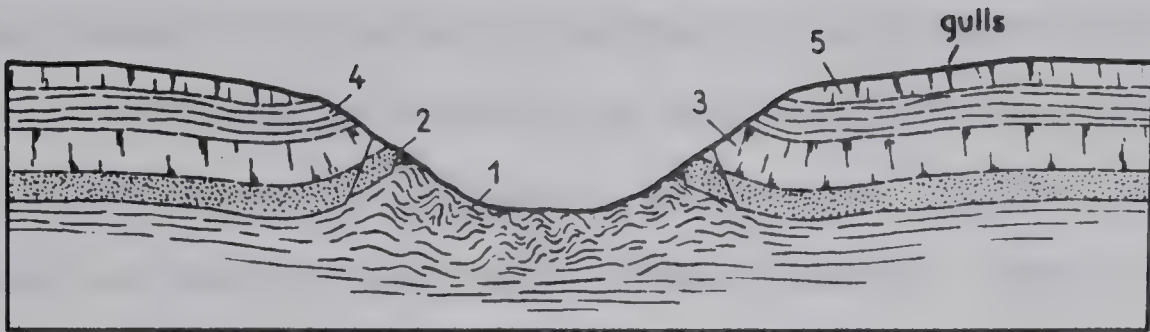




- |  |   |
|--|---|
| <p><b>Plan :</b></p> <ul style="list-style-type: none"> <li>(A) Embankment.</li> <li>(B) Spillway.</li> <li>(C) Canal outlet.</li> <li>(D) Road.</li> <li>(E) September 3, 1965, leakage and slough.</li> <li>(F) Open cracks.</li> </ul> <p><b>Section :</b></p> <ul style="list-style-type: none"> <li>(1) Dam crest.</li> </ul> | <p><b>Right Abutment Detail.</b></p> <ul style="list-style-type: none"> <li>(2) Downstream abutment slope.</li> <li>(3) Abutment slope at dam centerline.</li> <li>(4) Bedrock surface at dam centerline.</li> <li>(5) Upstream abutment slope.</li> <li>(6) Lower limit of grout acceptance.</li> <li>(7) Open cracks.</li> <li>(8) Approximate location of leak.</li> <li>(9) Grout holes.</li> </ul> |
|--|---|

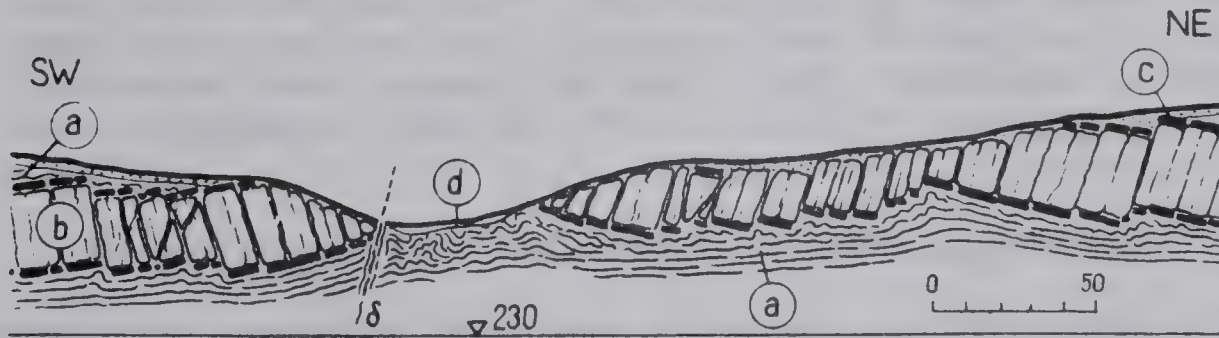
FIG. 3.2 STRESS RELIEF JOINTS AT FONTENELLE DAM, WYOMING  
( BELLPORT, 1967 )





Bulging of the Lias clays in the valley bottom near Northampton in Central England:  
1 — Lias clays, 2 — sandstones of Northampton Beds, 3 — Lincolnshire limestones, 4,5 — shales  
and limestones of the Oolite Series (Hollingworth, 1944).

(after Hollingworth et al, 1944)



Squeezing-out of marly shales on the valley bottom of the Lucina river near Ostrava;  
a — marly shales (Lower Cretaceous), b — tæschénite, c — contact metamorphosed slates.  
d — disturbed shale beds in the valley bottom (Záruba, 1956).

### VALLEY BULGES DOCUMENTED IN EUROPE - ATTRIBUTED TO PERIGLACIAL CONDITIONS





Phenomena analogous to valley bulges had previously been noted in cutoff trenches constructed at damsites in the Pennine Mountains in the north of England. Watts (1906) noted foldings in the shale bedrock in the trench for Langsett Dam in the Little Don Valley and "some curiously contorted snake-like bands" composed of soft material in the shale which were attributed by Watts to lateral pressure. All traces of these foldings disappeared in the lowest section of the 90 foot deep cutoff trench. Watts (1906, p. 672) recommended that:

"When a trench is bottomed, it should be immediately covered so as to prevent the floor from lifting in the center. It is a common occurrence in shaly ground for the floor to lift, especially if kept open for some time before refilling. When it begins to rise laminated beds sound "drummy" and, sometimes after long exposure, the effect is felt to a depth of 20 inches."

Lapworth (1911) describes bedrock exposed in a number of dam core trenches at sites located in the north of England. Numerous dam sections in the Carboniferous rocks of the Pennines showed a buckling up or wrinkling of the strata below the center of the valley; often extending to considerable depth and producing extensive fracturing and faulting in the rocks. The net result was a general opening of the rocks to freer percolation of water which necessitated the construction of deep cutoff trenches.

Horizontal displacement towards the valley occurred at these sites as noted by Lapworth (1911, p. 38).

"In the Derwent Valley these wrinkles are of great depth; and evidence of horizontal sliding is very



clear, pieces of shale from trial headings driven hundreds of feet into the hillside being perfectly polished by the movement."

The disturbance of beds dies out with depth and thick intact units of rock appear to protect the underlying material.

Sandeman (1918) describes wrinkles or folds in key-trenches at the Howden and Derwent Dams in the Derwent Valley. The bedrock at these sites is the Yoredale Rocks (Carboniferous) which consist of beds of shale ranging from several feet to a few inches in thickness, alternating with beds of sandstone usually less than 2 feet in thickness but occasionally attaining 7 or 8 feet.

Sandeman (1918, p. 155) describes the features at Howden Dam in the following terms:

"The Yoredale beds are wrinkled or folded in the valley-bottoms and also sometimes to a less extent a little higher up. Sometimes the strata are curved into a long roll without being faulted, but in the bottom of the valley they are tilted up sharply, as shown in Figure 3.4 (author's notation) where not only are they raised up sharply but also the central part is reduced to a powdered mass."

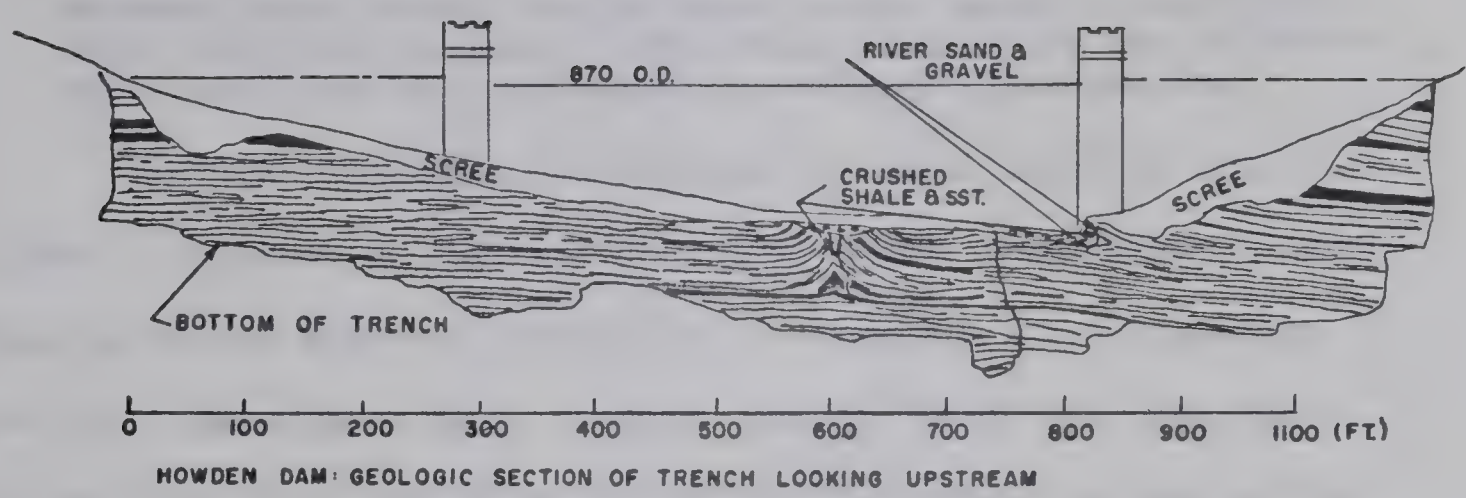
The zone of disturbance decreased with depth and few signs of disturbance were visible at the bottom of the 70 ft. deep trench.

Headings driven into the hillsides at Howden Dam found "the strata explored consisted mostly of broken shale, the rifts in which were in places as much as 6 to 8 inches in width" (Sandeman 1918, p. 161). The bedrock under the hillsides was broken by numerous small step-faults dipping at about 60 degrees towards the valley as shown in Figure 3.4. The downthrow of the faults was towards the valley

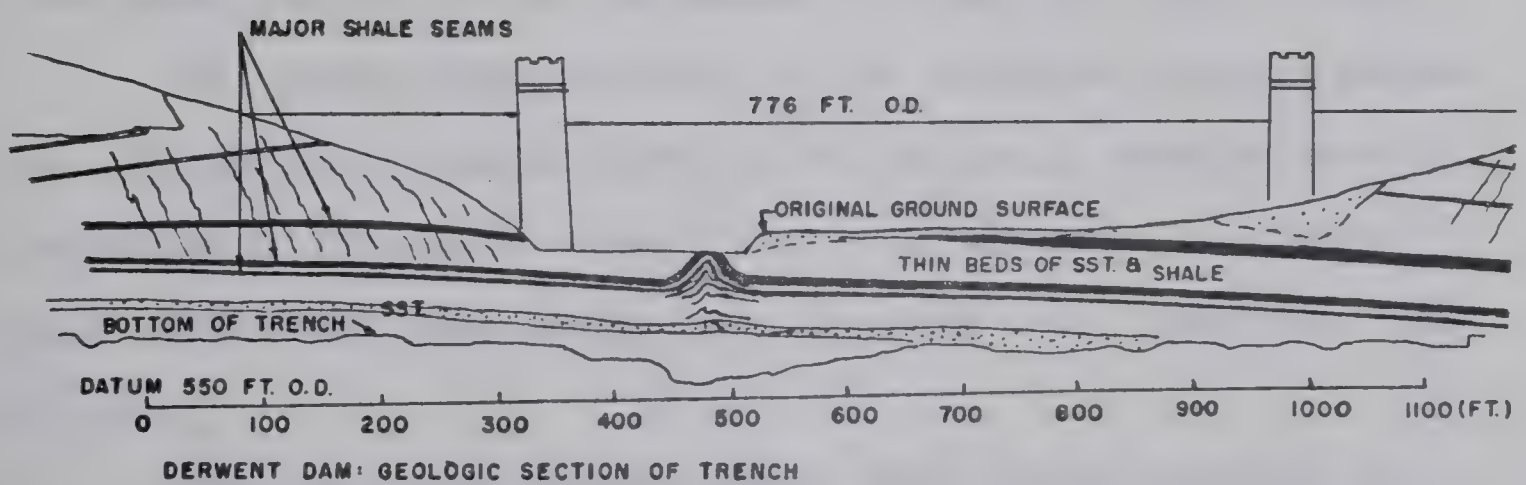








- MAIN SHALE BANDS
- ▨ SANDSTONE
- ▤ INTERBEDDED SHALES & SANDSTONE



(AFTER SANDEMAN, 1918)

SCALE: 0 80 160 FT.

GEOLOGIC SECTIONS OF DAM TRENCHES - DERWENT VALLEY

FIG. 3.4



and Lapworth (1918, p.196) stated:

"The joints and faults, instead of being parallel to those on the other side of the valley, were each inclined towards the center of the valley. Now that showed that those faults and cracks were connected with the valley itself and were therefore the effects of local and not regional or tectonic movements."

Valley bulging, as defined by Hollingworth et al., (1944), appears to differ from the cases described in the Pennine Mountains in the north of England as a crushing of the hard competent rock occurs rather than the apparent plastic failure and flow which has occurred in the softer rocks in Northamptonshire. Rowe (1968) describes a bulged valley bottom at Stauton Harold Dam near Derby, England. Figure 3.5 shows a geological section through the dam centerline. The bedrock is identified as sandstones and shales of Carboniferous age. The overlying shales and mudstones are described as having weathered into clays and have been pushed up to the ground surface by "hill creep".

The undrained strength of the deformed bedrock below the valley floor varied from 12 to 30 p.s.i. with a mean strength of 17 p.s.i. Overlying this material is a dark grey weathered shale which was fissured into lumps the "size of dice".

Kellaway and Taylor (1952) show valley bulging in the East Midlands of England to date from Pleistocene times and consider periglacial effects, especially the formation of horizontal ice lenses below the valley floor, to be the primary cause of the bulging. Differential rebound was discarded as a mechanism in this area due to the low relief





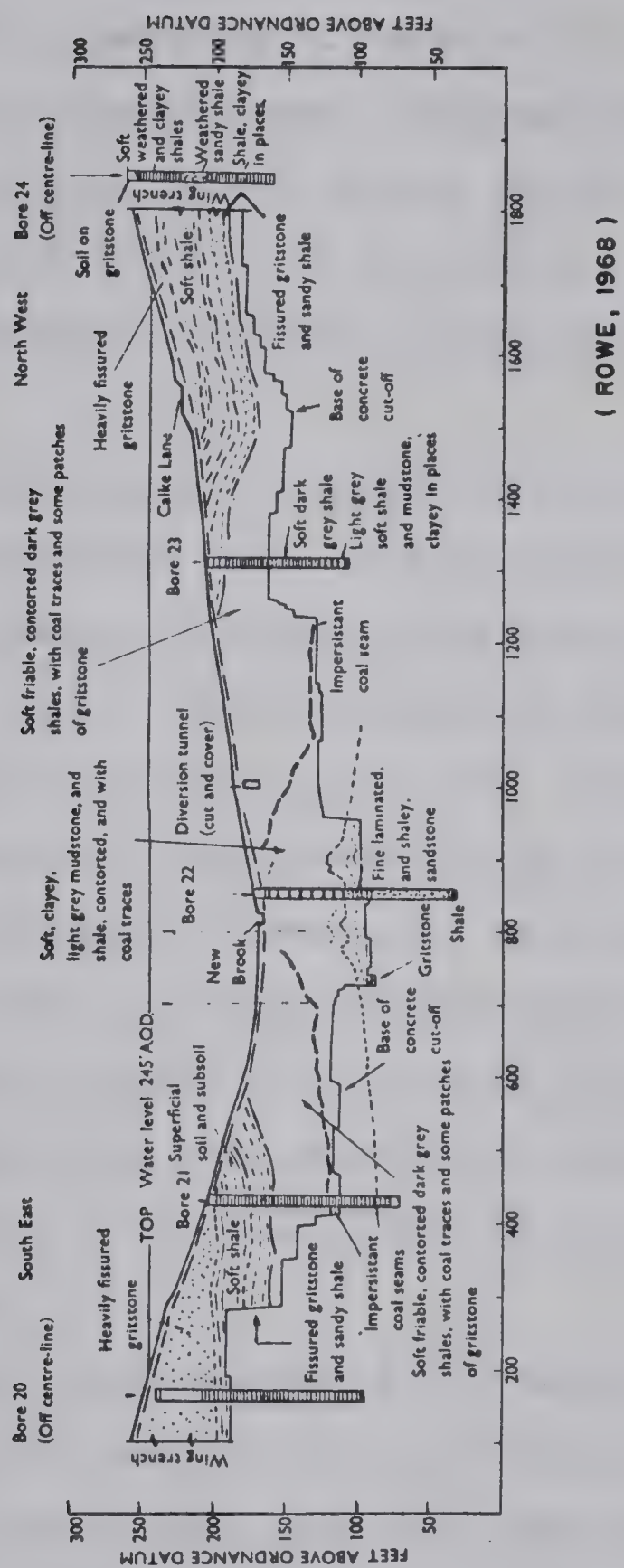


FIG. 3.5 STAUTON HAROLD DAM, ENGLAND: CUTOFF TRENCH SECTION



in the area with valley depth typically 80 to 100 feet. Evidence pointing to a periglacial cause of the bulged valleys included undisturbed gravel terraces which show no sign of folding overlying bulged valleys and the fact that postglacial valleys show little or no evidence of bulging while bulging is strongly developed in preglacial or interglacial valleys.

Little is known about the growth of ice lenses in bedrock and most documented cases of disturbance of stratified materials, by former intensive frost action, occur in overburden (Sharp, 1942). Several cases are documented showing the effects of ice wedging in rock. Schaefer (1948) records the occurrence of involutions in the Cretaceous shale of the Colorado Group in Montana. Vertical fissures presently infilled with surficial material were noted to a depth of 13 feet and a number of horizontal infilled fissures occurred several feet down from the bedrock surface suggesting horizontal layers of ice were formed in association with vertical ice wedges.

Yardley (1951) describes how frost wedging has lifted blocks up to 25 feet in diameter through vertical distances of more than 12 feet from flat exposures of crystalline rocks on the Canadian Shield north of Great Slave Lake. The movement occurred along joints and foliation planes and was best developed in fine textured quartz-mica schist and phyllite exposures in regions of low relief, where drainage is poor. The frost-thrusting of these





blocks was attributed to water freezing along horizontal joints.

It is generally accepted that cambering and valley bulging in Britain is a phenomena of Pleistocene date (Hutchinson, 1968; Higginbottom and Fookes, 1970) but the theory that periglacial phenomena are the cause of the bulged valleys has not been universally accepted in the engineering geology literature. Possible factors contributing to valley bulging listed by Higginbottom and Fookes (1970) are:

1. preferential development of ground ice in the valley bottom.
2. build-up of excess hydrostatic pressure below the valley floor.
3. behaviour of swelling clays.
4. rebound of the valley floor associated with removal of overburden load.

Zaruba (1956) describes analogous phenomena noted in the Oltul and Tarnava Mare river basins in Rumania. Tertiary clayey sediments flooring these basins have been forced up into gentle anticlines arranged parallel with the direction of the river. The term "valley anticlines" has been used to describe these features and their origin is ascribed by Zaruba to "lithostatic forces, analogously to salt dome formation." Sections of several bulged valleys are given by Zaruba (1956) in the Bohemian Cretaceous formation and the Carpathian Flysch, one of which is illustrated in Figure 3.3. Mechanisms postulated by Zaruba to explain the bulging include:



1. plastic deformation of the underlying clayey rocks under differential load.
2. swelling due to load removal.

The bulging at a damsite in the Carpathian Mountains resulted in differential movements between beds of shale as described by Zaruba (1956, p. 512).

"The resulting deformation consists in many slight differential shifts along the bedding planes of the fragments of shales. In the disturbed zones these fragments take the shape of small lenses separated by smooth planes covered with clayey films. The movement has a plastic character as partial differential movements do not form a uniform shear plane so that it does not result in a sudden sliding movement of the mass. . . . The instability of the slope becomes perceptible within a longer period of time, when the more or less continuous deformations reach measurable values."

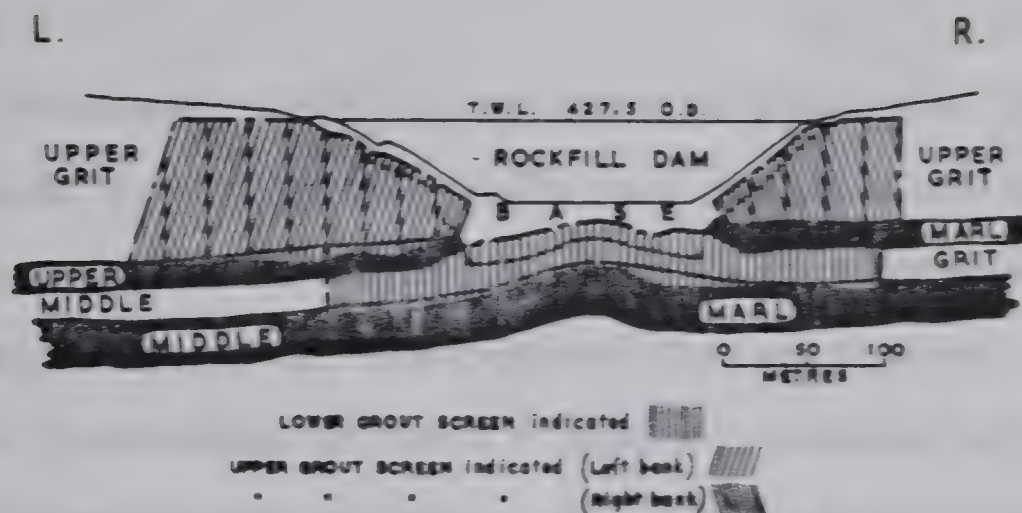
The occurrence of plastic deformation in the bulged bedrock affected the grouting of the dam foundation. High grouting pressures caused uplift and further disturbance of the shales by penetrating "along the differential shear planes for a long distance from the grout holes in all directions."

A number of dam foundation sections showing bulged valleys in England are given by Walters (1962). Other relevant sites illustrated include Ghrib Dam, located 60 miles south-west of Algiers in North Africa, which shows a well developed bulge below a valley cut through a grit (sandstone) and marl sequence as shown in Figure 3.6. Watauga Dam, also shown in Figure 3.6, and located in Tennessee, shows no evidence of bulging. The valley at

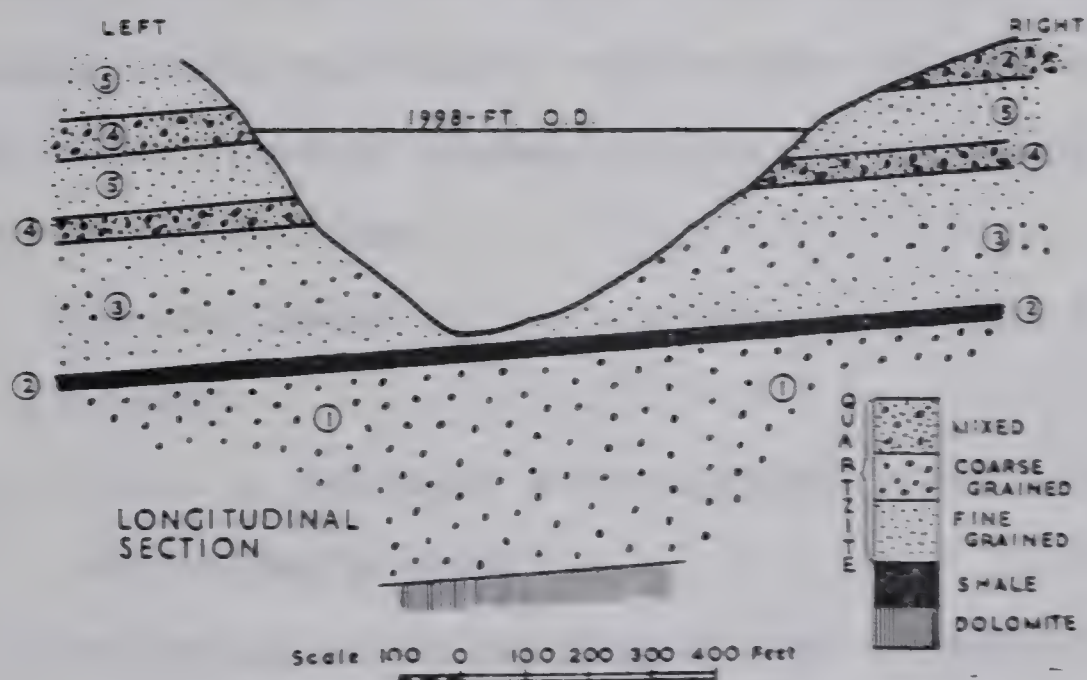








### GHRIF DAM FOUNDATION - ALGERIA



### WATAUGA DAM - TENNESSEE VALLEY AUTHORITY

(after WALTERS, 1962)

CROSS SECTIONS OF RIVER VALLEYS  
SHOWING AN ANTICLINE BELOW  
THE BED OF THE RIVER

FIG. 3.6



this site has downcut through an extremely stiff quartzite-shale sequence which has unconfined compressive strengths in the range of 20,000 p.s.i. (quartzite) to 9,000 p.s.i. (shale).

Ferguson (1967) noted tension fractures (previously described) in the valley walls and compression fractures below the valley floor in dam foundations exposed in the Allegheny Plateau of the eastern United States. The bedrock is flat-lying to gently dipping sedimentary rock which ranges from highly variable coal measures to uniform Devonian shales. Most of the rocks are cemented and relatively hard with the weakest rock being a compaction, nonbedded, indurated clay. Many of the valleys were downcut to their greatest extent by glacier meltwater at the end of the Pleistocene.

Features noted in dam trenches below the valley floor included:

1. gouge or mylonite along bedding plane breaks in the valley bottom.
2. an upwarping or arching of beds towards the center of the valley resulting in a slight flattening of the dip of the beds.
3. thrust faulting of rigid limestone beds below the valley floor.
4. tension failures of near surface beds due to arching.





The features, illustrated in Figures 3.1 and 3.7, are ascribed by Ferguson (1967) to release of high lateral stresses above valley bottom level and buckling of the strata below the valley floor due to high lateral pressures.

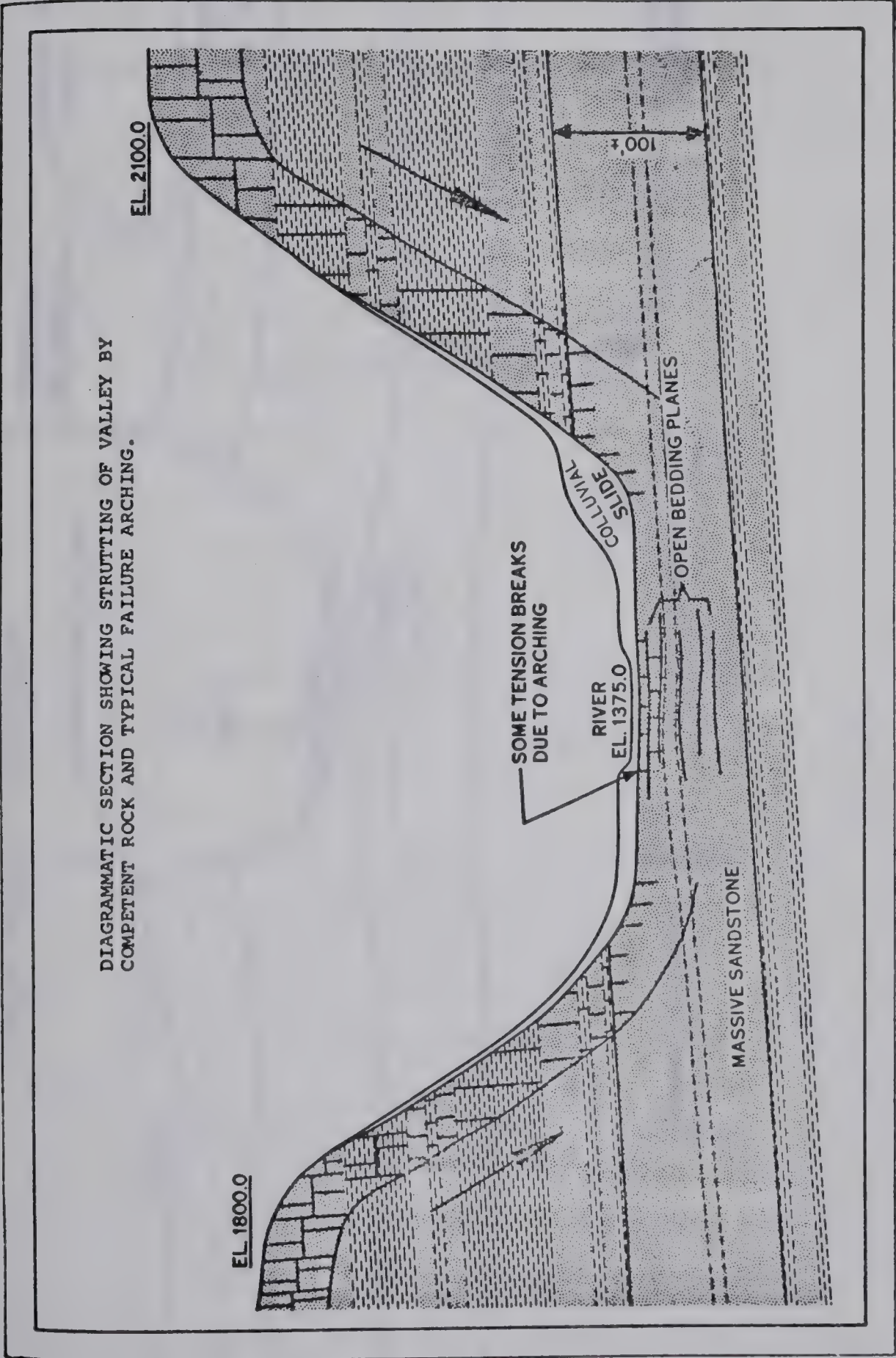
### 3.3 Case Histories Showing Rebound in the Study Area

An airphoto survey of landslide activity along the Pembina and North Saskatchewan Rivers in Alberta (Matheson, 1970) revealed the frequent occurrence of a rise in the ground surface immediately adjacent to the valley. This feature was visible under stereoscopic examination of air-photos (scale 1 inch = 2640 feet) and occurred frequently where the river valley was incised in a postglacial channel through a region of low topographic relief. A typical section is shown in Figure 3.8. The feature is termed a "raised valley rim".

Elongated sloughs and depressions trending parallel with the valley wall and located several hundred yards back from the valley edge frequently occurred in conjunction with the raised valley rim. In some cases tributary gulleys were observed to run parallel to the main valley before entering it at a right angle. These drainage features are associated with the raised valley rim and will be discussed in Chapter VII of this thesis.

The rise in ground surface adjacent to the valley is due to rebound of the valley floor. Evidence to support this theory is presented in the results of a study of





( FERGUSON, 1967 )

FIG. 3.7 FEATURES NOTED IN DAM CUTOFF TRENCHES IN THE ALLEGHENY PLATEAU







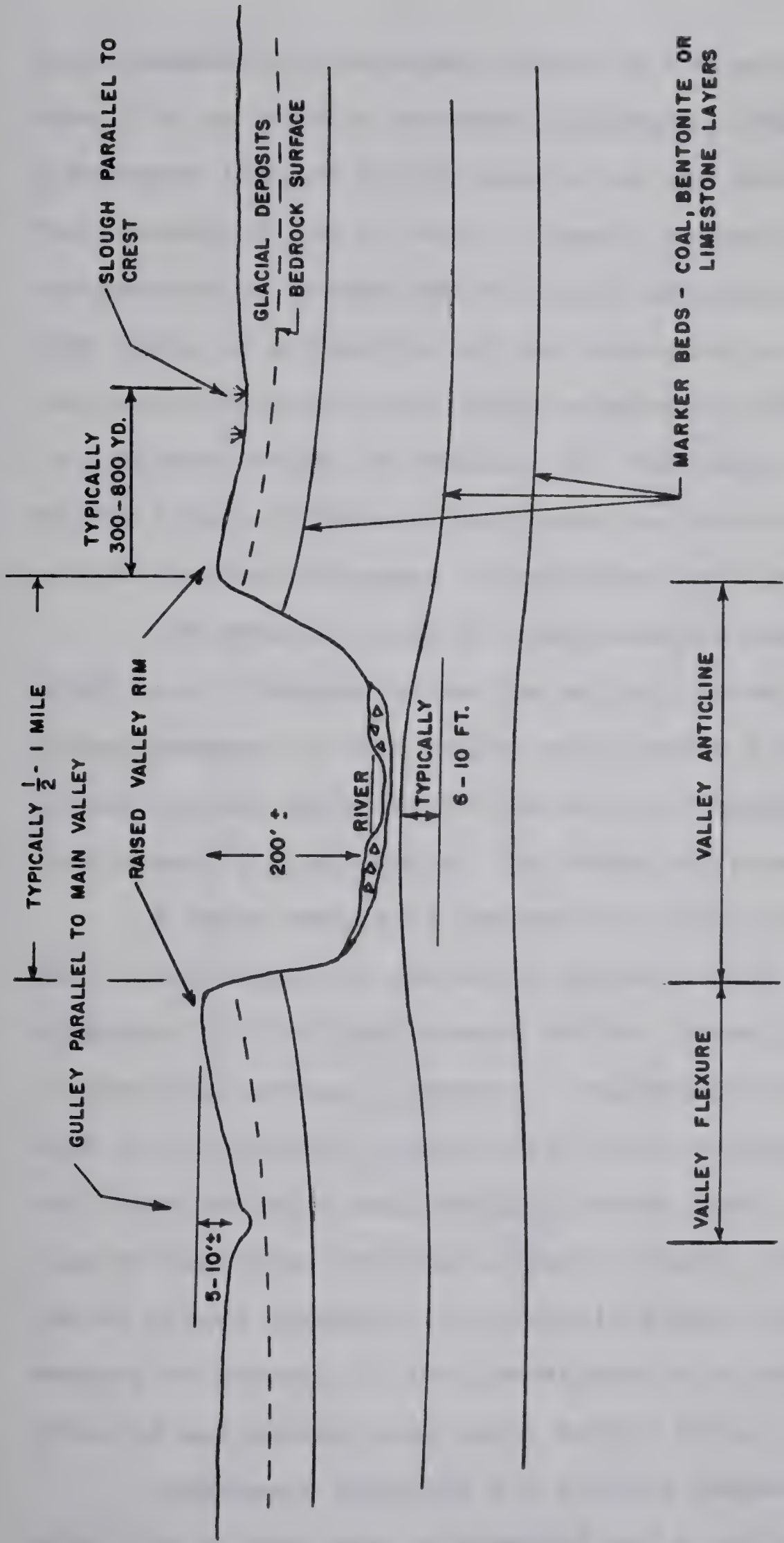


FIG. 3.8 IDEALIZED SECTION ILLUSTRATING FEATURES RESULTING FROM VALLEY FORMATION



displacements and stresses caused by the excavation of a trench in an elastic material (Dibiagio, 1966). The displacements induced by the excavation are shown in Figure 3.9. The excavation can be seen to result in vertical rebound of the excavation bottom and an inward movement of the excavation walls as a function of the stress relieved. A rise in the ground surface immediately adjacent to the excavation is predicted which is reduced, for the particular geometry of the finite difference grid used in this study, by relief of high lateral stresses as indicated by high value of  $K_0$ .

The general trend of displacements observed in the study area - rebound below the valley bottom, evidence of inward movement of the valley walls and a rise in the ground surface adjacent to the valley - agrees with the displacements predicted by the theory of elasticity.

A large amount of rebound must have occurred below the valley bottom to produce a raised valley rim visible on airphotos if the displacement pattern shown in Figure 3.9 is even qualitatively correct. The bedrock of the study area is flat-lying, usually free from tectonic disturbance and often contains well defined marker beds. Therefore, a line of testholes drilled across a valley, such as for a dam or bridge investigation, should reveal significant amounts of rebound if the investigation is sufficiently detailed and marker beds exist at the site.

Government agencies and private companies engaged in this type of work were approached and a collection of valley





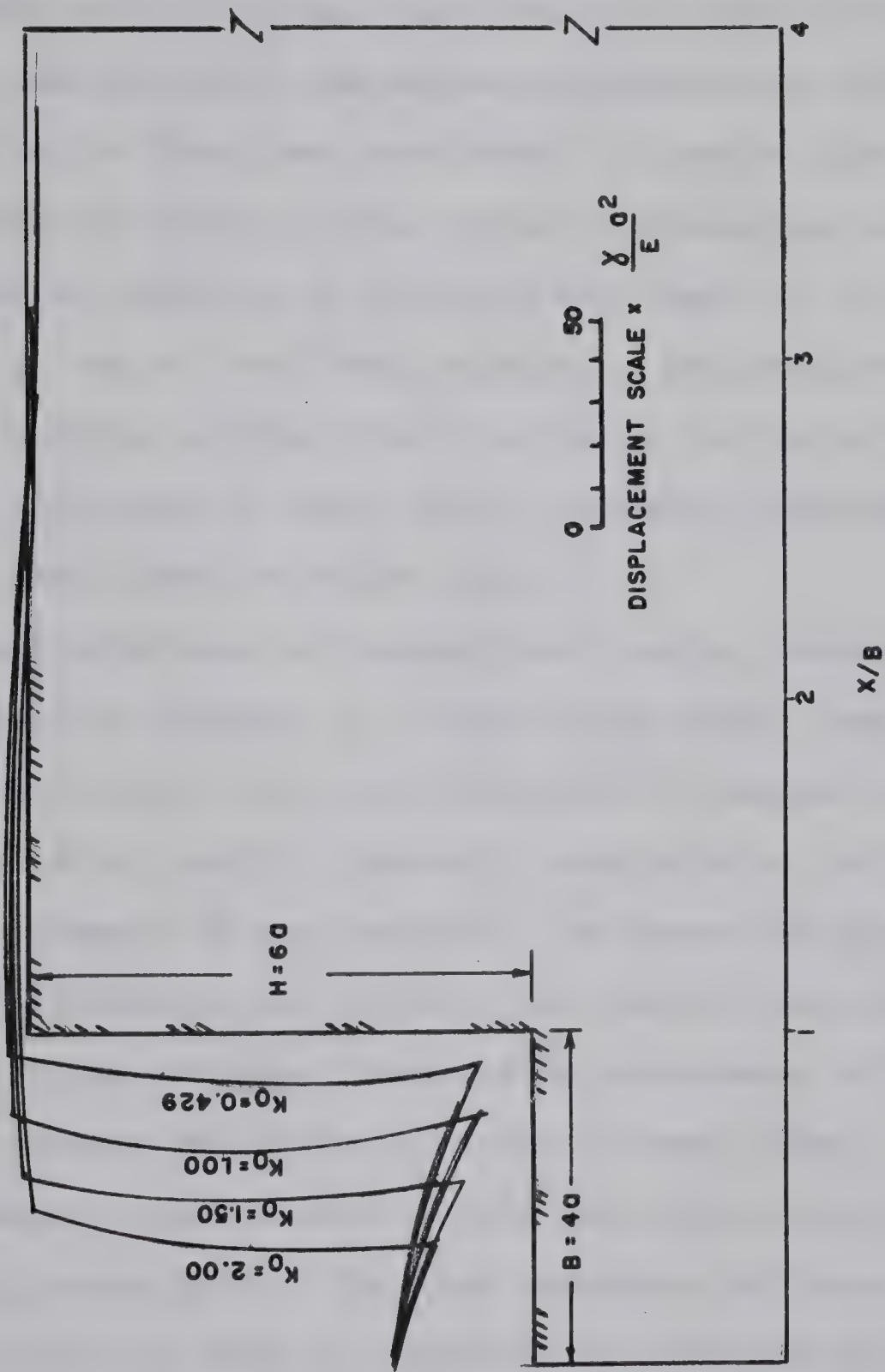


FIG. 3.9 DISPLACEMENTS DUE TO EXCAVATION INTO AN ELASTIC MASS FOR DIFFERENT VALUES OF  $K_0$  (DIBIAGIO, 1966)



geologic cross-sections, primarily from damsite investigations, was compiled from drilling records. At almost every site where sufficient drilling had been done to detail the stratigraphy accurately and correlation of beds between testholes was possible, unmistakable evidence of rebound below the bed of the river was noted. A gentle rise of the beds towards the valley center occurs although no evidence of buckling or faulting of the beds was found in the test-hole data at any of the sites studied in the project area. An upward warping of the strata in the valley walls towards the river was noted in cases where extensive drilling had been done back from the valley edge.

The limitations of conventional coring techniques was discussed in Chapter II. Cases exist where loss of core in one testhole precluded tracing of a marker bed over the entire valley width. However, knowledge of the depositional environment of the bedrock, the degree of lateral continuity of bedding at the site and the drilling techniques used enables one to make a reasonable assessment of the amount of rebound which has occurred in most cases.

Several other factors affect the evaluation of data from a particular site. The most important of these is the amount of drilling done on a particular site and the layout of the testholes. A typical preliminary drilling program for a damsite investigation is shown in Figure 3.10. Few testholes are usually drilled back from the abutments and the abutment testholes are usually drilled to a few feet





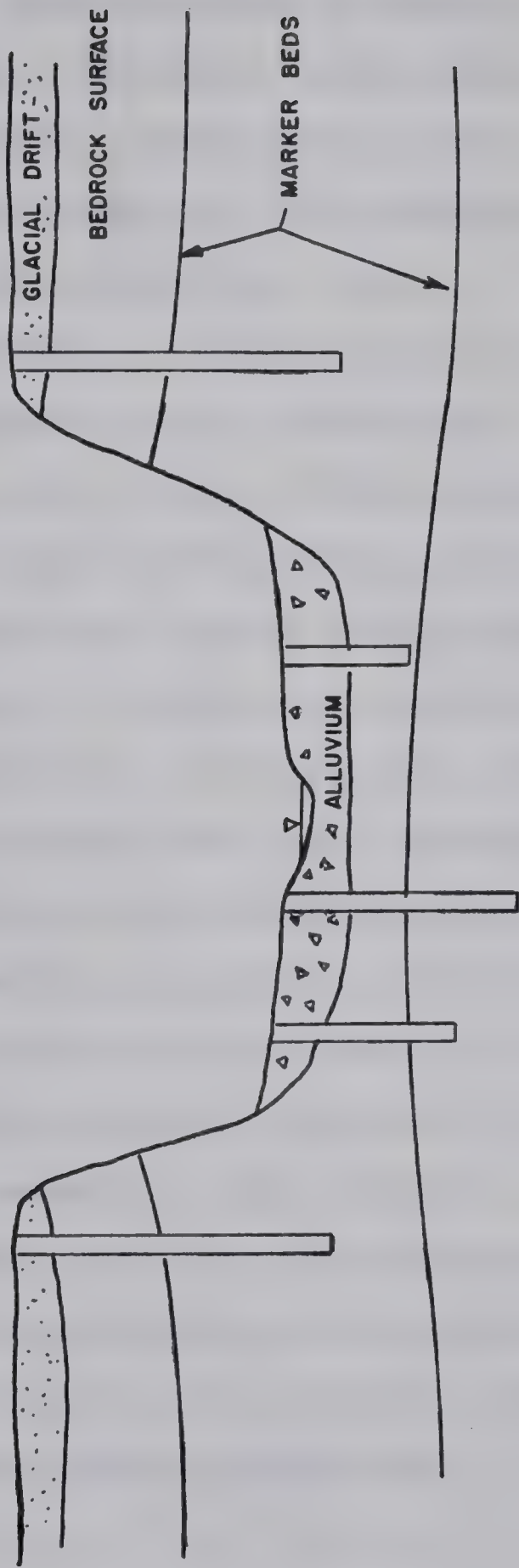


FIG. 3.10 TYPICAL PRELIMINARY DAMSITE DRILLING PROGRAM



below river level. Recovery from valley bottom testholes is often low, as has been discussed in Chapter II, with frequent loss of core. Therefore, cases where a marker bed can be traced over the entire section with reliability are few and cases documenting the entire sequence of valley anticline and valley flexure are rare.

A second factor in evaluating previously compiled stratigraphic sections is the conventional engineering method of plotting the valley profile on a natural scale. Most sections have been plotted using equivalent vertical and horizontal scales or using a slight reduction of horizontal scale - 2 or 3 vertical to 1 horizontal. Thus, a rise in a marker bed of a few feet over a horizontal distance of several hundred feet is not immediately apparent unless one is looking specifically for this feature.

In this section cases where evidence of valley rebound is found in the Cretaceous bedrock of the study area are discussed. The geological section of the valley is given along with details of site location, bedrock type and properties, and details of the drilling program. Sites where evidence is not detailed clearly enough to permit analysis of displacements are included in Appendix A. All sections are viewed looking downstream.

1. Hairy Hill Damsite: Hairy Hill Damsite is located on the North Saskatchewan River some 80 miles downstream of Edmonton, Alberta in Section 12, Township 57, Range 14 West



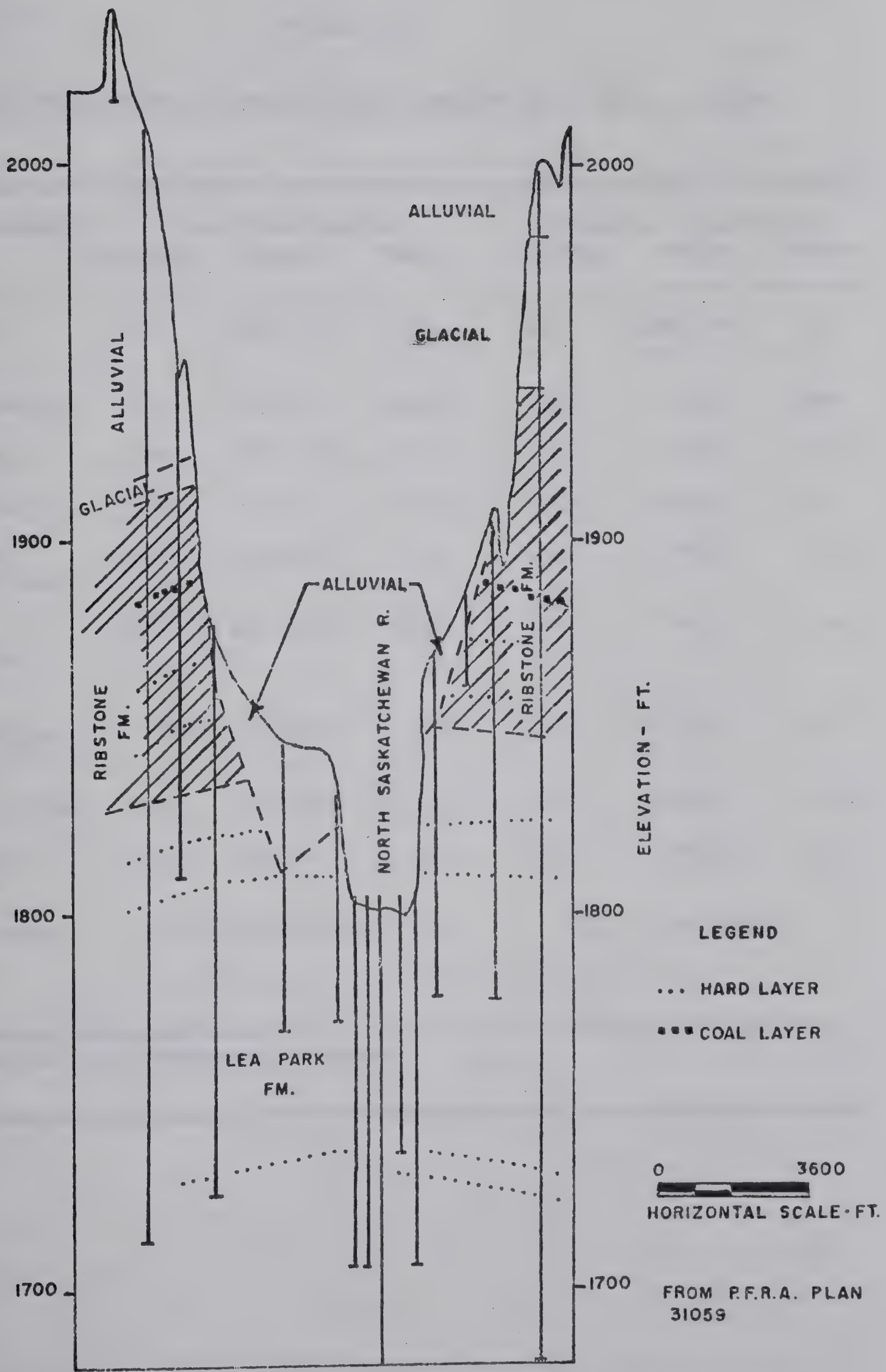


of the 4th Meridian (12-57-14-W4). The site was investigated by the Prairie Farm Rehabilitation Agency (P.F.R.A., 1970b). At the site the valley is about 200 feet deep and about one mile wide at the top. No significant floodplain exists and the river occupies most of the valley floor which is about 900 feet wide. A terrace lies north of the river some 20 to 50 feet above river level and terrace remnants lie south of the river.

Two bedrock formations of Upper Cretaceous age exist at the site. The upper Ribstone formation consists mainly of uncemented to poorly cemented sandstone while the lower Lea Park formation is a grey marine shale with occasional thin carbonaceous sandstone and silt lenses or layers. Layers of very hard calcareous limestone or sandstone, which serve as marker beds, occur in both formations. Correlation of these beds indicates some 6 feet of rebound has occurred in the center of the valley with respect to the upland testholes as shown in Figure 3.11.

Properties of the bedrock at this site are given in Table 3.1. Core recovery in the Ribstone formation averaged 50 to 60 percent whereas in the Lea Park formation an average core recovery of over 90 percent was achieved. In the Ribstone formation less than 25 percent of the core was greater than 4 inches in length; the rock quality designation (RQD) of this formation was 'very poor' (Deere, 1964). In the Lea Park formation the percentage core recovery greater than 4 inches in length ranged from 25 to 50 percent; a RQD





MARKER BED PROFILES - HAIRY HILL DAMSITE

FIGURE 3.11

COURTESY P.F.R.A.





TABLE 3.1

## BEDROCK PROPERTIES AT HAIRY HILL DAMSITE (P.F.R.A., 1970b)

Test or Property	Lea Park Shale			Ribstone Sandstone		
	Average	Range	Tests	Average	Range	Tests
Wet Density p.c.f.	129	118-137	529	124	104-130	155
Water content %	18	11-36	1340	20	7-33	408
Liquid limit	86	51-115	73	23	7-33	16
Plastic limit	21	16-27	73	23	17-33	16
Unconfined strength (p.s.i.)	134	13-427	35	16	1-51	12
Pocket Penetrometer (p.s.i.)	250	40- 250	478	69	7-213	28
Secant modulus (p.s.i. x 10 <sup>3</sup> )*	6.3	1.2-16.7	30	1.1	0.1-3.7	12
% Fines .074 mm.	97	83-100	42	27	10-43	24
% Colloidal .002 mm.	45	25-62	42	10	5-21	14
Activity Ratio	1.41	1.07-1.60	41	.30	0.09-0.67	7

\* Note: Secant modulus taken at 1/3 to 1/2 of ultimate strength in unconfined compression tests.



of "poor".

A horizontal separation along bedding planes between adjacent bedrock types such as sandstone and shale occurred repeatedly in the core. Minor fracturing and jointing with some slickensided surfaces was observed on some of the breaks in the shale core.

Strength testing on 6 inch core samples of Lea Park shale gave peak effective strength parameters from triaxial tests of  $\phi' = 43^\circ$  and  $c' = 0 - 23$  p.s.i. Direct shear tests gave a residual angle of shearing resistance of  $7.5^\circ$  with zero cohesion after 1.0 to 2.0 inches of displacement.

Consolidation tests indicate that the shale is heavily preconsolidated with an estimated preconsolidation pressure of 12.5 to 29 t.s.f. Swelling pressures of 15 to 19 p.s.i. occurred in the shale. The values of secant modulus obtained from unconfined compression tests are smaller than those found for the Bearpaw shale at Gardiner or Travers Dam as shown in Table 3.2.

TABLE 3.2  
SECANT MODULI FROM UNCONFINED COMPRESSION TESTS

Site	Bedrock	E (p.s.i.)	
		Average	Range
Travers Dam	Bearpaw shale	30,000	--
Gardiner Dam	Bearpaw shale	16,500	7,000 - 26,000
Hairy Hill	Lea Park shale	6,300	1,200 - 16,700





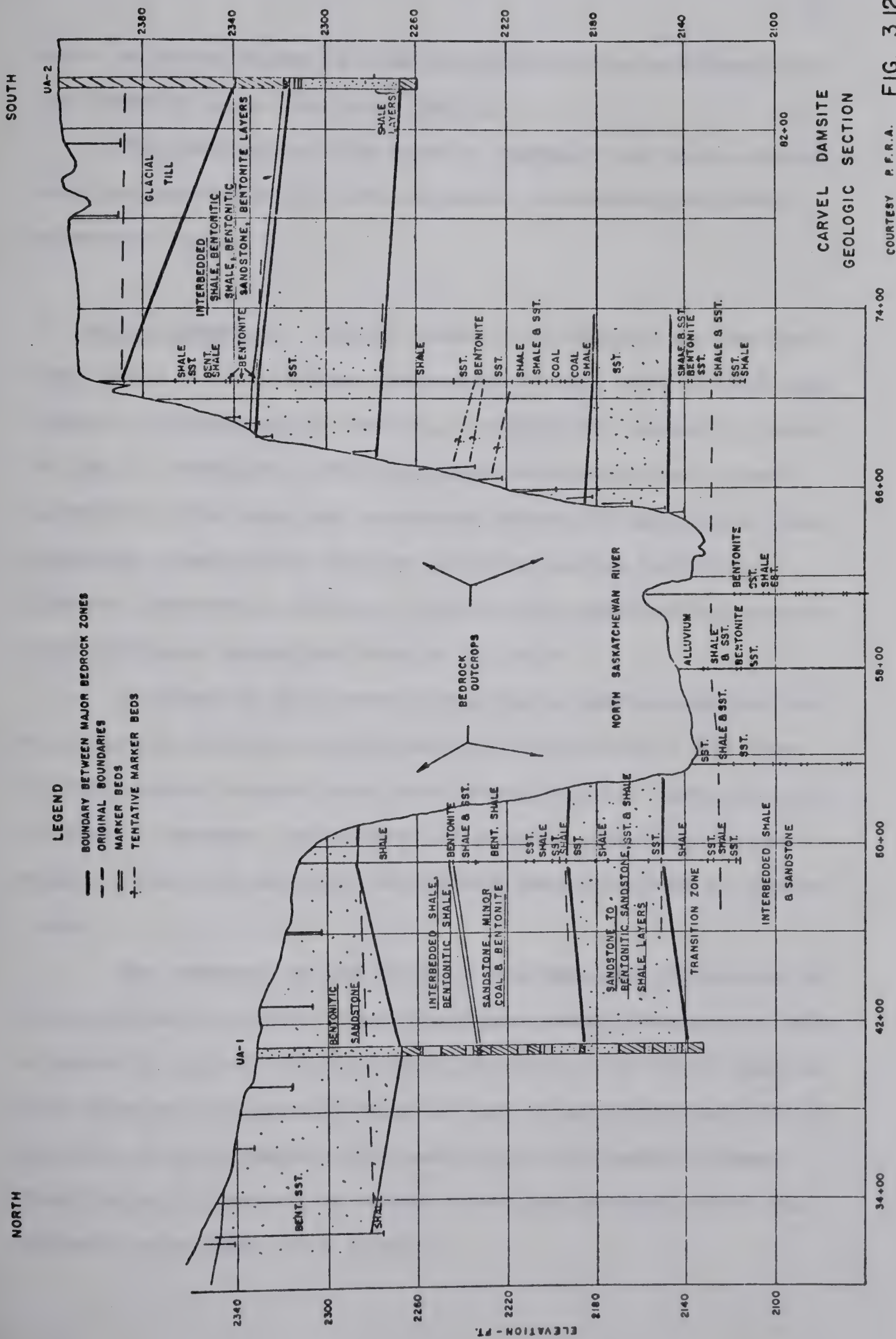
2. Carvel Damsite: Carvel Damsite is located on the North Saskatchewan River about 26 miles southwest of Edmonton, Alberta in Section 34, Township 50, Range 2, West of the 5th Meridian. The site was investigated by the Prairie Farm Rehabilitation Agency (P.F.R.A., 1969b).

The valley at the site is about 280 feet deep and 1800 feet wide at the top. The river occupies most of the valley floor which is about 1100 feet wide.

The bedrock at the site is the Edmonton formation (Upper Cretaceous) consisting of interbedded layers of sandstone, bentonitic sandstone, bentonitic shale, bentonite, sandy shale and coal with some calcareous and ironstone nodules or layers. Bentonite is a prevalent constituent throughout most of the beds. Details of core recovery, bedrock properties and a discussion of slope stability at the site are given in Chapter II of this thesis.

A study of the drilling results obtained by P.F.R.A. indicated that 5 to 6 feet of rebound has occurred below the valley bottom although no distinct marker beds were noted below river level. Two testholes were drilled as part of this thesis to extend the drilling coverage on this site; these testholes are shown as UA-1 and UA-2 on the geologic section, Figure 3.12. These two testholes were drilled about 1000 feet back from the valley edge and show a marked upwarping of the beds towards the river which cannot be explained on the basis of regional dip of the bedrock





COURTESY P.F.R.A. FIG. 3.12





which is about 20 to 40 feet per mile to the southwest in the Edmonton area (Carlson, 1967).

The bedrock at the site is heavily overconsolidated. Swelling pressures of 8 to 22 p.s.i. were obtained from oedometer tests.

3. Ardley Damsite: Ardley Damsite is located on the Red Deer River some 40 miles downstream of the City of Red Deer, Alberta in Sections 20 and 29, Township 38, Range 23, West of the 4th Meridian. The proposed structure has a crest length of 8700 feet and a maximum height of 220 feet. The site was investigated by the Water Resources Division, Alberta Government (A.W.R., 1968) during 1967-68 to supplement previous investigations of P.F.R.A.

A total of 24 diamond drill holes were cored on the site during 1967-68 (1,277 feet of NX core and 1,293 feet of HWF) using conventional double-walled core barrels. A handcut to expose unweathered overburden and bedrock was made in the left abutment about 600 feet upstream of centerline.

The bedrock at the site is the Edmonton formation of Upper Cretaceous age. The strata are nearly horizontal with a westerly dip of about 16 feet per mile. Up to 75 feet of till overlay the bedrock west of the river while only 10 to 15 feet of till mantles the bedrock on the east abutment. Some 10 to 20 feet of alluvial sands and gravels cover the bedrock below the river channel.



A large inactive landslide exists on the right abutment of the site. A soft, apparently remoulded shale was encountered in some drill holes at a depth of 20 feet below the riverbed and this was considered to be "an active zone at the base of the slump."

Shale samples from below the river were found to have a liquid limit of 60-80, a plastic limit of 15-35 and a wet unit weight of 110-140 p.c.f. The natural water content of these shales varied from 20 to 40 percent. Bentonite occurs in seams up to 30 inches thick below the river and has a relatively low strength (pocket penetrometer strengths of about 2 t.s.f.) with liquid limits of 200 - 300, plastic limits 40 - 50 and a natural water content somewhat greater than the plastic limit. Direct shear tests on bentonite samples showed considerable variation but average peak angles of shearing resistance were about  $33^{\circ}$ . Residual angles of shearing resistance averaged  $10^{\circ}$ . Two consolidated-undrained triaxial tests on shale and bentonitic shale samples gave initial tangent moduli of 12,000 p.s.i. and 8400 p.s.i. respectively.

The shale underlying the proposed spillway location on the west abutment had a natural water content of 15 to 20 percent and wet unit weights typically over 135 p.c.f. The higher density and lower water content of the bedrock below the abutments indicates that a considerable amount of rebound has occurred below the valley bottom.





A centerline geologic section showing the testhole logs is shown in Figure 3.13. A study of this section shows an apparent rise of the beds of about 8 feet below the river although correlation of bentonite beds is difficult due to frequent loss of core below the valley bottom.

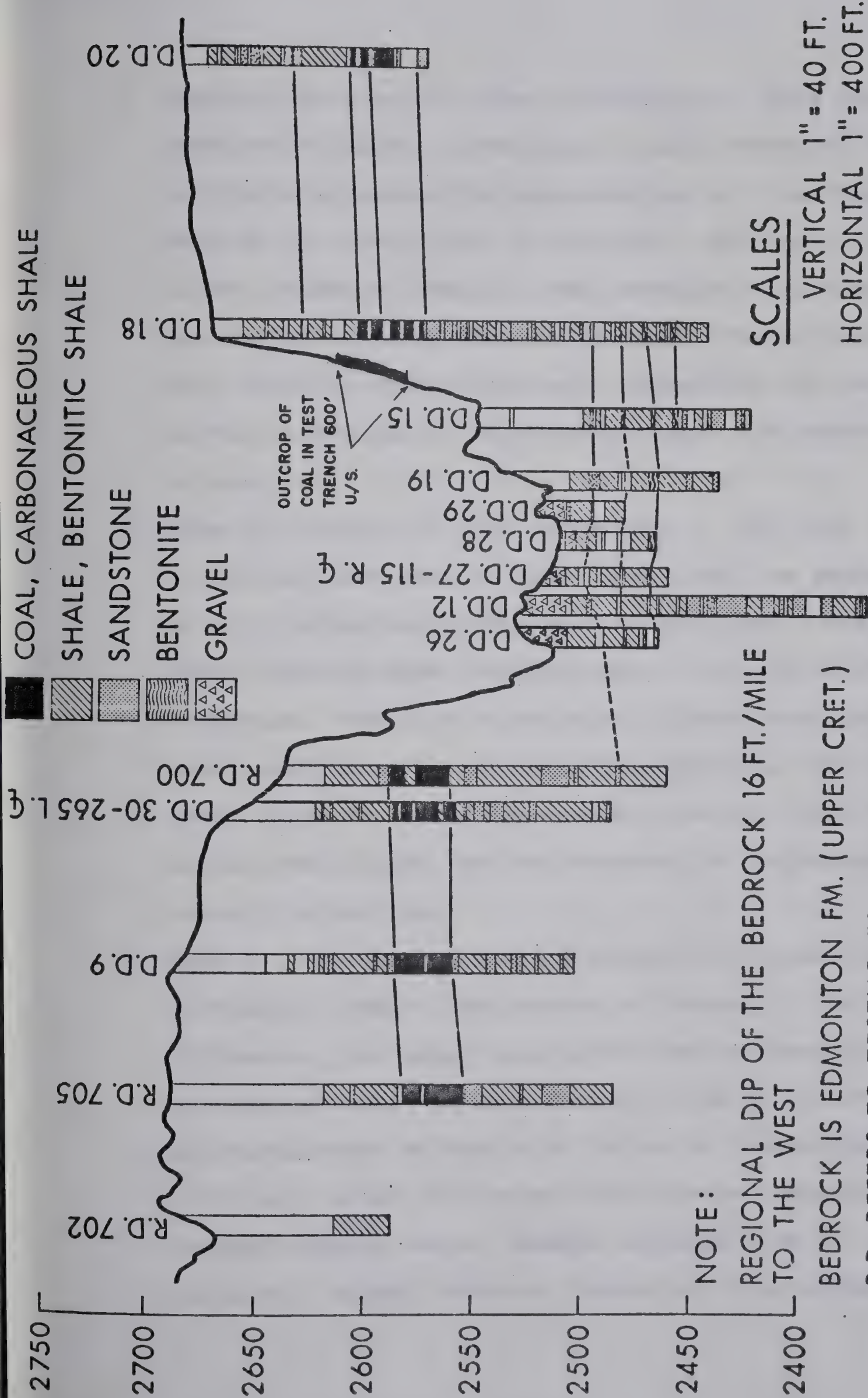
No upwarping of the 20 feet thick Ardley coal seam in the abutments is evident from the testholes until the elevation of the coal outcrop in the abutment trench is plotted on the profile. The bed outcrops about 12 feet above the level predicted from testhole data.

Three 48 inch diameter testpits were drilled into the valley bottom in 1969 to study the bedrock conditions below the valley (Brooker and Associates, 1969). Details of the method are given in Chapter II.

The bedrock was divided into 4 main zones or units on the basis of texture and apparent degree of disturbance. Detailed observations of the rock were made in Testpit 1 only.

1. Zone 1 - 14.5 to 26.5 feet in Testpit 1: The rock consists of disturbed, fractured siltstone which consists of hard pieces in a clay-like matrix. The siltstone is interbedded with soft bentonitic sandstone and thin beds of purer bentonite. Bedrock contacts in the upper portion of this zone rise at between 15 to 25 degrees towards the valley center and strike approximately parallel with the valley thalweg.





ARDLEY DAMSITE  
STRATIGRAPHY & TESTHOLES

FIG. 3.13







2. Zone 2 - 26.6 to 31.5 feet in Testpit 1: This zone consists of black, carbonaceous, badly fractured shale, soft pliable bentonitic sandstone and a 6 inch bentonite seam at the lower limit of the zone. The lower limit of the sandstone exhibits some secondary structure consisting of a blocky fracture pattern. The contacts in this zone are regular and well defined and the nature of the rock exhibits considerably less disturbance than in zone 1.
3. Zone 3 - 31.5 to 44 feet in Testpit 1: The rock is stratified dark grey to black shale with the exception of silty brown shale from 38.5 to 40.5 feet. The black shale exhibits some fissility and is usually hard or very hard. The rock is relatively intact with some units exhibiting a random fracture pattern. The silty brown shale has a dry appearance, crumbles readily between the fingers and was observed to disintegrate rapidly on wetting.
4. Zone 4: The three arbitrary bedrock divisions observed in Testpit 1 were also present in Testpit 3. At Testpit 2, however, the upper zone identified as lumpy siltstone was not present. In both Testpit 2 and 3 a fourth zone was encountered at depths of 24 and 36 feet respectively. This unit, which lies below intact shale, consists of crushed organic shale. Blocks obtained from the auger had a dry, crumbly texture consisting of an unconsolidated



matrix containing hard black particles with shiny, slick surfaces.

The stratigraphic section obtained from correlating testhole information with results of the large diameter testpits is shown in Figure 3.14. A single anticlinal rise of the beds towards the valley center of about 12 feet occurs; this value is a minimum for the amount of rebound occurring at the site as a considerable amount of rebound would occur immediately below the edge of the valley, outside the area shown in Figure 3.14.

4. James MacDonald Bridge, Edmonton, Alberta: The James MacDonald bridge was constructed across the North Saskatchewan River in downtown Edmonton, Alberta during 1970-71. The foundation investigation was conducted by R.M. Hardy and Associates Ltd. of Edmonton, Alberta.

The river lies in a valley about 200 feet deep and 3/4 mile wide at the site. In the valley bottom the river has carved a channel about 50 feet deep and 600 feet wide through the alluvial floodplains which cover the floor of the valley.

The bedrock at the site is the Edmonton formation (Upper Cretaceous) consisting of sandstone, shale, carbonaceous shale and coal layers. Most of the bedrock is hard with pocket penetrometer strengths in excess of 4.5 t.s.f.; some softening of the upper few feet of the shale has occurred with pocket penetrometer strengths as low as 3





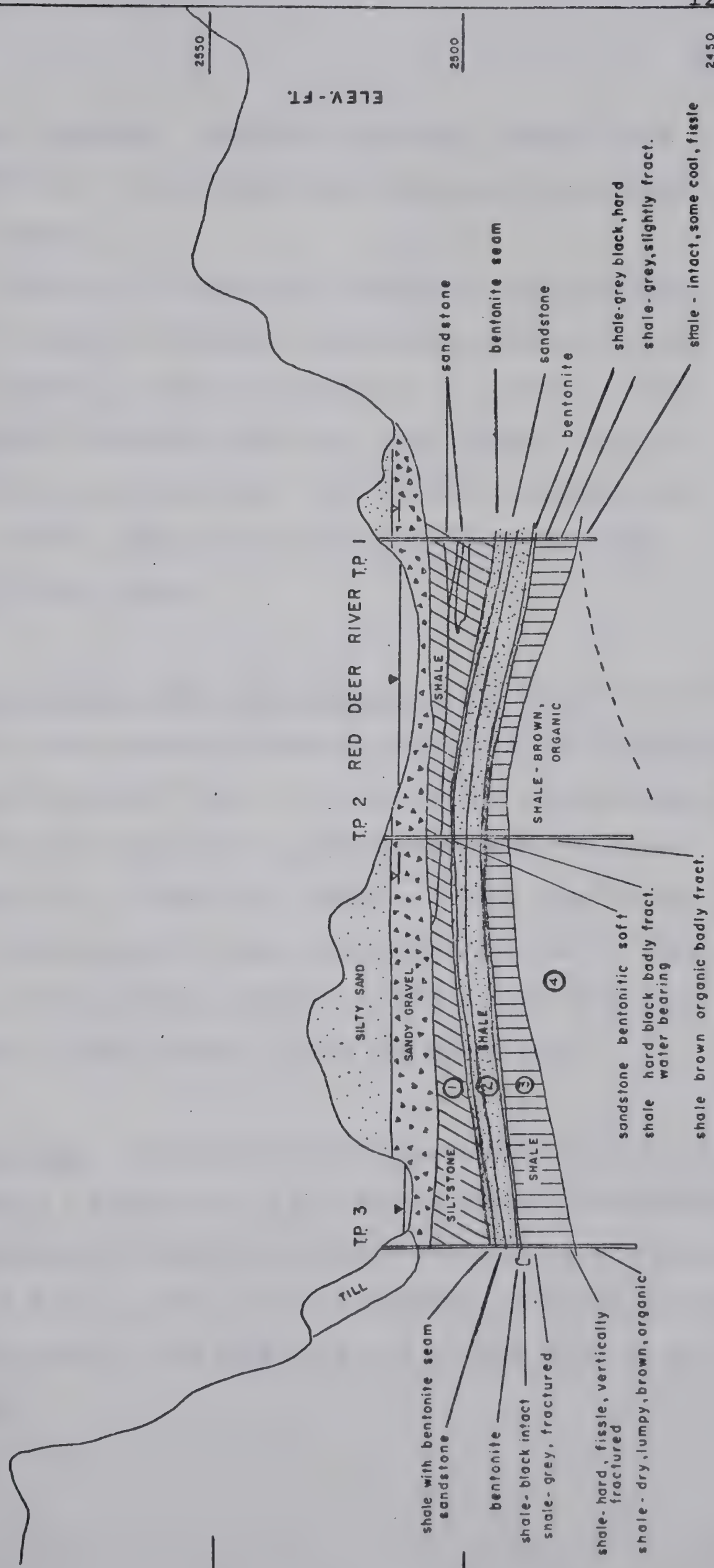
2600

2550

2500

2450

ELEV.-FT.



NOTE: TRACED FROM E.W. BROOKER & ASSOC. PLAN E-86-A-2

(1)-(4) ARBITRARY BEDROCK ZONES

HORIZONTAL SCALE- FT.

0 50 100 150

ARDLEY DAMSITE

STRATIGRAPHIC SECTION FROM  
LARGE DIAMETER TESTPITS

FIG. 3.14



t.s.f. being recorded. Swelling pressures ranging from 0.19 to 0.37 t.s.f. were found from oedometer tests made on 4 core samples.

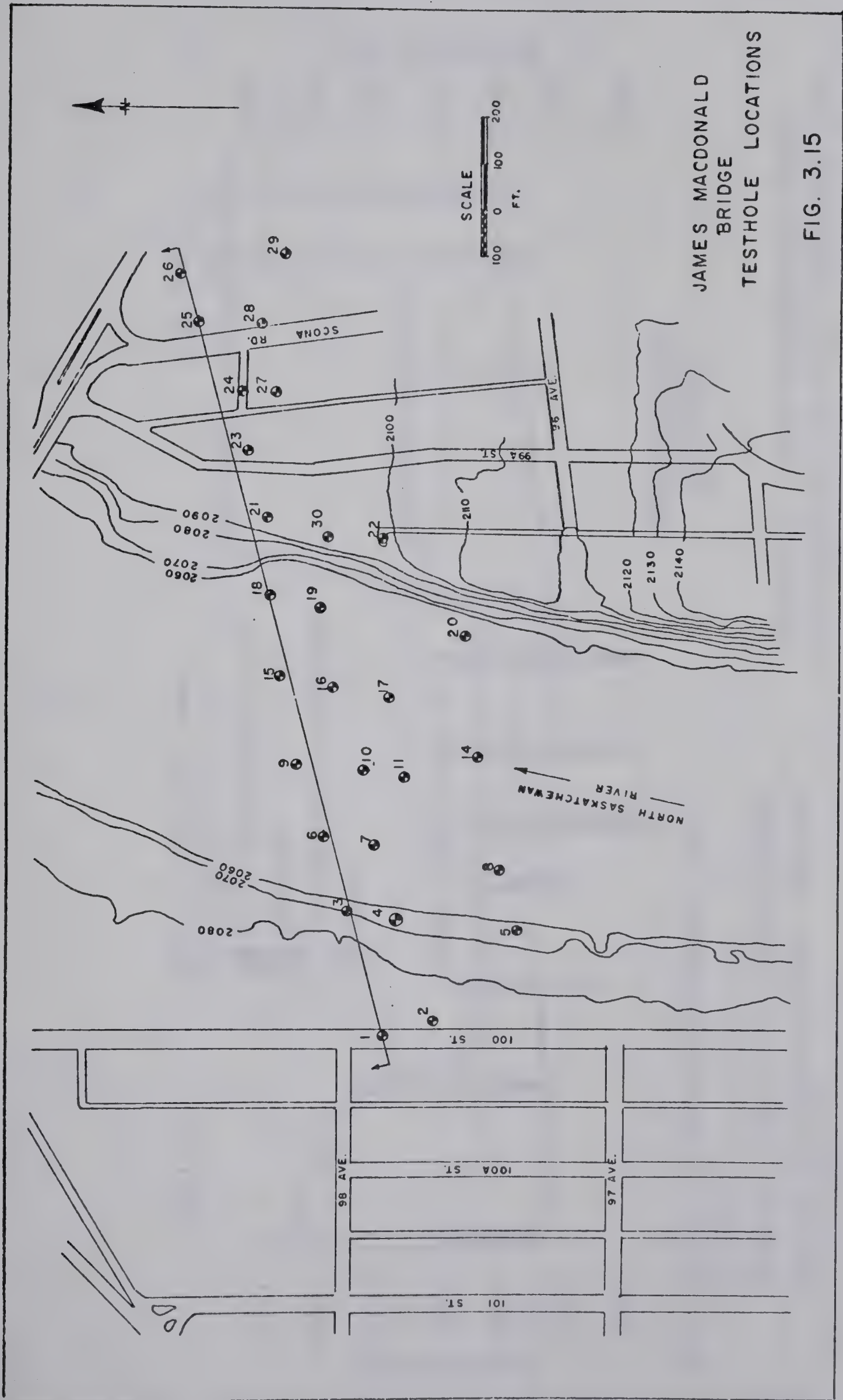
The location of testholes drilled on this project are shown in Figure 3.15 and a centerline profile across the river channel is shown in Figure 3.16. About 4 feet of differential rebound across the river channel can be observed by tracing coal beds. The section includes only the river channel and rebound below the floodplain and valley wall is not shown.

5. Capilano Bridge, Edmonton, Alberta: The Capilano bridge is located in east-central Edmonton several miles downstream of the James MacDonald site. The centerline stratigraphic section shown in Figure 3.17, provided by Reid, Crowther and Partners Ltd. of Edmonton, shows a 4 foot rise in an upper coal bed located 10 feet below the river bed. This anticlinal flexure is not evident in two deeper coal beds located about 60 and 80 feet below the river bed.

6. Boundary Dam: Boundary Dam was constructed by P.F.R.A. on Long Creek, a tributary of the Souris River, approximately 3 miles southwest of Estevan, Saskatchewan during the period 1956-1958 (P.F.R.A. 1956a, P.F.R.A. 1959a). The dam is an earthfill structure 1100 feet long and 95 feet high at maximum section.



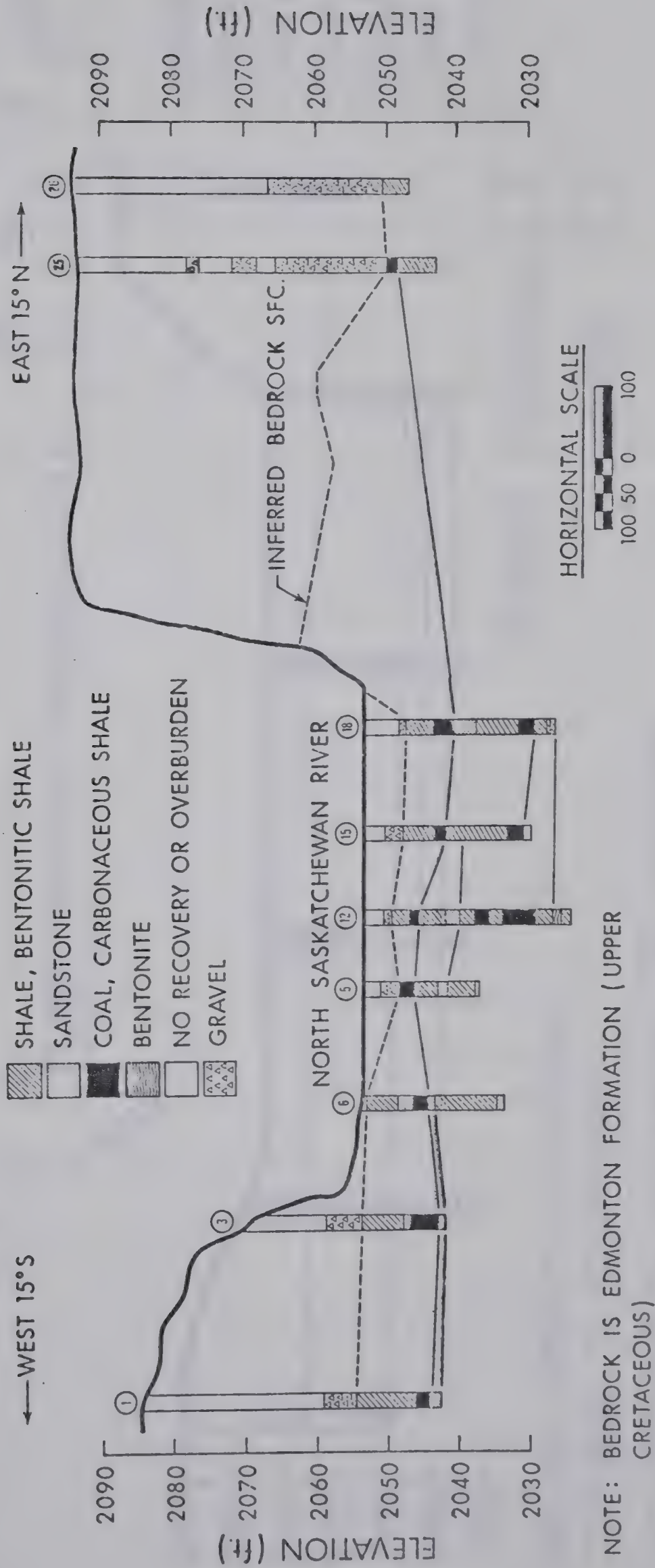




JAMES MACDONALD  
BRIDGE  
TESTHOLE LOCATIONS

FIG. 3.15





NOTE: BEDROCK IS EDMONTON FORMATION (UPPER CRETACEOUS)

ELEVATIONS FROM CITY OF EDMONTON DATUM  
REGIONAL DIP OF BEDROCK APPROX. 20FT./MILE  
TO THE SOUTHWEST

PROPOSED JAMES MACDONALD BRIDGE  
VALLEY BOTTOM PROFILE & TESTHOLES LOGS

FIG. 3.16





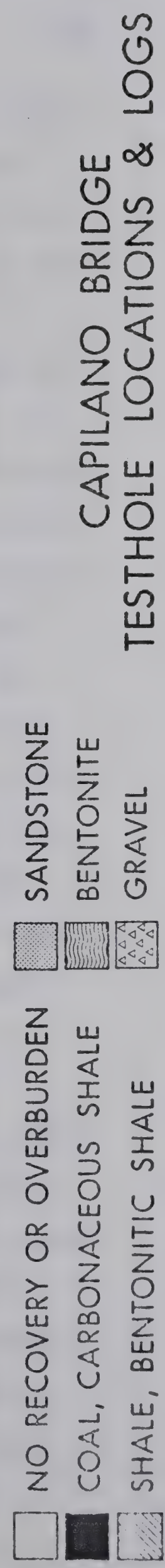
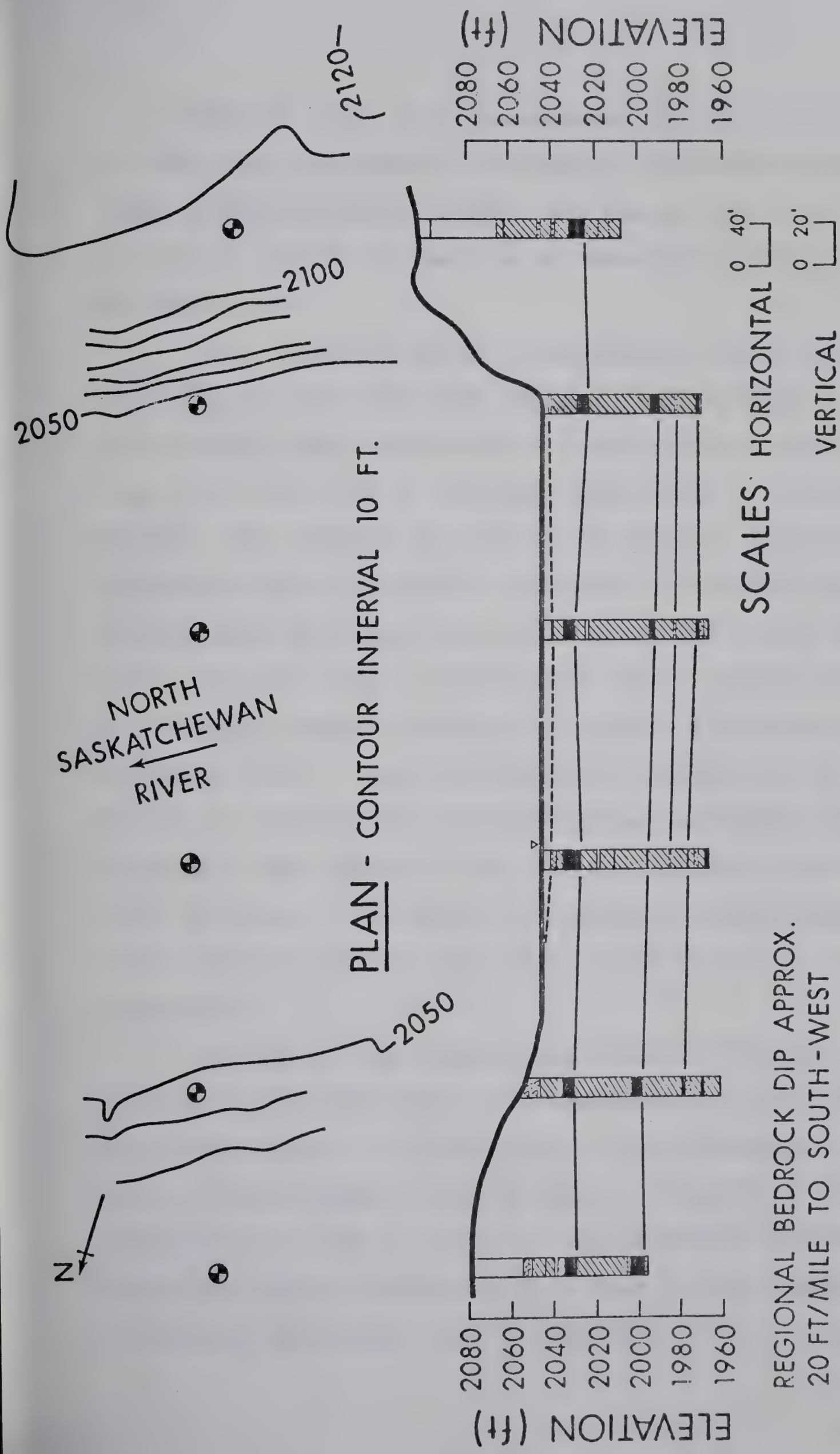


FIG. 3.17

CAPILANO BRIDGE  
TESTHOLE LOCATIONS & LOGS



Several sites were investigated in a 10 mile reach of Long Creek upstream of its junction with the Souris River in the preceding decade. The dam was built on Site 4; a geologic section of the site is contained in Chapter II as Figure 2.24.

Long Creek has carved a postglacial valley some 90 feet deep and 1000 feet wide through a thin veneer of glacial deposits and bedrock of the Tertiary Ravenscrag Formation (the equivalent of the Fort Union Group in the United States). The bedrock is composed of sandy to clayey shales, siltstones and fine-grained sandstones of Tertiary age. Several beds of lignite coal occur along the valley and serve as marker beds. The beds are poorly lithified and more closely resemble partially indurated fine sands, silts and sandy clays. A preliminary geology report on the site (P.F.R.A., 1955) states "stratification is erratic and individual beds appear to dip abruptly and pinch out over short distances - the result of current channelling and later infilling during times of sediment deposition in freshwater."

A study of the stratigraphy at Site 4 (Figure 2.24) shows a considerable amount of rebound has occurred below the valley bottom. A series of coal beds present at elevation 1730-1740 shows a rise of about 10 feet below the valley bottom. The coal zone in the abutments (elevation 1790-1800) shows a rise of 8 to 10 feet in the immediate vicinity of the valley wall on both sides of the valley.





The bedrock surface on either side of the valley rises 5 to 8 feet within 100 feet of the valley edge although no surface expression of the flexure occurs.

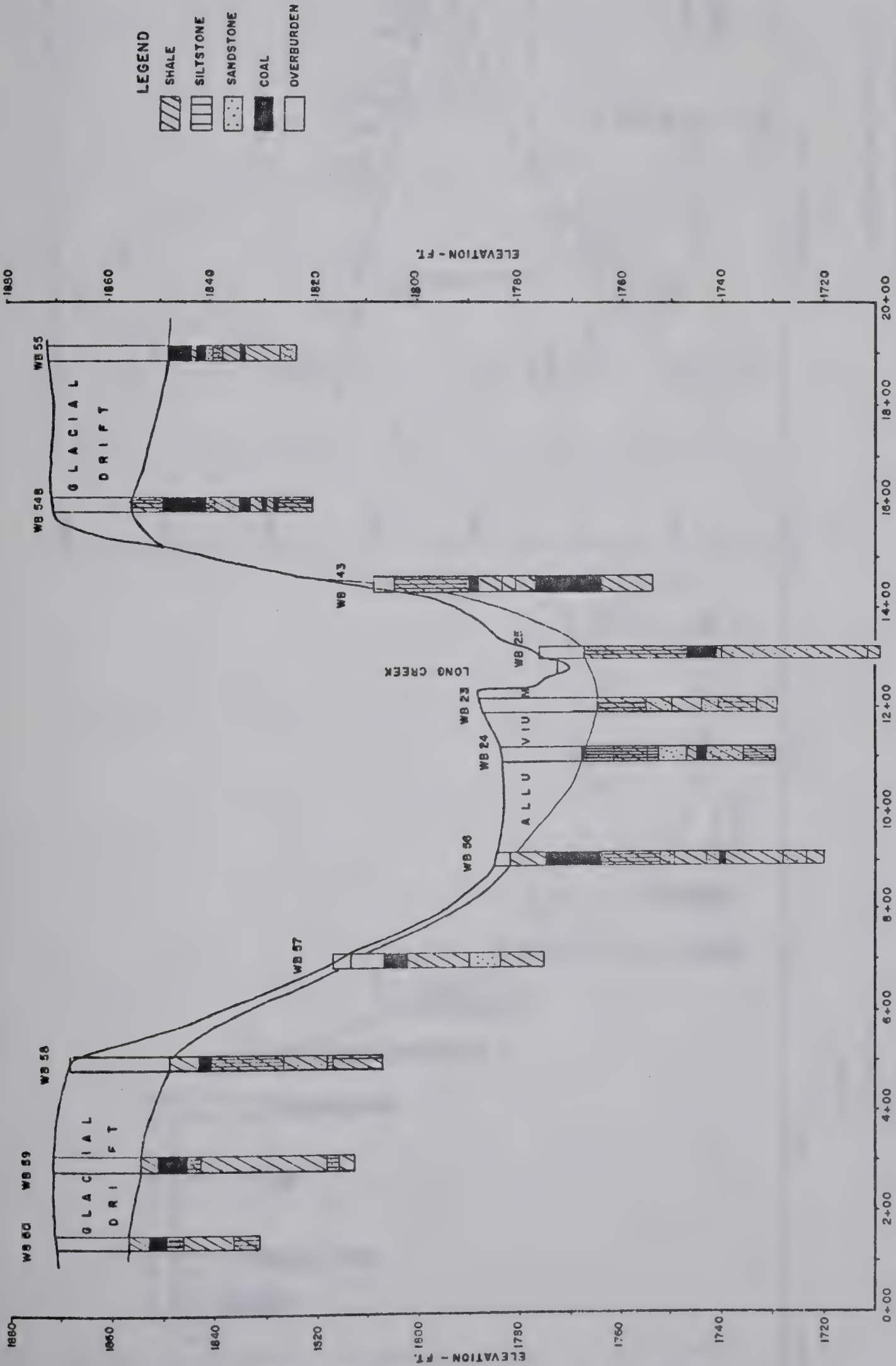
Thus evidence of both a valley anticline and valley flexure is present at this site. No raised valley rim exists at this site although evidence of it is found in behaviour of the bedrock surface. Surface expression of this feature may have been removed by erosion.

Similar behaviour of the bedrock occurs at Site 2 located some 5 miles upstream in Section 28, Township 1, Range 8, West of the 2nd Meridian as shown in Figure 3.18. Rebound of at least 4 feet has occurred below the river valley as evidenced by alluvial removal by the stream of most of the lower coal seam (elevation 1760-1775). Coal is present below the toe of slope on both sides of the valley in testholes WB56 and WB43 and the bottom of the coal is at approximately elevation 1763. The three testholes in the valley bottom (WB24, WB23 and WB25) show the bottom of the coal at, or above, elevation 1767.

The spillway testholes at this site, as shown in Figure 3.19, show the same behaviour between testholes WB66 and WB67 with about 5 feet of rebound occurring over a horizontal distance of 100 feet.

The physical properties of the Ravenscrag formation are shown in Table 3.3. No values of E are reported for the bedrock but, in view of the low unconfined strengths, the bedrock should have a low modulus of elasticity.



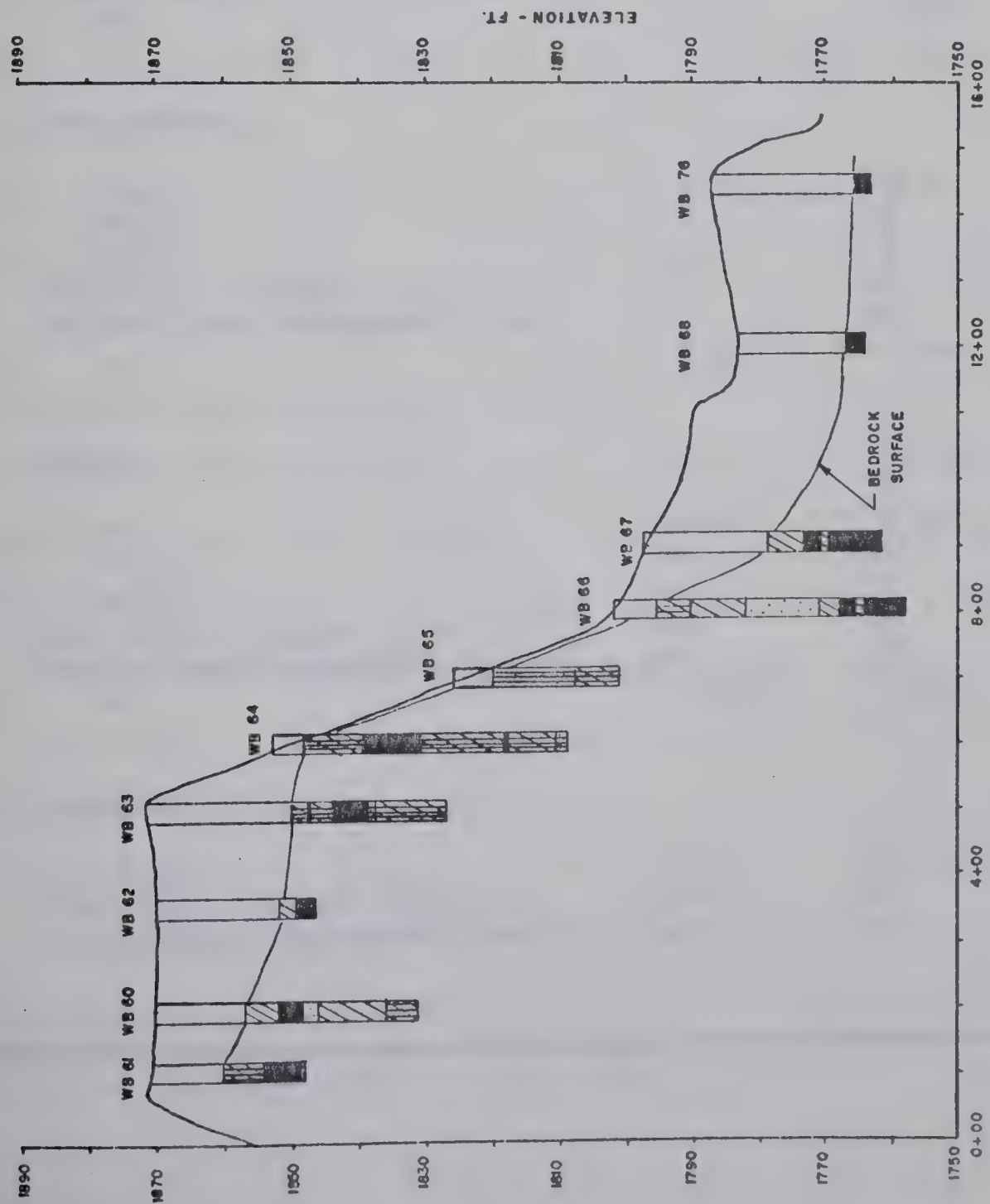
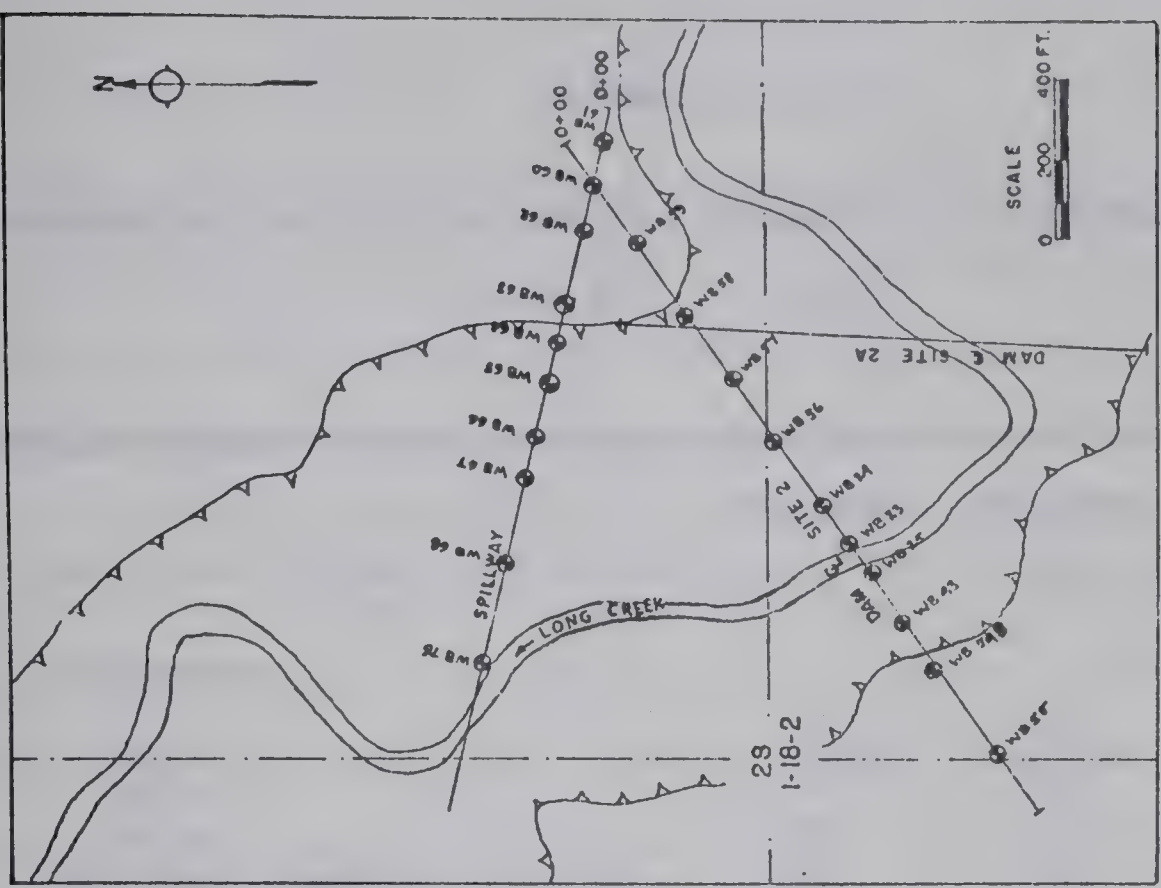


BOUNDARY DAM SITE 2  
GEOLOGIC PROFILE  
COURTESY P. F. R. A.

FIG. 3.18







BOUNDARY DAM SITE 2  
LOCATION PLAN & SPILLWAY SECTION

COURTESY P.F.R.A.

FIG. 3.19



TABLE 3.3

PROPERTIES OF THE RAVENSCRAG FORMATION AT BOUNDARY DAM  
(P.F.R.A., 1956a)

	Maximum	Minimum	Average
1. Siltstone			
W <sub>n</sub> %	30.8	14.6	22.4
W <sub>L</sub> %	173	111	135
W <sub>p</sub> %	29	19	25
Dry unit weight (p.c.f.)	111	83	99
Unconfined strength (p.s.i.)	160	31	80
e	1.15	0.63	0.77
2. Sandstone			
W <sub>n</sub> %	23.9	17.8	20.5
W <sub>L</sub> %	96	58	76
W <sub>p</sub> %	20	19	20
Dry unit weight (p.c.f.)	102	92	98
Unconfined strength (p.s.i.)	113	65	86
e	0.83	0.49	0.69
3. Shale			
W <sub>n</sub> %	39.2	9.4	23.0
W <sub>L</sub> %	180	106	134
W <sub>p</sub> %	29	22	24
Dry unit weight (p.c.f.)	108	85	98
Unconfined strength (p.s.i.)	176	53	97
e	0.93	0.56	0.71
4. Lignite Coal			
W <sub>n</sub> %	53.2	10.3	30.3
Dry unit weight (p.c.f.)	78	60	68
Unconfined strength (p.s.i.)	112	16	54





Confirmation of the upward flexure of the beds in the valley wall due to valley bottom rebound is given in Plates 2.1 and 2.2 in Chapter II. These views of the east core trench at the dam show a distinct rise in the coal seams towards the valley.

Indirect evidence on the effects of lateral stress relief was observed in the cutoff trenches excavated into the valley walls. The coal seams and bedrock above the coal seams were generally observed to be weathered and fissured adjacent to the valley sides, however the condition improved with distance into the abutments. The coal seams and bedrock at the farthest point of penetration of the cutoff (about 1200 ft. back from the valley wall) appeared quite impervious although jointing of the coal and bedrock was still in evidence (P.F.R.A., 1959a).

7. Rocky Mountain House, Site A: Rocky Mountain House Damsite A was investigated by Whitmore and Associates Ltd. (1968) for the Water Resources Division, Alberta Government. The site is located on the North Saskatchewan River in Sections 7, 8 and 12, Township 40, Range 7, West of the 5th Meridian. The North Saskatchewan River flows north at the site through a valley about 120 feet deep and 2 miles across.

The bedrock at the site is the Paskapoo formation (Tertiary). The area lies close to the center of the Alberta syncline where strata are flat lying or have dips



of a few to a few tens of feet per mile. The closest known faulting, marking the eastern edge of the disturbed belt of the foothills, lies in Section 19, Township 39, Range 8; more than 8 miles west of Rocky Mountain House.

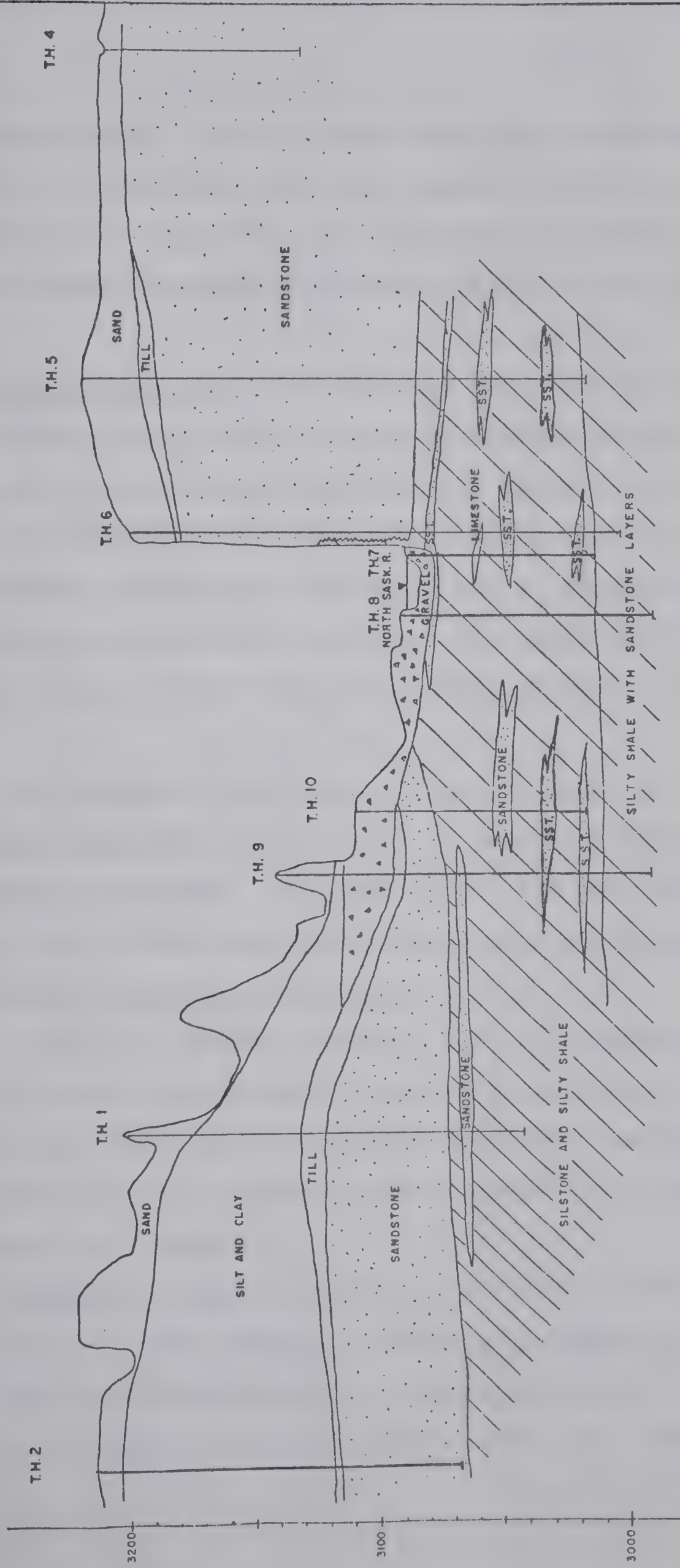
The bedrock can be divided into two units: an upper sandstone unit of up to 103 feet in thickness and a lower unit consisting of siltstones, lenses of silty shale, sandstones and conglomerate. A centerline geologic section is shown in Figure 3.20. No continuous marker beds were identified at this site, however, a thin band of limestone was found in testholes 6 and 7. The limestone occurred some 2 feet higher in testhole 7, below the riverbed, than in testhole 6 below the east abutment. The bottom contact of the sandstone shows a rise towards the valley center. The base of the sandstone unit outcrops some 37 feet above the level found from the testholes. This feature may be due to a fault or to unusual depositional environment at the time of deposition. However, all features at the site point to a considerable, although indeterminate, amount of rebound as having occurred.

Some of the shale cores from the lower bedrock unit had shiny, smooth slickensided surfaces. Joints in the cores from the sandstone members of the bottom unit were scarce and no slickensides were observed.

No strength testing on bedrock samples from this site was reported. However, work at another damsite in the Paskapoo formation, located on the McLeod river some 15 miles south of Whitecourt, Alberta (Lockwood Survey







NOTE: BEDROCK IS PASKAPOO FM. (TERTIARY)  
 : TRACED FROM WHITMORE & ASSOC. (1968)  
 DWG. 19A

SCALES  
 VERT. 0 20'  
 0 400'  
 HORIZ.

CENTERLINE STRATIGRAPHIC  
 SECTION - ROCKY MOUNTAIN HOUSE  
 DAMSITE A

FIG. 3.20



Corporation, 1967), found average unconfined compressive strengths for sandstone and shale samples of 2430 p.s.i. and 3770 p.s.i. respectively. Consolidation tests on shale samples yielded swelling pressures from 9.5 to 28 t.s.f.

8. St. Mary River Dam: The St. Mary River Dam was constructed on the St. Mary River in southern Alberta during 1946-1951 by the Prairie Farm Rehabilitation Agency (P.F.R.A., 1961). The dam is located about 5 miles northwest of Spring Coulee, Alberta in Sections 1 and 2, Township 5, Range 24, West of the 4th Meridian. The earthfill dam has a crest length of 2530 feet and a maximum height of 193 feet.

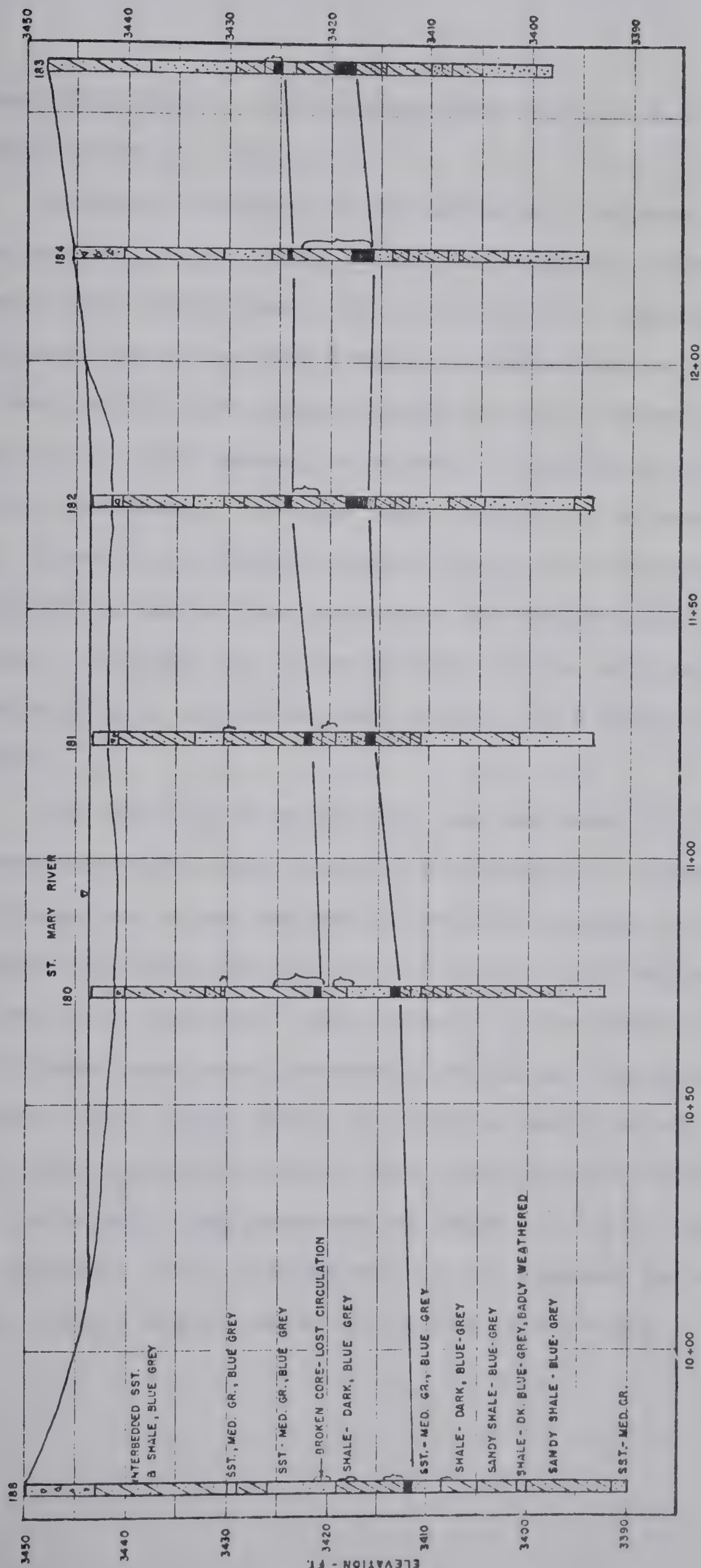
The bedrock at the site is the non-marine St. Mary formation (Upper Cretaceous) which is contemporaneous with the Edmonton formation. The beds dip to the west at approximately 1 to 2.5 feet per 100 feet and consist of interbedded sandy shales and clayey sandstones.

A geologic section through a line of testholes drilled 700 feet downstream of centerline is shown in Figure 3.21. Two layers of carbonaceous shale serve as marker beds and show a gentle rise of about 1 or 2 feet below the river channel.

Unconfined compression tests conducted on core samples (P.F.R.A., 1945) showed an average strength of 2010 p.s.i. and an average modulus of elasticity of  $1.0 \times 10^6$  p.s.i. with a range from 0.2 to  $3.8 \times 10^6$  p.s.i. Measured







ST. MARY DAM  
GEOLOGIC SECTION - 700 FT.  
DOWNSTREAM OF CENTERLINE

COURTESY - P. F. R. A.

FIG. 3.21



values of Poisson's ratio ranged from 0.02 to 0.4 with an average value of 0.128.

Indirect evidence of the effects of stress relief were present in the condition of the bedrock in the diversion tunnels and cutoff trench (P.F.R.A., 1961). Entrance and exit excavations for the diversion tunnel had to be carried 150 feet and 50 feet respectively into the exposed bedrock before rock sound enough to tunnel in was found. The first 220 feet of tunnel from the inlet had to be supported with steel I beams and wooden lagging due to the weathered and fractured nature of the rock near the valley wall. By comparison, only the top 10 to 20 feet of the vertical control tower shaft was fractured badly enough to require timber support.

The key trench at the dam was cut about 10 feet into bedrock below the river channel by blasting. Seepage into the trench was along horizontal bedding planes. It was observed the rock was extremely fractured and broken up. The resulting surfaces, particularly in the harder sandstone formations, were extremely jagged and contained numerous large voids along the bedding and fracture planes which often extended several feet into the formation. In many instances, displacements of large blocks of rock were also evident. This disturbance of the bedrock below the river channel was believed to be due to blasting.





9. Fort Peck Dam: The experience of the U.S. Army Corps of Engineers with the Bearpaw formation at Fort Peck Dam has been discussed in Chapter II. No complete stratigraphic section of the site has been published, however, a center-line section along the spillway published by Fleming et al. (1970) is shown in Figure 3.22. A rise of the 'G' bentonite layer is broken by numerous steeply-dipping faults which are considered to be due to massive slumping (Fleming et al., 1970).

The rise in the bentonite layer is not a depositional feature due to the flat-lying nature of the bedrock in the area. It appears unlikely that all of the rise in elevation of the bentonite layer is due to landslide activity as the dominant mode of slope failure in the study area is translational. The rise in elevation of the bentonite bed is consistent with the mechanism of vertical rebound due to stress relief - only the magnitude of the rebound appears anomalous.

10. Garrison Dam: The 6 or 7 feet of rebound which has occurred in the Fort Union Group below the Missouri River valley at Garrison Dam is discussed in Chapter II. The logs of the two testholes illustrating this feature are given in Figure 3.23. The amount of rebound below the valley bottom, given by Smith and Redlinger (1953), is the difference in elevation between coal beds in these two testholes; a considerably larger value of rebound has









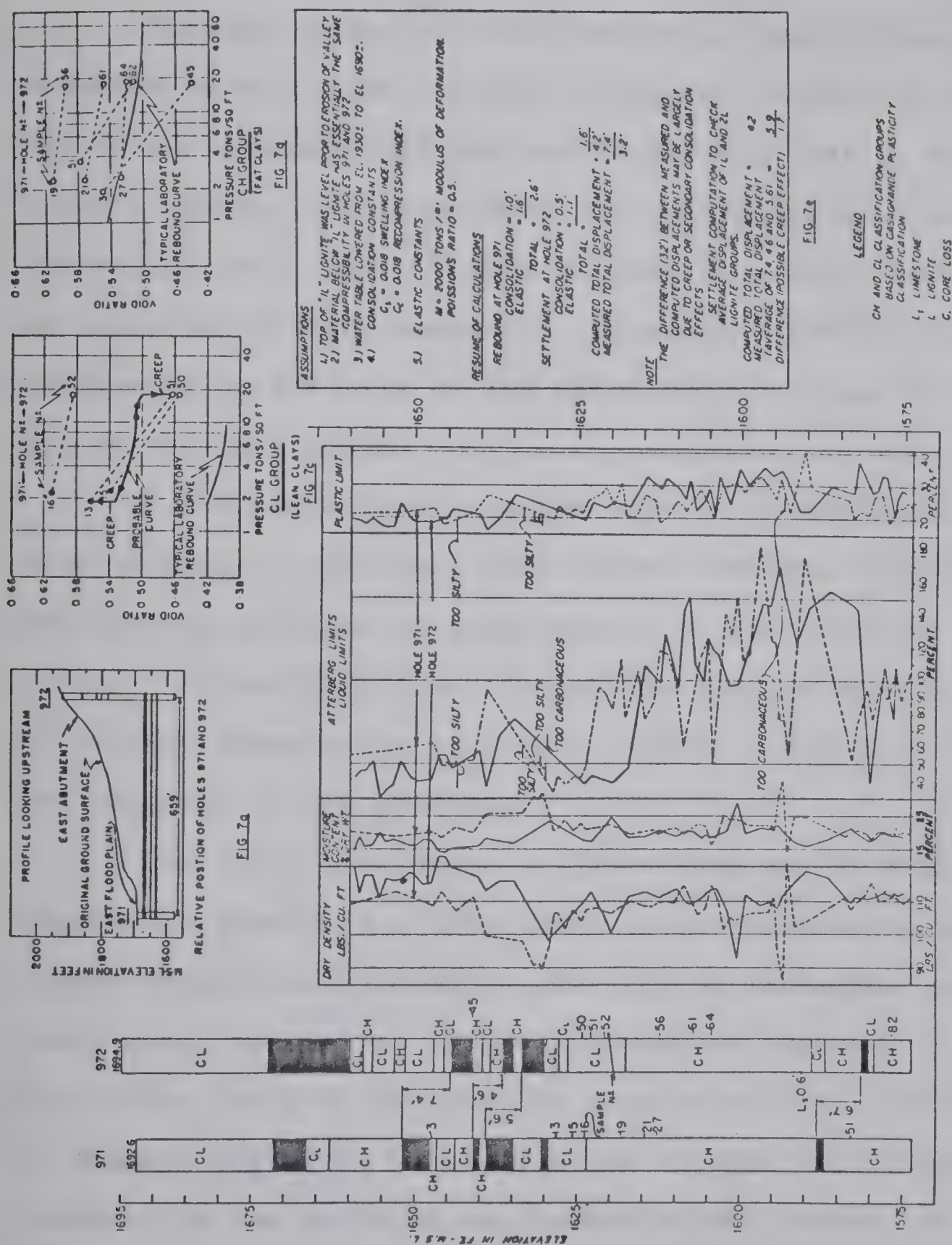


FIG. 3.23 REBOUND OBSERVATIONS AND CALCULATIONS, EAST ABUTMENT OF GARRISON DAM ( FLEMING ET AL., 1970 )



probably occurred as no data is available on the behaviour of the beds between testhole 971, at the toe of valley wall, and the valley center.

Further evidence of the amount of rebound which has occurred at this site is given in Figure 3.24 which shows the centerline geologic section (U.S.C.E., 1946). No single lignite bed can be traced over the entire distance across the valley but a rise of some 20 feet in lignite beds can be observed in both abutments. Since no evidence exists of old landslide activity at the site, the rise can only be due to valley flexure.

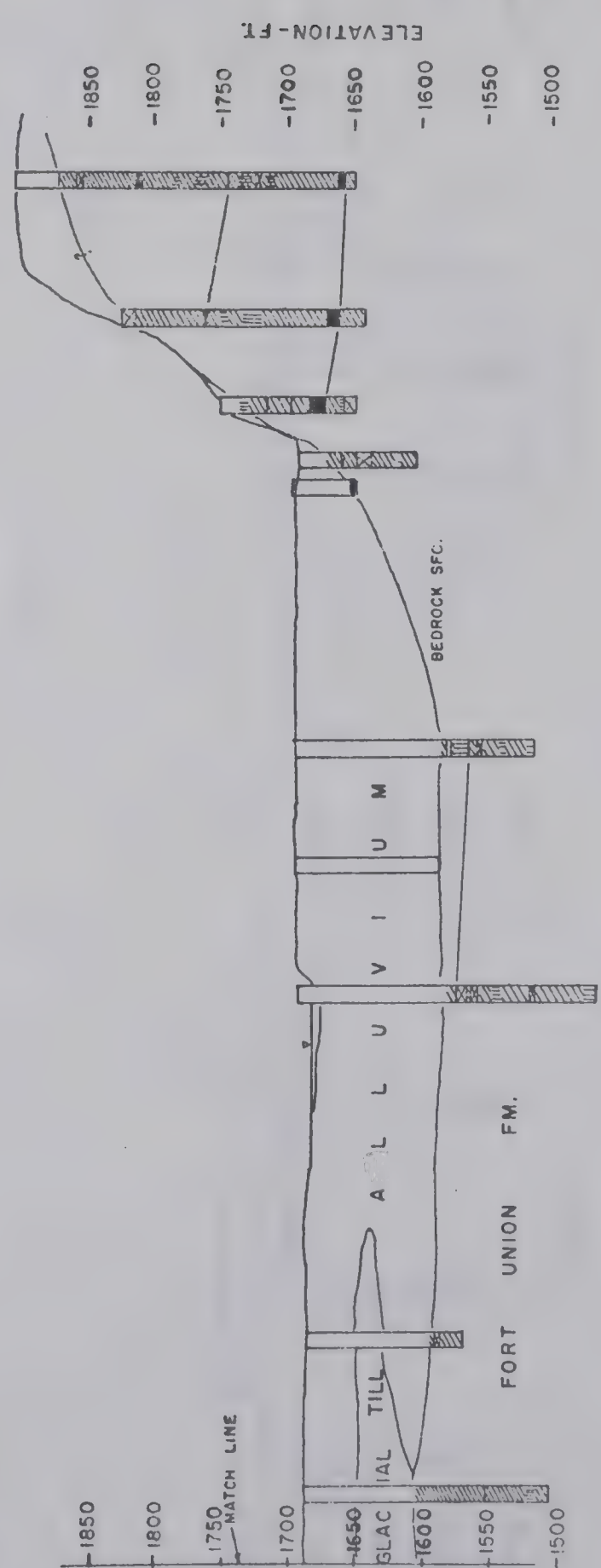
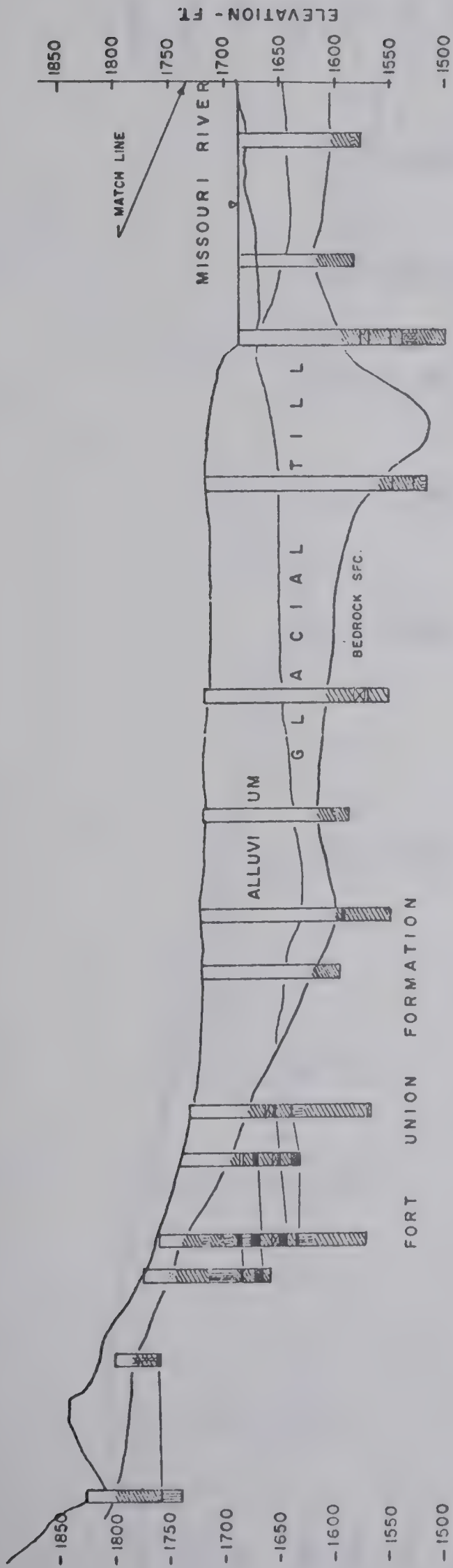
A similar rise of lignite beds in the abutment can be seen in Figure 3.25 where the geologic section of the spillway and two profiles at right angles to the spillway are given. A clearly defined rise of the lignite beds of close to 30 feet towards the valley is visible. Figure 3.26 gives the location of the profiles.

The Fort Union Group is flat-lying and it does not appear the upwarping of the beds can be ascribed to depositional environment, tectonic activity or landslide activity. Local minor structural irregularities are reported in the Fort Union Group at the site by Fleming et al., (1970) but it appears difficult to explain the uniform valley flexure observed on the basis of any mechanism but rebound of the bedrock due to valley formation.

The properties of the Fort Union Group have been previously discussed in Chapter II. The bedrock exhibits







**LEGEND**

- LIGNITE
- SILTSTONE OR SILT
- NO RECOVERY
- CLAY OR CLAYSTONE

HORIZONTAL SCALE (FT.) 0 300

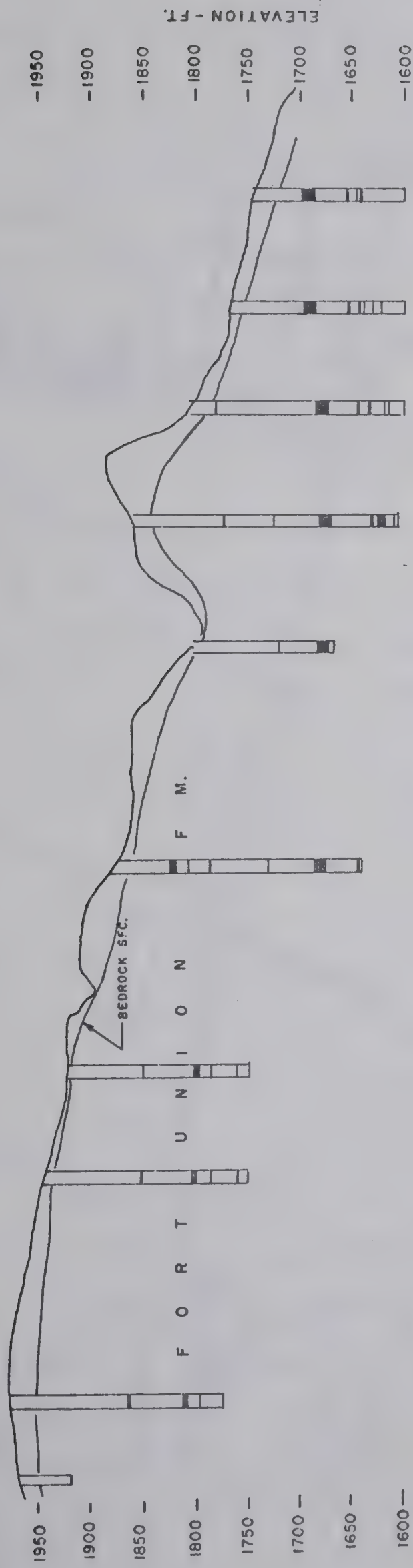
NOTE - ONLY LIGNITE SEAMS THICKER THAN 6 INCH SHOWN

GARRISON DAM  
GEOLOGIC SECTION  
PARALLEL TO DAM AXIS

COURTESY - U.S. ARMY CORPS OF ENGINEERS

FIG. 3.24

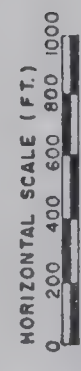




LEGEND

■ LIGNITE

NOTE - ONLY LIGNITE SEAMS THICKER THAN 6 INCHES SHOWN



GARRISON DAM  
SPILLWAY GEOLOGIC SECTIONS  
SHOWING MAJOR LIGNITE SEAMS

COURTESY - U.S. ARMY CORPS OF ENGINEERS

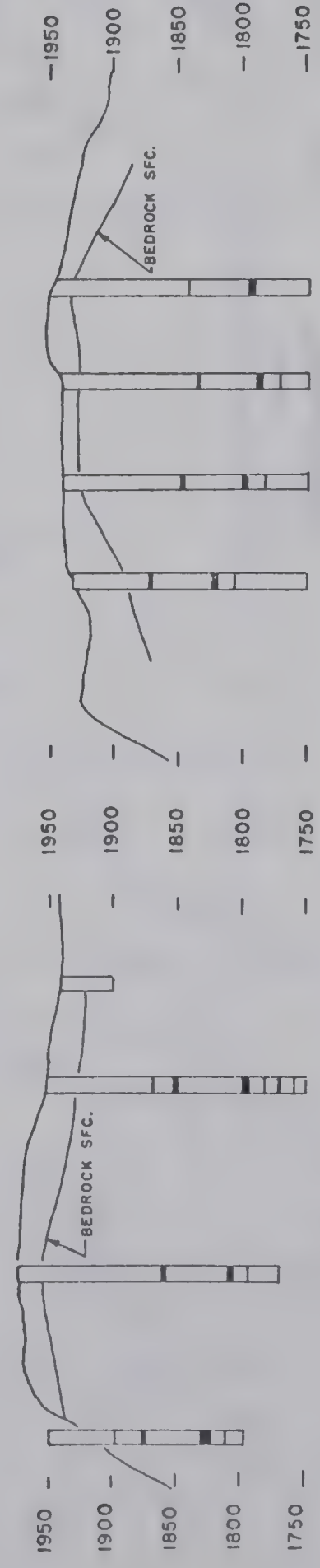
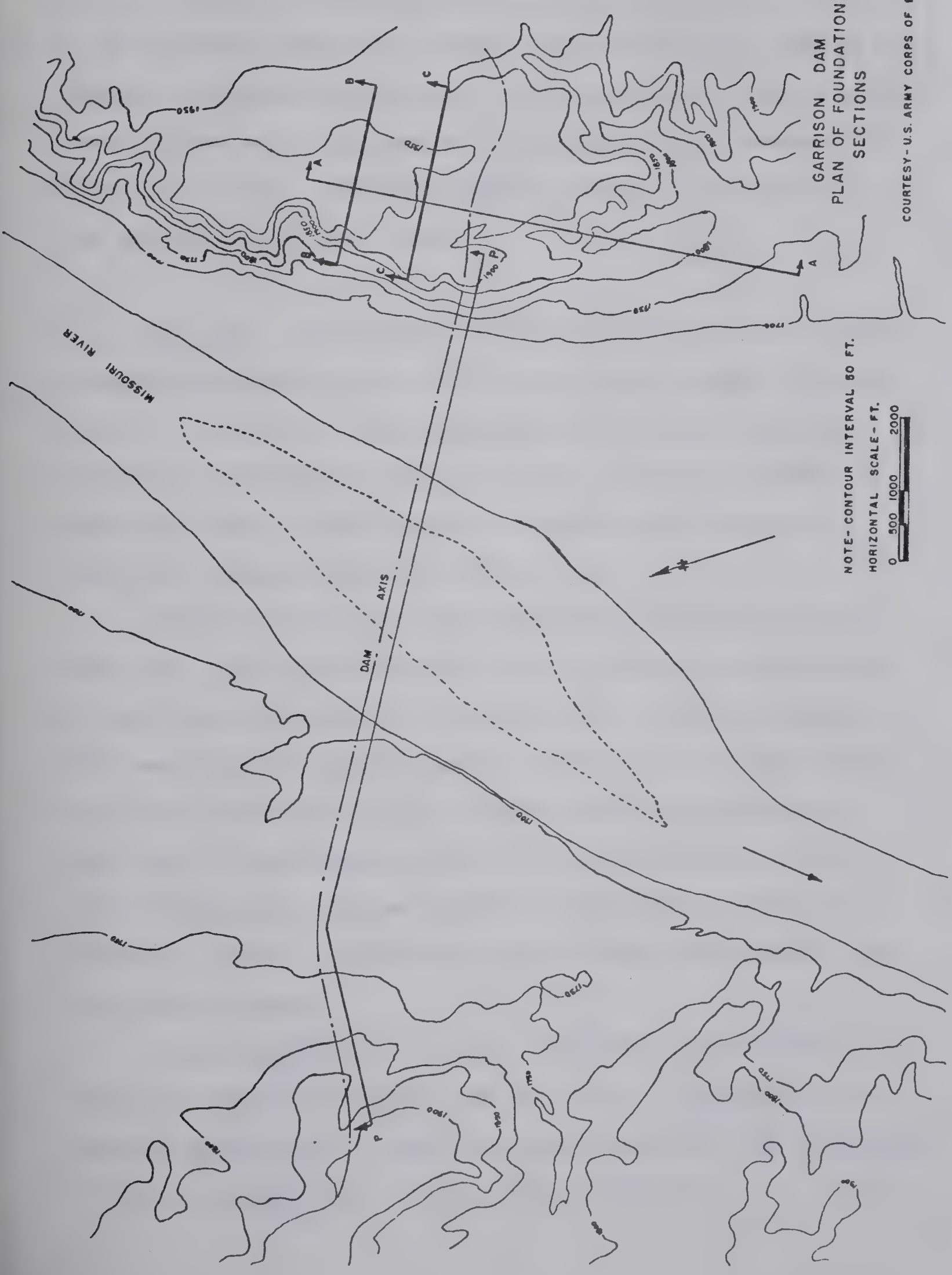


FIG. 3.25







GARRISON DAM  
PLAN OF FOUNDATION  
SECTIONS

NOTE- CONTOUR INTERVAL 50 FT.  
HORIZONTAL SCALE- FT.  
0 500 1000 2000

COURTESY- U.S. ARMY CORPS OF ENGINEERS

FIG. 3.26



a low modulus of elasticity ranging from 2880 to over 28,800 p.s.i. Constant stress-ratio triaxial tests gave a value of  $E$ , at a stress ratio of one-half, of 28,800 p.s.i. which was adopted for design purposes. The formation is heavily over-consolidated with an apparent preconsolidation pressure of 80 to 100 t.s.f. Oedometer tests indicated a compression and swelling index of 0.018.

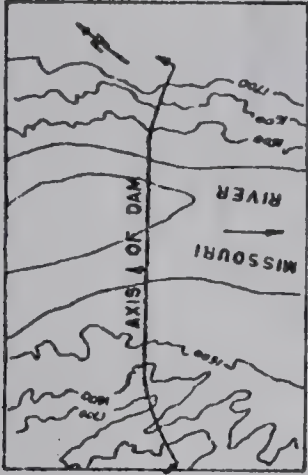
11. Oahe Dam: A discussion of the behaviour of the Pierre shale during construction of Oahe Dam is included in Chapter II. A detailed examination of the testhole logs contained in the Definite Project Report (U.S.C.E., 1948) indicates that a large amount of rebound has occurred below the Missouri Valley at this site.

Figure 3.27 shows the centerline geologic section of the site. An excellent marker bed is present in the form of the Crow Creek Marl. A 40 foot rise in the elevation of this marl bed is evident on both sides of the river valley. As at Fort Peck Dam, it is likely that the elevation of this bed is disturbed by the widespread slumping which has occurred adjacent to the valley in the Pierre formation; however a general trend for a rise in the bed towards the river can be seen.

Detailed logs of sections on either side of the river are given in Figure 3.28 and 3.29. A marked rise in the marl bed occurs in one testhole indicating the occurrence of slide activity with a rotational component.







Scale - ft.  
0 2000 4000 6000  
LOCATION

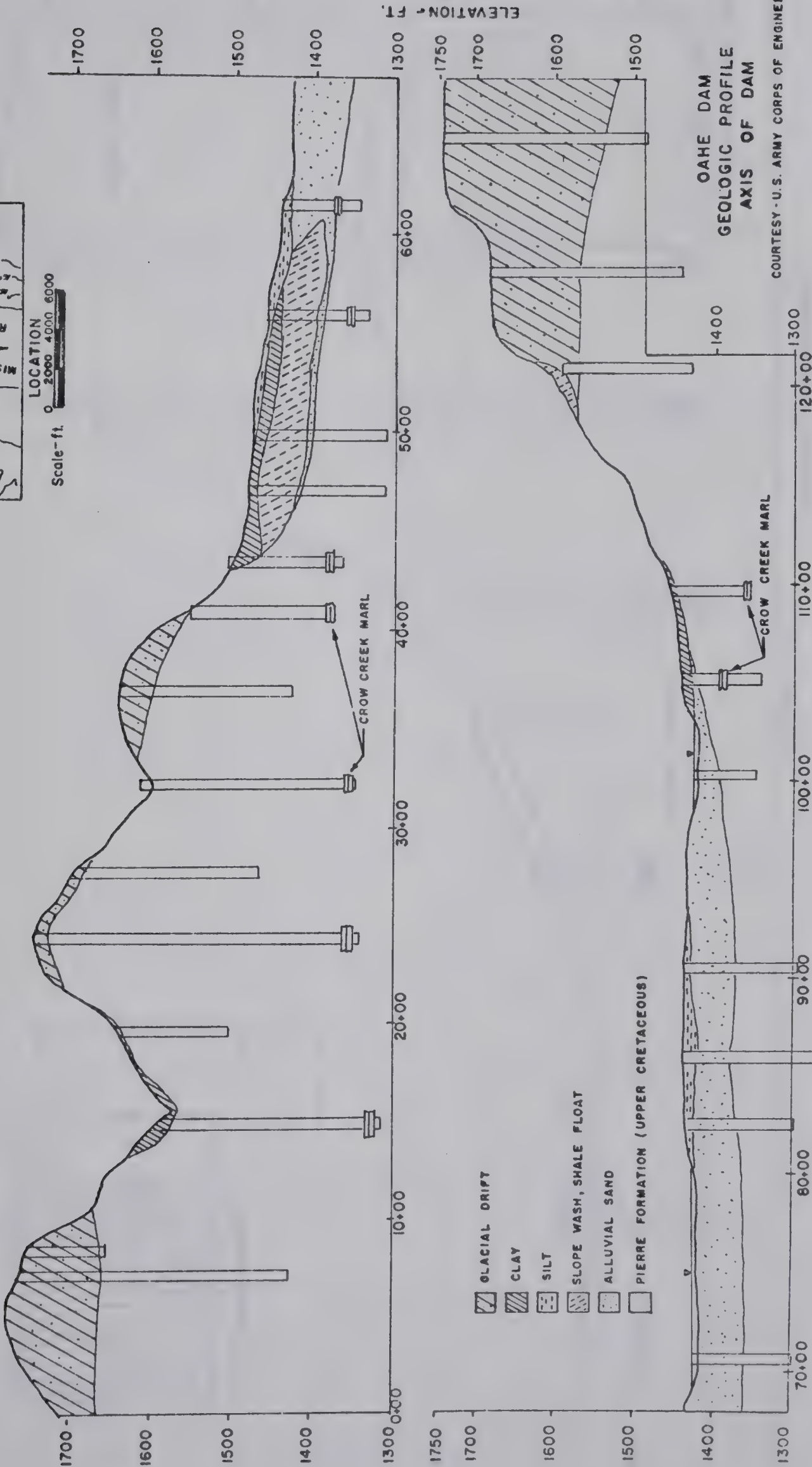


FIG. 3.27



- LEGEND
- CROW CREEK MARL
  - PIERRE SHALE
  - JOINT
  - LOST CORE
  - SLICKENSIDE

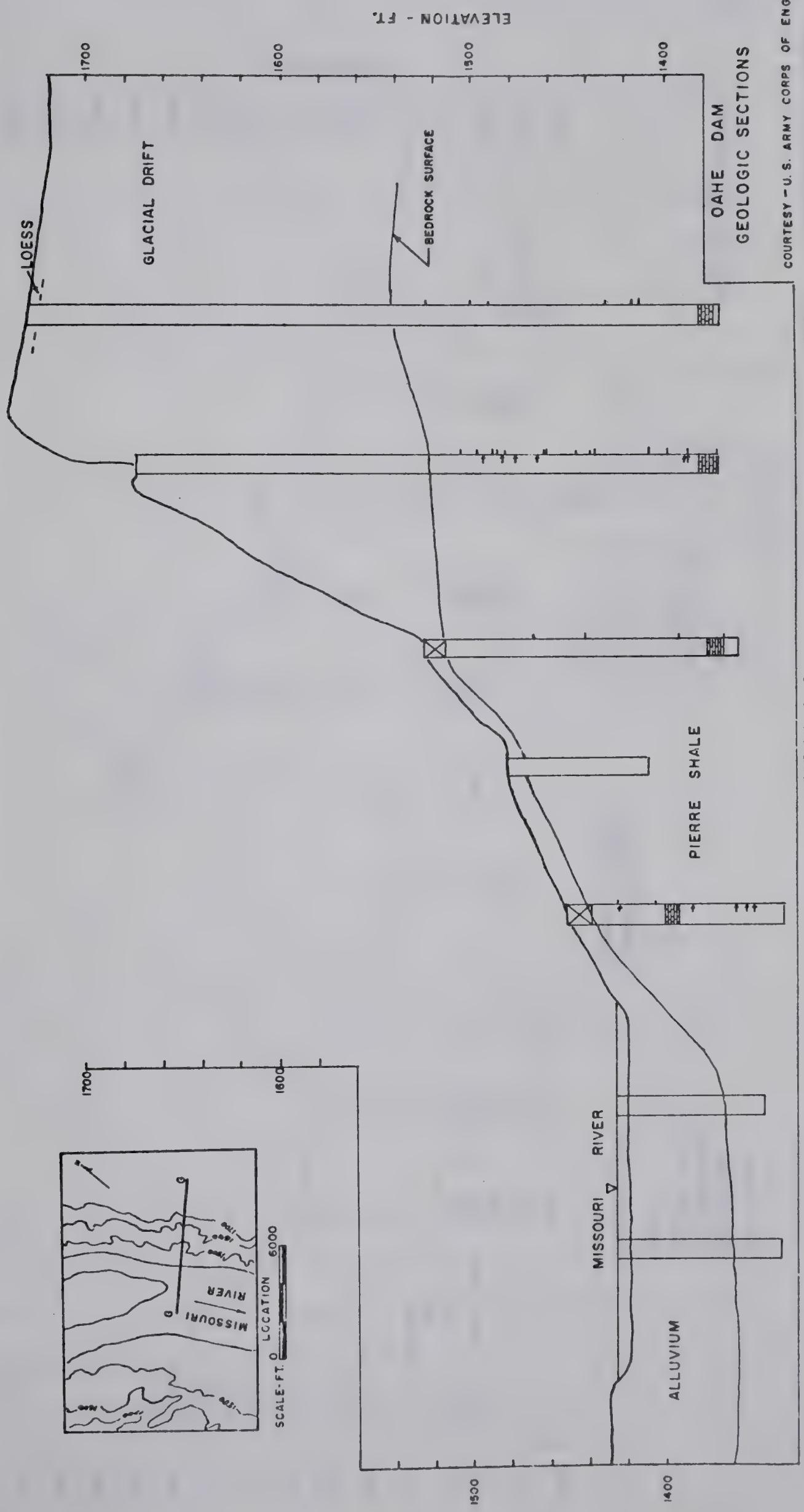
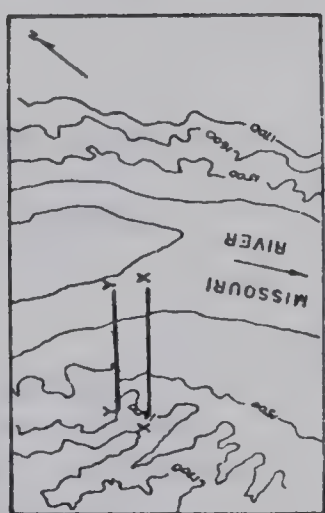
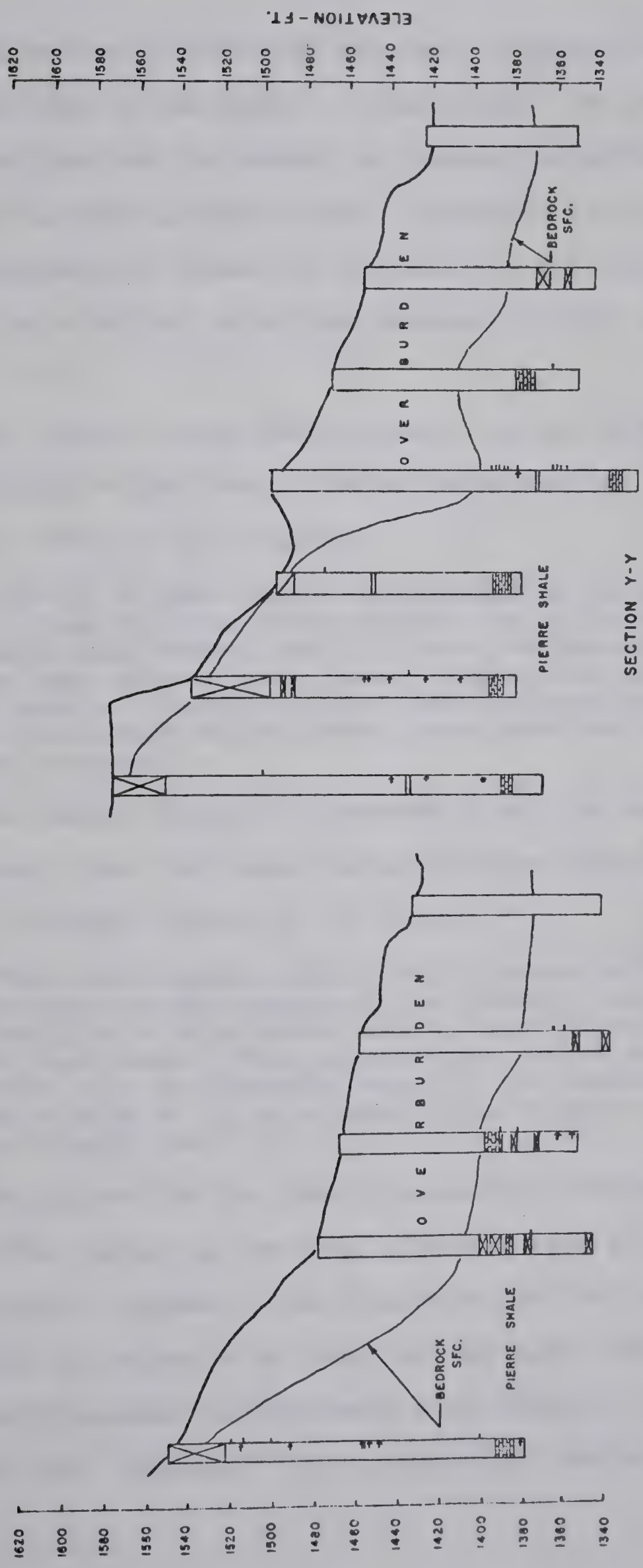


FIG. 3.28







OAHÉ DAM  
GEOLOGIC SECTIONS

COURTESY - U. S. ARMY CORPS OF ENGINEERS

FIG. 3.29



The abutment testholes were not extended far below river level due to the depth of the valley. No marker bed clearly delineating the amount of rebound occurring below the valley bottom has been found. However, it would appear that a considerable amount of rebound, in the order of tens of feet, has occurred below the Missouri Valley at this site.

The rebound along the Missouri has produced a well defined raised valley rim. The Definite Project Report (U.S.C.E., 1948, p. 11) states:

"On the top of the bluffs the topography is almost flat. From the rim of the bluffs the surface slopes landward thus leaving the rim edge the highest portion of the left side of the river. Subsurface explorations made at the top of the left abutment indicate that the bedrock shale almost parallels the present ground surface."

The raised valley rim extends along the east side of the Missouri River for some distance either side of the damsite. Crandell (1958, p. 4) noted:

"The most notable topographic feature of the Pierre area is the trench of the Missouri River, which is from 2 to 4 miles wide and, in most places, 300 to 400 feet deep. When approaching the trench from the east, one is scarcely aware of its presence within a mile or 2, in places a few hundred yards of the trench rim."

The raised rim is clearly visible on the east side of the river valley as the west side has been dissected by numerous small streams. The raised valley rim has been accentuated by deposits of loess on the east side of the river which decrease in thickness with distance back from the valley rim. However, in certain areas the effect is





visible on both sides of the valley. Figure 3.30 shows a profile across the Missouri Valley 2 miles downstream of the dam taken from 20 foot contour maps given by Crandell (1958). The same phenomena occurs elsewhere along the Missouri as "at many places in the State, upland surfaces immediately adjacent to the trench slope away from the Missouri River" (Crandell, 1958, p. 52).

12. Bowman-Haley Damsite: Bowman-Haley Damsite is located on the North Fork of the Grand River in Section 24, T.129N, R.101W, Bowman County, North Dakota about 6 miles upstream of the town of Haley, North Dakota. The site has been investigated by the U.S. Army Corps of Engineers (U.S.C.E., 1963b).

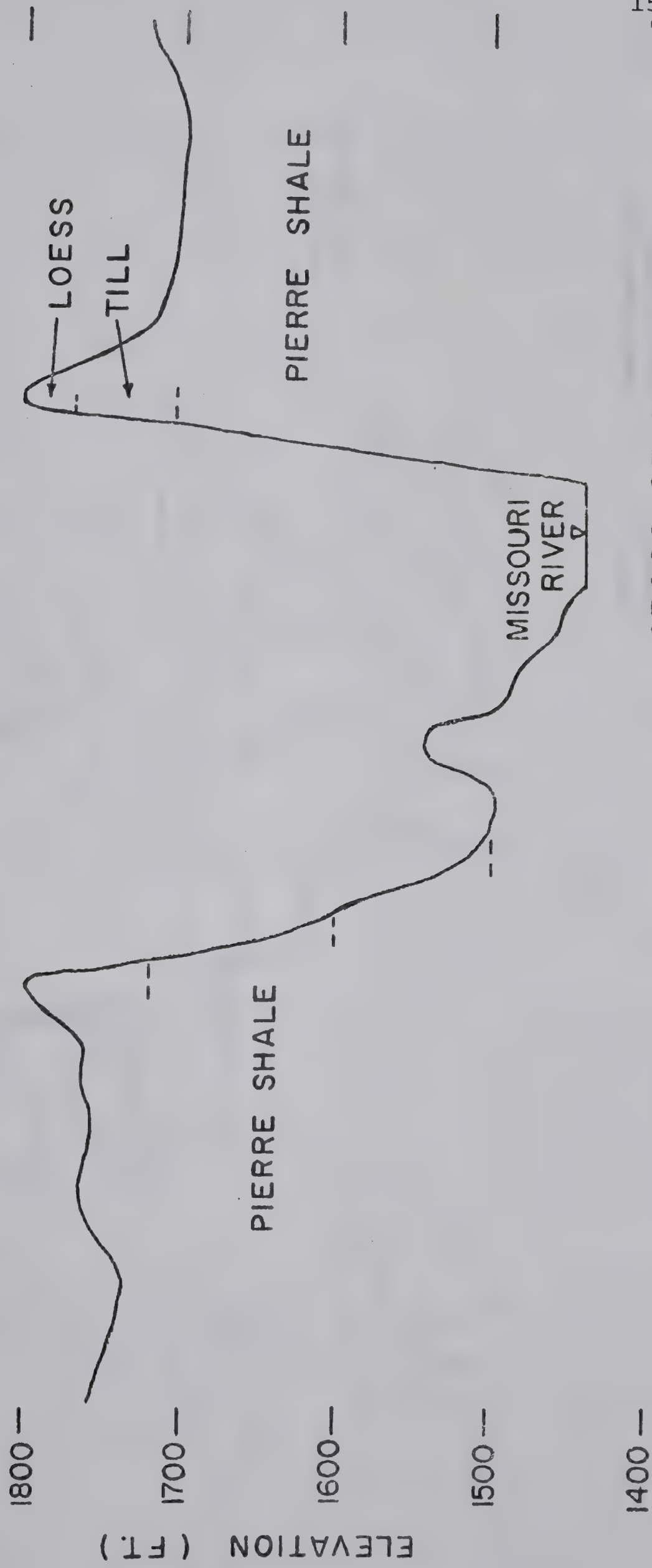
The area was unglaciated during the Pleistocene. The river lies in a one mile wide valley about 150 feet deep with flat valley sides. The bedrock at the site is the Ludlow formation of the Fort Union Group (Tertiary). Field investigations consisted of two rotary bore holes which used a 5 3/8 inch diameter double-tube core barrel and 22 churn drill borings made with a 4 or 6 inch diameter open-end drive barrel. Location of the testholes is shown in Figure 3.31.

The Ludlow formation consists of poorly indurated, interbedded clays, sands and silts with soft to hard thin-bedded calcareous sandstones, soft shales and lignite beds. Five lignite beds varying in thickness from 1 to 6 feet



S 68° W

N 68° E



CROSS-SECTION OF THE  
MISSOURI RIVER VALLEY

FIG. 330

Horizontal scale  
(miles)

From U.S.G.S. Maps

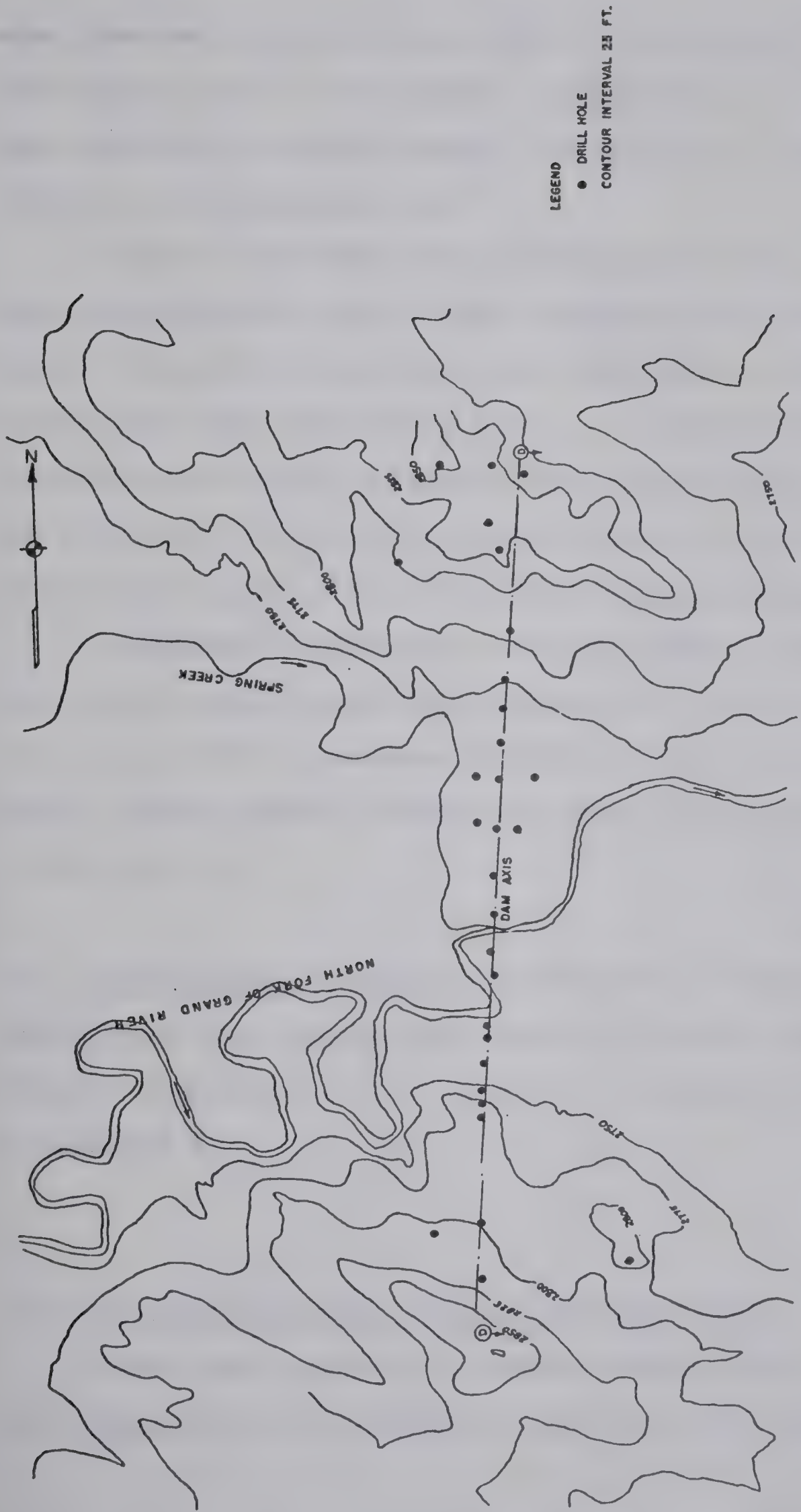




BOWMAN - HALEY DAM  
PLAN OF BORINGS

COURTESY - U.S. ARMY CORPS OF ENGINEERS

FIG. 3.31





were observed in the borings which served as marker beds. The regional dip of the bedrock is reported as 10 to 20 feet per mile to the northeast. No evidence of faulting exists in the immediate area.

Figure 3.32 shows the centerline geologic section. The orientation of lignite bed C indicates a slight regional dip to the north on which has been superimposed an upwarping of the beds under the valley sides. An asymmetric anticline some 20 feet high occurs under a gravel terrace on the left side of the valley indicating most of the rebound occurred during the early stages of valley downcutting.

Unconfined compression tests on samples from between the A and B lignite beds gave strengths of from 1.43 to 1.75 t.s.f. with an average strength of 1.56 t.s.f. The initial tangent moduli ranged from 80 to 168 t.s.f. (1110 to 2340 p.s.i.)

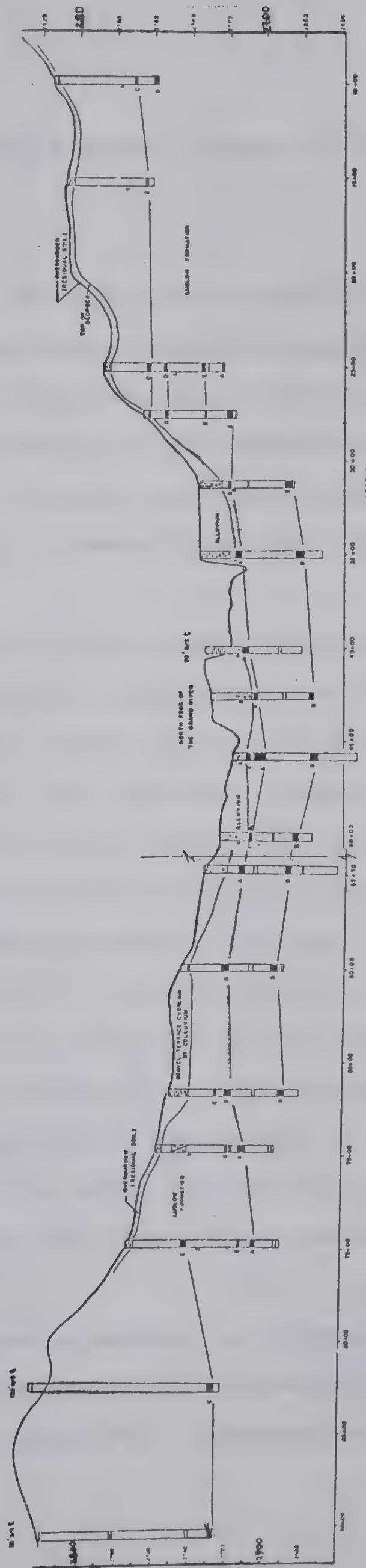
13. Miscellaneous Sections: A discussion of sites where insufficient drilling or the absence of marker beds precluded definite observation of the amounts of rebound is included in Appendix A.

### 3.4 Case Histories From Outside the Study Area

Data from a number of damsites outside the study area was collected in the course of this study and is included in







BOWMAN - HALEY DAM SITE  
 GEOLOGIC SECTION  
 COURTESY U. S. ARMY CORPS OF ENGINEERS  
 FIG. 3.32



this section where evidence of valley rebound is of particular interest.

1. Portage Mountain Dam: Portage Mountain Dam is located on the Peace River in north-eastern British Columbia some 12 miles west of the town of Hudson Hope. The dam was designed by International Power and Engineering Consultants Ltd. (I.P.E.C.) for the B. C. Hydro and Power Authority. The geology of the site is discussed by Dolmage and Campbell (1963).

The dam is situated one mile below the entrance to the Peace River Canyon where the river is 600 to 700 feet in width and flows between a right canyon wall 150 feet high and a left canyon wall 300 feet high. From the top of the left canyon wall the ground rises to the top of Portage Mountain. On the right bank a bedrock plateau 150 feet above river level underlies part of the dam.

The bedrock at the site consists primarily of non-marine sandstone, siltstones and shales of the Dunlevy and Gething formations (Lower Cretaceous). The average strike of the beds is approximately N48°W and the dip is 5 to 10 degrees to the southwest. No major faults occur at this site. The general geology and topography of the site is shown in Figure 3.33.

The principal sandstone members in the Dunlevy formation are designated by the prefix "N" and within the Gething formation by the prefix "E". Sandstone members

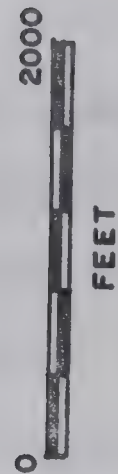




DUNLEVY FM

APPROX. DAM OUTLINE

- SANDSTONE
- SHALE
- PEACE RIVER COAL SEAM

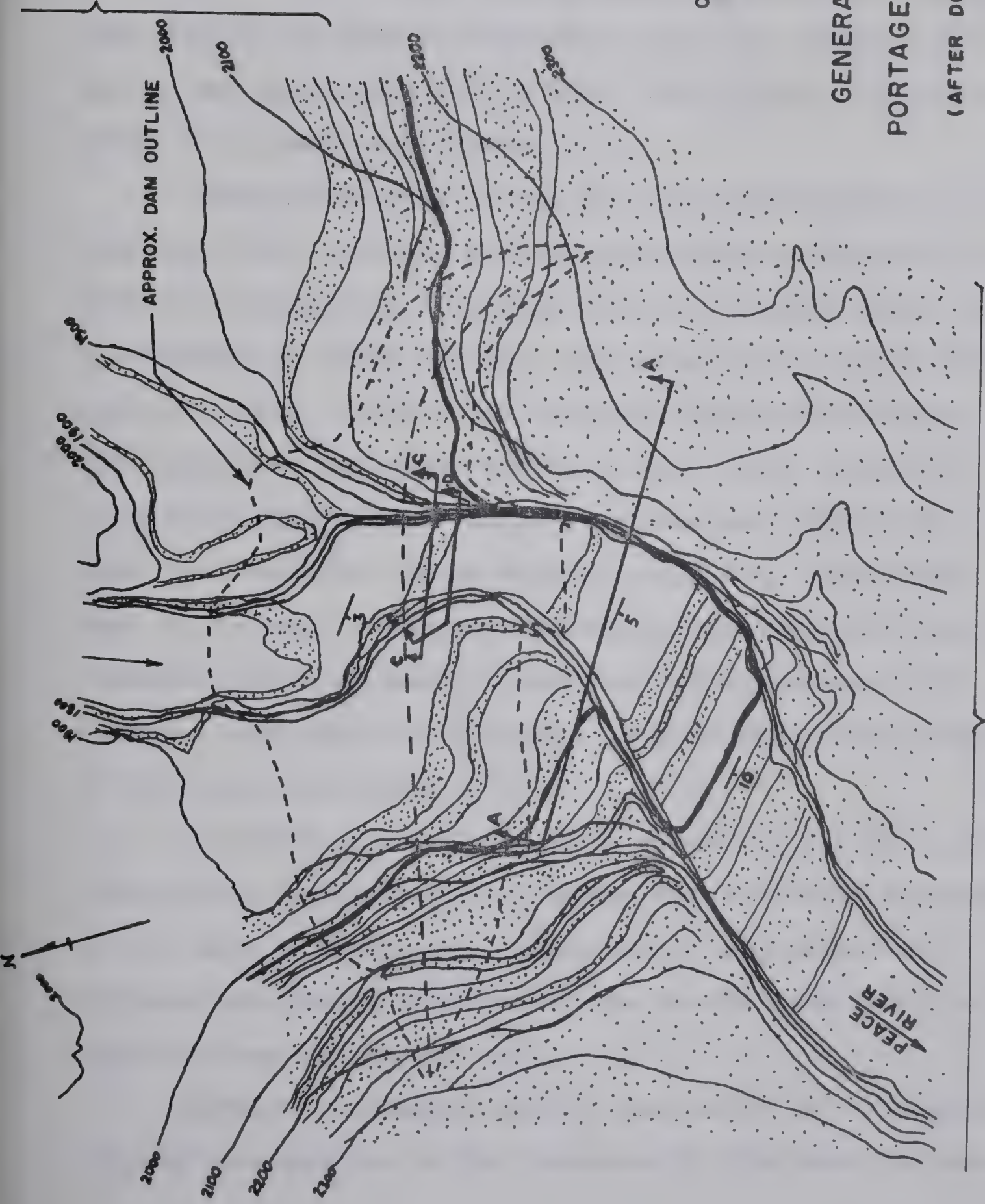


# GENERAL GEOLOGY PORTAGE MOUNTAIN DAM

(AFTER DOLMAGE & CAMPBELL, 1963)

GETTING FM.

FIG. 3.33





commonly pass gradationally into shale members. A shale member is therefore given the same designation as the underlying sandstone member; for example the N4 shale lies between the N4 sandstone and N3 sandstone (Imrie, 1967). The contact between the Dunlevy and Gething formations has been set at the base of the Peace River coal seam; a prominent and continuous bed of coal 7 to 10 feet in thickness which is an excellent marker bed.

Seams were noted in the N5 sandstone below the river-bed which were infilled with alluvial sand and gravel to a maximum thickness of 12 inches (I.P.E.C., 1965; Imrie, 1967). No evidence of these features was noted during the drilling program (Imrie, 1971). The infilled seams occur along bedding planes and pinch and swell over short distances bringing projections of solid overlying and underlying rock into contact. These features (I.P.E.C., 1965) have been attributed to vertical stress relief (rebound) with chemical and/or mechanical disintegration enlarging the openings once they were formed. No sand seams were observed in the shale horizons.

A number of sand seams were mapped in the N3 sandstone on the right abutment plateau but none were in excess of one inch in thickness. Imrie (1967) suggests these features are due to buckling of the strata under high horizontal stress in the bedrock.

Another structural feature indicative of sliding of one bed over another is the presence of thin gouge or mylonite







seams in various coal or shale horizons. These seams parallel the bedding, are 1/8 to 3 inches in thickness and are considered to be due to bedding plane slip associated with folding (Imrie, 1967). Other features noted by Imrie (1967, p. 23-24) include:

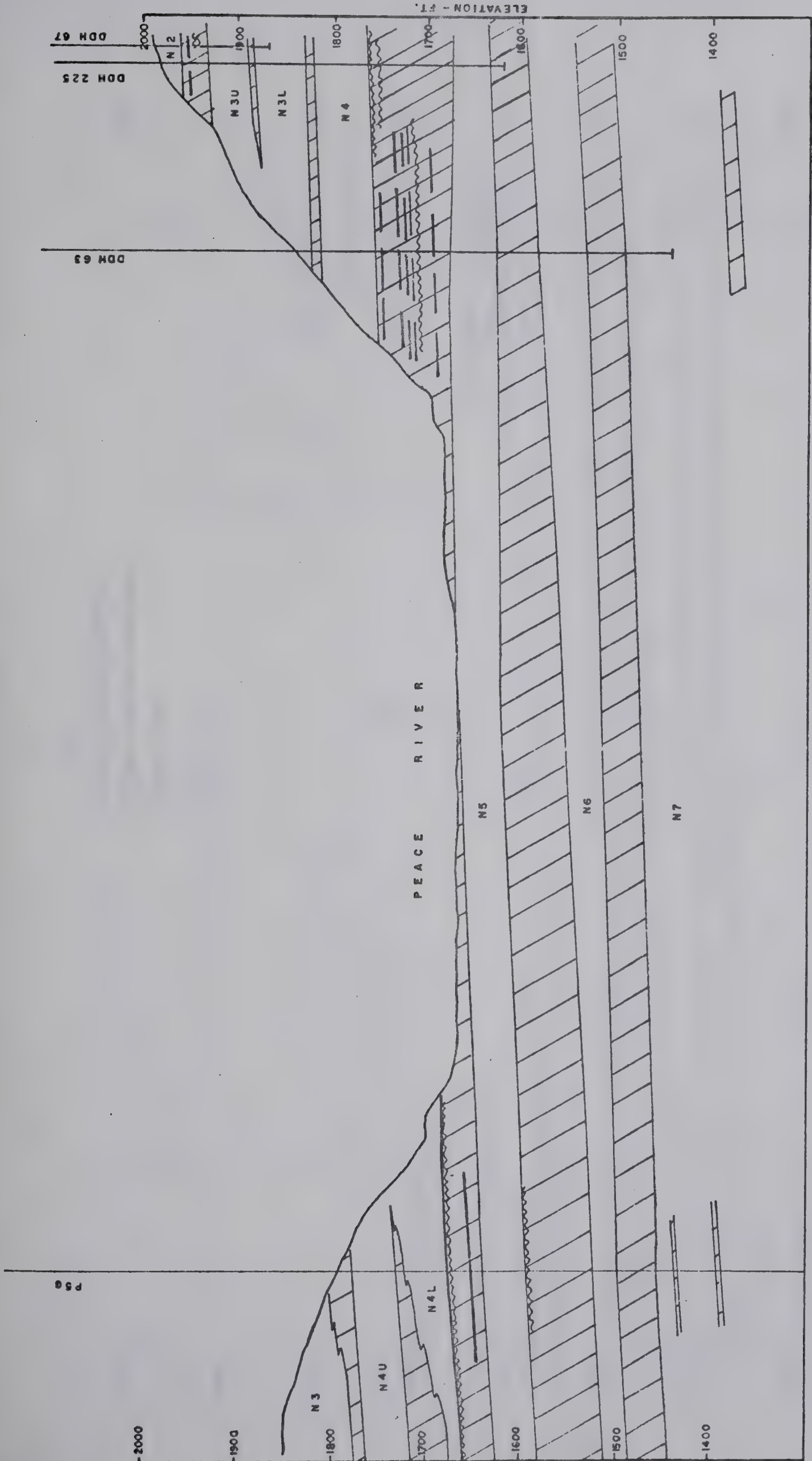
"local monoclinal warps, well-developed cleating in the coal and poor to well-developed jointing in the siltstone and shale. Shearing is common at the base of thicker coal seams. Joints are generally absent in the massive sandstones."

Two geologic sections of the valley bottom are given in Figures 3.34 and 3.35. A change in dip of the beds on either side of the valley is evident and an upwarping of the beds of about 15 feet appears to occur. This evidence cannot be regarded as conclusive in view of the gradational nature of the beds.

A geologic section across the valley downstream of centerline is given in Figure 3.36. A flattening in the dip of the Peace River coal seam occurs in the right abutment and the orientation of marker beds below the bedrock plateau on the left abutment indicates the existence of both rebound and valley flexure. The absence of the Peace River coal seam in testholes 422 and 424 indicates a steepening of the dip of the strata below the left valley wall.

Unconfined compression tests on rock cores gave strengths ranging from 16,400 p.s.i. to 19,800 p.s.i. for the sandstone and from 11,800 p.s.i. to 16,800 p.s.i. for the shale. Initial tangent moduli ranged from 2.2 to 2.6





NOTE-TRACED FROM B.C. HYDRO PLAN U-3042-S2187

SCALE - 0 100 FT.

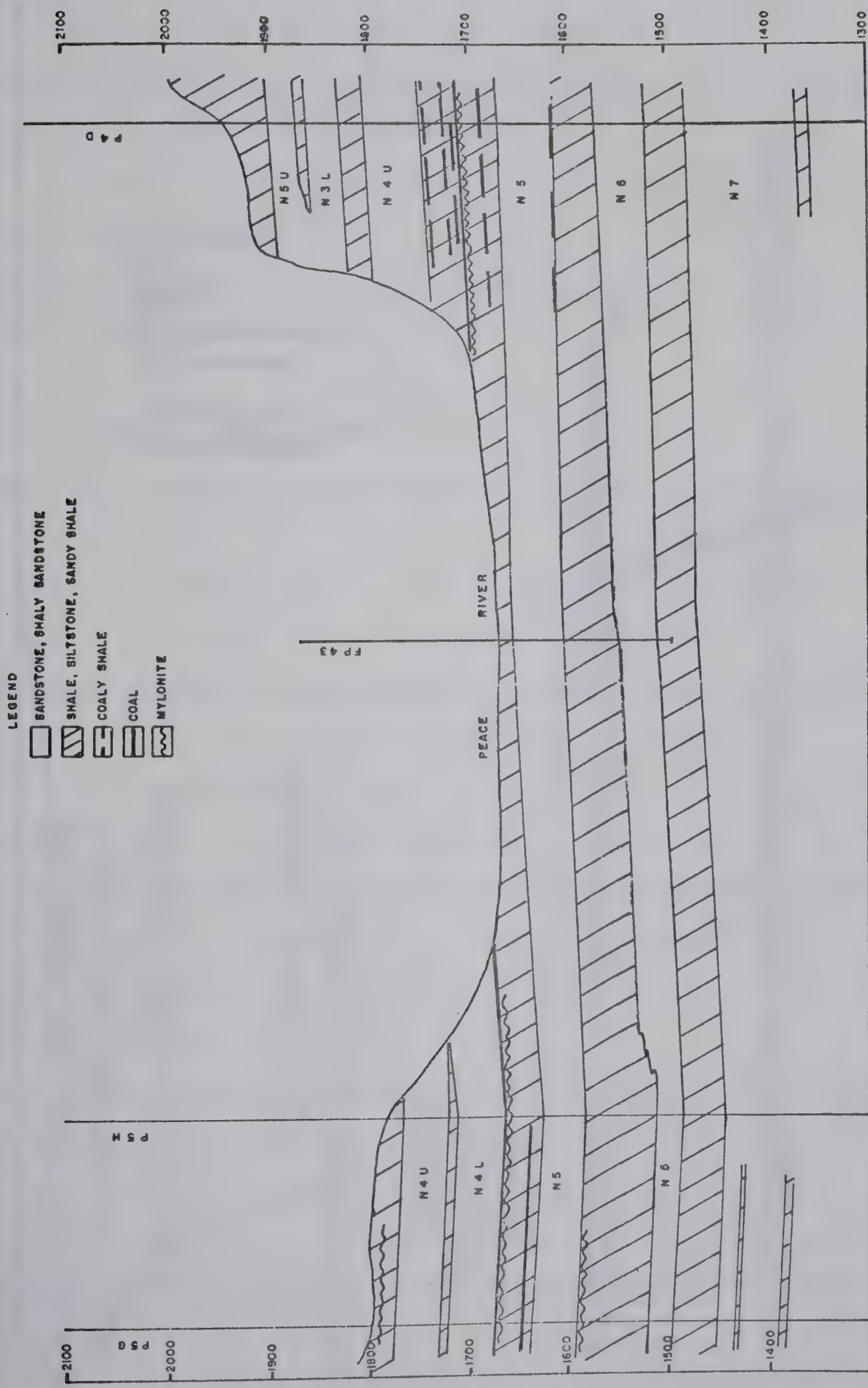
- LEGEND
- SANDSTONE, SHALY SANDSTONE
  - SHALE, SILTSTONE, SANDY SHALE
  - COAL
  - MYLONITE

PORTAGE MOUNTAIN DAM  
GEOLOGIC SECTION C-C

COURTESY I.P.E.C. FIG. 3.34



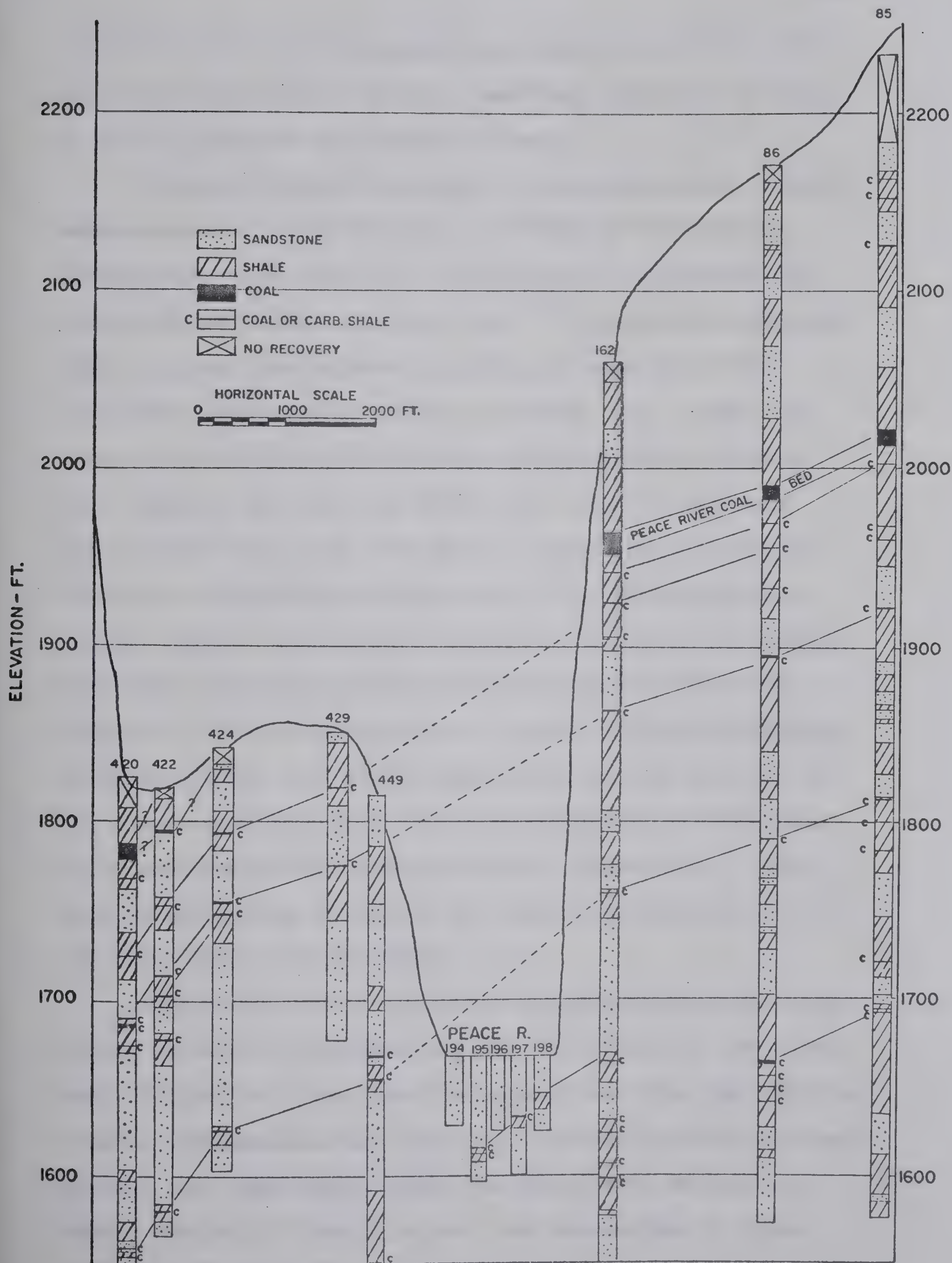




PORTAGE MOUNTAIN DAM  
GEOLOGIC SECTION D-D

FIG. 3.35





PORTAGE MOUNTAIN DAM - GEOLOGIC SECTION A-A

COURTESY I.P.E.C.

FIGURE 3.36





$\times 10^6$  p.s.i. for the sandstone and from 4.4 to  $5.6 \times 10^6$  p.s.i. for the shale. Average swelling pressures of about 12 p.s.i. occurred in oedometer tests.

During 1964-65, Professor N. Hast conducted in-situ measurements of rock stresses. A total of 307 stress measurements were taken in 7 testholes by the overcoring stress-relief method (Imrie, 1967). The results indicated that stresses in-situ were much higher than could be accounted for by gravitational stresses. At a depth of 450 feet in the powerhouse area, the horizontal stresses were found to be 1920 and 1070 p.s.i. and the vertical stress was found to be 1050 p.s.i.; much greater than the weight of overburden at this point. In the central and eastern section of the powerhouse, the direction of maximum horizontal stress was  $N76^{\circ}E$  which agrees well with the normal to the Portage Mountain - Butler Ridge anticlinorium which is  $N80^{\circ}E$ . The stress magnitudes at the west end of the powerhouse were lower and the orientations were apparently changed by the proximity of the canyon wall. The maximum horizontal stress at this point trends  $N20^{\circ}E$  while the canyon wall trends  $N16^{\circ}E$ .

Sources of error in stress measurements by the overcoring method are discussed by Merrill (1963, p. 349); the most critical of which are the assumptions that the rock is elastic, homogeneous and isotropic and the elastic constants derived from laboratory tests are applicable to in-situ rock. However, it would appear the assumption of large horizontal compressive stresses at Portage Mountain is



justified. These forces may be tectonic in origin and due to the Laramide orogeny which formed the Rocky Mountains.

2. Three Rivers Damsite: Three Rivers Damsite is located in south-western Alberta on the Oldman River in Section 17, Township 7, Range 29, West of the 4th Meridian about 6 miles northeast of the town of Pincher Creek, Alberta. The site has been investigated by the Prairie Farm Rehabilitation Agency (P.F.R.A., 1965a).

The Oldman River has cut a 200 foot deep canyon 800 feet wide at the site through bedrock of the Porcupine Hills formation (Tertiary), close to the transitional contact with the underlying Willow Creek formation (late Upper Cretaceous or early Tertiary). The Porcupine Hills formation consists of fine-grained, cross-bedded sandstone with interbedded shaly clays. The Willow Creek formation consists of thin alternating beds of sand, clay and sandy clay with harder beds of grey and buff sandstone towards the top of the formation. The dip in the area is negligible as the site lies close to the trough of the Alberta syncline. No faults are reported in the area.

The sandstone is generally fine-grained, very hard and characterized by low water contents and high densities. Unconfined compressive strengths range from 8300 to 19,780 p.s.i. and averaged 12,100 p.s.i. for 16 tests. Moduli from these tests ranged from 560,000 to 1,320,000 p.s.i. and averaged 850,000 p.s.i.





The shales were generally hard and slate-like with low water contents and high densities. Unconfined strengths ranged from 3175 p.s.i. to 8690 p.s.i. and averaged 5340 p.s.i. for 5 tests. Moduli from these tests ranged from 200,000 p.s.i. to 540,000 p.s.i. and averaged 390,000 p.s.i.

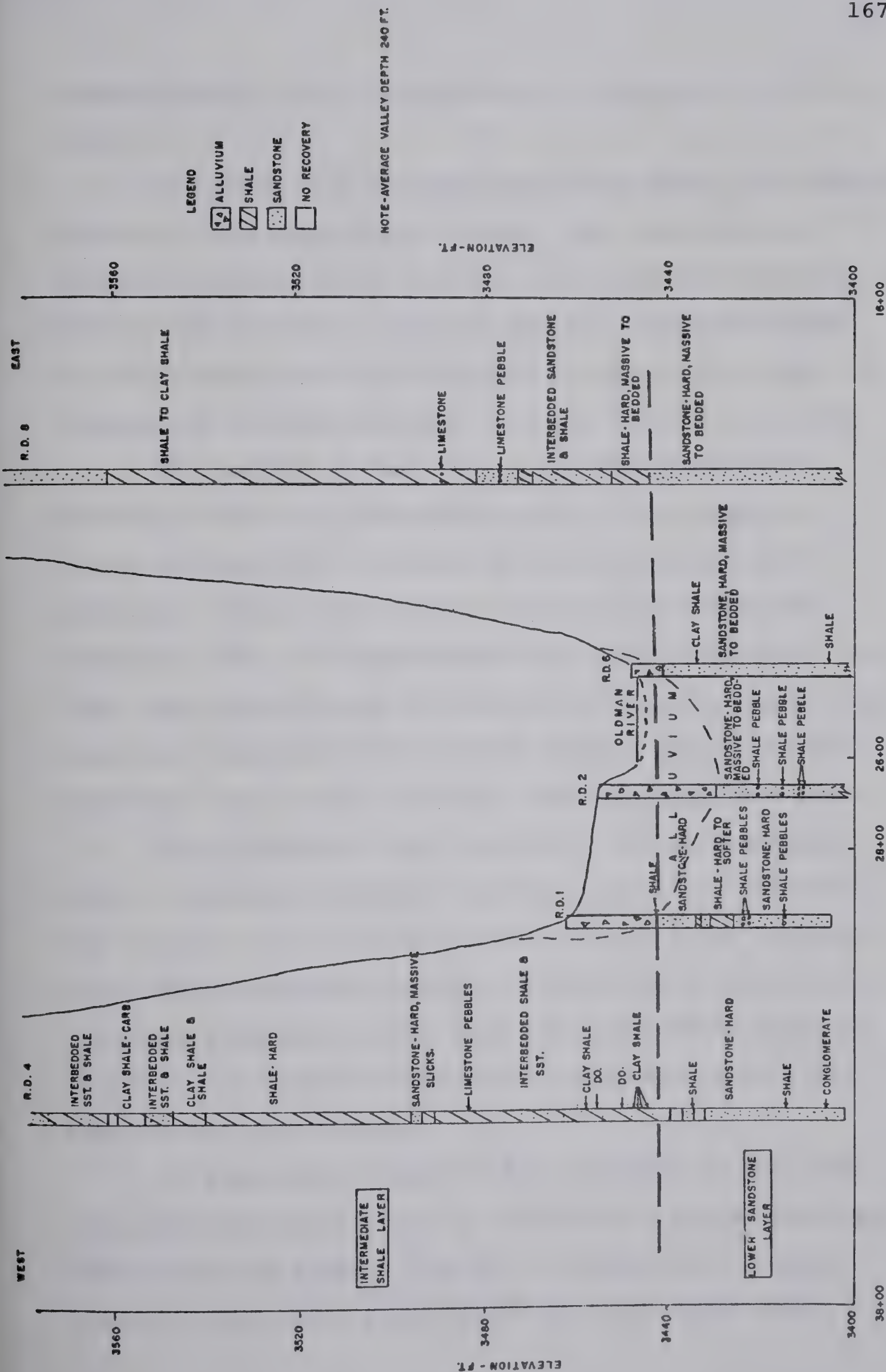
Eleven rotary drill holes were cored using double-walled core barrels. A centerline geologic section of the valley bottom is shown in Figure 3.37. Core recovery averaged between 70 and 80 percent. No water losses occurred during the drilling of testholes RD1 and RD6. A 100 percent water loss occurred in RD2 at a depth of 40 feet.

Marker beds are poor at this site with no coal or bentonite beds noted during the drilling program. However, a layer of shale pebbles noted in the sandstone in testholes RD4, RD1, and RD2, at elevation 3415, indicates little or no rebound as having occurred below the valley floor; however this correlation must be regarded as tentative. Since the bedrock below the valley is described as hard and firm, moisture contents are as low as in the abutment testholes at a similar elevation below the valley floor and no extensive fracturing apparently occurs, it would appear that an insignificant amount of rebound, in the order of inches rather than feet, occurs at this site.

3. Twelvepole Creek Damsite: Twelvepole Creek Damsite is located on Beech Forks, a tributary of Twelvepole Creek, 6.5 miles south of Huntingdon, West Virginia. The site has been



THREE RIVERS DAMSITE  
GEOLOGIC SECTION  
COURTESY - P. F. R. A. FIG 3.37







investigated by the U.S. Army Corps of Engineers (U.S.C.E., 1969a).

The Beech Fork drainage basin lies within the Kanswaha section of the Appalachian Plateau. The area has been extensively dissected by erosion and a dendritic drainage pattern has resulted. The area was not glaciated during the Pleistocene and the overburden on the valley slopes is composed of colluvium derived from the weathered bedrock.

The bedrock at the site is the Monongahela and Conemaugh series of Pennsylvanian age. The Conemaugh series was deposited in repeated marine advances and retreats. Marker beds include the Elks Lick limestone (elevation 606), the Upper Ames shale (elevation 565), the lower Ames shale facies (elevation 532) and the Brush Creek limestone (elevation 472). These members are generally persistent and can be correlated over the immediate area.

The lithologic units consist of clays, indurated clays, claystones, shales, sandstones and thin limestones. The regional dip is to the northwest at 50 to 72 feet per mile. The Parkersburg Syncline trends  $N65^{\circ}E$  and passes 0.7 miles southeast of the site. This structure gives the strata in the immediate vicinity of the dam a dip of 11 feet per mile to the east.

No faulting is known to have occurred in the area. Two major joint sets occur in the area and strike  $N80^{\circ}W$  and  $N30^{\circ}E$  with dips ranging from 80 to 90 degrees. A minor system of two joints strike  $N50^{\circ}W$  and  $N10^{\circ}E$  with dips



ranging from 70 degrees to the vertical.

The investigations at the site included 114 NX core borings, eight 4 inch core borings and eleven 6 inch core borings. All coring was performed using a standard, double tube, rotary core barrel. A rise in the Brush Creek limestone of about 5 feet occurs below the valley bottom and a distinct upwarping of beds on either side of the valley is visible in Figure 3.38.

It is possible that actual fracturing and failure of the beds below the valley center has occurred at this site from the unusual stratigraphy and truncated beds immediately below the valley centerline. However, this cannot be confirmed due to the limitations inherent in conventional drilling techniques as discussed in Chapter II.

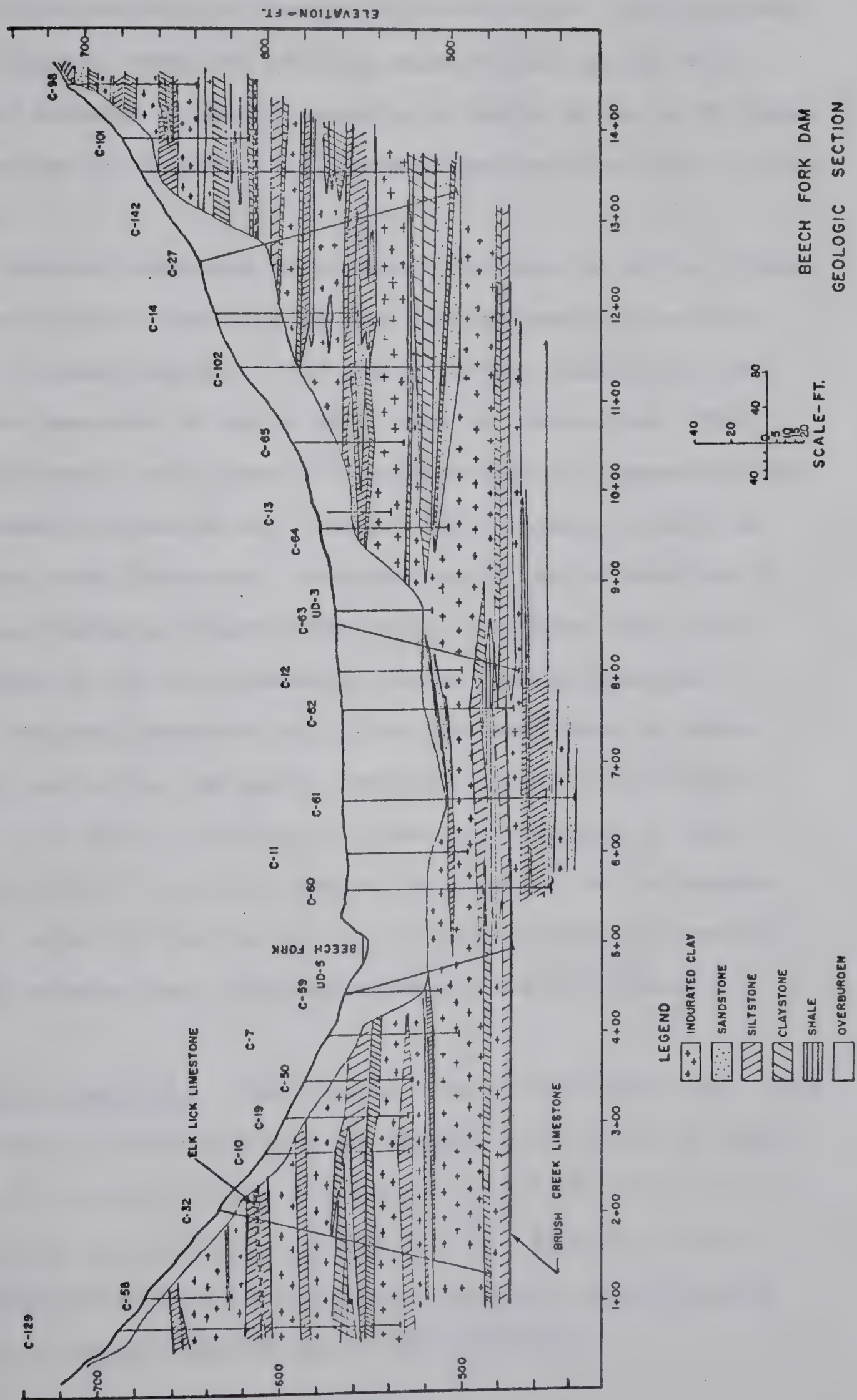
One unconfined compression test, conducted on shaly sandstone from testhole C-133 at elevation 556, gave a strength of 1012 p.s.i. and a tangent modulus at 0.2 percent strain of 135,000 p.s.i.

4. Smithville Damsite: Smithville Damsite is located on the Little Platte River about 1 mile north of Smithville, Kansas. The site was investigated by the U.S. Army Corps of Engineers (U.S.C.E., 1969b).

The Little Platte River Valley is in a mature stage of development with the river meandering across a 1300 feet wide floodplain. The valley has a maximum depth of 150 feet and gently sloping sides. The river flows over about 55







BEECH FORK DAM  
GEOLOGIC SECTION

COURTESY - U.S. ARMY CORPS OF ENGINEERS  
FIG. 3.38



feet of Pleistocene and recent alluvium which overlies bedrock. Glacial deposits overlies much of the upland with till and outwash deposits reaching a depth of up to 95 feet. Loess of up to 20 feet in thickness mantles the till in the uplands.

Bedrock consists of alternating beds of shale, limestone and minor sandstone of the Lansing and Kansas City Groups (Pennsylvanian). The depth to the Cambrian or Precambrian basement is about 2500 feet at this site. The shales present are termed a clayshale and are comparatively soft, usually fissile and contain thin lenses or beds of siltstone and limestone. Average unconfined strengths of the shale members ranged from under 6 to over 100 t.s.f. No strengths for the limestone members were reported.

Regional bedrock dip is to the northwest at about 50 feet per mile. No major faulting occurs in the area. Figure 3.39 shows a centerline geologic section of the valley bottom. A slight upward inclination of the strata on both sides of the valley is visible indicating several feet of rebound has occurred below the valley floor.

5. Other Damsites: Other cases from outside the study area, where insufficient drilling or lateral continuity of beds exists to clearly define the behaviour of the strata below the valley, are included in Appendix A. Several cases of anomalous structures in the shale-limestone Pennsylvanian bedrock of Kansas and Missouri are discussed.

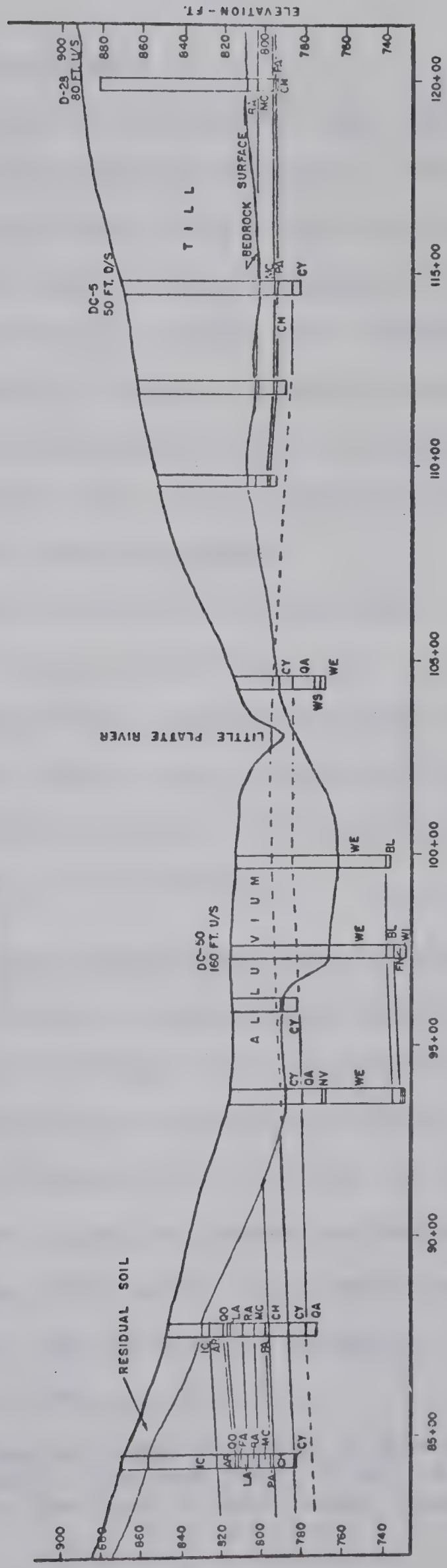




LEGEND

IC-ISLAND CREEK SHALE	WYNADOTE FM.
AR-ARGENTINE LIMESTONE	
OO-QUINDARO SHALE	
FA-FRISBIE LIMESTONE	
LA-LANE SHALE	
RA-RAYTOWN LIMESTONE	IOLA FM.
MC-MUNCIE CREEK SHALE	
PA-PAOLA LIMESTONE	
CH-CHANUTE SHALE	DRUM FM.
CY-CEMENT CITY LIMESTONE	
QA-QUIVIRA SHALE	
WV-WESTERVILLE LIMESTONE	
WE-WEA SHALE	
BL-BLOCK LIMESTONE	CHERRYVALE FM.
FM-FONTANA SHALE	

KANSAS CITY GROUP



SMITHVILLE DAM  
GEOLOGIC PROFILE

COURTESY - U. S. ARMY CORPS OF ENGINEERS

FIG 3.39



### 3.5 Evidence of Lateral Movement

The cases documented in the previous two sections, combined with the cases discussed in Chapter II, show that vertical rebound is a ubiquitous feature below the river valleys in the study area and in other regions of the world, where river valleys have downcut through soft sedimentary bedrock. Indirect evidence of lateral rebound exists in the form of tension joints paralleling the valleys but no direct estimate of the amount of lateral rebound which has occurred can be made from these features.

Indirect evidence on the relative magnitude of lateral movements due to river valley formation is available in the form of displacements induced by artificial excavation. Measurements taken using a tiltmeter are discussed in Chapter V, observations of a more qualitative nature will be discussed in this section.

1. Test Drift, South Saskatchewan River Dam: The test tunnel constructed at the South Saskatchewan River Dam has been previously discussed in Chapter II. A report on an inspection of the tunnel during construction (Allen, 1949) stated that a horizontal excavation of 40 feet had been made at the portal of the tunnel to remove weathered shale to allow mining to begin. The tunnel intercepted several broken zones in the rock and evidence of movement in the rock was noted by Allen (1949, p. 5).

"There is a definite disturbed zone in the tunnel especially between Sta. 1+00 and Sta. 1 + 36. Evidence of movement in the rock in the tunnel excavation





is shown by bent and broken vertical timbers in the tunnel. In this movement the soft, semi-plastic rock has squeezed around the timbers. There is also definite evidence that the rock in the roof of the tunnel has moved outwards in the valley and toward the portal of the tunnel, because the tops of the timbers from the portal, at least as far as Sta. 1 + 36, have moved towards the portal from a minimum up to about 10 inches. The greatest movement occurs between Sta. 1 + 20 and Sta. 1 + 22.

Furthermore, between Sta. 0 + 50 and Sta. 1 + 22 and especially between Sta. 1 + 13 and Sta. 1 + 22, the broken zones, which are slip planes, appear to rise towards the portal and the river, whereas, between Sta. 1 + 36 and the face of the tunnel on November 14, at Sta. 1 + 68, the slickensided broken zones appear to rise to the west. This suggests there may be a curved plane, concave downward, defining an unstable block which may still be moving."

Data compiled on completion of the test drift (P.F.R.A., 1951) indicated no perceptible increase in water content immediately adjacent to the tunnel compared to initial water contents indicating that the movements noted in the shale were not due to swelling. Surveys using conventional methods were unable to detect any instability of the slope above the tunnel. It would appear then that the movements towards the portal, noted in the tunnel, were due to lateral rebound resulting from removal of the 40 feet of weathered shale at the portal.

2. Mangla Dam: Lateral expansion of the tunnels at Mangla Dam in West Pakistan due to horizontal rebound resulting from excavation has been recorded by Khan and Naqvi (1967). Tunnel number 2 at the site was drilled while the power station tailrace excavation was still in progress. The



first steel tunnel-liner section was installed when the excavation was at elevation 938 feet. The last liner section was installed when the elevation of the excavation base was 880 feet. During the period of excavation to final grade, at elevation 802 feet, the tunnel expanded downstream about 4 inches over a lateral distance of 660 feet.

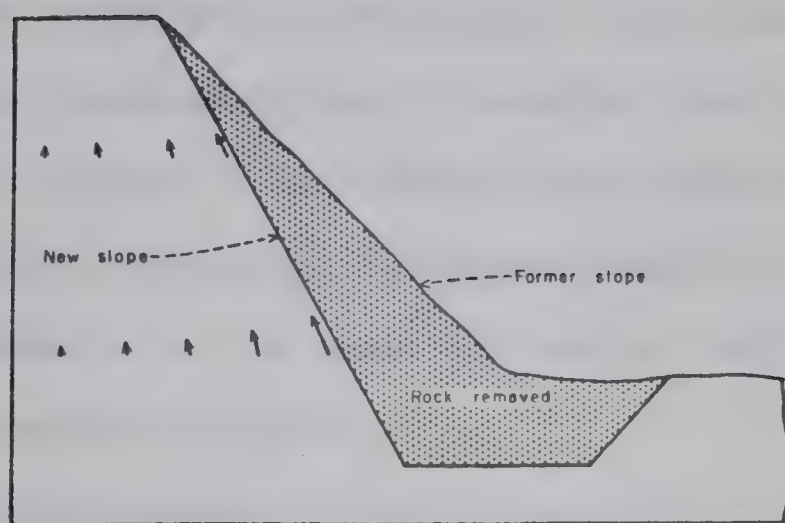
Plate bearing tests and measured values of rebound and settlement, assuming a semi-infinite, homogeneous, isotropic elastic media, indicated a modulus of elasticity of about 100,000 p.s.i. for the Siwalik formation.

3. Kimbley Open-Pit Mine, Nevada: An extensive field and laboratory program of investigation was undertaken by the U.S. Bureau of Mines at the Kimbley open-pit mine in Nevada. During 1966, the west wall of the pit was steepened from an average slope of 45 degrees to a slope angle which reached a maximum of 61 degrees. The pit was deepened from 500 feet to about 550 feet.

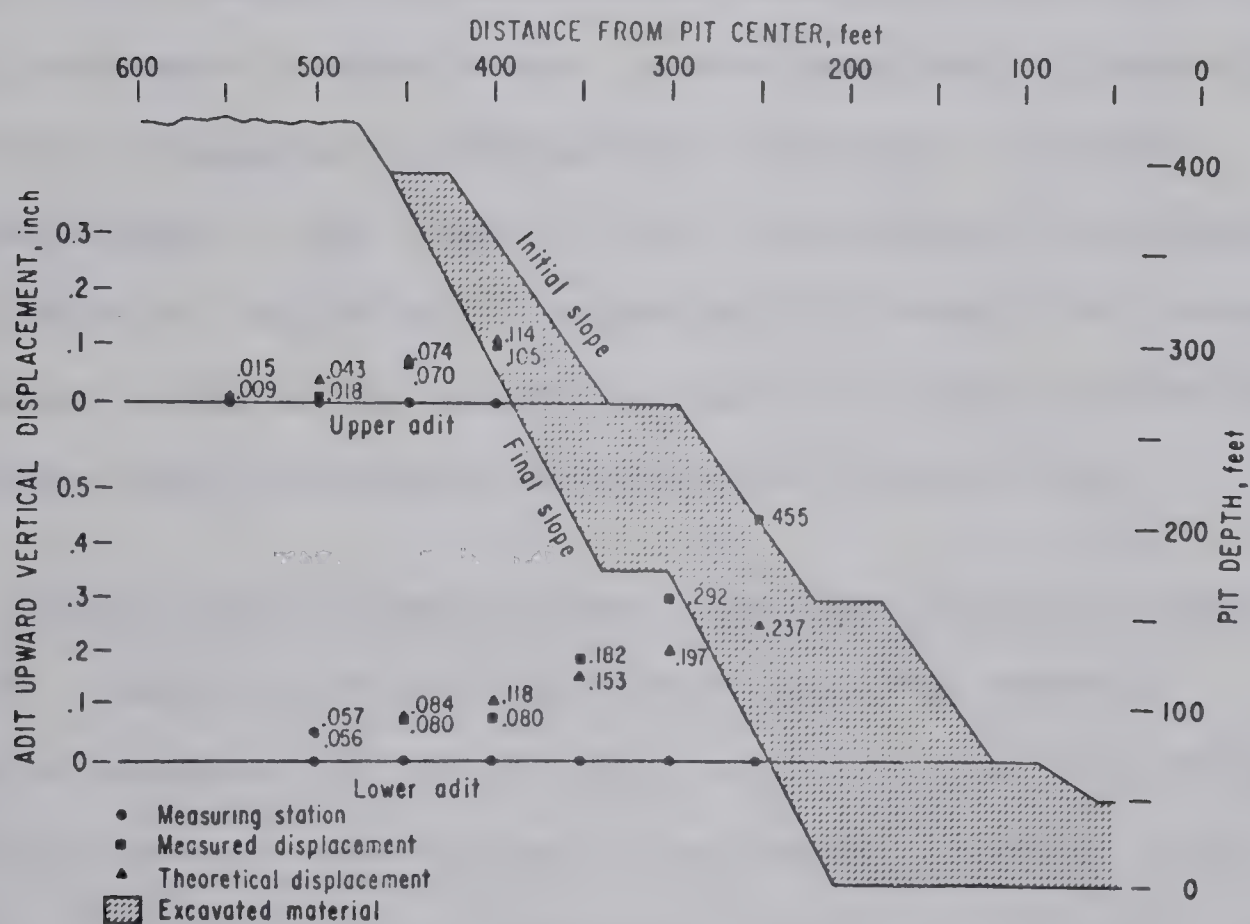
An extensive program of in-situ stress measurement, before the excavation began, showed the stress field in the area to be due to gravitational forces only with no evidence of tectonic stress. The vertical stress averaged 1 to 1.1 p.s.i. per foot of depth and the horizontal stresses were about two-thirds of the vertical stress (Merrill, 1968). The excavation and slope steepening resulted in a displacement upward and into the wall as illustrated in Figure 3.40.







— Illustrative section showing gross movement of the pit wall.  
(MERRILL, 1968)



(BLAKE, 1968)

FIG. 3.40 DISPLACEMENTS DUE TO EXCAVATION AT THE KIMBLEY OPEN-PIT MINE, NEVADA



Finite element studies of the slope modification (Blake, 1968) predicted the general trend and magnitude of displacements reasonably well provided the rock was assumed to be gravity loaded. Any excess horizontal stress field, due to tectonic forces or overconsolidation, would cause the displacements of the rock in the pit wall to be directed up and out towards the pit.

The observations at the Kimbley Pit are of interest as they show clearly the occurrence of upward flexure of the pit wall in response to rebound of the excavation bottom. The observed displacements agreed qualitatively with finite element results from a two-dimensional plane-strain analysis utilizing a homogeneous, isotropic, linearly elastic model. The result of any excavation in an overconsolidated or tectonically stressed rock should be lateral movement towards the excavation as a function of the stress relieved and the modulus of elasticity of the rock.

#### 4. Stratigraphic Observations Along the Missouri River:

Field evidence strongly indicating the occurrence of lateral movement along the Missouri River has been documented by the U.S. Army Corps of Engineers (Fleming et al., 1970). Slopes in the 5 bedrock formations along the upper Missouri River, the Colorado, Fort Union, Claggett, Bearpaw and Pierre formations, were mapped and borings made on one slope from each formation. In several cases a second test-hole was drilled halfway down the slope in a slide zone to sample failed rock while the first testhole was placed on





the valley scarp back from any evident slide activity. A summary of the observations on the occurrence of slickensides in the cores shows:

1. Colorado Group - No slickensides were found in the cores examined in the laboratory although a few were noted in the field.
2. Claggett Formation - One boring penetrated 148 feet of Judith River sandstone before reaching the Claggett shale. The lower part of the Judith River and the upper 50 feet of the Claggett contained several slickensided zones. Three other slickensided zones were found at greater depth in the Claggett formation in conjunction with bentonite layers. A shallower boring, drilled at mid-slope encountered numerous slickensides, gouge and bedding tilted up to the near vertical.
3. Bearpaw formation - The boring located at the top of the slope contained scattered slickensides through the 405 feet sampled with a significant gouge zone at a depth of 264 feet. The mid-slope boring contained zones of slickensides somewhat more intense than those in the upper boring. Numerous slickensides and broken material were identified in the Bearpaw just above the contact with the underlying Judith River sandstone.
4. Fort Union Group - A few slickensides were found in the field associated with lignite beds. No slickensides were found in the laboratory specimens.



5. Pierre Formation - Two borings were drilled in the Pierre. Scattered slickensides were noted in both borings with a marked increase in moisture content, with some slickensides, just above the contact with the underlying Niobrara chalk.

The presence of slickensides is attributed by Fleming et al. (1970) to lateral movements due to stress relief caused by valley formation. The concentration of slickensides found in conjunction with bentonite beds and near the contacts between lithologically different units, illustrates the effects of differential movements between strata with different moduli of elasticity.

The stability of valley slopes in the area studied appears to correlate well with the observed presence of slickensides. Valley slopes in the Pierre, Bearpaw and Claggett are characterized by slump topography and their stability appears to be controlled by residual strength parameters (Fleming et al., 1970). The testholes in these formations were characterized by slickensides. Valley slopes in the Colorado and Fort Union Groups are more stable and have a relative scarcity of slickensides. The Colorado Group consists of shale with scattered bentonite layers but also contains numerous very thin siltstone layers. It is suggested by Fleming et al., (1970) that the siltstone layers increase the stability of the slope "by increasing the cross-bed shear strength and possibly by decreasing lateral expansion in the formation." The Fort Union Group





contains lignite and sandstone layers which provide increased drainage, increase cross-bed strength and would also serve to reduce lateral movement.

5. James MacDonald and Beverly Bridges, Edmonton, Alberta:

During 1970-71 two bridges were constructed across the North Saskatchewan River in Edmonton, Alberta; the James MacDonald bridge in downtown Edmonton (the stratigraphy of which has been previously discussed) and the Beverly bridge in eastern Edmonton. Only a few feet of alluvium overlies bedrock below the river channel and the pier and abutment excavations for these bridges afforded an excellent opportunity to view the bedrock below and adjacent to the river and to observe any effects of valley formation.

One pier excavation was inspected at the James MacDonald bridge and three pier excavations and the west abutment excavation were inspected at the Beverly Bridge. A complete description of the geology exposed is given in Appendix B. A brief summary of the more important observations will be given in this section.

The east pier at the James MacDonald bridge was visited on October 7 and 8, 1970. Two circular holes about 25 feet in diameter were excavated with backhoe and dragline 14 feet into bedrock below the river bed. The stratigraphy exposed is discussed in Appendix B. Jointing exposed consisted of well defined horizontal joints along bedding planes and tight, near vertical joints which terminated in the horizontal jointing system.



A number of the horizontal joints between different bedrock units and between units of shale or sandstone were characterized by a thin ( $\frac{1}{4}$  to  $\frac{1}{2}$  inch thick) soft clay gouge zone. These zones were soft with a pocket penetrometer strength of about 0.5 t.s.f. and had a moisture content close to the plastic limit of the material. A pocket knife blade could be driven to its full length into these zones under only slight pressure. The rock contacts above and below these zones were observed to be smooth and polished, however no slickensides or striae were observed. Vertical joints were tight and did not exhibit any softening.

Similar features were noted in all three bridge pier excavations inspected at the Beverly bridge during August-October, 1971. The soft zones were found developed along horizontal bedding planes in a hard, competent, fine-grained sandstone. Most of the zones could be traced for some 100 feet around the entire circumference of the pit wall.

Pier 2 at the Beverly bridge was typical of the excavations visited on this project. The stratigraphy exposed is illustrated in Figure 3.41 and consisted mainly of hard competent sandstone. Two main gouge zones were observed in this pit, one located about 1.5 feet above the floor of the excavation between two sandstone beds and a second located about 6 feet above the floor of the pit at the contact between a 3 inch thick ironstone bed and the underlying sandstone. Plates 3.1 and 3.2 show the outcrop







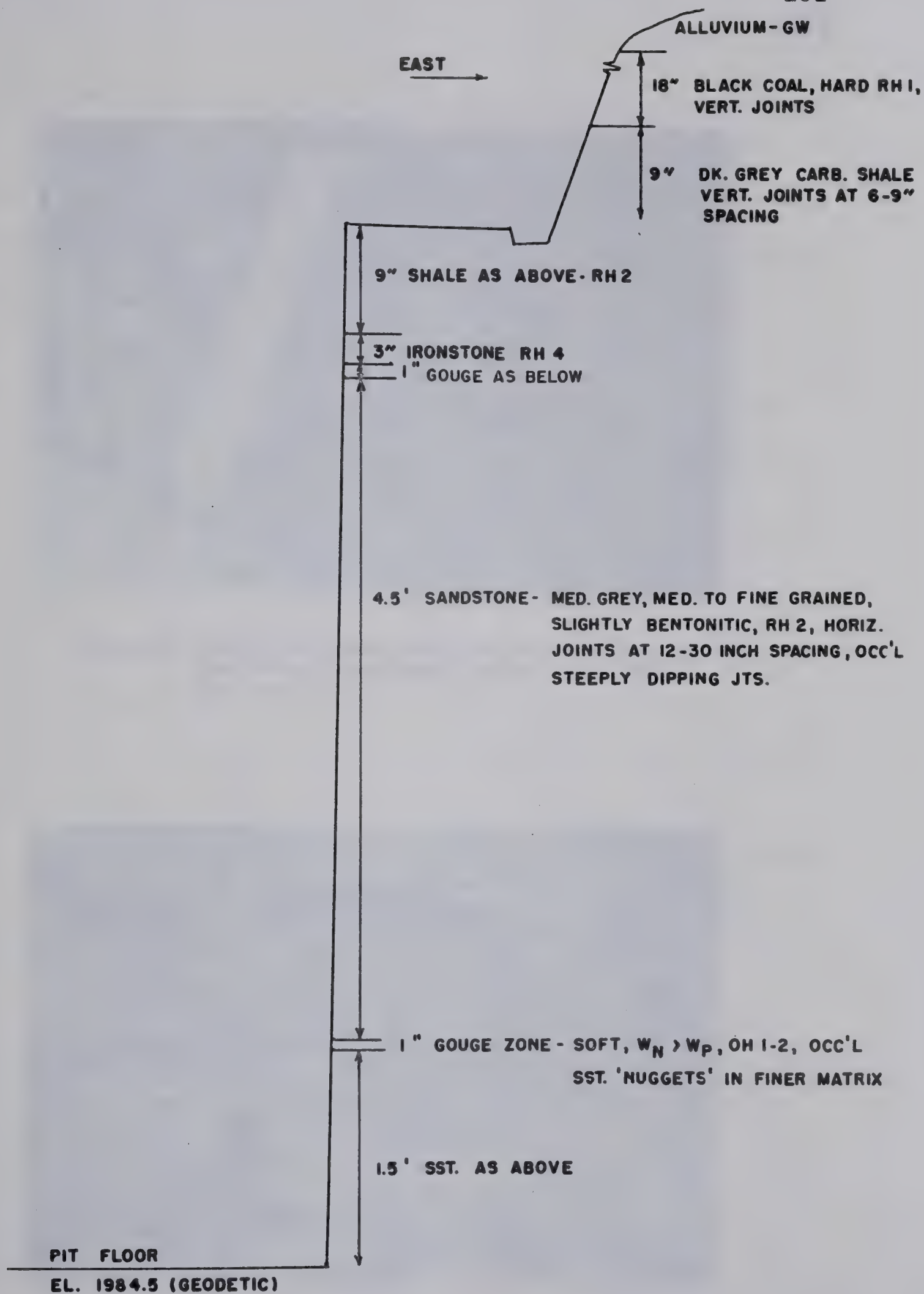


FIG 3.41 GEOLOGIC SECTION, EAST WALL, PIER 2, BEVERLY BRIDGE





Plate 3.1 View of the lower gouge zone on the east wall, Pier 2 excavation, Beverly bridge. Note knife for scale.



Plate 3.2 Closeup of the gouge zone shown in Plate 3.1.







of the lower gouge zone in the east wall of the excavation.

A block sample removed from the bottom gouge zone showed, upon drying, a slight polish indicative of slickensides on the bottom contact of the soft zone with the underlying fine-grained sandstone. This feature could not be seen in the field due to the high moisture content of the gouge zone. The presence of polish and slickensides shows that differential movement has occurred between the rock units below the river. The frequency of occurrence of these soft layers and their nature strongly suggests that they have resulted from lateral movement between the beds. The vertical joints end, as has been mentioned, in horizontal joints developed along bedding planes and no measurement of the amount of movement from joint offsets was possible. No similar features were observed in the bedrock exposed above river level in the west abutment excavation (Appendix B) or in any outcrops in the bedrock of the study area previously visited (Thomson and Matheson, 1970a).

A bentonite bed varying in thickness from 2 to 6 inches was exposed in the west abutment excavation for the Beverly bridge some 60 feet above river level. A smooth, slickensided failure plane was observed on both the top and bottom bentonite-shale contacts both in the field and in a block sample taken to the laboratory for detailed inspection. The striae on these failure surfaces pointed directly towards the river. Plate 3.3 shows the lower bentonite-shale contact in the field and Plate 3.4 shows this contact



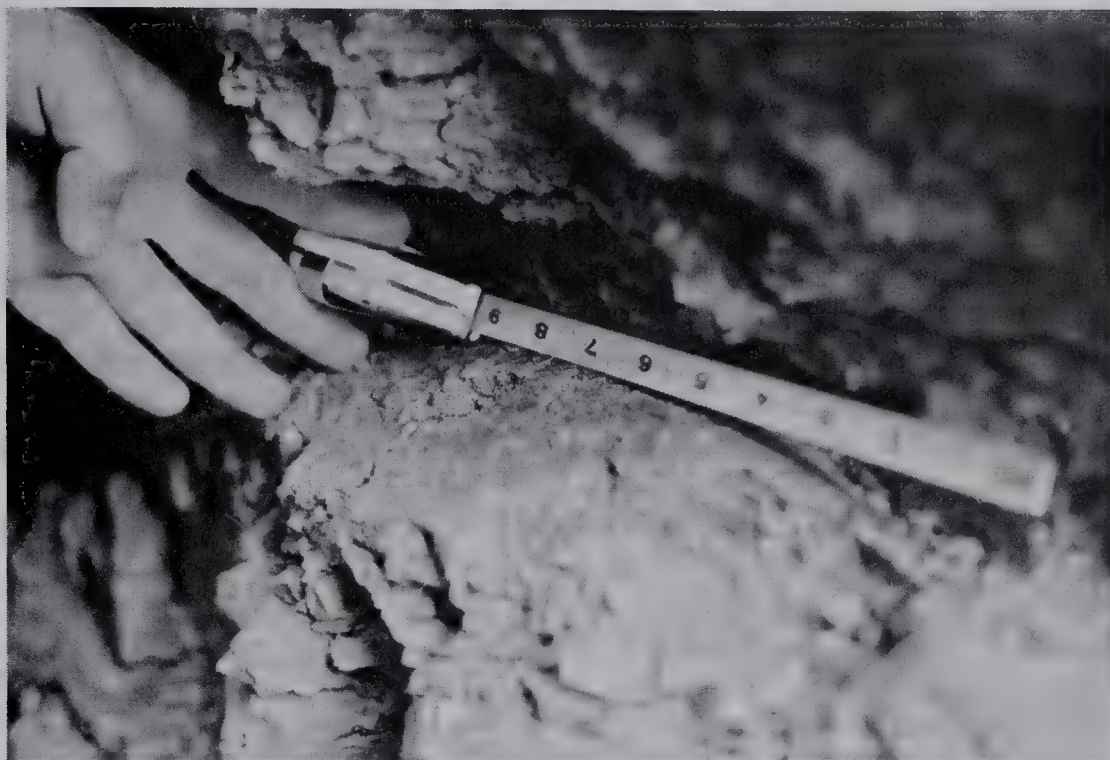


Plate 3.3 View of the slickensided lower shale-bentonite contact in the west abutment excavation of the Beverly bridge.

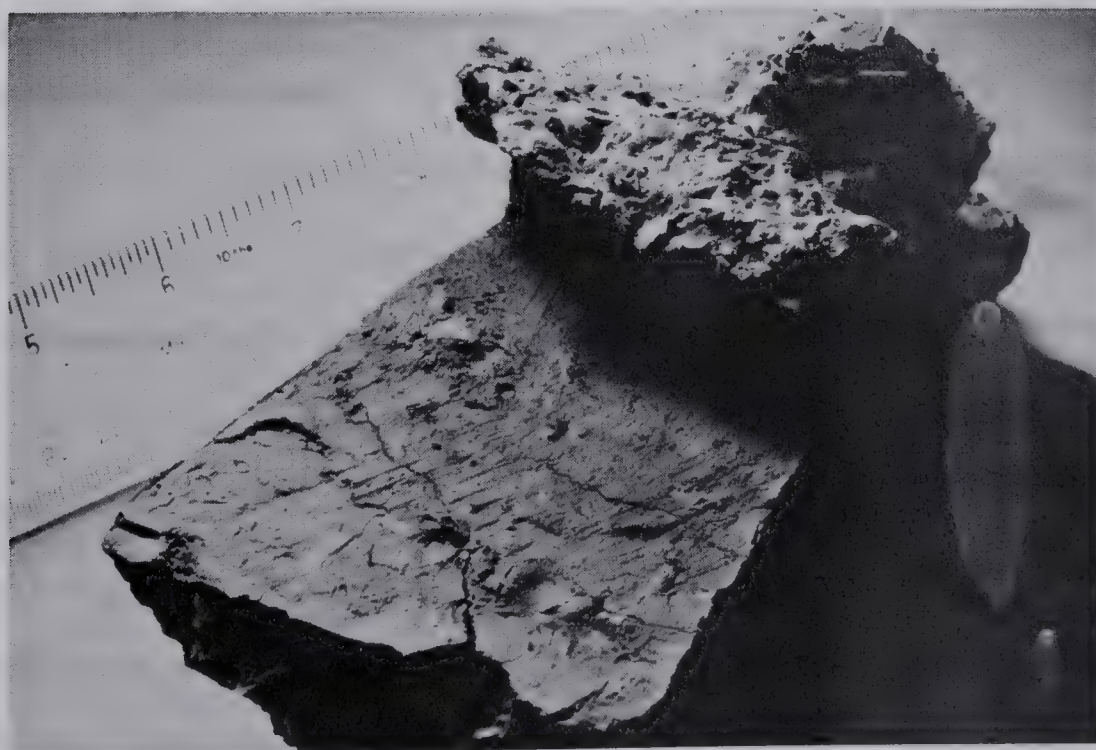


Plate 3.4 View of the shale-bentonite contact cut from the block sample taken in the west abutment excavation at the Beverly bridge. Note slickensides and striae.







when most of the superincumbent bentonite has been removed.

The bentonite was photographed in the field and sampled some 6 to 8 feet back from a near-surface landslide which has developed along the valley wall at this point. These surfaces, which are obviously at the residual strength, were not sheared by any previous landslide or mass-movement process. Details of stratigraphy, sample location and observations are given in Appendix B.

6. Summary: The observations from the South Saskatchewan River Dam test drift, Mangla Dam and the Kimbley Pit show that excavation into overconsolidated bedrock will result in lateral movement towards the excavation as well as rebound of the excavation bottom and upwarping of the rock adjacent to the excavation. The observations made by Fleming et al., (1970) along the Missouri River show that differential movement resulting in slickensides (or actual failure of the rock in-situ decreasing the strength from peak to residual) occurs across bentonite layers or at contacts between rock units of different lithology when a river valley is excavated into the bedrock of the study area. The breakage of cores at the contacts between different rock units, noted by P.F.R.A. at damsites along the North Saskatchewan River, appears to have a similar cause.

The apparent correlation of slope stability with slickenside occurrence along the Missouri River appears to relate the in-situ shear strength of a formation with the amount of lateral rebound which has occurred. The features



noted adjacent to and below the North Saskatchewan River at Edmonton appear to result from lateral differential movement between bedrock units and across bentonite layers. The result, in the case of the bentonite layer observed at the Beverly bridge, is failure in-situ and a decrease in strength to the residual. Subsequent slope stability is then governed by the residual strength parameters (at least along horizontal bedding planes), the occurrence of these pre-sheared layers, and the conventional factors such as piezometric level, slope height, and slope inclination. It is of interest to note that the bentonite layers markedly affect the piezometric conditions in the valley wall as discussed in Appendix B.

### 3.6 The Raised Valley Rim

The rise of the ground surface immediately adjacent to the valley edge has been previously discussed and this feature is due to rebound which occurs below the valley bottom. Evidence to support this mechanism is given by DeJong (1971) who monitored rebound occurring below the 46 feet deep foundation excavation for the A.G.T. complex in downtown Edmonton, Alberta, which is cut through dense glacial till. A maximum rebound of about 3 inches occurred in the excavation center; rebound points established on a building 20 feet back from the excavation edge showed a heave of about 0.3 inch.





WEST

EAST

VERT. MOVEMENT (FT.)

.10  
.05  
.00

.10  
.05  
.00

CIVIL ENGINEERING BLDG.

STIFF OVERCONSOLIDATED DIAMICTON (TILL-LIKE MATERIAL)

TRENCH

30'

20'

DENSE SANDS (BED OF GLACIAL LAKE EDMONTON)

SCALE (FT.) 0 5 10 20

1 - 2 FT. IRON PIN

FIG. 3.42 REBOUND ADJACENT TO UTILITY TRENCHES, U. OF A. CAMPUS



effect of postglacial erosion cannot be studied quantitatively - in some cases it appears to accentuate the raised rim while in other cases it appears to obliterate it. However, the feature was observed with such frequency that it was considered of interest to document its occurrence.

A brief airphoto study of sections of the Peace, Wapiti, Smokey, Little Smokey, Athabasca, Red Deer and South Saskatchewan Rivers was made. Field trips were made during the summer of 1970 to several of these areas to obtain profiles perpendicular to the valley edge to assess the relative magnitude and frequency of occurrence of this phenomena. A study of the finite element displacements shown in Figure 3.10 reveals a decrease in the amount of vertical rebound adjacent to the excavation for high values of  $K_0$ ; it was hoped a combination of field measurements of raised rim profiles, valley cross-sections and use of the finite element method would yield information on the in-situ stress conditions existing in the respective bedrock formations. Details on the areas visited and the profiles obtained are given in Appendix C. Figure 3.43 shows a map of the Province of Alberta showing areas where evidence of the raised valley rim has been observed.

Two valley cross-sections illustrating the effect are shown in Figures 3.44 and 3.45. Figure 3.44 shows profiles taken on both sides of the South Saskatchewan River at Redcliff, Alberta, 5 miles upstream of Medicine Hat. The banks of the South Saskatchewan River for about 15 miles





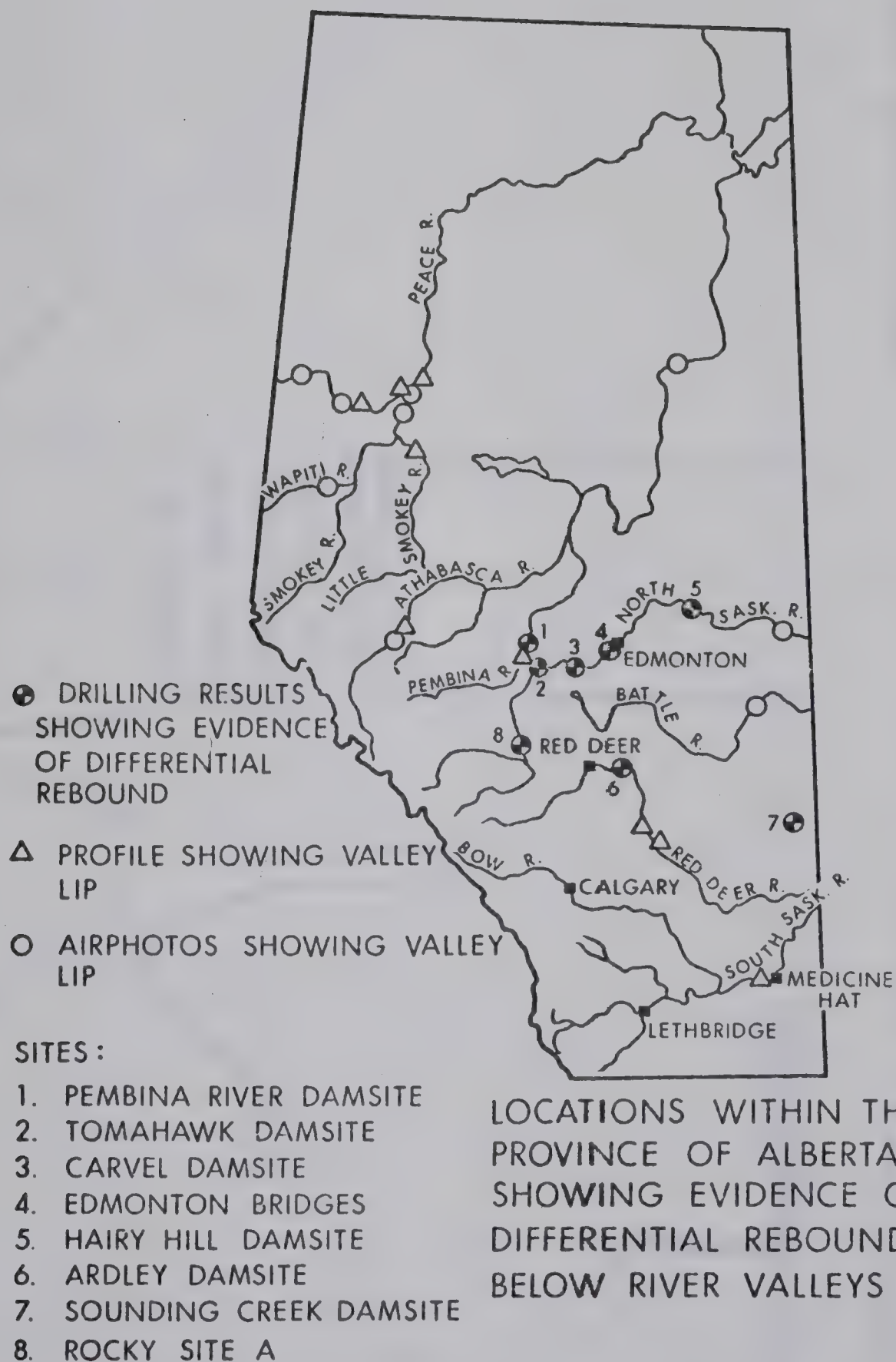


FIG. 3.43

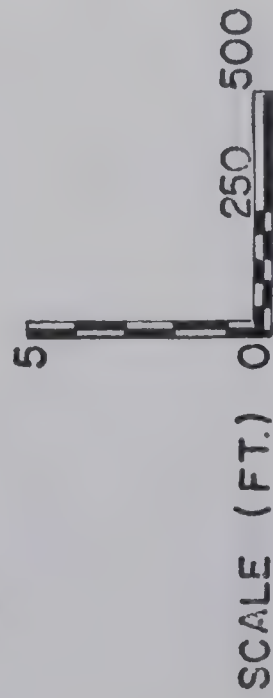


SOUTH

NORTH

PARALLEL TRIBUTARY

VALLEY OF  
THE SOUTH  
SASKATCHE-  
WAN RIVER  
1400 YD. WIDE  
200 FT. DEEP



PROFILE SOUTH SASK. 2  
SOUTH SIDE OF RIVER AT REDCLIFF

PROFILE SOUTH SASK. 1  
NORTH SIDE OF RIVER AT REDCLIFF

FIG. 3.44





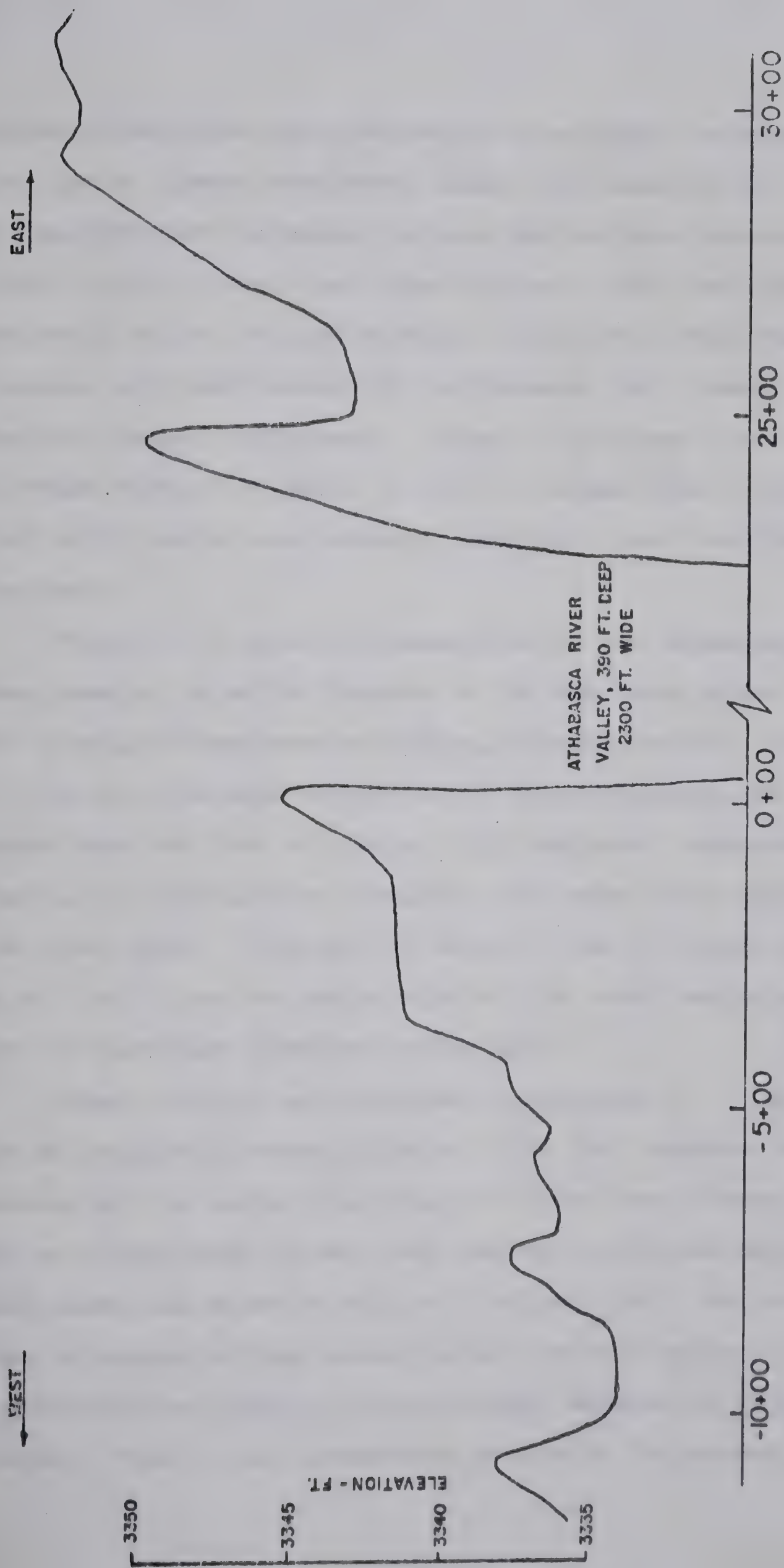


FIG. 3.45 ATHABASCA-OLDMAN DAMSITE PROFILE, LINE DD



upstream of Medicine Hat provided an area where the raised valley rim is almost continuous along both sides of the river except where tributary valleys and coulees intersect the main valley. The river flows through a 200 feet deep postglacial valley incised through a relatively thin veneer of glacial till and bedrock of the Foremost and Oldman formations (Upper Cretaceous). Figure 3.44 shows a rise in the ground surface of about 12 feet on either side of the valley which begins approximately 1800 feet back from the valley edge.

Figure 3.45 shows the centerline of the Athabasca-Oldman Damsite (line DD) located on the Athabasca River about 40 miles downstream of Hinton, Alberta (A.W.R., 1969a). The river cuts through a postglacial canyon incised 390 feet through about 40 feet of glacial till and hard, cemented sandstone of the Paskapoo formation with some shale occurring below river level. The profile shows a rise in ground surface of 3 to 6 feet on either side of the river beginning about 150 feet back from the valley edge.

Other profiles are included in Appendix C. A compilation of results is shown in Table 3.4. The increase in elevation of the valley rim relative to the mean ground level on either side of the river valley is plotted against valley width and depth in Figures 3.46 and 3.47. An increase in height of the raised valley rim with valley depth and width occurs although a considerable scatter of results is noted. This is not unexpected in view of the number of





TABLE 3.4

## COMPILATION OF RIM SURVEY RESULTS

River	Bedrock	Overburden Type	Thickness	Age	Valley Characteristics Width(ft.) Depth(ft.)	Slopes	Rim Height(ft.)	D <sub>c</sub> (ft.)
1. Pembina	Paskapoo & Edmonton	Till Silts	20 ft.	Postglacial	1,100 150	2:1	6	400
2. Peace River	-	Silts Till	60 ft.	Postglacial incised into preglacial	16,000 500	10:1	15	10,000
3. Tributary to Peace	-				5,000 500	4:1	2	300
4. Little Smokey	Puskaskau formation	Till	200 ft.	Postglacial?	3,000 300	6:1	3	900
5. Claypit 14	Oldman formation	Till	20 ft.	Excavation	600 70	4:1	1.2	35
6. South Saskatchewan (4) (5) (3) (1) (2)	Oldman	Till	20 ft.	Postglacial	4,200 325 4,200 325 5,700 300 4,200 200 4,650 200	3:1	9 21 5 13 16	800 3,100 700 1,800 1,800
7. Cypress Hills	Ravenscrag Frenchman Whitemud	Tertiary Gravels	50 ft.	Postglacial	6,000 600		1	250
8. Michichi Creek	Edmonton formation	Till	30 ft.	Postglacial	1,300 250	1:1	4	70
9. U. of A. trenches	-	Till?(20') Sand below		Excavation	17 30	4:1	0.04	100
10. Athabasca-Oldman DD	Paskapoo	Silts Till	50 ft.	Postglacial	2,300 390	1:1	8	600
11. Missouri 1	Pierre shale			Postglacial	17,000 360		40	2,500

Note: D<sub>c</sub> refers to the horizontal distance from valley edge to the point of upward rise of the ground sfc.



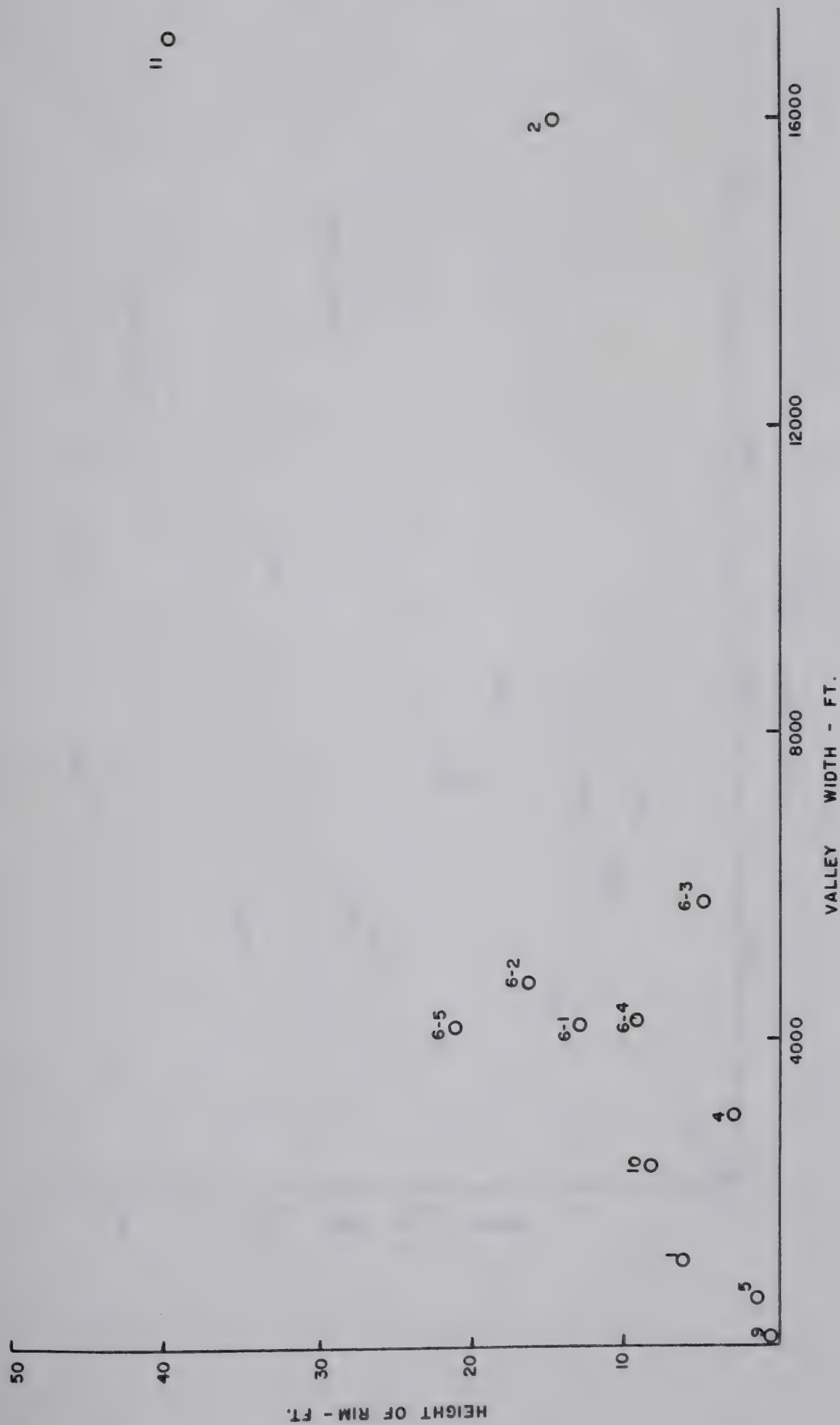


FIG. 3.46 HEIGHT OF RAISED RIM VERSUS VALLEY WIDTH





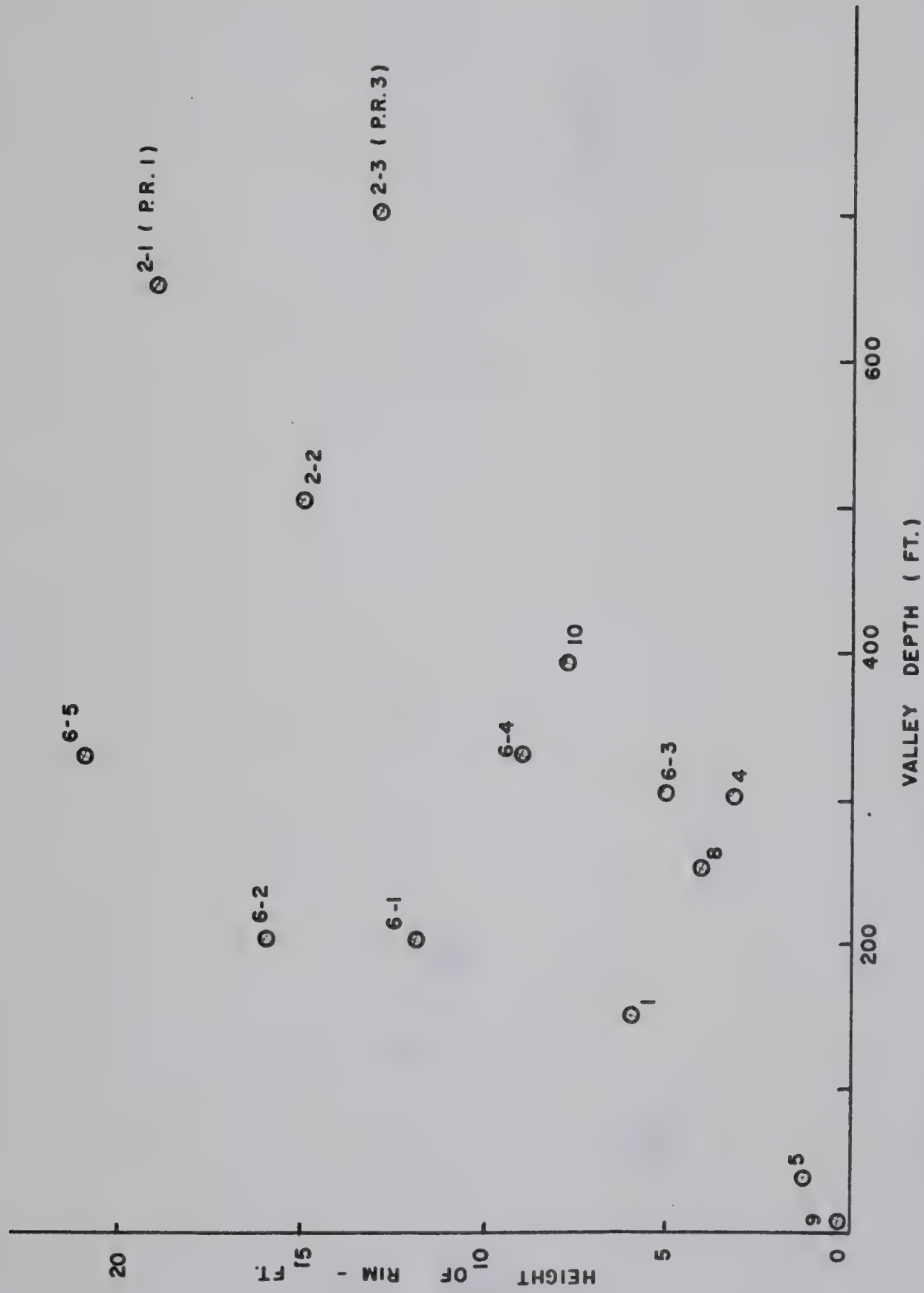


FIG. 3.47 HEIGHT OF RAISED RIM VERSUS VALLEY DEPTH



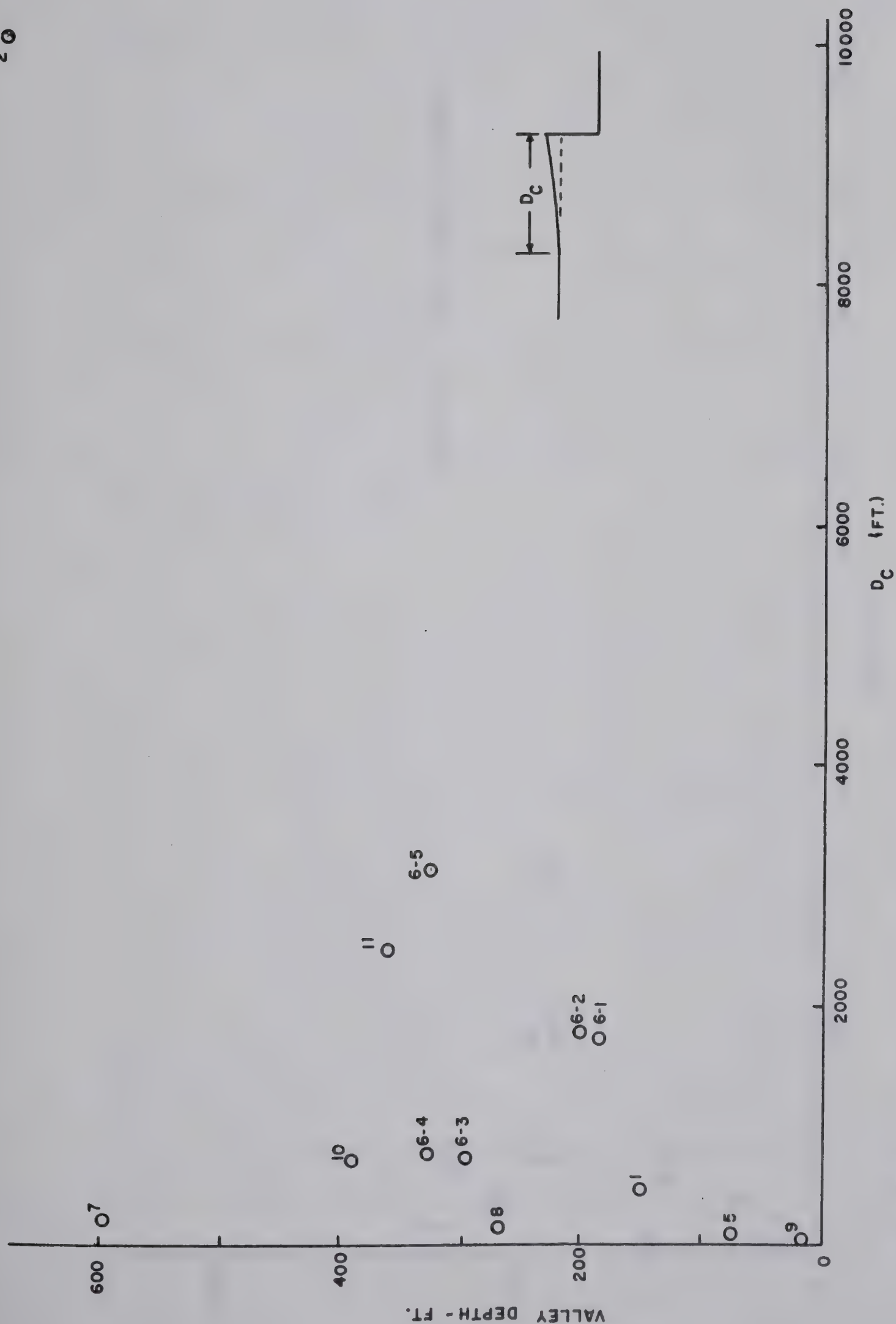


FIG. 3.48 WIDTH OF RAISED RIM VERSUS VALLEY DEPTH





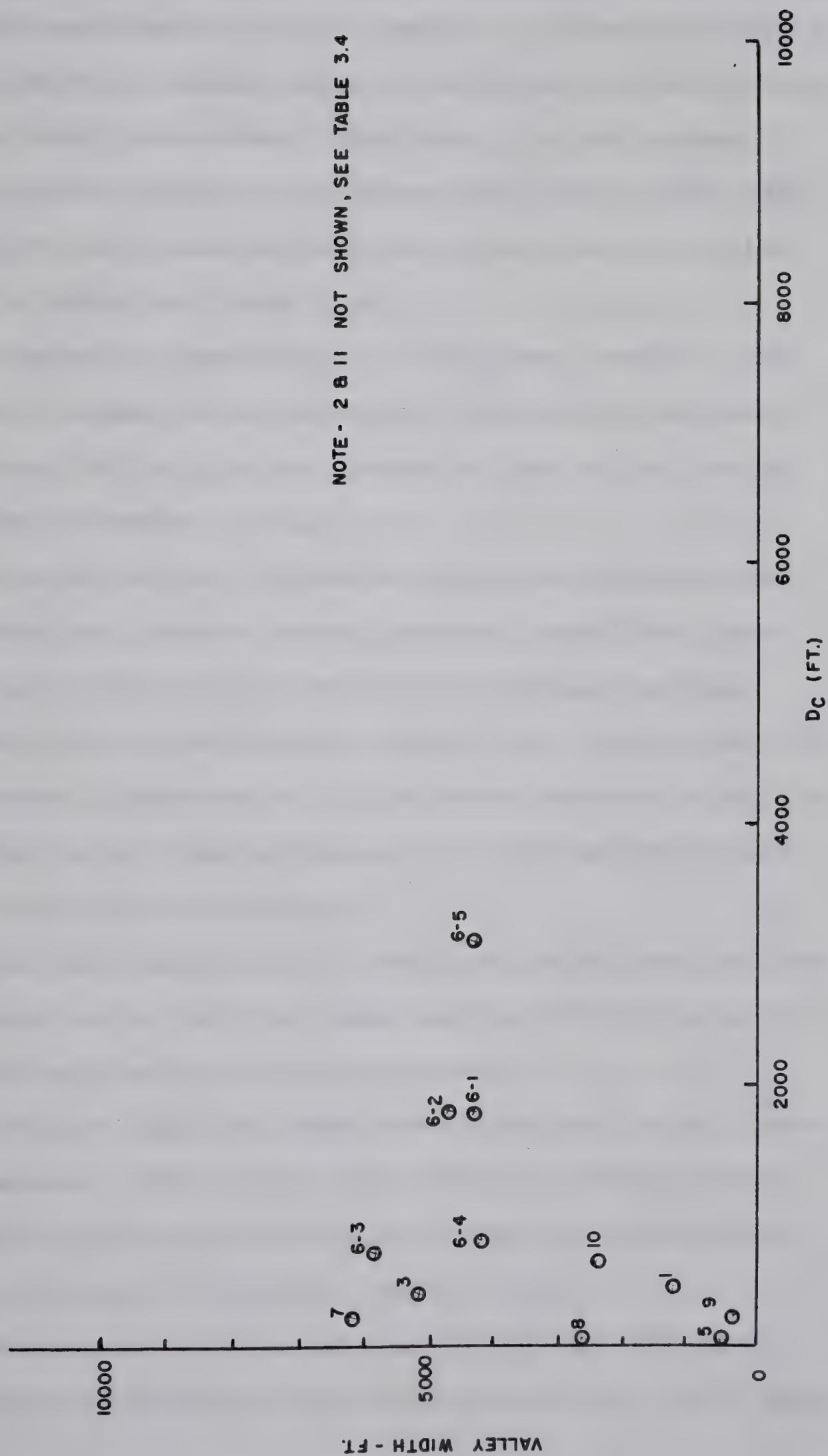


FIG. 3.49 WIDTH OF RAISED RIM VERSUS VALLEY WIDTH



variables, which have been mentioned previously, which would affect the development of this feature. A general trend to a greater width of raised rim with valley depth can be noted in Figure 3.48. No evident relationship exists between width of raised valley rim (distance from valley edge back to the point the ground surface begins to rise) and valley width as is shown in Figure 3.49.

A number of topographic features were noted on air-photos which appear to be associated with the development of the raised valley rim and rebound of the valley bottom.

These features include:

1. sloughs and wet depressions paralleling the valley edge and located several hundred yards back from the valley rim at the point the ground surface begins to rise into the valley rim. In a number of cases, a depression in the ground surface parallels the valley edge and appears to be associated with the raised rim effect.
2. parallel gulleys and tributaries which parallel the main valley wall for some distance before entering the main valley at right angles.
3. reversed drainage where the valley rim is well pronounced. Drainage is away from the valley trench and only a few major tributaries have breached the valley rim to enter the main valley.
4. development of flooded depressions and swamps on terraces elevated well above the present river level.





Rapid downcutting of the river channel has produced rebound along the river edge of the elevated terrace which contributes to the formation of swamps and sloughs on these terraces.

These features will be discussed in more detail in Chapter VII of this thesis. Several general points regarding the occurrence of the raised valley rim were noted in the course of the study.

1. The feature is best developed immediately above a steep, stable valley wall. For example, along the Pembina River the feature was best developed immediately above the outside of meander bends where the valley wall was inclined at about 1:1. Typically, no evidence of a raised rim was present above slip-off slopes where the valley wall was inclined at about 5:1.
2. A number of the valleys visited, notably the Peace River between Dunvegan and Peace River town and the Red Deer River in the vicinity of Drumheller, showed little or no sign of a raised rim along the main valley. However, a raised rim occurred along valleys and coulees tributary to the main valley.
3. The raised rim appears to be best developed where glacial deposits are thin.

The raised valley rim is surface expression of flexure in the bedrock of the valley walls. At a number of the dam-sites discussed previously, notably Hairy Hill, Carvel and



Boundary, clear evidence of upwarping of the strata in the valley walls exists from drilling results but no raised valley rim occurs. At Hairy Hill Damsite the irregular surface topography has obscured the effect while erosion has apparently removed the raised rim at Carvel Damsite and Boundary Dam.

Valley flexure should cause bedrock strata, if initially flat-lying, to dip gently into the valley wall on both sides of the valley. This phenomena has been noted by Underwood (1964) in the Niobrara formation along the Missouri river as discussed in Chapter II. Attempts to measure this effect in outcrops along several river valleys in Alberta met with little success due to the scarcity of outcrops undisturbed by slumping and the absence of marker beds where a dip could be measured to the required accuracy.

However, at several locations in the study area, valley flexure can be observed in the field. The upwarping of the coal beds towards the valley at Boundary Dam, Plates 2.1 and 2.2, has been discussed previously. A similar feature is visible in an apparently undisturbed outcrop of the Edmonton formation in a highway cut on the north bank of the Sturgeon River near Gibbon, Alberta, approximately 17 miles northeast of Edmonton. A view of the outcrop is shown in Plate 3.5 which consists of white-weathering bentonitic sandstone interbedded with several thin grey bentonite layers. A rise in the beds towards the valley is visible.







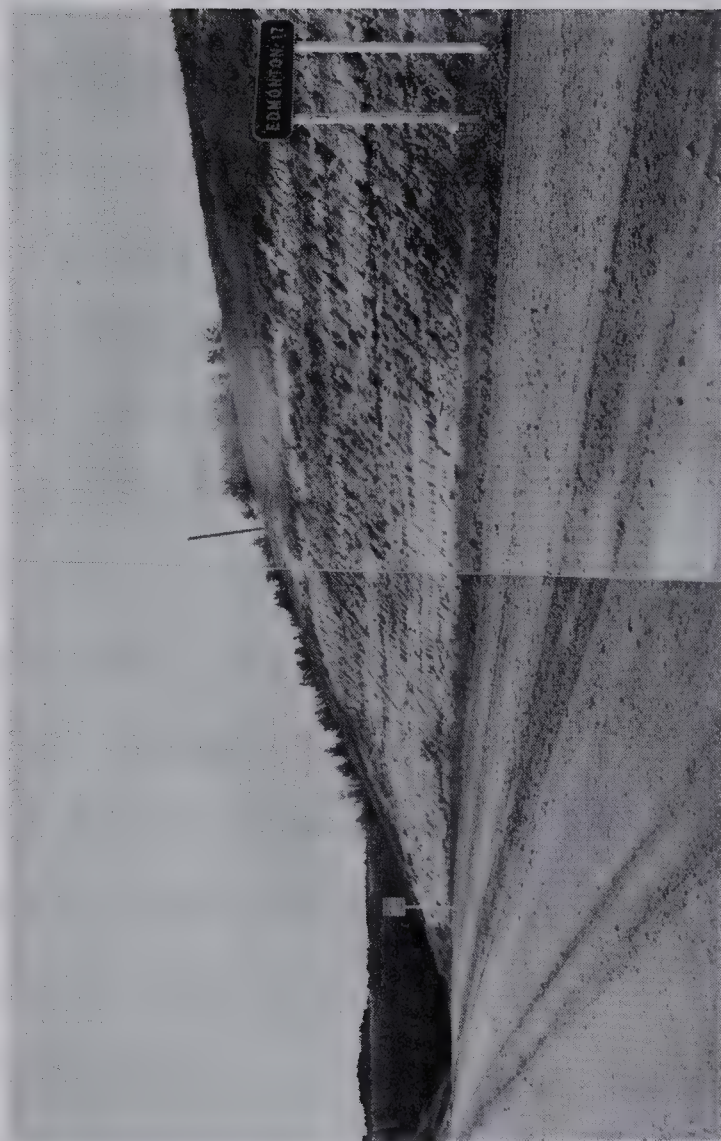


Plate 3.5 View of the west side of a roadcut on Highway 37 near Gibbons Alberta. Note the slight rise in the beds towards the valley of the Sturgeon river in the background.



A survey made on the outcrop of one of the bentonite beds, located approximately halfway up the slope, is shown in Figure 3.50. The regional dip of the bedrock is 20 to 40 feet per mile to the southwest (Carlson, 1966) and a flattening of dip and actual rise of the marker bed occurs as the valley is approached. No evidence of slumping was visible in the outcrop. It should be noted that no equivalent road-cut exists on the south side of the Sturgeon Valley at this point and it was not possible to observe the behaviour of the strata on the opposite side of the river.

Local variations in dip or 'rolls' have been documented in the Edmonton formation (Pearson, 1959) and are considered due to ice movement during the Pleistocene. It is possible that the upwarping of beds noted at Gibbons and Boundary Dam is due to local variation in dip due to ice movement or depositional environment. The weight of evidence showing the ubiquitous occurrence of valley rebound, valley flexure and raised valley rim makes this a somewhat remote possibility.

No attempt was made in this study to document the frequency of occurrence of a raised valley rim along a given section of river although in certain areas, such as along the South Saskatchewan River near Redcliff, Alberta, the raised rim occurred along most of the valley crest for a number of miles. Plate 3.6 shows a view of the raised valley rim near Drumheller.

The feature is certainly very common along the Missouri





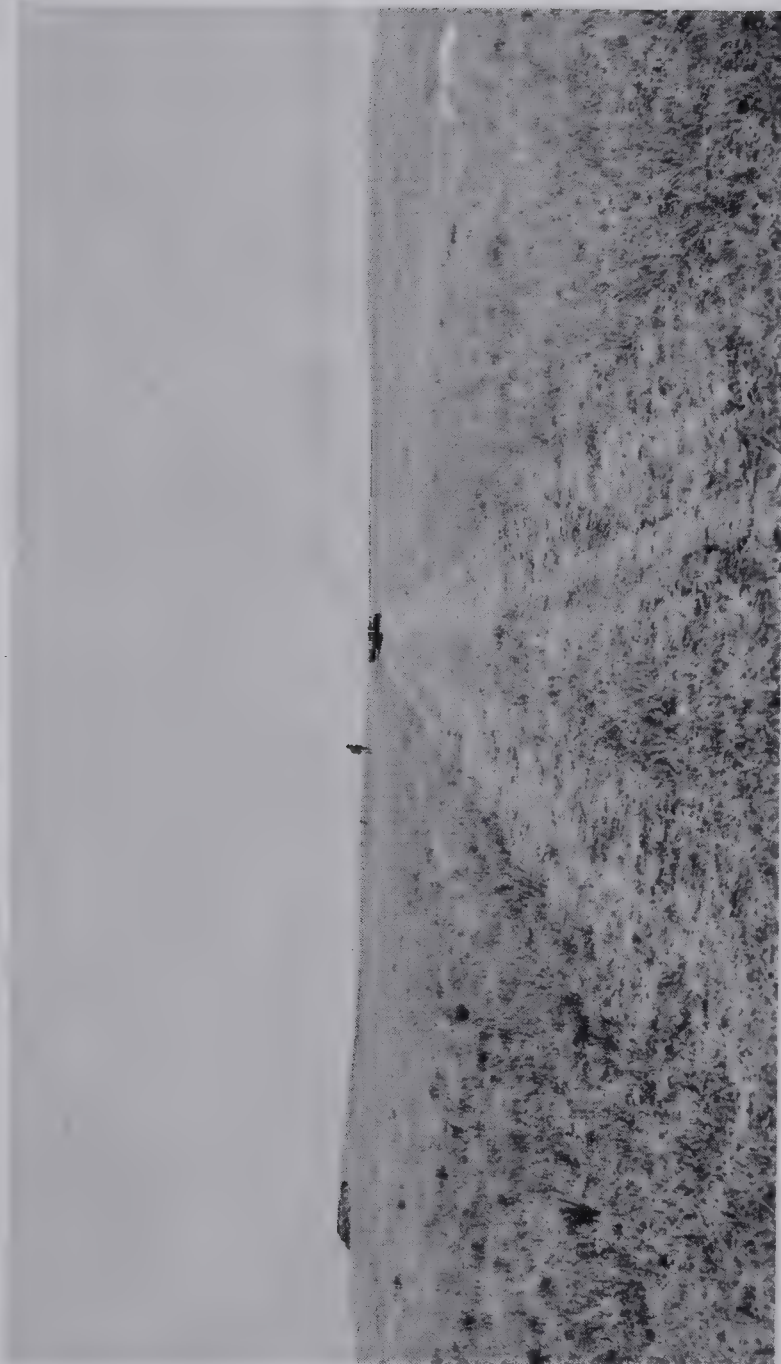


Plate 3.6 View of raised valley rim near Drumheller Alberta with the valley of Michichi Creek to the left of the photo. The photo is taken looking south along the neck of land where profiles M 1 - M 4 were surveyed.



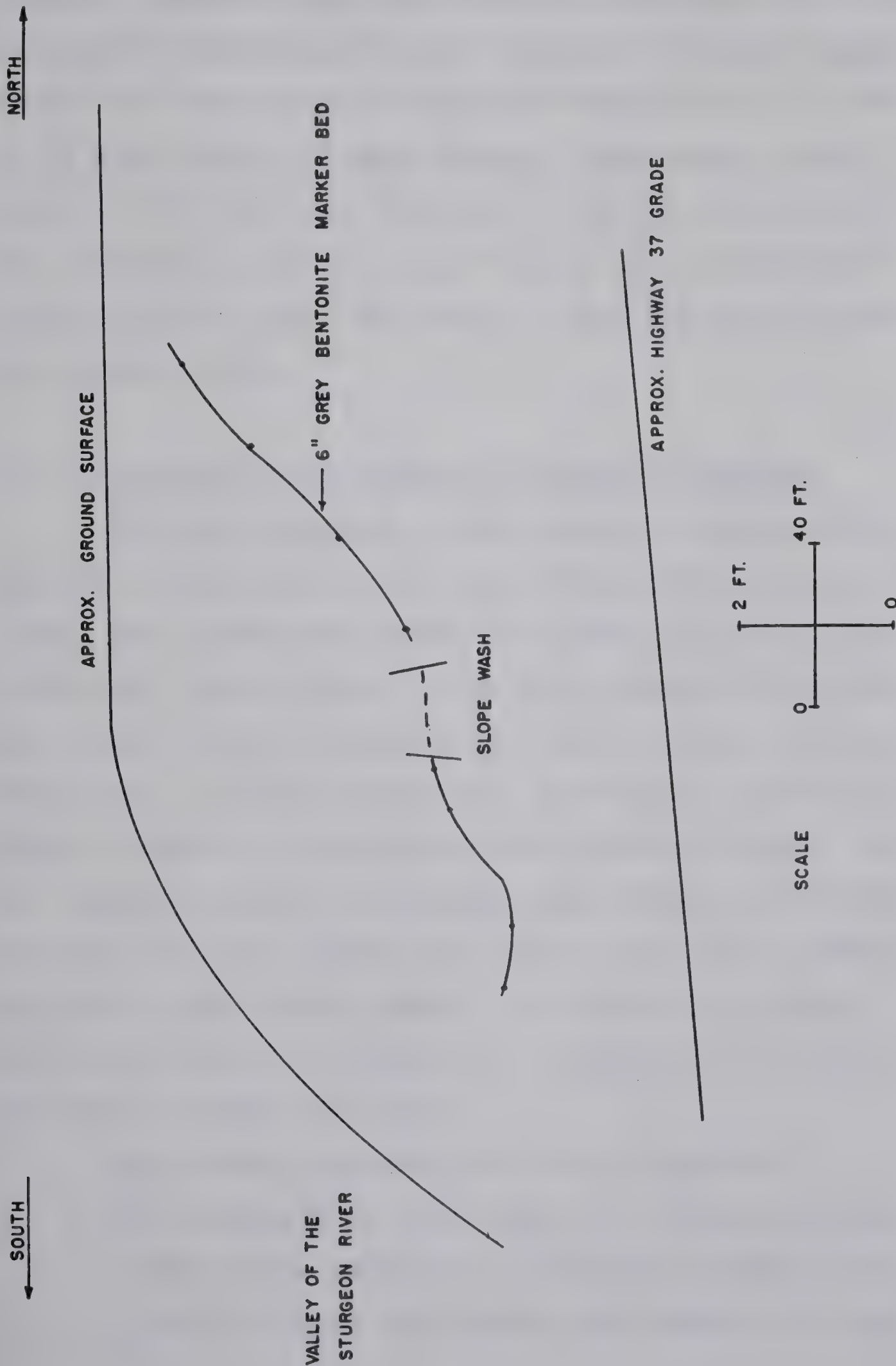


FIG. 3.50 SECTION OF HIGHWAY 37 CUT NEAR GIBBONS ALBERTA





River in South Dakota as was discussed previously in this chapter. Raised valley rims are also prevalent along other reaches of the Missouri River. Profiles of slopes mapped by the U.S. Army Corps of Engineers (Fleming et al., 1970) at 23 sites along the upper Missouri show raised valley rims at 9 of the sites, no rims at 3 of the sites and at the remaining 11 sites the profile was not extended back from the valley crest far enough to show the behaviour of the ground surface.

### 3.7 Discussion of the Geologic Evidence of Rebound

The data presented in this chapter indicates that wherever a major river valley has downcut through the relatively soft, overconsolidated, Cretaceous bedrock of the study area, large amounts of vertical rebound occur below the valley bottom accompanied by valley flexure and, in some cases, a raised valley rim. Faulting or crushing of beds, as noted in the Pennines and Allegheny Plateau, do not appear to occur in the study area although some disturbance of the upper bedrock was noted in the large diameter testpits at the Ardley Damsite. No evidence of plastic failure or bulging as documented in England and Europe has been noted in the study area.

Two primary problems must now be considered:

1. The mechanism(s) which cause the valley anticlines noted in the study area, the valley bulges in England and Europe and failure and crushing of strata



documented below the valleys in the Pennines and the Allegheny Plateau.

2. The effects of this behaviour on the properties of the bedrock below and adjacent to the valley.

Mechanism of Rebound: It would appear that three distinct types of feature have been documented below river valleys in various parts of the world. The "wrinkles" noted by Watts (1906), Lapworth (1911) and Sandeman (1918) below valleys in the Pennines in England occur in hard competent rock. Sandeman (1918) notes rock from the Millstone grits, which immediately overlies the Yoredale Rocks in the valley bottom, was quarried and used to build the Derwent and Howden dams. The unit weight of the quarried rock varied from 137 to 150 p.c.f. and it had a "crushing strength from 400 to 500 tons per square foot" (Sandeman, 1918, p. 165). The rocks in-situ appear to have failed in a brittle mode with a sharply defined buckle located under the center of the valley.

The valley bulges discussed by Hollingworth et al., (1944) and Zaruba (1956) occur in soft plastic shales or clays. Evidence of plastic failure and flow have been documented. The observations of Rowe (1968) at Staunton Harold dam indicate the rock below the valley has either failed under high lateral stress or been badly weathered. The presence of shale fissured into "lumps the size of dice" and a low undrained strength (a mean of 17 p.s.i.) indicates some process has greatly reduced the strength and competency





of the rock.

The observations of Ferguson (1967) on dam core trenches in the Allegheny Plateau indicate thrust-faulting of competent members and plastic failure and flow of weaker members.

A number of mechanisms have been proposed to explain the cause of these features. Lapworth (1911) attributed the broken and contorted strata below valley bottoms to landslide activity on either side of the valley although other possible causes mentioned included the weight of the sides of the valley and high lateral pressure crushing the strata below the valley.

Hollingworth et al., (1944, p. 27) considered the valley bulges in the Northampton Ironstone field to be due to differential loading as the "excess load on either side of the valley would cause a squeezing out of the clay towards the area of minimum load with a consequent forcing up of the rocks in the valley bottom". Weathering of the rocks, swelling of the clay due to wetting and loading of the valley walls by ice during the later stages of glaciation were also considered possible mechanisms of bulging. Kellaway and Taylor (1952) consider the valley bulges to be due to formation of ice-lenses as has been previously discussed.

Mechanisms suggested by Zaruba (1956) to explain valley bulging include plastic deformation of the underlying clayey rocks under differential load and swelling due to load removal.



Ferguson (1967) considers the folding and thrust-faulting noted below river valleys in the Allegheny Plateau to be due to high lateral stresses which fail the rock below the river valley in a manner analogous to a strut in compression.

Several of the proposed mechanisms appear somewhat unlikely. Landslide behaviour at the Beverly bridge is described in Appendix B and it appears unlikely that slide activity could cause the features noted in the pier excavations at this site. Landslides occur at a number of sites in the study area where a well defined valley anticline is documented but, as will be discussed later, it appears more likely that they are the result of this feature, not the cause of it. High artesian pressures may be postulated as the cause but none exist presently at Staunton Harold dam (Rowe, 1968).

Periglacial phenomena may be the dominant mechanism which formed the valley bulges in Britain and Europe, however, insufficient knowledge presently exists on the mechanism of formation of ice lenses in bedrock to allow a qualitative analysis of this mechanism.

Two main mechanisms exist which can be evaluated using present knowledge of the mechanics of materials.

1. Failure of the rock below the valley under high lateral stresses in a manner analogous to buckling of a laterally loaded strut.
2. Vertical rebound of the rock below the valley bottom





due to removal of superincumbent overburden and bedrock. The rebound would have both immediate and time-dependent (or swelling) components.

The mechanism of folding and fracturing of laterally loaded strata has been studied by various geologists using elastic and visco-elastic theory as discussed by Ramsay (1967). The theory of elasticity has been used by Price (1967) to study the initiation of folds and buckling of bedrock in the upper portion of the earth's crust where temperatures and confining pressure are relatively low.

The Euler buckling criteria was used by Price (1967) where the force to initiate buckling ( $P_{\text{critical}}$ ) was taken as:

$$P_{\text{critical}} = \frac{\pi^2 EI}{L^2} \quad (3.1)$$

where  $E$  is the modulus of elasticity of the rock,  $L$  is the length of rock unit and  $I$  the moment of inertia. For a rectangular strut  $I = d^3b/12$  where  $d$  is the depth and  $b$  is the width of the unit.

If a bed of rock of depth  $d$  and length  $l$  below the bottom of a valley is considered and it is assumed that no cohesion acts across the bottom contact of this bed then the stress required to initiate buckling using this criteria is:

$$\sigma_{\text{Critical}} = \left( \frac{\pi^2 E}{12 \frac{L}{d}} \right)^2 \quad (3.2)$$



Euler's buckling criteria ignores the effect of the weight of strut and any vertical pressure due to superincumbent rock or overburden.

The critical stress required to initiate buckling is shown in Figure 3.51 for lengths of strut of 500 and 1000 feet, moduli of elasticity of 100,000 and 1,000,000 p.s.i. and thicknesses of bed up to 20 feet. The results indicate that buckling of the upper layers below the valley could occur under lateral stresses of a few hundred p.s.i. if the bedrock is divided into a layered medium with no cohesion between the beds.

A more representative criteria would include the self-weight of the strut. Goldstein (1927) found for a clamped strut there is stability for any length when

$$R < \sqrt{4KB} \quad (3.3)$$

where R is the buckling force, B is the flexural rigidity and K is the force (on unit weight) resisting buckling. The critical stress, below which buckling cannot occur, is shown in Figure 3.52 for E varying from 10,000 p.s.i. to 1,000,000 p.s.i. This figure shows buckling is not possible in a competent stratified rock mass unless lateral stresses in the order of several thousand p.s.i. exist and the rock is bedded into individual layers a few feet thick.

Information on in-situ stresses and a detailed description of stratigraphy and bedrock properties at a location is scarce. However, data from Portage Mountain Dam





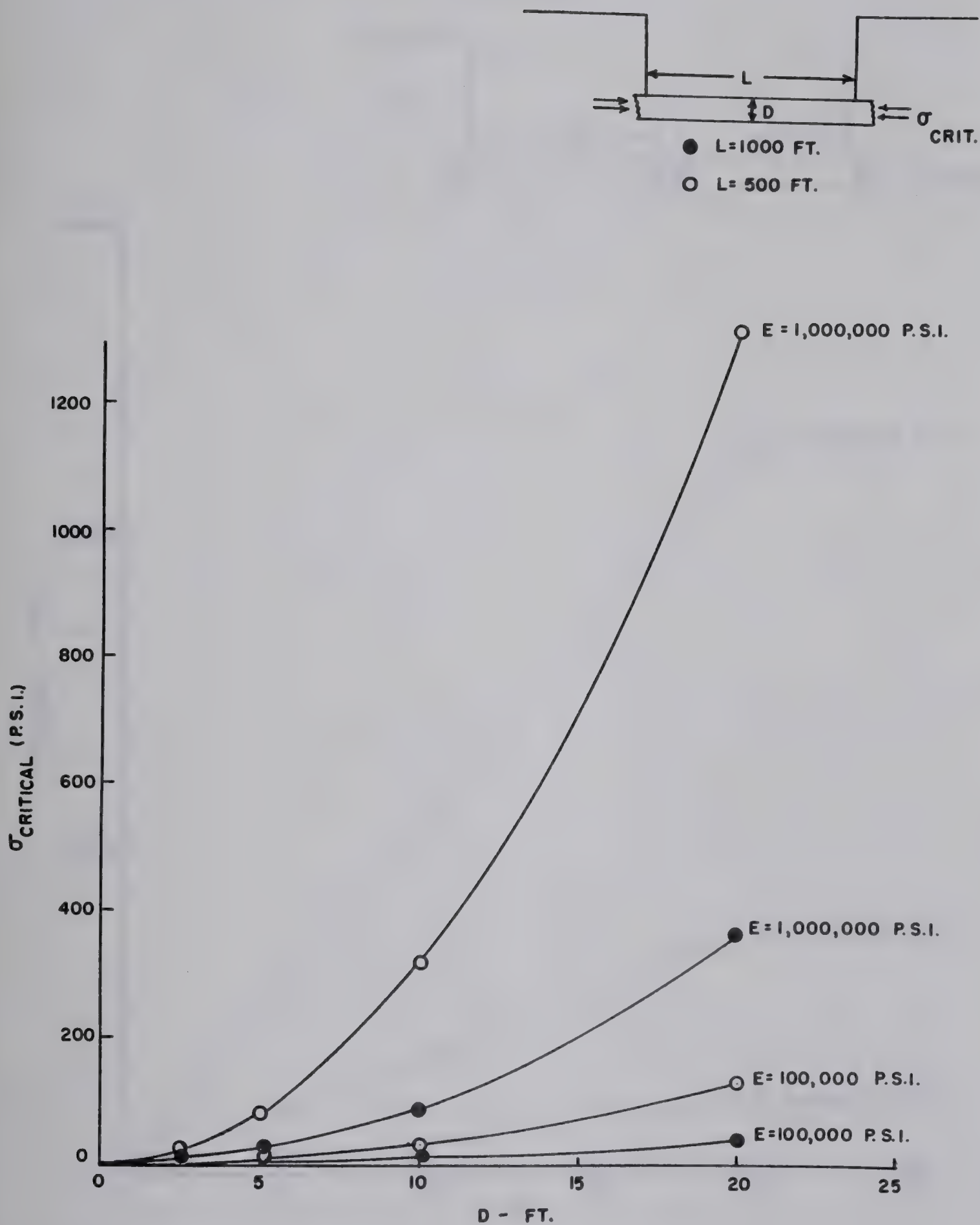


FIG. 3.51 CRITICAL STRESS FOR BUCKLING TO OCCUR (EULER'S CRITERION )



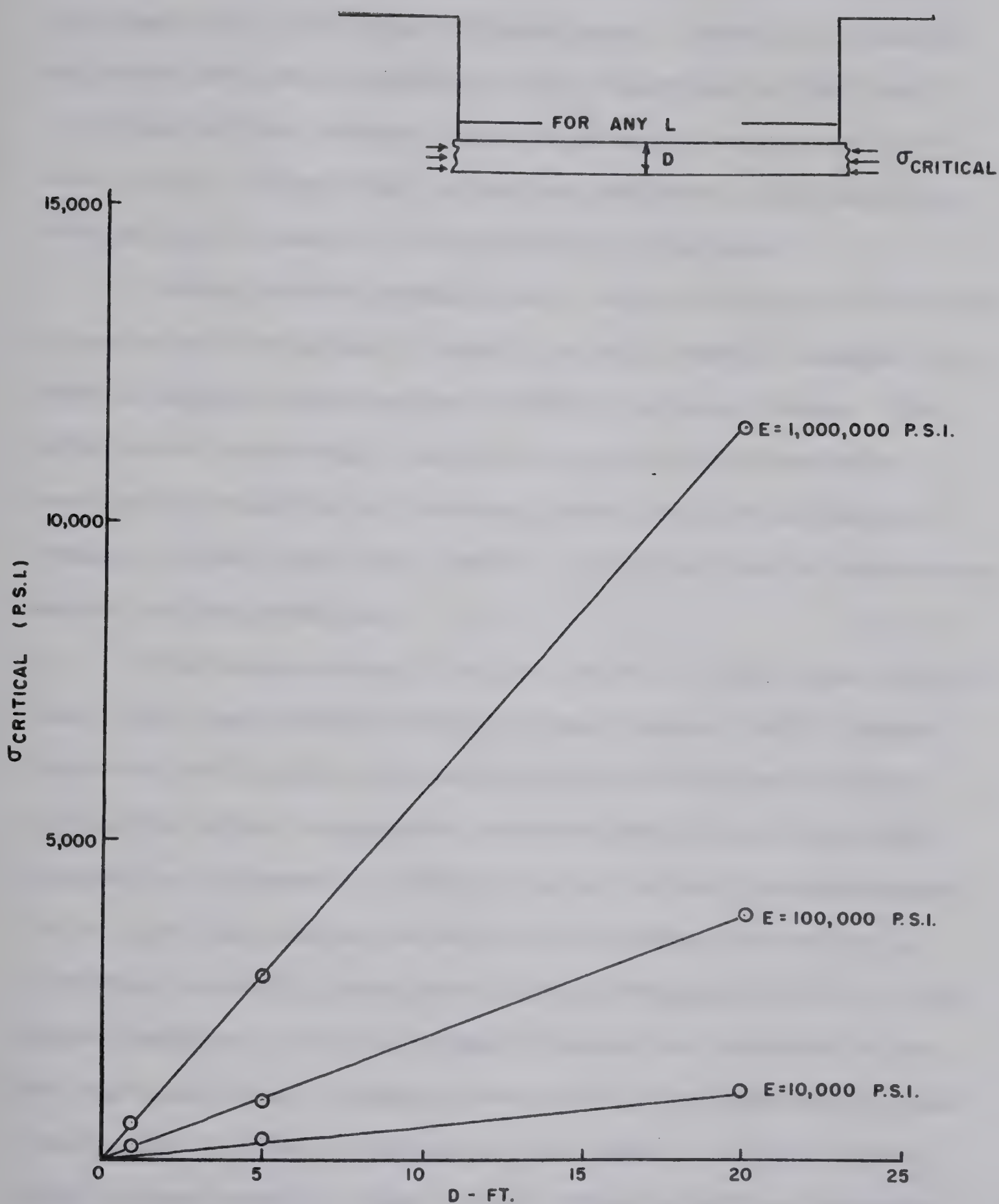


FIG. 3.52 CRITICAL STRESS FOR BUCKLING TO OCCUR IF SELF WEIGHT IS INCLUDED





indicates maximum lateral stresses in the order of several thousand p.s.i. do exist at this site. Assuming a modulus of elasticity of 1,000,000 p.s.i., buckling in the top 3 or 4 feet of the bedrock appears possible using the Goldstein model. The Euler criterion indicates that buckling of the top 30 feet of the bedrock is possible.

These results assume that, over the depth of buckling, there exists an intact, ideally elastic member bounded by a bottom bedding plane across which no cohesion acts. The effects of frictional forces along the bottom surface, sequential buckling of several layers and the effects of joints in the layer are ignored. Interbedding of the strata would inhibit buckling.

The observations from the Derwent Valley dams (Sandeman, 1918) and Portage Mountain Dam (Imrie, 1967), where alluvial infillings were observed along bedding planes, indicates actual separation between beds below the valley bottom has occurred. Buckling under lateral stress appears to be the only mechanism which could cause this effect. The open bedding planes described by Ferguson (1967, p. 64) below valleys in the Allegheny Plateau are apparently due to the same cause. These three areas, the Pennines in England, the Allegheny Plateau in the eastern United States and Portage Mountain Dam in the foothills of the Canadian Rockies, may have high tectonic lateral stresses due to ancient or present mountain building. Numerous cases where high lateral stresses have been measured underground are



reviewed by Jaeger and Cook (1969) and horizontal stresses of relatively large magnitude (several thousand p.s.i.) have been measured at moderate depths in Sweden, Australia and Portugal.

Indirect evidence of high lateral stress at shallow depth is given by Coates (1964) due to the cracking and 8 foot heave of the floor of an open pit mine cut 50 feet deep into thick bedded limestone. An analysis using the Euler buckling criterion indicates that a horizontal stress field of about 2000 p.s.i. caused buckling. The method of analysis used is only a first approximation to actual conditions but it is of interest to note that this figure is close to the values of lateral stress measured at Portage Mountain Dam.

It appears unlikely that lateral stresses of such magnitude to cause buckling (upwards of 1000 p.s.i.) exist in the Cretaceous bedrock below the valleys of the study area as the lateral stresses acting in-situ are apparently due only to overconsolidation. An average amount of material removed by erosion during the Tertiary would be in the order of 2000 feet. Thus, bedrock now existing below a 300 foot deep valley would have had an overconsolidation ratio of close to 8 prior to valley formation. Data published by Brooker and Ireland (1963) (given in Figure 2.4) indicates the coefficient of earth pressure at rest would be about 1.2 for bedrock with an angle of shearing resistance of 25 degrees. Thus, lateral stresses immediately







below the valley bottom should not exceed 400 p.s.i. Some increase in lateral stress may occur due to the stress-concentrating effect of the valley (Jaeger and Cook 1969, p. 361) but for most of the valleys in the study area this effect should not be large. A study of the buckling criteria including self-weight, shown in Figure 3.52, indicates that lateral buckling of more than the top few feet of the bedrock is not possible if lateral stresses in the order of 500 p.s.i. are present.

Buckling of the bedrock under high lateral stresses appears to be physically possible mechanism. However, initiation of buckling leads to an inward movement of the ends of the buckled layer which would cause a sharp reduction of the force causing the buckling. For buckling to continue, and lead to extreme flexure of the bedrock, would indicate that the force causing the buckling would have to increase to the critical to cause further movement. Whether the tectonic forces, which presumably have caused the deformations at Portage Mountain Dam, in the Pennines and in the Allegheny Plateau, behave in this fashion cannot be confirmed as little is presently known about their nature or origin.

Documented evidence indicates that buckling can occur below river valley bottoms. This phenomena was observed at the discharge tunnel excavation at Underbank Dam in the Little Don Valley which has been previously discussed (Watts, 1906). The trench was excavated at the toe of the valley wall



parallel to the valley axis. The floor of the 18 feet deep excavation appears to have buckled under high lateral pressure. Separation of beds occurred and actual tensile failure of the rock due to the folding occurred as "the anticlinal part of the folded rock was quite 'drummy', and lines of fracture ran along the ridge" (Watts, 1906, p. 675-676). High artesian pressures may have contributed to the buckling as testholes showed "a copious flow of artesian water many feet above the bed of the river" (Watts, 1906, p. 674).

The presence of relatively high lateral stresses may explain the presence of the disturbed zones noted in the bedrock at Ardley damsite (Section 3.3) and at the James MacDonald bridge (Appendix B) where apparent disturbance in a siltstone bed located between two more competent beds was observed. Terzaghi (1961) considered the upper 40 feet of the London Clay at Bradwell to have failed due to high lateral stresses with  $K_0$  approaching  $K_p$  (the coefficient of earth pressure for passive failure). Yudhbir (1969) found that shear failure of overconsolidated samples can occur during unloading in the oedometer test.

The data presented indicates that several modes of failure of bedrock below river valleys are possible. Data gathered indicates that the bedrock below the valleys in the Pennines, the Appalachian Plateau and the Peace River at Portage Dam may have failed by buckling under high lateral stresses which are probably tectonic in origin.





The bulged valleys noted in Britain and Europe may be due to formation of ice lenses associated with periglacial conditions or to high lateral stresses causing plastic failure and large deformations. Observations presented by Rowe (1968) from Staunton Harold Dam indicates the bedrock has failed, however, insufficient evidence on site geology and bedrock properties exists to permit an analysis of the mechanism of valley bulging.

Both field observations and the simple elastic analysis indicates that buckling is not the dominant mechanism which formed the valley anticlines in the study area. A factor pointing to the dominant mechanism being rebound due to stress relief, besides the qualitative agreement with displacements predicted using finite elements and the theory of elasticity, is the correlation of magnitude of rebound with stiffness of the bedrock. Table 3.5 summarizes the cases documented and laboratory results available on the modulus of elasticity of the bedrock at each site which are, in most cases, tangent or secant moduli from unconfined compression tests. The laboratory determination of  $E$  is effected by numerous factors as will be discussed in Chapter IV; the modulus of elasticity from an unconfined compression test serves merely as an approximate indication of the relative stiffness of the rock.

Table 3.5 shows a marked trend for larger amounts of rebound to occur below valleys cut into bedrock with a low modulus of elasticity. The maximum amounts of rebound in



TABLE 3.5

COMPILATION OF MAXIMUM VALUES OF REBOUND AND REPORTED VALUES OF E

Site	Maximum Rebound (ft.)	$\delta/H$	E (p.s.i.)
1. Ardley Damsite	12	.08	8,400-12,000 p.s.i.
2. Boundary Dam	6	.07	-
3. Carvel Damsite	5	.025	26,100 p.s.i. (shale) 53,000 p.s.i. (sandstone)
4. Hairy Hill Damsite	6	.033	6,300 p.s.i. (Lea Park)
5. Portage Mountain Dam	15	.075	$2.4-5.3 \times 10^6$ p.s.i.
6. Rocky A Damsite	4	.036	-
7. Sounding Creek	5	.125	-
8. St. Mary Dam	1.5	.01	$1 \times 10^6$ p.s.i.
9. Three Rivers Damsite	0.5	.002	$0.6 \times 10^6$ p.s.i.
10. Tomahawk Damsite	7	.035	15,000 p.s.i. (sandstone)
11. Pembina 3A Damsite	5	.038	44,800-75,600 p.s.i.
12. James MacDonald Bridge	4	.08	-
13. Garrison Dam	20	.09	14,000-40,000 p.s.i.
14. Gavins Point	7	.05	20,000 p.s.i.
15. Bowman-Haley	20	.12	1,540 p.s.i.
16. Twelvepole Creek Damsite	5	.022	135,000-150,000 p.s.i.
17. Smithville Damsite	6	.06	Limestone $5 \times 10^5$ p.s.i.
18.*A. G. T. Excavation	0.25	.007	6,000-20,000 p.s.i.
19.*South Saskatchewan Dam	-	.007	18,000 p.s.i.

\* Artificial excavation





the valley centers range from about 3 to over 10 percent of the valley depth for sites where  $E$  of the rock is less than 50,000 p.s.i. Artificial excavations which have been discussed in Chapter II typically show values of rebound of less than one percent of the excavation depth showing the importance of time on the amount of rebound measured at a given site. The time-dependent rebound, over the centuries the valleys have existed, has contributed the major proportion of the vertical rebound. This component of rebound, or 'swelling', can be considered as elastic rebound as the rate of rebound due to 'swelling', several decades after completion of the Fort Peck spillway, is a function of the stress removed (Fleming et al., 1970). However drained rather than undrained moduli would be required to predict the ultimate value of rebound.

The rebound in the valley center can be approximated as one dimensional rebound. Assuming the bedrock to act as a linearly elastic material, the one dimensional rebound  $\delta$  is:

$$\delta = \int_0^z \frac{\Delta\sigma}{E} dz \quad (3.4)$$

where  $\Delta\sigma$  is the stress relieved by valley formation,  $E$  is the modulus of elasticity of the bedrock and  $z$  is the depth of rock contributing to the rebound. This simple model assumes a homogeneous isotropic elastic mass; in nature  $E$  should increase with depth (Chang and Duncan, 1970) and



should become completely rigid, for practical purposes, at some finite depth. The assumption of a constant value of  $E$  acting over a depth  $z$  is therefore a simplifying assumption and results from the one-dimensional model must be interpreted accordingly.

The rebound  $\delta$  is given by:

$$\delta = \frac{\gamma H z}{E} \quad (3.5)$$

where  $\gamma$  is the average unit weight of rock removed during valley excavation and  $H$  is the valley depth. Thus, the rebound expressed as a percentage of valley depth is:

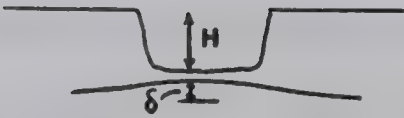
$$\frac{\delta}{H} = \frac{\gamma z}{E} \quad (3.6)$$

A series of curves for assumed thicknesses of elastic material  $z$  are shown in Figure 3.53 assuming  $\gamma$  to be 144 p.c.f. The values of rebound from Table 3.5 can be seen to follow the general trend as predicted by the one-dimensional rebound model. This model overestimates rebound as it assumes no decrease of  $\Delta\sigma$  with depth. However, at shallow depths the error is small although at a depth to valley width ratio of 1.0 the one-dimensional model will overestimate rebound by about 41%.

The two sites departing from this trend are Portage Mountain Dam in British Columbia and Smithville Damsite in Kansas. Both are located in a different geologic environment; the sites in the study area have elastic rebound as the mechanism of formation of the valley anticline while Portage Mountain and Smithville apparently have another mode of formation for their anticlinal structures.







NOTE- SEE TABLE 3.5 FOR SITE NUMBERS

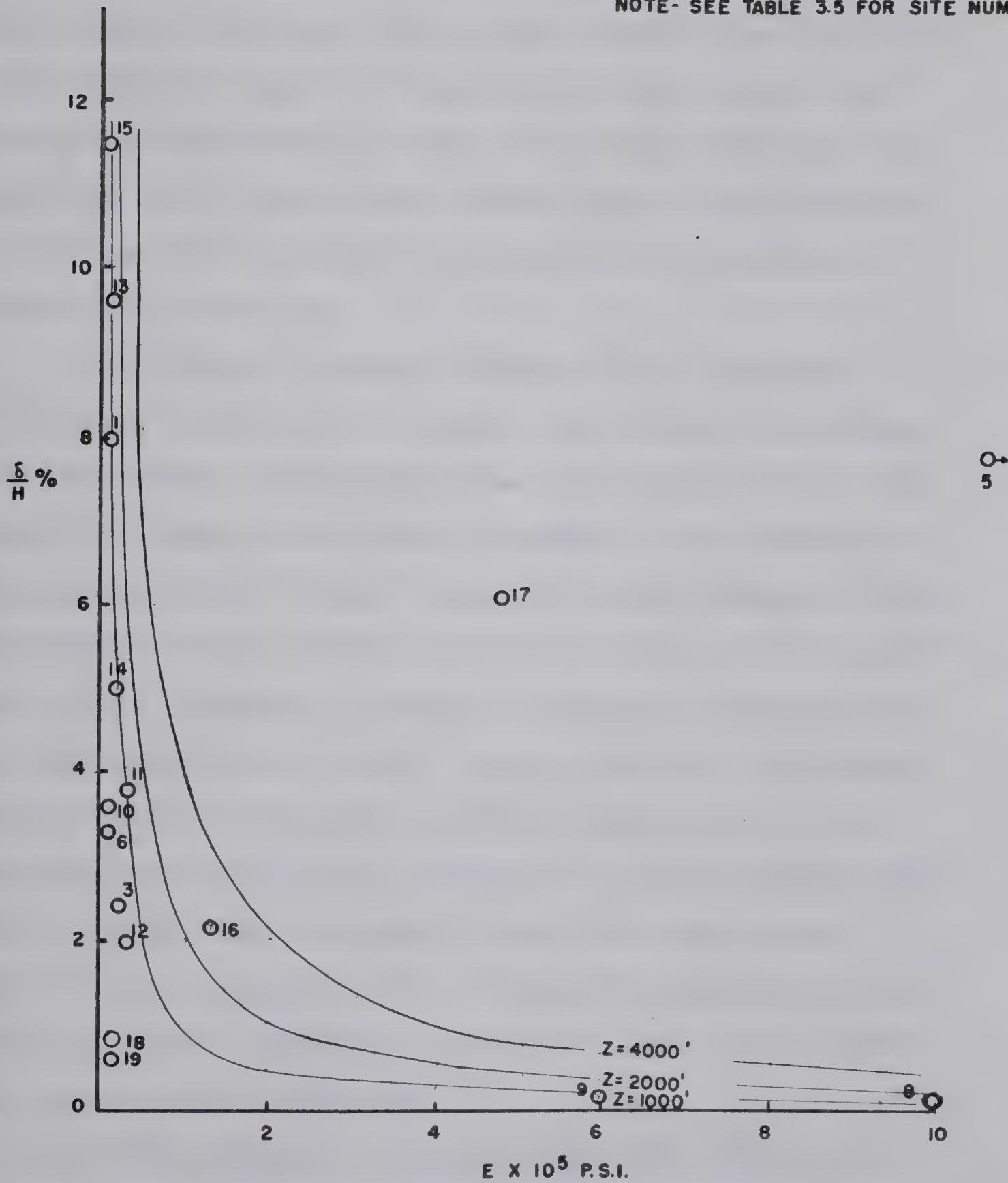


FIG. 3.53 NORMALIZED MAXIMUM VALUES OF REBOUND VERSUS E



The Effects of Rebound: The downcutting of a river valley through a sedimentary rock sequence which has a low modulus of elasticity will result in vertical rebound of the valley bottom as a function of  $E$  of the bedrock and the magnitude of the stress relieved. Valley anticlines, with associated valley flexure, appear to underlay all the valleys cut through the Cretaceous bedrock of the study area and the magnitude of the rebound can be approximated by the ratio of the depth of valley to the inverse of the modulus of elasticity of the rock.

The effects of valley bulging on the design of engineering structures in England and Europe is discussed by Zaruba (1956) and Higginbottom and Fookes (1970). The buckling of beds in the valley bottoms of the Pennines is discussed by Watts (1906), Lapworth (1911), Sandeman (1918) and Walters (1962) and has necessitated the excavation of deep cutoff trenches to provide a positive cutoff through the previous buckled strata. Larger immediate settlement of dams placed on bulged or buckled foundations can be expected than for similar structures placed on intact bedrock. In the event grouting is used for underseepage protection at a damsite, the presence of bulged beds would lead to a marked increase in the grout take and may modify the entire grouting program.

No comprehensive discussion has been found in the literature as to the effect of valley bulging on the slope stability of the valley walls. The references quoted





previously by Lapworth (1911), Sandeman (1918) and Zaruba (1956) show clearly that large differential movements have occurred between beds under the valley and valley walls. Ferguson (1967) noted the occurrence of mylonite or gouge along bedding planes which is apparently due to lateral movement between the beds. These differential displacements have apparently been large enough to shear the rock to the residual for considerable distances back into the hillside with "pieces of shale from trial headings driven hundreds of feet into the hillside being perfectly polished by the movement" (Lapworth 1911, p. 38). The occurrence of landslides in the valley walls correlated so well with the occurrence of buckled beds that Lapworth considered the disturbance in the bedrock to be due to slide activity.

Sliding between beds was noted by Sandeman (1918, p. 155-156) in the Yoredale Rocks below the Derwent valley.

"An examination of the section of this wrinkling of the ground surface - which was more marked on the southern side of the trench, where there was a double folding - will show that there must have been considerable sliding of one stratum upon another, and that this sliding was a maximum at the top of the broken strata - in the centre of the disturbance - and at a minimum at the bottom, where it will be observed the beds gradually become more nearly horizontal."

Landslide activity is a common feature in the area as described by Sandeman (1918, p. 155).

"The Derwent Valley and the adjoining Ashop Valley contain many old landslides, and one at the junction of the two valleys is very extensive, being apparently 3/4 mile in length. The Ashop Valley in particular for a considerable distance shows signs of continuous landslides."



The relative displacements between beds noted by Sandeman (1918), Zaruba (1956) and Ferguson (1967) appears to be due largely to the mechanism of flexural slip due to folding, as is discussed in Chapter V. The slickensiding of shale in the trial drift noted by Lapworth (1911) may be due to flexural slip combined with the effects of differential lateral movements due to lateral stress relief.

Observations made at the bridge sites in Edmonton, Alberta reveal similar, although less strikingly defined, features. The presence of mildly polished gouge zones below the river bed shows lateral movement has occurred between the strata. The slickensided surfaces in the bentonite bed in the valley wall shows that the residual strength can be reached adjacent to a valley by processes other than previous sliding. Three mechanisms appear likely to explain the observed slickensides on a mechanical basis.

1. Unrestrained swelling of the bentonite towards the valley wall due to absorption of water percolating down through the fractured bedrock. This mechanism lies outside the scope of this thesis and is discussed in detail by Eigenbrod (1972).
2. Differential displacement across the bentonite layer due to stress relief and elastic rebound. The stiffness, and hence modulus of elasticity, of the bentonite is much lower than that of the surrounding bedrock and stress relief and rebound should result in relatively large shear strains across the weak layer.







3. Flexural slip between strata due to folding as a function of thickness of bed and change in dip.

Field evidence exists to support the occurrence of these mechanisms. The high moisture contents and softened upper shale noted during study of the bentonite bed at the Beverly bridge (Appendix B) indicates swelling has occurred, in the upper portion of the bentonite layer at least. The well defined failure surfaces on both contacts of the bentonite bed are consistent with failure occurring due to rigid restraint along the bentonite-shale contacts while the bentonite expands towards the river. The increase in thickness of bentonite layers towards the banks of the Missouri River in the Niobrara chalk (Underwood, 1964) shows clearly that a considerable amount of swell can occur in bentonite layers adjacent to a valley wall.

The occurrence of secondary failure planes and the inclusions of hard shale in the bentonite matrix appear to be the results of large differential movements across the bentonite layer due to stress relief.

The review of data published on landslide activity in the study area in Chapter II indicates that the stability of most of the valley slopes in the study area, in the weaker formations at least, are governed by residual strength or a strength appreciably less than the peak. The presence of sheared surfaces along bed contacts and bentonite layers strongly suggests that the landslides, which are controlled



by the residual strength, are the result and not the cause of these features. The data presented shows that the strength of the bedrock has been reduced to the residual by mechanisms due to valley formation - flexural slip due to rebound and large differential movements across bentonite layers. Subsequent slope stability is then largely dependent upon groundwater conditions and height and inclination of slope. The presence of bentonite layers at the residual strength does not preclude the existence of high valley walls inclined at a steep angle provided the piezometric level is low as has been discussed in Chapter II.

Further discussion on the engineering implications of the points discussed in this chapter will be given in Chapter VI. Regardless of cause, the results of rebound due to valley formation, lateral movements of the valley walls and flexural slip, have results which affect the stability of the valley walls and the design and construction of any engineering works which may be undertaken in or adjacent to the valley.





## CHAPTER IV

### FINITE ELEMENT ANALYSIS OF RIVER VALLEY FORMATION

#### 4.1 Introduction

The cases documented in Chapters II and III show that the unloading due to a large excavation, either artificial or natural, results in an upward rebound of the excavation floor and an inward movement of the excavation walls. A change in stress due to the excavation occurs throughout the adjacent soil or rock mass. The displacements resulting from the excavation and the final state of stress in the material adjacent to the excavation can be found if the excavation (or valley) is cut in a linearly elastic material.

The one-dimensional elastic analysis in Chapter III indicates that elastic rebound is the dominant mechanism in the formation of the valley anticlines noted in the study area. Therefore, this chapter will analyze the displacements which will result from river valley formation in a homogeneous, isotropic elastic material using a range of elastic and in-situ stress parameters appropriate to the bedrock of the study area.

The stress-strain behaviour of soil and rock and the factors which influence the determination of the modulus of elasticity of these materials will be reviewed. The displacements due to elastic rebound for a typical



valley section in the study area are found by use of the finite element method. The effects of valley geometry, depth of finite element grid and increase in  $E$  with depth on displacements are evaluated.

#### 4.2 The Stress-Strain Behaviour of Soil and Rock

The theory of elasticity, discussed in such standard texts as Chou and Pagano (1967) and Timoshenko and Goodier (1970), assumes that the material possesses characteristic elastic constants, the modulus of elasticity ( $E$ ) and Poisson's ratio ( $\nu$ ). In an ideal elastic material  $E$  and  $\nu$  are material properties. Most soils and rocks depart markedly from this assumption and the stress-strain behaviour of the bed-rock of the study area is extremely complex. A value of  $E$  and  $\nu$  is not a fundamental property of a soil or rock but rather a value which describes the response of the sample under a particular set of conditions.

Laboratory Determination of  $E$ : No standard procedure exists for the determination of the modulus of elasticity of a bed-rock sample in the laboratory. Standard engineering practice is to derive  $E$  from the stress-strain curve of unconfined or undrained triaxial tests. Results are reported as a tangent or secant modulus. The tangent modulus is the slope of a line tangent to the stress-strain curve at some point while the secant modulus is the slope of a line connecting two points on the curve. Unloading of the sample usually results in a steeper stress-strain curve







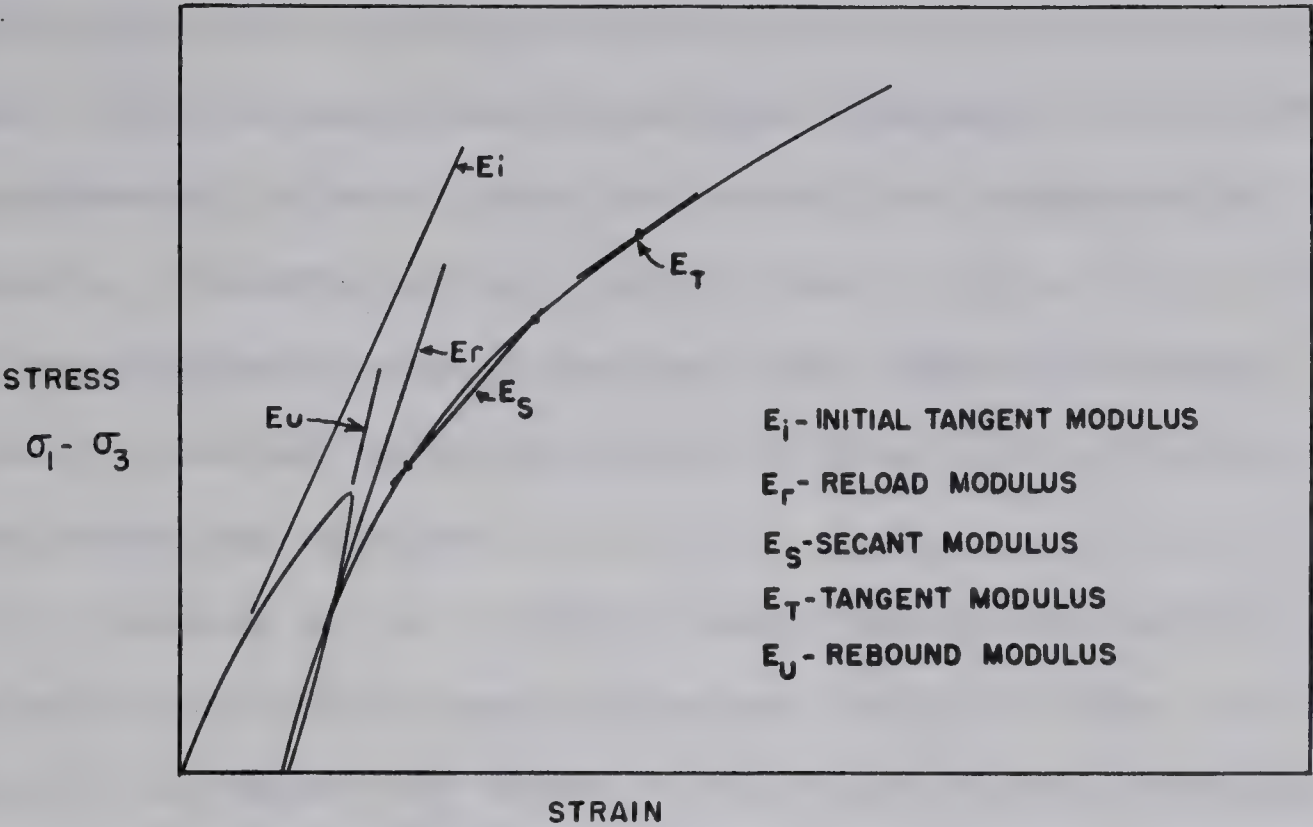
and, hence, gives a higher rebound modulus than initial loading. A typical stress-strain curve is shown in Figure 4.1.

Research by Ward et al., (1959), Ladd (1964), Ward et al., (1965), Soderman et al., (1968), Hendron et al., (1970) and others has shown that large variations exist between laboratory values of  $E$  for a given soil or rock depending upon a number of factors which are discussed below.

1. Shear Stress Level: Ladd (1964) noted that a reduction occurred in  $E$  with increasing stress level for both normally consolidated and overconsolidated soils, with a marked reduction as the sample approached failure. Duncan and Chang (1970) show that the assumption that soils have a hyperbolic stress-strain curve leads to a procedure where the tangent modulus at any stress level can be calculated from the initial tangent modulus. Soils or rocks, where a high percentage of their shear strength is mobilized, will be characterized by a low value of  $E$  and a high displacement will result from a given stress change.

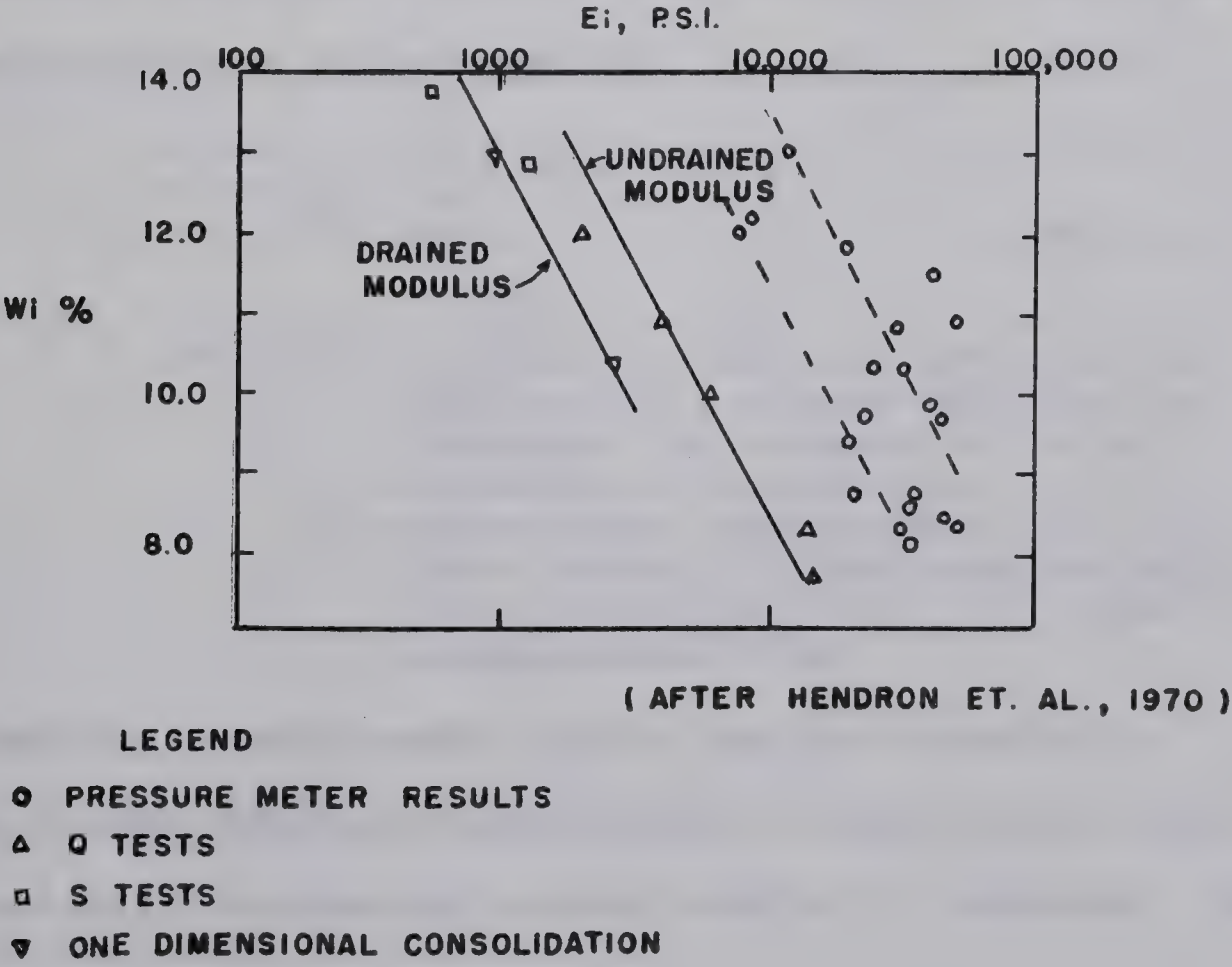
2. Test Type and Drainage Conditions: Ladd (1964) found that undrained triaxial tests on normally consolidated clay samples yielded moduli approximately two to three times greater than unconfined compression test results. Consolidated-undrained triaxial tests, consolidated





TYPICAL STRESS - STRAIN RELATIONSHIP - FIGURE 4.1

FIELD AND LABORATORY MODULI - FIGURE 4.2







initially to the in-situ vertical effective stress, gave moduli five to six times those from undrained tests and approximately eleven times the unconfined compression results. Soderman et al. (1968) found, for a clay till in southern Ontario, moduli derived from consolidated-undrained triaxial tests to be two to four times greater than undrained results.

Hendron et al., (1970) found the drained moduli, for soft shale of Pennsylvanian age from a bridge site in Ohio, to be about one third to one half of the undrained moduli for specimens at the same initial water content as shown in Figure 4.2.

3. Confining Pressure: Janbu (1963) found that the initial tangent modulus (defined as  $M$  by Janbu) of soil and rock samples increases with vertical effective stress in the triaxial test. It was found:

$$M = m \sigma_a \left( \frac{\sigma'}{\sigma_a} \right)^{1-a} \quad (4.1)$$

where  $m$  = a modulus number in the order of  $10^5$  to  $10^6$  for hard rock but decreasing for increasing porosity  
 $\sigma_a$  = atmospheric pressure  
 $a$  = an exponent approaching unity for rock, about 0.5 for sand and silt and approaching zero for normally consolidated clay

Makhlouf and Stewart (1965) found a hyperbolic increase in the modulus of elasticity of sand in the triaxial test with increasing lateral confining pressure. No



variation of  $E$  with maximum principal stress was noted.

Mahtab and Goodman (1968) found an increase in initial tangent modulus with confining pressure for samples of schistose gneiss and Berea sandstone.

Chang and Duncan (1970) found both the initial tangent and the unloading or rebound modulus of overconsolidated sand, clay and siltstone of the Tulare formation in California, to be related to lateral effective confining pressure by the relationship:

$$E = K P_a \left( \frac{\sigma'_3}{P_a} \right)^n \quad (4.2)$$

where  $K$  = a modulus number

$n$  = an exponent

$P_a$  = atmospheric pressure

$\sigma'_3$  = lateral effective confining pressure

4. Sample Disturbance: Sample disturbance has been shown to have an important effect on laboratory determination of  $E$  for borehole samples. Comparison of undrained triaxial test results on borehole and block samples by Ward et al., (1959), Ward et al., (1965) in the London Clay showed that soil sampling by conventional techniques led to a marked reduction in  $E$ . Lo et al., (1970) found, for an overconsolidated lacustrine clay in Ontario, the moduli, from block samples, derived from consolidated-undrained triaxial tests were four to seven times those from borehole samples.





Soderman et al., (1968) found a higher rebound modulus in the undrained triaxial test for till samples carved from 4 inch diameter Shelby tubes than from 2 inch diameter Shelby tubes. Rebound moduli were higher from block samples than from any of the Shelby tube samples indicating that cycling the load does not remove all the effects of sample disturbance. The reduction in  $E$  was most marked in samples taken from small diameter tubes.

5. Stress Path: The modulus of elasticity should be determined for stress increments corresponding to those which occur in the field and the test should start from the values of stress existing in-situ (Ladd, 1964). Conventional triaxial testing procedure determines a loading modulus, usually an initial tangent or a secant modulus at a stress level of  $1/2$  to  $1/3$  the failure stress. Simons and Som (1969) show that this procedure gives a secant modulus of 5,300 p.s.i. for a sample of blue London Clay in the undrained triaxial test. An analysis taking the probable in-situ stress conditions and stress path into account gave  $E = 12,800$  p.s.i.

The modulus found from unloading is commonly much higher than the initial loading modulus. Kohn (1965) studied the elastic properties of a dense glacial till in northern Saskatchewan in a testing program which compared the results of unconfined compression tests and undrained triaxial tests with the results of in-situ plate-loading



tests and moduli derived from rebound and settlement observations. The results are shown in Table 4.1. Unconfined compression moduli are larger than the initial values of E from the undrained triaxial tests. The triaxial test results show a rapid increase in E with load cycling. Laboratory results are appreciably smaller than values of E derived from plate-bearing tests and field observations.

TABLE 4.1

VALUES OF E FROM SQUAW RAPIDS (KLOHN, 1965)

Test Type	Average E (p.s.i.)
Unconfined compression	21,000
Undrained triaxial-initial loading	11,000
-rebound	48,300
-reload	25,400
In-situ Plate Bearing Tests-initial loading	72,000
-rebound	112,000
-reload	214,000
Rebound Observations*	140,000
Settlement Observations*	155,000
* Assuming $\nu = 0.30$	

6. Anisotropy: Overconsolidated soils are not isotropic and E is commonly found to be greater in the horizontal





than in the vertical direction. Barden (1963) showed that anisotropy will affect displacements measured for loading, or unloading, at the surface of an anisotropic mass; in excavation problems the rebound measured in the field should be somewhat less than the value calculated using values of  $E$  derived from vertical samples.

The ratio of  $E$  (horizontal) to  $E$  (vertical) varies from 1.2 to 2.3 for the London Clay (Ward et al. 1959, Ward et al. 1965). Lo et al., (1970) found the modulus ratio to be about 1.4 for an overconsolidated glacio-lacustrine clay in southern Ontario.

Wright (1969) found the Pepper shale (Cretaceous) from the Waco Dam in Texas (Van Auken 1963, Beene 1967) to be highly anisotropic with undrained secant moduli at 50 percent of the deviator stress at failure averaging 2460 p.s.i. for vertical samples and 7250 p.s.i. for horizontal samples. Samples of Bearpaw shale from the Fort Peck Dam in Montana showed horizontal undrained moduli to be an estimated two or three times greater than moduli from vertical samples.

7. Time Effects: Thixotropy is the increase in strength measured in the laboratory with time at constant composition. Ladd (1964) shows this effect is significant only in remolded soils or normally consolidated clays having a high liquidity index.



The rate of strain during testing normally or over-consolidated clay samples in the undrained and consolidated-undrained tests is shown by Ladd (1964) to have some effect upon the modulus. Lo et al., (1970) reports very small rate effects on values of  $E$  from consolidated-undrained tests on overconsolidated lacustrine clay.

Field Determination of  $E$ : Methods have been derived to measure  $E$  in the field in view of the large number of factors which affect the laboratory determination of the modulus of elasticity. A value of  $E$  can be derived from a plate-bearing test. This method suffers from several limitations:

1. the value of  $\nu$  must be measured or assumed.
2. the soil or rock mass is usually assumed to be a semi-infinite, homogeneous, isotropic, elastic material.
3. only a small segment of the soil or rock mass is stressed as plates much in excess of 12 inches diameter are too unwieldy for common use.

An alternative method involves measuring the rebound of an excavation center and applying Steinbrenner's equation (Terzaghi 1943, Harr 1966) to derive a value of  $E$  acting in the field. The displacement at the surface of the unloaded area is given by:

$$W = \frac{2aq}{E} (1 - \nu^2) K \quad (4.3)$$





where  $W$  is the rebound at the excavation surface,  $q$  is the intensity of load relieved,  $\nu$  is Poisson's ratio and  $E$  is the modulus of the homogeneous, isotropic semi-infinite elastic mass assumed in the derivation of this expression.  $K$  is an influence factor dependent upon the dimensions of the unloaded area.

Measurements of displacement permit  $E$  to be calculated if  $\nu$  is known or assumed. The two main defects in this approach are the difficulty in allowing for complicated field boundary conditions and the assumption of a semi-infinite homogeneous elastic mass. Laboratory values of  $E$  have been shown to increase with confining pressure, hence  $E$  should increase with depth in the field. Therefore, moduli derived from Steinbrenner's equation will be an average of the actual variation of  $E$  with depth and will be considerably higher than laboratory values of  $E$  determined at zero or low confining pressure. Agreement of laboratory moduli and values of  $E$  derived from field observations is thus unlikely for soil or soft rock.

The effect of depth of elastic material has been studied by Egorov (reported by Harr, 1966) who tabulated values of  $K$  for use in Equation 4.3 for a homogeneous elastic body underlain at depth  $Z$  by a rigid base. Results are presented for both the no friction case ( $\tau = 0$ ) and the case of no displacement ( $u = 0$ ) along the contact with the rigid base.



Comparison of Field and Laboratory Values of E: A number of documented cases exist where laboratory values of E have been compared to moduli derived from field behaviour. Poor agreement is generally found which can be expected in view of the many factors which influence laboratory derived moduli and the assumptions, implicit in Steinbrenner's equation, which are at variance with actual conditions existing in the field.

Simons (1957) studied the behaviour of two buildings founded on normally consolidated soil in Norway. Values of E were determined at half the failure deviator stress from unconfined compression tests and consolidated-undrained triaxial tests consolidated to the in-situ vertical effective stress. The moduli from the triaxial tests were two to four times the field derived moduli and the unconfined compression moduli were  $1/3$  to  $1/5$  of the field results.

Serota and Jennings (1959) derived a value of E of 1200 t.s.f. for London Clay from rebound measurements taken in a 27 foot deep excavation. Initial tangent moduli from undrained triaxial tests ranged from 80 to 400 t.s.f.

Bozozuk (1963) derived values of E for the Leda clay from rebound measurements in excavations for the Ottawa sewage treatment plant. Field results agreed well with the maximum initial tangent modulus from unconfined compression tests on block samples if  $\nu$  were assumed equal to 0.40. This correspondence appears fortuitous in view of the factors previously discussed.







The elastic properties of the dense glacial till studied at Squaw Rapids by Klohn (1965), have been given in Table 4.1. Field moduli derived from Steinbrenner's equation are approximately 7 times those found in unconfined compression tests and 6 times those found from undrained triaxial tests. The moduli derived from field observations of rebound and settlement were approximately twice those found from plate-bearing tests on initial loading.

Peterson (1965) reported the value of  $E$  for the Bearpaw shale at the South Saskatchewan River Dam to vary from 7000 p.s.i. in laboratory undrained triaxial tests to over 30,000 p.s.i. derived from rebound measurements assuming  $\nu = 0.50$ .

Meigh and Greenland (1965) compared the results of plateloading tests, pressuremeter tests and laboratory tests in the Coal Measures mudstone and sandstone, Keuper marl and Bunter sandstone in England. A reasonable correspondence occurred between modulus values obtained from plate-bearing tests and the results of the Menard pressuremeter. Laboratory tests on open-drive samples were considerably different due to sample disturbance.

Ward et al., (1968) studied the properties of the Middle Chalk in Norfolk, England. Moduli from full scale loading tests, using a water filled tank 18.3 meters high and 18.3 meters in diameter, compared well with moduli from plate-loading tests carried out in the bottom of auger holes 3 feet in diameter. The actual displacement pattern



measured under the loaded tank showed that displacements were localized around the loaded area far more than could be predicted using a homogeneous elastic model. The behaviour is consistent with the theoretical predictions of Gibson (1967) for an elastic material whose stiffness increases with depth.

A plot of values of  $E$  calculated from vertical strains measured under the tank center (assuming  $\nu = 0.10$ ) is shown in Figure 4.3. Some of the variation of  $E$  with depth is due to weathering of the chalk, which decreases with depth, while the remainder of the increase in  $E$  with depth is due to an increase in lateral confining pressure.

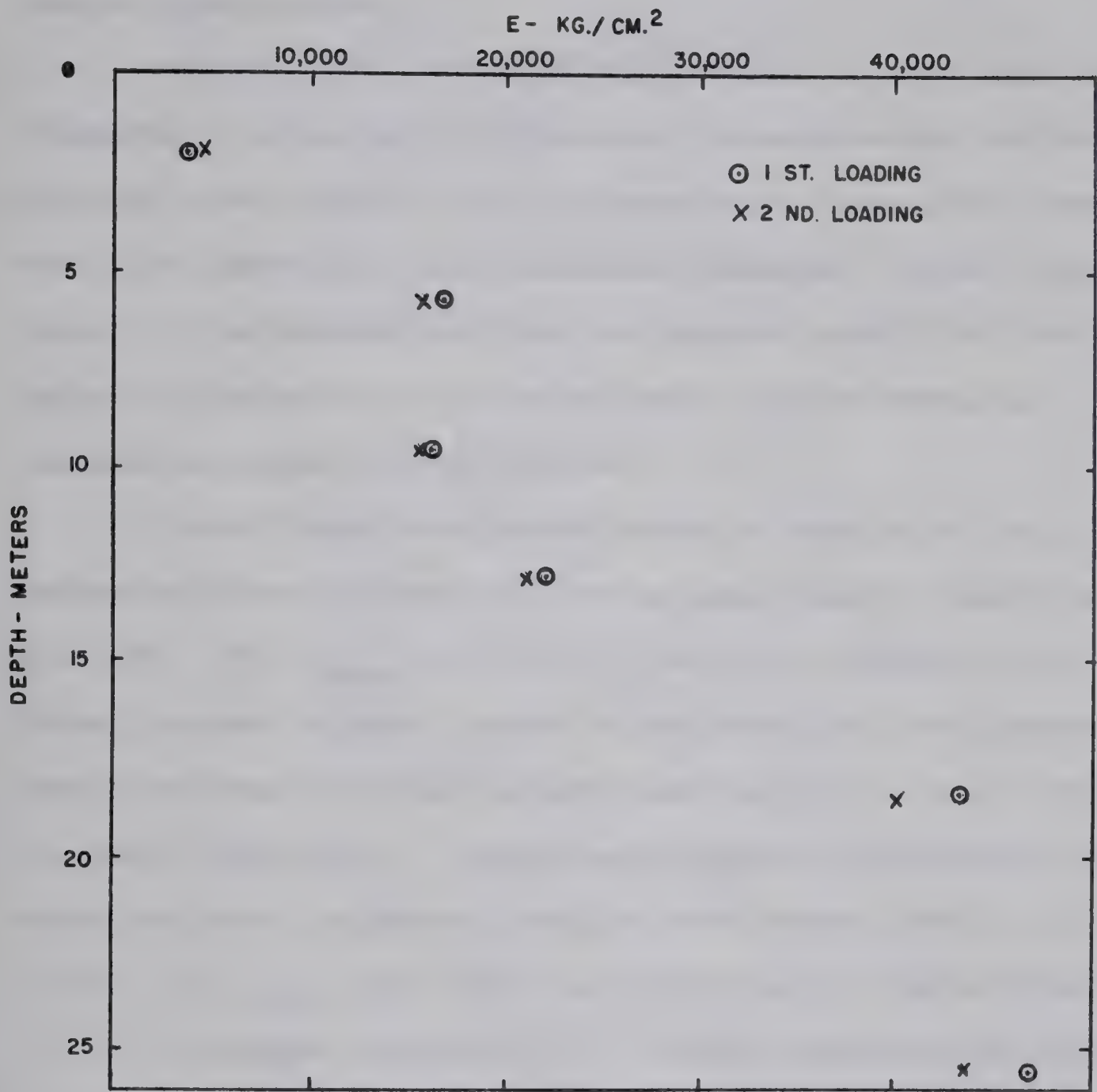
Hendron et al., (1970) found that pressuremeter tests in shale of Pennsylvanian age in Ohio gave results considerably higher than laboratory moduli as shown in Figure 4.2. The pressuremeter moduli are an undrained value and the difference between these results and laboratory undrained moduli is considered due to anisotropy, as the strata are stressed horizontally with the pressuremeter, and sample disturbance.

The test results were to be applied to prediction of bridge pier settlements and a drained modulus would be appropriate for design. The authors recommend that either the laboratory drained moduli be tripled or that  $1/3$  the pressuremeter results be used. In the absence of laboratory drained tests or in-situ pressuremeter tests, it was recommended that undrained laboratory moduli be used in









( AFTER WARD, BURLAND & GALLOIS, 1968 )

NOTE - E CALCULATED FROM IMMEDIATE VERTICAL STRAINS BELOW TEST TANK CENTER  
-  $\nu$  ASSUMED EQUAL TO 0.10

VARIATION OF E WITH DEPTH IN THE MIDDLE CHALK AT MUNDFORD, NORFOLK

FIG. 4.3



the calculation of settlements to allow for the effects of sample disturbance.

DeJong (1971) studied the rebound of a 40 feet deep foundation excavation in Edmonton, Alberta which was cut through dense glacial till to preglacial sands and gravels overlying bedrock of the Edmonton formation (Upper Cretaceous). The bedrock surface was approximately 10 feet below the excavation bottom and most of the measured rebound occurred in the bedrock.

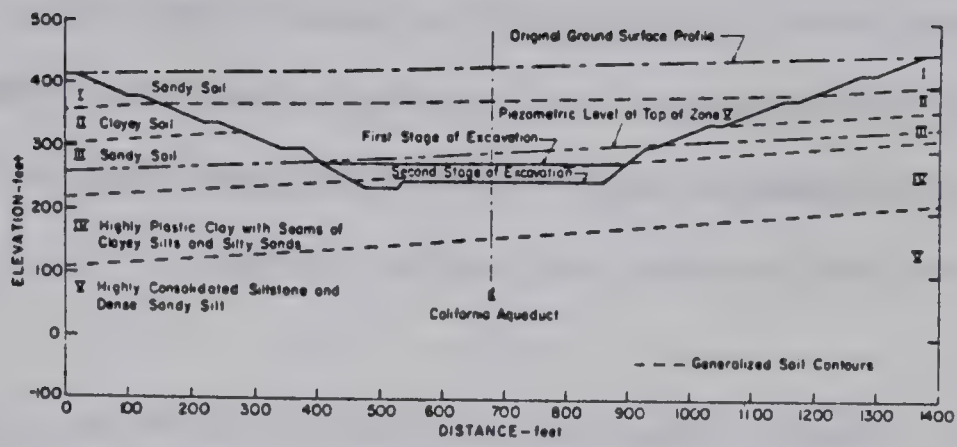
Consolidated-undrained tests on samples of soft sandstone from Pitcher tube cores gave tangent moduli at  $\frac{1}{3} (\sigma_1' - \sigma_3')$  max. of 14,800 p.s.i. and 10,450 p.s.i. Three drained triaxial tests on mudstone and soft sandstone gave a maximum observed tangent modulus at  $\frac{1}{2} (\sigma_1' - \sigma_3')$  of about 5000 p.s.i. Unconfined compression tests on mudstone and soft sandstone samples gave secant moduli at  $\frac{1}{4} (\sigma_1 - \sigma_3)$  max. of 3,500 and 8,000 p.s.i. respectively.

A maximum rebound of 2.7 inches was observed in the excavation center. A computer solution utilizing Steinbrenner's equation gave an average derived modulus of about 54,000 p.s.i. The use of laboratory moduli would obviously lead to a large over-estimate of field rebound if Steinbrenner's equation is used to predict excavation behaviour.

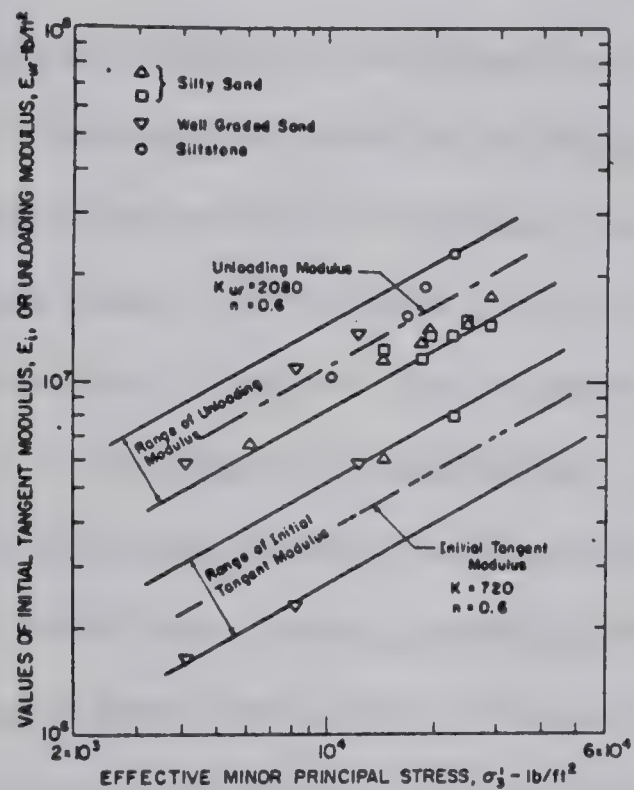
Chang and Duncan (1970) describe movements monitored during construction of a 200 foot deep excavation, shown in Figure 4.4(a), for the Buena Vista Pumping Station in California. The excavation was made in moderately overconsoli-



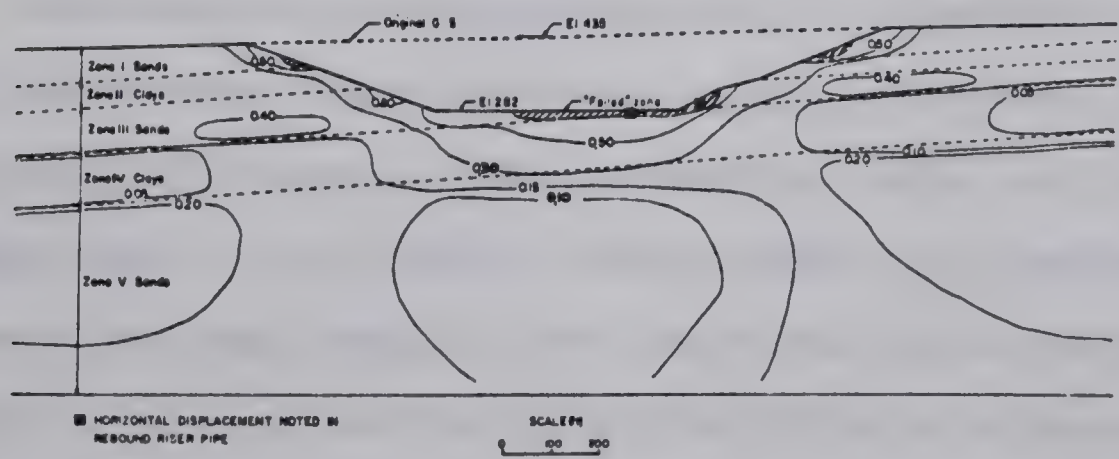




A - GENERALIZED PROFILES ALONG SECTION A-A, BUENA VISTA PUMP-  
ING PLANT SITE



B - VARIATIONS OF VALUES OF INITIAL TANGENT MODULUS AND UN-  
LOADING MODULUS WITH EFFECTIVE MINOR PRINCIPAL STRESS FOR BUENA  
VISTA SANDY SOILS



C - CONTOURS OF MOBILIZED STRENGTH  $[(\sigma_1 - \sigma_3)/(\sigma_1 - \sigma_3)_f]$  AFTER  
EXCAVATION

FIGURE 4.4 DATA FROM THE BUENA VISTA PUMPING PLANT (CHANG & DUNCAN, 1970)



dated sands, silts and clays of the Tulare formation which are about 4000 feet deep at the site. A maximum vertical rebound of 2.43 feet was observed in the excavation center of which about  $1/3$  occurred after the excavation was completed.

Consolidated-undrained and drained triaxial tests on Pitcher tube samples showed that both the initial tangent modulus and the rebound modulus increase with lateral effective confining pressure as shown in Figure 4.4(b). A finite element program was used to simulate the excavation sequence in which the modulus assigned to each element was calculated on the basis of stress level, effective lateral confining pressure and whether the element was undergoing primary loading, unloading or reloading. The predicted values of rebound agreed fairly well with observed values of rebound with 2.24 feet being predicted in the excavation center versus 2.43 feet measured. Figure 4.4(c) shows the contours of strength mobilized after the excavation is completed indicating that elastic equilibrium is maintained throughout most of the soil mass around the excavation.

This article is noteworthy as it illustrates a number of factors which influence  $E$  acting in-situ and shows that the finite element method can take into account at least some of the factors which affect  $E$ . However, the agreement between predicted and measured displacements is unusual in view of the fact that the effects of anisotropy and sample disturbance were ignored. A simple one-dimen-





sional elastic analysis (Matheson and Koppula, 1971) indicates that the position of the bottom base of the finite element grid has some influence on the displacements predicted at the excavation base, even when the effect of increase in  $E$  with depth is allowed for. Chang and Duncan (1970) place the rigid base of the finite element grid 600 feet below the bottom of the 200 feet deep excavation; the agreement between observed and predicted behaviour may be fortuitous with the effects of sample disturbance being cancelled by the boundary conditions of the finite element grid used.

### Summary

The cases discussed in this section show that laboratory values of  $E$  are affected by many factors and are typically much lower than field derived moduli. The use of laboratory parameters in Steinbrenner's equation will lead to a gross over-estimate of excavation rebound; the performance of the Buena Vista excavation indicates that laboratory derived values of  $E$  may yield a good approximation to field behaviour if the effects of stress level, confining pressure and stress path are allowed for in the testing and analysis procedure. The problem of proper location of the boundaries of the finite element grid remains to be resolved.

Documented evidence indicates that plate-bearing tests will give a result in good agreement with the value



of  $E$  acting in-situ. Pressuremeter tests give very similar results in the one case documented and it appears that this technique offers a relatively quick and inexpensive means of finding the undrained value of  $E$  acting in-situ.

#### 4.3 Finite Element Simulation of River Valley Excavation

Little information is available on the values of  $E$ ,  $\nu$  and  $K_0$  acting in-situ in the bedrock of the study area. Little is known about typical values of drained and undrained moduli and the in-situ stress conditions which will govern the behaviour of the rock mass in-situ. Thus, any analysis of river valley formation in the study area must, of necessity, include a number of simplifying assumptions.

A number of the bedrock formations in the study area are relatively homogeneous, others are extremely heterogeneous with rapid changes in lithology and horizontal beds of bentonite. Analysis of the effects of change in lithology would require the ability of specifying layers with different elastic parameters. The finite element method was adopted in view of these factors as the effects of non-homogeneity and complicated boundary conditions can be handled readily, which is not the case with the finite difference method used by Dibiagio (1966) to study displacements and stress changes induced by excavation of a vertical trench into a homogeneous, isotropic elastic mass. Displacement of the valley walls can be studied by the finite element method which is not the case







for the computer solution by DeJong (1971) of Steinbrenner's equation.

Method of Analysis Adopted: The finite element method was originally developed to study problems in solid mechanics and is described in standard texts such as Zienkiewicz and Cheung (1967) and Holand and Bell (1970). The method is well suited to the solution of excavation problems in geotechnical engineering as each element in the finite element grid can be assigned a different value of  $E$  and  $\nu$  and different geometric and stratigraphic configurations can be represented easily. A brief description of the basic steps in the finite element method is given in Appendix D.

In this study of river valley formation, it was assumed at the outset that the valley was excavated into a homogeneous, linearly elastic material. Moduli reported from most of the projects documented are mainly from unconfined compression tests and serve merely as an approximate guide to the relative stiffness of the rock. Little or no data is available for the formations of the study area on the rate of increase of  $E$  with confining pressure, in-situ stress conditions, the effect of stress path, stress level and sampling disturbance. Therefore, a simplified model was chosen, the limitations of which have been discussed previously.

The procedure to simulate river valley excavation is discussed in Appendix D. The vertical stress prior to



excavation was assumed equal to the weight of the superincumbent overburden. The lateral stress was assumed to vary linearly with depth and be equal to  $K_0$  (the coefficient of earth pressure at rest) times the vertical stress. Total and effective stresses are synonymous in this analysis as the effect of pore water is ignored.

Thus the vertical and horizontal stresses at depth are given by:

$$\sigma_v = \gamma z \quad (4.4)$$

$$\sigma_h = K_0 \gamma z \quad (4.5)$$

where  $\gamma$ , the unit weight of the soil or rock, was assumed to be 150 p.c.f. Excavation results in the removal of stress from the excavation face which is equivalent, for a linearly elastic material, to the application of a surface traction perpendicular to the excavation surface equal to the stress relieved. Deformations occur within the elastic media and a stress change occurs throughout the material adjacent to the excavation which must be added to the initial stress field to produce the final state of stress.

Brown and King (1966) show that an excavation in a homogeneous isotropic, linearly elastic material can be simulated in one step, giving the same results as a sequential excavation procedure such as used by Duncan and Dunlop (1969) and Chang and Duncan (1970).

The finite element program used for the analysis of





valley formation is described in Appendix D. It was originally written by Wilson (1963) for plane-stress analysis of solid mechanics problems. It has since been modified for plane-strain conditions and automatic generation of nodes and elements. The author further modified the program for superposition of the stress changes induced by the excavation on the initial state of stress. Constant strain triangles are used in the program. Appendix D contains instructions for the use of the program, details on setting up a finite element grid for a typical problem, coding procedure and a listing of the program written in Fortran IV as used on the IBM model 360/67 computer. Results from the example are presented to allow any future user of the program to validate his results.

The program gives the final stress field around the valley; this has not been studied in detail as it duplicates previously published work (Duncan and Dunlop 1969) and the displacements resulting from valley formation are of prime interest for comparison with the cases documented in Chapter III.

The displacements and stresses obtained from the program have been compared with closed-form solutions, finite difference results and published finite element results. A satisfactory agreement was found and will be discussed in the next section.



Comparison of Results: A finite difference study of the displacements and stresses induced in a homogeneous, isotropic elastic medium by excavation of a rectangular trench has been referred to previously (Dibiagio, 1966). A finite element grid was used to simulate the finite difference grid; dimensions of the two grids were identical although the finite element grid used a somewhat larger element size.

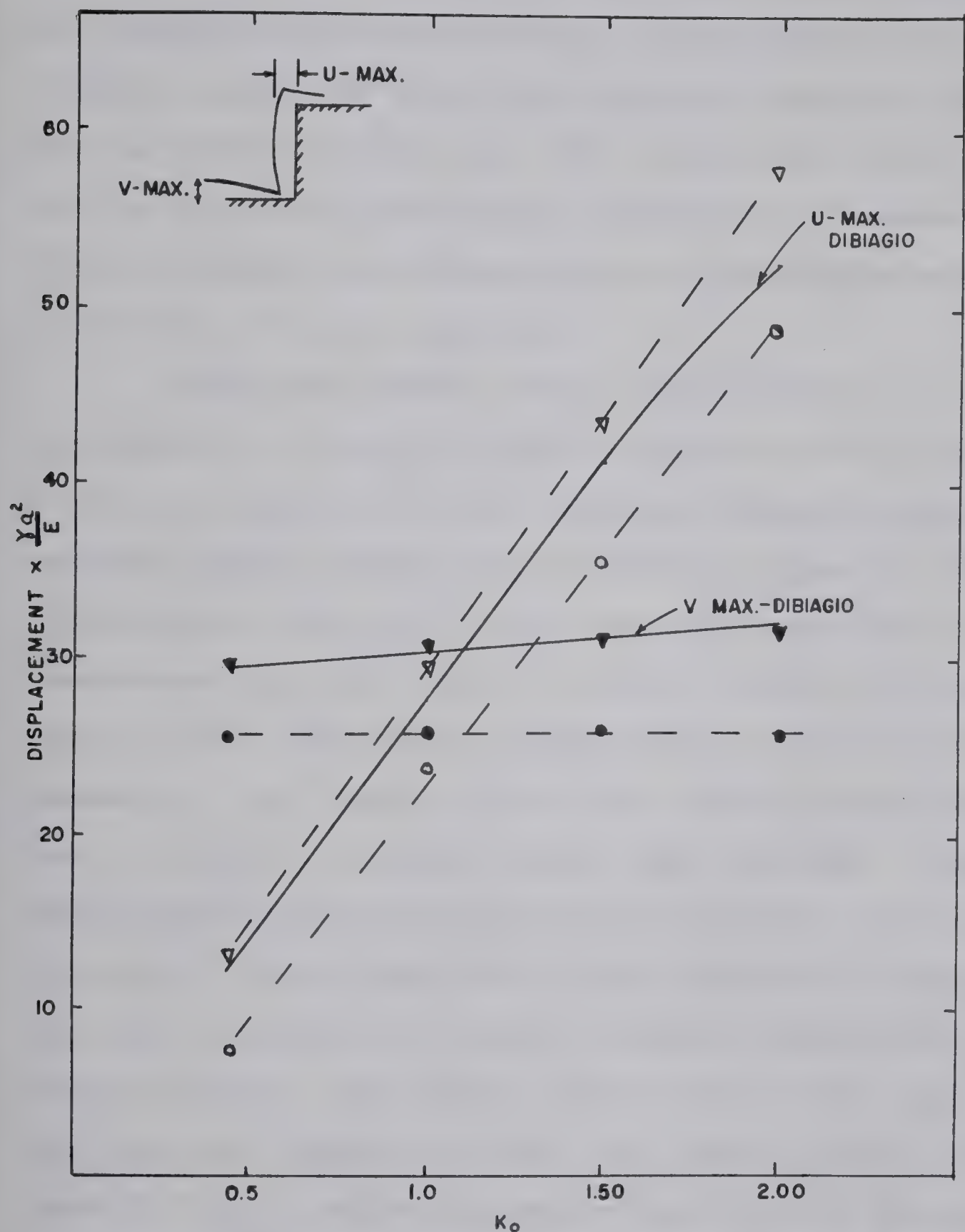
The results of the two methods are compared in Figure 4.5 for identical values of  $E$ ,  $\nu$  and  $K_0$ . Dibiagio used the condition of  $\gamma_x = 0$  (free movement in the x direction) along the bottom rigid boundary of the finite difference grid which results in somewhat higher values of rebound for the bottom of the cut than for the case of fixing the nodes on the bottom of the grid in both x and y. The finite element program gives practically identical values of excavation bottom rebound for values of  $K_0$  ranging from 0.429 to 2.00. A slight divergence occurs in the lateral movements of the excavation wall for increasing values of  $K_0$  and is apparently due to the stress boundary conditions used by Dibiagio on the vertical edge of the finite difference grid.

Closed form solutions are available for the displacements of a loaded strip (Harr, 1966). The maximum rebound, in the center of a valley 2000 feet wide, should approximate the rebound in the center of a strip 2000 feet wide loaded with a traction equal to the weight of over-









FINITE ELEMENT RESULTS		
U - MAX	V - MAX	BOTTOM BOUNDARY CONDITIONS
○	●	$U = 0$
▽	▼	$\tau = 0$

NOTE - FINITE ELEMENT GRID 3 USED  
TO DUPLICATE DIBIAGIO'S (1966)  
FINITE DIFFERENCE GRID

COMPARISON OF FINITE  
ELEMENT & FINITE DIF-  
FERENCE DISPLACEMENTS

FIGURE 4.5



burden removed from the valley floor.

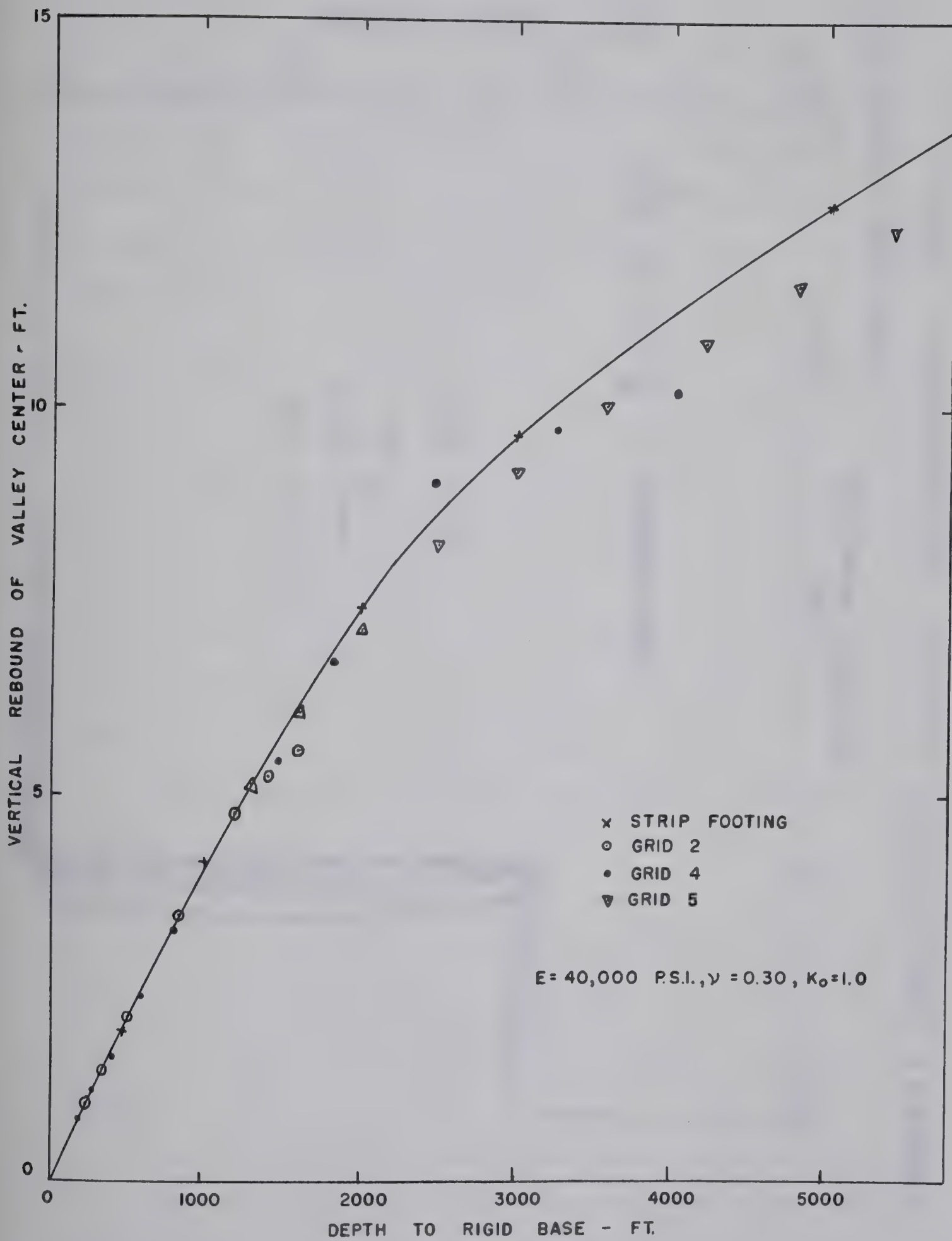
Values of rebound were calculated using Equation 4.3 for various depths to rigid base and are compared to finite element results for grids with different depths to rigid base as shown in Figure 4.6. The results are seen to be very similar and illustrate the effect of the boundary conditions used in the mathematical model on displacements for a given set of input parameters.

Duncan and Goodman (1968) studied stresses and displacements in a linearly elastic rock mass due to a vertical cut using an excavation sequence program based upon constant strain quadrilateral elements. Figure 4.7 shows displacements which will occur due to an excavation in a homogeneous rock mass for  $\nu = 0.20$  and values of  $K_0$  ranging from 0 to 2.0. The finite element grid, illustrated in Appendix D, is a replica of the grid used by Duncan and Dunlop although a coarser element mesh was used. Displacements from the two programs agreed to within a few percent; contours of stress agree well in the interior of the grid with some difference in results occurring towards the excavation boundary. The maximum shear stress at the toe of the slope was reported by Duncan and Goodman (1968) as about  $0.6 \frac{\gamma H^2}{E}$ , while the program used in this investigation gave about  $0.54 \frac{\gamma H^2}{E}$ .

The program used by Duncan and Goodman (1968) adjusts boundary node stresses using a method described by Duncan,



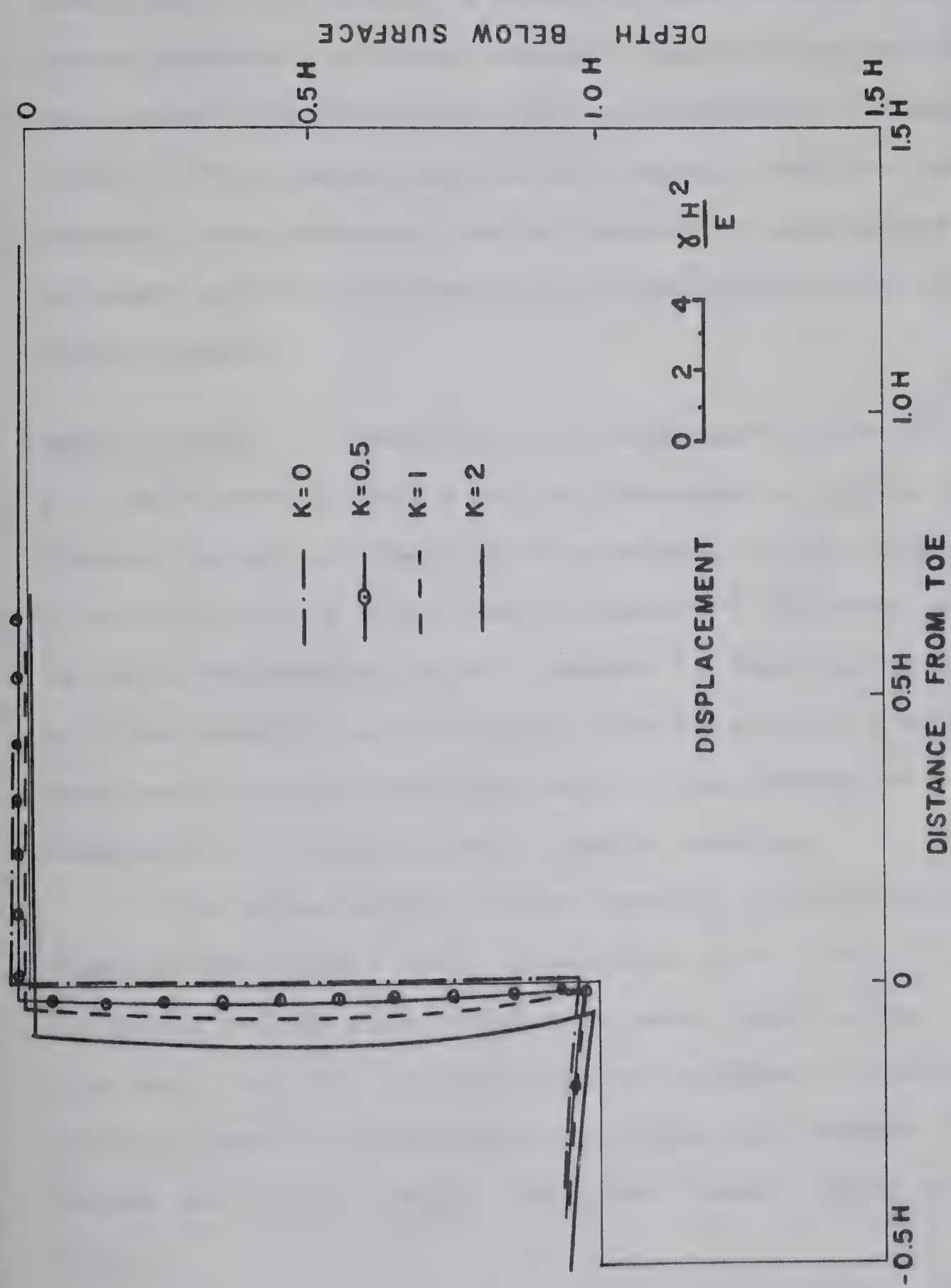




REBOUND IN VALLEY CENTER  
VERSUS DEPTH TO RIGID BASE

FIGURE 4.6





( AFTER DUNCAN & GOODMAN, 1968 )

FIGURE 4.7 DISPLACEMENTS ADJACENT TO HOMOGENEOUS VERTICAL CUT





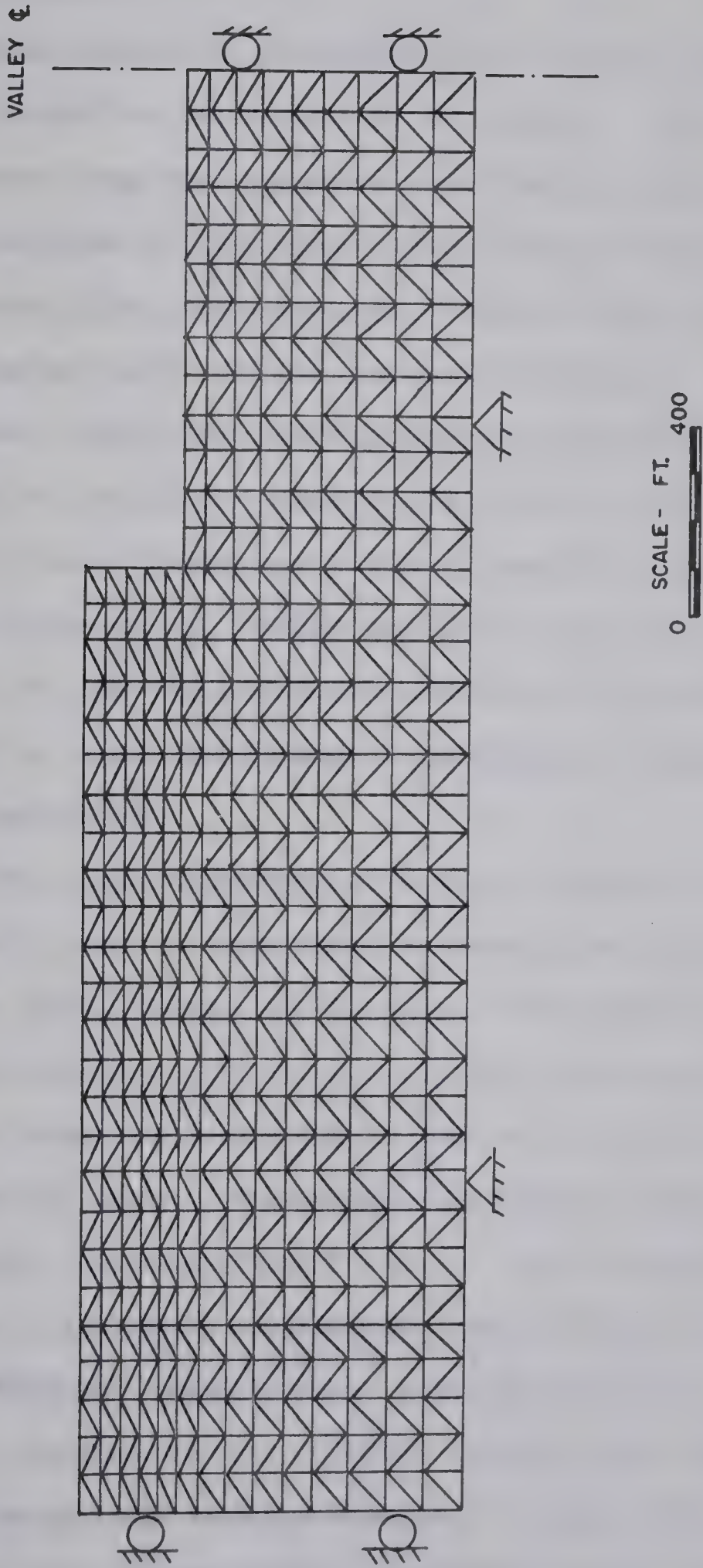
Dunlop and Seed (1968), as boundary node stresses derived from a program utilizing constant strain triangles contain an inherent approximation error as described by Wilson (1963). The program used in this thesis does not correct boundary node stresses; the difference is considered insignificant as the displacements are not affected to any appreciable extent.

Model Adopted: A number of finite element grids (Figure 4.8) were used in this study to represent a typical post-glacial valley incised into the bedrock of the study area. A valley width of 2000 feet and depth of 200 feet was taken as being representative of a number of damsites where drilling results are available. Vertical valley walls were used initially and the bedrock was assumed to be homogeneous, isotropic and linearly elastic.

The nodes on the bottom boundary of each grid were fixed in both the x and y directions ( $u = 0$ ,  $v = 0$ ) and the nodes on the side boundaries were fixed in the x direction only ( $u = 0$ ). This procedure conforms to previous finite element work reported by Duncan and Goodman (1968), Duncan and Dunlop (1969), Chang and Duncan (1970) and others.

The discussion of laboratory and field testing for E in Section 4.2 suggests that laboratory moduli serve as a lower bound for the value of E acting in the field (if a homogeneous grid is used to model field behaviour) while





FINITE ELEMENT REPRESENTATION OF A VALLEY WITH  
VERTICAL SIDES - GRID ONE

FIGURE 4.8







field moduli derived from Steinbrenner's equation serves as an upper bound.

The amount of drainage which has occurred since valley formation is difficult to assess. The rate of valley downcutting was apparently extremely rapid with most of the valleys in the study area reaching their present depth soon after deglaciation - some 15,000 to 25,000 years ago. The majority of the bedrock formations in the study area have a very low coefficient of permeability and drainage of an intact section of shale would take thousands of years (Koppula, 1970). However, stress relief and the presence of joints and fractures in the immediate vicinity of the valley would increase the permeability of the rock to a marked extent immediately adjacent to the valley perimeter.

Thus, the question of whether drained or undrained values of  $E$  act is important as data previously described (Hendron 1970, DeJong 1971) shows that the drained moduli are approximately  $1/3$  to  $1/2$  of the undrained moduli.

A wide range of moduli are reported for the bedrock of the study area. Undrained laboratory moduli range from 6500 p.s.i. to over 30,000 p.s.i. Field moduli, which represent undrained conditions, range from about 30,000 p.s.i. (Bearpaw shale) to as high as 100,000 p.s.i. (Pierre shale). Hendron et al., (1970) suggest the use of undrained moduli to analyze drained loading problems, unfortunately none of the moduli reported in the study area are



an unloading modulus. Therefore, the modulus of elasticity used in the finite element analysis was varied from 10,000 p.s.i. to 80,000 p.s.i. to cover the range of possible values.

Practically no information is available on  $\nu$  for the bedrock of the study area. Values of  $\nu$  from unconfined compression tests on core samples of the St. Mary formation (Upper Cretaceous) from the St. Mary Damsite in southern Alberta show considerable variation but generally range from 0.05 to 0.20 (P.F.R.A, 1945).

It should be noted that  $\nu$  is dependent upon drainage conditions. A soft saturated clay is nearly incompressible under undrained conditions and hence a value of  $\nu$  of approximately 0.50 is appropriate to use in an undrained analysis of an excavation made into this material. If unloading occurs over a long period of time, drainage occurs and the resulting volume change causes a reduction in  $\nu$ .

Such data that is published indicates a relatively low value of  $\nu$  is appropriate for drained conditions. Chang and Duncan (1970) found  $\nu = 0.20$  for the Buena Vista sandy soils in drained triaxial tests. A considerable scatter of results was noted and there appeared to be no trend toward variation in  $\nu$  with increasing confining pressure. However, Mahtab and Goodman (1968) observed an increase in  $\nu$  with deviator stress for samples of schistose gneiss and Berea sandstone. It was noted that the rate of increase of  $\nu$  decreased with confining pressure.







In view of the almost total lack of data on  $\nu$  in the bedrock of the study area, a range of  $\nu$  from 0.48 (to simulate undrained behaviour in soft, saturated clay-shales) to 0.10 was used in the analysis.

The stress history of the bedrock has been discussed in Chapter II and only one in-situ measurement of vertical and lateral stresses is recorded - the measurement of  $K_0$  equal to 1.50 at the South Saskatchewan River Dam. However, in view of the large depths of material removed by erosion during the Tertiary period and the depth of ice (as high as 5000 feet) the area was covered with during the Pleistocene, values of  $K_0$  could be appreciably higher than 1.50. Thus, a range of  $K_0$  from 0.43 to 3.00 was used in the analysis to cover all likely states of in-situ stress.

#### 4.4 Displacements Due To Valley Excavation In A Homogeneous Elastic Rock

Grid 1 (Figure 4.8) was used initially to simulate the valley. The rigid base of the finite element grid was placed 600 feet below the valley bottom and the lateral boundary was placed 2,000 feet back from the valley edge so that its position would have little influence upon displacements in the vicinity of the valley.

The displacements obtained from this study have not been put into non-dimensional form by dividing by  $\frac{\gamma H^2}{E}$ . A direct measure of displacement appears to be of more interest in this study since field rebound values exist for



valleys of similar geometry.

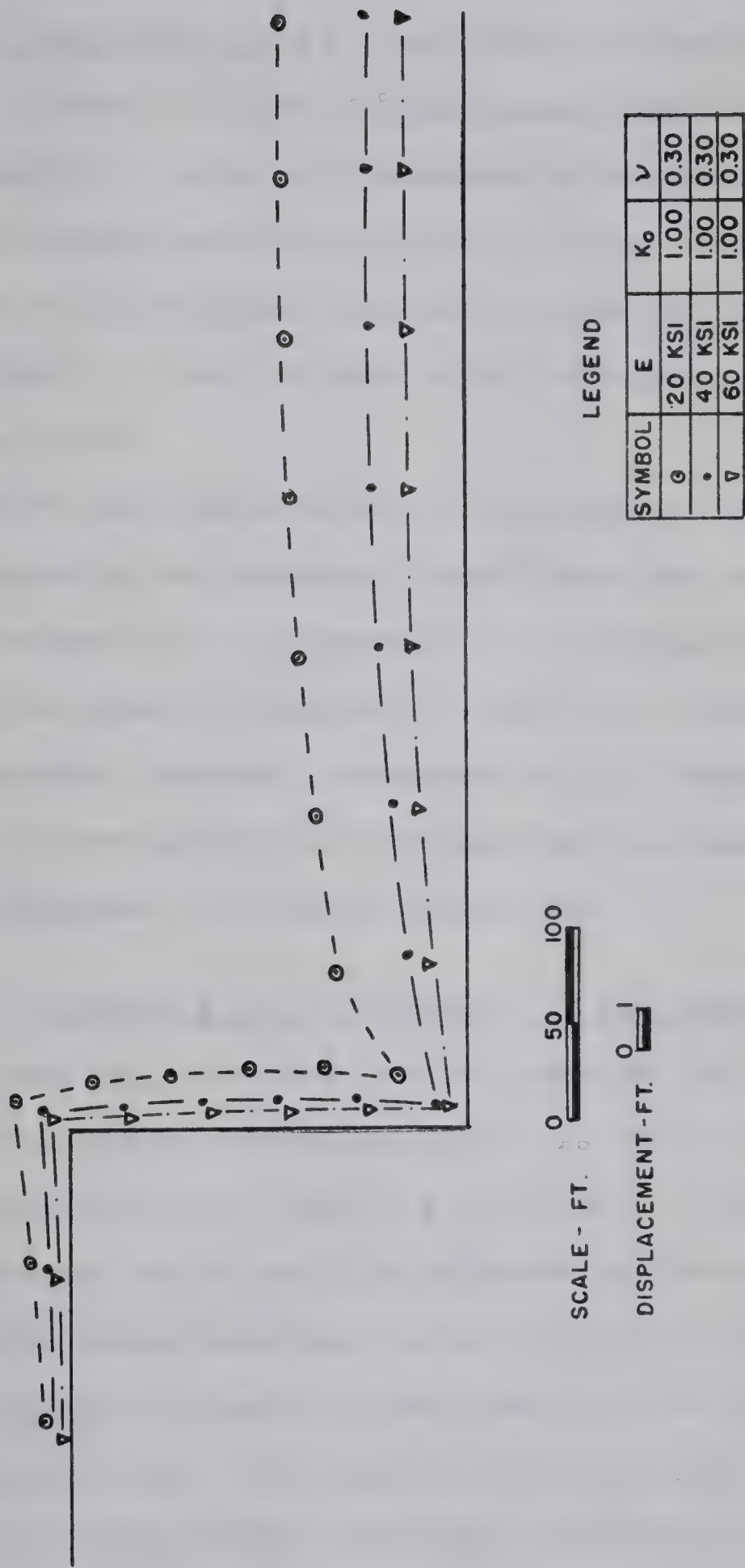
Effect of Variation in E: Figure 4.9 shows the displacements which will occur in the vicinity of the valley wall due to valley excavation for a homogeneous grid with  $K_0 = 1.00$ ,  $\nu = 0.30$  and values of E of 20,000 p.s.i., 40,000 p.s.i., and 60,000 p.s.i. Excavation of the valley produces an upward rebound of the valley floor, an inward movement of the valley walls and a gentle rise in the ground surface as one moves towards the valley edge. In effect, the general form of field observations documented in Chapter III is reproduced by the finite element analysis. The magnitude of displacements, for constant values of  $K_0$  and  $\nu$ , is a function of the reciprocal of E with displacements increasing with lower values of E.

The valley anticlines documented in Chapter III characteristically show the rebound at the valley center as being at least 3 percent of the valley depth (6 feet for this grid). Therefore, a value of E of somewhat less than 20,000 p.s.i. would be required to produce valley anticlines of the magnitude observed in the study area.

The displacement pattern for low values of E, given in Figure 4.9, shows that the majority of the rebound in the valley bottom occurs over the first 50 feet out from the valley wall. A change in the dip of the bedding planes of close to 2 degrees would be observed in the field for  $E = 20,000$  p.s.i. if the model used perfectly simulated field behaviour.







DISPLACEMENTS DUE TO VALLEY  
EXCAVATION - GRID ONE

FIGURE 4.9



Effect of Variation in  $\nu$ : The effect of variation in  $\nu$  is shown in Figure 4.10 for a homogeneous grid with  $E = 40,000$  p.s.i. and  $K_0 = 1.00$ . A considerable variation in displacement occurs which indicates that the actual determination of  $\nu$  is of some importance. However, the effect of a variation in  $\nu$  can be seen to be secondary compared to a variation in  $E$ .

Vertical displacement is reduced for high values of  $\nu$  corresponding to undrained conditions and is maximized for low values of  $\nu$  corresponding to drained conditions. The results given in Figures 4.9 and 4.10 indicate that the time-dependent rebound, characteristic of excavation behaviour, is associated with drainage and the change in  $E$  and  $\nu$  from undrained to drained conditions.

Change in Surface Profile Adjacent to the Excavation: The surface profile, from the lateral edge of the finite element grid to the top of the valley wall, is shown in Figure 4.11 for a variation in  $K_0$  from 0.43 to 3.00. A high value of  $K_0$  suppresses the raised rim adjacent to the valley wall. Figure 4.12 shows that the raised valley rim is maximized at low values of  $E$  and is a manifestation of rebound in the valley bottom. The distance back from the valley edge to the point the valley rim begins to rise is independent of  $E$  with a variation in  $E$  effecting only the height of the raised rim.







SCALE- FT.  
0 50 100

DISPLACEMENT - FT.  
0 1

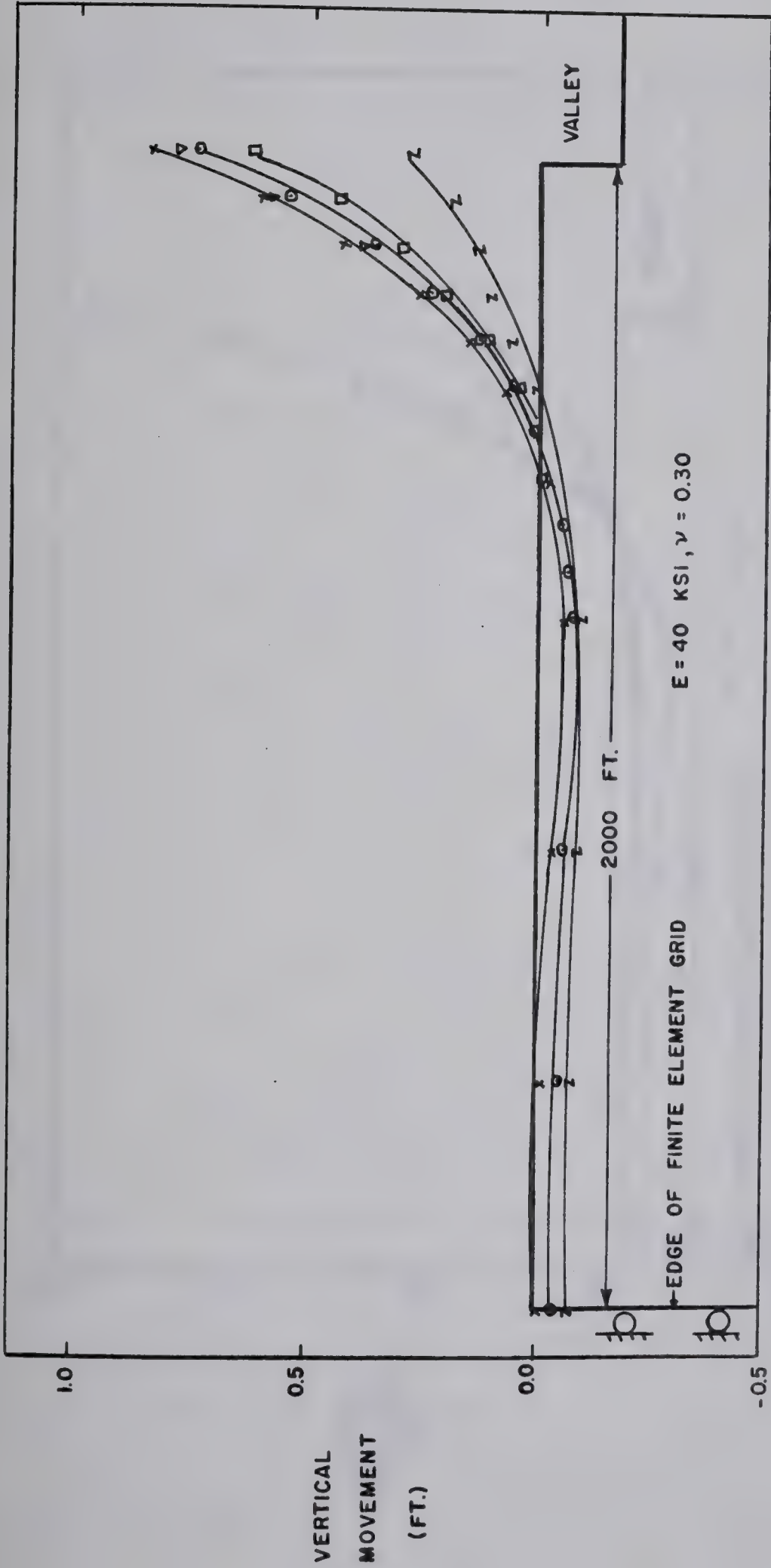
LEGEND

SYMBOL	E	K <sub>o</sub>	ν
•	40 KSI	1.00	0.10
⊙	40 KSI	1.00	0.30
Δ	40 KSI	1.00	0.40

DISPLACEMENTS DUE TO VALLEY  
EXCAVATION - GRID ONE

FIGURE 4.10





LEGEND

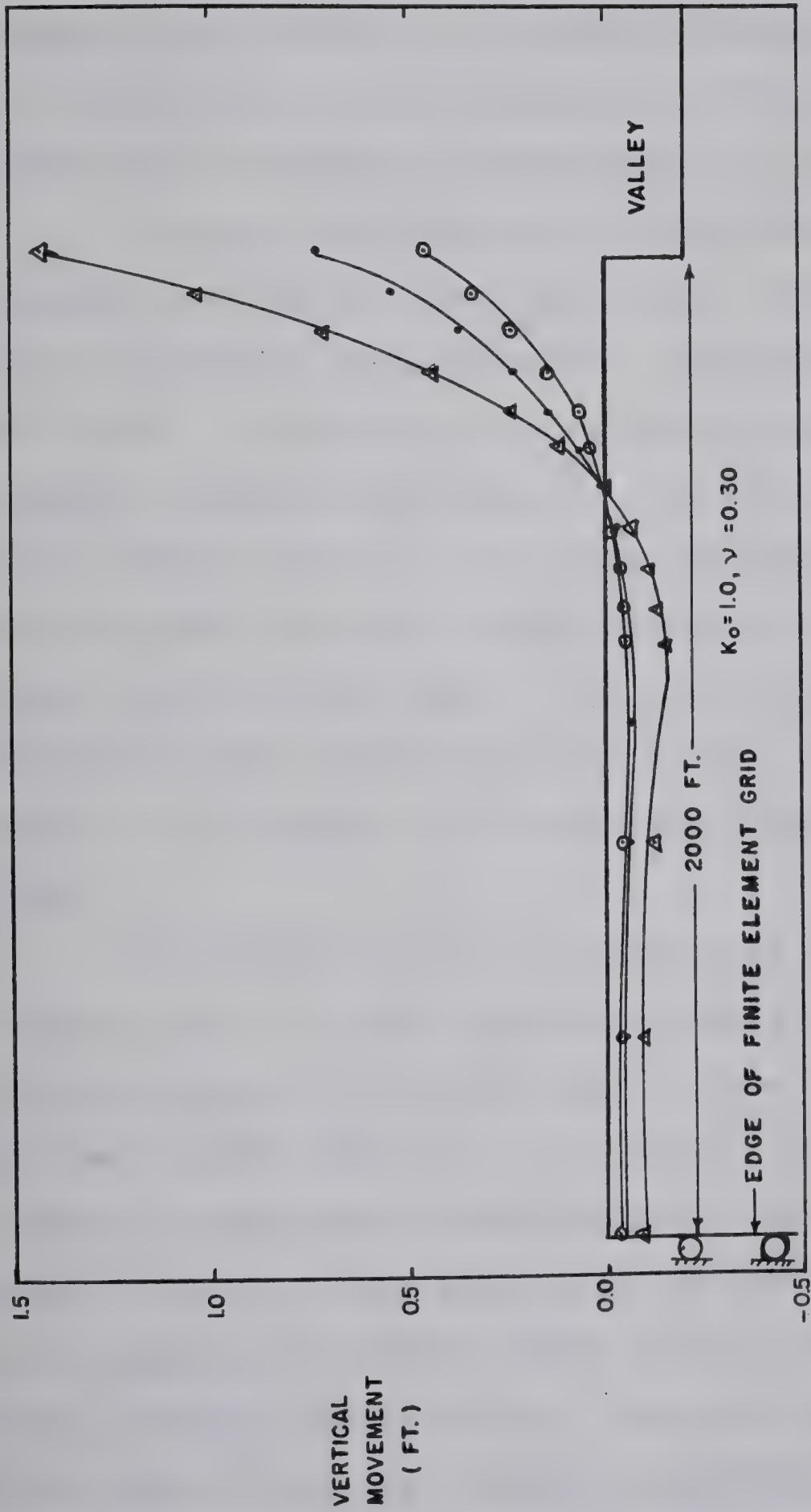
SYMBOL	$K_0$
z	3.00
□	1.50
○	1.00
▽	0.75
x	0.429

VERTICAL DISPLACEMENT OF THE GROUND  
ADJACENT TO THE RIVER VALLEY - GRID I

FIGURE 4.11







LEGEND

SYMBOL	E
△	20 KSI
·	40 KSI
○	60 KSI

VERTICAL DISPLACEMENT OF THE GROUND  
ADJACENT TO THE RIVER VALLEY-GRID I

FIGURE 4.12



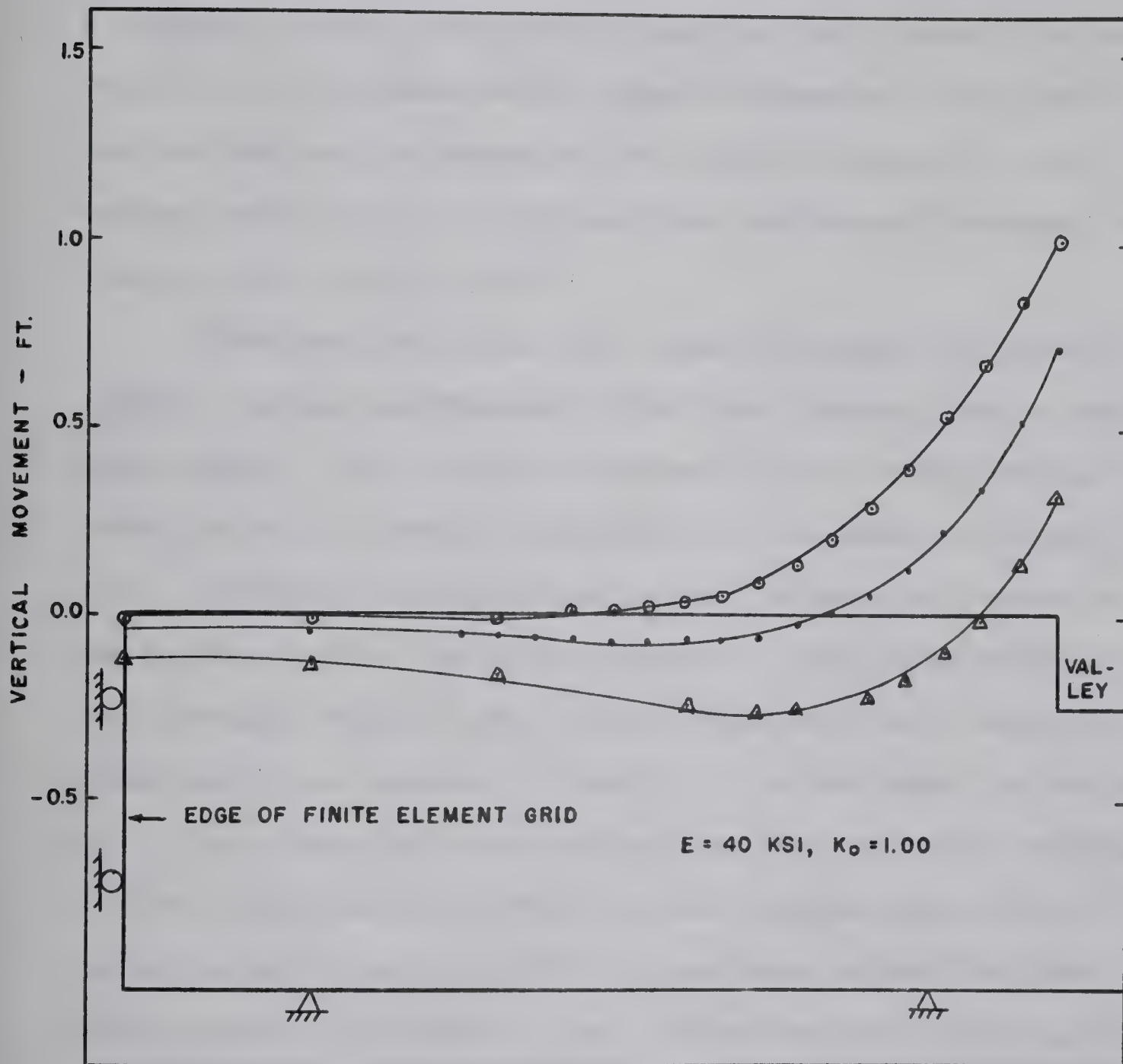
Figure 4.13 shows the surface profile adjacent to the valley for a variation in  $\nu$ . The raised rim is maximized at low values of  $\nu$  simulating drained conditions. The distance back from valley edge to the beginning of the raised rim is shown to be sensitive to a variation in  $\nu$ .

A valley rim formed soon after valley formation, assuming a relatively low value of  $K_0$ , will be controlled by the undrained parameters which results in a high value of  $E$  and  $\nu$ . The result is a relatively small rise in the surface adjacent to the valley. The use of drained parameters will lead to a 2 to 3 fold increase in the height of the raised rim and a marked increase in the distance back from the valley edge to the point the ground surface starts to rise. A high value of  $K_0$  will suppress the height of the valley rim and slightly reduce its base width.

The raised valley rims documented in Appendix C indicate that at least partially drained conditions exist in the bedrock of the study area in view of the magnitude of the features measured in the field. The apparent increase in magnitude and definition of the raised rims from south to north in the study area may be due to more complete drainage of bedrock below valleys formed in the early stages of deglaciation. However, the numerous factors which affect the ultimate topographic surface adjacent to the valley - initial local relief, weathering,  $K_0$ ,  $E$ ,







LEGEND	
SYMBOL	$\nu$
$\Delta$	0.40
.	0.30
$\circ$	0.10

VERTICAL DISPLACEMENT OF THE  
GROUND ADJACENT TO THE RIVER  
VALLEY - GRID ONE

FIGURE 4.13



and  $\nu$  - make it impossible, at this time, to explore more fully the implications of this feature.

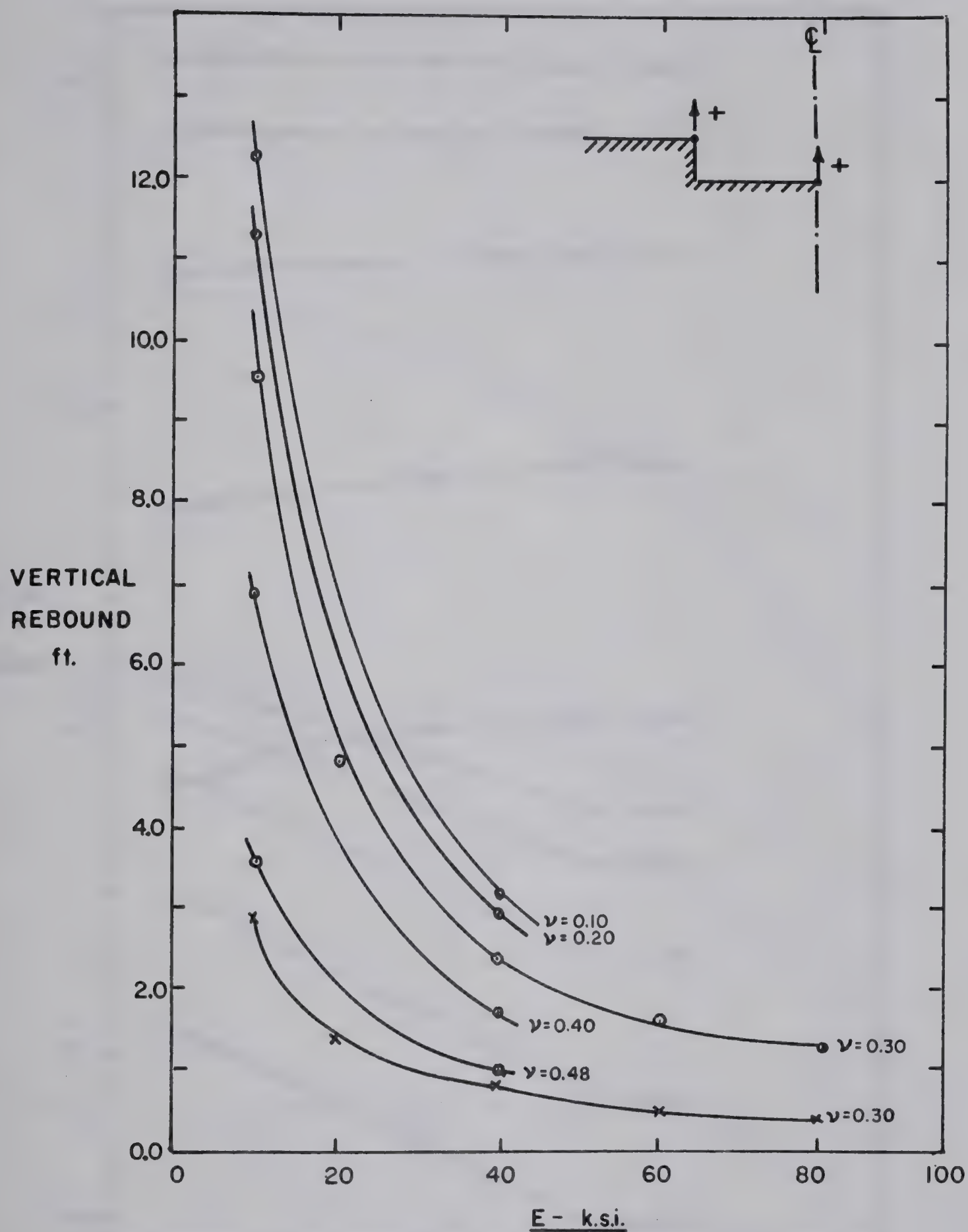
#### Effect of Input Parameters on Maximum Vertical Rebound:

A clearer picture of events occurring, as a result of variation of one or more of the input parameters ( $E$ ,  $\nu$  and  $K_0$ ), can be obtained by studying the maximum rebound in the valley center and the vertical and horizontal movement of the top and toe of slope.

The results agree with those reported by Dibiagio (1966), Duncan and Goodman (1968) and Duncan, Dunlop and Seed (1968). The vertical rebound in the valley center is found to be an inverse function of  $E$  as shown in Figure 4.14. Rebound due to stress relief is seen to become a negligible factor for high values of  $E$  and thus valleys cut through bedrock with a high value of  $E$  will exhibit practically no rebound. Figure 4.15 shows that the value of  $K_0$  has practically no effect upon the vertical rebound of the valley center. The vertical displacement of the valley edge is about  $1/3$  of the maximum rebound in the valley center (for Grid 1) at low values of  $\nu$  although the relationship is affected by  $K_0$  to some extent. A downwarping of the ground surface adjacent to the valley is predicted for values of  $K_0$  greater than 0.75 for undrained conditions ( $\nu = 0.48$ ) as shown in Figure 4.16. A reduction in  $\nu$  to 0.20 or 0.30 will result in suppression of the rim for values of  $K_0$  as high as 3.0. Duncan and Goodman (1968)







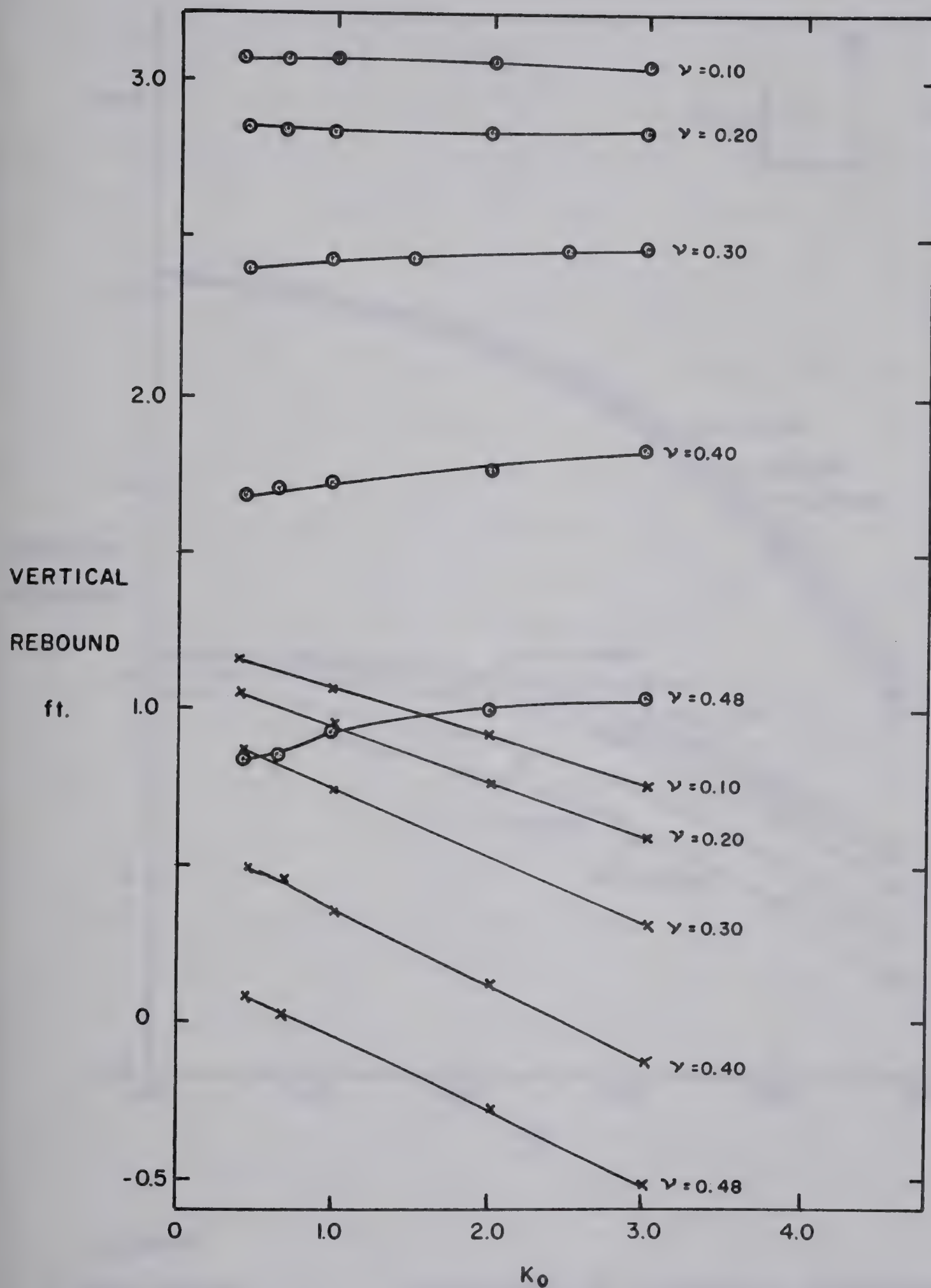
### LEGEND

- VALLEY CENTER
- x VALLEY EDGE

VARIATION OF VERTICAL DISPLACEMENT  
WITH E - GRID 1,  $K_0 = 1.00$

FIGURE 4.14



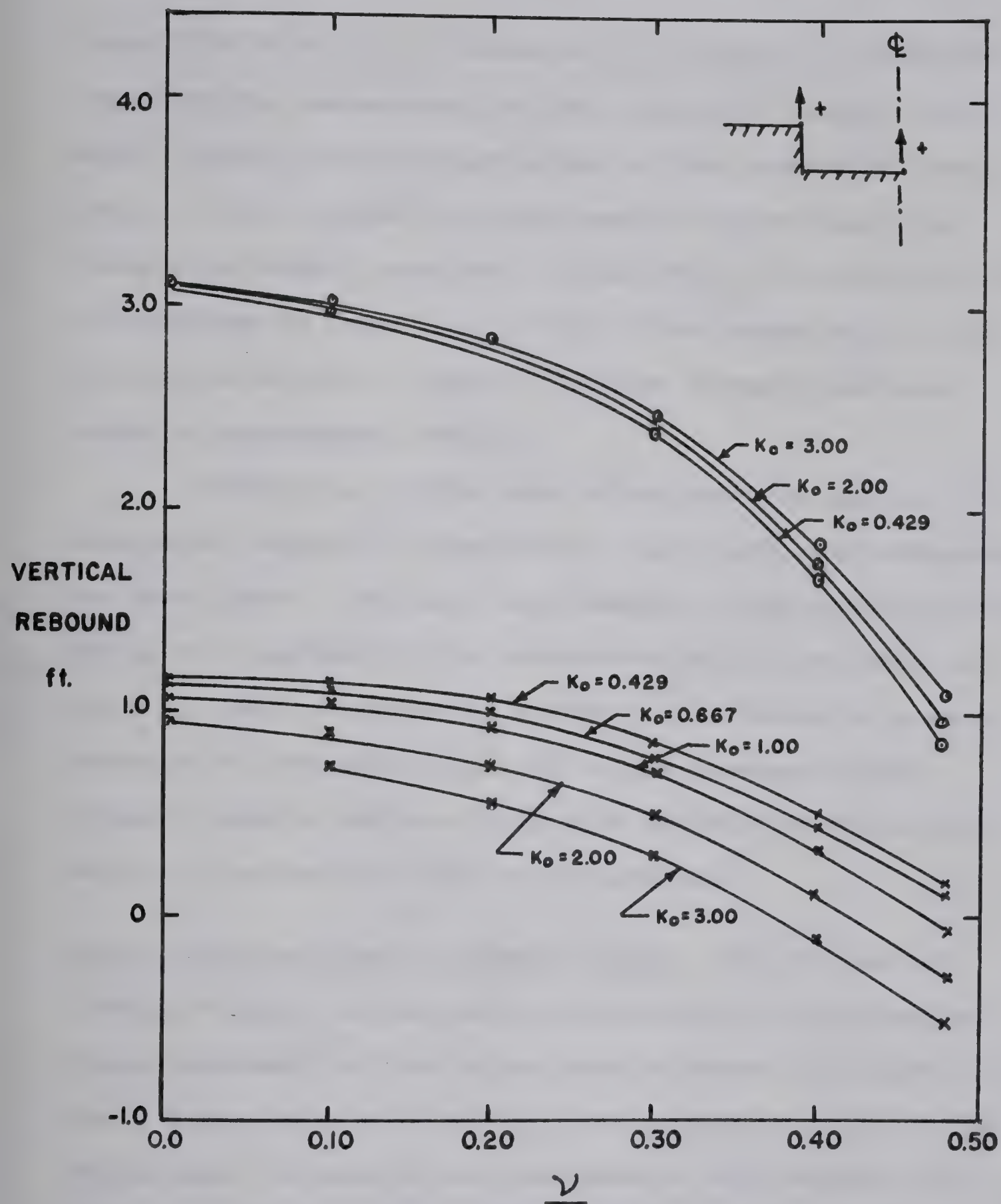


VARIATION OF VERTICAL DISPLACEMENT  
WITH  $K_0$  - GRID I,  $E = 40$  KSI

FIGURE 4.15







VARIATION OF VERTICAL DISPLACEMENT  
WITH POISSON'S RATIO - GRID I,  $E=40$  KSI

FIGURE 4.16



found, for  $\nu = 0.20$ , a value of  $K_0$  of about 1.5 would be required for downwarping of the valley rim using a grid with a depth to rigid base equal to the excavation depth. Grid 1, with a depth to rigid base of three times the excavation depth, requires a value of  $K_0$  of close to 5 for downwarping to occur if  $\nu = 0.20$ . The comparison illustrates the effect of depth of finite element grid when using a homogeneous section.

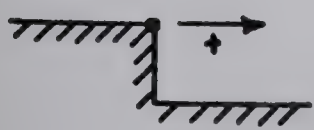
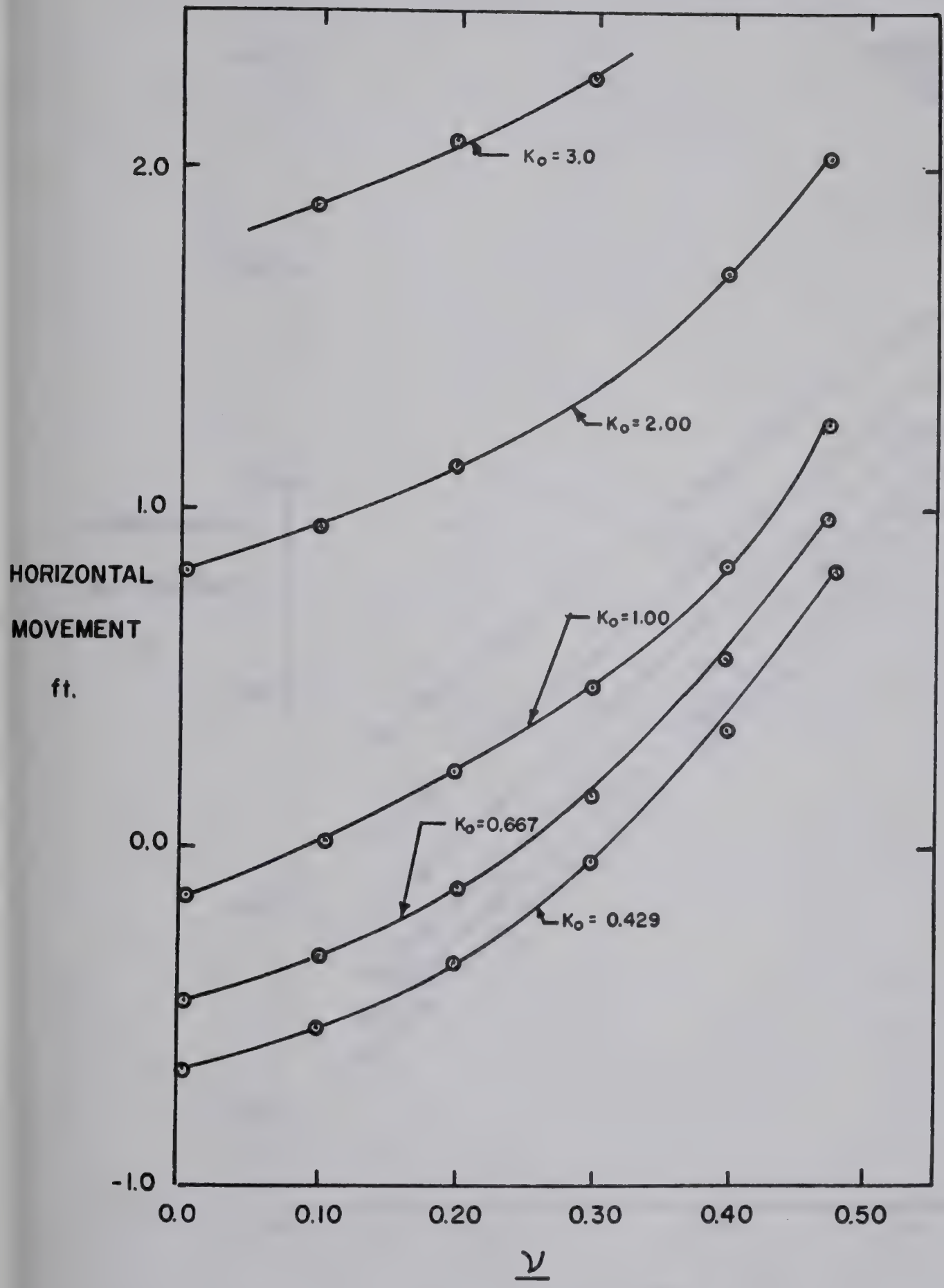
Downwarping of the edge of excavations cut in soft, saturated, normally consolidated clays have been documented by Peck (1969). Vertical settlements of the ground surface of up to 2 percent of the excavation depth have been recorded. This phenomena is commonly attributed to plastic yielding of the clay at toe of slope; however finite element results indicate that some of this behaviour may be due to undrained elastic displacements.

Lateral Movement Due to Stress Relief: The release of lateral stress, due to valley downcutting, will cause an inward movement of the valley edge as shown in Figure 4.17. For a given value of  $E$  and  $K_0$ , the inward movement of the valley wall is seen to be a maximum at high values of  $\nu$ . Lateral movement of the valley edge is a direct function of  $K_0$  as shown in Figure 4.18. Maximum movements in the order of 2 to 3 feet will occur at high values of  $K_0$  if  $E = 40,000$  p.s.i.

The effect of a variation in  $E$  is shown in Figure 4.19 for  $K_0 = 1.00$  and  $\nu = 0.30$ . The inward lateral movement



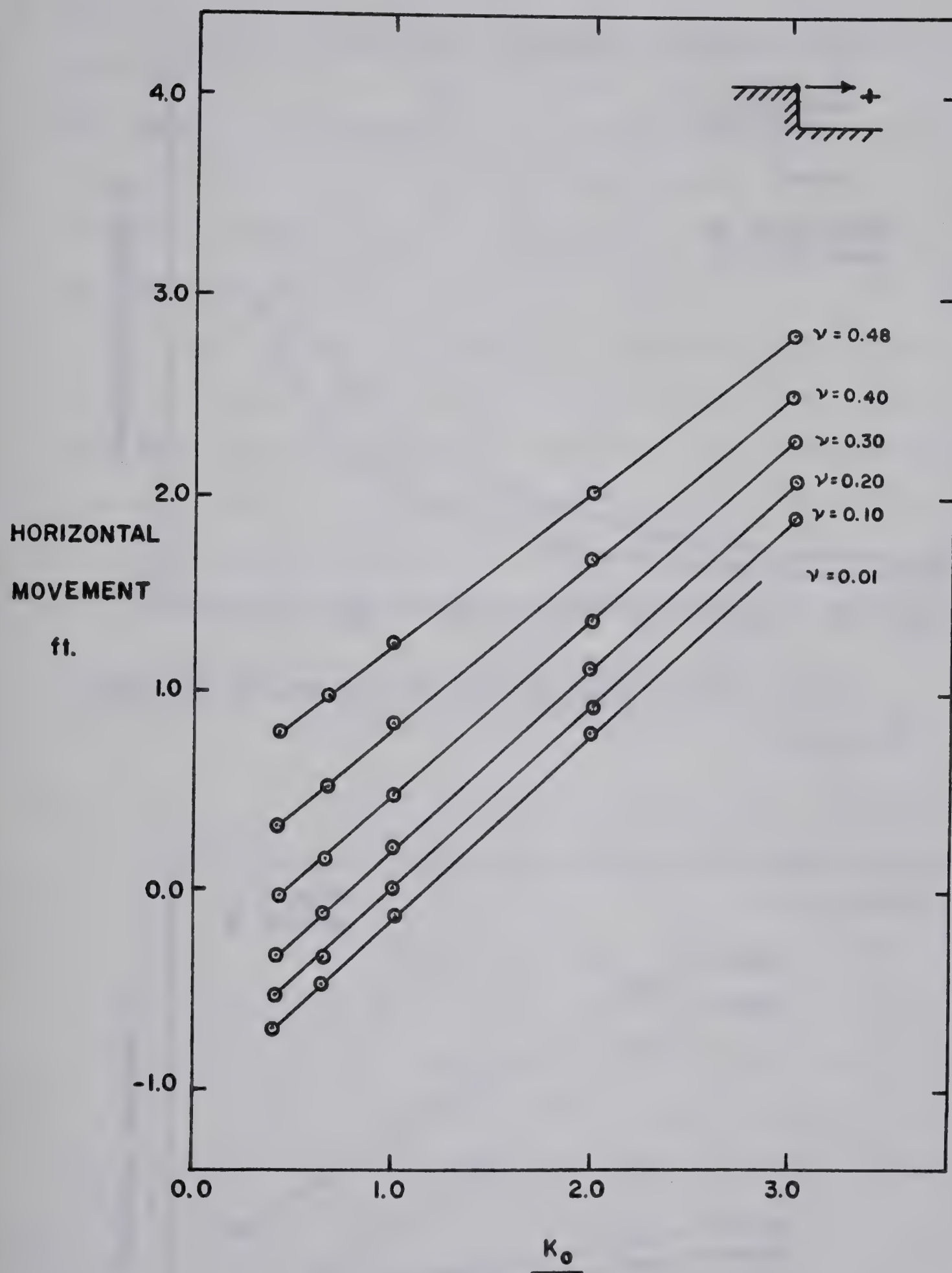




HORIZONTAL MOVEMENT OF VALLEY  
EDGE - GRID I , E=40 KSI

FIGURE 4.17



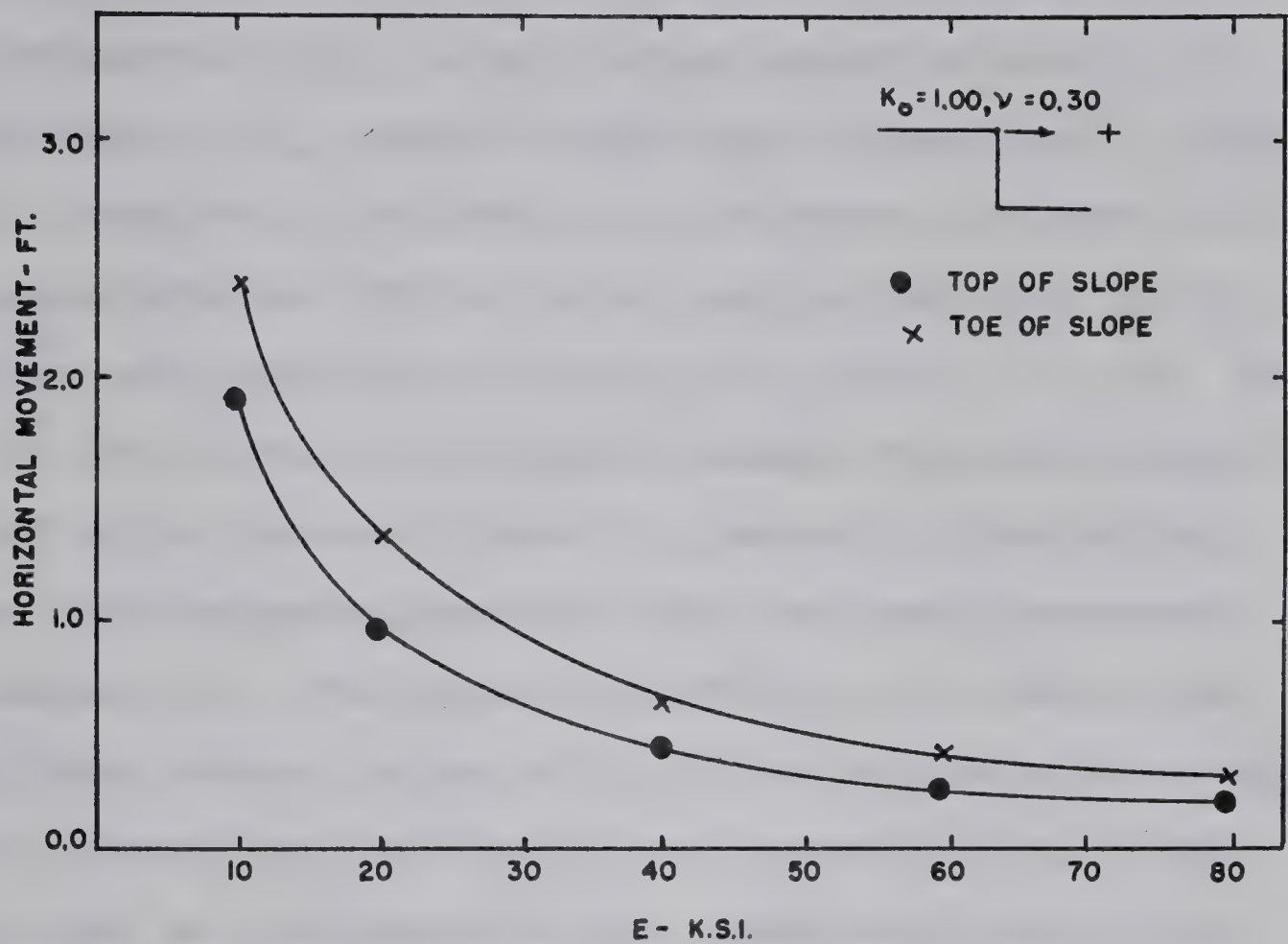


EFFECT OF  $K_o$  ON HORIZONTAL MOVEMENT  
OF VALLEY EDGE - GRID I,  $E=40$  KSI

FIGURE - 4.18

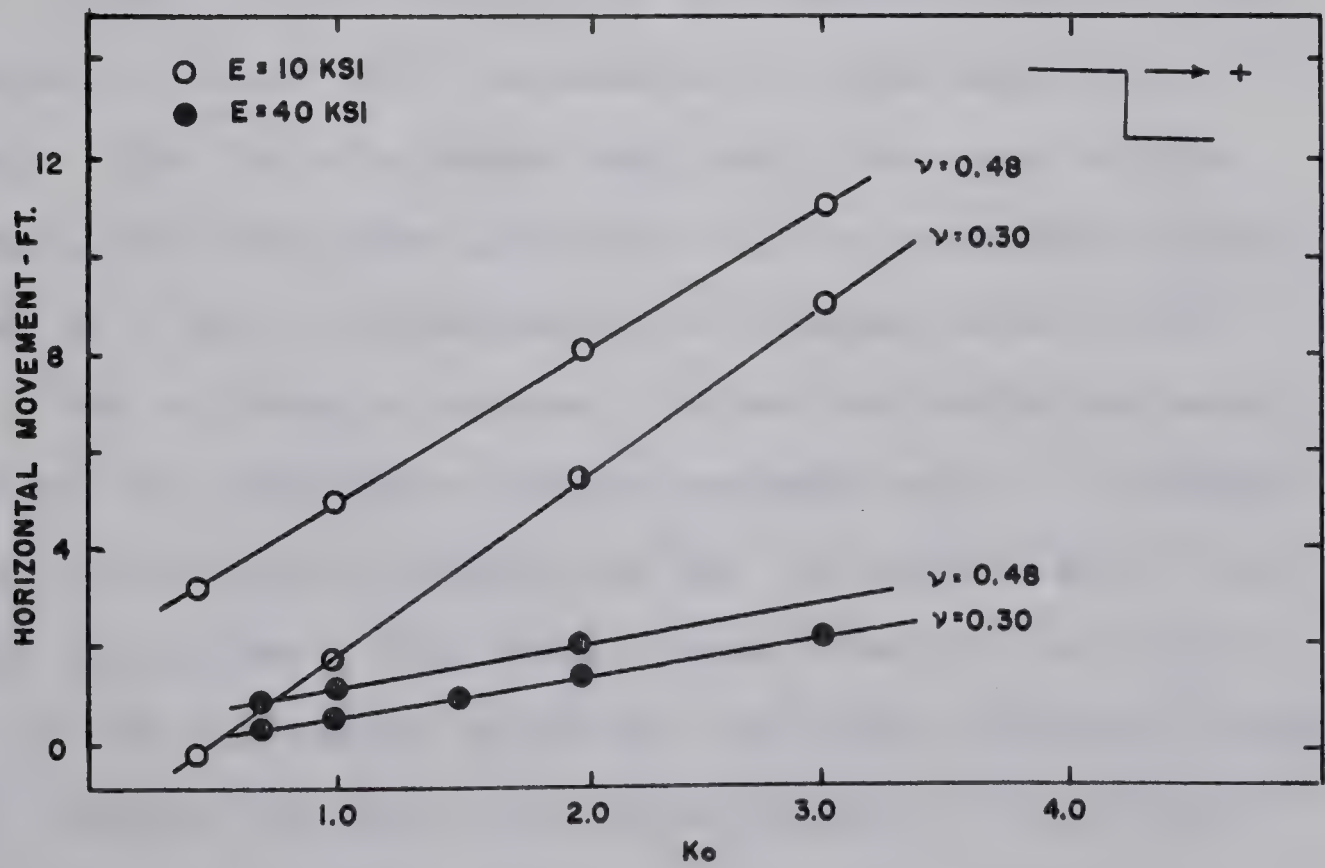






VARIATION OF HORIZONTAL DISPLACEMENT WITH E - GRID I

FIG. 4.19



VARIATION OF HORIZONTAL DISPLACEMENT WITH  $K_o$  - GRID I

FIG. 4.20



of the top and toe of slope are shown to be a function of the reciprocal of  $E$ . A much larger inward movement, for high values of  $K_0$ , occurs at the top of slope for  $E = 10,000$  p.s.i. than for  $E = 40,000$  p.s.i. as shown in Figure 4.20. An inward movement of the valley wall in the order of 10 feet is predicted for  $E = 10,000$  p.s.i. and  $K_0 = 3.00$ . The use of  $E = 10,000$  p.s.i. gives a maximum vertical rebound in the valley center of about 3.2 percent of the valley depth which compares favorably with the cases documented in Chapter III. The value of 10,000 p.s.i. is much lower than field deduced values of  $E$  for the bedrock of the study area, however the field moduli are essentially undrained moduli and are influenced by the assumptions implicit in Steinbrenner's equation as has been previously discussed.

Discussion: The valley anticlines noted below postglacial river valleys in the study area are formed primarily as a function of  $E$  and  $\nu$  of the bedrock and the depth of the valley. The finite element analyses, discussed in this chapter, show that the anticline will be maximized by low values of  $E$  and  $\nu$  corresponding to drained conditions.

The difference between drained and undrained moduli explains the difference between maximum values of rebound noted in artificial excavations and the magnitude of the valley anticlines. The former range from 0.5 to 1.0 percent of the excavation depth and the latter typically range from 3 percent of the valley depth upwards. Artificial





excavations are open for a relatively short period of time and little time exists for drainage to occur in the bedrock mass below the excavation; therefore, an undrained modulus controls the measured deformations and a much smaller value of rebound occurs than in the case of natural valleys which have existed for many thousands of years.

This concept explains why a large proportion of the measured field rebound in the cases discussed in Chapter II is time-dependent and why most of the total rebound measured occurs in the top few feet of the bedrock below the excavation bottom. Drainage of the upper few feet of the bedrock surface occurs and reduces the modulus acting from undrained to drained conditions which results in the major proportion of the rebound occurring near the bedrock surface. This process is still occurring in some cases and the continuing slow rebound noted at Garrison, Oahe and Fort Peck Dams (Chapter II) appears to be due to continuing 'modulus change' at greater depths.

The analysis of the Buena Vista excavation (Chang and Duncan, 1970) assumes either zero or total drainage of the material around the excavation. The excavation was open for approximately one year and it appears unlikely that anything approaching complete drainage occurred, particularly at a considerable depth below the excavation bottom and in the thick clay zones present in the stratigraphic profile. The predicted displacements, which agreed closely with observed behaviour, were based on fully



drained parameters again indicating the possible effects of the position of the finite element grid.

The finite element studies using Grid 1 show that a value of  $E$  in the order of 10,000 p.s.i. is required to produce valley anticlines and raised valley rims of the magnitude of those observed in the field. This figure agrees reasonably well with the range of undrained laboratory moduli for bedrock of the study area but it is well below field derived moduli.

#### 4.5 Effect of Depth to Rigid Base

No study has yet been published on the effect of increasing the depth of the finite element grid in excavation simulation. All previous finite element excavation studies have used a comparatively shallow depth to rigid base. Duncan and Goodman (1968) and Duncan and Dunlop (1969) used a depth of homogeneous elastic material below the bottom of the excavation equal to the depth of excavation. Chang and Duncan (1970) used a depth to rigid base equal to three times the depth of excavation, as has been mentioned previously. The depth to rigid base in most previous finite element work appears to have been dictated more by computer storage capacity than by any evidence on what constitutes proper simulation of field conditions.

In certain field problems, a position for the bottom base of the finite element grid can be obtained from a study of the geologic profile. An example, discussed







previously, is the Ottawa sewage plant excavation (Bozozuk, 1963) where some 90 feet of soft Leda clay overlies limestone. The modulus of the bedrock would be many times that of the clay and the interface could be taken as the bottom rigid base of the finite element grid with some degree of confidence.

No such clear-cut delineation exists in the field cases documented in Chapter III. Throughout the study area, many thousands of feet of sedimentary rock overlies the Precambrian basement. Thus, if a homogeneous finite element grid is used to study river valley formation, the position of the rigid base of the grid will be arbitrary. The value of  $E$  required to give observed values of rebound for a given valley section will be a function of the depth of the finite element grid. Therefore, use of any mathematical model, assuming a homogeneous elastic medium, to derive values of  $E$ ,  $\nu$  and  $K_0$  acting in-situ will not yield unique solutions.

Grids 2, 4 and 5 (Figure 4.21) were used to study the effect of depth to rigid base. The depth to rigid base was varied from 1600 to 0 feet below valley bottom by progressively setting the modulus of the lower rows of elements to a very high value ( $0.4 \times 10^9$  p.s.i.), thus simulating a rigid base. The validity of this 'high modulus' technique was checked by two runs where the node points, at the chosen depth to rigid base, were fixed in  $x$  and  $y$  along the top of a row of elements where a high

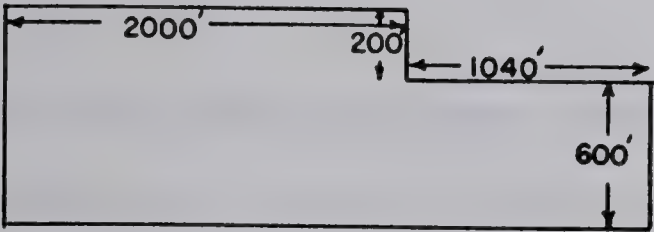


GRID NO.

SKETCH

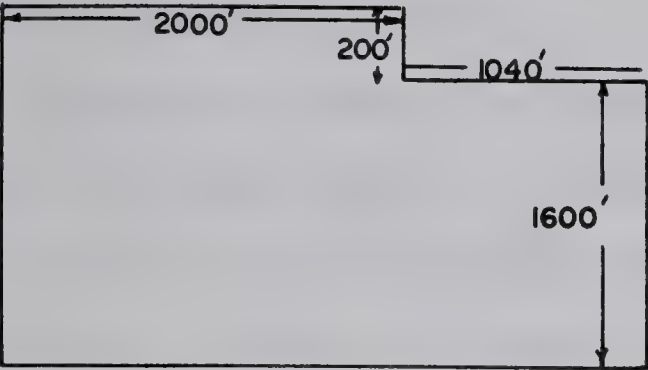
USE

1



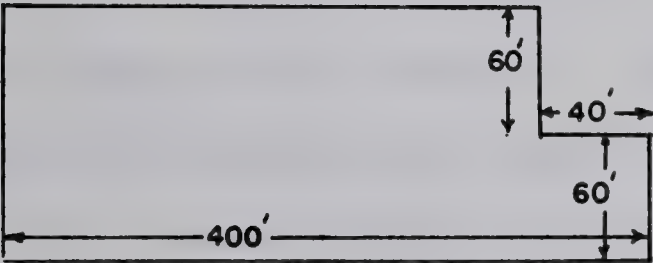
VARIATION OF  $E, \nu, K_0$

2



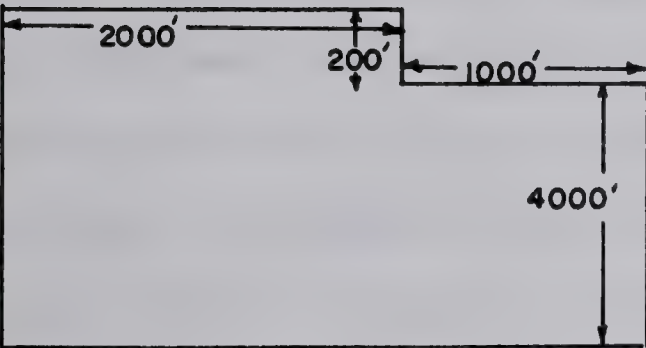
VARIATION OF  $E$  WITH DEPTH  
VALLEY WIDTH, DEPTH, & WALL  
INCLINATION

3



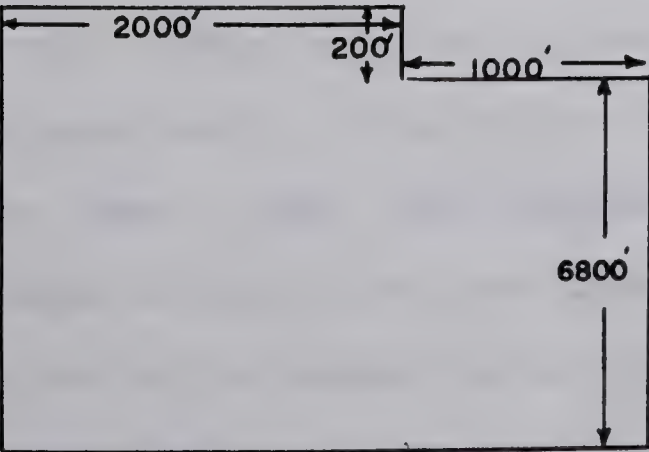
COMPARISON WITH RESULTS  
REPORTED BY DIBIAGIO (1966)

4



EFFECT OF DEPTH TO RIGID  
BASE

5



EFFECT OF VARIATION IN  $E, \nu, K_0$   
AND DEPTH TO RIGID BASE

FINITE ELEMENT GRIDS

FIGURE 4.21





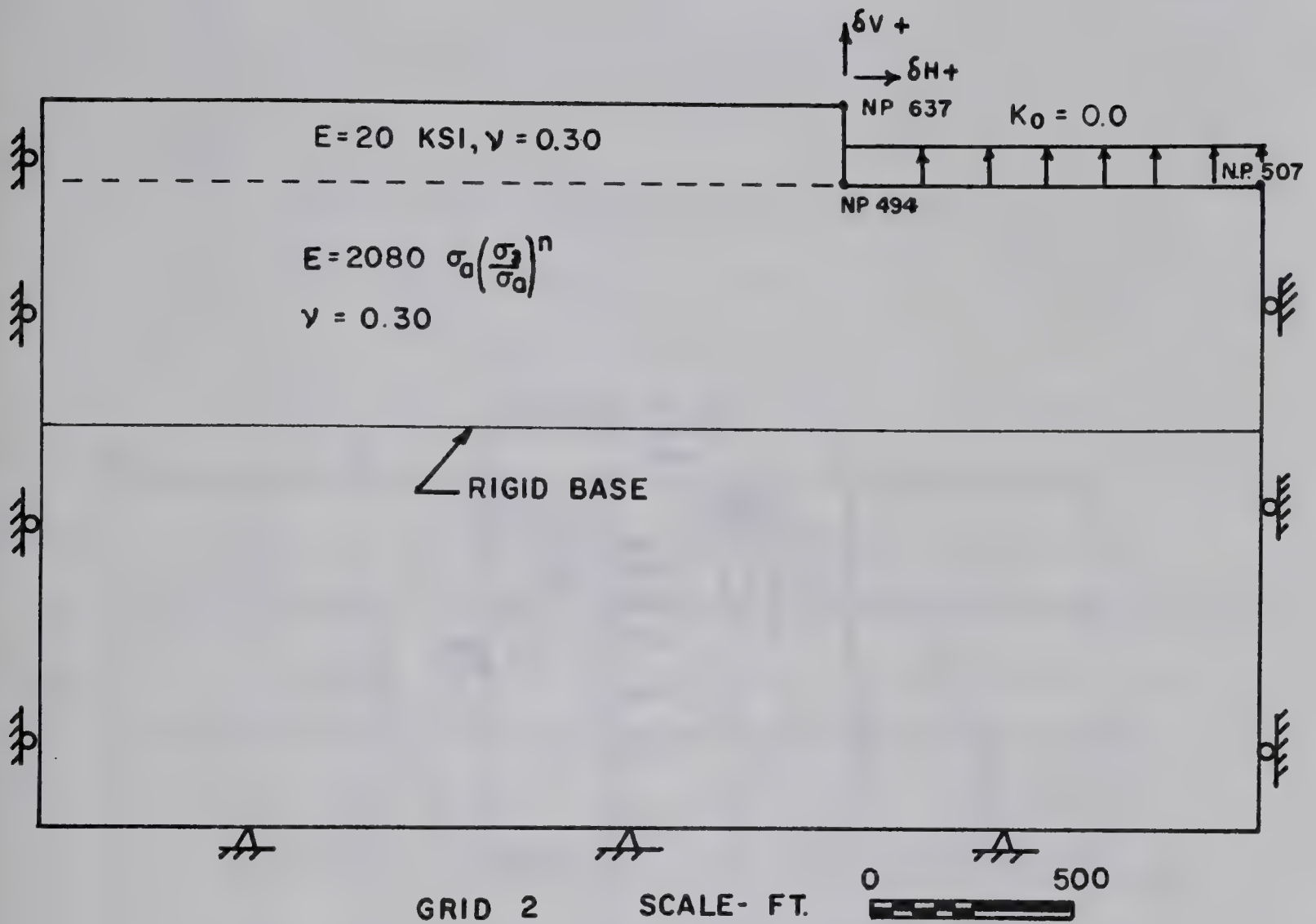
modulus had previously been used to simulate a rigid base. The results are shown in Figure 4.22 and the difference in displacements between the two techniques is negligible around the valley periphery.

Figure 4.6 shows the effect of depth of finite element grid upon values of rebound in the valley center for a given set of input parameters ( $E = 40,000$  p.s.i.,  $\nu = 0.30$ ,  $K_0 = 1.00$ ). A linear relationship exists between maximum rebound in the valley center and depth to rigid base up to a depth of 1200 feet. Further deepening of the finite element grid leads to a decrease in the rate of increase of rebound with depth to rigid base.

The reason for this phenomena is shown in Figure 4.23 where the principal stress changes induced in a homogeneous, isotropic, elastic material under a strip load are shown. A valley 2000 feet wide will thus, on formation, induce changes in vertical stress of up to 20% of the stress relieved on the valley floor at a depth of over 6000 feet. Changes in lateral stress are shown to decrease much more rapidly with depth.

The correspondence between maximum rebound in the valley center and the rebound in the center of a 2000 foot wide strip loaded with an equivalent traction has been discussed previously. The closed form solution for a strip footing (Harr, 1966) and computer solutions are identical to a depth of 1200 feet and show that rebound in the valley center is not affected, to any appreciable degree, by the restraining effect of the valley walls.





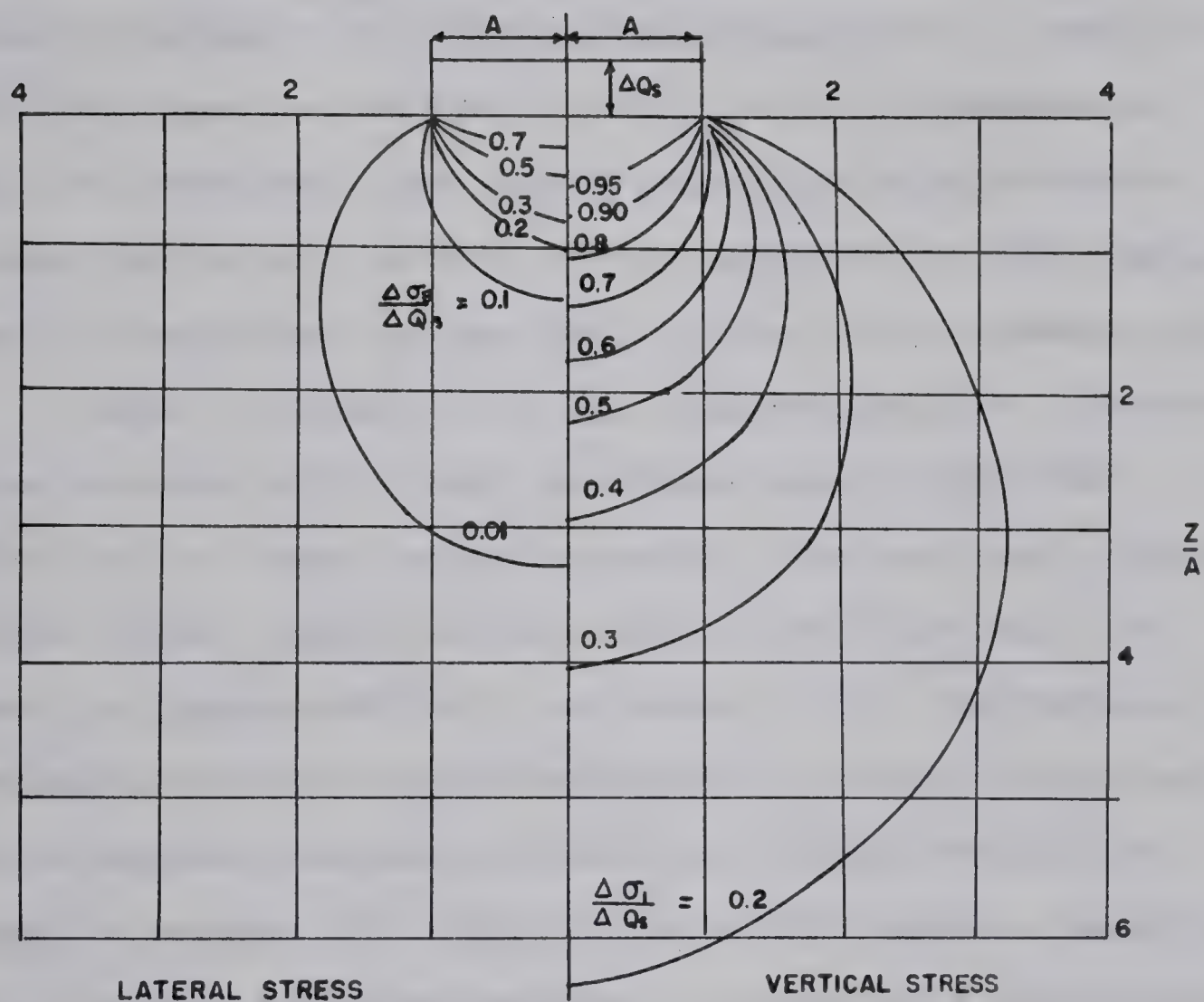
METHOD OF FIXING RIGID BASE	NP 507 δV FT.	TOE OF SLOPE-NP 494		TOP OF SLOPE- NP 637	
		δH FT.	δV - FT.	δH - FT.	δV- FT.
FIXITY OF NODES IN X & Y	0.8892	0.0328	0.4120	-0.1857	0.3293
HIGH MODULUS ( $.4 \times 10^9$ P.S.I.)	0.8896	0.0326	0.4124	-0.1856	0.3294

## COMPARISON OF METHODS OF FIXING RIGID BASE-GRID 2

FIGURE 4.22







( LAMBE AND WHITMAN, 1969 )

CHANGE IN PRINCIPAL STRESS  
UNDER A STRIP LOADING

FIGURE 4.23

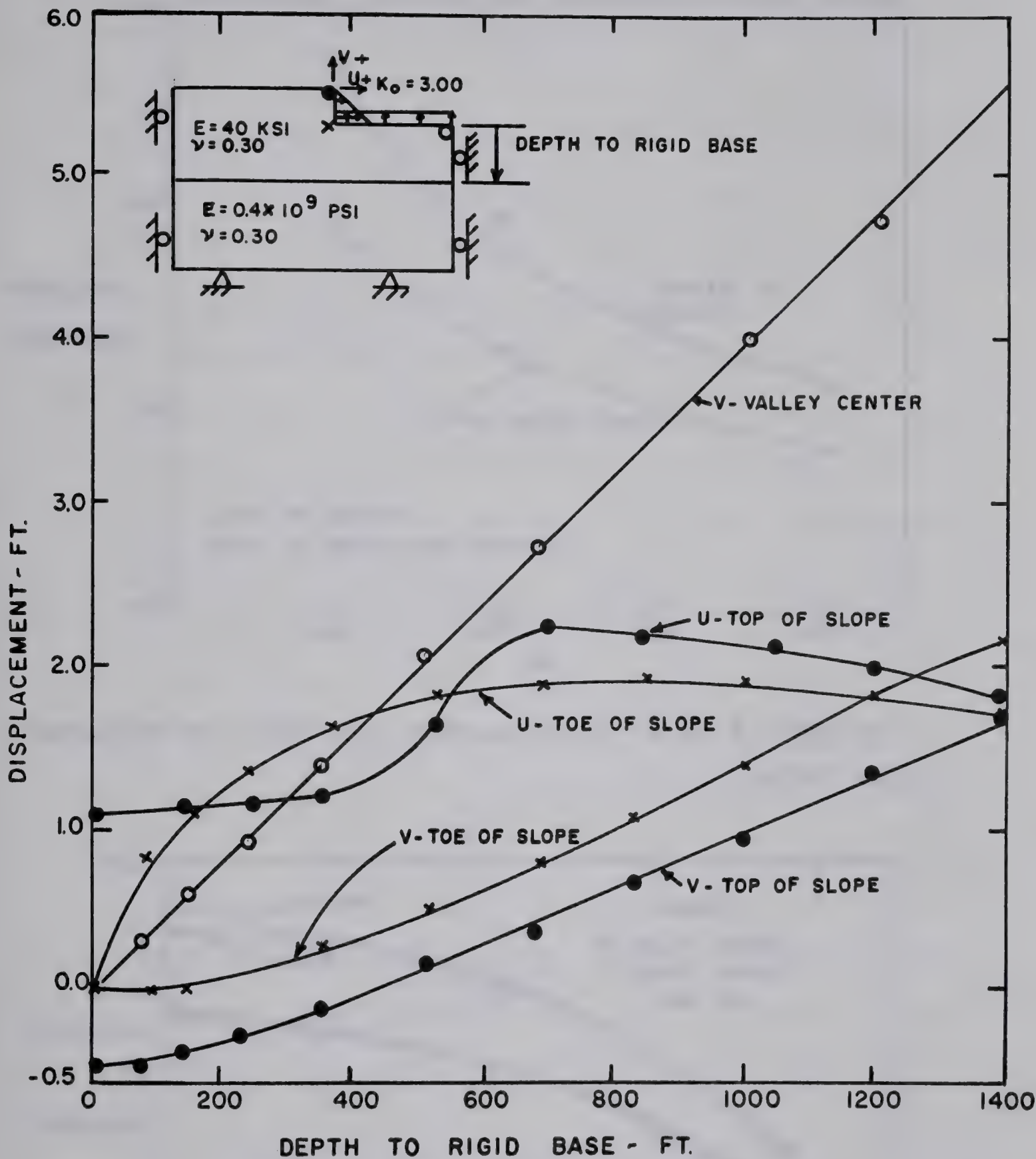


The effect of depth to rigid base on the movement of the valley center and toe and top of slope is shown in Figure 4.24. The vertical rebound of the valley center and top of slope vary approximately linearly with the depth to the rigid base. The inward movement of both top and toe of slope increases with depth to rigid base until a depth of about 800 feet is reached at which point the movements begin to decrease. The entire pattern of displacements around the valley, as well as the magnitude of the displacements, is effected by the depth of the finite element grid.

Grid 5 (Figure 4.21) was used to simulate a homogeneous section with a depth to rigid base of 6800 feet which is 3.4 times the valley width. The vertical rebound of the valley center and the top of the valley wall is shown in Figure 4.25 for a variation in  $E$ . The vertical rebound of the top of the valley wall is about 70 percent of the maximum rebound in the valley center compared to about 30 percent for Grid 1 (Figure 4.21) where a depth to rigid base of 600 feet was used. A value of  $E$  of approximately 80,000 p.s.i. would have to be used in Grid 5 to produce the magnitude of the valley anticlines documented in Chapter III. The difference between this figure and the 10,000 p.s.i., which would produce the same maximum rebound in the valley center (about 3 percent of the valley depth) when used in Grid 1, graphically illustrates the limitations of trying to deduce  $E$  from measured values of excavation rebound.



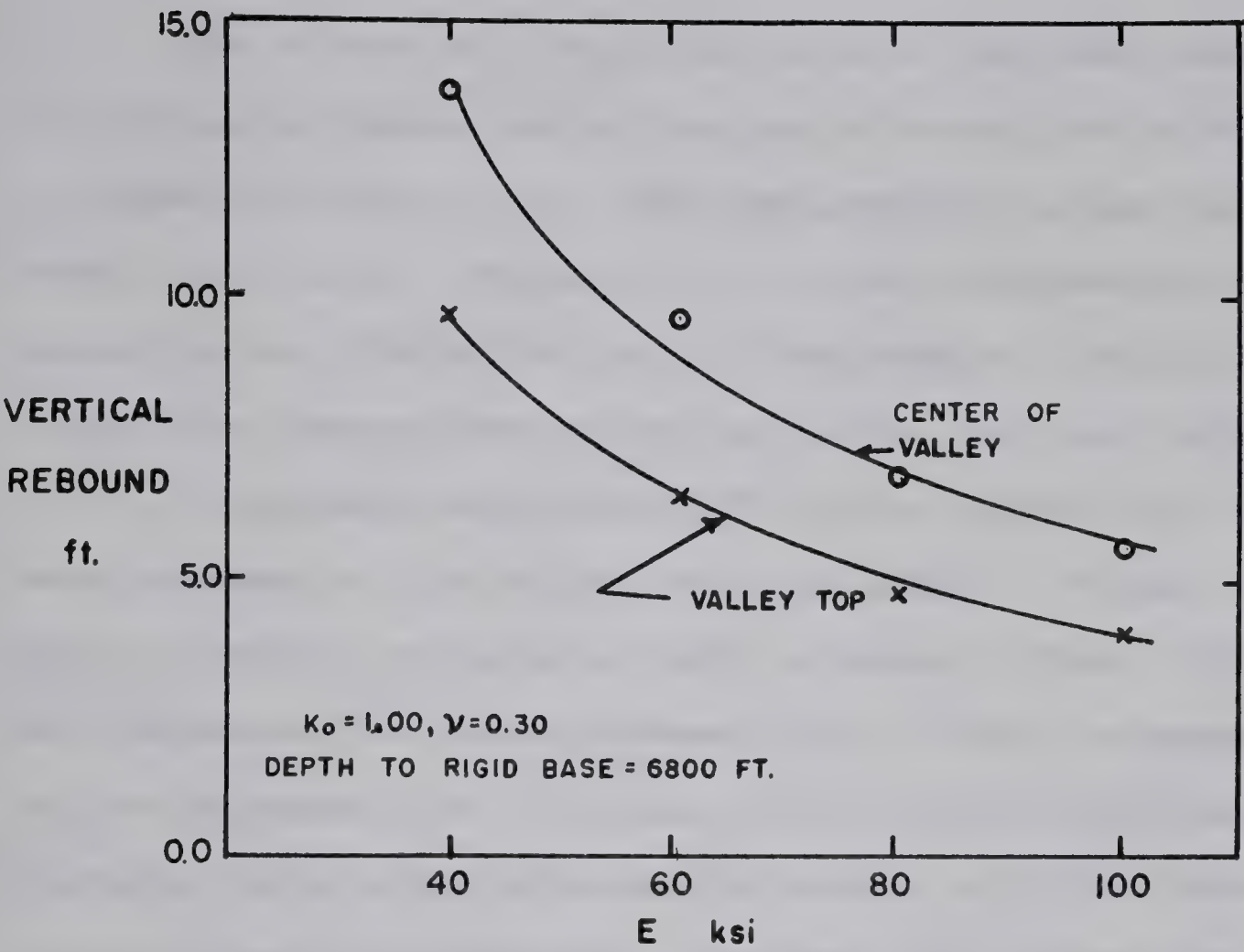




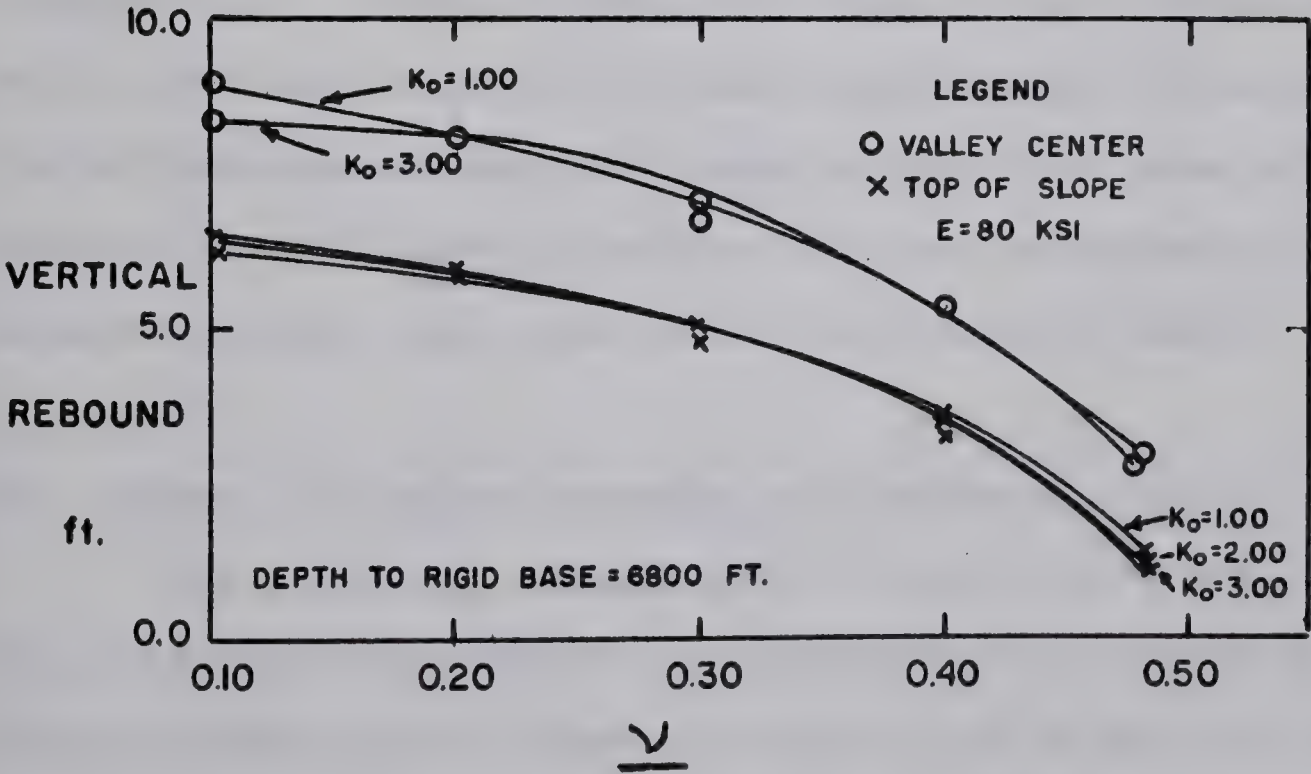
DISPLACEMENTS VERSUS DEPTHS  
TO RIGID BASE - GRID TWO

FIGURE 4.24





VARIATION OF VERTICAL DISPLACEMENT WITH E - GRID 5  
FIGURE 4.25



VARIATION OF VERTICAL DISPLACEMENT WITH  $\nu$  - GRID 5  
FIGURE - 4.26



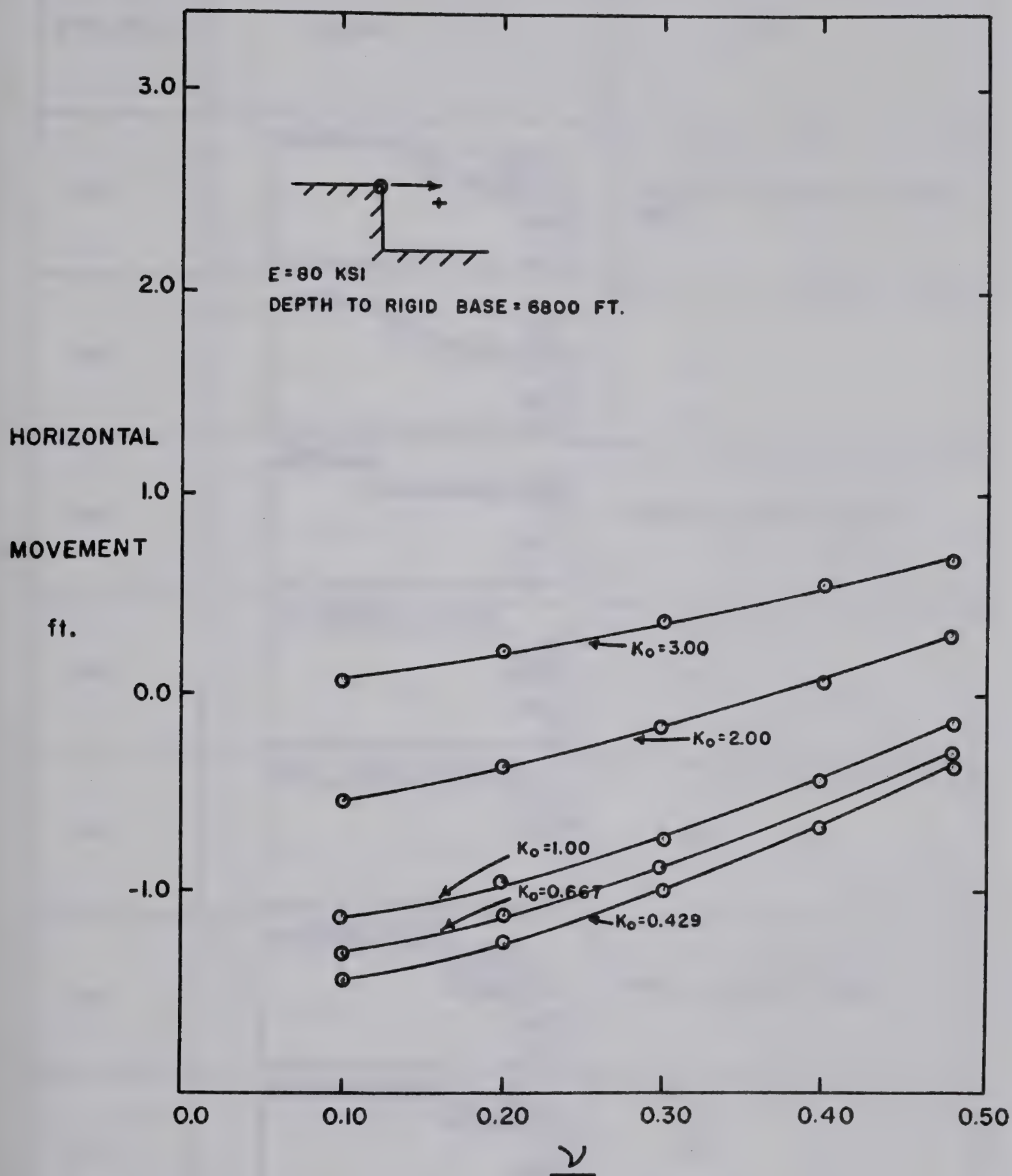


The effect of a variation in  $\nu$  on vertical rebound, in the valley center and at the top of slope for Grid 5, is shown in Figure 4.26. The displacements follow the same trend as in Grid 1 (Figure 4.16) but are considerably less sensitive to a variation in  $K_0$ . The results from Grid 5 predict no downwarping of the valley rim for high values of  $\nu$ . Extremely high values of  $K_0$  are required for inward movement of the valley walls as shown in Figure 4.27. This behaviour contradicts field evidence by Kwan (1971) who documented an inward movement of 1.5 inch, accompanied by the appearance of a tension crack 21 feet back from the vertical face, which preceded failure of a 32 foot deep test cut made in lacustrine clays and tills at Welland, Ontario. Similar behaviour was noted by Underwood (1964) in the Niobrara chalk at Fort Randall Dam as discussed in Chapter VII. It would therefore appear that a relatively shallow finite element grid best approximates the actual field displacement pattern around excavations when a homogeneous grid is used although sufficient evidence to conclusively prove this point does not presently exist.

#### 4.6 Effect of Valley Geometry and Increase in E with Depth

The effect of valley width, valley depth and the slope of the valley walls was studied by use of the seven finite element grids shown in Figure 4.28 as well as results previously obtained from Grid 2 (Figure 4.21).



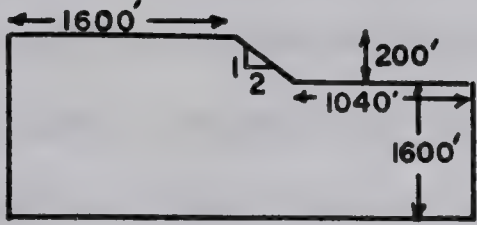
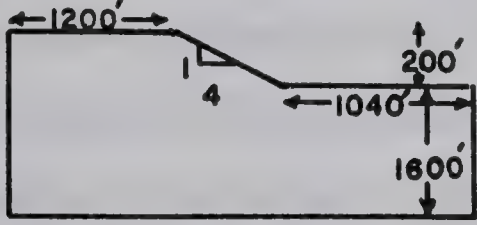
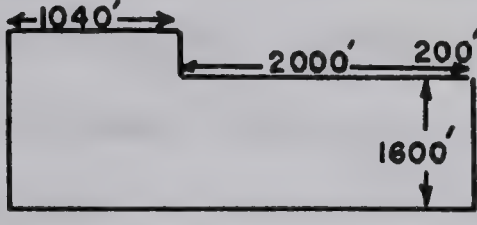
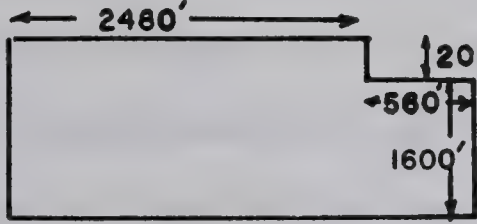
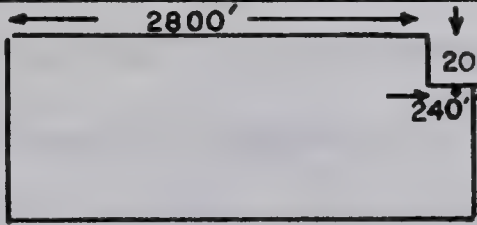
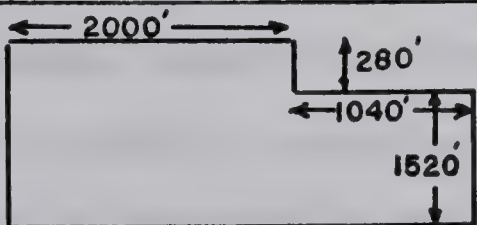
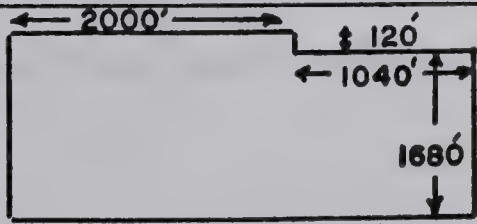


EFFECT OF POISSON'S RATIO UPON  
 HORIZONTAL DISPLACEMENTS-GRID 5

FIGURE 4.27





GRID NO.	SKETCH	USE
2 A		EFFECT OF SLOPE OF VALLEY WALL.
2 B		DO.
2 M		EFFECT OF VALLEY WIDTH
2 N		DO.
2 O		DO.
2 X		EFFECT OF VALLEY DEPTH
2 Y		DO.

FINITE ELEMENT GRIDS USED TO STUDY  
EFFECT OF VALLEY WIDTH, DEPTH & SLOPE

FIGURE - 4.28



Effect of the Valley Wall Inclination: The effect of the inclination of the valley walls was studied using Grids 2A and 2B (Figure 4.28) which have 2:1 and 4:1 slopes respectively and a valley bottom width of 2080 feet and a valley depth of 200 feet. Depths to rigid base of 520 and 1600 feet were used to study the effects of this factor.

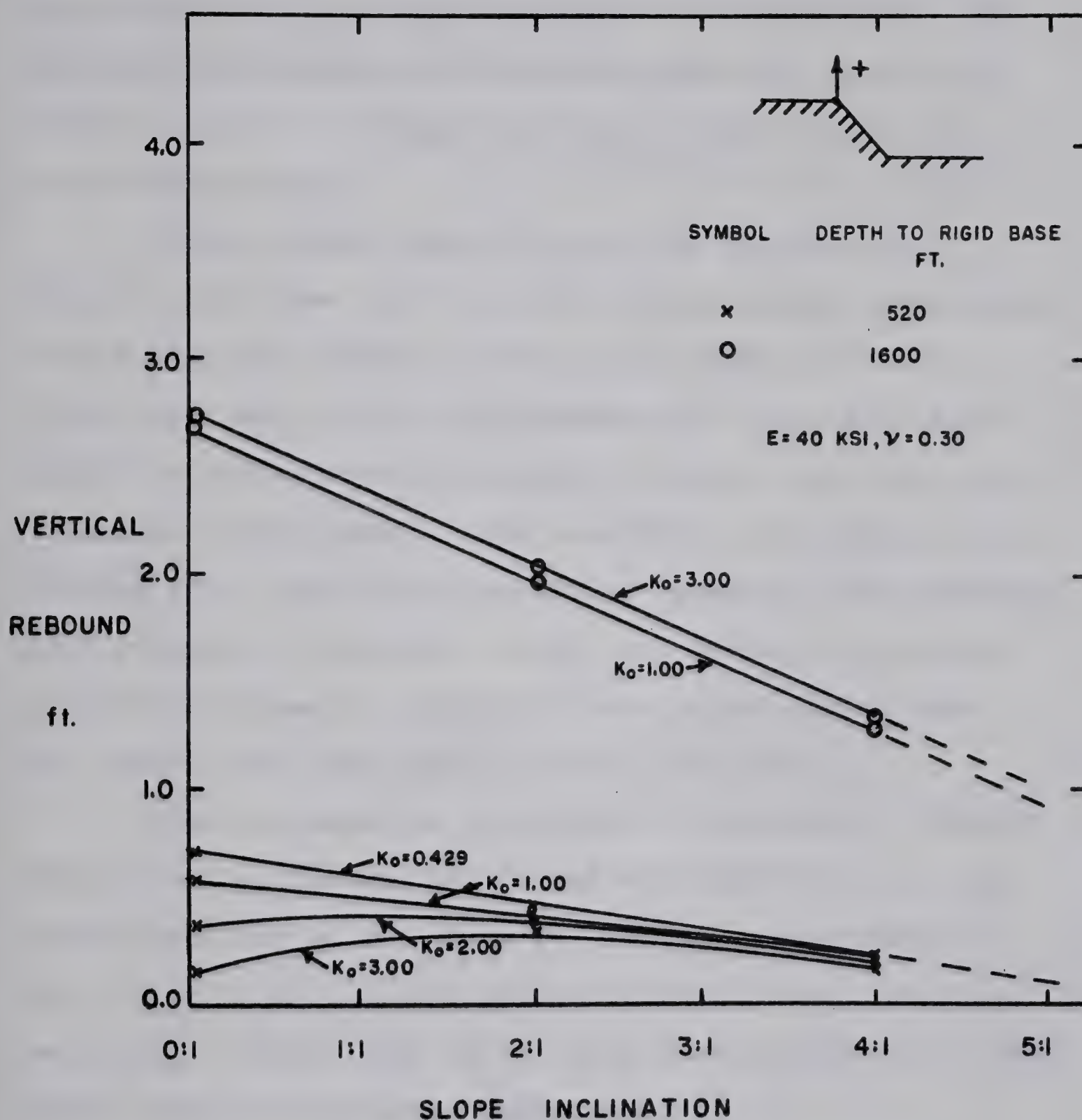
Figure 4.29 shows that flattening the valley wall reduces the vertical displacement at the valley edge and would thus reduce the height of the raised valley rim. This reduction is most marked using a grid with a large depth to rigid base; for a shallow grid the reduction in raised valley rim is dependent upon  $K_0$  to some degree. However, it can be seen that a valley with sides sloping at 6:1 or 8:1 would exhibit an extremely small raised rim. The flattening of the valley walls had almost no effect upon rebound in the valley center.

These results agree with field observations documented in Appendix C. The raised valley rim was observed to be more pronounced along the Pembina River above steep banks on the outside of meander bends. Little evidence of a raised rim was observed along gently sloping sections of valley wall on this and other river valleys in the Province of Alberta.

Effect of Valley Width: Grids 2M, 2N and 2O (Figure 4.28) were used to study the effect of valley width. Vertical walls were assumed, the valley depth was taken as 200 feet







EFFECT OF VALLEY WALL INCLINATION  
UPON VERTICAL DISPLACEMENT OF  
THE VALLEY EDGE - GRIDS 2, 2A, 2B

FIGURE 4.29



and the valley width was varied from 480 to 4000 feet. Depths to rigid base of 520 and 1600 feet were used. The vertical displacements of the valley edge and center are shown in Figures 4.30 and 4.31 for the shallow and deep grids respectively.

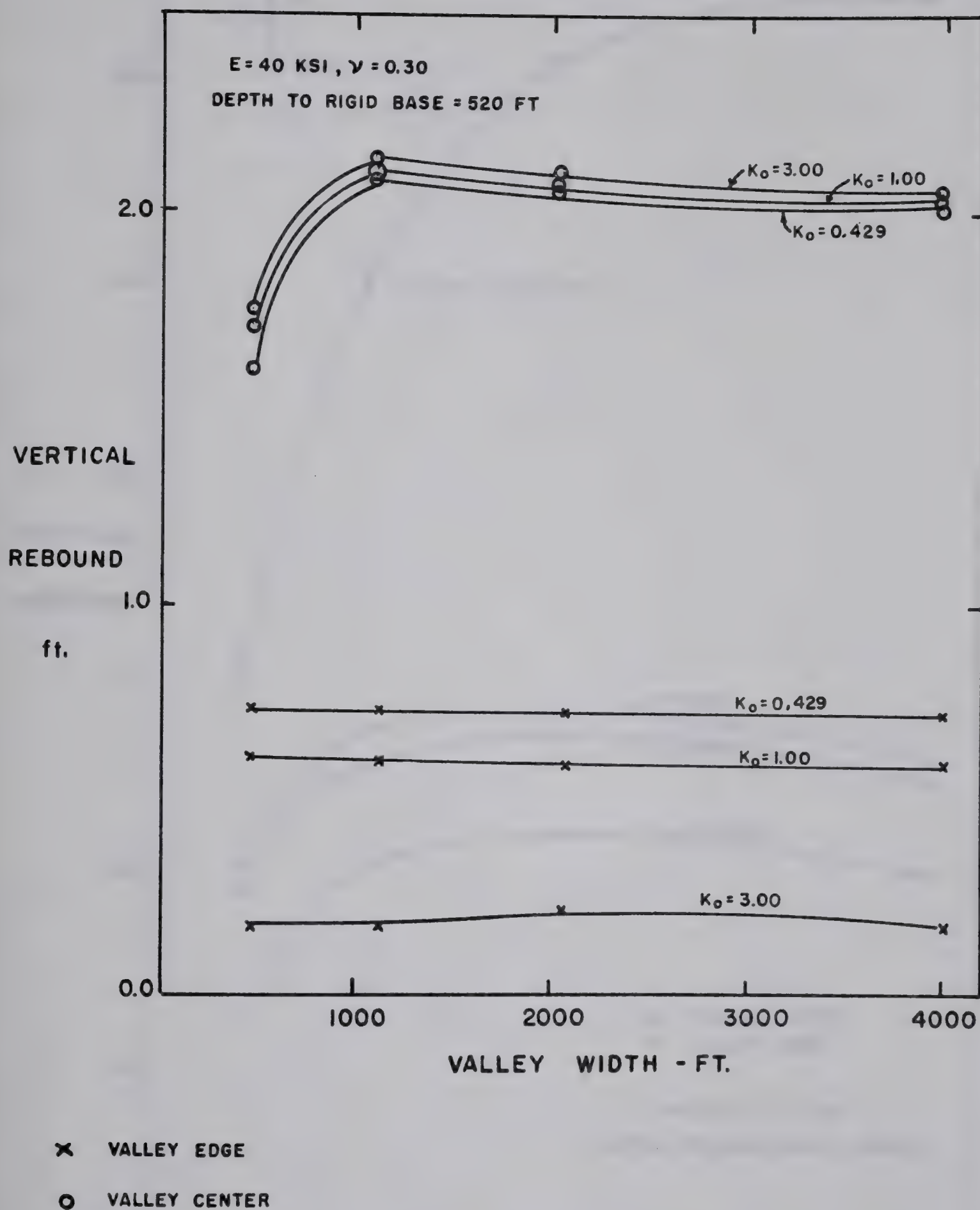
Finite element results using the shallow grid (Figure 4.30) show that the valley width has no appreciable effect upon the rebound in the valley center and little effect upon the vertical displacement of the valley edge until the valley width is reduced to below 1000 feet (five times the valley depth). The results for the deeper grid (Figure 4.31) show that a variation in valley width affects both rebound in the valley center and on the valley edge. A marked decrease in rebound at both points begins when the valley width decreases to below 1000 feet.

Field evidence on this point is ambiguous. The well defined valley flexure and raised rim noted along the Missouri River may be due, in part, to the extreme width of the valley (2 to 4 miles) although other factors, such as valley age and the time which has elapsed since valley formation, may be of greater importance.

Effect of Valley Depth: The effect of valley depth was studied by Grids 2X and 2Y (Figure 4.28) which have a depth of 280 and 120 feet respectively. The effect of valley depth on displacements for average depths to rigid base of 440 and 1520 feet is shown in Figure 4.32.



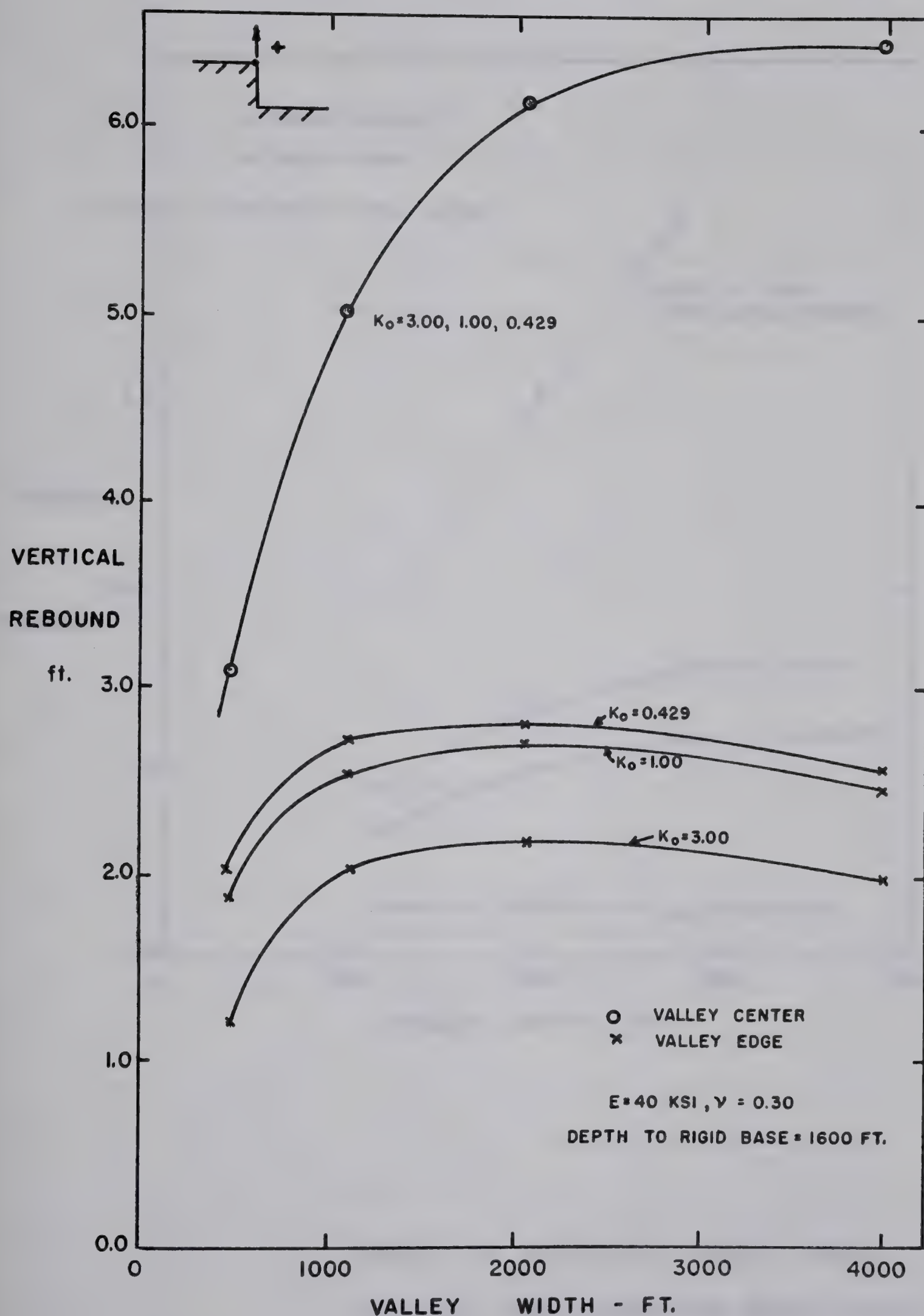




EFFECT OF VALLEY WIDTH UPON VERTICAL  
 DISPLACEMENTS - GRIDS 2,2M,2N,2O

FIGURE 4.30



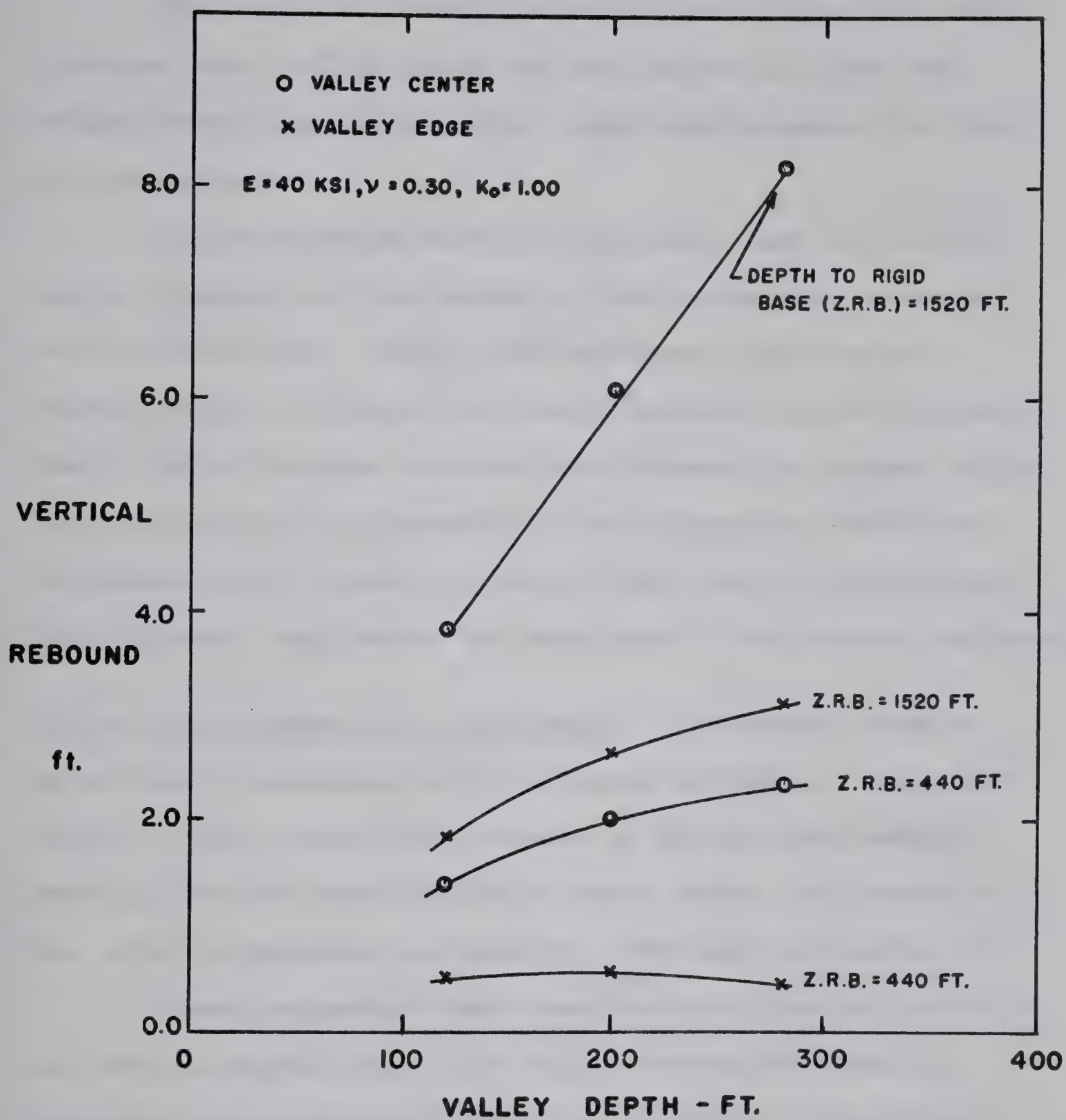


EFFECT OF VALLEY WIDTH UPON REBOUND

FIGURE 4.31







EFFECT OF DEPTH OF VALLEY UPON  
VERTICAL DISPLACEMENTS-GRIDS 2,2X,2Y

FIGURE 4.32



The vertical rebound of the valley center and edge increase with valley depth for the deeper grid but the valley depth has little effect upon displacements for the shallower grid.

Field evidence strongly indicates that the valley center rebound and the height of the raised rim increase with valley depth. Smith and Redlinger (1953) note a higher value of rebound for deeper excavations at Garrison Dam. The difference in magnitude between the raised valley rim at clay pit 14 (Appendix C) and along the South Saskatchewan River appears to be at least partly due to excavation depth (and hence the magnitude of the stress relieved).

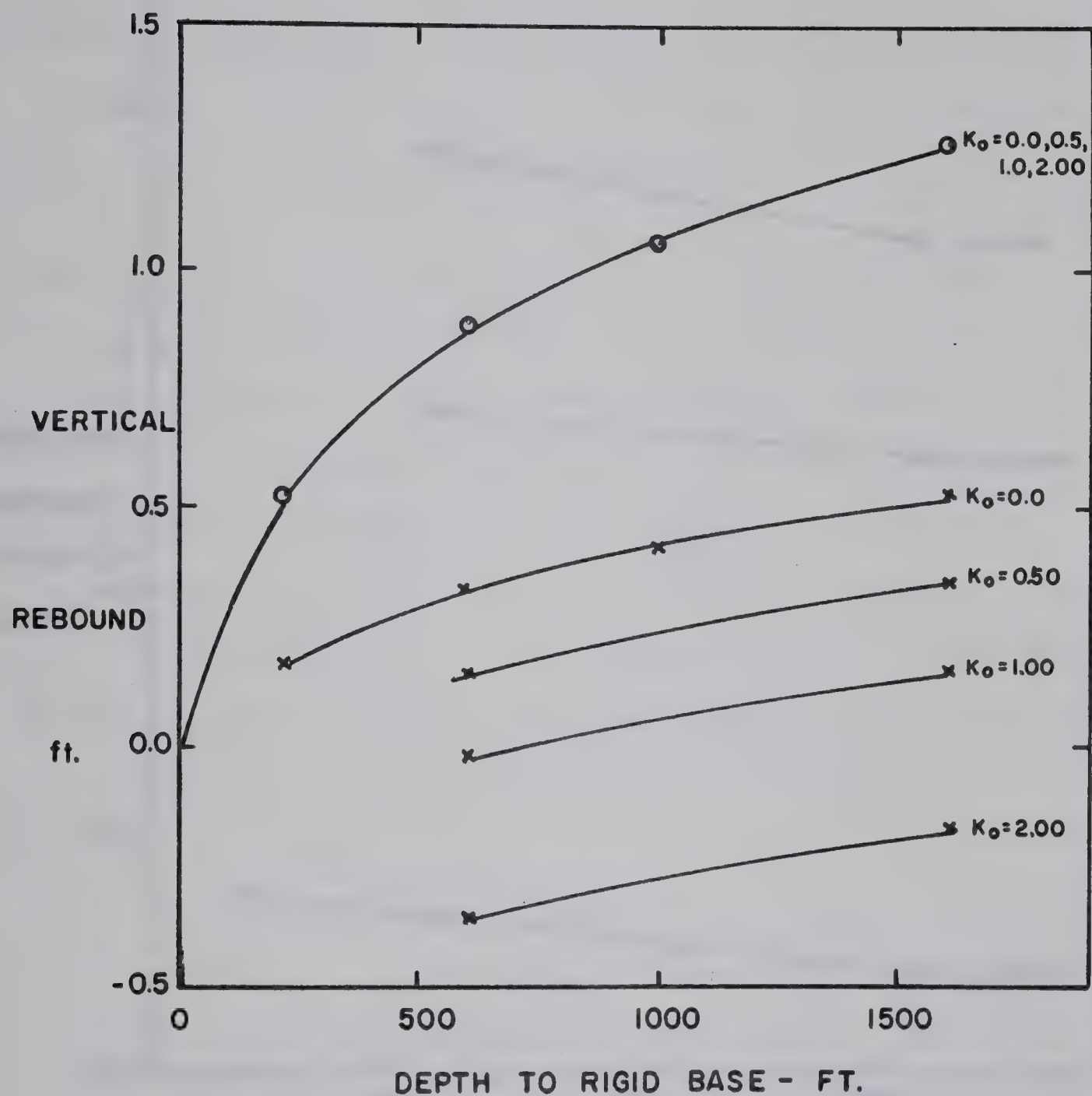
Effect of Increase in E with Depth: Laboratory studies show that E increases with confining pressure. Chang and Duncan (1970) found the increase in the drained rebound modulus for the sandy soils at Buena Vista, California to be given by Equation 4.2 with  $K = 2080$  and  $n = 0.60$ .

These parameters were used to calculate values of E at various depths below the valley bottom for Grid 2, assuming zero porewater pressure. The rate of increase in vertical rebound of the valley center, with increasing depth to rigid base, was found to be much slower than for a homogeneous grid as shown in Figure 4.33. The depth to rigid base has little effect upon horizontal movements of the valley rim as shown in Figure 4.34.

These results show that the boundary conditions become much less critical in a finite element analysis of







o VALLEY CENTER

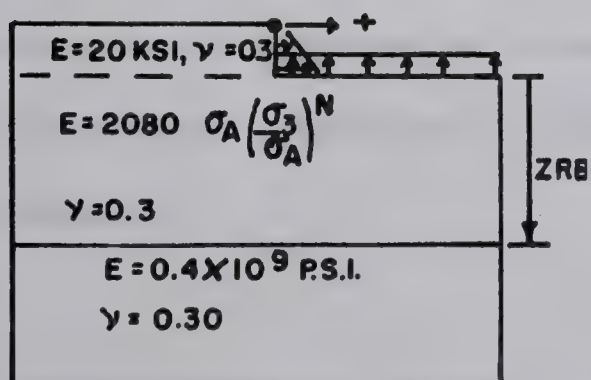
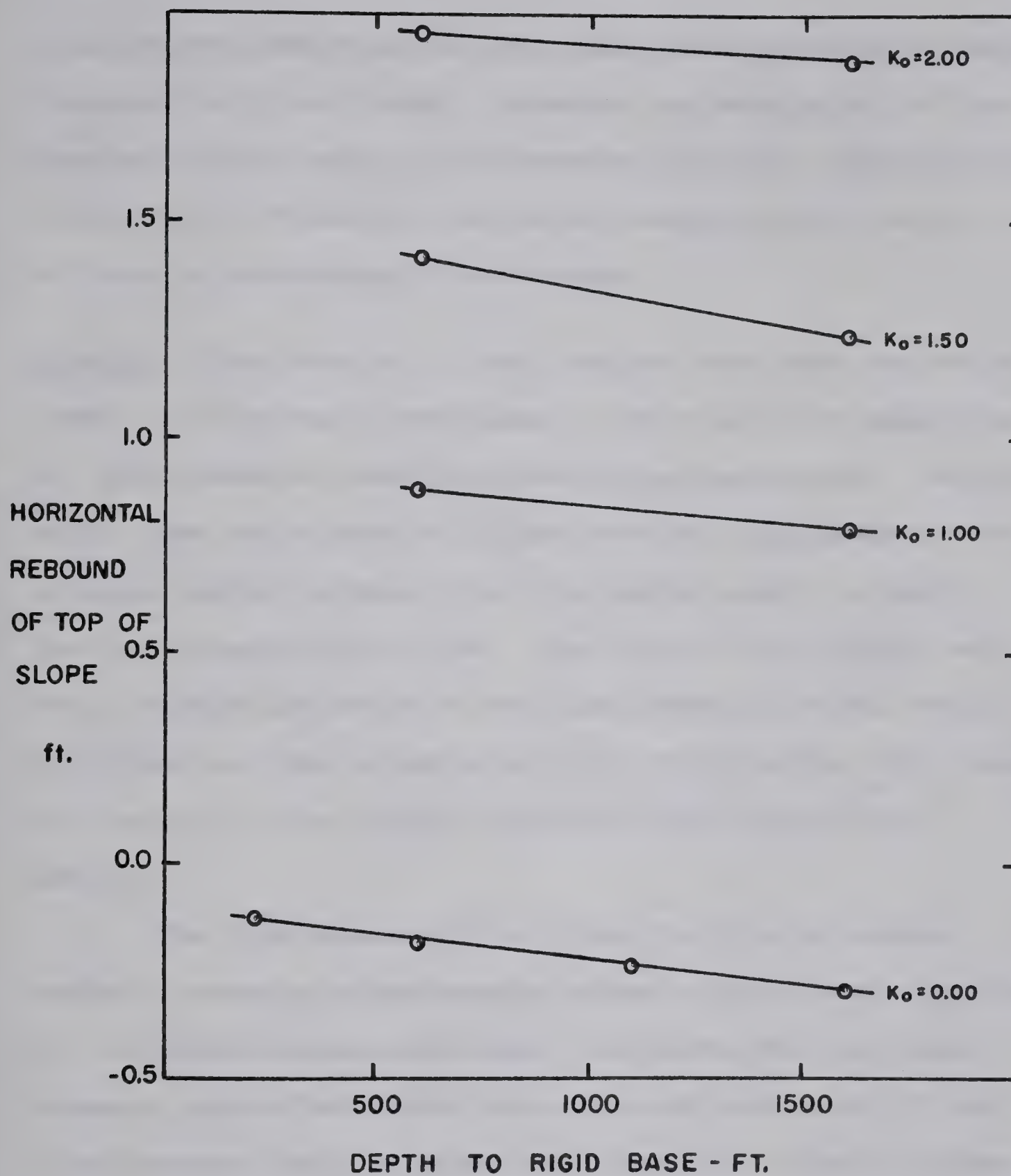
x VALLEY EDGE

NOTE-  $E$  INCREASES WITH DEPTH  
AS IN FIG. 4.34,  $\nu = 0.30$

EFFECT OF DEPTH TO RIGID BASE  
ON VERTICAL DISPLACEMENTS-GRID 2

FIGURE - 4.33





EFFECT OF DEPTH TO RIGID  
BASE, NON-HOMOGENEOUS GRID

GRID 2 - E INCREASING WITH DEPTH

FIGURE 4.34



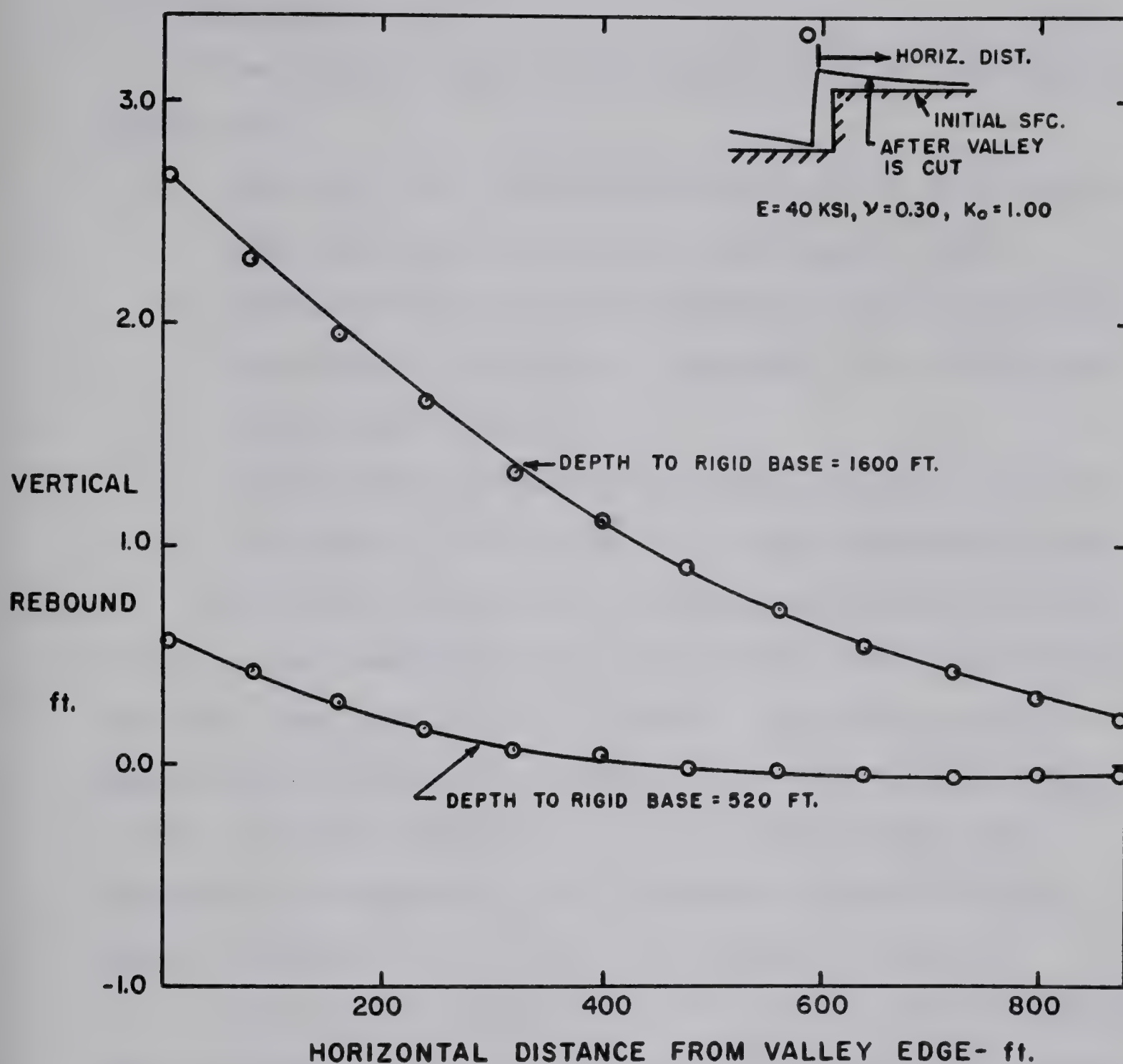


rebound problems when the rock mass has a relatively rapid increase in  $E$  with depth. However, no data exists at present as to the rate (s) of increase of  $E$  with depth in the study area. Therefore, no further work was done on the effects of increasing  $E$  with depth.

Summary: The results in this section show that the valley depth is of primary importance in governing the magnitude of displacements resulting from valley excavation. Valley width does not appear to affect vertical displacements to a large degree provided that the valley width to depth ratio is greater than five. The slope of the valley wall has a marked influence on the displacements at the top of the slope and the presence of flat valley walls will reduce the height of the raised valley rim by a significant amount.

The displacements found from the finite element method, assuming a homogeneous elastic grid, are a function of the depth of the grid used. The depth of the finite element grid effects both the magnitude and sense of the displacement field as shown in Figure 4.35, where surface profiles back from the valley edge are given for a given set of elastic parameters and depths to rigid base of 520 and 1600 feet. Entirely different shapes of raised valley rim result.





EFFECT OF DEPTH TO RIGID BASE ON  
VERTICAL DISPLACEMENTS ADJACENT  
TO THE VALLEY - GRID 2

FIGURE 4.35





#### 4.7. Discussion

The standard steps in the solution of an engineering problem are:

1. Adoption of a mathematical model which approximates the physical situation to a reasonable degree.
2. Evaluating the relevant material properties of the problem in the field or laboratory and using these results in the model.
3. Evaluating the theoretical results in view of the reliability of the model and input parameters used.

The review of present knowledge concerning analysis of excavation problems shows that a satisfactory mathematical model does not exist at present. The finite element method shows promise of becoming a tool which will result in the reliable prediction of excavation behaviour but insufficient knowledge of the parameters acting in the field precludes full use of its potential at present.

Laboratory testing may yield useable input parameters for the finite element method but it is clear that insufficient knowledge exists at present on the effects of sample disturbance and variation of  $E$  with stress level, confining pressure and drainage conditions. Implicit in the reliable use of the finite element technique is the need for a reliable, standardized method of measuring stresses in-situ.

The finite element results obtained from the use of a homogeneous, isotropic grid must be evaluated as being results from an extremely simplified model. However, a



number of points of interest are apparent.

1. Values of  $E$  derived from field measurements are a function of the boundary conditions of the grid used when the size of the region represented by the finite element grid is limited. Results from a homogeneous, isotropic grid are extremely dependent upon depth to rigid base. Therefore, attempts to deduce  $E$  or  $K_0$  acting in-situ from displacements observed in the field will not yield meaningful results until a better knowledge exists of the appropriate boundary conditions to use in the grid. This knowledge can only be gained through instrumentation of field excavations.
2. The difference in magnitude between the rebound observed in artificial excavations and the rebound which has occurred below the river valleys in the study area appears primarily due to the time scale involved and the difference between undrained and drained moduli. The time-dependent rebound or 'swelling' documented in many artificial excavations is a result of drainage and consequent reduction in  $E$ . The magnitude of the valley anticlines in the study area indicates that drained parameters control the features documented in this thesis.
3. Analysis of river valley formation, using a relatively shallow homogeneous finite element grid, appears to present a reasonable picture of the displacements which have occurred in nature. A





value of  $E$  of approximately 10,000 p.s.i. appears to give a displacement pattern similar to that observed in the field. This value of  $E$  compares reasonably well with laboratory undrained values of  $E$  for the bedrock from the study area. Thus, allowing for the effects of sample disturbance, the value of 10,000 p.s.i. appears to be a reasonable figure for the drained value of  $E$  for the weaker formations in the study area.



## CHAPTER V

### STRESS RELIEF AND LATERAL DISPLACEMENT

#### 5.1 Introduction

The cases documented in Chapter III show that rebound due to valley excavation is a ubiquitous feature below the river valleys cut in the Cretaceous bedrock of the Western Plains of Canada and the U.S.A. The amount of rebound appears to be largest where the bedrock has a low modulus of elasticity.

The data presented in Chapter II shows that the Cretaceous bedrock of the study area has a low modulus of elasticity and is highly overconsolidated. Therefore, the lateral stress released when a valley is cut should be greater than the vertical stress and the lateral rebound should be greater than the vertical rebound, provided that the rock is not highly anisotropic. No field exploration method can give a direct measure of the amount of the lateral rebound that has occurred adjacent to a river valley. However, indirect evidence is present in the form of vertical joints which parallel the valley wall as noted by Crandell (1958), Bradley (1963), Underwood (1964), Ferguson (1967), Wilson (1970). DeBeer (1969) and Kwan (1971) record the formation of vertical joints parallel to excavation walls in cuts made in overconsolidated clay in Belgium and glacial and lacustrine deposits near Welland, Ontario.





The Cretaceous bedrock of the study area consists of interbedded sandstone, shale, bentonite and coal layers, some of which are continuous over a considerable distance. The sections presented in Chapter III show many sites where the bedrock would better fit the model of a layered medium than a homogeneous mass. Several engineering implications arise when the formation of a valley anticline and lateral stress relief in a layered medium are considered. Flexural slip would occur between beds due to the folding accompanying vertical rebound. Differential movements would occur between beds of different lithology due to differences between the modulus of elasticity of the beds.

In this chapter, the literature available on lateral movements in soil and rock due to excavation is summarized. The mechanism of flexural slip is reviewed and the magnitude of movements, due to valley rebound, is examined. The finite element method is used to study displacements which occur across a bentonite layer due to valley excavation and slope flattening.

## 5.2 Literature Review

Case histories of measured vertical rebound due to excavation are given in Chapter IV. Fewer documented instances of lateral movement exist in the literature since these have not been usually observed in detail until the last decade when the use of inclinometers (Wilson, 1970) became common.



Terzaghi (1950) gives an example of a landslide developing due to lateral rebound in an excavation for the Swir III Dam east of Leningrad, U.S.S.R. A cut made in a stiff, greenish Devonian clay, overlying a lower very stiff, sandy clay, caused an expansion of the Devonian clay over the lower sandy clay of about 1 foot in 6 hours. The expansion of the Devonian clay caused fissuring of an upper till layer which led, following heavy rains, to a flow slide in the upper till.

Underwood (1964) reported lateral displacements occurring across bentonite layers in the Niobrara chalk (Upper Cretaceous) at Fort Randall Dam on the Missouri River. Differential horizontal rebound at Gavins Point Dam, between the Niobrara chalk and the underlying Carlile shale, produced tension cracks in the chalk adjacent to a spillway excavation.

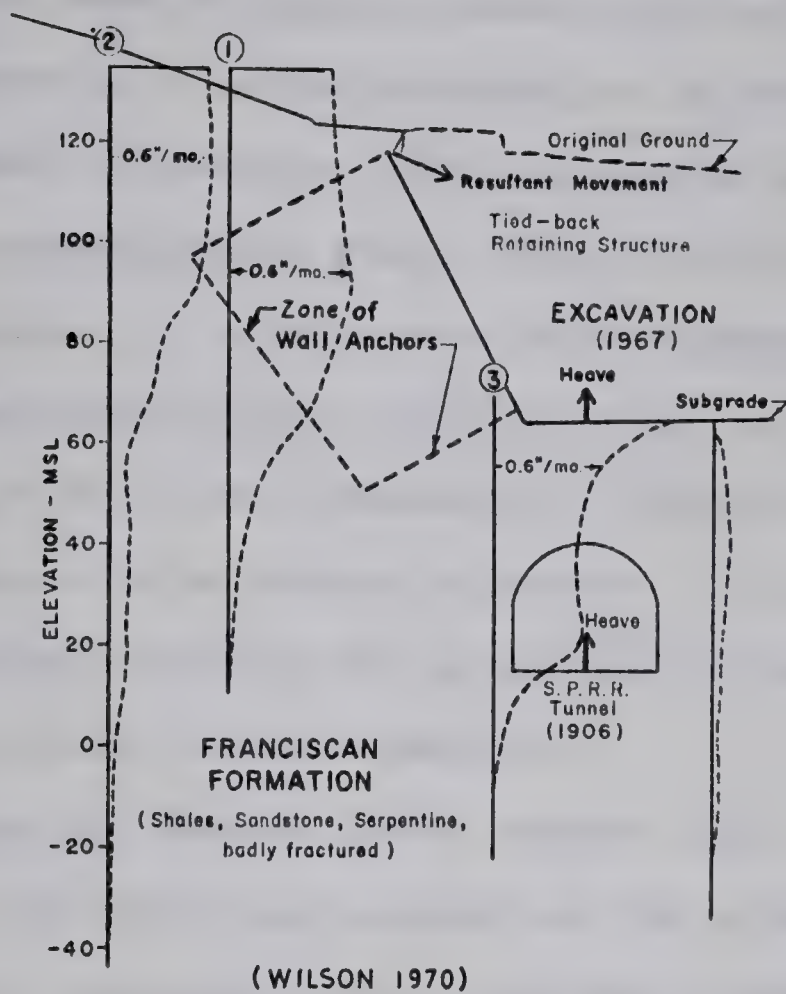
Feld (1966) discusses lateral movements noted in a deep excavation in limestone (180 feet deep, 20 feet wide) at Niagara Falls. The side walls of the trench moved in sufficiently to bend cross-beams set in for machinery support. A similar pit on the Canadian side of the falls experienced about 4 inches of lateral movement.

Wilson (1970) gives a number of well-documented cases showing lateral movement due to excavation. Figure 5.1 shows displacements which occurred due to a freeway excavation made into the Franciscan formation in San Francisco. Figure 5.2 shows displacements which occurred









—MOVEMENTS AT POTRERO TUNNEL, SAN FRANCISCO

FIG. 5.1

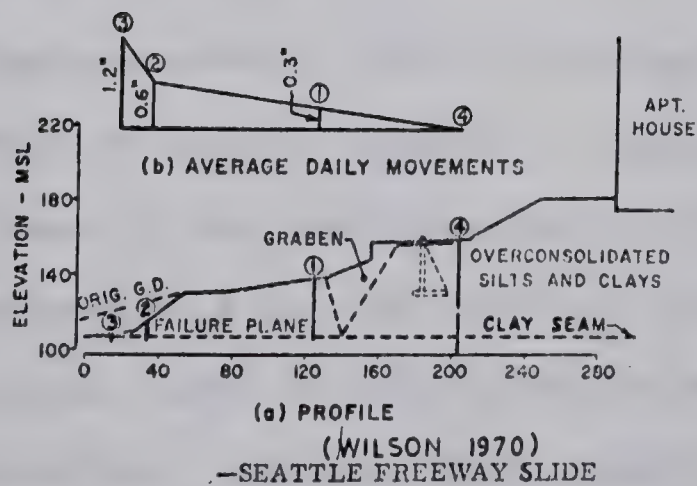


FIG. 5.2



along a thin seam of highly plastic clay which appeared to form the base of a slide generated by a shallow excavation for a freeway in Seattle. The excavation was made in a highly overconsolidated stiff silt and plastic clay.

Figures 5.3 and 5.4 show displacements measured along a landslide failure surface which was initiated by a freeway excavation near Minneapolis, Minnesota. The movement was found to be occurring within a thin seam of bentonite confined between two stringers of limestone, 17 feet below the bottom of the excavation.

Chang and Duncan (1970) report large lateral movements at a 200 feet deep excavation for a pumping plant at Buena Vista, California which has been previously discussed in Chapter IV. Two rebound gages were observed to have their tops sheared off with horizontal offsets of 1.35 feet occurring towards the center of the excavation. The offsets occurred at an elevation approximately 48 feet below the excavation bottom.

Inclinometers showed sharp, differential movements of 1 inch or less at several depths in apparently random directions. Three of the inclinometers indicated relative horizontal displacements in the order of 1 to 2 inches in a nearly horizontal layer of clay located beneath the bottom of the excavation. Wilson (1970) suggested that these offsets were due to concentrated shear stresses developing along the neutral axis of the layer, in a manner similar to





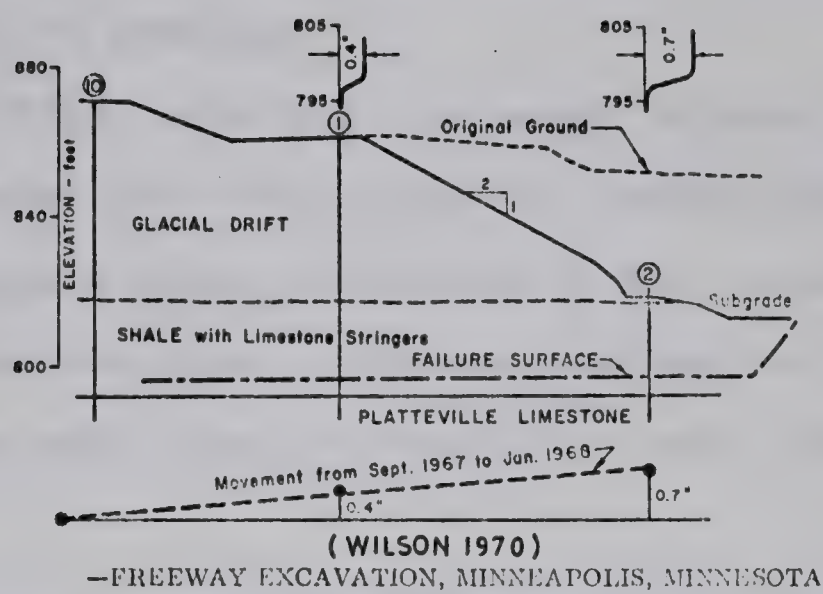


FIG. 5.3

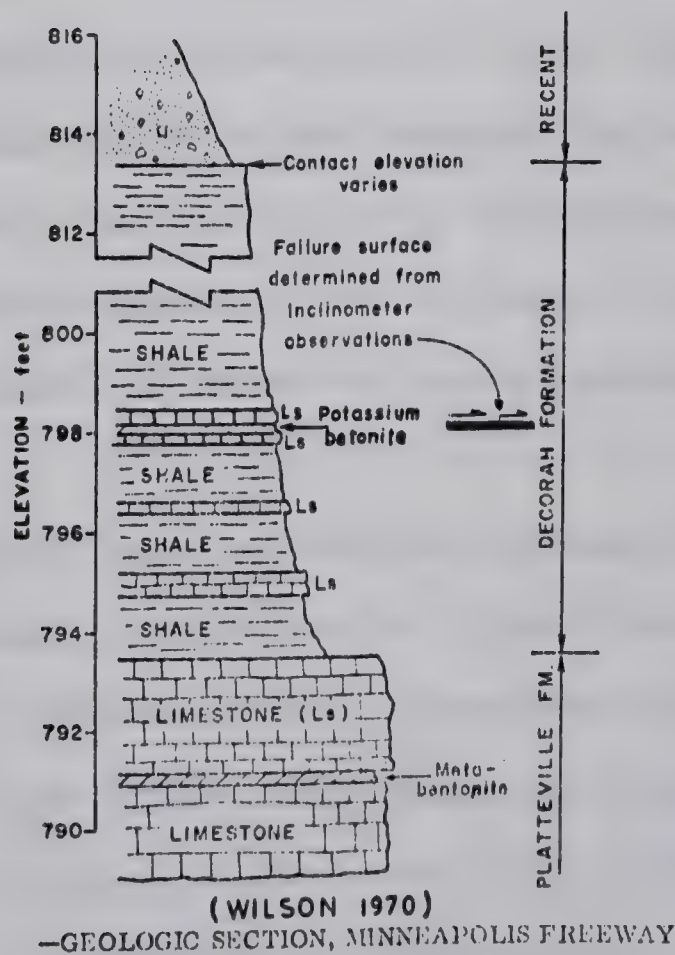


FIG. 5.4



shear stresses developing along the neutral axis of a thick beam subjected to bending.

Chang (1969) reported that minor offsets of about 1.5 inch occurred near the top of the impervious clay layer, immediately below the bottom of the excavation. A general tilt of the slope indicator casings was noted with the top tilted away from the excavation with respect to the bottom.

In summary, recent field measurements, using inclinometers, show that significant lateral displacements often result towards an excavation if a cut is made into a soil or rock mass. The displacements are more marked in a highly overconsolidated soil or rock mass or in a soil or rock mass with a low modulus of elasticity. In a layered material, unequal displacements at the boundaries of lithologic units appear to result in differential displacements, or shear strains, between layers. The presence of a weak layer appears to result in movement being concentrated in, or at, the layer.

The engineering implications of stress relief in layered media has been recognized in a qualitative fashion by several authors. Kenney (1967) suggested that a contributory cause of the Vajont rockslide was movement between layers due to stress relief resulting from formation of the river canyon. Movement of rock towards the valley resulted in differential shear strains. As a result, clay zones were formed between certain beds of rock with a





strength at the residual angle of shearing resistance ( $\phi'_r$ ). The presence of these weak zones controlled the subsequent stability of the rock mass.

Suklje (1969, p. 449) noted that the massive Gradot landslide in Macedonia occurred along a slightly inclined contact between overlying silty deposits and a clay base. The basic cause of the slide was postulated to be the erosive action of the Vataša River deepening its bed and causing "unequal creep deformation" between the two strata overcoming the "cohesion" of the soil.

### 5.3 Flexural Slip

Structural geologists have recognized that many sedimentary strata have well developed plane-parallel stratification and this inherent weakness often controls the type of internal deformation which occurs during folding and buckling of the rock. During the folding of a sequence of sedimentary rock, such as shown in Figure 5.5, the outer layers slip over the inner layers. Slickensides have been formed in sedimentary rock folds due to this process (Ramsay, 1967). The amount of flexural slip, between two beds of thickness  $x$ , is given by Norris (1967) as

$$\text{Interbed slip} = \frac{x \theta \pi}{180} \quad (5.1)$$

where  $\theta$  is the change in dip of the bed in degrees.<sup>1</sup> The mechanics of interbed slip for an anticlinal structure are shown in Figure 5.6. The maximum interbed slip occurs at

---

<sup>1</sup>The flexural slip mechanism assumes no change in length of beds during rebound and may somewhat overestimate slip below the valley bottom.



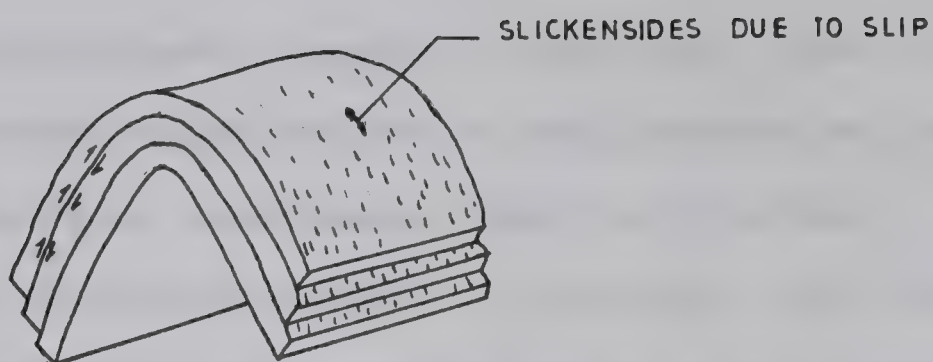
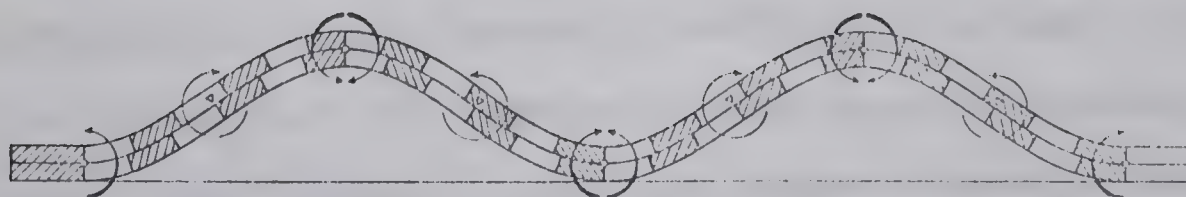


FIG. 5.5 FLEXURAL SLIP FOLDING (AFTER RAMSAY, 1967)



Schematic diagram showing mechanics of folding of a two-layered model; axis of rotation  $\bigcirc$ , inflection  $\nabla$ , sense of external rotation  $\curvearrowright$ , (fat arrow) and sense of rotation by interlaminar slip  $\curvearrowright$ .

FIG. 5.6 INTERBED SLIP DUE TO FOLDING (AFTER NORRIS, 1967)





the points of inflection on the limbs of the anticline and the interbed slip is zero at the top of the anticline below the valley center.

Geotechnical engineers appear to have been slow to appreciate the possible significance of this mechanism in the reduction of shearing resistance along a potential failure plane from peak to residual. It was not until 1966 that Skempton (1966) noted that the low value of  $\phi'$ , which must have been acting along the failure surface of the Vajont slide, could be the result of bedding-plane slip due to tectonic folding of the bedrock.

The rebound of the bottom of river valleys and artificial excavations has been documented in Chapters III and IV. Provided the valley has been cut in a layered sequence of rock, flexural slip should occur as a function of the change in dip, due to rebound, and the bed thickness. The maximum interbed slip due to folding can be calculated using Equation 5.1 for layers of varying thickness and is shown in Figure 5.7 for changes in dip up to 6 degrees. A relatively small change in dip can induce a considerable amount of interbed slip for a deposit with widely separated bedding planes; for example, a change in dip of 3 degrees due to rebound would cause a maximum interbed slip of over 3 inches on the limb of the valley anticline for a bed thickness of 5 feet.

Average bed thickness and vertical rebound between adjacent boreholes may be obtained from the profiles given



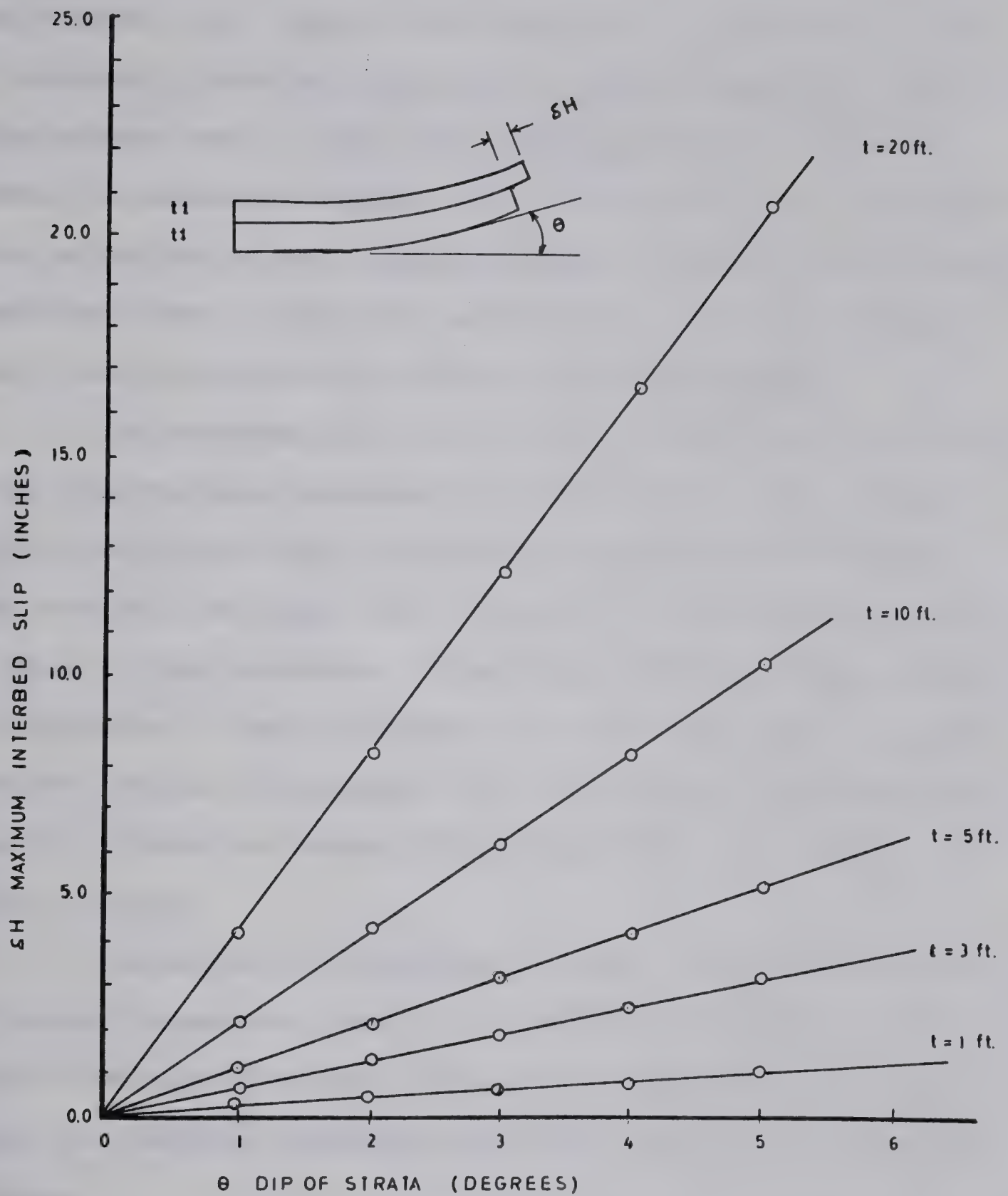


FIG. 5.7 MAXIMUM INTERBED SLIP DUE TO FOLDING A HORIZONTAL STRATIFIED SEQUENCE OF ROCK





in Chapter III. Hence, for certain of the damsites cited, a reasonably good estimate of the maximum change in dip of the bedrock can be made from simple geometry. Table 5.1 shows the maximum interbed slip for various bed thicknesses. The selection of bed thickness poses a problem as horizontal bedding planes, which act as planes of weakness, are normally not indicated by standard coring techniques.

The observations from the two bridge sites in Edmonton, Alberta were discussed in Chapter III. In a given stratigraphical unit, horizontal bedding planes occurred at intervals of from 1 to 2 feet in the shale and from 2 to 5 feet in the sandstone. Therefore, for the bridge sites at Edmonton, a bed thickness of 2 to 4 feet would be appropriate for use in Equation 5.1. The maximum interbed slip due to folding at these sites should then lie between 0.4 and 0.7 inch.

Larger bed thicknesses, however, could be expected in other formations than in the Edmonton formation. If a bed thickness of 10 feet occurred at Garrison or Boundary Dam, the maximum interbed slip could easily reach several inches.

Underwood (1964) discusses three large dams constructed by the U.S. Army Corps of Engineers on the Missouri River where the bedrock is the Niobrara chalk of Upper Cretaceous age. The chalk is a horizontally bedded formation interbedded with layers of bentonite which are up to 3 inches thick. These bentonite beds are continuous over



TABLE 5.1

FLEXURAL SLIP DEVELOPED DUE TO VALLEY REBOUND  
FOR SITES IN THE STUDY AREA

Site and Location	Vertical Rebound (Ft.)	Estimated $\Delta\theta$	Bed Thickness (Ft.)	Maximum Interbed Slip $\delta H$ (inch)
James Macdonald Bridge (Edmonton)	2.5	0.88 <sup>o</sup>	2 4	0.37 0.74
105 St. Bridge (Edmonton)	2.5	0.86 <sup>o</sup>	2 4	0.37 0.74
Hairy Hill Damsite (North Saskatchewan River)	6.0	0.33 <sup>o</sup>	2 10	0.14 0.70
Carvel Damsite - Valley Wall (North Saskatchewan River)	-	0.40 <sup>o</sup>	5 10	0.42 0.84
Ardley Damsite (Red Deer River)	7.2	1.04 <sup>o</sup>	2 10	0.44 2.18
Rocky Site A (North Saskatchewan River)	1.4	0.42 <sup>o</sup>	2 10	0.17 0.88
Garrison Dam-Abutment (Missouri River)	-	1.0 <sup>o</sup>	10	2.09
Boundary Dam (Long Creek, Saskatchewan)	-	3.0 <sup>o</sup>	2 10	1.26 6.28





long distances and some have been traced over 20 miles. The bedding, as exposed in the river valley, was nearly always inclined downward at  $2^{\circ}$  to  $5^{\circ}$  towards the bluffs. The finite element analyses in Chapter IV showed that an upwarping of beds in the valley wall results from vertical rebound of the valley bottom.

Figure 5.7 indicates that a considerable amount of interbed slip will occur due to a change in dip of 2 to 5 degrees. At Fort Randall Dam, excavation of deep cuts in the chalk resulted in a reported vertical rebound of 3 to 4 inches. Small but definite offsets or overthrusts, of the higher over the lower beds, were noticed in the excavation sides. Offsets across a bentonite seam caused a sharp bend in the column pipe of a deep well, drilled 10 feet back from the face of the powerhouse excavation. Gages set across all prominent bentonite seams exposed during the excavation showed that, after initial rebound, movement subsided rapidly.

Underwood (1964) attributes the lateral movements to release of lateral stress. This is undoubtedly an important mechanism and may dominate in this case but the displacement pattern, offset of higher over lower beds, is exactly the behaviour predicted by the flexural slip mechanism. If the chalk units acted as intact layers, separated at wide intervals by thin, continuous bentonite beds, a study of Figure 5.7 shows that a considerable amount of interbed slip could occur due to a small rebound at the base of the excavation.



Some of the documented behaviour could be due to this mechanism as shown in Figure 5.8. If the chalk beds were assumed to be 10 feet thick and the vertical rebound caused a change in dip of  $\frac{1}{2}$  degree, then a maximum interbed slip of 1.1 inches could occur.

The excavation slopes in the Niobrara chalk at Fort Randall remained stable after the lateral movements. Natural slopes along the river were noted to stand in high vertical cliffs and it is apparent that slope stability in this formation is unaffected by lateral stress relief or flexural slip due to rebound. This point will be discussed in some detail in Chapter VI of this thesis.

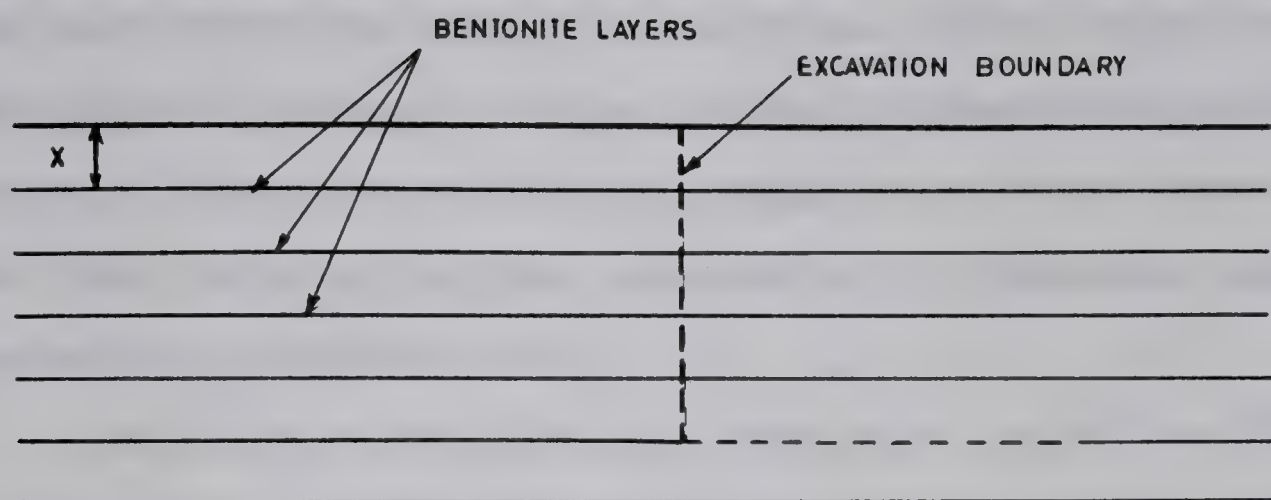
The discovery of shear zones in the bedrock at the Mangla Dam project in West Pakistan caused a considerable change in the design of the project (Binnie et al., 1967). The nature of these shear zones, and other discontinuities in the Siwalik formation at the site, has been discussed by Fookes (1965) and Fookes and Wilson (1966). One of the major sets of discontinuities noted at Mangla were shear zones, consisting of planes within the clay strata of the Siwalik formation where relative movement had occurred along bedding planes due to folding induced by the orogeny of the Himalaya Mountains in Plio-Pleistocene times.

The shear zones vary in thickness from a few millimeters to over one meter. In the thinnest of the zones, movement is concentrated in one plane where in the wider zones, the bedrock has been sheared into a number of lenses.

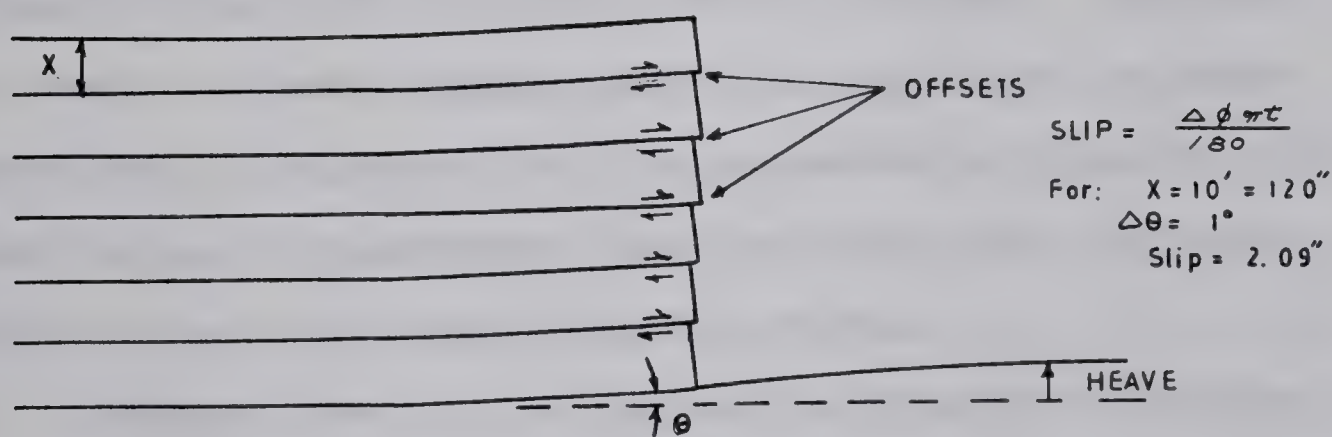








(a) BEFORE EXCAVATION



(b) AFTER EXCAVATION

FIG. 5.8 MECHANISM OF OVERTHRUSTING DUE TO FLEXURAL SLIP FOLDING



Shear zones were found in two out of three clay beds and some beds contained more than one zone. These zones have been traced for over 1500 feet without encountering an end to them. Shear tests on block samples from these zones show that the clay has been sheared to its residual angle of shearing resistance ( $\phi'_r$ ).

The beds at the site dip north-east at  $10^\circ$  to  $15^\circ$ . A study of the stratigraphy, given by Binnie et al. (1967), shows the bed thickness at Mangla to range from 5 to 20 feet. Assuming an average bed thickness of 10 feet and an average dip of 15 degrees, the interbed slip due to folding can be calculated from Equation 5.1 as 2.6 feet. At Jari damsite (22 kilometers to the east) the dip of the beds is approximately 45 degrees. The amount of flexural slip between 10 foot beds is predicted as 7.8 feet. Although the cause of these features might be attributed to other mechanisms, it appears that the mechanism of flexural slip would induce displacements along existing beds sufficient to shear the rock in-situ to the residual.

Another case, illustrating the effects of folding of bedrock, is given by Anderson and Schuster (1971), who describe numerous landslides which have occurred mobilizing the residual strength in the clay-shale interbeds of the Columbia River Valley in Oregon and Washington. The bedrock in the area consists of interbedded basalt and clay-shale beds. The sequence has been highly folded and, in some cases, faulted by tectonic activity which produced





"bedding plane slips" which are planar, heavily slickensided fissures which roughly parallel the bedding of the basalts. The clay-shales have peak and residual angles of shearing resistance of  $44^{\circ}$  and  $10^{\circ}$  respectively.

In 1964, two highways and two railroads were re-routed through this area. Twelve slopes failed during construction of which nine were planar movements at residual strength along pre-existing failure surfaces. These failures were 'wedge' shaped with a block moving downward along a nearly flat horizontal surface, parallel to the bedding of the clay shales. The other failures occurred along random fissures and appeared to have a rotational failure surface. The rate of displacement of each failure was low with days and sometimes weeks necessary for movements of a few feet to occur.

The cases discussed show that flexural slip will occur in a layered bedrock sequence when large scale folding, due to tectonic activity, occurs. There appears to be no reason why interbed slip should not occur, although on a much reduced scale, due to the formation of the gentle anticlinal structures below the valley bottoms of the study area. The amount of rebound, which has been noted in the case histories described in Chapter III of this thesis, could result in a maximum of several inches of interbed slip.

Data on the strength parameters, acting along the beds following displacements of this magnitude, is meagre.



Tests from Mangla show that the strength has been reduced to the residual after displacements which, if caused by flexural slip, vary from 2.6 feet at Mangla to 7.8 feet at Jari, for an assumed bed thickness of 10 feet.

The lithologic nature of the bedrock appears to control the amount of displacement across a discontinuity required to reach residual ( $\phi'_r$ ). Norris (1967) shows the interbed slip which occurred in the limestone Queensway folds at Ottawa, Ontario to be in the order of 1 inch. However "abundant polish and slickenside striae on bedding" were noted and indicate that the small amount of movement had reduced the angle of shearing resistance along the bedding to the residual.

Studies on joint surfaces in the London Clay (Skempton and Petley, 1967) indicate that joints formed by brittle fracture (no evidence of any shearing displacements) have essentially  $\phi'_p$  acting across the joint with little or no cohesion. However, very small shearing movements, of the order of a few millimeters, are sufficient to reduce  $\phi'$  to its residual value. James (1970, p. 88) found, for samples of unweathered Oxford Clay, seven reversals in the shear box, on samples perpendicular to the bedding, produced less of a decrease in strength than one reversal along the bedding planes which caused a drop in strength 90 percent of the amount from peak to residual.

Patton (1971) reported on the results of shear tests, done by Kanji at the University of Illinois, where a lower







residual strength was mobilized at failure along a kaolinite-limestone interface than was found for either the intact limestone or the kaolinite. Patton (1971) considered this 'interface' effect as being of considerable importance in field stability problems as shear adjacent to a very stiff material leads to a more rapid particle alignment and hence, rapid development of the residual strength.

#### 5.4 Finite Element Analysis of Lateral Movements Across a Weak Layer

Several well documented cases have been cited where lateral movements and landslides have occurred along a bentonite layer. Bentonite seams are common in the Upper Cretaceous bedrock of the study area and are discussed in Chapter II. Bentonite beds, of up to 2 feet in thickness, have been reported in the Bearpaw formation at Fort Peck Dam in Montana by Fleming et al., (1970). Babet (1966) reports bentonite beds in the Bearpaw formation in southern Alberta which have thicknesses of over 10 feet. Bentonite beds of up to 18 inches in thickness occur in the Pierre formation at Oahe Dam on the Missouri River (Fleming et al., 1970). Bentonite beds, 5 to 10 feet in thickness, are not uncommon in the Edmonton, Oldman and Wapiti formations of Alberta. Yudhbir (1969) and Scott and Brooker (1968) considered that the presence of bentonite layers has an extremely detrimental effect upon slope stability.

The finite element program described in Chapter IV



was used to study the effect which a bentonite layer would have upon displacements caused by valley excavation. Grid 1A, Figure 5.9, was used to study the effect of a 10 feet thick bentonite layer located either at the toe of slope (layer "A") or 40 feet below the valley bottom (layer "B"). A similar approach was used by Duncan and Goodman (1968) as part of a program to study the effect of joints upon rock slope stability.

A valley 200 feet deep and 2000 feet wide was used to simulate the dimensions of a typical post-glacial valley of the study area. Initially, vertical valley walls were chosen. A modulus of elasticity of 10 k.s.i. and a Poisson's ratio of 0.30 were used for the homogeneous section of the grid to give a valley anticline similar to that found in nature.

The value of 10 k.s.i. for E appears to agree reasonably well with the undrained moduli of the weaker formations of the study area and is considerably in excess of the drained values of E reported by DeJong (1970) for a bentonitic sandstone from the Edmonton formation. Thus, use of this figure to represent drained (or long term) displacements of the homogeneous bedrock appears reasonable as 9.61 feet of rebound in the valley center (3.2 percent of valley depth) results from use of this value in a homogeneous grid, which falls within the range of field behaviour documented in Chapter III.

The value of  $\nu$  of 0.30 was chosen arbitrarily to







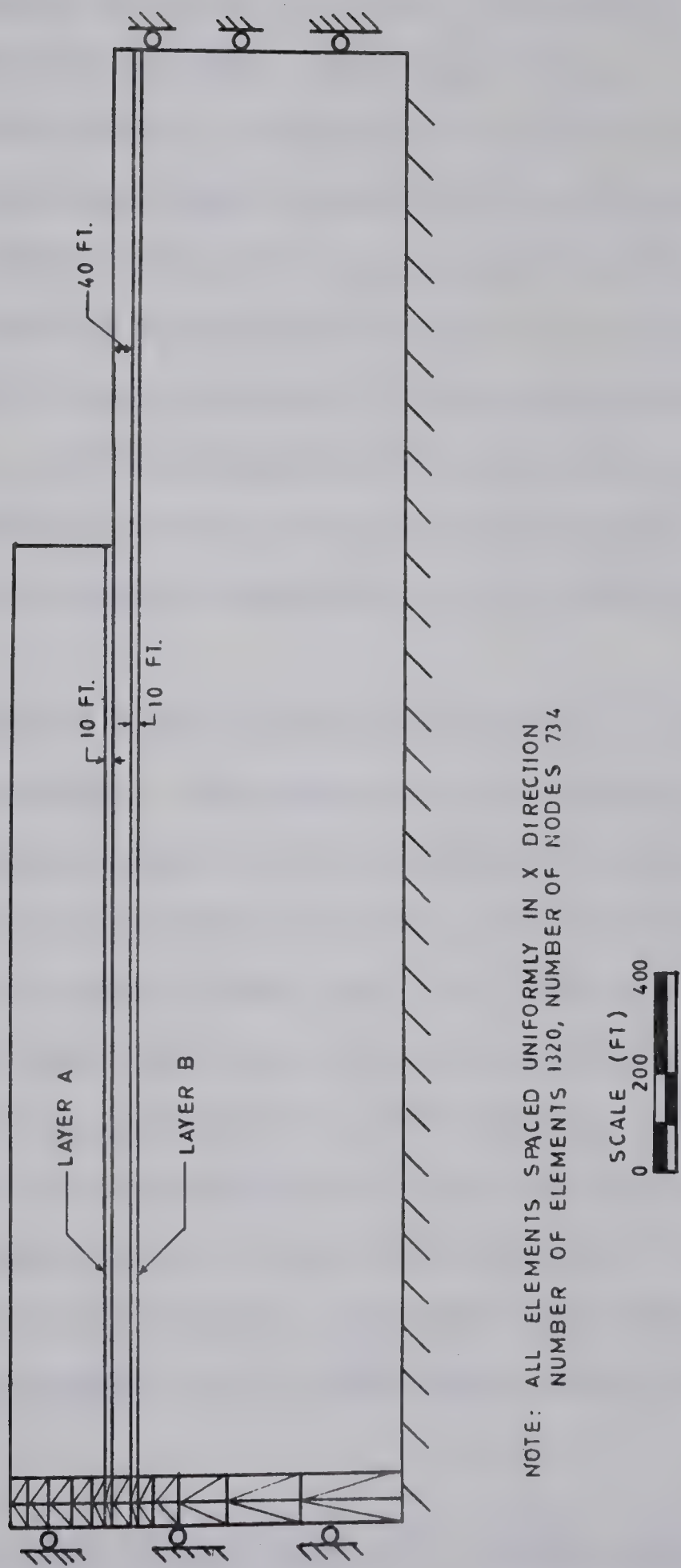


FIG. 5.9 GRID 1A



represent drained behaviour as no reliable data is available for the bedrock of the study area. Variation in this parameter should not markedly effect the results.

No triaxial moduli are reported for bentonite. However, field observations (Appendix B) show the material to be markedly softer than the surrounding bedrock and it would appear that the drained modulus of this material may be 1/10 or 1/100 of the value of  $E$  of the surrounding bedrock. Swelling, due to adsorption of groundwater, would lead to a considerable volume increase and would be simulated by use of a very low value of  $E$  in the bentonite layer.

Low values of  $E$  were used successively in the two thin layers to simulate the presence of a bentonite bed. The modulus of elasticity of the simulated bentonite layer ( $E_L$ ) was reduced successively to 0.10, 0.01 and 0.001 of the modulus of the rest of the grid ( $E$ ). Values of  $K_0$  of 0.50, 1.00, 2.00 and 3.00 were used to study the effect of the degree of overconsolidation of the bedrock. Initially, a value of  $\nu$  of 0.30 was used for the entire grid although the effect of variation in  $\nu$  was later studied. The effect of distance to lateral boundary, distance to bottom boundary, width and position of the weak layer were also investigated.

Differential Movement Across Layer "A" Through 'Toe of Slope: Layer "A" was used to simulate a horizontal bentonite





layer 10 feet thick, with its base level with the valley bottom. A study of the nodal displacements following excavation shows the top of layer "A" moving further towards the valley than the bottom at a given section. This leads to a differential displacement ( $\delta H$ ) across the layer which, when divided by the layer thickness, gives the average shear strain  $\gamma$  across the layer. Figures 5.10 to 5.13 inclusive show the differential displacements across this layer for  $K_0 = 0.50, 1.00, 2.00$  and  $3.00$ . Large differential displacements, or shear strains, occur due to stress relief; this effect is a maximum at the toe of slope and decreases with distance into the slope. The amount of differential displacement across the bentonite layer increases with  $K_0$ . The use of high values of  $K_0$  and low ratios of  $E_L/E$  results in high shear strains occurring for considerable distances back from the toe of slope. The differential movement for a homogeneous section ( $E_L/E = 1.00$ ) is seen to be negligible in Figure 5.10 and 5.11. For cases where the weak layer is very thin, the differential movement is effectively the interbed slip.

The maximum interbed movement occurs at the toe of the slope. The effect of  $K_0$  and  $E_L/E$  upon differential movement at the toe of the slope is given in Figure 5.14 and 5.15. The effect of  $K_0$  is shown to be of prime importance, especially where the ratio  $E_L/E$  is low. For example, consider the case where  $E_L/E = 0.01$ . The differential movement in a normally-consolidated deposit ( $K_0 = 0.6$ )



GRID 1A  
 $K_0 = 0.50$

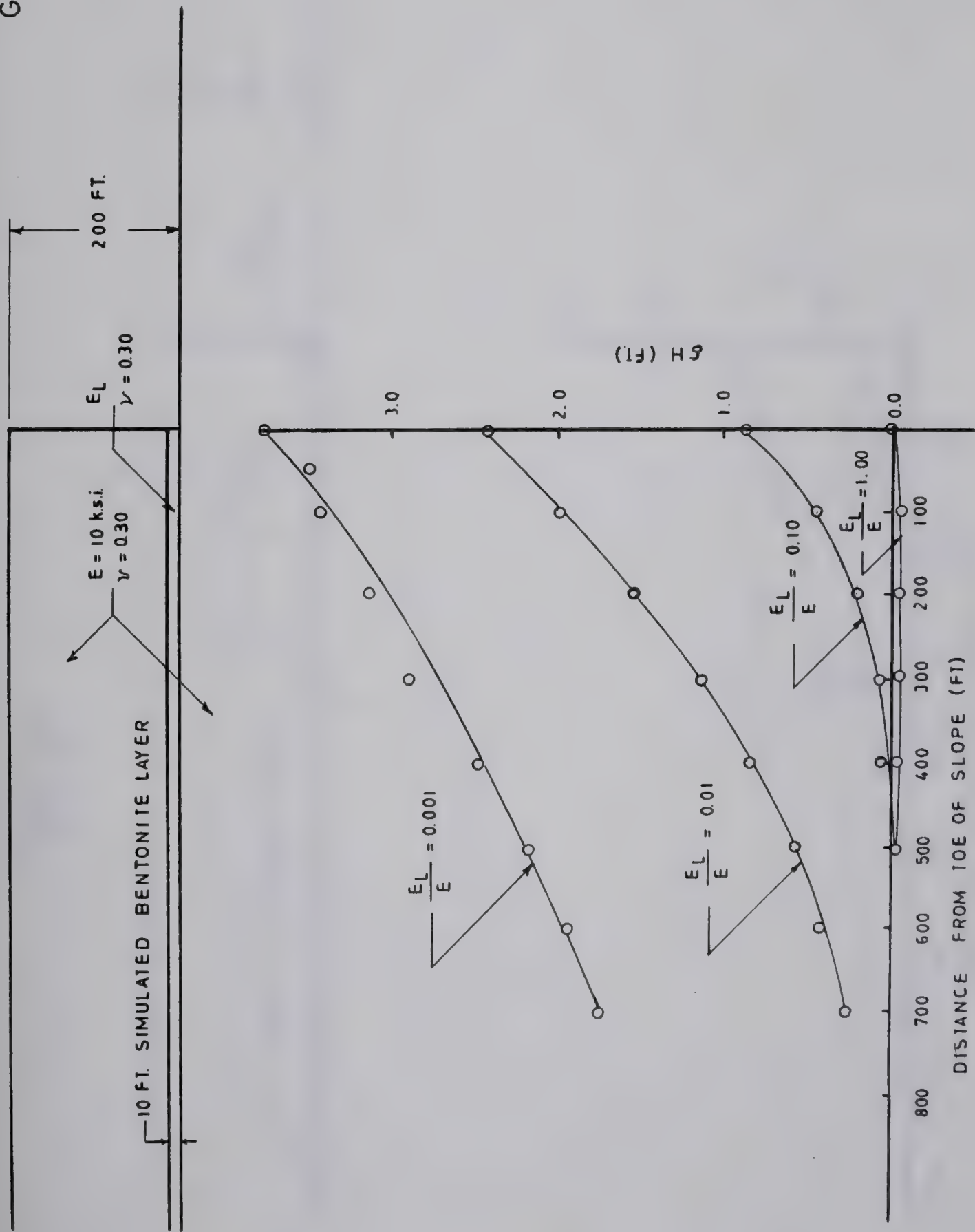


FIG. 5.10 DIFFERENTIAL DISPLACEMENTS ACROSS BENTONITE LAYER ( $K_0 = 0.50$ )





GRID 1A  
 $K_0 = 1.00$

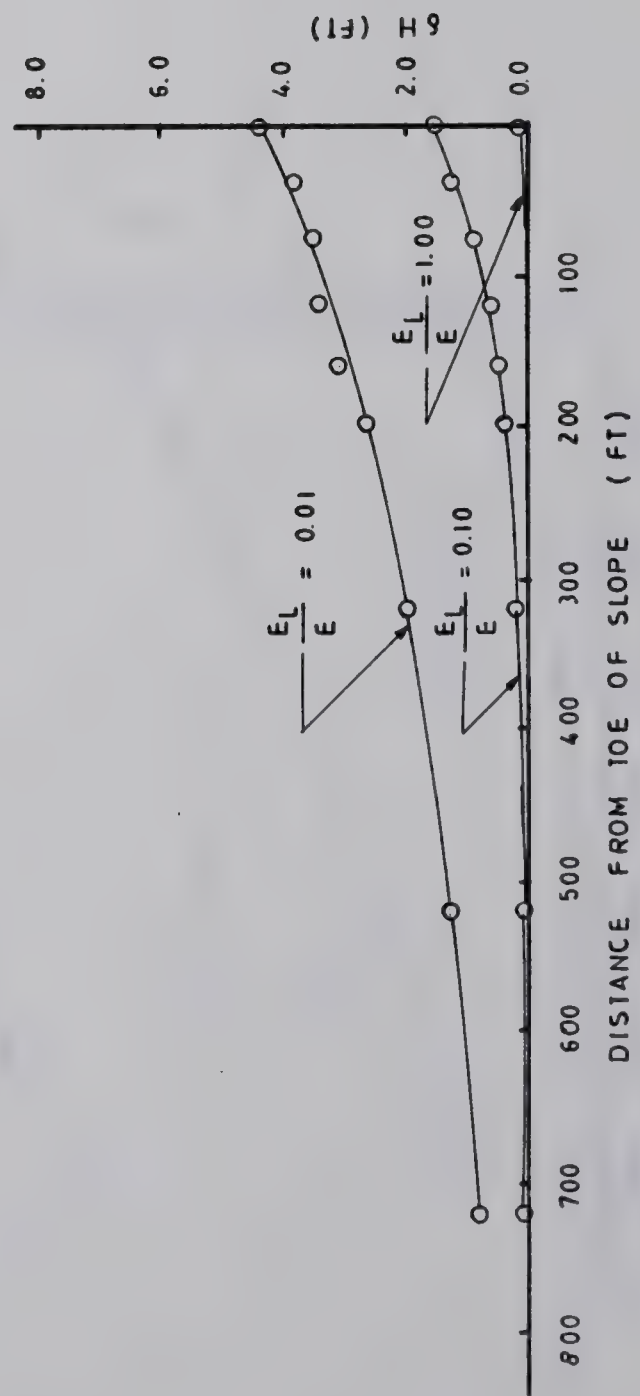
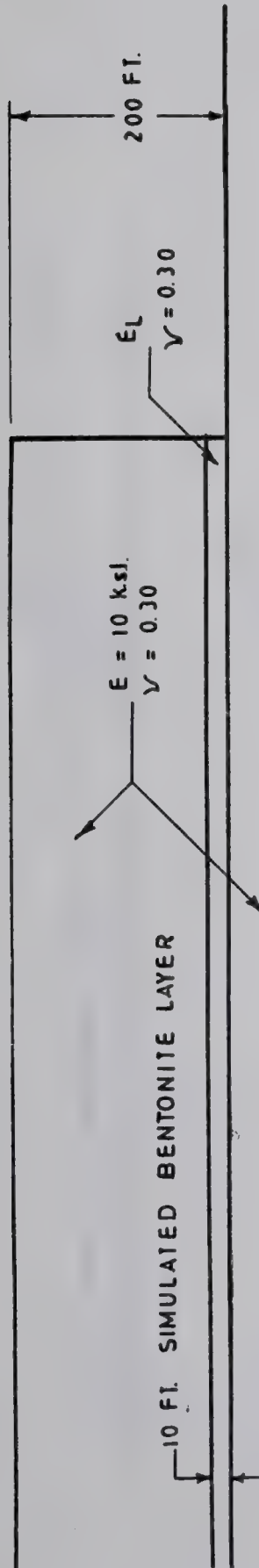


FIG. 5.11 DIFFERENTIAL DISPLACEMENTS ACROSS BENTONITE LAYER ( $K_0 = 1.00$ )



GRID 1A  
 $K_0 = 2.00$

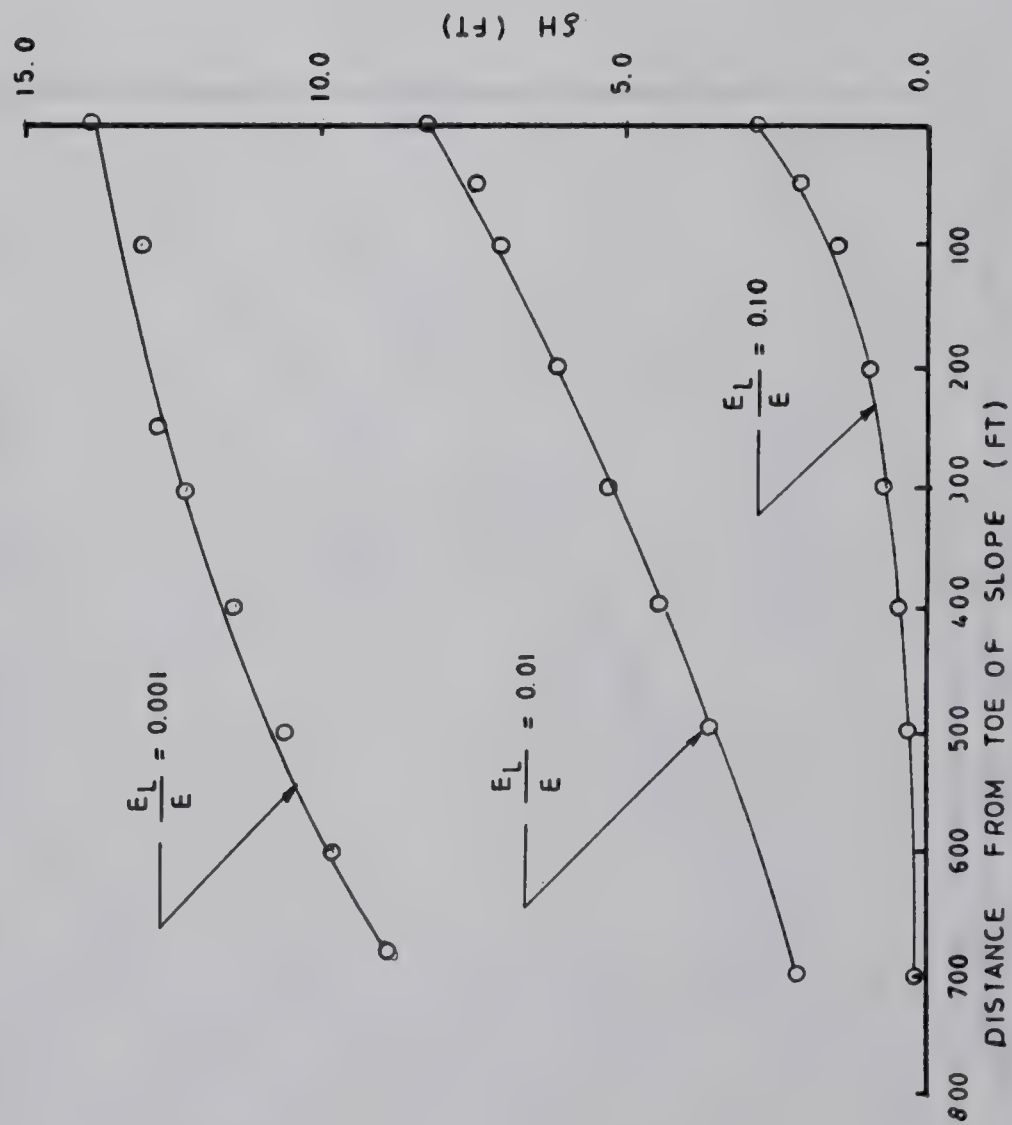
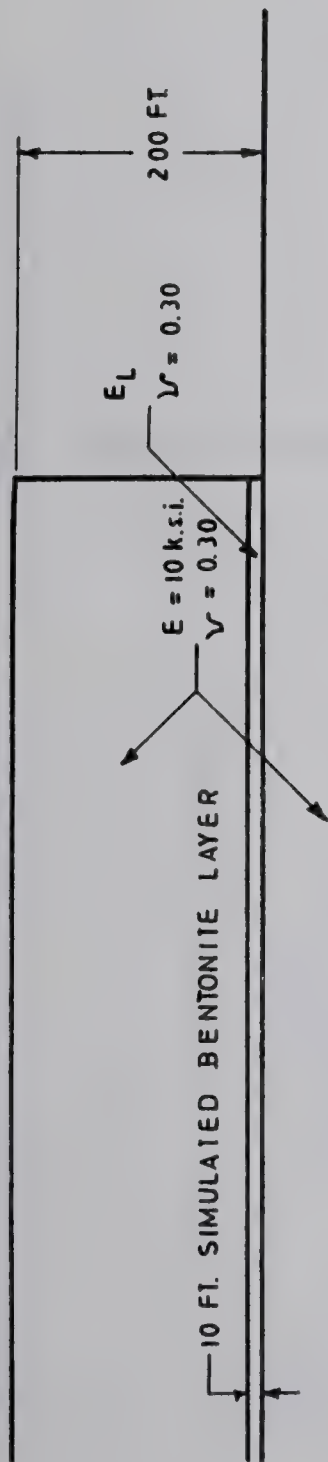


FIG. 5.12 DIFFERENTIAL DISPLACEMENTS ACROSS BENTONITE LAYER ( $K_0 = 2.00$ )





GRID 1A  
 $K_0 = 3.00$

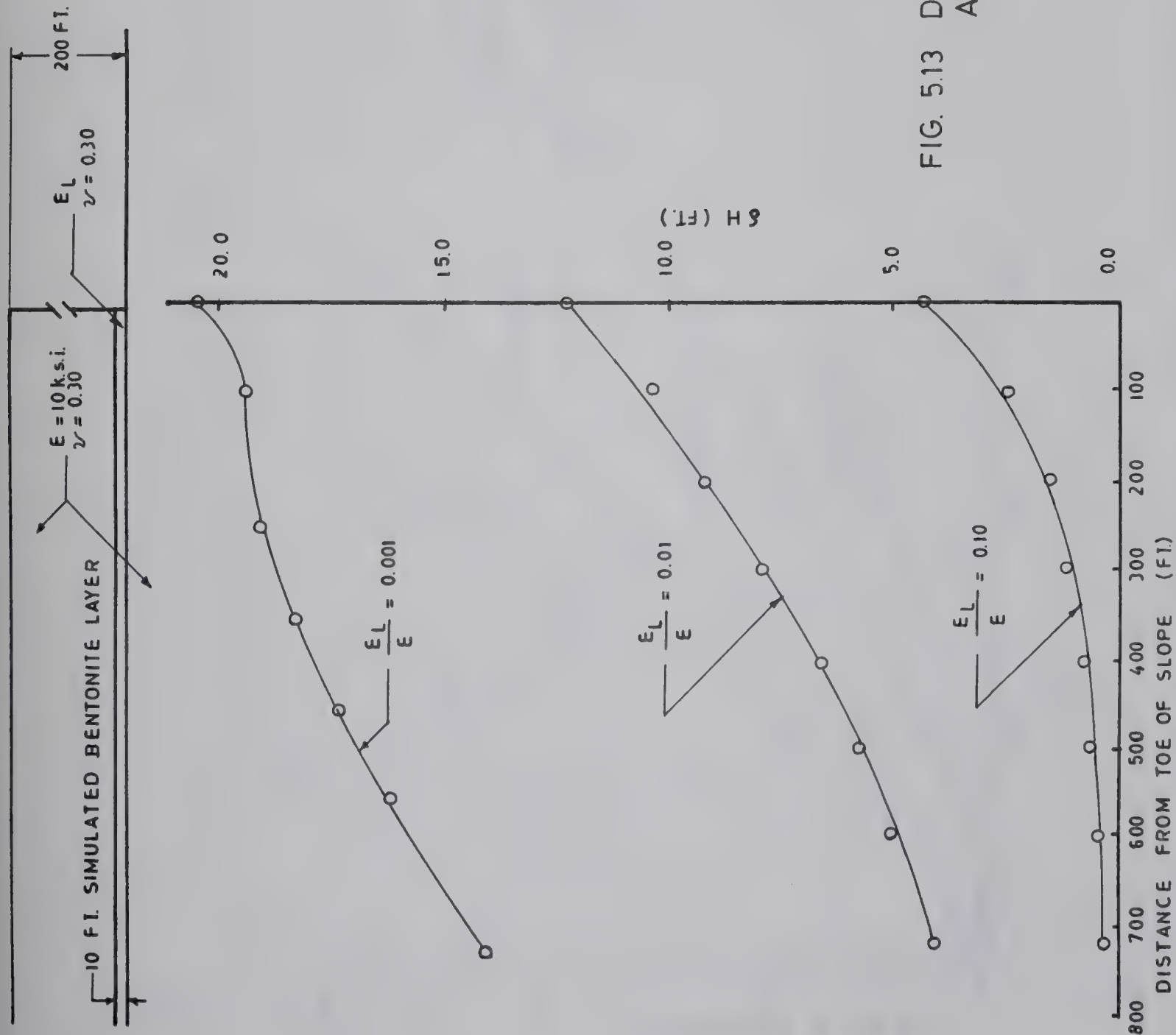


FIG. 5.13 DIFFERENTIAL DISPLACEMENTS  
 ACROSS BENTONITE LAYER  
 $K_0 = 3.00$



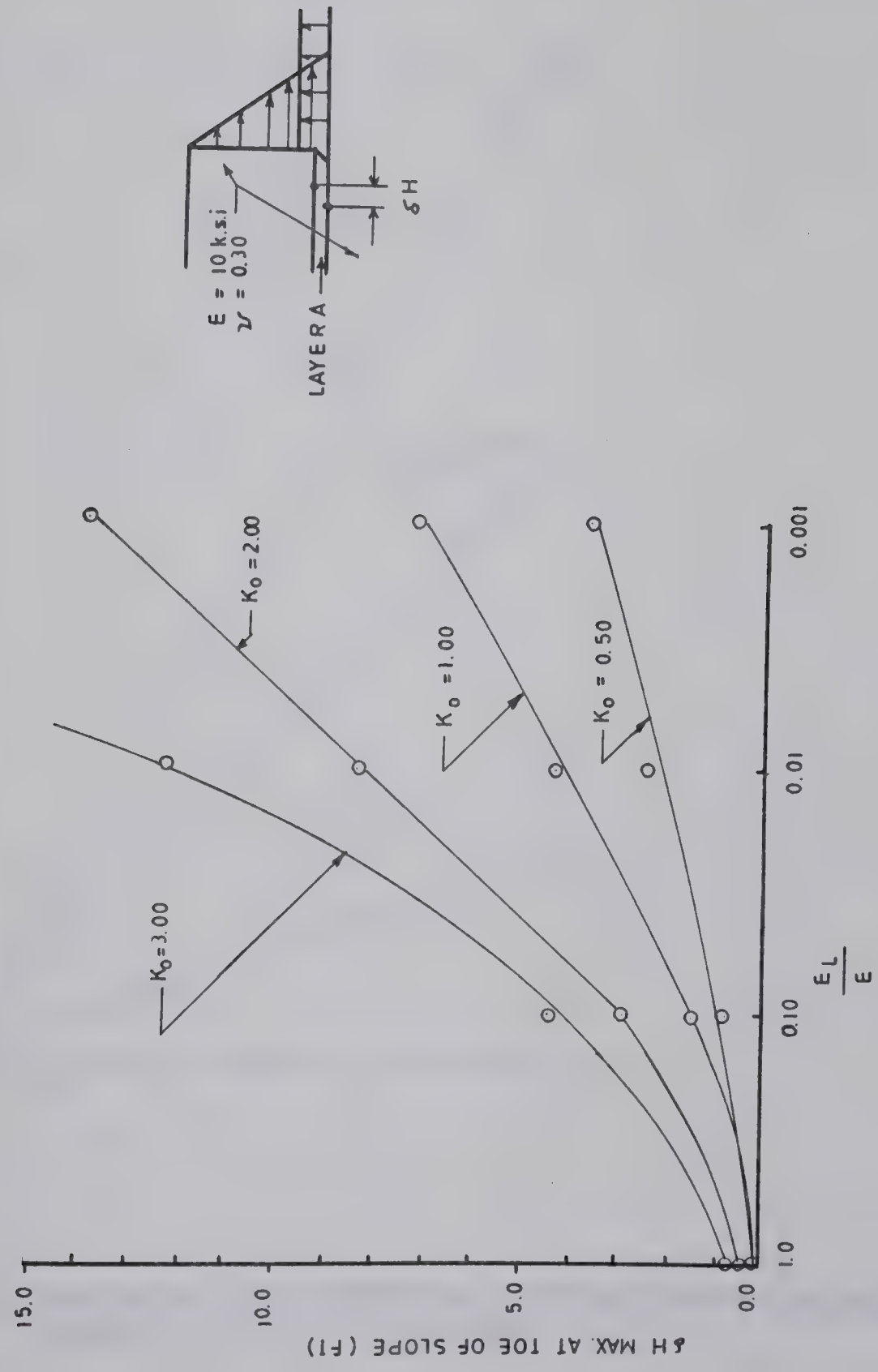


FIG. 5.14 MAXIMUM DIFFERENTIAL DISPLACEMENT ACROSS LAYER "A" AT TOE OF SLOPE





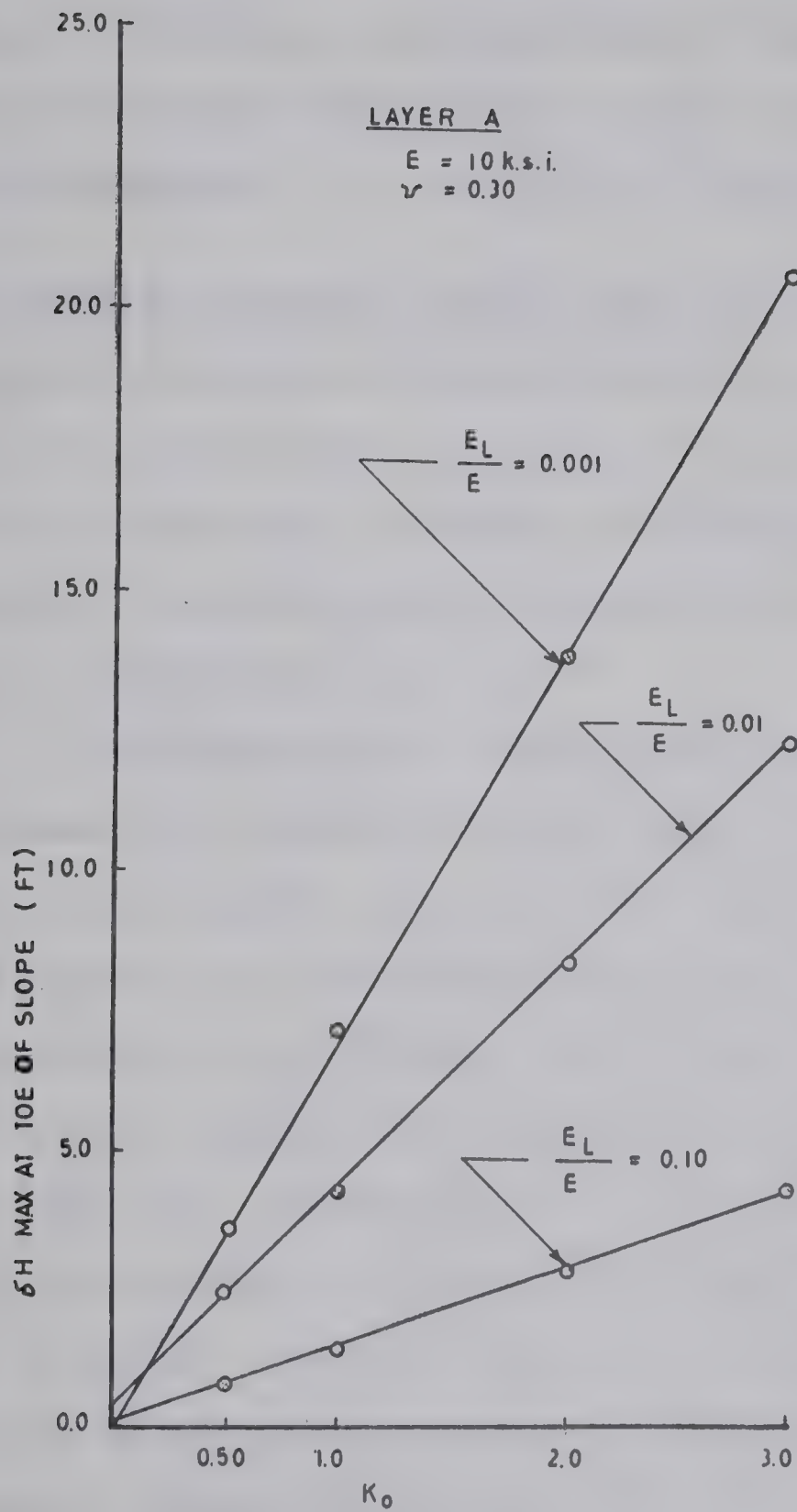


FIG. 5.15 MAXIMUM DIFFERENTIAL DISPLACEMENT ACROSS LAYER "A" AT TOE OF SLOPE



would be about 2.5 feet across layer "A" at the toe of the slope. In a highly overconsolidated deposit ( $K_o = 3.00$ ) the differential displacement at the toe of the slope would be approximately 13.3 feet giving a shear strain of 133%.

#### Differential Movement Across Layer "B" Below the Valley

Bottom: The effect of valley excavation on a weak layer below the valley floor was studied by placing layer "B", a 10 foot thick row of elements, 40 feet below the valley bottom. The same range of parameters were used as in the study reported for layer "A".

The differential displacement across the layer increases to a maximum below the toe of the slope and then decays rapidly to zero at the valley center as shown in Figure 5.16. The differential displacements are again a function of  $E_L/E$  and  $K_o$ . The effect of  $E_L/E$  and  $K_o$  upon the maximum differential movement are shown in Figures 5.17 and 5.18. The presence in layer "B" of a low value of  $E_L/E$  results in a large differential movement below the toe of slope. If layer B has a ratio of  $E_L/E$  of 0.01, the maximum differential movement will be about 5 feet for a normally consolidated deposit ( $K_o = 0.6$ ) compared to 13 feet for a highly overconsolidated deposit with  $K_o = 3.00$ .

#### Effect of Modulus of Elasticity of the Grid Upon Differen-

tial Movements: An increase in the modulus of elasticity of the grid, using  $E_L/E$  ratios of 0.10 and 0.01, caused a decrease in the amount of differential movement across





GRID 1A

- $\nu = 0.30$
- $\bullet = E_L/E = 0.01$
- $\circ = E_L/E = 0.10$

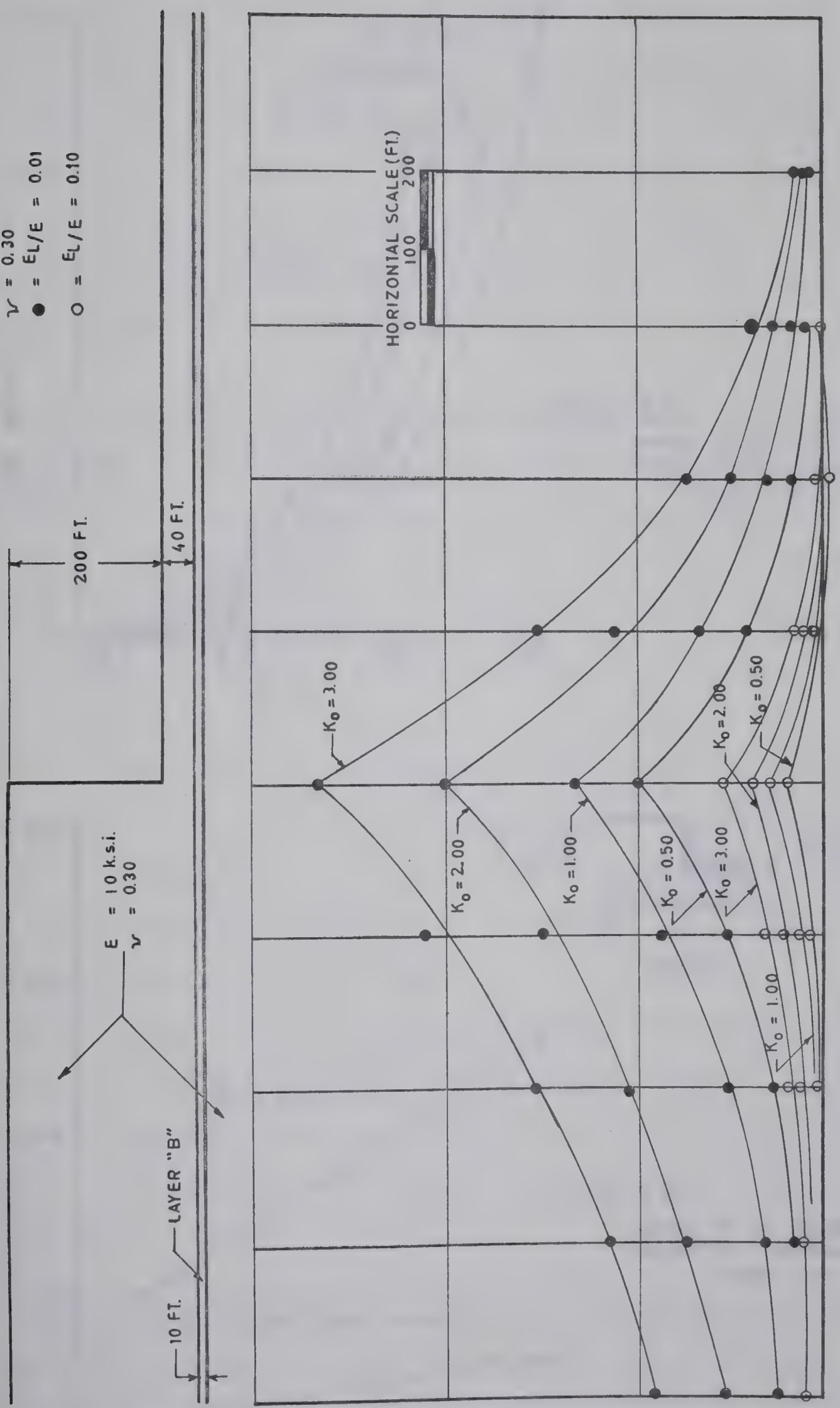


FIG. 5.16 DIFFERENTIAL DISPLACEMENT ACROSS LAYER "B"



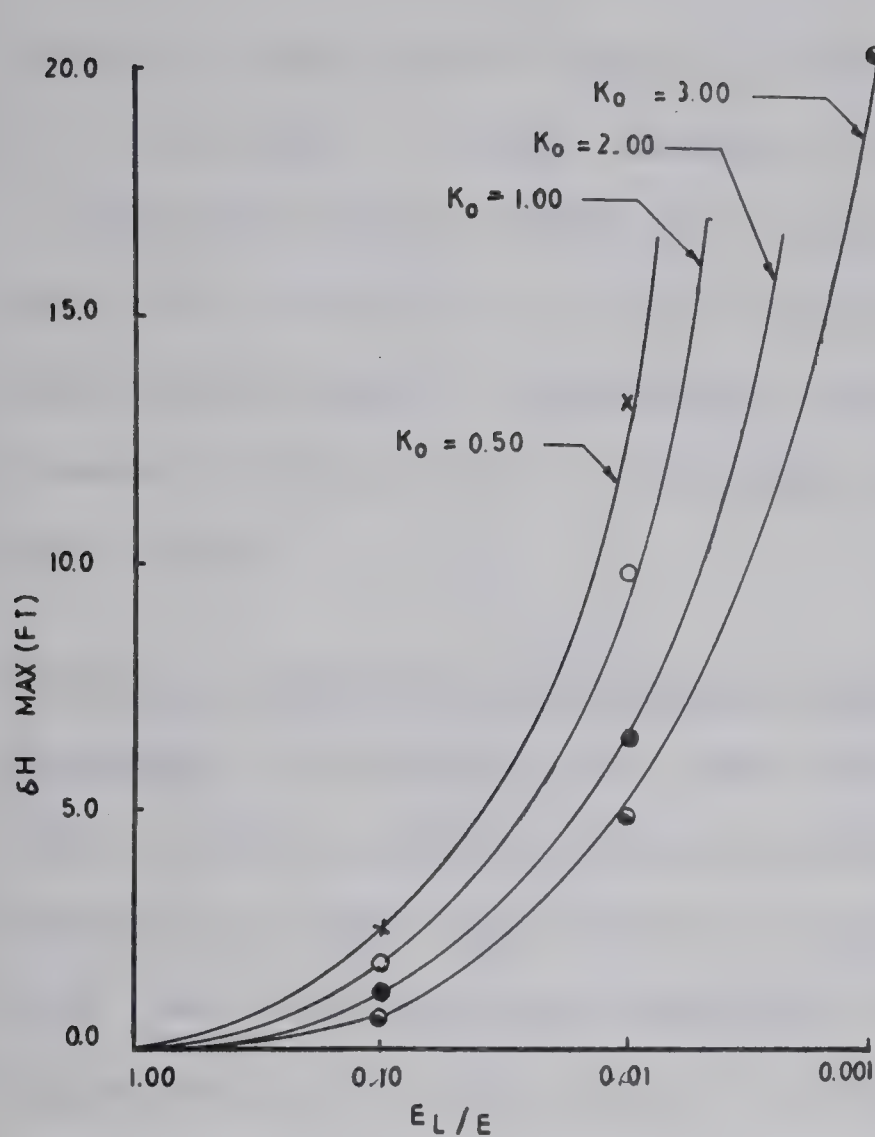


FIG. 5.17  
EFFECT OF  $E_L/E$  ON MAXIMUM  
DIFFERENTIAL MOVEMENT -  
LAYER "B"

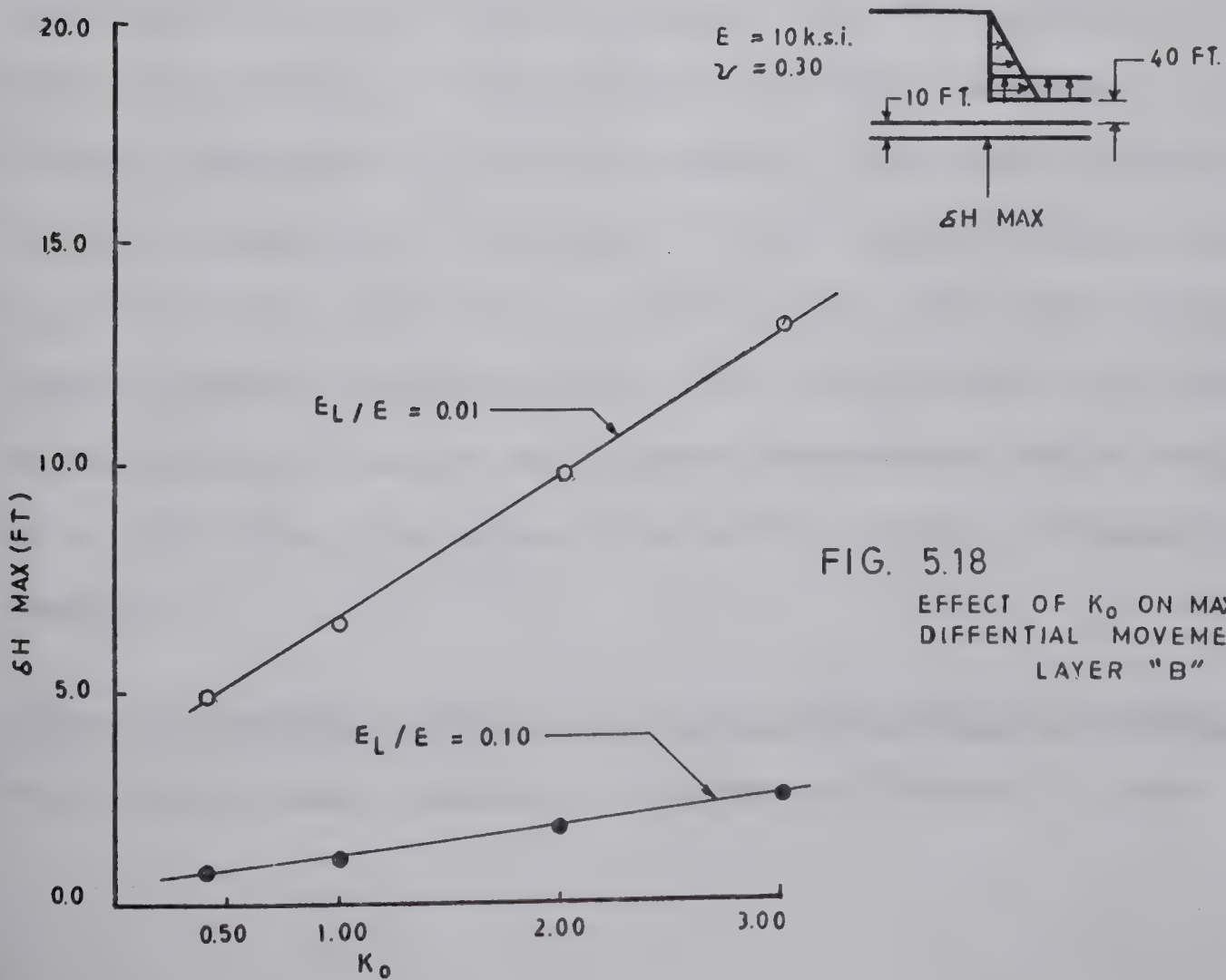


FIG. 5.18  
EFFECT OF  $K_0$  ON MAXIMUM  
DIFFERENTIAL MOVEMENT -  
LAYER "B"





layers "A" and "B" as shown in Figures 5.19 and 5.20 for  $K_0 = 1.00$  and  $\nu = 0.30$ . However, a high value of  $K_0$  and a low value of  $E_L/E$  would still give large values of  $\delta H$ , even for a value of  $E$  in the order of 30 to 40 k.s.i.

which would appear a reasonable value, in view of the discussion in Chapter IV, to simulate undrained behaviour of the valley.

#### Effect of Variation of Poisson's Ratio $\nu$ Upon Differential

Movement: A variation in  $\nu$  was found to have only a secondary effect upon the maximum differential movements.

Figure 5.21 shows the effect of varying  $\nu$  for the entire grid from 0.48 (undrained behaviour) to 0.10. A minor variation in  $\delta H$  at the toe of the slope for the layer "A" can be seen to occur.

The value of  $\nu$  for layer "A" was varied from 0.48 (undrained) to 0.10 while keeping  $\nu$  for the remainder of the grid constant. The results are shown in Figure 5.22. A small increase in  $\delta H$ , at the toe of the slope, occurs for an increase in  $\nu$  of layer "A" for the parameters used ( $K_0 = 1.00$ ,  $E = 10$  k.s.i.,  $E_L/E = 0.10$ ). The small variation in results indicates that the actual value of  $\nu$  used in the analysis is not of primary importance and selection of  $\nu = 0.30$  for the entire grid should yield reasonable results.

#### Effect of Boundary Position on the Differential Movement:

The finite element studies reported in Chapter IV show



GRID 1A

$K_0 = 1.0$

$\gamma = 0.30$

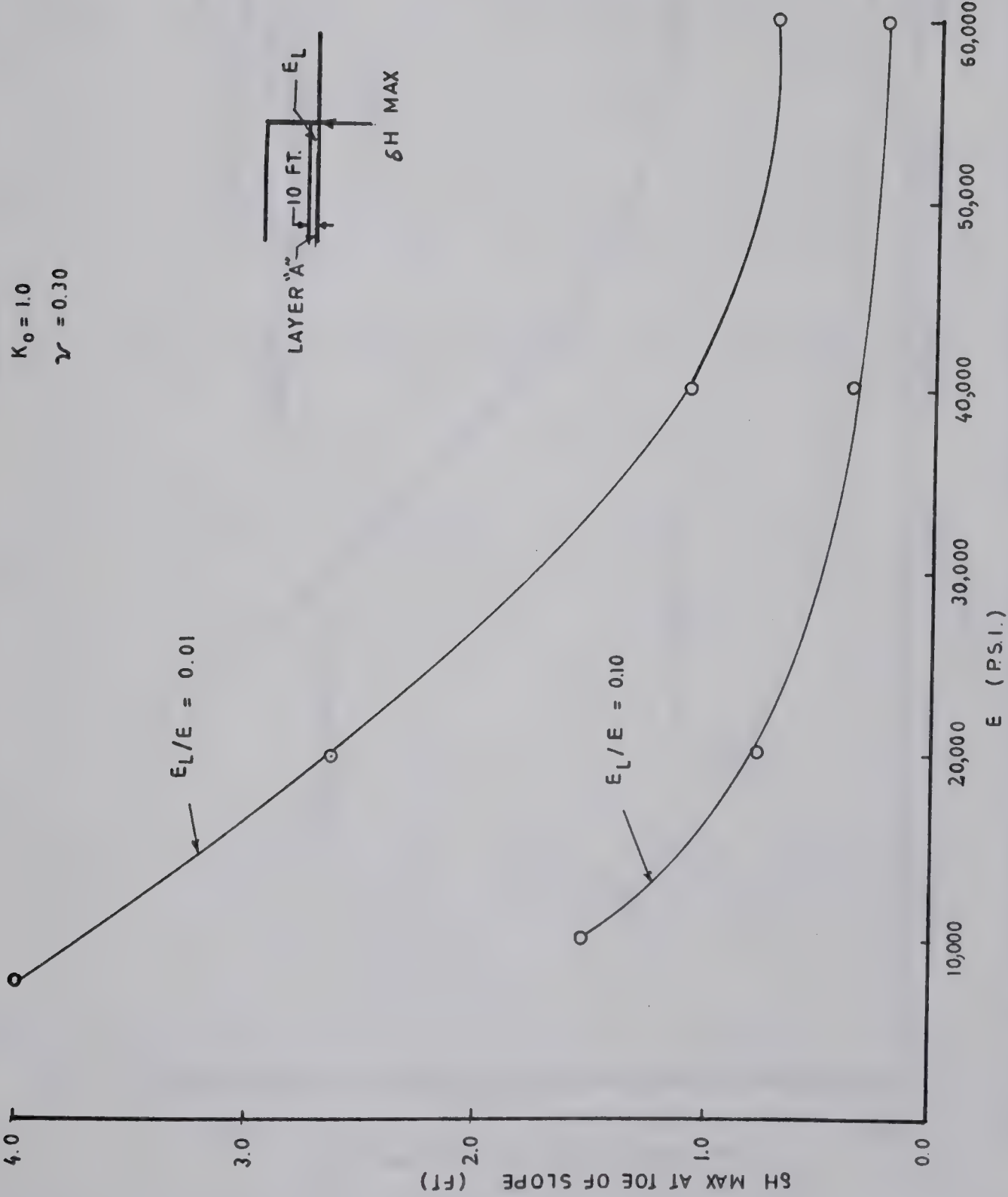


FIG. 5.19 MAXIMUM DIFFERENTIAL DISPLACEMENT ACROSS LAYER "A"





GRID 1A

$K_0 = 1.0$

$\nu = 0.30$

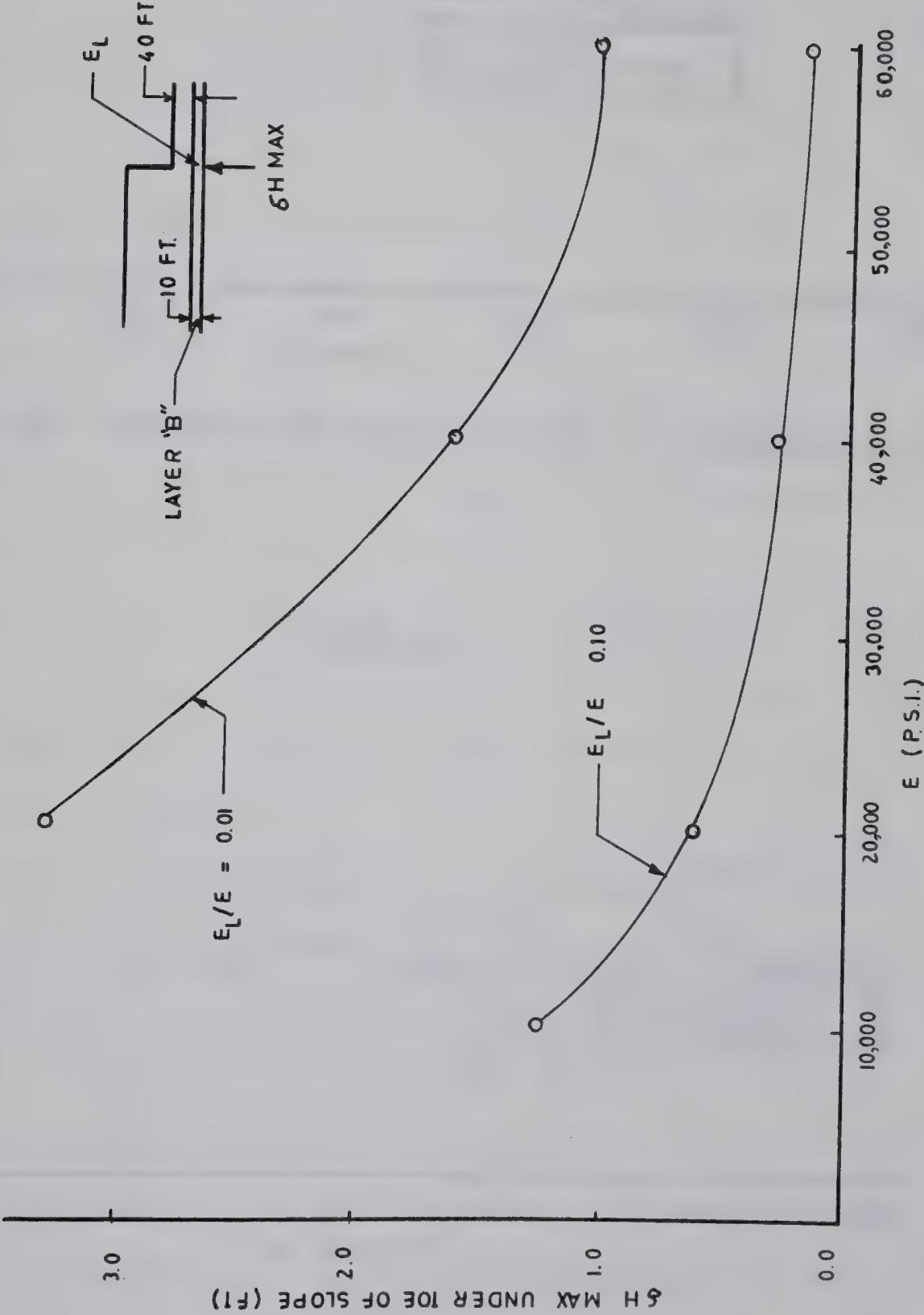
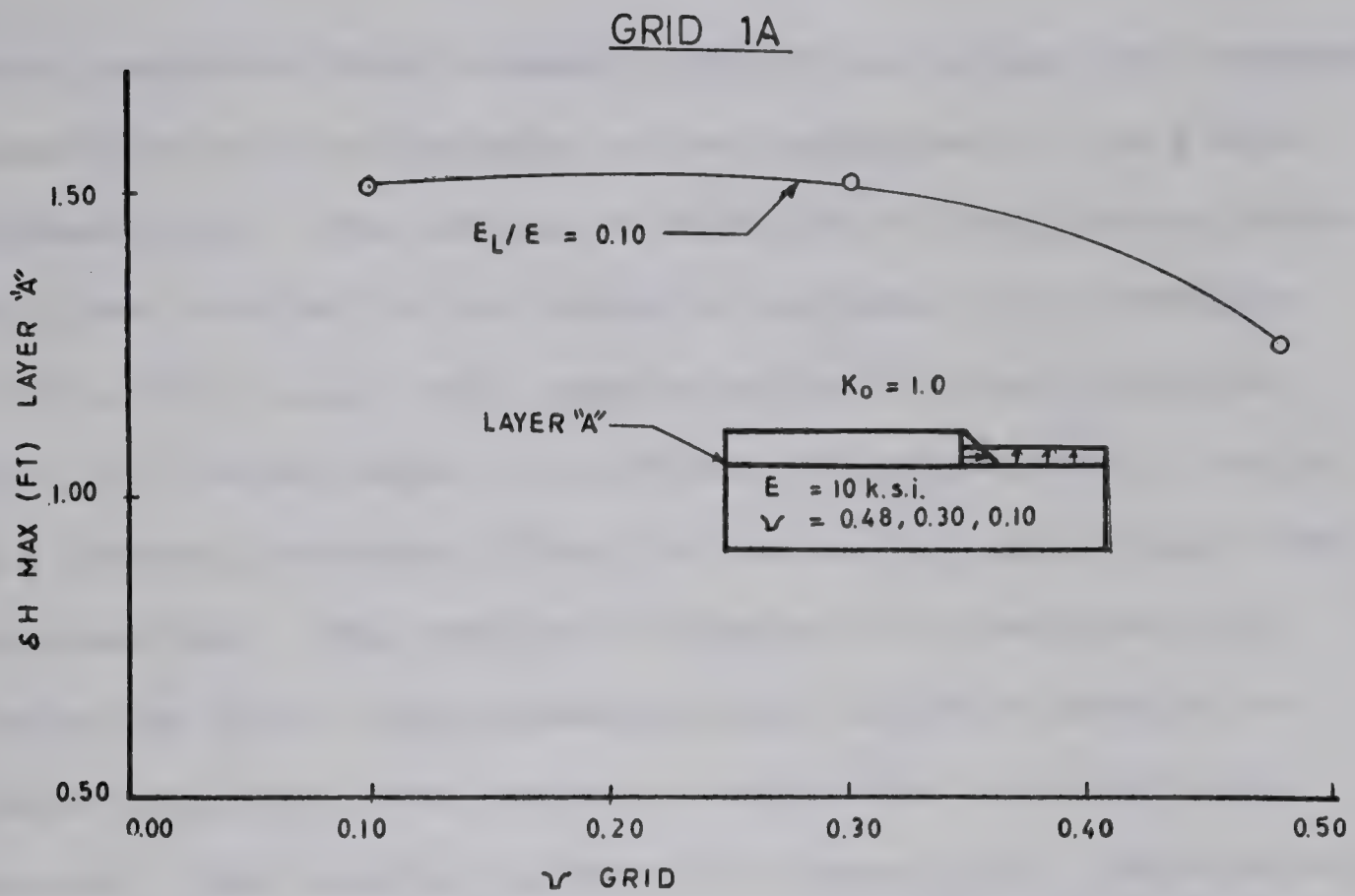
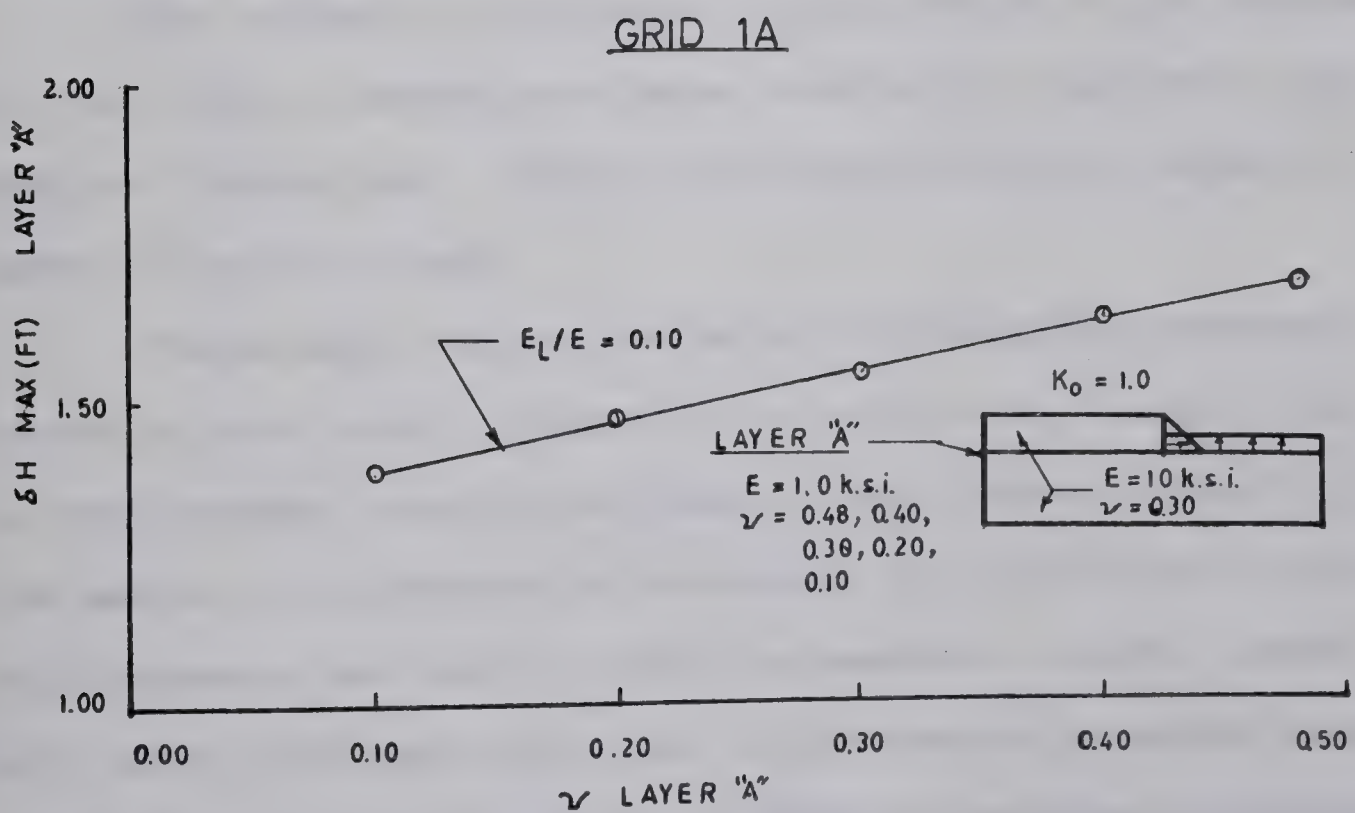


FIG. 5.20 MAXIMUM DIFFERENTIAL DISPLACEMENT ACROSS LAYER "B"



FIG. 5.21 EFFECT OF VARIATION IN  $\nu$ -HOMOGENEOUS SECTIONFIG. 5.22 EFFECT OF VARIATION IN  $\nu$ - LAYER "A"





that predicted displacements around the valley are extremely sensitive to the distance to the boundaries of the finite element grid. The effect of distance to the lateral boundary was studied by assigning an extremely high modulus ( $1.0 \times 10^8$  p.s.i.) to elements beyond a given distance from the valley edge. The effect of progressively moving the lateral boundary closer to the valley edge could then be observed. The results in Chapter IV show that this technique gives displacements which are very similar to those resulting from actually fixing the boundary node points. The results, plotted in Figure 5.23, indicate only a slight decrease in maximum displacement at, or below, the toe of the slope for layers "A" and "B" for a decrease in the distance to the lateral boundary.

The effects of distance to the bottom rigid boundary of the finite element grid were studied by the same 'high modulus' technique. Figure 5.24 shows that the effect of depth of grid is small.

Therefore, the variation in differential movement across a weak layer appears to be relatively insensitive to the boundary conditions used in the finite element grid. The amount of differential movement, obtained from a given grid geometry and set of input parameters, can be viewed with more confidence than the displacements obtained from a homogeneous grid, which are a direct function of distance to the boundary of the finite element grid.



## GRID 1A

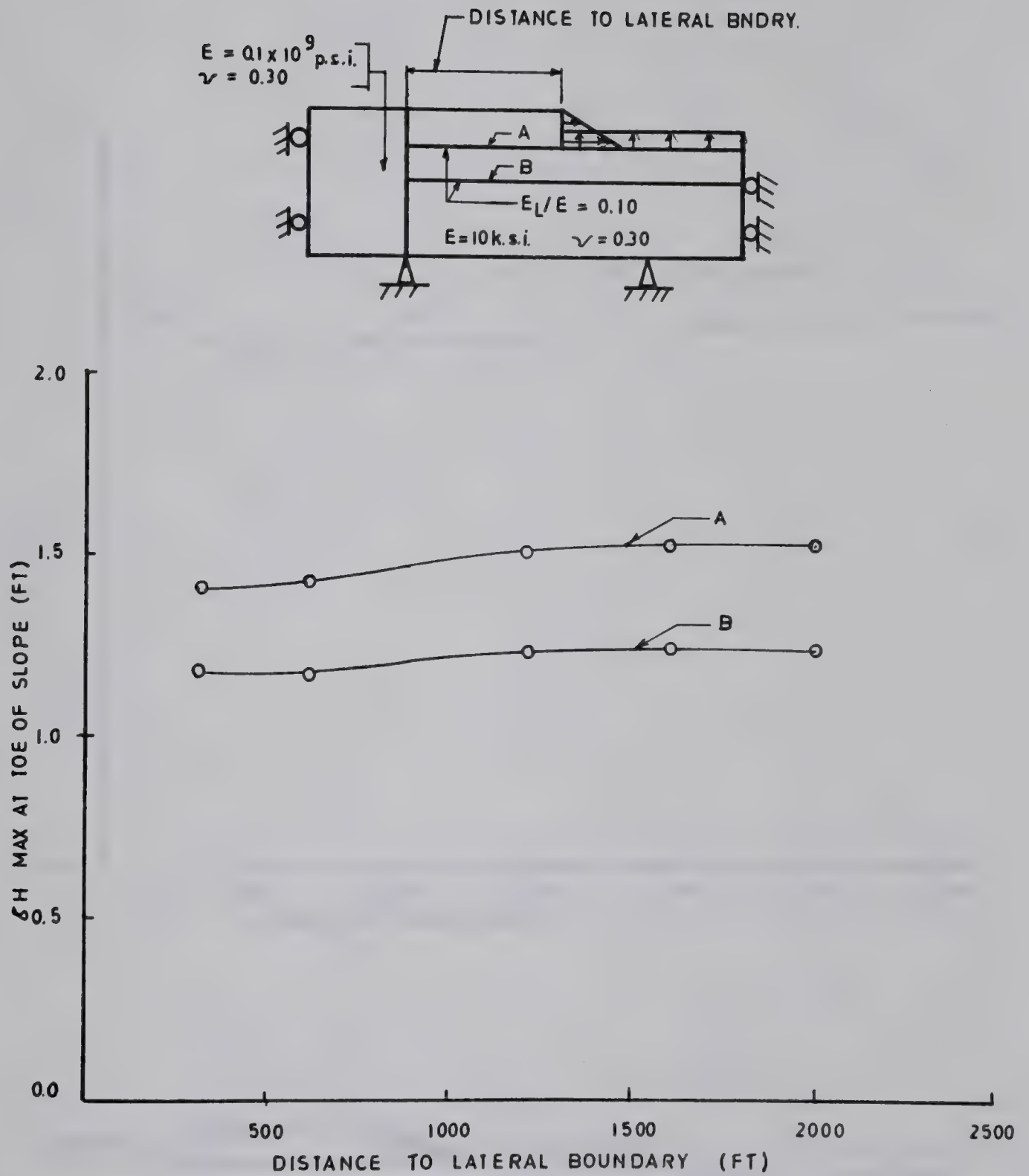


FIG. 5.23 EFFECT OF DISTANCE TO LATERAL BOUNDARY





## GRID 1A

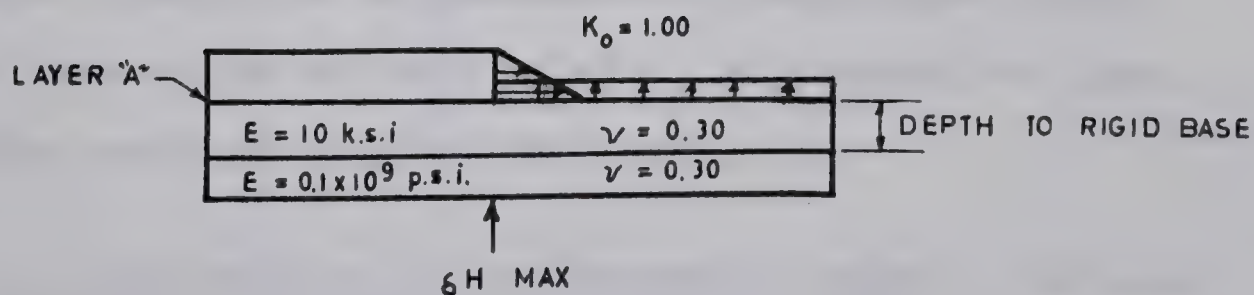
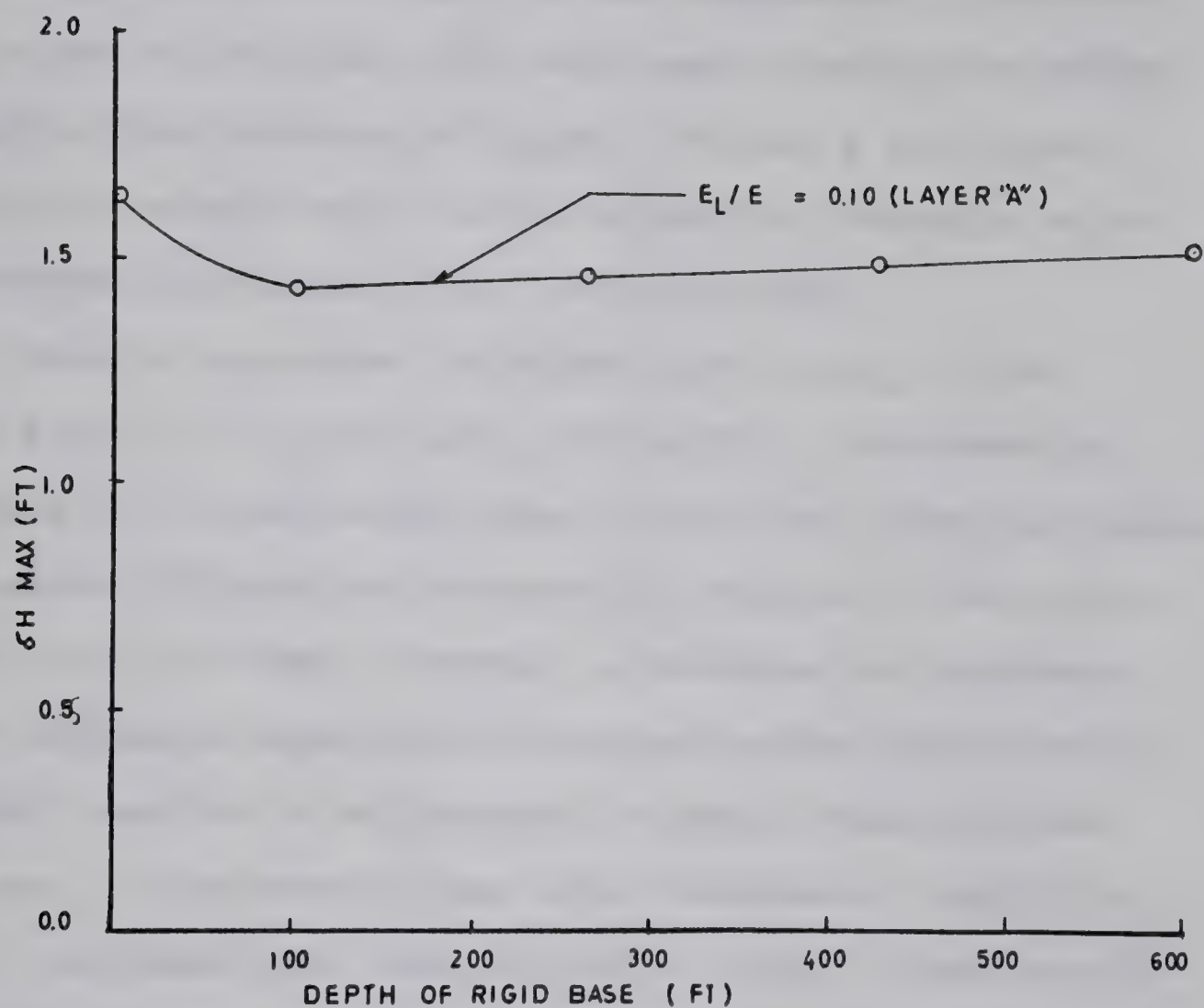


FIG. 5.24 EFFECT OF DEPTH TO RIGID BASE ON MAXIMUM DIFFERENTIAL DISPLACEMENT



Effect of Width of the Weak Layer: The results of the previous section showed that the differential movement in the region of the toe of the slope was not influenced to a large degree by the distance to the boundaries. Therefore, Grids 8 and 8A (Figure 5.25) were used to study the effect of varying the thickness of layer "A" from 2 to 12 feet, keeping the aspect ratio of the triangular elements below the recommended figure of 5:1 (Wilson, 1963).

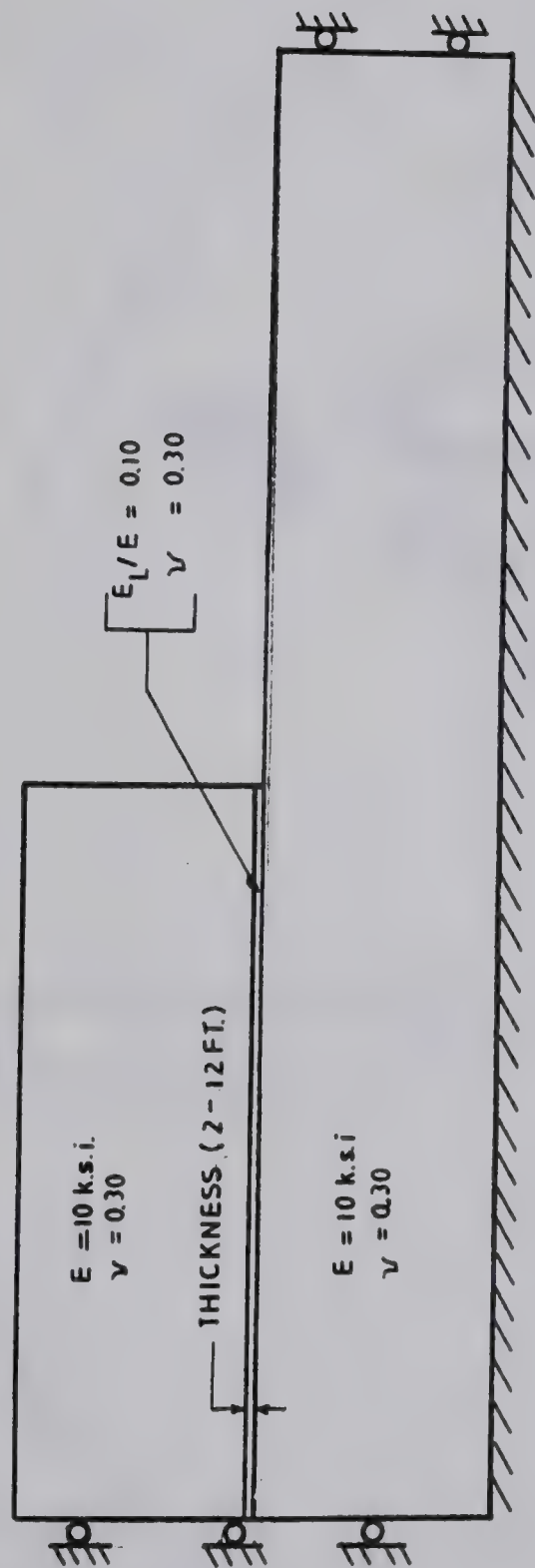
Results are shown in Figure 5.26 for  $K_O = 1.00$ ,  $E = 10 \text{ k.s.i.}$ ,  $\nu = 0.30$  and  $E_L/E = 0.10$ . A decrease in thickness of the bentonite layer from 12 to 2 feet decreases the maximum differential movement at the toe of the slope from 2.2 to 1.05 feet. However, a decrease in thickness of the bentonite layer, while decreasing the differential movement, results in an increase in shear strain across the layer. A decrease in the layer thickness, from 12 to 2 feet, increased the shear strain at toe of slope from 20 to 53 percent.

It would therefore appear that the thickness of the bentonite layers are of considerable importance, with thinner beds being of more critical importance to slope stability problems than thicker beds.

Effect of the Position of the Bentonite Layer: The location of the bentonite layer, above or below the valley floor, was studied using Grids 1A and 8. The effect of the position of a 10 feet thick bentonite layer above the







NOTE: NUMBER OF ELEMENTS = 720  
NUMBER OF NODE POINTS = 430

FIG. 5.25 GRID 8 & 8A



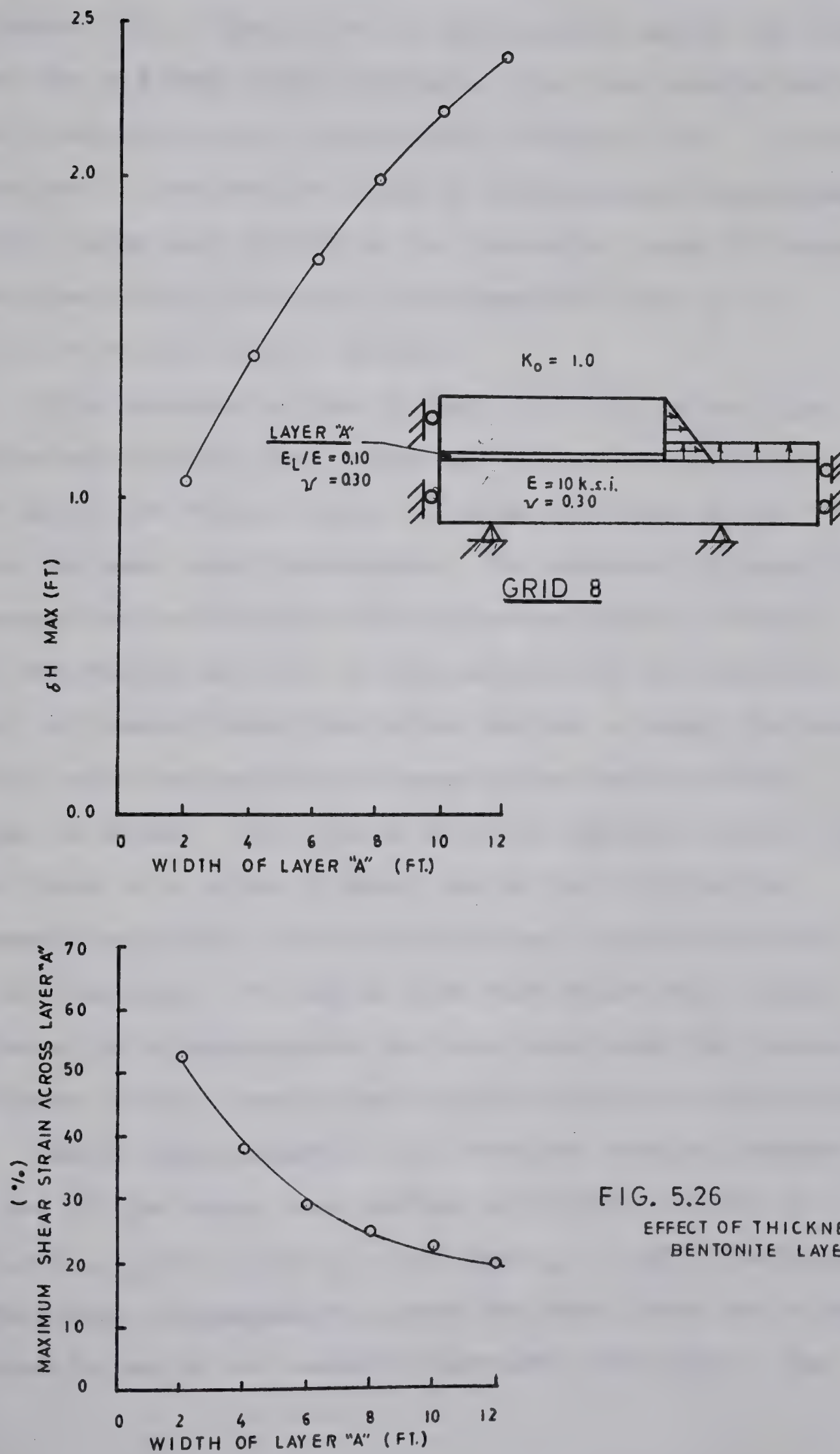


FIG. 5.26  
EFFECT OF THICKNESS OF  
BENTONITE LAYER





valley floor was studied using Grid 1A. Results are shown in Figure 5.27. The effect of the position above the valley floor for a 4 feet thick bentonite layer was studied using Grid 8 and results are also shown in Figure 5.27. A rapid reduction in the maximum value of differential displacement at the valley wall occurs as the bentonite layer is raised above the valley floor for the parameters used ( $E = 10$  k.s.i.,  $\nu = 0.30$ ,  $E_L/E = 0.10$ ).

The position of the 10 feet thick bentonite layer was varied from 390 feet below the valley bottom to 90 feet above the valley floor, as shown in Figure 5.28, using the same input parameters. The maximum differential movement occurs when the top of the weak layer is level with the valley bottom. As the position of the bentonite layer is lowered below the valley bottom, a sharp decrease in  $\delta H$ , occurring across the layer below the toe of the slope, is noted. The rate of decrease rapidly lessens and stabilizes at a value of about 60% of the differential movement found when the bentonite layer occurred at the toe of the slope. It can be seen that relatively large differential displacements can occur even when the bentonite layer is at a considerable depth below the valley bottom.

Nodal displacements, on a vertical section through the toe of the slope, are plotted in Figure 5.29 for  $E = 10$  k.s.i.,  $E_L/E = 0.10$ ,  $\nu = 0.30$  and  $K_O = 1.00$ . The large differential displacements across the weak layer are clearly visible and do not markedly decrease with depth. Two



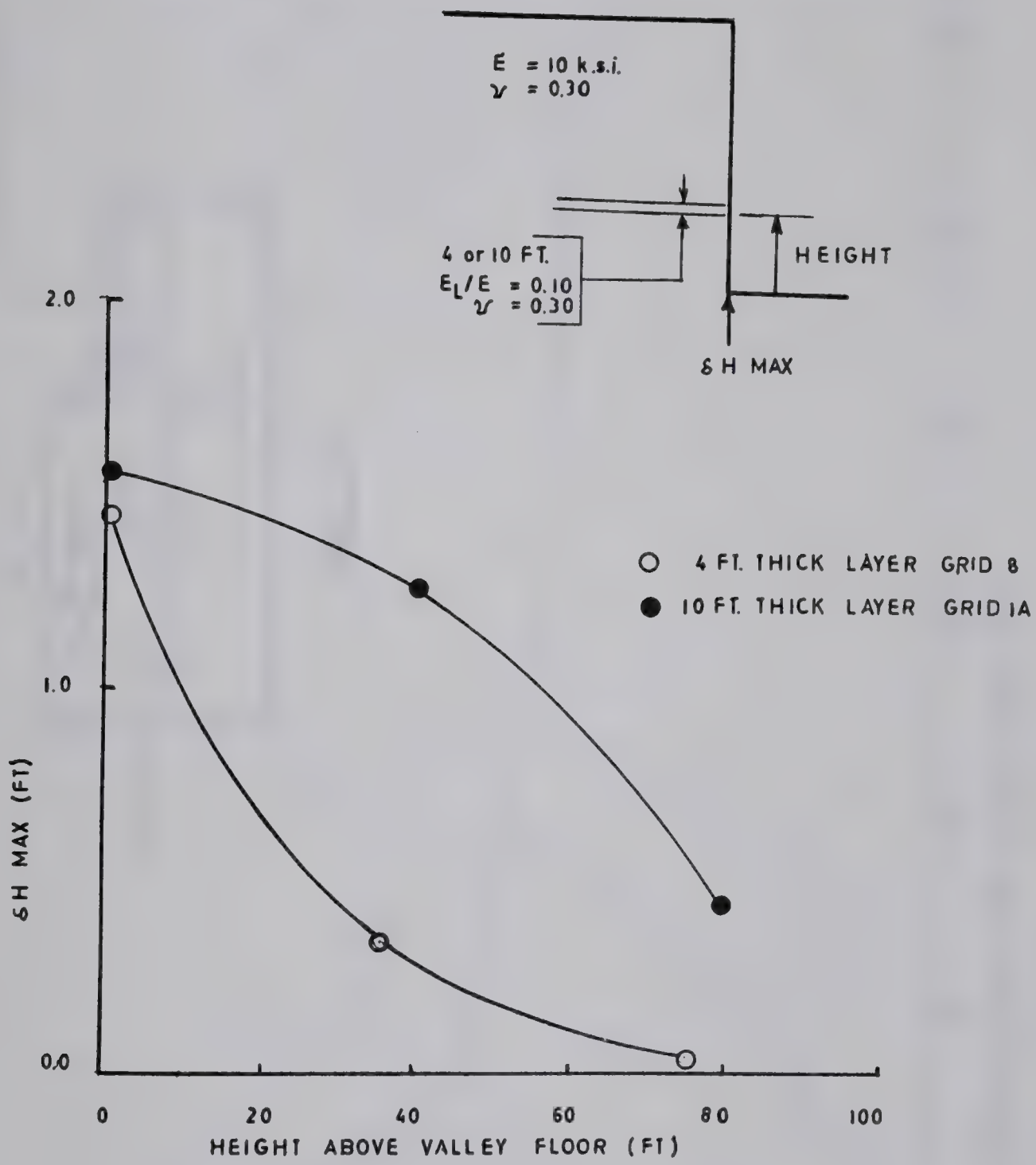


FIG. 5.27 EFFECT OF LOCATION OF BENTONITE LAYER IN VALLEY WALL





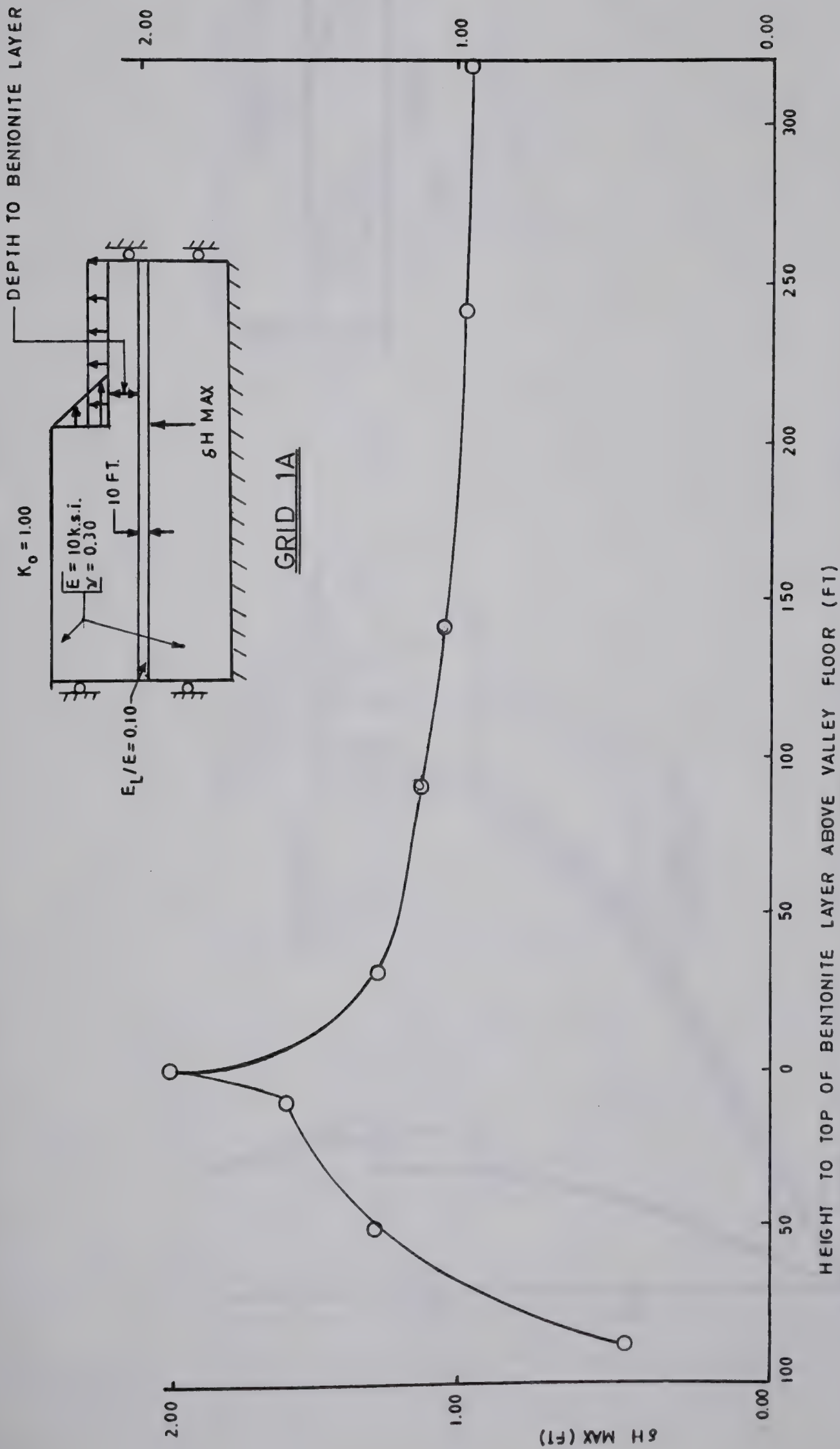


FIG. 5.28 EFFECT ON MAXIMUM DIFFERENTIAL DISPLACEMENTS OF LOCATION OF BENTONITE LAYER



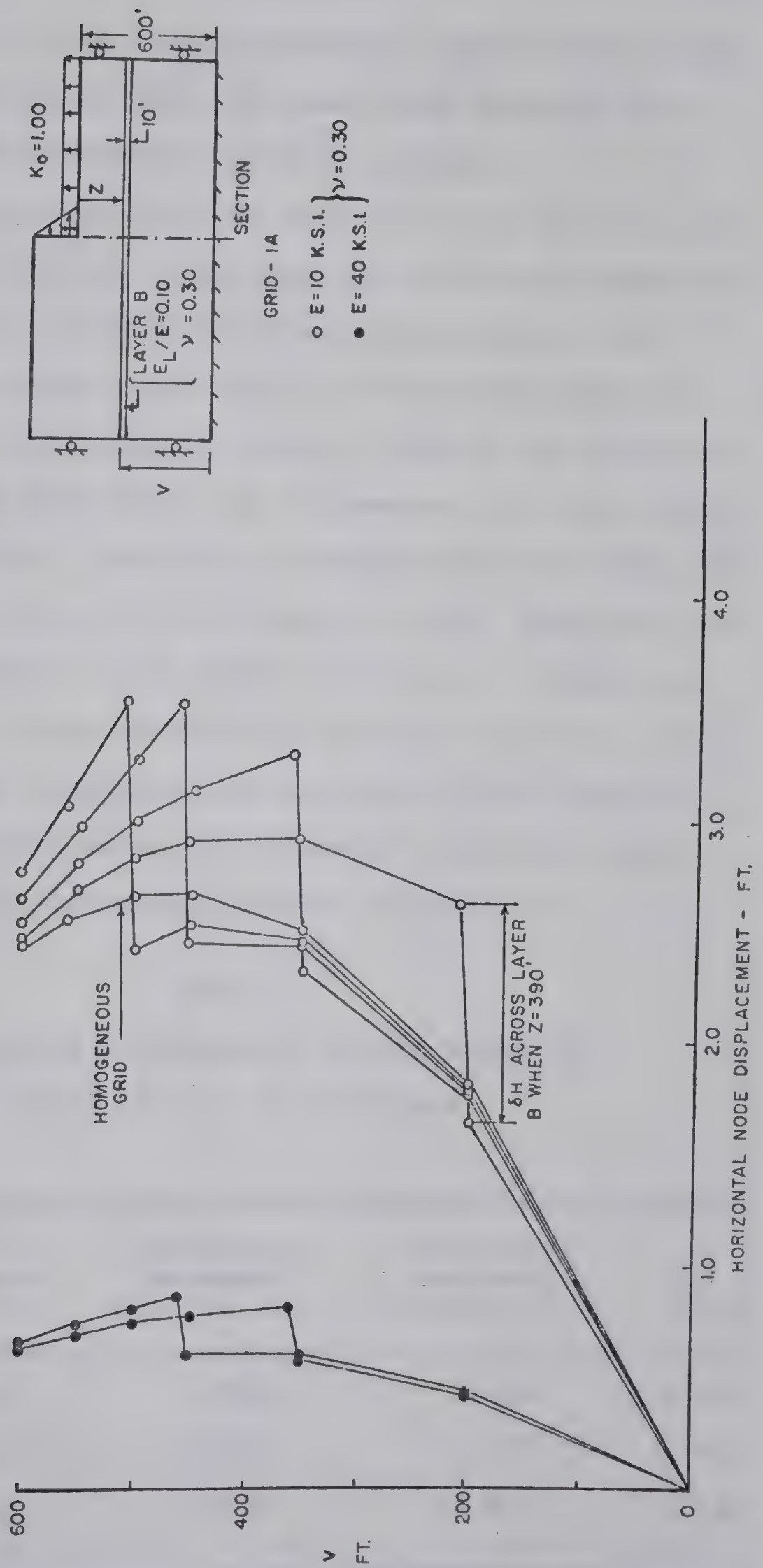


FIG. 5.29 HORIZONTAL NODAL DISPLACEMENT ON A SECTION THROUGH TOE OF SLOPE





cases, using  $E = 40 \text{ k.s.i.}$  to simulate displacements under undrained conditions, show the same trend although the differential displacements are much reduced.

It is important to note that it is the presence of a layer with a modulus lower than the surrounding material which causes the large differential displacements and shear strains across a thin row of low modulus elements. Figure 5.30 illustrates this point. Grid 1A was modified to place the 10 foot thick row of elements 240 feet below the valley bottom. Initially, a homogeneous grid was used with  $E = 10 \text{ k.s.i.}$ ,  $\nu = 0.30$  and  $K_0 = 1.00$ . The thin layer was then assigned a value of  $E = 1.0 \text{ k.s.i.}$  A third run was made using a homogeneous grid with  $E = 1.0 \text{ k.s.i.}$  with all other input parameters the same as in the first two trials. The differential displacement across the layer under the toe of the slope is shown in Table 5.2.

TABLE 5.2  
DIFFERENTIAL DISPLACEMENT ACROSS LAYER "B"  
BELOW THE TOE OF THE SLOPE

E Grid (k.s.i.)	E Layer (k.s.i.)	Horizontal Movement N.P.224 (Ft.)	Horizontal Movement N.P.163 (Ft.)	$\delta H$ (Ft.)
10.0	10.0	2.556	2.502	0.054
10.0	1.0	3.297	3.325	0.927
1.0	1.0	25.558	25.016	0.542



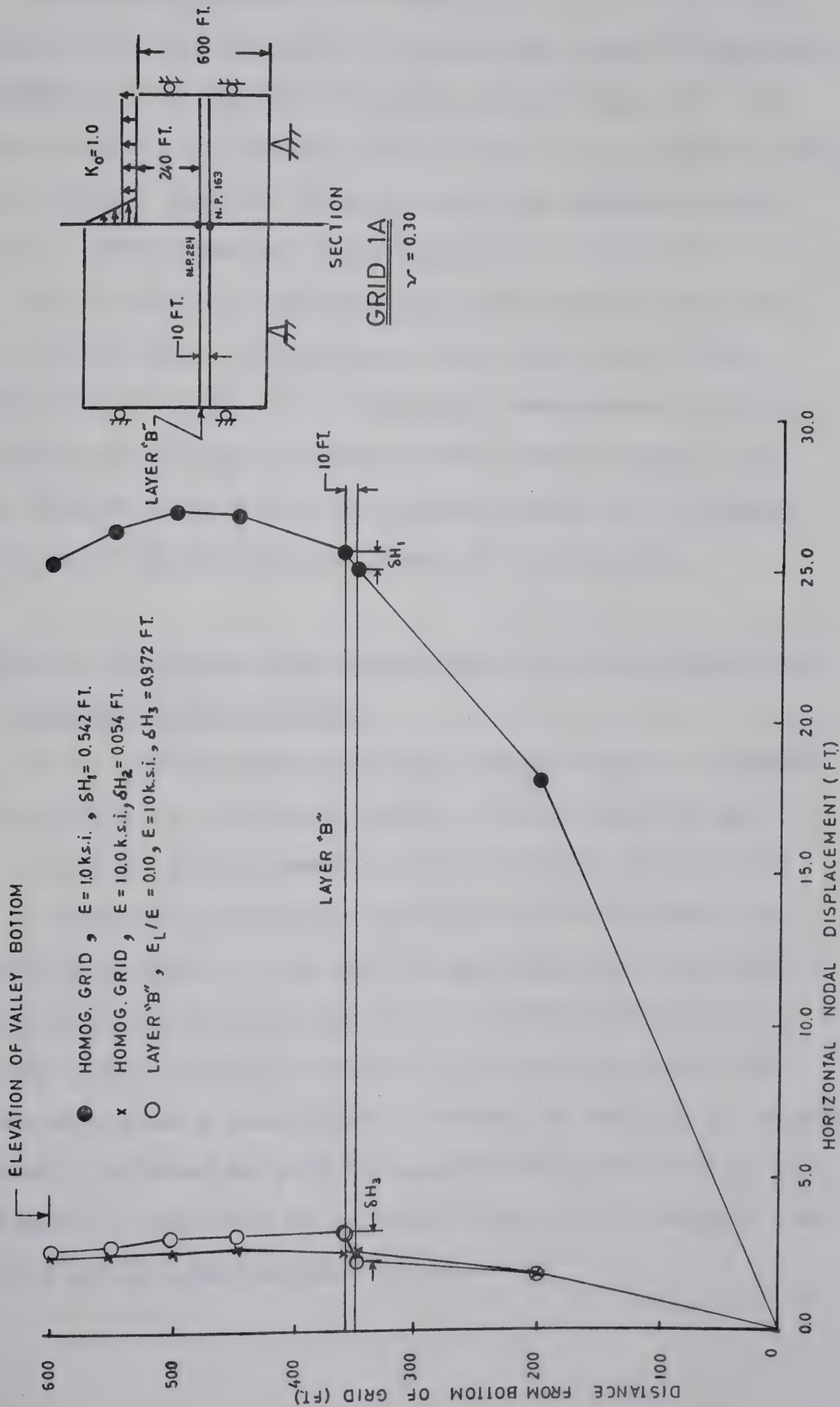


FIG. 5.30 HORIZONTAL NODAL DISPLACEMENT ON SECTION THROUGH TOE OF SLOPE





In the case where a low modulus of 1.0 k.s.i. was assigned to the entire grid, a relatively large differential displacement of 0.542 feet occurred across layer "B". An increase in E of the entire grid to 10.0 k.s.i. reduced this to 0.054 feet. However, keeping the rest of the grid at 10.0 k.s.i. and lowering the modulus of the layer to 1.0 k.s.i. ( $E_L/E = 0.10$ ), resulted in a differential displacement of 0.972 feet. Therefore, a weak zone with a low modulus of elasticity in an otherwise homogeneous section can be seen to act as a 'shear-strain concentrator' in a manner analogous to a hole in a plate acting as a 'stress concentrator' in the classic theory of elasticity.

#### 5.5 Effect of Valley Wall Inclination and Slope Flattening on Differential Movement

River valleys and artificial excavations are seldom cut vertically for any great depth. Slide activity and other agents of mass movement will eventually flatten the slope to some angle dependent upon the shear strength of the rock, the depth of cut and the groundwater conditions. Two finite element grids were used to study the effect of slope angle and slope flattening on the differential displacements across a weak layer. Natural or artificial slopes are often flattened as part of construction activity or in an attempt to stabilize an existing slide or to improve the stability of an oversteepened slope.



Grid F, illustrated in Figure 5.31, was used to simulate a valley 200 feet deep and 1280 feet wide cut with a vertical wall. Grid FL, illustrated in Figure 5.31, simulates a valley of the same depth and bottom width but with 2:1 sides. In both grids a 10 foot bentonite layer is simulated 50 feet below the valley bottom.

The differential displacements, due to cutting the valley with a vertical wall, are shown in Figure 5.32 for the input parameters of  $E = 10 \text{ k.s.i.}$ ,  $\nu = 0.30$ ,  $E_L/E = 0.10$  and values of  $K_0$  ranging from 0.667 to 3.00. As discussed before, results are dependent upon  $K_0$ . The maximum differential movement occurs below the toe of the slope and for  $K_0 = 3.00$ , approximately 3.05 feet of differential movement occur.

The differential movements due to cutting the valley at the 2:1 slope are shown in Figure 5.33. Large values of differential displacement occur some distance back into the slope from the toe of the slope but are less than for the case of vertical excavation. For  $K_0 = 3.00$ , about 2.3 feet of maximum differential movement occurs compared to 3.05 feet for the case of vertical excavation using the same input parameters.

Effect of the Slope Flattening: The effect of flattening the slope from the vertical (Grid F) to a 2:1 slope (Grid FL) can be studied by taking nodal stresses from Grid F along the proposed 2:1 slope, converting them to nodal





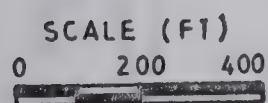
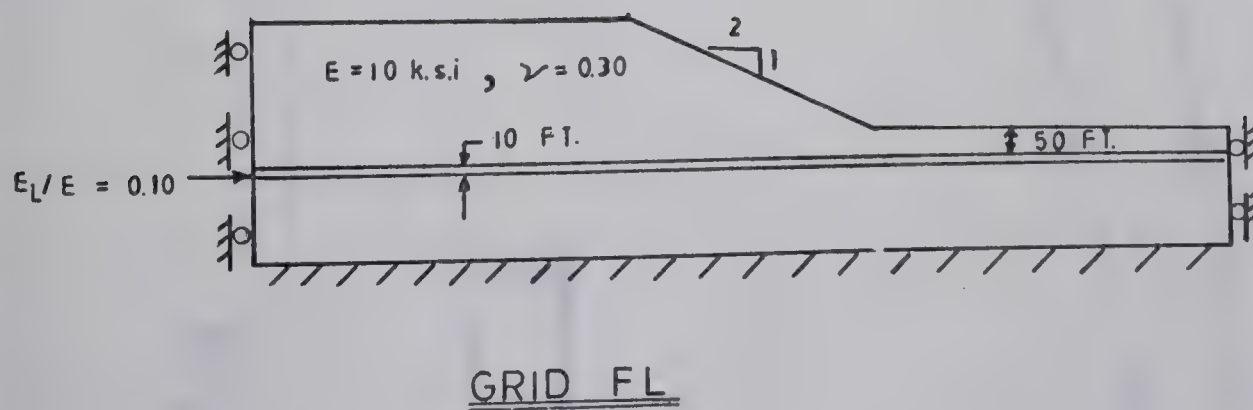
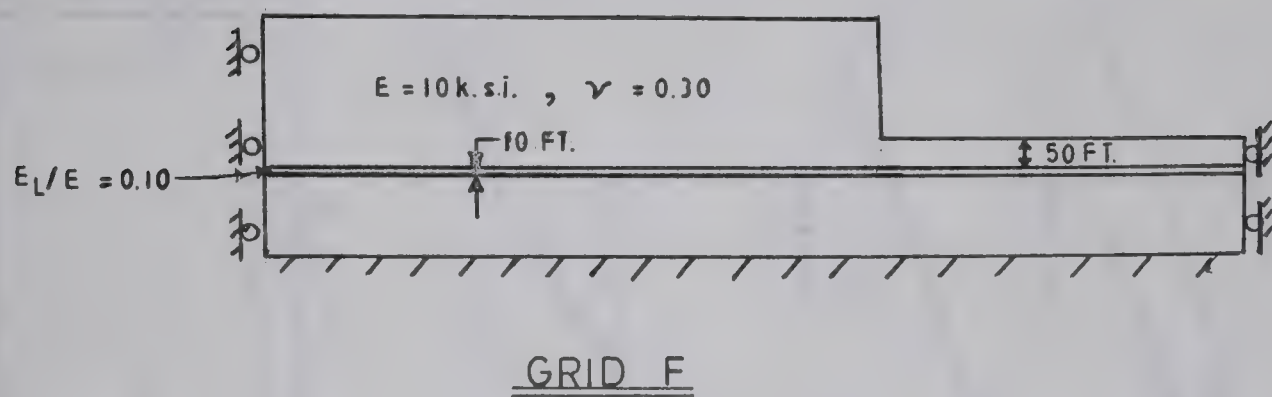


FIG. 5.31 GRIDS F & FL



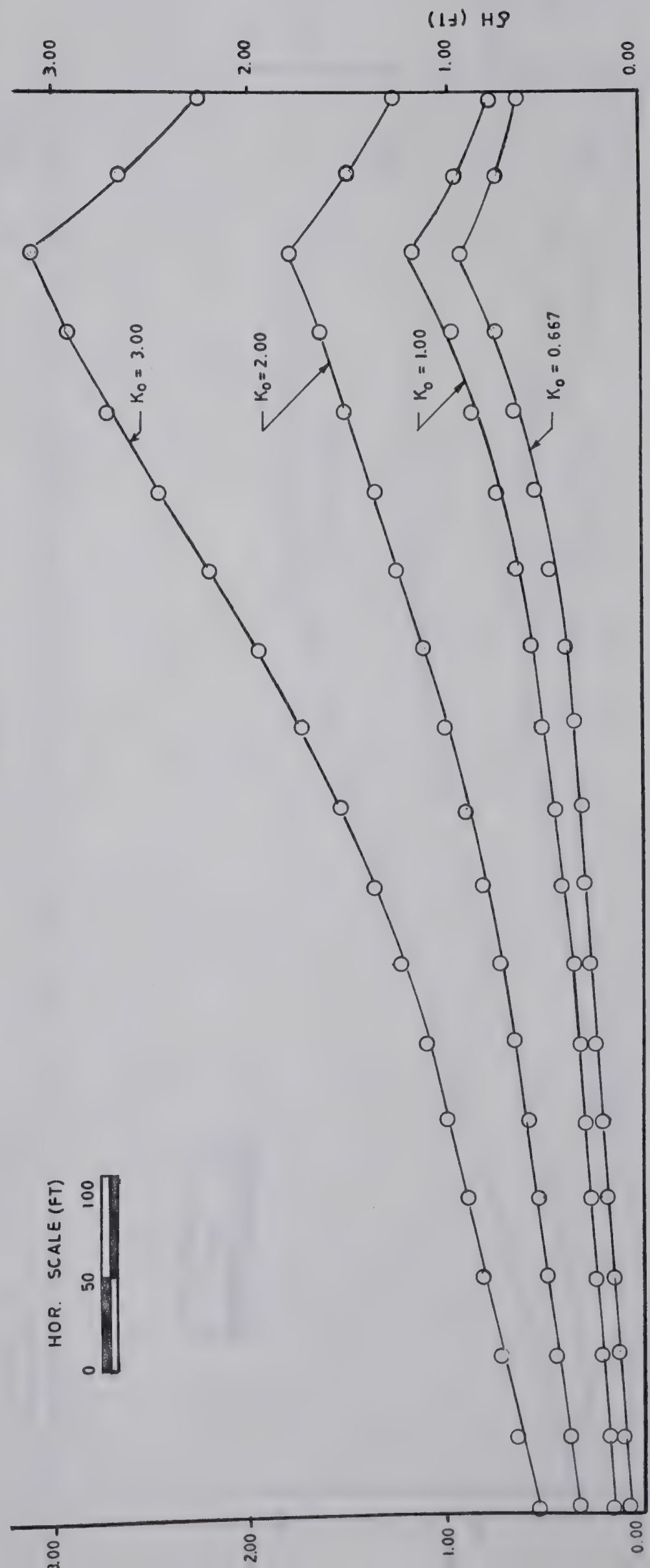
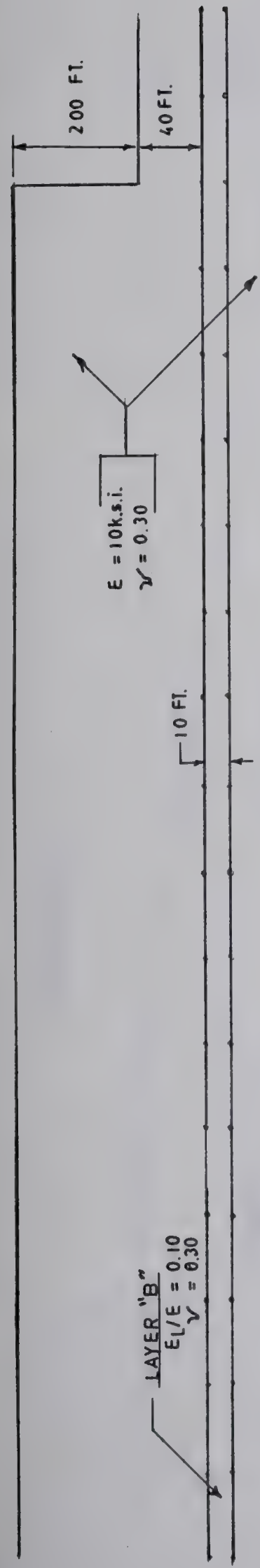
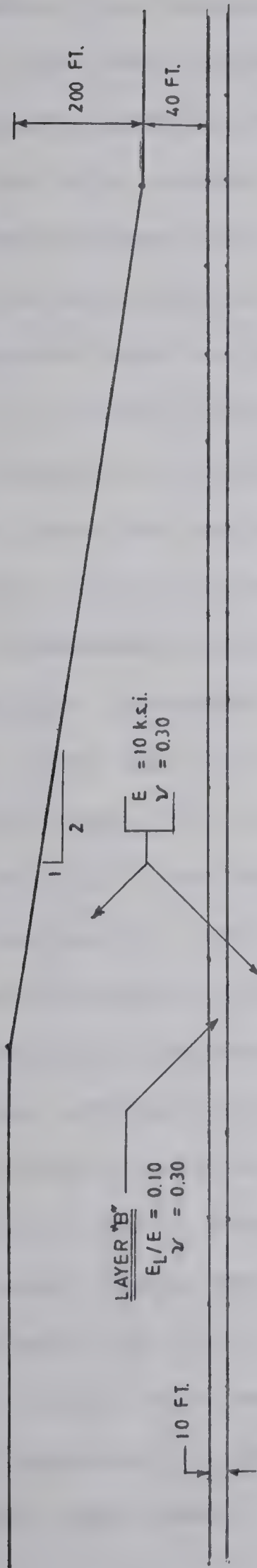


FIG. 5.32 DIFFERENTIAL DISPLACEMENTS ACROSS LAYER "B" DUE TO A VERTICAL EXCAVATION





# GRID FL



HOR. SCALE (FT)

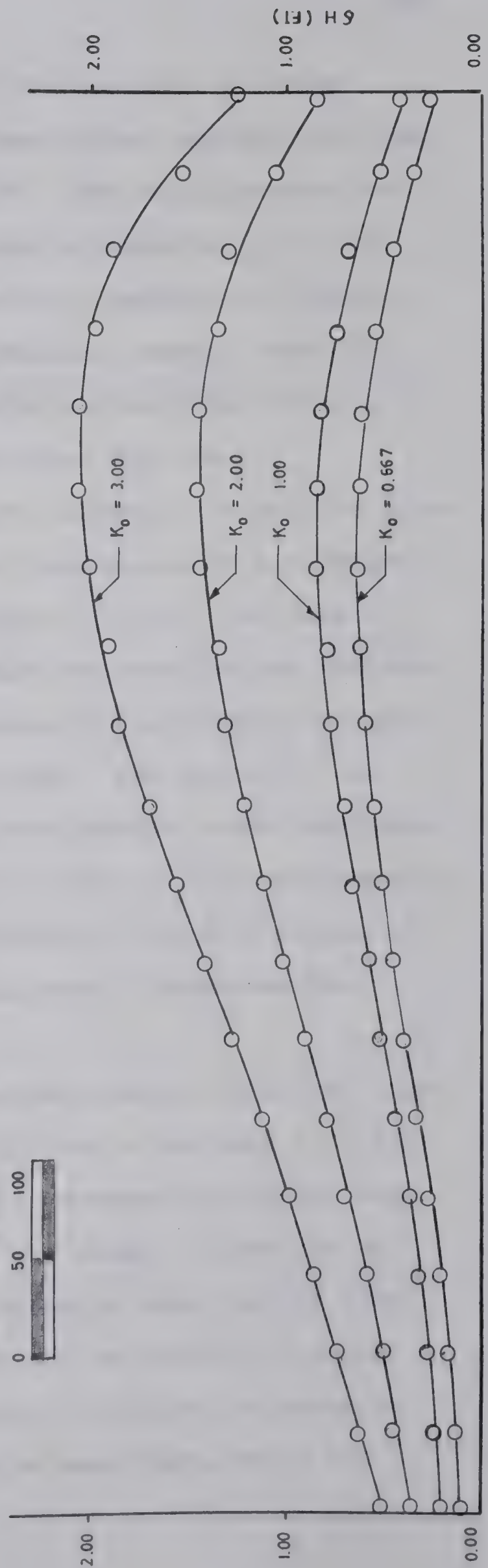


FIG. 5.33 DIFFERENTIAL DISPLACEMENTS ACROSS LAYER "B" DUE TO DIRECT EXCAVATION TO A 2:1 SLOPE



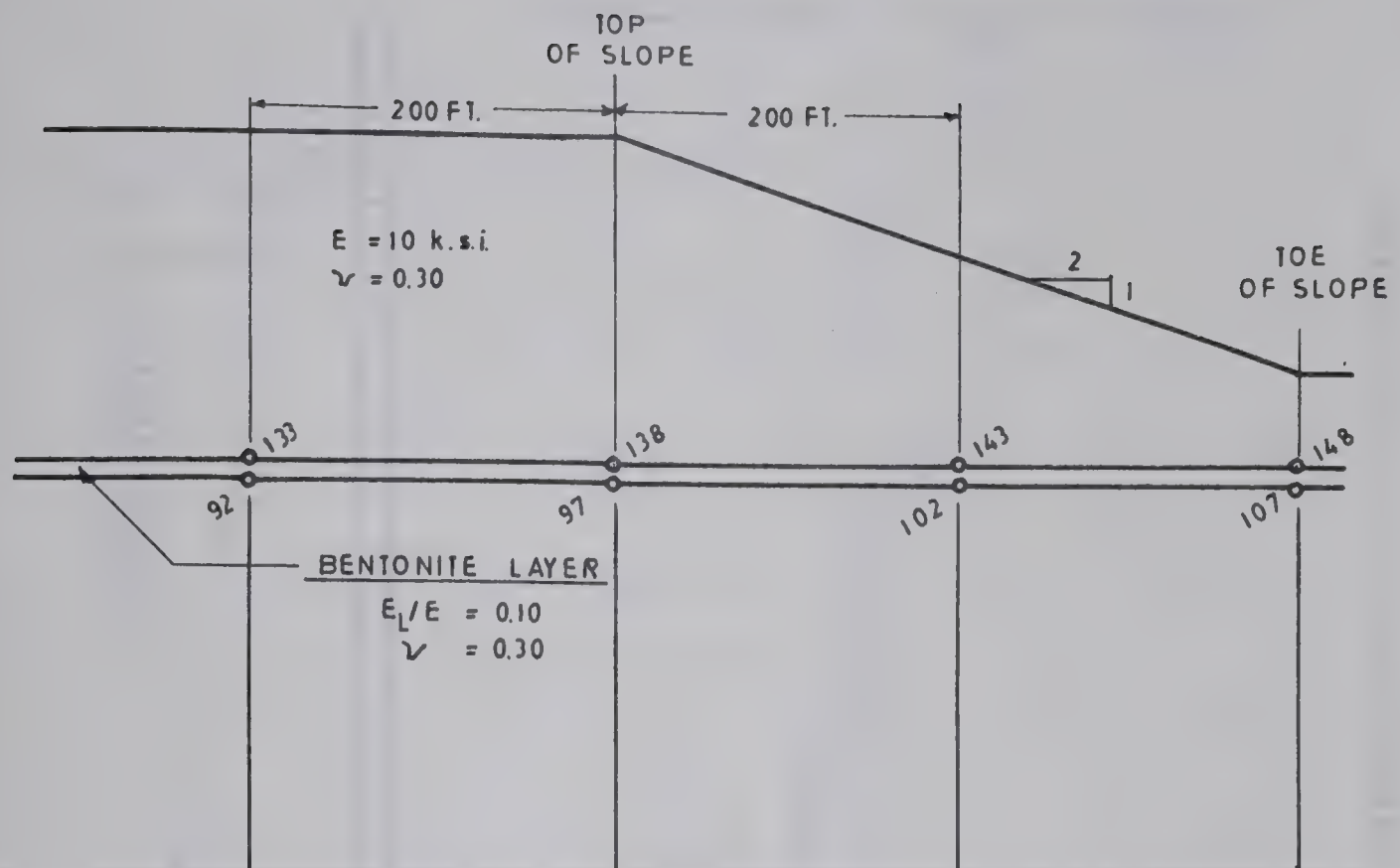
forces making due allowance for the presence of shear stresses, and then reversing these forces and applying them as a boundary traction to Grid FL. The displacements obtained from this process are added algebraically to displacements obtained from the vertical excavation (Grid F) and, by the principle of superposition, should equal the displacements found by use of Grid FL when the valley is cut to a 2:1 slope in one step rather than two.

Differential displacements across the bentonite layer resulting from the two different approaches to excavating a 2:1 valley wall are shown in Figure 5.34 for the case  $K_0 = 2.00$ . A reasonably good agreement between the two methods is found with a maximum difference in displacement of about 0.1 feet below the toe of the slope. The source of the discrepancy appears to be that the boundary nodal stresses found from Grid F are somewhat in error. The approximation errors inherent in use of the constant-strain triangle are discussed by Wilson (1963), this case illustrates the limitations of this element.

The differential displacements which will occur due to flattening of the valley wall from a vertical to a 2:1 slope, are given in Figure 5.35. Movement along the bentonite layer, below the toe of the slope, is seen to be negative with the top of the bentonite layer moving away from the valley with respect to the bottom of the layer. This is analogous to the process of reversal of shear in the direct shear test. It can be seen that, while the







STEP 1 VERTICAL EXCAVATION	$\delta H$ (FT)			
	0.367	0.654	1.114	1.794
STEP 2 SLOPE FLATTENING	0.012	0.140	0.241	- 0.459
SUM $\delta H$ 2-STEPS	0.379	0.794	1.355	1.335
EXCAVATION TO 2:1 SLOPE (1-STEP)	0.431	0.911	1.356	1.383
ERROR	12.1%	12.9 %	0.8 %	3.8 %

FIG. 5.34 COMPARISON OF A ONE STAGE TO A TWO STAGE  
EXCAVATION PROCESS ( $K_0 = 2.00$ )



# GRID FL

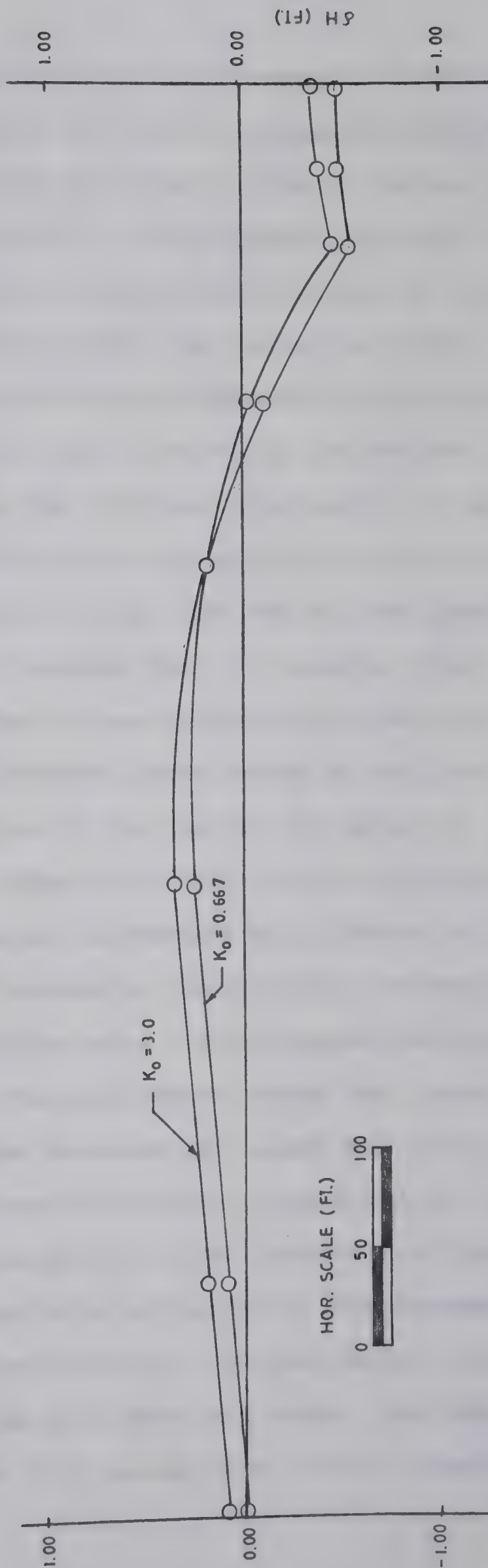


FIG. 5.35 DIFFERENTIAL DISPLACEMENTS ACROSS LAYER "B" DUE TO FLATTENING SLOPE FROM VERTICAL TO 2:1





algebraic sum of the differential displacements across the bentonite layer is the same for the two stage excavation procedure as for excavation directly to the 2:1 slope, the vertical excavation followed by slope flattening will lead to larger cumulative sums of the absolute values of the differential displacements across the bentonite layer.

The cumulative sum of the differential displacements across the bentonite layer due to vertical excavation, plus the further displacement due to slope flattening, is shown in Figure 5.36. The differential displacement across the bentonite layer is maximized under the toe of the slope. Comparison with the displacement due to a single stage excavation to a 2:1 slope (Figure 5.33) shows that the total differential displacement experienced by the bentonite layer in the region of the toe of the slope is approximately twice as large using the two stage excavation process. Only a minor difference in differential displacement across the bentonite layer exists between the two methods below the valley edge and the upper portion of the slope. A marked difference occurs under the lower half of the slope and for some distance out under the river valley. The effect is seen to be most pronounced at high values of  $K_0$ ; for example at  $K_0 = 3.00$ , excavation directly to a 2:1 slope would lead to a differential displacement across the bentonite layer of about 1.8 feet under the toe of the slope. Excavation to a vertical slope, and then subsequent flattening to 2:1, would give a total cumulative



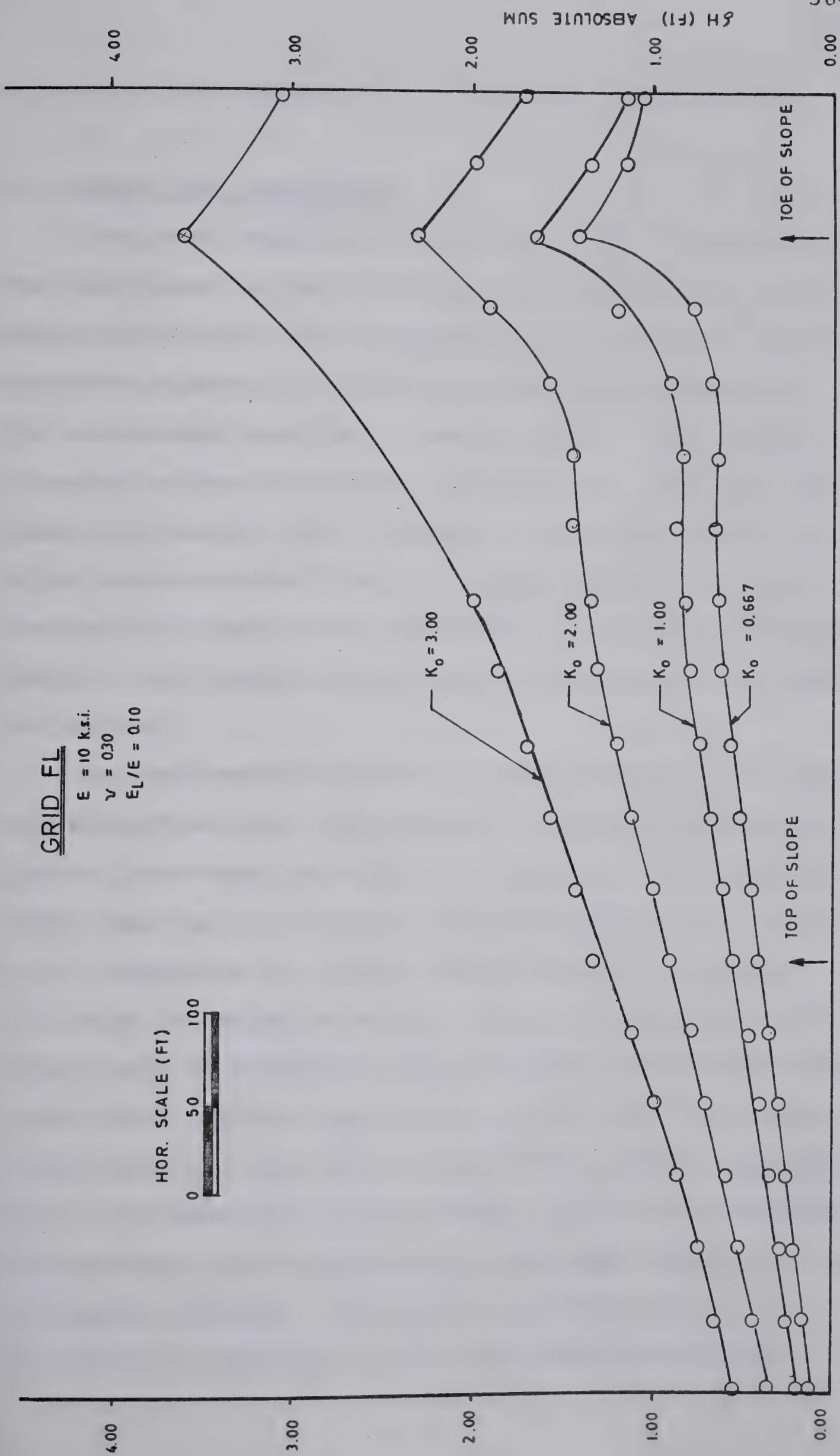


FIG. 5.36 CUMULATIVE DIFFERENTIAL DISPLACEMENTS ACROSS LAYER "B" DUE TO VERTICAL EXCAVATION AND SLOPE FLATTENING





differential displacement of 3.5 feet at the same point.

## 5.6 Summary and Discussion

The cases documented in Section 5.2 of this chapter show that large lateral displacements can occur due to an excavation and that these displacements appear to be concentrated at bentonite layers and changes in lithology. The slickensides observed in bedrock cores, concentrated at bentonite beds and changes in lithology, from the sites along the Missouri River (Fleming et al., 1970) appear to be due to concentrated lateral rebound leading to failure in-situ of the bedrock and subsequent polishing and slickensiding as the strength along these discontinuities fell to the residual.

The two mechanisms studied in this chapter, flexural slip and differential rebound across a layer weak with a modulus lower than the surrounding bedrock, qualitatively predict much of the observed field behaviour in the study area. Rebound of the valley bottom results in interbed slip below and adjacent to the valley. Differential movements should be maximized on the limb of the resulting anticlines and a maximum value of slip in the order of several inches appears likely for the cases documented in the study area. The release of lateral stress leads to the resulting displacements being concentrated across weak layers in a non-homogeneous material. This effect is maximized for low (or drained) values of  $E$ , a low ratio of  $E$  of the weak



layer to  $E$  of the surrounding material, and high values of  $K_0$ . The shear strain generated by this mechanism would apparently only reach significant values where there exists a horizontally bedded, highly overconsolidated soil or rock which has a low modulus and continuous thin layers characterized by a very low value of  $E$ . This description aptly describes a number of the formations of the study area.

The formation of a river valley in the study area, therefore, will generate extremely high differential displacements across horizontal planes of weakness. Data on the amount of displacement in the field, necessary to shear the bedrock in-situ to the residual, is virtually non-existent. However, the documented behaviour of the landslides in the study area suggests that failure in-situ has occurred and that the residual parameters acting along the horizontal base of the slides have been produced by mechanisms associated with valley formation. Subsequent slope stability is then controlled by other factors such as piezometric level and slope height.

The finite element simulation of slope flattening indicates that the differential movements (or shear strains), which occur across a weak layer, are a function of the excavation sequence used. Excavation to a steep slope and subsequent flattening produces a greater cumulative shear strain across the weak layer than direct excavation to the final slope configuration. Provided that the shear strain resulting from the initial steep cut was sufficient to







reduce the strength acting across the weak layer to below the peak, slope flattening will result in a further drop in strength due to the additional cumulative strain generated by the further excavation necessary to flatten the slope. This phenomenon may explain the marked tendency in the study area for slope flattening and minor toe excavations to generate landslides as discussed in Chapter II. A number of interesting possibilities for the analysis of natural slopes and for the future design of excavated slopes arise from these concepts and will be discussed in Chapter VI.



## CHAPTER VI

### CIVIL ENGINEERING APPLICATIONS

#### 6.1 Introduction

This chapter will discuss the application of the results of this study to problems of slope stability in the study area and, in a more general fashion, to stability problems in overconsolidated fissured clays and shales elsewhere. Implications for the design of such engineering structures as earth dams, bridge piers and cofferdams will be noted and illustrated by several examples.

#### 6.2 Summary of Thesis Results

The literature review presented in Chapter II on the nature of the bedrock of the study area shows that the bedrock of the study area is characterized by:

1. high lateral stresses.
2. low values of E.
3. a low coefficient of permeability.
4. ubiquitous horizontal planes of weakness in the form of bentonite layers and bedding planes.

The review of landslide activity in the Cretaceous bedrock of the study area shows that:

1. a progressive decrease in strength appears to be acting along river valleys.





2. the bedrock is extremely sensitive to unloading and excavation induced landslides are common.
3. the landslides commonly have a long horizontal base controlled by a horizontal plane of weakness.
4. most of the slides analyzed have a strength at, or close to, the residual acting along the horizontal base of the slide.
5. the landslides frequently occur in conjunction with bentonite beds, with the bottom surface of the slide mass moving in, or along, a bentonite bed.

The case histories, presented in Chapter III on the magnitude of rebound which has occurred below the valleys of the area, clearly show that large vertical, and hence, lateral deformations have occurred during valley formation due to stress relief and subsequent rebound. The finite element results in Chapter IV indicate that a low, or drained, value of  $E$  must have been acting to produce the magnitude of displacements observed in the field. The difference between drained and undrained moduli appears to explain the difference in magnitude of rebound below artificial excavations and the river valleys of the study area.

The present river valley walls are, therefore, not a static feature but have undergone large vertical and lateral displacements since valley formation. Postglacial valleys were formed by rapid downcutting at the end of the Pleistocene. The immediate rebound which accompanied valley formation would be controlled by the undrained



modulus of the bedrock and was comparatively small; the final equilibrium conditions would be controlled by the drained modulus which is characteristically  $1/2$  or  $1/3$  of the undrained modulus. The present valleys are geologically young and calculations given by Koppula (1970) show that high negative pore pressures could still exist below a postglacial valley carved into relatively impervious bedrock. Therefore, time-dependent rebound may, in some areas, still be going on although at an imperceptible rate.

The bedrock of the study area has dominant horizontal planes of weakness in the form of bedding planes and bentonite layers. The displacements due to valley formation can result in flexural slip between beds below and adjacent to the valley, due to the formation of the valley anticline and valley flexure. This phenomena is reviewed in Chapter V and displacements between the beds, in the order of one to two inches, appear probable for the cases documented.

The relief of lateral stress will result in an inward movement of the valley wall. The presence of thin beds of bentonite or bentonitic shale, with a modulus lower than the surrounding bedrock, has been shown to result in the development of high shear strains across the weak layers. The magnitude of these movements, for input parameters representative of the weaker formations of the study area, appears sufficient to lead to a large reduction in strength for a considerable distance back from the







valley edge. The field observations documented in Appendix B, the correlation between slickenside occurrence and the presence of bentonite layers or lithologic change (Fleming et al., 1970), and the separation of cores at points of lithologic change noted by P.F.R.A. (Chapter II) support the mechanistic picture presented by the flexural slip mechanism and the finite element analysis.

Thus, in summary, the experience recorded in the study area shows that most of the landslides which occur along the river valleys are controlled by shear strengths at, or close to, those predicted by residual parameters. Processes associated with valley formation (flexural slip and stress relief) have apparently caused this reduction of strength in-situ.

### 6.3 Application to Slope Stability in the Study Area

Review of existing theory: A feature characteristic of overconsolidated, fissured clays is the decrease in stability of a cutting with time. Terzaghi (1936) proposed that excavation involved release of lateral stress which led to a subsequent opening of joints and fissures and allowed an accumulation of water in these openings. A softening of the clay on the walls of the joints and fissures led to a decrease in strength of the soil mass with time and subsequent failure.



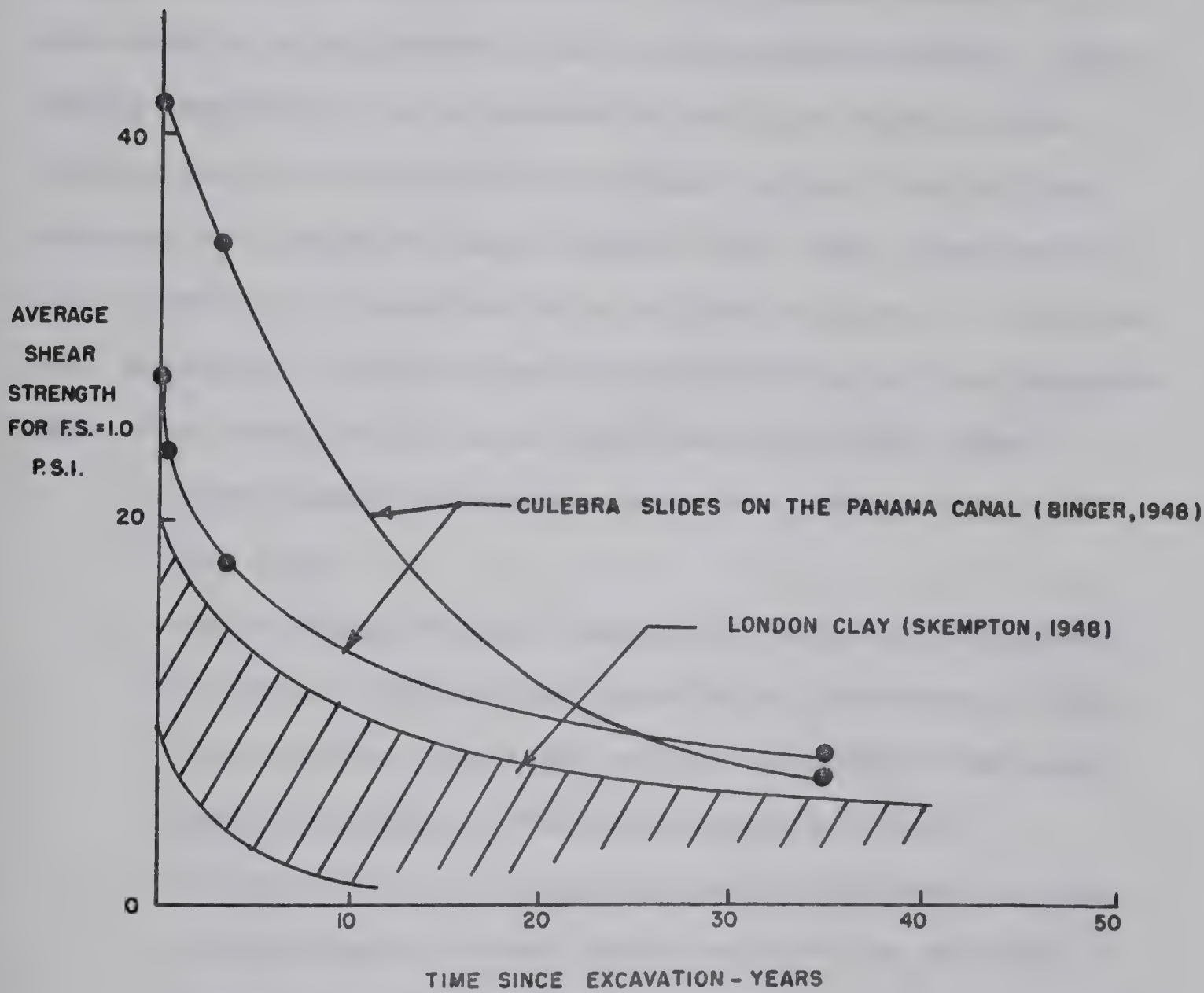
Skempton (1948) and Cassell (1948) documented the decrease in stability with time for cuttings in the London Clay, using the  $\phi = 0$  method of analysis, and found the undrained strength acting at failure to be much lower than indicated by laboratory tests. Binger (1948) found a similar drop in strength for the Panama Canal slides in the Cucaracha shale. Figure 6.1 illustrates the decrease in strength with time required for a factor of safety of unity, computed using the  $\phi = 0$  method of analysis.

Studies of landslide case histories in England, using effective stress analyses (Henkel and Skempton, 1954, Henkel, 1957 and others), showed that the effective cohesion acting in the field was often less than measured in the laboratory. This finding led to the theory that the effective peak frictional strength ( $\phi'_p$ ) controlled slope stability with the cohesion tending to zero with time. However, as has been discussed previously, numerous landslides have occurred in overconsolidated clays which cannot be explained by laboratory peak strengths. The use of residual strength parameters (Skempton, 1964) explains previously documented failures which have occurred at exceptionally low strengths.

Residual strength provides a basis for the analysis of movements which occur along a pre-existing failure surface. However, the decay of strength with time and the retrogressive nature of many landslides in overconsolidated clays suggests a mechanism, or mechanisms, by which the







DECAY OF STRENGTH IN EXCAVATIONS IN  
OVERCONSOLIDATED CLAY

FIG. 6.1



strength of a cutting is reduced with time.

Bjerrum (1966) presented a theory of progressive failure to explain the difference between field and laboratory strengths in overconsolidated plastic clays and clay shales. The clay is assumed to have a large amount of recoverable strain energy due to its stress history. Excavation results in an expansion of the clay towards the cutting and a concentration of shear stress, due to the presence of a discontinuity in the clay mass, results in the progressive formation of a failure surface at the residual strength. Progressive failure leading to the development of a continuous failure surface will occur when:

1. local shear stresses exceed the peak strength of the clay.
2. the advance of the failure surface is accompanied by local differential strains in the zone of shear failure that are large enough to strain the clay past the peak on its stress-strain curve.
3. the clay shows a large and rapid decrease in shear strength with strain after failure has occurred.

Bjerrum (1966) considers that overconsolidation produces diagenetic bonds which alter the clay structure and produce the characteristically stiff and brittle overconsolidated clays and clay-shales. Weathering destroys diagenetic bonds and releases stored strain energy and hence, produces high lateral stresses. Therefore, the relative propensity of an overconsolidated clay for progressive





failure is assumed to depend upon the strength of the diagenetic bonds, the degree of weathering, and the locked-in strain energy.

Bjerrum considers creep (defined as movements which occur at an imperceptible rate) as a phenomenon related to the slow volume expansion which accompanies the liberation of stored strain energy in the zone of weathering. Creep is considered to result in a lateral expansion which can ultimately lead to the development of a continuous failure surface and the ultimate failure of the slope.

The theory of progressive failure provides a qualitative method of explaining the behaviour of slopes in overconsolidated clay as:

1. failures typically start at the toe of the slope and progress inward as shown by deBeer (1969) and, in highly overconsolidated shales, are often composed of a number of retrogressive slide blocks (Hayley, 1968).
2. failures are often controlled by strengths lower than the laboratory peak values.
3. failures often occur along a horizontal plane at the base of weathering.

Considerations of progressive failure have been invoked by a number of authors (Peck 1967, D'Appolonia et al., 1967, Beene 1967, Conlon and Isaacs 1970 and others) to explain differences between field and laboratory strengths. Laboratory results, noted by R. J. Conlon



(unpublished) and reviewed by Peck (1967), indicate that the strain at peak strength is dependent upon normal pressure with somewhat larger strains being necessary to mobilize the peak strength at intermediate, rather than at low or high normal stress. It can therefore be postulated that the top and lower portions of a failure surface will have failed (or be past the peak of the stress-strain curve) while the central portion is still mobilizing its peak strength. Considerations such as these have led Conlon and Isaacs (1970, p. 26-27) to state:

"The peak strengths of individual soil elements simply cannot be mobilized simultaneously along a potential failure surface because, as it is now generally accepted, the failure of practically every soil mass is progressive failure."

The concept of progressive failure does not, however, appear to apply in every case studied. Skempton (1970) notes that the strength controlling first-time slides in London Clay cuttings is controlled by a value of  $\phi'$  close to the peak value of  $20^\circ$ , although values of  $c'$  have decreased to close to zero (termed the fully softened value). Skempton considers that relatively small displacements are required to reduce the London Clay to its fully softened condition ( $c' = 0$  and  $\phi'_s = \phi'_p$ ). No smooth continuous failure surface has yet developed at this stage although a complex of minor shears probably exists. Movements in the field in the order of 2 to 3 feet are considered necessary to generate a continuous, smooth failure surface.







The fully softened strength ( $c' = 0$ ,  $\phi' = \phi'_p$ ) is considered to be the limit of strength reduction for first-time slides in the London Clay and probably many other fissured clays. However, slides in overconsolidated, non-fissured clays at Lodalen (Sevaldson, 1956) and Kimola (Kankare, 1969) and in non-fissured clay till at Selset (Skempton and Brown, 1961) occurred at strengths close to the undisturbed peak value. Skempton (1970) considers this behaviour is due to the absence of fissures or other structural discontinuities.

Skempton (1970, p. 323) concludes that:

"Clays with a higher degree of over-consolidation or a greater tendency to expand, following stress relief, may suffer a greater drop in strength even before a first time slide occurs. In such materials the residual may indeed be the relevant limiting strength, as suggested by Bjerrum (1967). This would also be the case if, over an appreciable proportion of its length, the slip surface could follow a bedding plane or other discontinuities along which tectonic shearing has taken place."

Bishop (1971), however, considers stability analysis based on some mechanism of progressive failure to be the proper method of explaining first time failures in the London Clay.

Review of the Theory of Progressive Failure: The theory of progressive failure implies that the decrease in strength of the soil or rock mass is due to a process acting at selected points due to favorably located discontinuities.

Bjerrum (1966, p. 6) states:

"If the long term stability of all slopes in over-consolidated clays was governed by the residual



shear strength, wide areas in the United States and Canada where the clay shales outcrop would be as flat as a pancake, and, indeed they are not. Next to areas where slides have occurred, there are existing slopes which indisputably have been stable for hundreds of years with an inclination incompatible with an angle of shearing resistance as low as the residual value."

This conclusion is not supported by studies of landslide activity along the Pembina and South Saskatchewan Rivers of Alberta (Matheson, 1970; Roggensack, 1971) which showed that zones of high groundwater level correlated well with areas of intensive landslide activity. Studies on the valleys of the study area, by the U. S. Army Corps of Engineers (Fleming et al., 1970) and the Prairie Farm Rehabilitation Agency (P.F.R.A., 1969a), show that high, steep valley walls can exist, provided the water table is low, even if the residual strength exists along horizontal planes of weakness.

Zones of groundwater discharge, often associated with the upper surface of bentonite layers, were noted by Scott and Brooker (1968) in several of the slide zones studied in the Bearpaw formation or its stratigraphic equivalent in Western Canada. The observations at the Devon slide (Eigenbrod and Morgenstern, 1971) and at the Beverly bridge (Appendix B) show that groundwater conditions in the area are very complex with perched water tables commonly occurring due to the presence of bentonite layers.

The stability of natural valley slopes in the study area appear to be controlled by local groundwater conditions.







The presence of a low water table results in high, steep-sided, stable valley walls while a rise in the water table results in an increase in landslide activity.

The review of published data on landslide activity in Chapter II shows that the majority of the landslides in the study area are controlled by strengths well below those predicted by peak parameters. The reduction in strength could be due to progressive failure; however, in view of the magnitude of the deformations which have accompanied valley formation in the area, it would appear that planes of weakness now exist along bentonite layers and bedding planes along which the shear strength has been reduced, in some cases, to the residual.

Other explanations for the observed behaviour are possible. It could be argued that all the slides documented are reactivations of fossil landslides or that movement of the glaciers, during the Pleistocene, sheared the bedrock in-situ to the residual. However, the relative absence of large fossil slumps in the Fort Union Group and Colorado formation along the Missouri River (Fleming et al., 1970) tends to weaken the first proposed mechanism. The slickensides and striae on the bentonite layer at the Beverly bridge (Appendix B) were observed to point directly perpendicular to the valley wall in an east-west direction. The direction of ice movement in the Edmonton area was from northwest to southeast (Geological Survey of Canada, 1967) and it thus appears unlikely that these features are due to ice movement.



Effects of Valley Formation on Slope Stability: An excavation made in overconsolidated clay will reduce the pore pressure adjacent to the excavation since the pore pressure coefficient  $A$  is low for overconsolidated soils. Very low or even negative pore pressures are possible. The decrease in pore pressure due to excavation has been inferred in the Boom Clay in Belgium (de Beer, 1969) and in the London Clay at Bradwell (James, 1970, p. 140). Pore pressure deficiencies have been measured in the Cucaracha shale at the site of the East and West Culebra slides on the Panama Canal (Lutton and Banks, 1970) and in the Gault Clay at Folkestone Warren in England (Wood, 1971).

Koppula (1970) showed that application of one-dimensional consolidation theory, to the excavation of a river valley into a saturated clay with a low permeability, predicts high negative pore pressures below the valley floor. Hence, negative pore pressures might still exist below a postglacial valley incised into a formation such as the Bearpaw or Pierre which has a low value of  $C_v$ . Negative pore pressures might be induced in the valley walls although dissipation would be more rapid in view of the effects of geologic structure, jointing and drainage path.

The initial excavation of the valleys at the end of the Pleistocene was rapid, hence it would appear correct to analyze the initial rebound accompanying valley formation using the undrained modulus of the bedrock. The presence of low or negative pore pressures result in a relatively







high value of  $E$  and the resulting rebound would be low - in the order of 0.5 to 1.0 percent of the valley depth. A relatively small change in dip along beds below and adjacent to the valley would result and a small amount of flexural slip between beds would occur. The shear strains, which would occur across bentonite layers and other planes of weakness due to release of lateral stress, would be relatively small.

Dissipation of the negative or low pore pressures would result in continuing time-dependent rebound whose ultimate magnitude is governed by the drained modulus of the bedrock. Thus, both flexural slip and shear strain across weak layers would increase with time. The behaviour of the slides in the study area indicates that sufficient shear occurs relatively soon after valley formation to significantly reduce the strength along critical planes of weakness.

James (1970) found that peak frictional parameters control first time failures in the London Clay; Lutton and Banks (1970) obtained similar results for analyses of the initial failures on the Panama Canal. Thus, it would appear that initial undrained displacements following excavation are not sufficient to reduce the strength parameters in the case of a relatively homogeneous overconsolidated clay. The absence of continuous, horizontal planes of weakness in the London Clay and Cucaracha shale appears important in understanding slide behaviour since only small



shear strains result from stress relief in homogeneous materials.

The release of lateral stress may result in tension joints forming parallel to the valley wall as is discussed in Chapter VII. Formation of these joints, along which there has been relatively little or no shear, would result in a decrease of cohesion across these surfaces to zero (Skempton and Petley, 1967) although it appears unlikely that any substantial decrease in  $\phi'$  would occur.

Therefore, formation of the valley would, depending upon the occurrence and location of bentonite beds and bedding planes at a given site, result in a series of potential failure surfaces along which a decrease in strength has occurred. The actual loss in strength would be a function of the geometry of the initial planes of weakness, the elastic properties of the bedrock, the in-situ stress relieved, the time since valley formation, and valley geometry.

An increase in the amount of flexural slip and shear strain across weak layers occurs with time, due to the change from undrained to drained conditions. This will tend to decrease stability with time.

The sequence of events following valley formation explains the occurrence of large, retrogressive landslides noted on the outside of meander bends in the study area (Matheson, 1970 and Roggensack, 1971). Active erosion of the river, on the outside of the meander bends, leads to







further release of vertical and lateral stress. The subsequent vertical and lateral rebound leads to a further decrease in pore pressure in the valley wall. Piezometer levels in the overconsolidated Gault Clay are appreciably lower than sea level at Folkestone Warren in England (Wood, 1971) and have apparently resulted from rapid landward erosion of the cliff by the ocean. The rapid lateral erosion of a river in the overconsolidated bedrock of the study area should produce similar results. In a deeply incised valley, oversteepening of the slope, combined with low strength values acting along horizontal planes of weakness, results in the initiation of a landslide.

A series of retrogressive slides are likely in this situation as gradual removal of the toe of the initial slide by river erosion results in further unloading of the rock landward of the failure surface. Subsequent rebound results in a further decrease in strength along critical planes and a retrogressive series of slides results as documented by Hayley (1968) at the Little Smokey bridge in northern Alberta. The gradual 'creep' of these slide blocks, along a failure surface now at the residual strength, is then due to gradual equalization of the low pore pressures and a gradual decrease of the effective stress on the failure surface as postulated by Wood (1971).

Several important points arise from consideration of the processes which accompany valley formation. Slopes presently existing in the study area are controlled by



planes which have been sheared in-situ to a strength lower than the peak. The differential displacement across these layers will vary with distance back from the valley wall, hence, the strength acting along these discontinuities will vary from place to place. The strength acting along these surfaces cannot be deduced from peak or residual strengths of the rock mass and thus, if a meaningful analysis of the stability of an existing slope is to be made, undisturbed samples must be obtained of critically located bentonite layers and bedding planes. Carefully controlled strength tests would then show the strength parameters which are currently acting.

Conventional drilling techniques (discussed in Chapter II) are often incapable of even locating the presence of critical bentonite beds and bedding planes in the bedrock. A much wider use of in-situ examination and sampling of the bedrock from test pits and drifts is required to locate zones across which failure in-situ has occurred.

Slope flattening, in a horizontally-bedded overconsolidated clay, appears undesirable from the point of view of slope stability as the additional shear strains induced across weak layers may lead to a further drop in strength (if the layer is not already at residual). The experience, of further slide activity being activated at Oahe Dam due to slope flattening, has been noted in Chapter II. The continuing creep of landslides, along a continuous failure surface at the residual strength, may not be due to the







release of stored strain energy as postulated by Bjerrum (1966) but may be due to a decrease in effective stress across the failure surface by the dissipation of excavation-induced low pore pressures.

#### 6.4 Application to Design Problems

Earth Dam Design: The processes which accompany valley formation have been discussed previously. Flexural slip along beds and shear strain across weak layers will result in sizeable displacements across bedding planes and bentonite layers in the upper portion of the bedrock below the valley bottom. Therefore, the bedrock below the valley bottoms in the study area can, from theoretical considerations and the field observations detailed in Appendix B, be expected to have residual strengths acting along bedding planes and bentonite layers. The presence of these critical layers will dictate the stability of any earth dams placed on the valley bottom.

Conventional coring techniques will not usually detect these controlling features; therefore, excavation of exploratory testpits and drifts is mandatory and field testing on a scale greater than presently used appears advisable. Dam sites located on horizontally-bedded, over-consolidated clays in other geologic locales may have similar features in the upper portion of the bedrock below the valley bottom and this possibility should be reflected



in the investigation techniques adopted.

Conservative sideslopes have been adopted for the design of major earthfill dams in the study area following the failure of Fort Peck Dam in 1938. Chapter II shows how subsequent designs were based on experience obtained from this failure or from considerations of natural slope inclination. Laboratory peak strength parameters were obtained but seldom used in the final design. The findings in this thesis appear to confirm the wisdom of this empirical process; the strength of the bedrock governing the stability of the dams and associated excavations has been reduced by processes associated with valley formation and design on the basis of peak parameters would, in all probability, result in failure.

The experience gained at Mangla Dam in West Pakistan is relevant to the present discussion. The occurrence of the shear zones in the clay members of the Siwalik formation has been discussed in Chapter V. The discovery of these weakened zones resulted in extensive redesign of the project (Binnie et al., 1967). No evidence of these zones were observed in the 3½ years of drilling before the main construction contract was let. During this period some 11,000 feet of percussion drilling (19 to 22 inch diameter) and 72,000 feet of small diameter rotary drilling were carried out for exploratory purposes (Binnie et al., 1968, p. 367).







A 600 foot long exploration adit was excavated prior to construction to assess the bedrock conditions in the future location of the diversion tunnels. Observations in the adit found (Binnie et al., 1968, p. 370):

"Thin bands of soft plastic clay were found within harder clay strata in the adit. This material squeezed out slightly, and a side adit was driven at one point at about river level to examine it further. As a result of this, it was concluded that the softening was the result of pressure release during excavation. Subsequent events proved that this conclusion was erroneous and, in fact, the soft clay has been identified as probably a shear zone in one of the lower clay beds which outcrops in the tailrace excavation."

This occurrence points out the advantages of in-situ observations, if interpreted correctly, and the advisability of using laboratory tests to augment field observations as shear tests, on block samples of the soft zone, would have revealed the low strengths acting in-situ.

Design of Bridge Piers and Cofferdams: The presence of the gouge zones, noted below river bottoms in the study area, have a marked effect upon the design and performance of such engineering works as bridge piers and cofferdams.

Harris (1971) reported that the end of construction settlements of the bridge piers of the James MacDonald bridge in Edmonton were about one inch, which was considerably more than predicted by analyses based upon the properties of the intact rock mass. The presence of several gouge zones below the base of the piers would account for this anomalous behaviour as these zones are filled with a



soft, apparently remoulded, highly compressible material. Settlements of this magnitude are unlikely to adversely affect the performance of the bridge but it may prove advisable, under certain conditions, to allow for behaviour of this nature.

Hendron (1971) described the occurrence of mylonite seams (seams infilled with a soft, plastic clay-like material) which were observed in the excavations for three cofferdams on the Ohio river in the U.S.A. These seams occurred at, or just inside, a shale-limestone contact some 10 to 20 feet below the bedrock surface. Slickensides were observed in these zones in the field and laboratory shear tests confirmed that the strength along these features was at the residual. No evidence of these zones were observed in the investigation drilling program.

Failure occurred at one of the sites with the cofferdam moving at least 75 feet into the excavation. At the other sites, no failures occurred but analyses showed that the presence of the mylonite seams reduced the factor of safety to below 1.10. Clearly this is undesirable and the limitations of standard investigation techniques are again revealed.

## 6.5 Summary

The discussion in this chapter emphasizes the practical significance of horizontal planes, at strengths well below the peak, below and adjacent to the river valleys in







the study area. The stability of engineering works such as earth dams and cofferdams are greatly affected by the presence of these features. Therefore, future design of these structures must proceed on the assumption that weakened planes exist below the river valleys and in the valley walls, until such time that detailed in-situ investigation provides reliable data on the strengths acting across bedding planes and bentonite layers.

Standard coring techniques have been shown to be usually incapable of even locating the presence of features which control the stability of both natural slopes and structures founded on the bedrock of the region. Present investigation techniques merely give a general picture of the geology of a site; stability analyses based upon samples of the rock mass appear, therefore, to be of little use. A vast improvement in drilling techniques or a much wider use of test drifts and pits appears necessary before meaningful stability analyses of natural and artificial slopes in the study area are possible.

The data presented suggests that progressive failure is not a dominant mechanism of loss of strength in highly overconsolidated clay which has dominant horizontal planes of weakness. Displacements across these layers due to flexural slip and stress relief appear to provide a better means of explaining observed behaviour.



## CHAPTER VII

### GEOLOGICAL APPLICATIONS

#### 7.1 Introduction

The valley anticlines, valley flexure and raised valley rims discussed in this thesis are geological features which can be explained by the application of the concepts of stress release and elastic behaviour of the bedrock. These features are ubiquitous in the study area and are therefore of significance to such areas of geology as stratigraphic interpretation, structural geology and geomorphology. A detailed analysis of the geologic consequences of river valley formation is outside the scope of this work, but a brief discussion will be given in this chapter on the effects that river valley formation in the study area have on stratigraphic interpretation of drilling results, structural geology features and geomorphological features, such as the drainage patterns which have developed adjacent to the valley wall since deglaciation.

#### 7.2 Local Stratigraphic Correlation of Drilling Results

The case histories presented in Chapter III show that the maximum rebound of the valley bottom typically ranges from between 3 and 8 percent of the valley depth for typical postglacial valleys cut into the Cretaceous bedrock of the study area. Upward flexure of initially







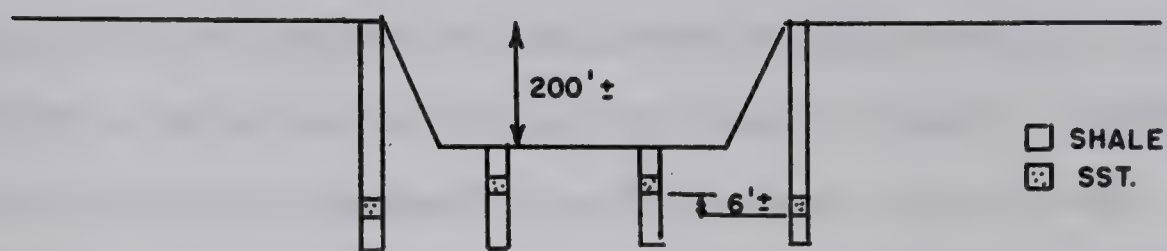
horizontal beds in the valley wall is predicted by the finite element method and is documented in a number of the case histories.

Therefore, the dip of any bedding plane measured on outcrops on the valley walls will not be the true bedrock dip of the overall region but will have been affected by the formation of the river valley. The change in orientation for most sites in the study area will be minor (in the order of 1 or 2 degrees) although Underwood (1964) noted a 2 to 5 degree downwards inclination of beds in the Niobrara chalk towards the bluffs, as has been previously discussed.

The occurrence and magnitude of the anticlines which underlie the valleys of the area must be considered when interpreting the drilling results from a section across a valley. Several cases were found in the examination of the initial interpretation of drilling results where erroneous stratigraphic interpretations resulted from ignoring the possibility of rebound of the bedrock below the valley bottom.

Figure 7.1(a) shows a simplified stratigraphic section from a preliminary damsite investigation. The bedrock at the site was mainly shale, however below the river level a 5 foot thick sandstone bed was encountered in all the testholes. The sandstone bed was encountered some 5 to 6 feet higher in the valley bottom testholes than in the abutment testholes and the original stratigraphic section was interpreted as in Figure 7.1(b).





(A) SIMPLIFIED DRILLING RESULTS



(B) INCORRECT INTERPRETATION



(C) PROBABLE STRATIGRAPHY

FIG. 7.1 DAMSITE STRATIGRAPHY





Samples from the sandstone layer from both abutment and valley bottom testholes had practically identical field descriptions, water contents and Atterberg limits. Sandstone layers are not normally satisfactory marker beds since they tend to pinch out over relatively small lateral distances. However, in view of the fact that the average  $E$  of the bedrock at the site was reported below 20,000 p.s.i., a valley bottom rebound of several percent of the valley depth can be expected. Therefore, it would appear that the stratigraphic interpretation shown in Figure 7.1(c) is correct; some 6 feet of vertical rebound has occurred at this site and the sandstone layer is continuous over the area investigated.

### 7.3 Application to Structural Geology

The valley anticlines and valley flexure illustrate a structural feature which is due to stress relief and related to topography, is widely spread and has received relatively little attention in the geologic literature. Intensive folding, discussed previously, in a dam trench in the Pennine Mountains in England (Watts 1906) and below river valleys in the Allegheny Plateau (Ferguson, 1967) has been observed to result in tensile failures of the bedrock at the axis of the anticline. These two cases illustrate that jointing can occur in the bedrock due to extreme anticlinal flexure of the bedrock below river valleys and artificial excavations although the mechanism of folding, in



these two cases, is apparently not simple elastic rebound.

The possibility of beds buckling under high lateral stress has been discussed in Chapter III. This appears a possible mechanism to account for the features noted in dam trenches in the Pennines and the Allegheny Plateau as well as at Portage Mountain Dam in the Rocky Mountain foothills of northeastern British Columbia. Other mechanisms may exist and these cases deserve further study. However, if the mode of formation of the features described in Chapter II is indeed buckling, then these cases provide qualitative data on the presence, nature and magnitude of high lateral stresses whose origin would appear to be tectonic.

The occurrence of steeply dipping joints paralleling valley walls has been discussed in Chapter II. It seems clear that these joints result from valley formation. The development of vertical tension cracks, adjacent to artificial excavations, has been documented by Kwan (1971) for lacustrine clay and till and by deBeer (1969) for the lightly overconsolidated Boom Clay in Belgium. Similar behaviour was observed in the Niobrara chalk by Underwood (1964, p. 30) at Gavins Point Dam who noted:

" . . . steep slopes were cut through chalk into the underlying Carlile shale. In the spillway at a location where the excavation resulted in a horizontal surface of chalk overlying a deep cut in the shale, the chalk developed tension cracks. As there was no vertical displacement at these cracks it was believed that the cracks were due to differential horizontal rebound between the chalk and the shale in which the much greater horizontal strain of the shale not only relieved all compression







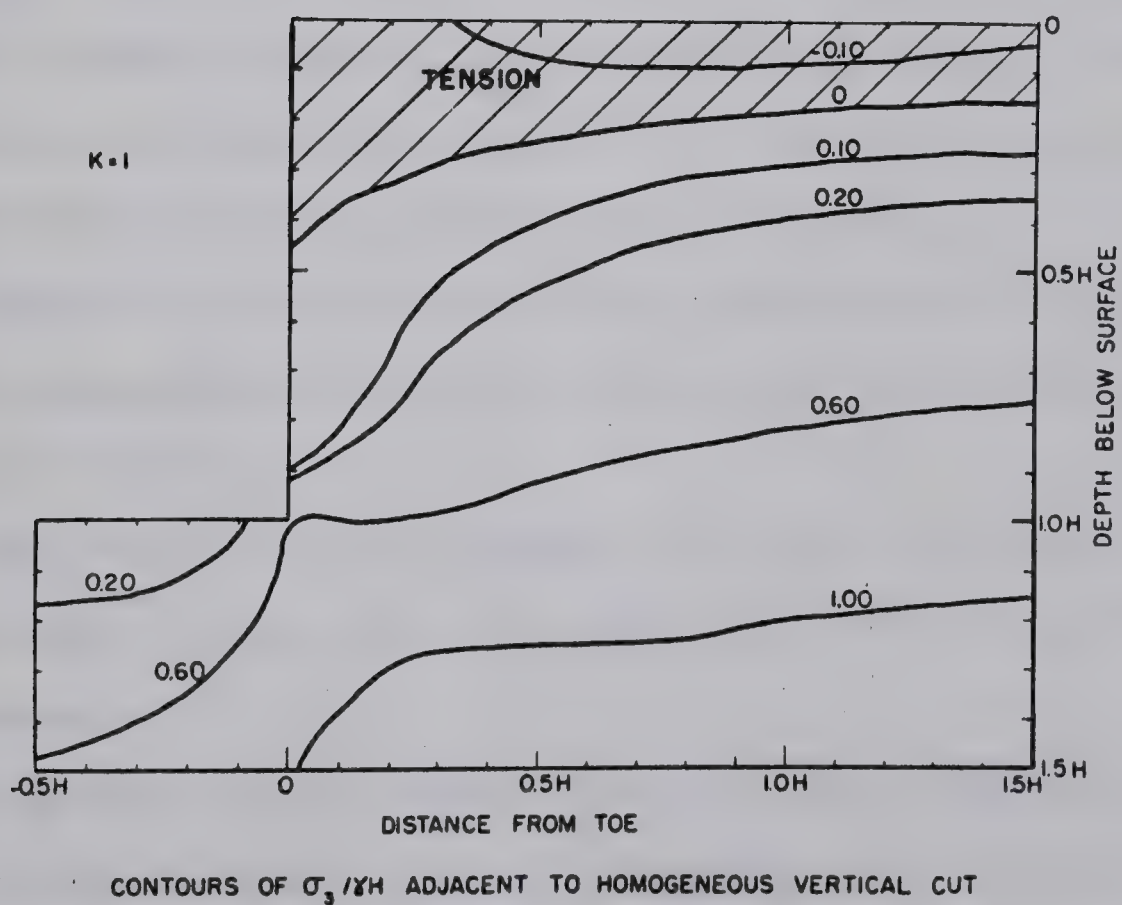
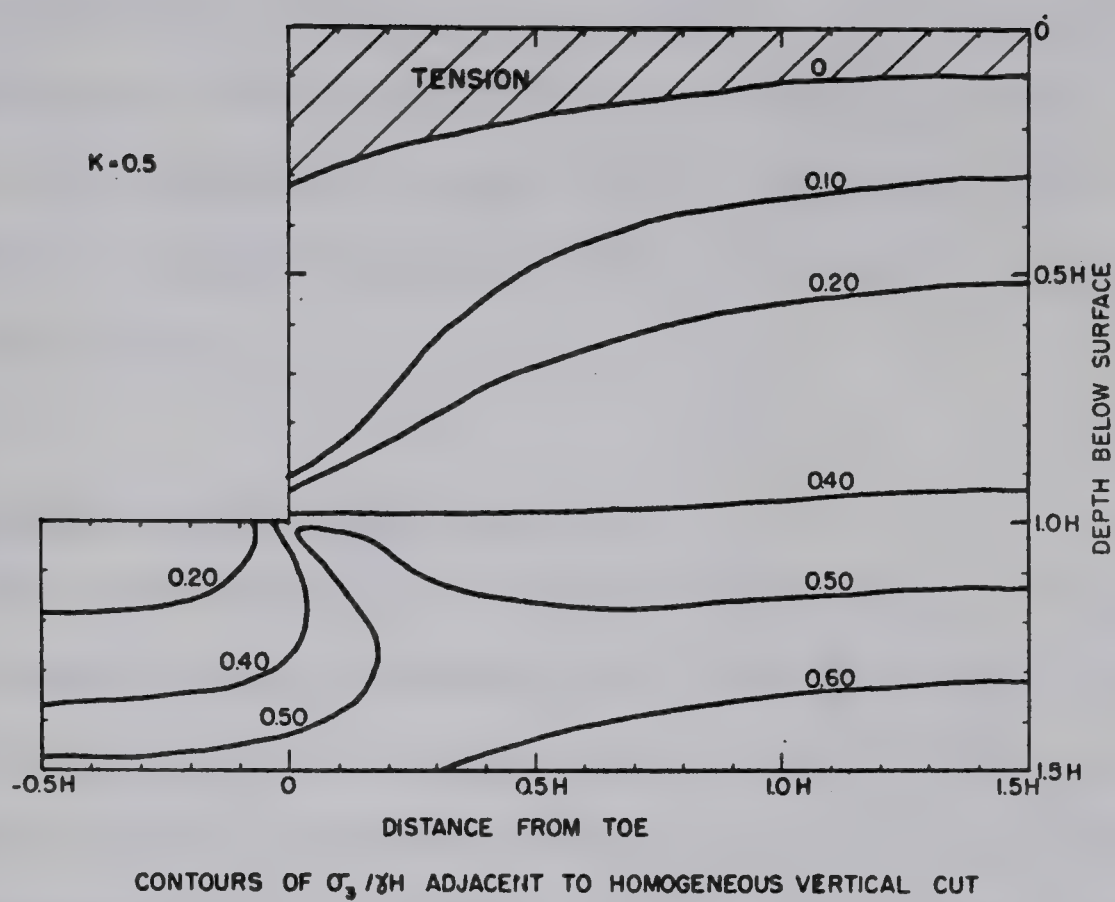
in the chalk but carried it over into tension, i.e. 'stretching' the chalk, as it were, and forming the tension cracks."

The finite element method provides a technique for analyzing the mode of formation of these joints. Duncan and Goodman (1968) noted that a tensile stress zone developed in an excavation wall as a result of excavation into a homogeneous elastic mass, as is illustrated in Figure 7.2. Most rocks are weak in tension and failure, or opening of existing joints and fissures, can be expected. The magnitude of the tensile stress increases with increasing values of  $K_0$  and hence the depth to which tensile stress will occur increases somewhat with larger values of  $K_0$ . These results qualitatively explain the development of tension failures parallel to the valley wall although extension of these joints to the elevation of the valley floor, as documented by Ferguson (1967), may be due to stress concentrations at the end of the tension joint leading to a continuing propagation of the tip of the joint.

The occurrence of 'mylonite' or 'gouge' zones, along bedding planes below or adjacent to river valleys in the study area, apparently results from interbed slip due to flexural folding and stress release. The presence of slickensided surfaces across bedding planes and bentonite layers appears to be an unloading phenomenon and is due to the processes of stress relief and rebound.

Large displacements have occurred adjacent to the river valleys since valley formation and the effects of





( DUNCAN &amp; GOODMAN, 1968 )

FIG. 7.2 DEVELOPEMENT OF TENSION ZONES ADJACENT TO A VERTICAL CUT





these displacements are clearly visible in the bedrock of the study area. The finite element studies show that the presence of a horizontal layer with a low modulus results in stresses, and hence strains, which are concentrated across this layer.

#### 7.4 Applications to Geomorphology

The occurrence of the raised valley rim in the study area provides a unique example of a landform whose occurrence and size can be predicted in a general fashion by application of the theory of elasticity. The occurrence and magnitude of this feature in the field is somewhat irregular and reflects the many variables which exist in nature and cannot be included in a theoretical analysis. However, a study of several areas where the feature is well developed shows that the raised valley rim, resulting from the formation of a major postglacial river valley in an area of very low local relief, has a pronounced effect upon the drainage pattern which has developed immediately adjacent to the valley.

The features which develop adjacent to the main valley depend largely upon the magnitude of the raised rim and include:

1. parallel gulleys which are generally a few hundred yards in length and are oriented parallel to the valley edge before approaching the main valley at right angles.



2. parallel tributaries which parallel the main valley for some distance before entering it. These features appear to represent a development of the initial parallel gulleys and are often located further back from the valley edge.
3. backwards drainage which occurs where the raised valley rim has developed to such an extent that drainage along the valley rim flows landward to a few main tributaries which enter the main valley at widely separated points.

The type of features developed, and hence the drainage pattern which develops adjacent to the valley, appears to depend on the height of the raised valley rim and hence the elastic properties of the bedrock, the depth and width of the valley and the time since valley formation. In areas where little evidence of the raised valley rim is found and the feature is sporadic in occurrence, the height of the raised rim is less than about 3 feet (such as along the Pembina River near Entwistle, Alberta) and no evidence of parallel drainage is noted. In areas where the raised rim is more continuous and ranges in height from about 3 to 15 feet (such as along the South Saskatchewan River upstream of Medicine Hat), parallel gulleys and tributaries become common as shown in Figure 7.3. A raised rim of greater magnitude (as along the Missouri River in South Dakota) leads to the development of backward drainage (Crandell, 1958).













The sequence of formation of these features is shown in Figure 7.4. Valley downcutting at the end of the Pleistocene results in initial undrained rebound which forms a rather small raised rim. In certain cases where the valley is deep and the undrained modulus is relatively low, as in the Pierre shale along the Missouri river, the raised rim was sufficiently high to cause runoff to flow landward thus forming a backward drainage system. In cases where the valley was shallower or the undrained modulus higher, a smaller raised rim resulted and was breached in places by ponded meltwater. Rapid downcutting formed a gulley, perpendicular to the main valley, through the raised rim and erosion in the trough, formed parallel to and behind the raised rim for high values of  $\nu$ , resulted in the formation of parallel gulleys and parallel tributaries.

A study of airphotos of the area shows that a number of the bedrock formations are considerably more susceptible to erosion by running water than the overburden. Removal of the overburden leads to rapid formation of deeply incised tributary valleys and badland topography in formations such as the lower Edmonton and Bearpaw. The parallel gulleys appear to occur mainly in the glacial deposits capping bedrock as soon after the bottom of the gulley reaches the bedrock, rapid erosion and slumping produces a system of parallel tributaries extending some distance back from the main valley. Rebound occurs adjacent to these tributaries and, as along Michichi Creek near Drumheller, Alberta, a





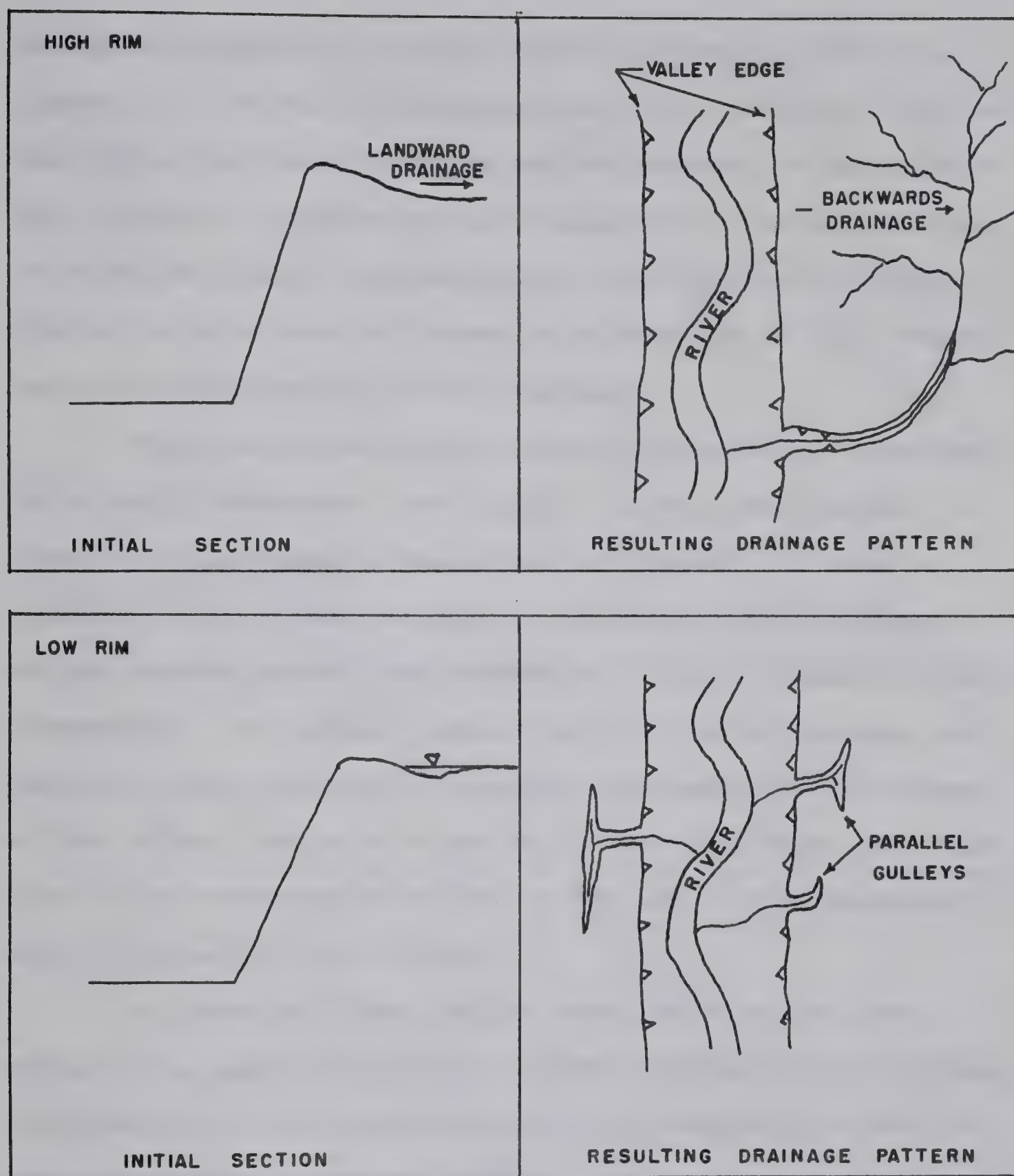


FIG. 7.4 DEVELOPEMENT OF DRAINAGE PATTERNS ADJACENT TO POSTGLACIAL RIVER VALLEYS



secondary system of parallel drainage forms as shown in Figure 7.5. Michichi Creek parallels the valley of the Red Deer River for some distance before entering it and secondary parallel tributaries and gulleys have formed parallel to Michichi Creek, indicating that the entire tributary system in this area is formed as a function of the events resulting from valley bottom rebound.

The occurrence of the features previously described is strongly dependent upon initial topographic relief. A number of the damsites described in Chapter III show no evidence of a raised valley rim although the occurrence of valley bottom rebound and consequent valley flexure is well documented. In certain cases, such as Carvel Damsite and Boundary Dam, postglacial erosion has removed all evidence of the effect while at other sites, such as Hairy Hill Damsite, high topographic relief in the area has suppressed all evidence of this feature.

Evidence of these valley edge features has been noted along many of the major river systems in the Province of Alberta and its occurrence along the Missouri River is well documented (Crandell, 1958). Raised valley rims doubtless occur elsewhere and serve as a visible indicator of the amount of valley bottom rebound which has occurred.

A second type of landform which are apparently influenced by rebound of the valley bottom are backwater swamps and sloughs which have been observed on high level terraces, now well above river level. These features are









normally ascribed to formation of natural levees along the edge of the main river channel. However, rapid downcutting of the river would lead to rebound resulting in a rise of the river edge of the terrace as shown in Figure 7.6 and it would appear that this mechanism would assist in the formation of features of this type which have been noted along the Athabasca and North Saskatchewan Rivers in Alberta.





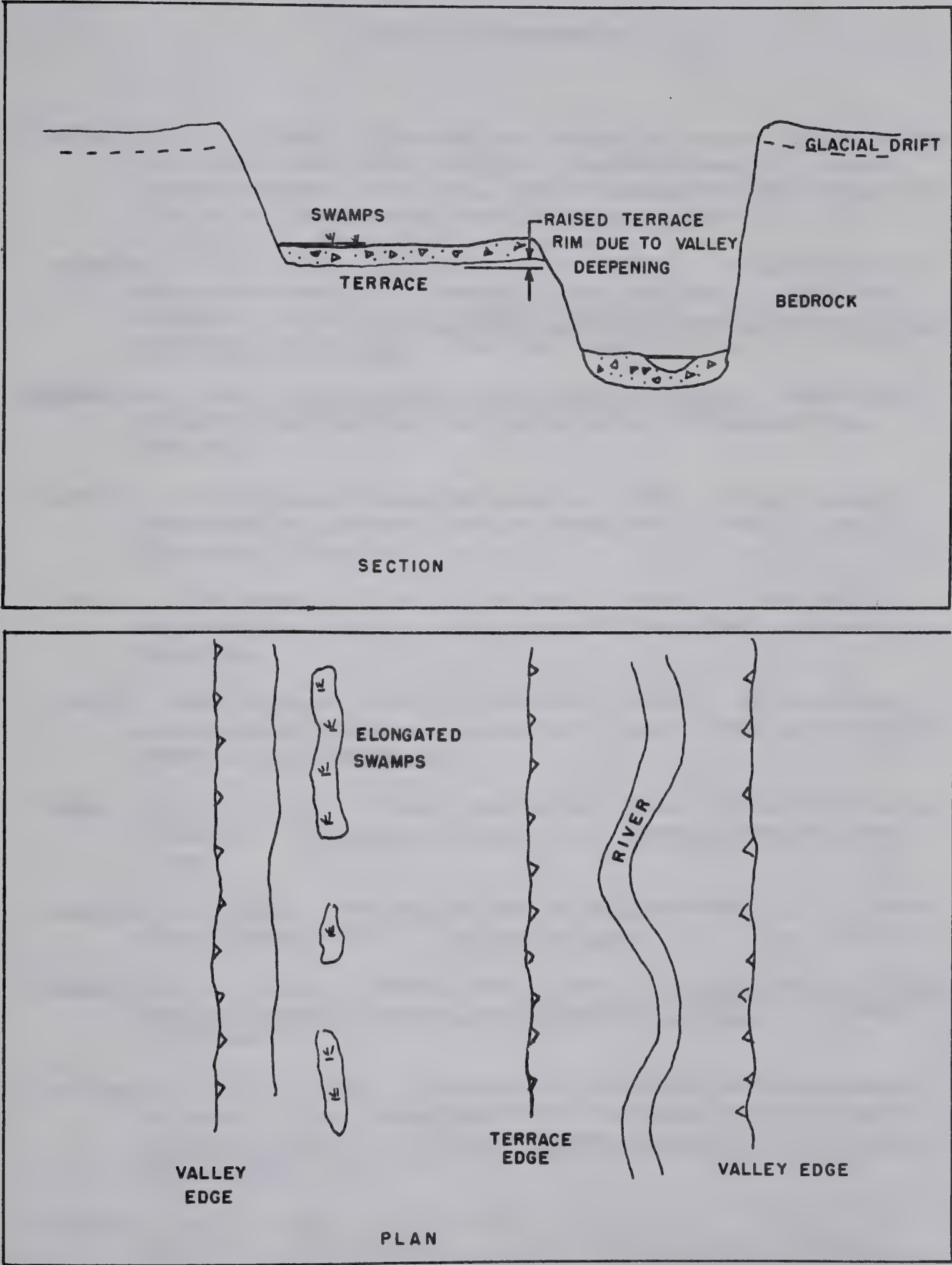


FIG. 7.6 FORMATION OF BACKWATER SWAMPS ON HIGHLEVEL TERRACES



## LIST OF REFERENCES

- Allen, J. A., 1949. "Geological notes on tunnel inspection, P.F.R.A., Site 10, Outlook, Saskatchewan". Unpublished report, P.F.R.A. Soil Mechanics and Materials Division, Saskatoon, Saskatchewan, 7 pp.
- Anderson, P. A. and Schuster, R. L., 1971. "Stability of clay interbeds - Columbia River valley". Meeting Preprint 1478, Joint ASCE - ASME Transportation Engineering Conference, Seattle, Washington, July 26-30.
- A.S.T.M., 1958. Procedures for Testing Soils. American Society for Testing and Materials, Philadelphia, 544 pp.
- A.W.R., Development Planning Branch, 1968. "Preliminary engineering report, Ardley Damsite". Vol. I and II, Edmonton, Alberta.
- A.W.R., Development Planning Branch, 1969a. "Preliminary engineering report, Athabasca-Oldman Dam", Edmonton, Alberta.
- A.W.R., Development Planning Branch, 1969b. "Preliminary engineering report, Horseguard Dam, North and South", Edmonton, Alberta, July.
- Babet, P. H., 1966. "Some characteristics of bentonite in Alberta". Research Council of Alberta Report 66-2, 25 pp.
- Barden, L., 1963. "Stresses and displacements in a cross-anisotropic soil". Geotechnique, 13, 3, p. 198-210.
- Beene, R. W., 1967. "Waco Dam slide". Journal of the Soil Mechanics and Foundations Division, ASCE, 93, SM4, p. 35-44.
- Bellport, B. P., 1967. "Bureau of Reclamation experience in stabilizing embankment of Fontenelle Earth Dam". Transactions of the Ninth International Congress on Large Dams, 1, p. 67-79.
- Binger, M. V., 1948. "Analytical studies of Panama Canal Slides". Proceedings of the Second International Conference in Soil Mechanics and Foundation Engineering, Rotterdam, 2, p. 54-69.





- Binnie, G. M. et al., 1967. "Mangla: Part 1: Engineering of Mangla". Proceedings of the Institution of Civil Engineers, 38, p. 343-544.
- Binnie, G. M., Clark, J. F. and Skempton, W. W. 1967. "The effect of discontinuities in clay bedrock in the design of dams in the Mangla project." Transactions of the Ninth International Congress on Large Dams, Istanbul, 1, p. 165-189.
- Bishop, A. W., 1955. "The use of the slip circle in the stability analysis of earth slopes". Geotechnique, 3, p. 7-17.
- Bishop, A. W., 1971. "The influence of progressive failure on the choice of the method of stability analysis". Geotechnique, 21, 2, p. 168-172.
- Bjerrum, L., 1966. "Mechanisms of progressive failure in slopes of overconsolidated plastic clays and clay shales". The Third Terzaghi lecture presented at the ASCE Conference on Structural Engineering, Miami.
- Blake, W., 1968. "Finite element model study of slope modification at the Kimbley Pit". Transactions of the American Institute of Mining Engineers, AIME, 241, p. 525-533.
- Bozozuk, M., 1963. "The modulus of elasticity of Leda Clay from field measurements". Canadian Geotechnical Journal, 1, 1, p. 43-51.
- Bradley, W. C., 1963. "Large scale exfoliation in massive sandstone of the Colorado plateau". Bulletin, Geological Society of America, 74, p. 519-527.
- Brooker, E. W., 1958. "Special Problems in Stability of Slopes". Unpublished M.Sc. thesis, Department of Civil Engineering. University of Alberta.
- Brooker and Associates, 1969. "The Ardley Testpit". Unpublished report submitted to the Water Resources Division, Alberta Government.
- Brooker, E. W. and Ireland, H. O., 1965. "Earth pressures at rest; related to stress history". Canadian Geotechnical Journal, 2, 1, p. 1-15.
- Brooker, E. W. and Lindberg, D. A., 1965. "Field measurement of pore pressure in high plasticity soils". Proceedings of the International Research and Engineering Conference in Expansive Clay Soils, 2, Texas A. and M. University.





- Brown, C. B. and King, I. P., 1966. "Automatic embankment analysis: equilibrium and instability conditions." Geotechnique, 16, 3, p. 209-215.
- Byrne, P. J. S., 1955. "Bentonite in Alberta". Research Council of Alberta Report No. 71, 20 pp.
- Carlson, V. A., 1966. "Bedrock Topography and Surficial Aquifers of the Edmonton District, Alberta". Research Council of Alberta Report 66-3.
- Casagrande, A., 1949. "Notes on swelling characteristics of clay shales". Harvard University.
- Cassel, F. L., 1948. "Slips in fissured clay". Proceedings of the Second International Conference on Soil Mechanics and Foundation Engineering, Rotterdam, 2, p. 46-49.
- Chang, C., 1969. "Finite element analyses of soil movements caused by deep excavation and dewatering". Unpublished Ph.D. thesis, University of California, Berkeley, 304 pp.
- Chang, C. Y. and Duncan, J. M., 1970. "Analysis of soil movement around a deep excavation". Journal of the Soil Mechanics and Foundations Division, ASCE, 96, SM5, p. 1655-1681.
- Chou, P. C., and Pagano, N. J., 1967. Elasticity; Tensor, Dyadic and Engineering Approaches, D. Van Nostrand Co., Princeton, New Jersey, 290 pp.
- Christian, J. T., and Whitman, R. V., 1969. "A one-dimensional model for progressive failure". Proceedings of the Seventh International Conference on Soil Mechanics and Foundation Engineering, Mexico City, 2, p. 541-545.
- Coates, D. F., 1964. "Some cases of residual stress effects in engineering work". State of Stress in the Earth's Crust ed. W. R. Judd, Elsevier, New York, p. 679-688.
- Collin, A., 1846. Landslides in Clay. Translated by W. R. Schriever, University of Toronto Press, Toronto, 1956.
- Conlon, R. J. and Isaacs, R. M. F., 1970. "Effect of sampling and testing techniques on the shear strength of a glacio-lacustrine clay from Welland, Ontario". Sampling of Soil and Rock, ASTM STP 483, American Society for Testing and Materials, p. 10-29.
- Crandell, D. R., 1958. "Geology of the Pierre Area, South Dakota". U. S. Geological Survey, Professional Paper No. 307, 83 pp.





- Crockford, M. B. B., 1951. "Clay deposits of Elkwater Lake area, Alberta". Research Council of Alberta Report No. 61, 102 pp.
- D'Appolonia, E., Alperstein, R., and D'Appolonia, D. J., 1967. "Behaviour of a colluvial slope". Journal of the Soil Mechanics and Foundations Division, ASCE, 93, SM4, p. 447-474.
- de Beer, E. E., 1969. "Experimental data concerning clay slopes". Proceedings of the Seventh International Conference on Soil Mechanics and Foundation Engineering, Mexico City, 2, p. 517-525.
- Deere, D. V., 1964. "Technical description of rock cores for engineering purposes". Rock Mechanics and Engineering Geology, 1, p. 16-22.
- DeJong, J., 1971. "Foundation displacements of multi-storey structures". Unpublished Ph.D. thesis, Department of Civil Engineering, University of Alberta, 251 pp.
- Dibiagio, E. L., 1966. "Stresses and displacements around an unbraced rectangular excavation in an elastic medium". Unpublished Ph.D. thesis, University of Illinois, 137 pp.
- Dolmage, V. and Campbell, D. D., 1963. "The geology of the Portage Mountain Damsite, Peace River, B. C." Transactions of the Canadian Institute of Mining and Metallurgy, 66, p. 308-320.
- Duncan, J. M. and Chang, C., 1970. "Nonlinear analysis of stress and strain in soils". Journal of the Soil Mechanics and Foundations Division, ASCE, 96, SM5, p. 1629-1653.
- Duncan, J. M., and Dunlop, P., 1969. "Slopes in stiff-fissured clays and shales". Journal of the Soil Mechanics and Foundations Division, ASCE, 95, SM2, p. 467-492.
- Duncan, J. M., Dunlop, P. and Seed, H. B., 1968. "Finite element analyses of slopes in soil". U. S. Army Waterways Experiment Station, Vicksburg, Contract Report S-68-6, University of California, Berkeley.
- Duncan, J. M. and Goodman, R. E., 1968. "Finite element analyses of slopes in jointed rock". U. S. Army Waterways Experiment Station, Vicksburg, Contract Report S-68-3, University of California, Berkeley, 276 pp.





- Eigenbrod, K. D., 1972. "Ph.D. thesis in preparation".  
Department of Civil Engineering, University of Alberta.
- Eigenbrod, K. D. and Morgenstern, N. R., 1971, "A slide in Cretaceous bedrock, Devon, Alberta". Presented at 2nd Annual Symposium on Stability for Open Pit Mining, Vancouver, B. C., November, 1971.
- Feld, J., 1966. "Rock movements from load release in excavation cuts". Proceedings of the First International Congress of the International Society of Rock Mechanics, Lisbon, 2, p. 139-140.
- Ferguson, H. F., 1967. "Valley stress release in the Allegheny Plateau". Bulletin of the Association of Engineering Geologists, 4, 1, p. 63-68.
- Fleming, R. W., Spencer, G. S., and Banks, D. C., 1970. "Empirical study of behaviour of clay shale slopes", Vol. I and II, U. S. Army Engineer Nuclear Cratering Group, Technical Report No. 15, Livermore, California, December 1970.
- Fookes, P. G., 1965. "Orientation of fissures in stiff overconsolidated clay of the Siwalik system". Geotechnique, 15, p. 195-206.
- Fookes, P. G. and Wilson, D. D., 1966. "The geometry of discontinuities and slope failures in Siwalik clay". Geotechnique, 16, p. 305-320.
- Geological Survey of Canada, 1967. "Glacial Map of Canada". Map No. 1253A, Scale 1:5,000,000, Department of Energy, Mines and Resources, Ottawa.
- Gibson, R. E., 1967. "Some results concerning displacements and stresses in a non-homogeneous elastic half-space". Geotechnique, 17, 3, p. 58-67.
- Gibson, R. E., and Henkel, D. J., 1954. "Influence of duration of tests at constant rate of strain on measured drained strength". Geotechnique, 4, p. 6-15.
- Goldstein, S., 1927. "The stability of a strut under thrust, when buckling is resisted by a force proportional to the displacement". Proceedings of the Cambridge Philosophical Society, 23, p. 120-129.
- Gould, J. P., 1960. "A study of shear failure in certain Tertiary marine sediments". Proceedings of the ASCE Research Conference on Shear Strength of Cohesive Soils, Boulder, p. 615-641.





- Hake, B. G. and Addison, C. C., 1954. "Use of bentonite beds as a marker formation". Western Canada Sedimentary Basin and Stratigraphy of the Plains of Southern Alberta, ed. L. M. Clark, American Association of Petroleum Geologists, p. 87-97.
- Hardy, R. M., 1963. "The Peace River Highway Bridge - a failure in soft shales". Highway Research Record 17, p. 29-39.
- Hardy, R. M., 1966. "Failure of the Peace Highway Bridge". Proceedings of the Fourth Annual Engineering Geology and Soils Engineering Symposium, University of Idaho, April, p. 49-59.
- Hardy, R. M., Brooker, E. W. and Curtis, W. E., 1962. "Landslides in overconsolidated clays". The Engineering Journal, 45, 6, p. 81-89.
- Harr, M. E., 1966. Foundations of Theoretical Soil Mechanics, McGraw-Hill, New York, 380 pp.
- Harris, M. C., 1971. "Personal Communication".
- Hayley, D. W., 1968. "Progressive failure of a clay shale slope in northern Alberta". Unpublished M. Sc. thesis, Department of Civil Engineering, University of Alberta.
- Hendron, A. J., 1971. "Unpublished lecture presented at The Analysis and Design of Rock Slopes short course," University of Alberta, Edmonton, August 23-27.
- Hendron, A. J., Mesri, G., Gamble, J. C., and Way, G., 1969. "Compressibility characteristics of shales measured by laboratory and in-situ tests". ASTM Special Technical Publication 477, p. 137-153.
- Henkel, D. J., 1957. "Investigations of two long-term failures in London Clay at Wood Green and Northolt". Proceedings of the Fourth International Conference on Soil Mechanics and Foundation Engineering, London, 2, p. 315-320.
- Henkel, D. J. and Skempton, A. W., 1954. "A landslide at Jackfield, Shropshire in overconsolidated clay." Geotechnique, 5, p. 131-137.
- Higginbottom, I. E. and Fookes, P. G., 1970. "Engineering aspects of periglacial features in Britain". The Quarterly Journal of Engineering Geology, 3, 2, p. 85-117.





- Holland, I. and Bell, K., 1970. Finite Element Methods in Stress Analysis, Tapir Forlag, Trondheim, Norway.
- Hollingworth, S. E., Taylor, J. H. and Kellaway, G. A., 1944. "Large scale superficial structures in the Northampton Ironstone Field". Quarterly Journal of the Geologic Society of London, 100, p. 1-44.
- Hutchinson, J. N., 1968. "Mass movement". The Encyclopedia of Geomorphology ed. Fairbridge, Reinhold, New York, p. 690.
- Hvorslev, M. J., 1949. Subsurface Exploration and Sampling of Soils for Civil Engineering Purposes. U. S. Army Waterways Experiment Station, Vicksburg, Mississippi, November, 521 pp.
- Imrie, A. S., 1967. "Analysis of the underground powerhouse arch at the Portage Mountain Dam". Unpublished M.Sc. thesis, Department of Geology, University of Alberta.
- Imrie, A. S., 1971. "Personal communication".
- I.P.E.C., 1965. "Memorandum on foundation geology, Portage Mountain development". International Power and Engineering Consultants Ltd., Vancouver, B. C.
- Iverson, N. L., 1970. "Discussion on 'Riverbank stability at the University of Alberta, Edmonton' by S. Thomson". Canadian Geotechnical Journal, 7, 2, pp. 169-170.
- Jaeger, J. C., and Cook, N. G. W., 1969. Fundamentals of Rock Mechanics, Methuen, London, 513 pp.
- James, P. M., 1970. "Time effects and progressive failure in clay slopes". Unpublished Ph.D. thesis, University of London, 210 pp.
- Janbu, N., 1963. "Soil compressibility as determined by oedometer and triaxial tests". Proceedings of the European Conference on Soil Mechanics and Foundation Engineering, Wiesbaden, 1, p. 19-25.
- Jennings, J. E., 1970. "A mathematical theory for the calculation of the stability of slopes in open cast mines". Planning Open Pit Mines, ed. Van Rensburg, South African Institute of Mining and Metallurgy, p. 87-102.
- Kankare, E., 1969. "Failures at Kimola floating canal in southern Finland". Proceedings of the Seventh International Conference on Soil Mechanics and Foundation Engineering, Mexico City, 2, p. 609-616.





- Kellaway, G. A. and Taylor, J. H., 1952. "Early stages in the physiographic evolution of a portion of the East Midlands". The Quarterly Journal of the Geological Society of London, 108, p. 343-366.
- Kenney, T. C., 1967. "The influence of mineral composition on the residual strength of natural soils". Proceedings, Geotechnical Conference on the Shear Strength Properties of Natural Soils and Rocks, Oslo, 1, p. 123-129.
- Kenney, T. C., 1967. "Stability of the Vajont Valley slope, discussion of 'The rock slide in the Vajont Valley' by L. Muller". Rock Mechanics and Engineering Geology, 7, p. 10-16.
- Khan, M. B. and Nagvi, S. A., 1967. "Foundation problems on Mangla Dam Project". Transactions of the Ninth International Congress on Large Dams, Istanbul, 1, p. 1115-1143.
- Klohn, E. J., 1965. "The elastic properties of a dense glacial till". Canadian Geotechnical Journal, 2, 2, p. 116-128.
- Knight, D. K., 1963. "Oahe Dam: Geology, embankment and cut slopes". Journal of the Soil Mechanics and Foundations Division, ASCE, 89, SM2, p. 99-125.
- Koppula, S. D., 1970. "The consolidation of soil in two dimensions and with moving boundaries". Unpublished Ph.D. thesis, Department of Civil Engineering, University of Alberta, 281 pp.
- Kwan, D., 1971. "Observations of the failure of a vertical cut in clay at Welland, Ontario". Canadian Geotechnical Journal, 8, 2, p. 283-298.
- Ladd, C. C., 1964. "Stress-strain modulus of clay in undrained shear". Journal of the Soil Mechanics and Foundation Division, ASCE, 90, SM5, p. 103-132.
- Lane, K. S. and Occhipinti, S. J., 1953. "Rebound gages check movement analysis at Garrison Dam". Proceedings of the Third International Conference on Soil Mechanics and Foundation Engineering, Zurich, 1, p. 402-405.
- Lapworth, H. 1911. "The geology of dam trenches". Transactions of the Institution of Water Engineers, 16, May, p. 25-51.





- Lapworth, H., 1918. "Discussion on 'The Derwent Valley Waterworks' by E. Sandeman". Minutes of Proceedings of the Institution of Civil Engineers, 206, p. 196.
- Lo, K. Y., Seychuk, J. L. and Adams, J. I., 1970. "A study of the deformation characteristics of a stiff fissured clay". ASTM Special Technical Publication 483, p. 60-76.
- Locker, J. G., 1969. "The petrographic and engineering properties of fine grained sedimentary rocks in central Alberta". Unpublished Ph.D. thesis, Department of Civil Engineering, University of Alberta.
- Lockwood Survey Corporation, 1967. 'Report on Damsite Investigations - McLeod River'. Unpublished report submitted to the Water Resources Division, Alberta Government, March.
- Lutton, R. J. and Banks, D. C., 1970. "Study of clay shale slopes along the Panama Canal: Report 1, East Culebra and West Culebra slides and the model slope". U. S. Army Waterways Experiment Station Technical Report S-70-9, 285 pp.
- MacKenzie, G. L., 1960. "The South Saskatchewan River Dam". The Engineering Journal, 43, 5, p. 50-55.
- Mahtab, M. A. and Goodman, R. E., 1968. "Stresses around wellbores in nonlinear rock". Society of Petroleum Engineers Journal, AIME, 243, p. 304-312.
- Makhlouf, H. M. and Stewart, J. J., 1965. "Factors influencing the modulus of elasticity of dry sand". Proceedings of the Sixth International Conference on Soil Mechanics and Foundation Engineering, Montreal, 1, p. 298-302.
- Matheson, D. S., 1970. "An airphoto survey of landslides along the Pembina River". Unpublished internal report, Department of Civil Engineering, University of Alberta, 57 pp.
- Matheson, D. S. and Koppula, S. D., 1971. "Discussion on 'Analysis of soil movement around a deep excavation' by C. Y. Chang and J. M. Duncan". Journal of the Soil Mechanics and Foundation Division, ASCE, 97, SM7, p. 1034-1036.
- Meigh, A. C. and Greenland, S. W., 1965. "In-situ testing of soft rocks". Proceedings of the Sixth International Conference on Soil Mechanics and Foundation Engineering, Montreal, 1, p. 73-76.





- Merrill, R. H., 1963. "In-situ determination of stress by relief techniques". State of Stress in the Earth's Crust, ed. W. R. Judd, American Elsevier, New York, p. 343-369.
- Merrill, R. H., 1968. "Bureau contribution to slope angle research at the Kimbley Pit, Ely, Nevada". Transactions, Society of Mining Engineers, AIME, 341, p. 513-524.
- Middlebrooks, T. A., 1942. "Fort Peck Slide", Transactions, American Society of Civil Engineers, 107, p. 723-742.
- Morgenstern, N. R., 1967. "Shear strength of stiff clay". Proceedings, Geotechnical Conference on Shear Strength Properties of Natural Soils, Oslo, 2, p. 59-69.
- Morgenstern, N. R. and Price, V. E., 1965. "The analysis of the stability of general slip surfaces". Geotechnique, 15, 79-93.
- Morgenstern, N. R. and Tchalenko, J. S., 1967. "Microscopic structures in Kaolin subjected to direct shear". Geotechnique, 17, 4, p. 309-328.
- Morgenstern, N. R. and Thomson, S., 1971. "Comparative Observations on the Use of the Pitcher Sampler in Stiff Clay". ASTM Special Technical Publication 483, p. 180-191.
- Norris, D. K., 1967. "Structural analysis of the Queensway folds, Ottawa, Canada". Canadian Journal of Earth Sciences, 4, p. 299-321.
- Painter, W. T., 1965. "An investigation of the Lesueur landslide, Edmonton, Alberta". Unpublished M.Sc. thesis, Department of Civil Engineering, University of Alberta.
- Patton, F. D., 1971. "Unpublished lecture presented at The Analysis and Design of Rock Slopes short course". University of Alberta, Edmonton, August 23-27.
- Pearson, G. R., 1959. "Coal resources for strip mining, Wabamum Lake district, Alberta". Research Council of Alberta Report 59-1, 55 pp.
- Peck, R. B., 1967. "Stability of natural slopes". Journal of the Soil Mechanics and Foundations Division, ASCE, 93, SM4, p. 403-417.
- Peck, R. B., 1969. "Deep excavations and tunnelling in soft ground". State of the Art Volume, Seventh International Conference on Soil Mechanics and Foundation Engineering, Mexico City, p. 225-290.





- Pennell, D. G., 1969. "Residual strength analysis of five landslides". Unpublished Ph.D. thesis, Department of Civil Engineering, University of Alberta, 166 pp.
- Peterson, R., 1954. "Studies of Bearpaw shale at a damsite in Saskatchewan". Proceedings of the American Society of Civil Engineers, Separate No. 476, 80, August.
- Peterson, R., 1958. "Rebound in Bearpaw shale, Western Canada". Bulletin, Geological Society of America, 69, p. 1113-1124.
- Peterson, R., 1965. "Discussion on 'The Elastic Properties of a Dense Glacial Till Deposit' by E. Kohn". Canadian Geotechnical Journal, 2, 2, p. 140.
- Peterson, R., Jaspar, J. L., Rivard, P. J., and Iverson, N. L., 1960. "Limitations of laboratory shear strength in evaluating stability of highly plastic clays." Proceedings of the ASCE Research Conference on Shear Strength of Cohesive Soils, Boulder, p.765-791.
- Peterson, R., and Peters, N., 1963. "Heave of spillway structures on clay shales". Canadian Geotechnical Journal, 1, 1, pp. 5-15.
- P. F. R. A., Soil Mechanics and Materials Division, (1945). "Rock Core Compression Tests, Proposed Site of St. Mary Dam", Saskatoon, Saskatchewan, March, 29 pp.
- P. F. R. A., Soil Mechanics and Materials Division (1949). "Report of Investigation of Permeability of Rock Foundation in the River Section Beneath St. Mary Dam", Saskatoon, Saskatchewan, April.
- P. F. R. A., Soil Mechanics and Materials Division (1951). "Report on Geological Test Drift", Saskatoon, Saskatchewan, December.
- P. F. R. A., Soil Mechanics and Materials Division, (1950). "Preliminary Soil Mechanics Report, Waterton Dam-sites", Saskatoon, Saskatchewan, April.
- P. F. R. A., Airphoto Analysis and Engineering Geology Division (1955). "Report on Preliminary Inspection Trip to the Proposed Boundary Damsite Area", Regina, Saskatchewan, August.
- P. F. R. A., Soil Mechanics and Materials Division (1956a). "Preliminary Soil Mechanics Report on Boundary Dam, Site 4", Saskatoon, Saskatchewan, January.





- P. F. R. A., Air photo Analysis and Engineering Geology Division (1956b). "Notes; Inspection of Test Drifts, Waterton Site No. 3", Regina, Saskatchewan, May.
- P. F. R. A., Soil Mechanics and Materials Division, (1958). "Waterton Damsite No. 3 and Outlet Canal, Supplementary Soil Mechanics and Materials Report", Saskatoon, Saskatchewan, May.
- P. F. R. A., Soil Mechanics and Materials Division (1959a). "Report on the Construction of Boundary Dam at Estevan, Saskatchewan", Saskatoon, Saskatchewan, May.
- P. F. R. A., Soil Mechanics and Materials Division (1959b). "Preliminary Soil Mechanics Report on Cameron Project, Damsite No. 2", Saskatoon, Saskatchewan, August.
- P. F. R. A., Soil Mechanics and Materials Division (1961). "Soil Mechanics Report, St. Mary Dam Construction", Saskatoon, Saskatchewan, March.
- P. F. R. A., Soil Mechanics and Materials Division (1965a). "Preliminary Soil Mechanics Report, Three Rivers Damsite, Oldman River Project", Saskatoon, Saskatchewan, May.
- P. F. R. A., Soil Mechanics and Materials Division (1965b). "Preliminary Soil Mechanics Report, Paddle River Damsite No. 7", Saskatoon, Saskatchewan, July.
- P. F. R. A., Geology and Air Surveys Division, (1969a). "Air Photo Interpretation of North Saskatchewan River Valley in Vicinity of Hairy Hill, Alberta", Regina, Saskatchewan, January.
- P. F. R. A., Soil Mechanics and Materials Division (1969b). "Soil Mechanics Report on Carvel Site", Saskatoon, Saskatchewan, August.
- P. F. R. A., Soil Mechanics and Materials Division (1969c). "Soil Mechanics Report on Tomahawk Site", Saskatoon, Saskatchewan, October.
- P. F. R. A., Soil Mechanics and Materials Division, (1969d). "Qu'Appelle Diversion to Souris River, Soil Mechanics Report, Proposed Rafferty Dam", Saskatoon, Saskatchewan, November.
- P. F. R. A., Soil Mechanics and Materials Division (1969e). "Preliminary Soil Mechanics Report, Crossfield Creek Project Site 3", Saskatoon, Saskatchewan.





- P. F. R. A., Soil Mechanics and Materials Division, (1970a). "Report on Cypress Hills Park, Belanger Creek Dam-site", Saskatoon, Saskatchewan, January.
- P. F. R. A., Soil Mechanics and Materials Division, (1970b). "Soil Mechanics Report on Hairy Hill Dam-site, North Saskatchewan River", Saskatoon, Saskatchewan, March.
- Pollock, D. H., 1962. "Geology of the South Saskatchewan River Project". The Engineering Journal, 45, 4, p. 37-46.
- Pope, J. R., and Anderson, M. W., 1960. "The strength properties of clays derived from volcanic rocks". ASCE Research Conference on Shear Strength of Cohesive Soils, Boulder, p. 315-340.
- Price, N. J., 1967. "The initiation and development of asymmetrical buckle folds in non-metamorphosed competent sediments". Tectonophysics, 4, 2, p. 173-201.
- Ramsay, J. G., 1967. Folding and Fracturing of Rocks, McGraw-Hill, New York, 568 pp.
- Rennie, R. J., 1966. "Residual strength of a clay-till applied to Little Smokey River landslide". Unpublished M.Sc. thesis, Department of Civil Engineering, University of Alberta.
- Ringheim, A. S., 1964. "Experience with the Bearpaw shale at the South Saskatchewan River Dam". Transactions, Eighth International Congress on Large Dams, Edinburgh, 1, p. 529-550.
- R. M. Hardy and Associates, 1966. "Report to Water Resources Division, Department of Agriculture, Government of Alberta, on Pembina Flood Control Project, Evansburg, Alberta". Vols. I and II, Edmonton, Alberta.
- Roggensack, W. D., 1971. "An airphoto study of landslides along the Oldman River and South Saskatchewan River in Alberta". Unpublished internal report, Department of Civil Engineering, University of Alberta, Edmonton, Alberta, October.
- Rowe, P. W., 1968. "The influence of geologic features of clay deposits on the design and performance of sand drains." Proceedings of the Institution of Civil Engineers, Supplementary Volume, Paper 70583.
- Rutherford, R. L., 1928. "Geology between North Saskatchewan and McLeod Rivers". Research Council of Alberta Report 19, 7 pp.





- Sandeman, E., 1918. "The Derwent valley waterworks". Minutes of Proceedings of the Institution of Civil Engineers, 206, p. 152-189.
- Serota, S. and Jennings, R. A. J., 1959. "The elastic heave of the bottom of excavations". Geotechnique, 9, 62-70.
- Sevaldson, R. A., 1956. "The slide at Lodalen, October 6th, 1954". Geotechnique, 6, 4, p. 167-182.
- Sharma, L., 1968. "Geotechnical Properties of Peace River glacial lake sediments". Unpublished M.Sc. thesis, Department of Civil Engineering, University of Alberta, 100 pp.
- Sharp, R. P., 1942. "Periglacial involutions in northeastern Illinois". Journal of Geology, 50, p. 113-133.
- Scott, J. S. and Brooker, E. W., 1968. "Geological and engineering aspects of Upper Cretaceous shales in Western Canada". Paper 66-37, Geological Survey of Canada, Department of Energy, Mines and Resources, Ottawa, 75 pp.
- Simons, N. E., 1957. "Settlement studies on two structures in Norway". Proceedings of the Fourth International Conference on Soil Mechanics and Foundation Engineering, 1, p. 431-436.
- Simons, N. E., and Som, N. N., 1969. "The influence of lateral stresses on the stress deformation characteristics of London Clay". Proceedings of the Seventh International Conference on Soil Mechanics and Foundation Engineering, Mexico City, 1, p. 369-377.
- Sinclair, S. R., Brooker, E. W., and Thomson, S., 1966. "Stability of clay shale slopes". Presented at the ASCE Conference on Stability and Performance of Slopes and Embankments, Berkeley, California, August 22-26.
- Sinclair, S. R. and Brooker, E. W., 1967. "The shear strength of Edmonton shale". Proceedings, Geotechnical Conference on Shear Strength Properties of Natural Soil and Rocks, Oslo, 1, p. 295-299.
- Skempton, A. W., 1961. "Horizontal stresses in an overconsolidated Eocene clay". Proceedings, Fifth International Conference on Soil Mechanics and Foundation Engineering, Paris, 1, p. 351-357.
- Skempton, A. W., and Brown, J. D., 1961. "A landslide in boulder clay at Selset, Yorkshire", Geotechnique, 11, 4, p. 280-293.
- Skempton, A. W., 1964. "Long-term stability of clay slopes". Geotechnique, 14, 2, p. 77-101.





- Skempton, A. W., 1966. "Bedding-plane slip, residual strength and the Vajont landslide". Geotechnique, 12, 1, p. 82-84.
- Skempton, A. W., 1970. "First time slide in overconsolidated clays". Geotechnique, 20, 3, p. 320-324.
- Skempton, A. W. and La Rochelle, P., 1965. "The Bradwell slip; a short-term failure in London Clay". Geotechnique, 15, 3, p. 221-242.
- Skempton, A. W. and Petley, D. J., 1967. "The strength along structural discontinuities in stiff clays". Proceedings, Geotechnical Conference on Shear Strength Properties of Natural Soils and Rocks, Oslo, 2, p. 29-46.
- Smith, C. K. and Redlinger, J. F., 1953. "Soil properties of Fort Union shale". Proceedings, Third International Conference on Soil Mechanics and Foundation engineering, Zurich, 1, p. 62-66.
- Soderman, L. G., Kim, Y. G., and Milligan, V., 1968. "Field and laboratory studies of modulus of elasticity of a clay till". Highway Research Board Research Record 243.
- Suklje, L., 1969. Rheological Aspects of Soil Mechanics. John Wiley and Sons, London, 570 pp.
- Tape, R. F., 1971. "Non-circular effective stress analysis of the Waco Dam slide". Unpublished M. Eng. report, Department of Civil Engineering, University of Alberta, 14 pp.
- Taylor, R. S., 1971. Atlas: Coal-mine workings of the Edmonton Area. Bulletin Commercial Printers, Edmonton, 33 pp.
- Terzaghi, K., 1936. "Stability of slopes in natural clay". Proceedings, First International Conference on Soil Mechanics and Foundation Engineering, 1, p. 161-165, Cambridge, Massachusetts, U.S.A.
- Terzaghi, K., 1943. Theoretical Soil Mechanics, John Wiley and Sons, New York, 510 pp.
- Terzaghi, K., 1950. "Mechanisms of landslides". Application of Geology to Engineering Practice (Berkey Volume) Geological Society of America, p. 83-123.
- Terzaghi, K., 1955. "Influence of geological features on the engineering properties of sediments". Harvard





Soil Mechanics Series No. 50; also in Economic Geology (Fiftieth Anniversary Volume) p. 557-618.

- Terzaghi, K., 1961. "Discussion on 'Horizontal stresses in overconsolidated Eocene clay' by A. W. Skempton". Proceedings, Fifth International Conference on Soil Mechanics and Foundation Engineering, Paris, 3, p. 144-145.
- Thomson, S., 1970. "Riverbank stability study at the University of Alberta, Edmonton". Canadian Geotechnical Journal, 7, 2, p. 157-168.
- Thomson, S., 1971. "Analysis of failed slope". Canadian Geotechnical Journal, 8, 4, p. 596-599.
- Thomson, S. and Matheson, D. S., 1970a. "Clay pits in southeastern Alberta". Internal Soil Mechanics Note 7, Department of Civil Engineering, University of Alberta, September, 19 pp.
- Thomson, S., and Matheson, D. S., 1970b. "The Dunphy landslide". Internal Soil Mechanics Note 8, Department of Civil Engineering, University of Alberta, 7 pp.
- Timoshenko, D. and Goodier, J. N., 1970. Theory of Elasticity, McGraw-Hill, New York, 567 pp.
- Underwood, L. B., 1964. "Chalk foundations at four major dams in the Missouri River Basin". Transactions of the Eighth International Congress on Large Dams, Edinburgh, 1, p. 23-45.
- Underwood, L. B., 1967. "Classification and identification of shales". Journal of the Soil Mechanics and Foundations Division, ASCE, 93, SM6, p. 97-116.
- Underwood, L. B., Thorfinnson, S. T. and Black, W. T., 1964. "Rebound in redesign of Oahe Dam hydraulic structures". Journal of the Soil Mechanics and Foundations, ASCE, 90, SM2, p. 65-86.
- U. S. C. E., Omaha District (1946). "Garrison Reservoir, Missouri River Basin, North Dakota, Basis of Design, Definite Project Report," Vol. I and Appendix I, II and III, Omaha, Nebraska, February.
- U. S. C. E., Omaha District (1948). "Oahe Dam and Reservoir, Definite Project Report, Appendix III - Geology", Omaha, Nebraska, February.
- U. S. C. E., Omaha District (1949). "Gavins Point Reservoir, Definite Project Report, Appendix III - Geology", Omaha, Nebraska, December.





- U. S. C. E., 1951. "Engineering Manual, Part CXIX, Chapter 2". U. S. Government Printing Office, Washington, D. C.
- U. S. C. E., Kansas City District (1954). "Pomona Dam and Reservoir, Hundred and Ten Mile Creek, Design Memorandum Geology", Kansas City, Missouri, July.
- U. S. C. E., Kansas City District (1956). "Tuttle Creek Dam and Reservoir, Big Blue River, Kansas, Design Memorandum No. 6 - Geology" Kansas City, Missouri, January.
- U. S. C. E., Kansas City District (1957). "Pomme de Terre Dam and Reservoir, Hundred and Ten Mile Creek, Kansas, Design Memorandum No. 3. Geology", Kansas City, Missouri, January.
- U. S. C. E., Kansas City District (1961). "Milford Dam and Reservoir, Republican River, Design Memorandum No. 8", Kansas City, Missouri, April.
- U. S. C. E., Kansas City District (1962). "Stockton Dam and Reservoir, Sac River, Missouri, Design Memorandum No. 3", Kansas City, Missouri, May.
- U. S. C. E., Kansas City District (1963a). "Kaysinger Bluff Dam and Reservoir, Design Memorandum No. 4. - Geology", Kansas City, Missouri, July.
- U. S. C. E., Omaha District (1963b). "Bowman - Haley Dam and Reservoir, North Dakota, Design Memorandum BH-2, Omaha, Nebraska, October.
- U. S. C. E., Omaha District (1966). "Cottonwood Springs Creek Dam and Reservoir, Design Memorandum No. CS-12", Omaha, Nebraska, June.
- U. S. C. E., Huntingdon District (1969a). Beech Fork Lake, Twelvepole Creek, West Virginia, Design Memorandum No. 6 - Dam, Spillway and Outlet Works", Huntingdon, West Virginia, May.
- U. S. C. E., Kansas City District (1969b). "Smithville Reservoir, Little Platte River, Missouri, Design Memorandum 3 - Geology", Kansas City, Missouri, September.
- U. S. C. E., Kansas City District (1970). "Omega Lake, Vermilion Creek, Kansas River Basin, Kansas, Design Memorandum No. 2 - Appendix A - Geology", Kansas City, Missouri, October.





- Van Auken, F. M., 1963. "Shear Strength of clay shales found in the southwestern U. S. A." Proceedings of the Second Panamerican Conference in Soil Mechanics and Foundation Engineering, Brazil, 1, p. 255-288.
- Walters, R. C. S., 1962. Dam Geology, Butterworths, London, 335 pp.
- Ward, W. H., Burland, J. B., and Gallois, R. W., 1968. "Geotechnical assessment of a site at Mundford, Norfolk, for a large proton accelerator". Geotechnique, 18, p. 399-431.
- Ward, W. H., Marsland, A. and Samuels, S. G., 1965. "Properties of the London Clay at the Ashford Common shaft: in-situ and undrained strength tests". Geotechnique, 15, p. 321-344.
- Ward, W. H., Samuels, S. G. and Butler, M. E., 1959. "Further studies of the properties of London Clay." Geotechnique, 9, p. 33-58.
- Watts, W., 1906. "Geological notes on sinking Langsett and Underbank Concrete Trenches in the Little Don Valley". Transactions of the Institution of Mining Engineers, 31, p. 668-678.
- Westgate, J. A., 1965. "Surficial geology of the Cypress Hills Area, Alberta". Research Council of Alberta Preliminary Report 65-2.
- Whitmore and Associates, 1968. "Rocky Mountain House Dam-site A, Technical Memorandum". Submitted to the Water Resources Division, Alberta Government, June, 55 pp.
- Wiesner, W. R., 1969. "Residual shear strength of over-consolidated clay shales". Unpublished M.Sc. thesis, Department of Civil Engineering, University of Saskatchewan, 168 pp.
- Wilson, E. L., 1963. "Finite Element Analysis of Two-Dimensional Structures". Structures and Materials Research, Report 63-2, University of California, Berkeley.
- Wilson, S. D., 1970. "Observational data on ground movements related to slope instability". Journal of the Soil Mechanics and Foundations Division, A.S.C.E. 96, SM5, p. 1521-1544.
- Wilson, S. D., and Hancock, C. W., 1959. "Horizontal displacement of clay foundations". Proceedings of the First Pan-American Conference on Soil Mechanics, Mexico City, Mexico, 1, p. 41-57.



- Wood, A. M. M., 1971. "Engineering aspects of coastal landslides". Proceedings of the Institution of Civil Engineers, 50, p. 257-276.
- Wright, S. G., 1969. "A study of slope stability and undrained shear strength of clay shales". Unpublished Ph.D. thesis, University of California, Berkeley, California, 347 pp.
- Yudhbir, 1969. "Engineering behaviour of heavily overconsolidated clays and clay shales with special reference to long-term stability". Unpublished Ph.D. thesis, Department of Geotechnical Engineering, Cornell University, 161 pp.
- Yardley, D. H., 1951. "Frost-thrusting in the Northwest Territories". The Journal of Geology, 59, p. 65-69.
- Zaruba, Q., 1956. "Bulged valleys and their importance for foundations of dams". The Transaction of the Sixth International Congress on Large Dams, New York, 4. p. 509-515.
- Zienkiewicz, O. C. and Cheung, Y. K., 1967. The Finite Element Method in Structural and Continuum Mechanics, McGraw-Hill, London.







## APPENDIX A

### MISCELLANEOUS GEOLOGIC SECTIONS



A number of geologic sections gathered showed insufficient evidence of rebound to allow any estimate to be made of the amount of rebound which has occurred below the valley bottom. In some cases, however, some indications of rebound exist. These cases are included in this Appendix to provide information on sites where lack of sufficient drilling to define the amount of rebound which occurs or where insufficient lateral continuity of beds exists to allow correlation of strata between testholes.

1. Damsites in Alberta: Drilling records of seven damsites located in western Alberta, where the bedrock is the Tertiary Paskapoo formation, were studied. Six of these sites, as shown in Table A.1, showed such variation in bedding that no correlation of strata across a valley section was possible. The exception was Rocky Mountain House, Damsite A which has been previously discussed in Chapter III.

A typical stratigraphic centerline for a damsite in the Paskapoo formation is shown in Figure A-1. Horseguard Damsite is located approximately 10 miles southeast of Rocky Mountain House, Alberta (A.W.R., 1969b). No marker beds occur in the bedrock and a rapid and erratic variation between sandstone and shale occurs reflecting the continental depositional environment of this formation.

Two damsites located further east in the Edmonton formation showed some evidence of rebound, however, the absence of marker beds immediately below the valley bottom





precluded their use as case histories. Paddle River Damsite (P.F.R.A., 1965b) is located on the Paddle River about 80 miles northwest of Edmonton. Some 60 feet of alluvium and interglacial deposits have infilled the valley bottom. Insufficient drilling was done on the abutments to show evidence of valley flexure and the valley bottom testholes penetrated only the upper 20 feet of the bedrock below the valley where no marker beds were encountered. An apparent correlation of thin shale and sandstone beds shows about 3 feet of rebound has occurred below the 100 foot deep valley; this figure must be regarded as tentative due to the absence of a reliable stratigraphic correlation.

A similar situation exists at the Tomahawk Damsite (P.F.R.A., 1969c) located on the North Saskatchewan River about 10 miles downstream of Drayton Valley, Alberta. No marker beds occur immediately below river level although a tentative correlation of shale and sandstone layers indicates a rebound of some 6 to 8 feet has occurred below the 220 foot deep valley.

Horizontal separation of bedding planes between different bedrock units occurred repeatedly in the core at Tomahawk as at the Carvel and Hairy Hill sites as discussed in Chapter II. A general correlation of drilling-water losses and the degree of weathering of the fractures in the core was noted. High water losses occurred in testholes adjacent to the abutments where the core was badly weathered



TABLE A.1

## ALBERTA DAMSITES IN THE PASKAPOO FORMATION

Site	Location	Comments	Source
1. Rocky Site E	Junction of the Clearwater and North Saskatchewan Rivers, 5 miles upstream of Rocky Mountain House	No correlation of beds possible due to rapid lateral change in bedding	A.W.R.
2. Rocky Site A	North Saskatchewan River 10 miles downstream of Rocky Mountain House	Apparent uplift of beds below river	A.W.R.
3. Horseguard	Horsguard Creek 10 miles south-east of Rocky Mountain House	No correlation of beds possible	A.W.R.
4. McLeod January	McLeod River 12 miles north-east of Edson	No correlation of beds possible	A.W.R.
5. McLeod	McLeod River 15 miles upstream of Whitecourt	No correlation of beds possible, insufficient drilling	A.W.R.
6. Athabasca-Oldman	Athabasca River at Oldman Creek, 40 miles downstream of Hinton	Insufficient drilling	A.W.R.
7. Crossfield	SE $\frac{1}{4}$ -14-28-28-W4	No correlation of beds possible	A.W.R.







while in testhole RD7, located about 1500 feet back from the valley edge, only negligible water losses were reported and the core from this hole showed little evidence of weathering.

A series of borings were done in downtown Edmonton for a new bridge across the North Saskatchewan River immediately downstream of the existing 105th Street bridge. A stratigraphic section, courtesy of R.M. Hardy and Associates Ltd., is shown in Figure A.2. A relatively sharp upwarping of the beds under the south bank of the river channel is apparent.

Cameron Damsite Number 2 is located in east-central Alberta on Sounding Creek some 6 miles northeast of Youngstown. The entire centerline geologic section is given in Figure A.3. The bedrock is the Bearpaw formation (P.F.R.A., 1959b).

No marker beds are present but an anomalous rise of sandstone in the lower portion of the valley bottom testholes occurs. No evidence of the sandstone is found below the left abutment and left toe-of-slope. Thus, if the sandstone bed shown in the valley bottom testholes was initially flat-lying and continuous, some 4 feet of rebound must have occurred below this 40 foot deep valley. However, insufficient drilling has been done on this site to prove this point and the variation in bed contact elevation may be a depositional feature.



No correlation of beds was possible at Waterton Dam on the Waterton River in south-western Alberta (P.F.R.A., 1958) due to the absence of marker beds.

Data on the 19th Baseline Damsite on the Smokey River in northwestern Alberta, provided by R.M. Hardy and Associates Ltd., revealed no direct evidence of rebound due to absence of marker beds in the Wapiti formation.

The site is located about 3 miles north of the Highway 34 bridge across the Smokey River east of Grande Prairie, Alberta. The valley is about 500 feet deep and 1 mile across. The bedrock has a relatively low modulus of elasticity ranging from 3000 p.s.i. to 13,000 p.s.i. in consolidated-undrained triaxial tests. From the data presented in Chapter III it would appear that a relatively large amount of rebound should have occurred at this site although direct geologic evidence is not available.

Indirect evidence of the occurrence of rebound is present in the moisture-content profile shown in Figure A.4. Moisture contents were taken at six inch intervals and show a marked increase in moisture content at, or near, unit contacts as far down as 100 feet below river level. This increase in moisture content appears to be due to interbed slip due to folding associated with rebound.

2. Damsites In Saskatchewan: Damsites located in Saskatchewan where no evidence of rebound was observed were the







Belanger Creek Damsite in southwestern Saskatchewan (P.F.R.A., 1970a) and the Rafferty Damsite located on the Souris River in southeastern Saskatchewan (P.F.R.A., 1969d). Only a preliminary drilling program has been conducted on these two sites and insufficient drilling exists to detail the stratigraphy.

The South Saskatchewan River Dam (Gardiner Dam) has been discussed in Chapter II. No marker beds occur in the Bearpaw formation at this site and no evidence on the amount of rebound can be directly obtained. Observations made by Allan (1949) in the testdrift on the west side of the river have been previously discussed in Chapter III. The rise in what Allan termed "failure surfaces" towards the portal of the drift could reflect an upwarping of initially horizontal weak bentonitic layers along which slides or differential movements subsequently developed. This point is hypothetical and no direct measurement of the amount of rebound at this site is available.

3. Damsites In The United States: Three of the main dams on the Missouri River, Fort Peck, Garrison and Oahe, show definite indications of large amounts rebound which have occurred below the valley bottom. A fourth main dam on the Missouri, Gavins Point, is located about 6 miles upstream of Yankton, South Dakota. The bedrock at the site is the Niobrara Chalk overlying the Carlile shale (U.S.C.E., 1949).



Figure A.5 shows the location of several geologic sections through the right abutment of this dam. Figures A.6 and A.7 give these sections. A rise of 5 to 10 feet in the contact between the Niobrara chalk and the Carlile shale occurs as the contact is traced out from under the abutment. No equivalent sections are available for the left abutment at this site.

Unconfined tests gave an average unconfined compressive strength of 750 p.s.i. for the Niobrara chalk and 240 p.s.i. for the Carlile shale. The modulus of elasticity from these tests averaged 112,000 p.s.i. for the Niobrara chalk and 20,000 p.s.i. for the Carlile shale.

Profiles of nine damsites, located in Kansas and Missouri, which were investigated by the U.S. Army Corps of Engineers, Missouri River Division, were studied and are summarized in Table A.2. At two of the sites, Smithville (discussed in Chapter III) and Pomona, a gentle anticline occurs below the valley bottom. However, at several of the sites, Milford and Onega Lake Site 4, the bedrock is flat-lying and no evidence of rebound can be observed. The bedrock at most of these nine sites is interbedded shale and limestone of Permian to Pennsylvanian age. At several sites, where the bedrock is limestone, an anomalous folding and brecciation occurs in the bedrock. These features may be depositional in origin or due to tectonic stresses.







TABLE A.2

DAMSITES INVESTIGATED BY THE U.S. ARMY CORPS OF ENGINEERS  
IN KANSAS AND MISSOURI, SOUTH OF THE STUDY AREA

Dam Site	Bedrock	Reliability of Strati- graphic In- terpretation	Structure Visible
1. Smithville (U.S.C.E., 1969b)	Interbedded limestone and shale	Good	Gentle anticline below valley
2. Milford (U.S.C.E., 1961)	Interbedded shale and limestone	Good	Flat lying, no uplift visible
3. Stockton (U.S.C.E., 1962)	Limestone	Fair	Anomalous rolls in bedrock below left abutment
4. Kaysinger Bluff (U.S.C.E., 1969a)	Dolomite	Good	Local folds and breccia
5. Pomona (U.S.C.E., 1954)	Interbedded shale and limestones	Fair	Gentle anticline below valley, apparently 20 ft. of rebound
6. Tuttle Creek (U.S.C.E., 1956)	Interbedded shale and limestone	Fair	Gentle anticline below valley, apparently 20 ft. of rebound
7. Pomme de Terre (U.S.C.E., 1957)	Dolomite	Fair	Anomalous down- warping below left abutment
8. Omega Lake Site 4 (U.S.C.E., 1970)	Interbedded limestone and shale	Fair	Flat lying, no uplift visible
9. Omega Lake Site 1 (U.S.C.E., 1970)	Interbedded limestone and shale	Fair	Apparent up- warping in right abutment only



An example of these unusual features occurs at Kay-singer Bluff Damsite on the Osage River about  $1\frac{1}{2}$  miles north of Warsaw, Missouri (U.S.C.E., 1963a). The river valley at the site is about 200 feet deep and 5000 feet wide. Bedrock at the site is a moderately hard, finely crystalline dolomite limestone of the Cotter-Jefferson City formation (Ordovician). The stratigraphy of the site has been mapped by dividing the bedrock at the site into 26 lithologic units.

The regional dip of the bedrock is in the order of 20 feet per mile to the west-northwest. No major faulting or bedrock anomalies are described in the geologic literature of the area. However, the drilling program revealed two extensive breccia zones and minor folding under the valley bottom. Figure A.8 shows the contours drawn on a distinctive and persistent contact between units 18 and 19 in the bedrock sequence at the site. Several folds with a magnitude of 5 to 10 feet occur except in the right abutment where a rise of some 35 feet over a horizontal distance of 700 feet occurs. A fault was noted in one of the borings in this section of the profile. The existence of two other faults was inferred from the behaviour of the 18-19 unit contact as shown in Figure A-9.

Extensive breccia zones were found below the left and right abutments. These zones consist of hard angular rock fragments enclosed in a softer shale matrix. Breccia







in these zones contained zones of very soft clay, slickensides and numerous fractures. In addition, borings outside the major breccia zones showed a bedding-plane breccia, generally less than 1 foot in thickness, which was considered to be due to minor faulting or solutioning along bedding planes.

In view of the nature of the rocks at this site, it would appear that they exhibit a high modulus of elasticity. Therefore the amount of elastic rebound due to valley formation would be a fraction of one percent of the valley depth and it appears that stress relief could not explain the folds and breccia zones existing at this site. It is striking, however, to note that the two breccia zones occur below the abutments, a point where change in dip due to elastic rebound would be a maximum. Stress concentration due to valley formation would be a maximum at these points and the breccia zones discussed could be due to failure and plastic deformation of the weaker members of the bedrock. The presence of breccia along bedding-planes may be due to differential movements between beds.

The site is located on the northwest side of the long elliptical bedrock dome of the Ozark Plateau which has its long axis extending northeast-southwest. It appears possible the features illustrated could be due to high tectonic lateral stresses. It is interesting to note somewhat similar disturbance to the bedrock below valleys in



areas which are, or have been, engaged in mountain building - the Pennines, the Allegheny Plateau and the foothills of the Rocky Mountains.





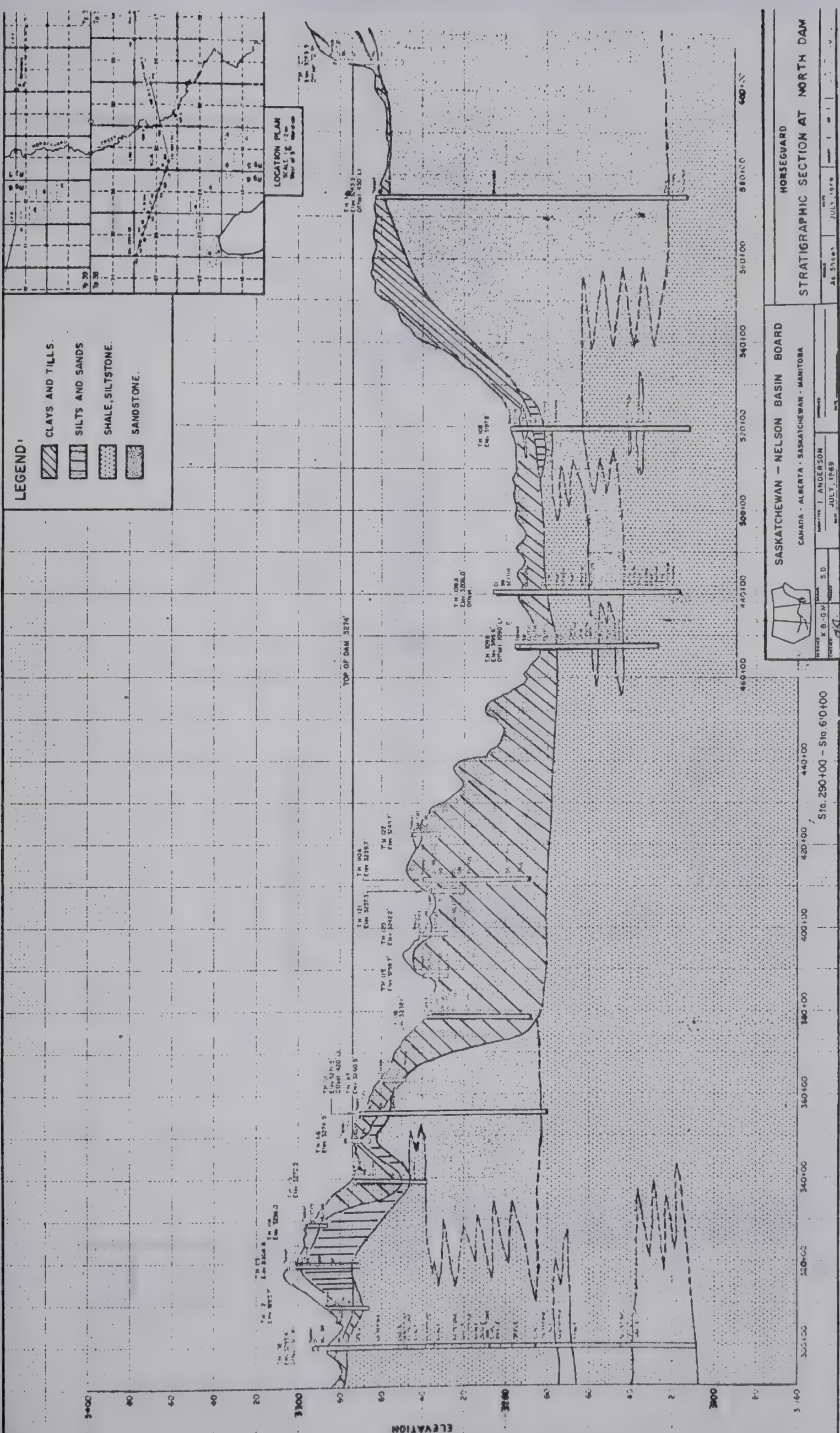


FIG. A.1 HORSESHOE DAMSITE GEOLOGIC SECTION



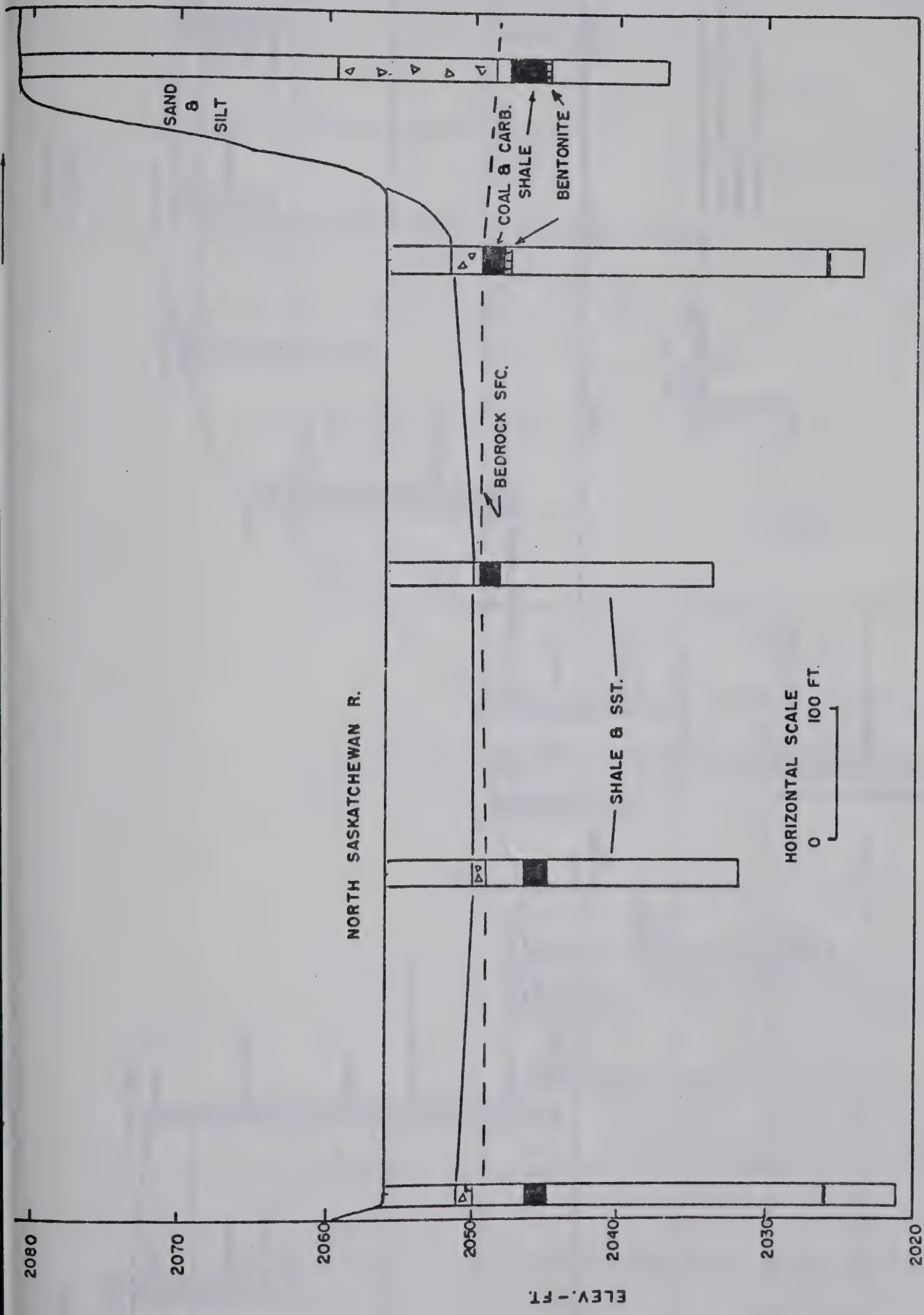


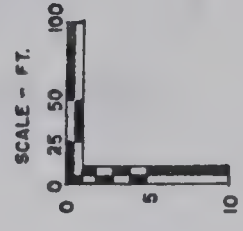
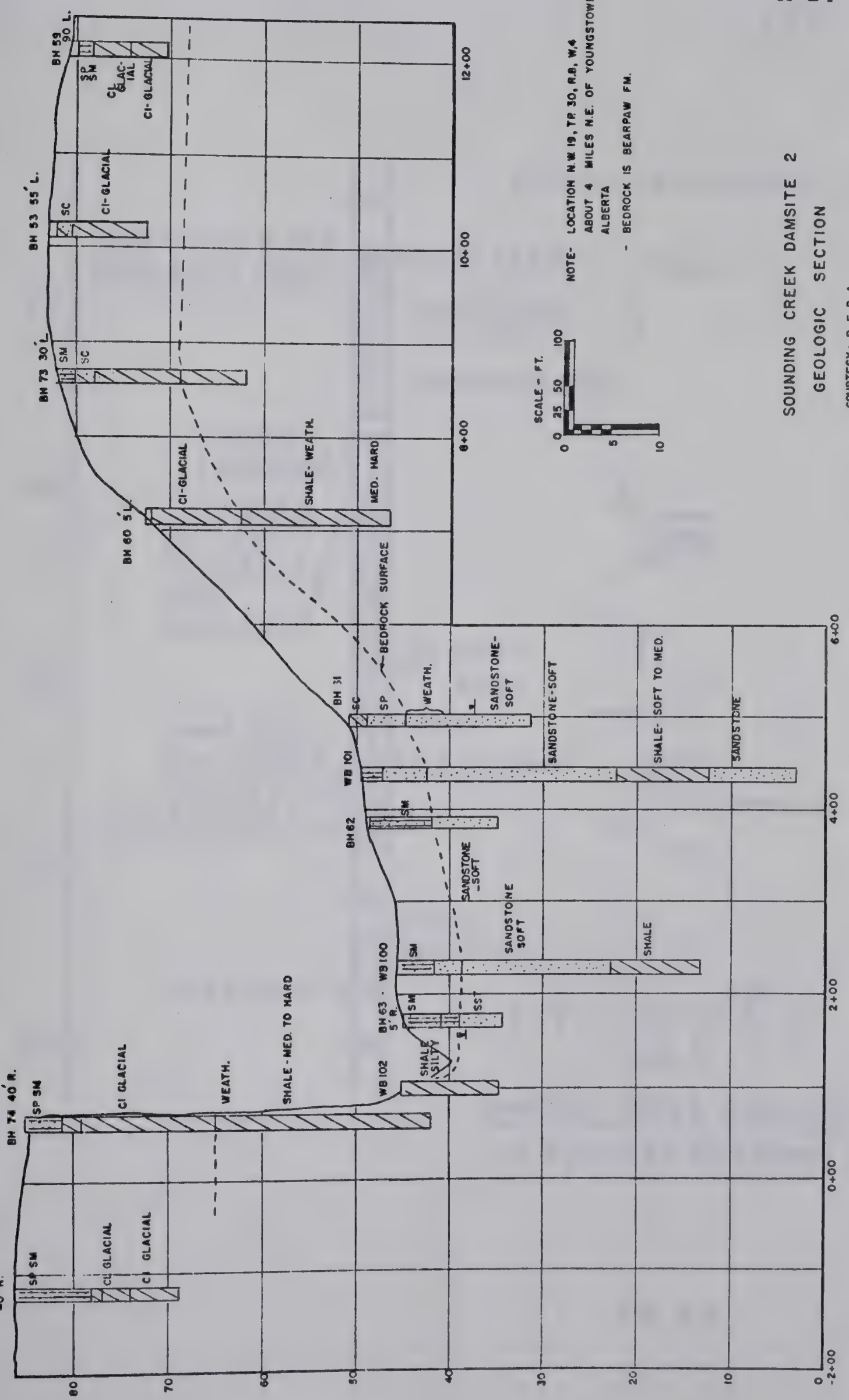
FIG. A.2 PROPOSED 105th ST. BRIDGE, EDMONTON ALBERTA (COURTESY R.M. HARDY & ASSOC.)





SOUTH 35° W

AM 96  
40' R.



NOTE- LOCATION N.W. 19, T.R. 30, R.B. W.4  
ABOUT 4 MILES N.E. OF YOUNGSTOWN  
ALBERTA  
- BEDROCK IS BEARPAW FM.

A-14

SOUNDING CREEK DAMSITE 2  
GEOLOGIC SECTION

COURTESY - P. F. R. A.

FIG. A.3



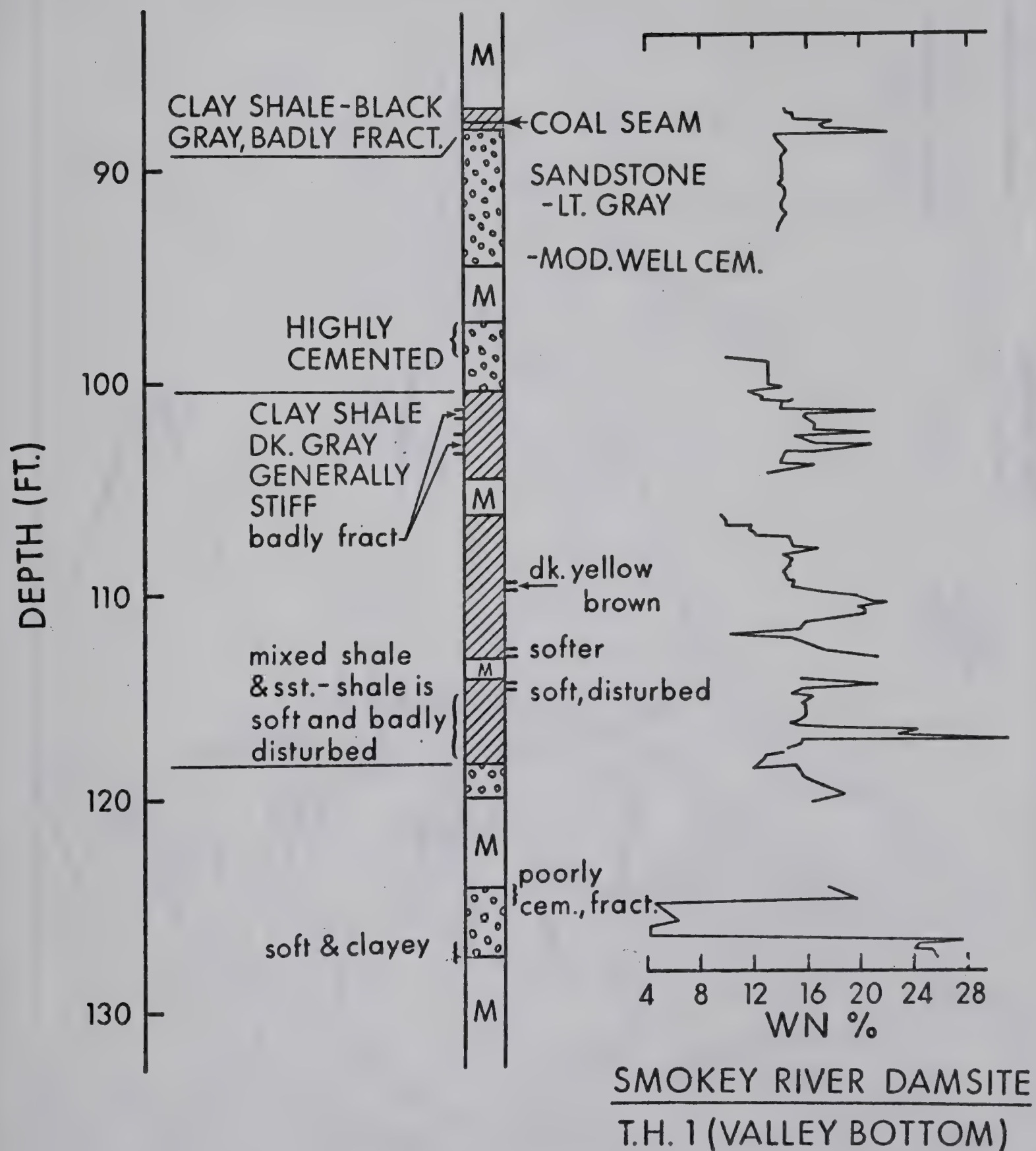


FIG. A.4





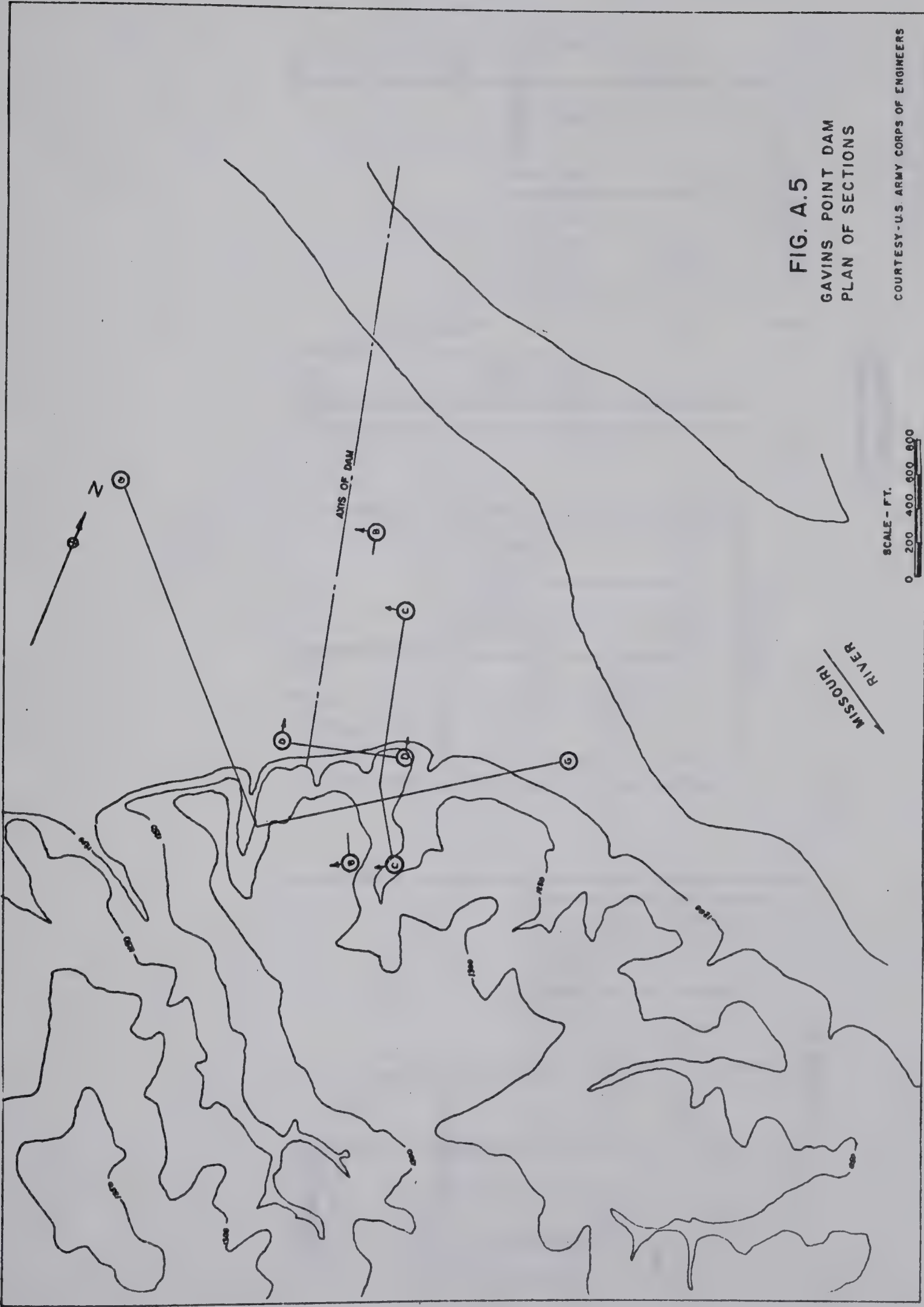
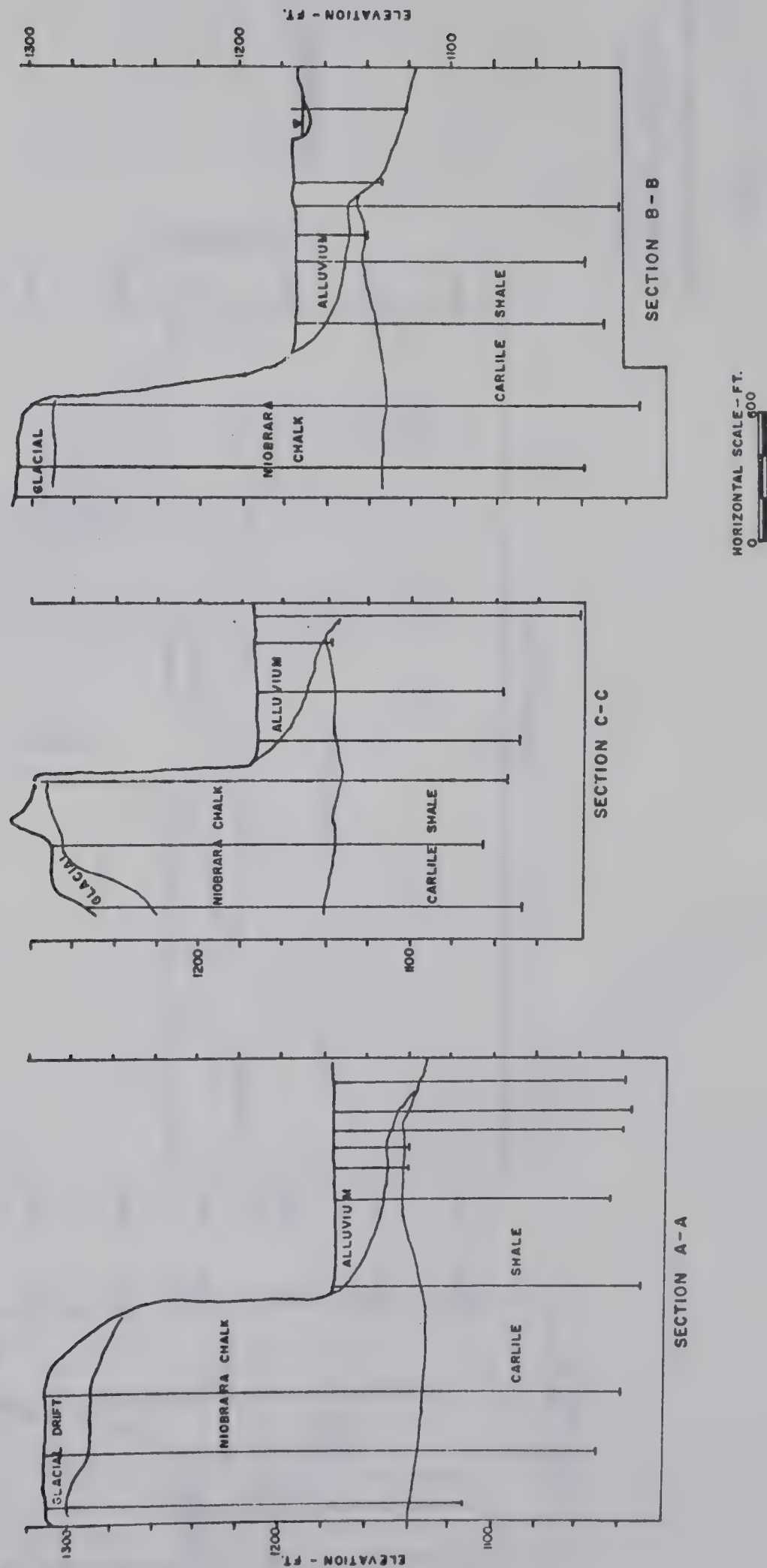


FIG. A.5  
GAVINS POINT DAM  
PLAN OF SECTIONS

COURTESY-U.S. ARMY CORPS OF ENGINEERS





GAVINS POINT DAM  
GEOLOGIC SECTIONS

FIG. A.6

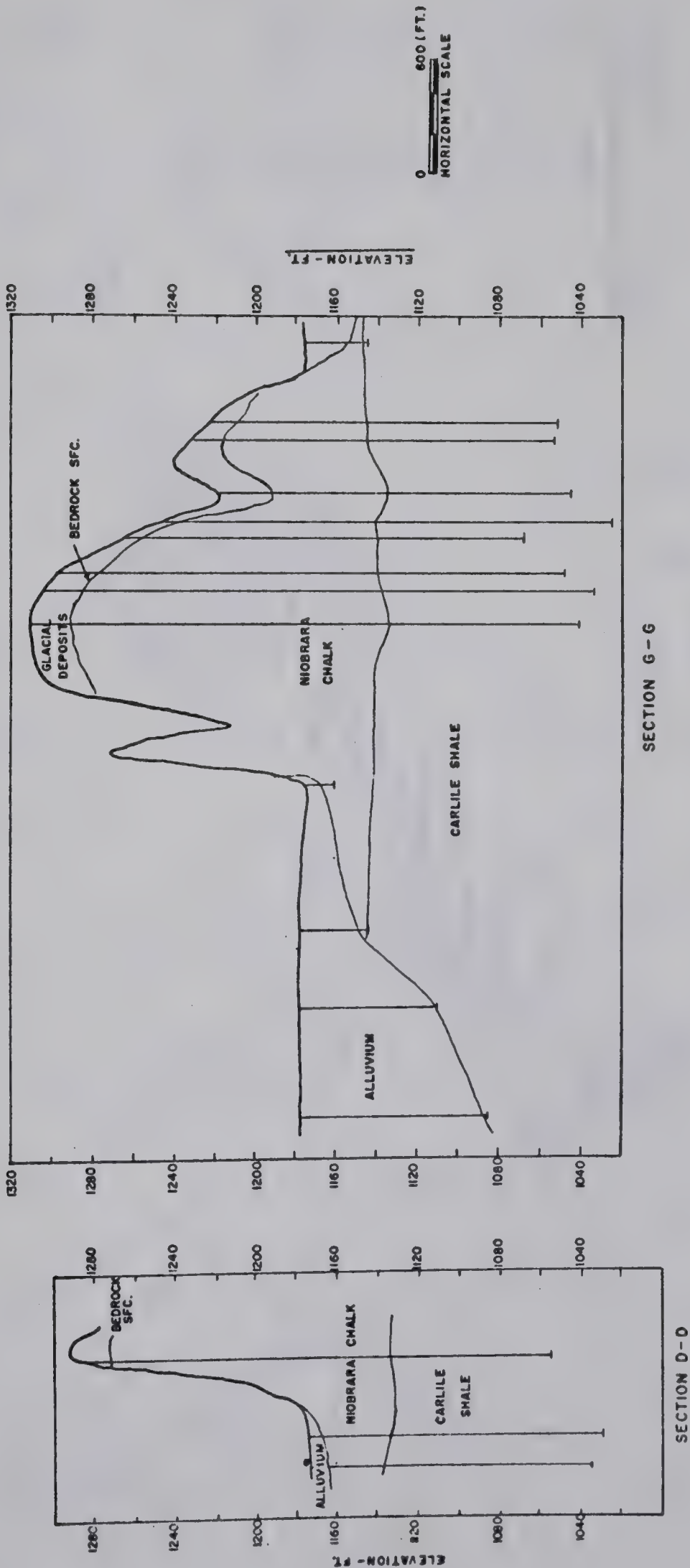




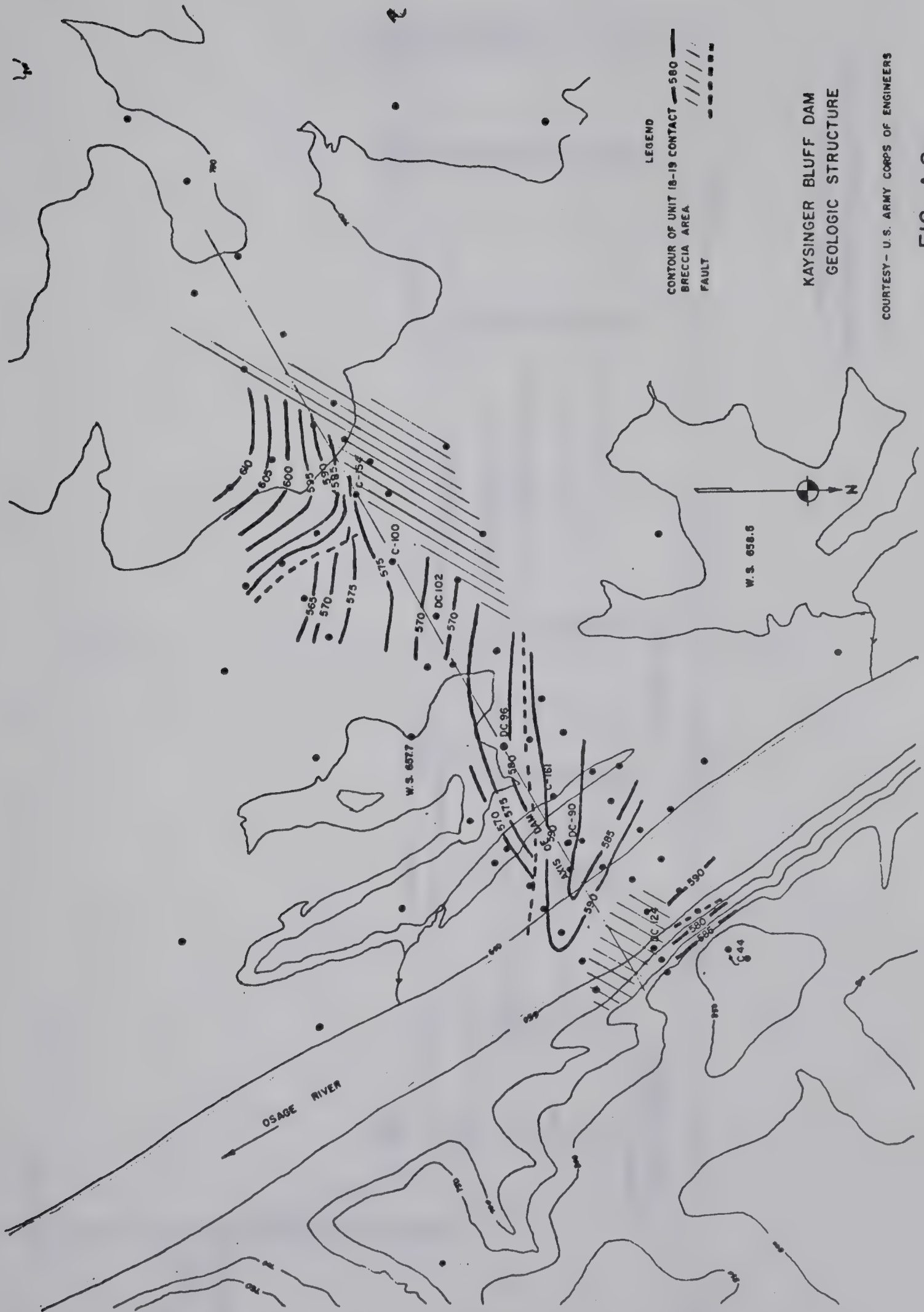
GAVINS POINT DAM  
GEOLOGIC SECTIONS

COURTESY - U.S. ARMY CORPS OF ENGINEERS

FIG. A. 7





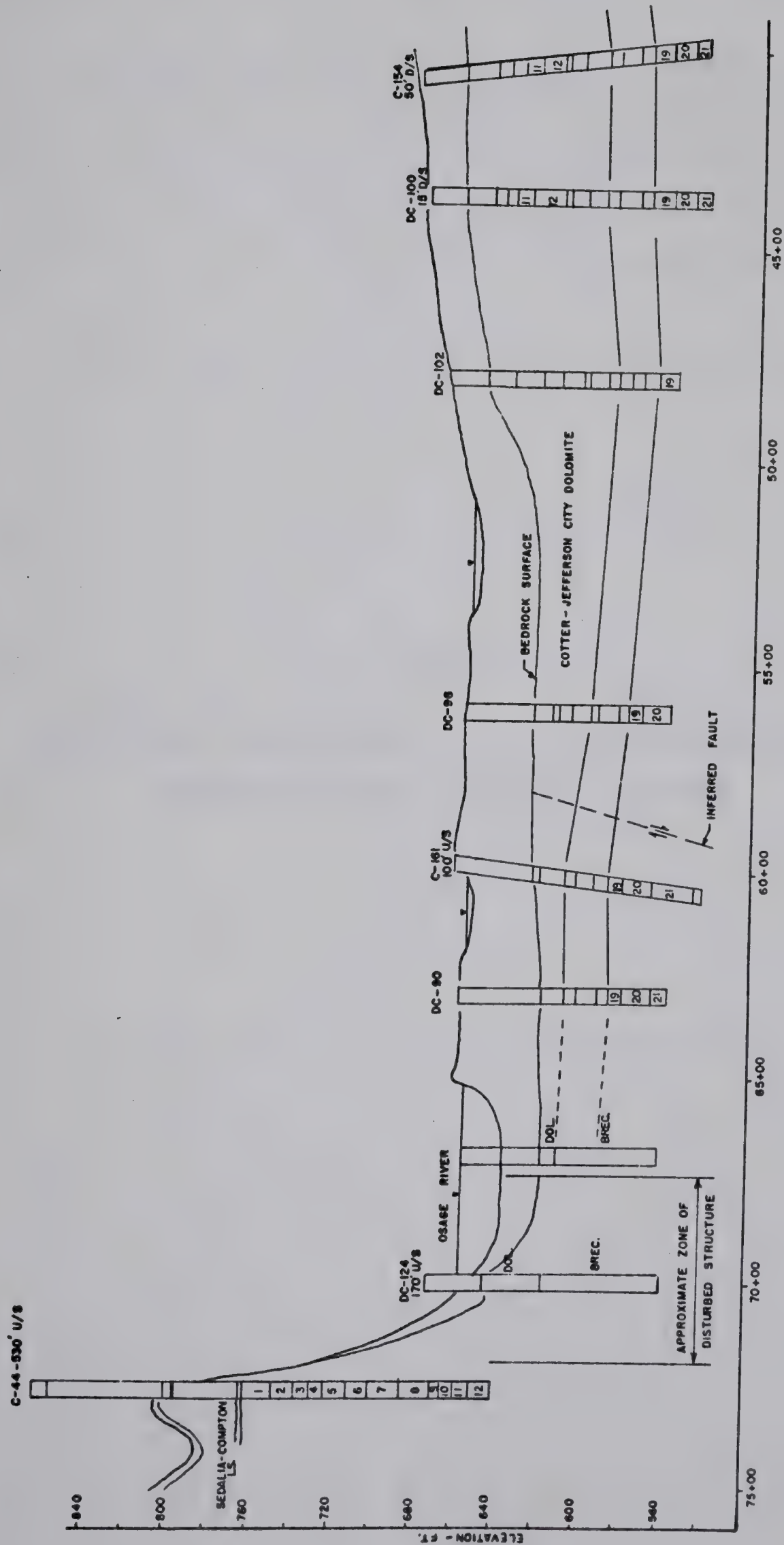


COURTESY - U.S. ARMY CORPS OF ENGINEERS

FIG. A.8







KAYSINGER BLUFF DAM  
VALLEY BOTTOM GEOLOGIC STRUCTURE

COURTESY U.S. ARMY CORPS OF ENGINEERS

FIG. A.9



APPENDIX B

GEOLOGICAL OBSERVATIONS AT THE JAMES MACDONALD AND  
BEVERLY BRIDGES, EDMONTON, ALBERTA





1. Introduction: During 1970-71 two bridges were constructed across the North Saskatchewan River in Edmonton, Alberta. The James MacDonald bridge was constructed across the river in downtown Edmonton immediately upstream of the existing Low Level bridge. The Beverly bridge is located about 200 yards upstream of the existing Highway 16 bridge in eastern Edmonton.

A few feet of alluvium overlies bedrock of the Edmonton formation (Upper Cretaceous) below the North Saskatchewan River in the Edmonton area. The bridge pier excavations were excavated from 7 to 14 feet into the bedrock below the bedrock surface and provided an excellent opportunity to view the bedrock below the river channel. One pier excavation was inspected at the James MacDonald bridge and three pier excavations and the west abutment excavation were inspected at the Beverly bridge.

2. Observations at the James MacDonald Bridge: Pier number 5, the east pier at the site, was excavated on October 7 and 8, 1970. The location of the site and the stratigraphic section across the channel are given in Chapter III of this thesis. The pier is located about 100 feet out into the channel from the east bank of the river. The pier excavation was carried out in two stages from inside an earth cofferdam. First, the alluvium and top few inches of bedrock was stripped from the base of the proposed pier. Then



two circular excavations about 25 feet in diameter were made using a backhoe and dragline some 14 feet into bed-rock. The rock was easily excavated and appeared to separate along pre-existing joints and fractures; very little disturbance to rock adjacent to the excavation appeared to result from the excavation procedure.

The sides and bottom of the pit were trimmed by hand using clay spades. Some two hours normally elapsed during this phase of the operation during which the rock on the walls of the excavation could be inspected and photographed. All strikes recorded are referenced to magnetic north; the declination of the magnetic north pole is about 23 degrees east in the Edmonton area. Values of rock hardness observed are referenced to the Panama Hardness Scale given in Table B.1.

(a) Observations in the south excavation: The south pit was excavated on October 7, 1971. The stratigraphy of the south wall of the pit is shown in Figure B.1. About 2 feet of alluvium overlay 6 feet of dark grey shale. Below the shale about 1.5 feet of fractured black carbonaceous shale forms a marker bed which was observed to dip at about 3 degrees to the northeast. Below the coal 2.7 feet of grey-green siltstone overlay 3.0 feet of grey, medium to coarse-grained sandstone. At the bottom of the excavation 0.6 feet of grey-green siltstone was visible. A view of the south face of this excavation is shown in Plate B.1.







The upper shale was fractured into blocks by three joint sets. The dominant set of joints occurred along horizontal bedding planes and were spaced at between 2 and 6 inches. Two steeply dipping joints striked at about  $N38^{\circ}$  and  $N30^{\circ}$  W. A sketch of the fracture pattern observed on the south edge of the pit is shown in Figure B.2.

The carbonaceous shale unit was badly fractured by predominantly horizontal joints at a 1 to 2 inch spacing. These joints were opened and provided most of the seepage into the excavation.

The siltstone below the carbonaceous shale was badly fractured on a 2 to 4 inch spacing. The upper 6 inches of the siltstone was very soft and pieces could be easily cut with a knife. The carbonaceous shale-siltstone contact was along an open softened joint in which a knife blade 3 inches long could be driven under very little pressure. The siltstone for about  $\frac{1}{4}$  inch below the contact was observed to be very soft and apparently disturbed.

A slickensided, polished surface was noted 1.3 feet above the bottom of the siltstone unit as shown in Plate B.2. The strike of this surface was  $N75^{\circ}W$  and the dip was  $13^{\circ}$  to the north. A knife blade could be easily driven into this fissure, along the slickensided surface, for several inches.

The upper 0.9 feet of the sandstone unit had horizontal joints spaced at  $\frac{1}{2}$  to 1 inch and was softer than



the lower portion of the sandstone. Several of these joints were open. The lower portion of the sandstone was intact with an occasional random joint. The 0.9 feet of rock visible below the base of the sandstone was hard and intact with an occasional random joint.

Seepage into the excavation appeared to be about 10 to 20 gallons per minute. Most of the seepage came from open joints in the carbonaceous shale and upper shale unit.

No detailed observations were made on the joints in the bedrock; however, it appeared the upper 10 feet of the bedrock had been disturbed by horizontal movement due to the presence of soft, open horizontal joints and the generally softer and more disturbed nature of the bedrock compared to the bottom 3 feet of sandstone and shale visible. The disturbed and badly fractured condition of the carbonaceous shale, siltstone and upper sandstone was anomalous as the top 6.2 feet of shale appeared hard and undisturbed despite the well developed jointing system previously described.

The softened joint in the sandstone unit defining the bottom of the apparent disturbance in the bedrock could be traced for about 10 feet along the south face of the pit; no attempt was made to follow this joint along the rest of the excavation periphery.

(b) Observations in the north excavation: The north excavation of pier 5 was inspected on October 8, 1970. The pit







dimensions and method of excavation were identical to the south excavation visited the previous day.

The stratigraphy exposed on the northwest side of the excavation is shown in Figure B.3. The stratigraphic sequence observed was very similar to that detailed in the south pit some 50 feet to the south. About 2 feet of alluvial gravels overlay 4.7 feet of dark grey shale. Below the shale 1.5 feet of black carbonaceous shale overlay 4.0 feet of medium grey sandstone. At the bottom of the excavation, 1.4 feet of dark grey siltstone was visible. The beds were observed to dip to the east-northeast at about 2 to 3 degrees.

The upper shale zone showed a prominent set of horizontal joints developed along bedding planes at 3 to 12 inch spacing. Two sets of near vertical joints occurred. On the northwest side of the excavation these joints strike at  $N70^{\circ} W$  and  $N40^{\circ} E$ . On the southeast corner of the excavation the joints were observed to strike at  $N20^{\circ} W$  and  $N60^{\circ} E$  and dip  $80^{\circ} W$  and  $85^{\circ} N$  respectively.

The horizontal joints in this unit were often characterized by a clay layer along the joints which consisted of 1/8 to 1/4 inch of soft, plastic clay which had a pocket penetrometer strength of about 0.5 t.s.f. and a moisture content slightly in excess of the plastic limit. These layers did not appear to be a depositional feature but due to differential horizontal movements between the shale units and were therefore termed gouge zones.



The upper portion of the shale unit was observed to have a 'nugget' structure and could be split into 1 - 2 inch pieces under moderate finger pressure along smooth, fresh, curved surfaces. This structure was present in the lower siltstone unit although not nearly as well defined.

The carbonaceous shale unit was highly fractured along predominantly horizontal bedding planes at 1 to 2 inch spacing. Joints occurred at other orientations but were continuous over several feet only. Vertical joints in this unit were not well pronounced and terminated on horizontal bedding plane joints.

The sandstone unit below the carbonaceous shale had a softened horizontal joint  $1/2$  to  $3/4$  inch wide located 1.9 feet below the top of the sandstone. Above this joint the sandstone appeared to be somewhat softened and disturbed as shown in Plate B.4. A few thin, poorly defined, tight near-vertical joints occur in the bottom section of the sandstone unit. These joints were difficult to trace over more than 1 or 2 feet.

The softened joint in the sandstone unit could be traced over the entire periphery of the pit. Pocket penetrometer readings on this layer varied from 2.5 to 3.5 t.s.f. while the sandstone either side had an estimated strength of more than 45 t.s.f.

The lower siltstone unit was hard with an occasional horizontal or steeply dipping joint. A thin gauge zone  $1/8$







inch thick occurred in this unit just above the excavation floor.

Seepage into the excavation was estimated at 5 to 10 gallons per minute with most of the seepage occurring through the badly fractured carbonaceous shale and along the top of the sandstone. Most of the joints in the upper shale were dry.

The disturbed and heavily jointed nature of the upper 8 feet of bedrock in this excavation indicated increasing movement of the bedrock with elevation. The soft horizontal clay-filled gouge zones were interpreted as field evidence of horizontal displacement across bedding planes. No measurement of joint offsets was possible as no unique set of vertical joints could be traced from one unit to the next.

### 3. Observations in the Pier Excavations at the Beverly

Bridge: The Beverly bridge site is located in eastern Edmonton about 500 feet upstream of the existing Clover Bar bridge which carries Highway 16 across the North Saskatchewan River. The river valley is approximately 140 feet deep and 1400 feet wide at this point. The river flows in a 700 foot wide channel against the west valley wall which shows evidence of near-surface slumping and has a natural slope of about 2:1.



Four piers were constructed for the Beverly bridge and are numbered from 1 to 4 from west to east. The site was visited periodically from July to October 1971 and observations on the bedrock were made in three of the pier excavations and the west abutment excavation.

(a) Pier 4 Excavation: Pier 4 is located near the east bank of the river channel and was the first pier constructed on the project. The pier excavation was made on August 4, 1971 and consisted of a pit approximately 60 feet long and 30 feet wide cut about 14 feet into the bedrock.

The stratigraphy exposed is shown in Figure B.4 and consists of 6 inches of soft, weathered, badly fractured coal overlying 1 foot of soft, fractured grey shale. The underlying bedrock consisted of 12 feet of medium grey, fine-grained sandstone. A dip to the east of about 3 degrees was visible. Prominent horizontal joints were observed developed along bedding planes spaced at 1 to 2 feet intervals and 2 sets of steeply dipping joints occurred which ran from one bedding plane to another. The vertical joints had smooth, slightly irregular surfaces and were tightly closed; a knife blade could not be pushed into them.

A number of the horizontal joints were characterized by softened gouge zones. On the northeast face of the excavation four of these zones occurred in the sandstone unit which could be traced over 10 feet along the excavation







wall. These zones were similar to those noted previously at the James MacDonald bridge and consisted of about  $\frac{1}{4}$  inch of soft plastic clay-like material which could be easily removed with the finger. The gouge at this site contained a fairly high proportion of sand and silt sized particles as it was gritty to the taste. Again, as at the other bridge, these zones did not appear to be a depositional feature.

On the west wall of the excavation a typical set of steeply-dipping joints had a strike of  $N45^{\circ} W$  and  $N43^{\circ} E$  and a dip of  $88^{\circ} E$  and  $81^{\circ} W$  respectively.

(b) Pier 1 Excavation: Pier 1 was the second pier constructed on this project and was inspected on August 30, 1971, several days after the concrete pier base had been poured, so that only the top few feet of bedrock was visible. Pier 1 is located near the toe of slope of the west valley wall.

The toe of a slide mass in the valley wall was exposed on the south (upstream) side of the excavation as shown in Plate B.5. The slide mass apparently moved out horizontally along the top of a black carbonaceous-shale bed some 5 feet below the riverbed and then rose up to the riverbed about 30 feet out from the toe of slope. Seepage along the failure surface and extensive brecciation of the bedrock immediately adjacent to the failure surface was noted.



The bedrock exposed on the west side of the excavation is shown in Figure B.5. The failure surface of the slide apparently lies some 4 feet above the base of this section and extensive brecciation of the bedrock results for some 18 inches below the base of the slide. Plate B.6 shows the intensive brecciation of the bedrock immediately below the failure surface on the east side of the excavation.

The effect of lateral stress relief due to excavation were visible along the west wall of the pit in the black carbonaceous shale unit. Blocks of carbonaceous shale were observed to have moved out along bedding plane joints from  $\frac{1}{4}$  to  $\frac{1}{2}$  inch towards the excavation as shown in Plate B.7.

Two steeply dipping joint sets occurred in the carbonaceous shale along with horizontal joints. The vertical joint set had strikes of  $N35^{\circ} E$  and  $N48^{\circ} W$  and dips of close to 90 degrees.

Seepage into the excavation was about 10 gallons per minute mainly from the south and southwest walls of the excavation along the slide failure surface. A slickensided surface was noted on the bottom of the bentonite seam below the carbonaceous shale unit on the west wall of the excavation.

A marked dip to the west occurs in the beds at this spot. The top of the carbonaceous shale outcropped at elevation 1995.3 (geodetic) on the east side of the pit while on the west side, over a distance of 40.2 feet horizontally, the outcrop elevation was 1994.5.







(c) Pier 2 Excavation: The excavation for pier 2 was inspected on September 8, 1971. The stratigraphy exposed and features observed in this excavation have been discussed in Chapter III.

A detailed inspection of the lower gouge zone in the southeast corner of the pit showed two thin clayey zones separated by a  $\frac{1}{2}$  inch thick layer of brecciated sandstone. A minor amount of seepage was noted occurring from this lower gouge zone. A general view of the excavation is given in Plate B.8.

(d) Pier 3 Excavation: The pier 3 excavation was inspected on October 19, 1971. The stratigraphy exposed is shown in Figure B.6 and consists of 0.6 feet of black coal fractured into 1 to 2 inch pieces immediately underlying the riverbed alluvium. Below the coal 3.2 feet of grey, moderately fractured siltstone overlay 6.3 feet of light grey, fine grained sandstone. A softened gouge zone occurred at the siltstone-sandstone contact and five more gouge zones were observed in the sandstone on the east face of the excavation.

A block sample was removed from the east wall with its upper surface forming the bottom of one of the gouge zones. No slickensides were observed in the field but, after drying in the laboratory, a distinct polish was observed on the sandstone - gouge zone contact.



#### 4. Observations in the West Abutment Excavation, Beverly

Bridge: An excavation some 40 feet long, 50 feet wide and 10 feet deep was made into the bedrock for the west abutment of the bridge. The excavation was first visited on July 27, 1971 and several subsequent visits were made to record further observations as construction progressed. Previous to the pier excavation some 30 feet of overburden had been removed by the construction of an approach cut to the bridge site.

A view of the north wall of the excavation is shown in Plate B.9 and a field sketch of the bedrock exposed is shown in Figure B.7. The failure surface of an apparently recent landslide is visible in the excavation near the valley wall as is evidence of faulting and a fossil landslide apparently dating back to the time of valley formation. Evidence of bedrock disturbance extends for about 15 feet back from the present valley wall.

The geology exposed on the south wall of the excavation, 50 feet to the south of the section previously discussed, is markedly different as shown in Figure B.8 and Plates B.10 and B.11. A block of dark-brown shale has apparently been upthrust immediately adjacent to the valley edge.

A sharply defined 2 to 3 inch thick bentonite bed was exposed near the base of the south side of the excavation. A well developed downward "smear" of bentonite





marked the intersection of the bentonite layer with a fossil near-surface landslide as shown in Figure B.8 and Plate B.12. The occurrence of bentonite being displaced along a slide failure surface has been noted previously in the Cretaceous bedrock of the study area (Thomson and Matheson, 1970b). A similar downdragging of the bentonite layer was noted on the rear of the shale block, as shown in Figure B.8, thus indicating this graben-like feature was formed by differential vertical movement.

Slope-flattening work during August and September showed several interesting features. Flattening of the slope immediately below the abutment excavation revealed the failure surface of the landslide along some of the slope as shown in Figure B.9. Down-dragging of coal from a 2 foot thick coal seam located about  $3/4$  of the way up the slope was revealed showing powdered coal included in the failure surface for greater than 20 feet below the outcrop elevation.

A block sample was cut from the bentonite layer on the south face of the excavation about 6 feet back from the slide scarp. A detailed examination of the block sample was made in the laboratory as will be detailed in the next section of this appendix. The site was visited on October 19, 1971 and a close examination was made of the bentonite seam exposed on the north face of the excavation some 6 feet back from the failure scarp. The bentonite had dried



and two well developed, smooth, flat, slickensided surfaces were observed with the slickensides and striae pointing east-west towards the river. These surfaces occurred at the top and bottom contacts of the bentonite layer.

A survey of airphotos showed no signs of slide activity or disturbance of the ground surface back from the valley edge. The disturbance in the abutment excavation is obvious from the data presented and three mechanisms appear probable.

1. The disturbance is due to the near-surface landslide activity developed along the valley wall.
2. The disturbance is due to stress relief associated with valley formation.
3. The disturbance is due to coal mining activity and caving of mine workings located back from the river bank.

The observations made in Pier 1 indicate that brecciation and disturbance of the bedrock occurs for a distance of about 18 inches from the failure surface. It would appear unlikely that the slide activity would cause the faulting noted in the bedrock for over 6 feet back from the failure surface.

The disturbance of the beds may be due to valley formation. The features noted on the north side of the excavation are step-faults and appear to roughly parallel







the existing valley wall. These features may have initially been tension fractures although the downward movement towards the valley cannot be explained by this single mechanism. It is of interest to compare these features with the step-faults, detailed by Sandeman (1918) at the Derwent Dam, which have been discussed in Chapter III.

Numerous coal mines have been worked along the North Saskatchewan River and examples of subsidence are given by Taylor (1971). At the site of the Beverly bridge, mine workings are shown to be continuous along both sides of the river (Taylor, 1971, p. 19-20) with mine workings extending back over  $\frac{1}{2}$  mile from the valley's edge. The west abutment of the Beverly bridge falls close to the intersection of two mines - number 1167 abandoned in 1942 and number 9 abandoned in 1923 - and reference is made to old workings found in drift entries along the river bank.

Caving of mine workings located some distance in from the valley wall would explain the anomalous features noted on the south abutment excavation wall with the dark brown shale mass being intact rock with the material landward of it having subsided. The north face of the excavation would then presumably be intact bedrock and not underlain by caved mine workings.

5. Observations on Block Sample, Beverly Bridge: Previous to cutting the block sample from the bentonite layer on the



south side of the excavation on July 27, 1971, a pocket penetrometer profile was taken across the bentonite layer in the field. The block sample was removed to the laboratory and dissected on July 29, 1971.

The observations made and natural moisture contents are shown in Figure B.10. Two flat, slickensided surfaces with well developed striae occurred on the top and bottom bentonite-shale contacts. Secondary failure surfaces occurred immediately above the top of the bentonite layer and in the center of the bentonite layer. These surfaces were smooth, slickensided and continuous over the entire length of the sample for some 12 inches. The surfaces were 'wavey' with an amplitude of about  $\frac{1}{2}$  inch. No striae were observed on them.

The shale above the bentonite layer was badly fractured with the degree of fracturing increasing with depth until the bentonite layer was reached. The shale above the bentonite for approximately 1 inch was softened into a soft brown clay as shown by the water content profile in Figure B.10. A decrease in moisture content with depth occurred through the bentonite layer with the highest moisture content, and lowest pocket penetrometer strength, immediately below the top bentonite-shale contact.

A close examination of the bentonite showed small, hard shale pebbles, up to  $\frac{1}{16}$  inch in size, embedded throughout the bentonite layer. Small pieces of pure







bentonite were observed in the upper softened shale above the bentonite layer up to  $\frac{1}{4}$  inch from the bentonite-shale contact. The shale for about  $\frac{1}{2}$  inch below the bentonite layer was brecciated into hard,  $\frac{1}{8}$  inch pieces which often had a thin bentonite coating.

6. Groundwater Conditions in the West Abutment, Beverly

Bridge: The preliminary inspection on July 27, 1971 showed an anomalously high water table at the site with seepage discharging from the slope some 20 to 30 feet below the valley crest. In October, 1971 a bench was constructed across the slope some 30 feet below the abutment which exposed the 2 foot thick coal seam shown in Figure B.9 and a portion of a slide failure surface. The slide surface, at this point, occurred along the contact between the coal seam and an overlying bentonite seam which varied from 1 to 3 inches in thickness. An actual down-warping of about 16 degrees was observed in the coal-bentonite contact at this point which appeared due to the landslide. The coal was well jointed but practically no seepage was observed from this bed along the 100 feet of outcrop visible.

A pit had been excavated about 20 feet upslope from the bench. Several inches of free water were visible in the bottom of this excavation which was estimated to be 7 or 8 feet deep and did not reach the coal seam. These



observations, coupled with the moisture contents noted in the bentonite seam, show that the bentonite layer was acting as a perfectly impervious cutoff and had a marked effect upon the groundwater conditions in the valley wall by causing a perched water table to form.

Bentonite layers often occur in conjunction with coal layers in the Edmonton formation. When they occur below a coal layer the superincumbent fractured coal acts as a drain and very little build-up of hydrostatic pressure occurs. A bentonite layer above a coal seam has the opposite effect and perched water table forms above the bentonite layer.

7. Results of Laboratory Testing: Samples of bedrock from the pier excavations at the Beverly bridge were tested to determine the index properties of the gouge zone material and the bedrock immediately above and below the softened zone. Samples were taken from the lower gouge zone in the southwest corner of the pier 2 excavation and from a gouge zone on the east side of the pier 3 excavation about 4 feet up from the pit floor.

A two pound bag sample of the softened gouge zone material was removed along a one foot section of the pit wall. A similar sample was taken immediately above and below the gouge zone. The liquid limit, plastic limit and gradation of each of the samples was found by standard soil testing procedures (A.S.T.M., 1958).





The Atterberg limits of the samples are shown in Table B.2. Results from the gouge zone lie between those from the bedrock above and below the zone; the range of results is small and indicates the softened material in the gouge zone has the same composition as the rock either side of the zone. The results of the hydrometer analyses, shown in Figure B.11, show a very similar grain size curve for material above, below and from the gouge zone. Thus, the softened bedding planes do not seem to be depositional in origin but rather appear to have resulted from lateral movement across horizontal bedding planes.

The results of the hydrometer analyses shown in Figure B.11 classify the bedrock as a coarse siltstone rather than a fine grained sandstone as it was described in the field.

TABLE B.2

## ATTERBERG LIMITS ON SAMPLES FROM THE BEVERLY BRIDGE

Site	Sample Location	W <sub>L</sub> %	W <sub>p</sub> %
Pier 2	Above gouge zone	57.2	24.3
	Gouge zone	66.8	26.2
	Below gouge zone	68.0	24.4
Pier 3	Above gouge zone	53.0	23.5
	Gouge zone	68.9	26.5
	Below gouge zone	70.2	27.4



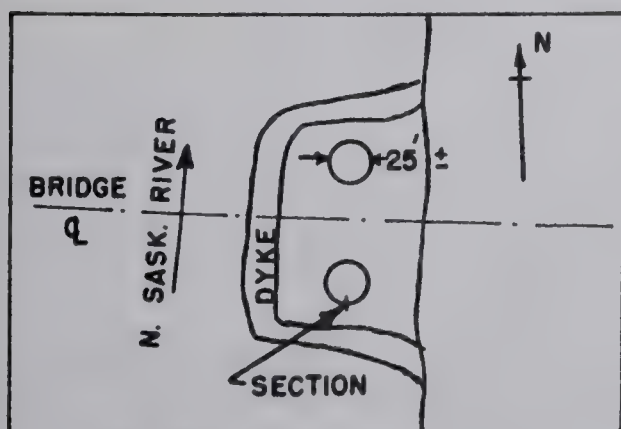
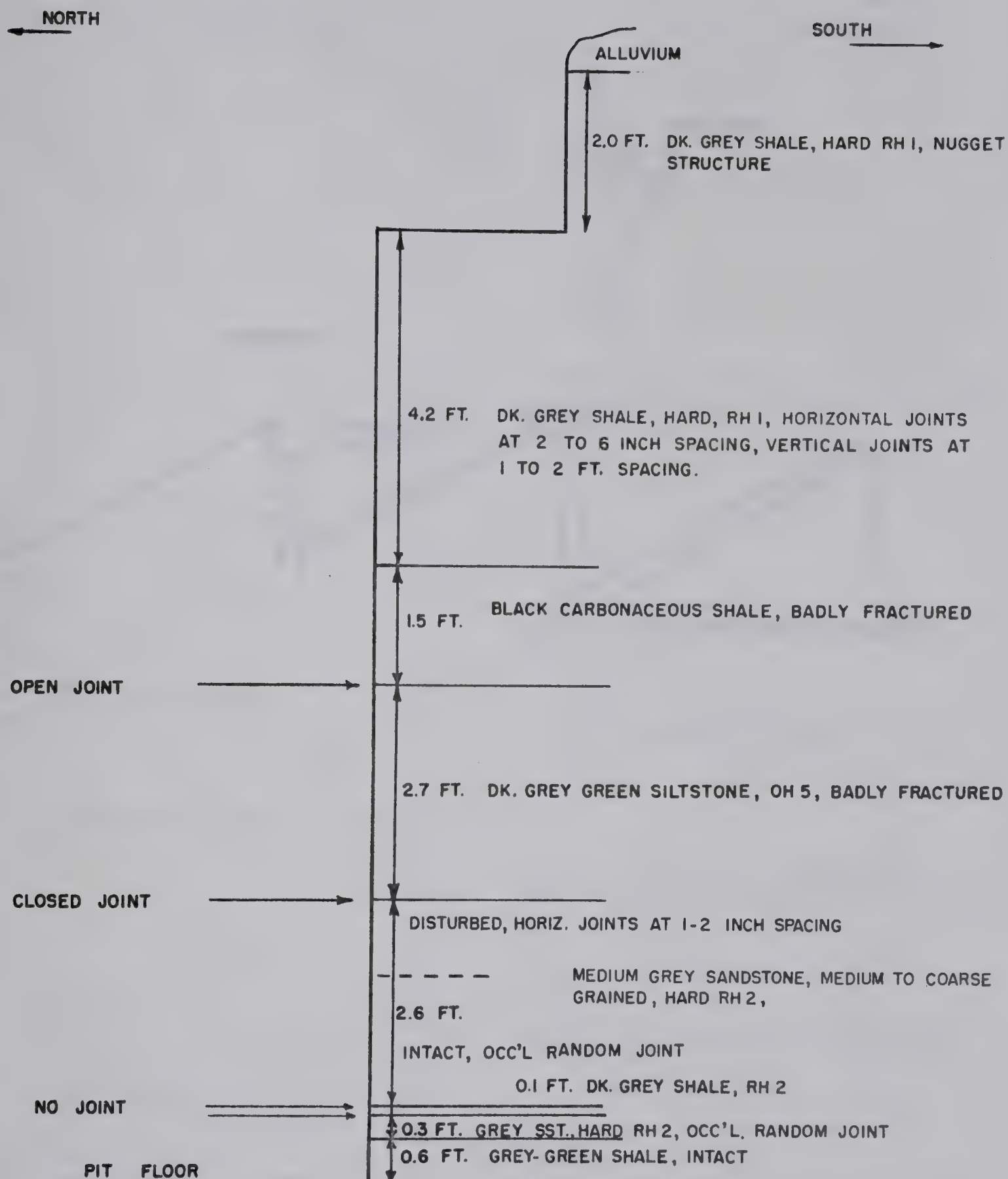
TABLE B.1

## DEFINITION OF THE PANAMA HARDNESS SCALE

Overburden		Pocket Pen- etrometer (P.P.) T.S.F.
OH-1	Easily squeezed through fingers. Consistency of fresh putty.	0-2
OH-2	Easily indented with finger point at moderate pressure.	2-10
OH-3	A pencil point can be readily pushed into sample.	10-20
OH-4	Difficult to take drive sample. Difficult to punch pencil point into sample.	20-30
OH-5	Material of near rock character.	30-40
Rock		
RH-1	Slightly harder than very hard overburden, rock-like character but crumbles or breaks easily by hand (some clay-shales and uncemented sandstones).	40-45
RH-2	Cannot be crumbled between fingers but can be easily picked with light blows of the geology hammer. (Some shales and slightly cemented sandstones and conglomerates.)	45 +
RH-3	Can be picked by moderate blows of geology hammer. Can be cut with knife.	
RH-4	Cannot be picked with geology hammer, but can be chipped with moderate blows of hammer.	
RH-5	Chips can be broken off only with heavy blows of the geology hammer.	





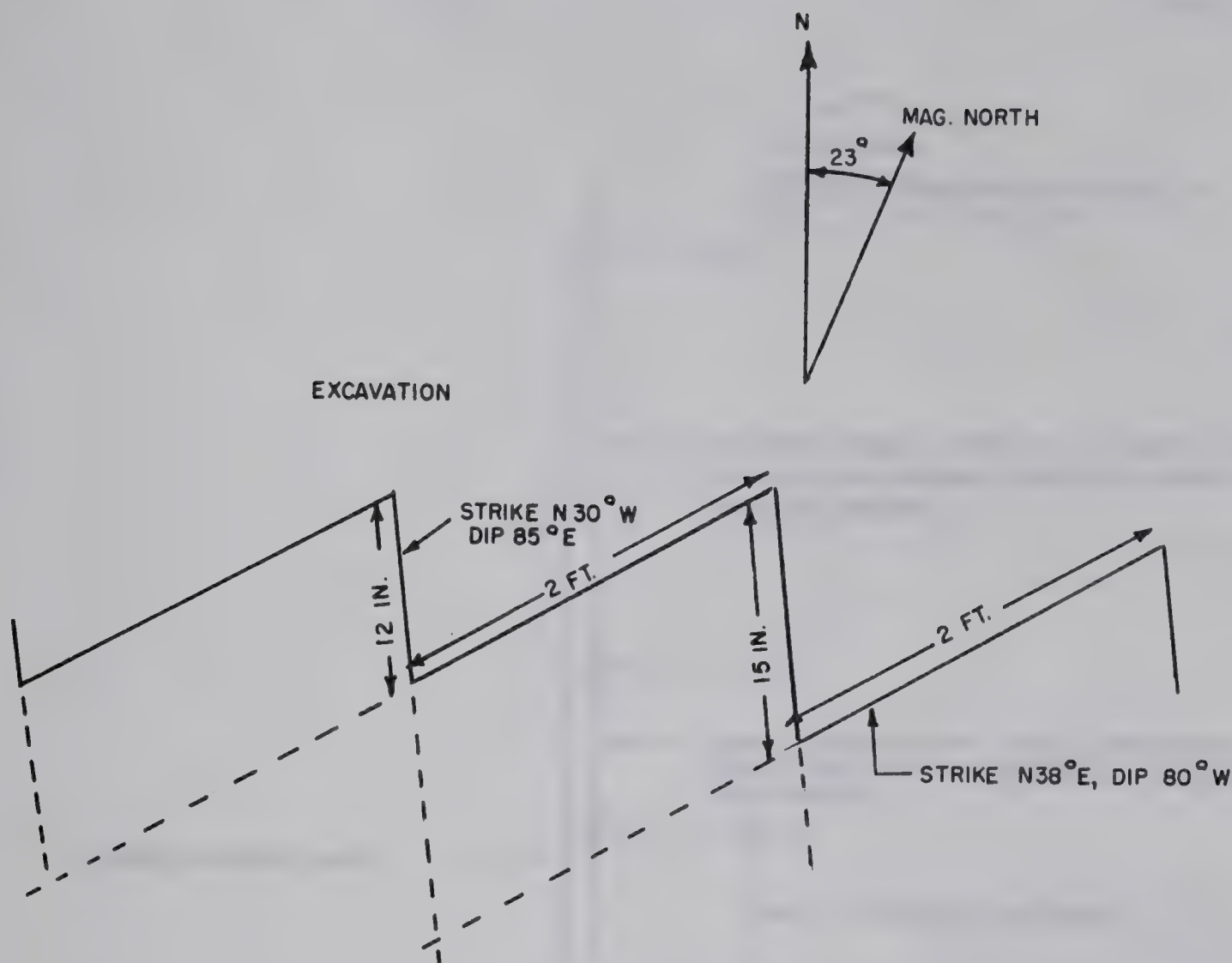


LOCATION SKETCH

STRATIGRAPHIC SECTION, EAST PIER  
EXCAVATION, JAMES MACDONALD BRIDGE

FIG. B.1



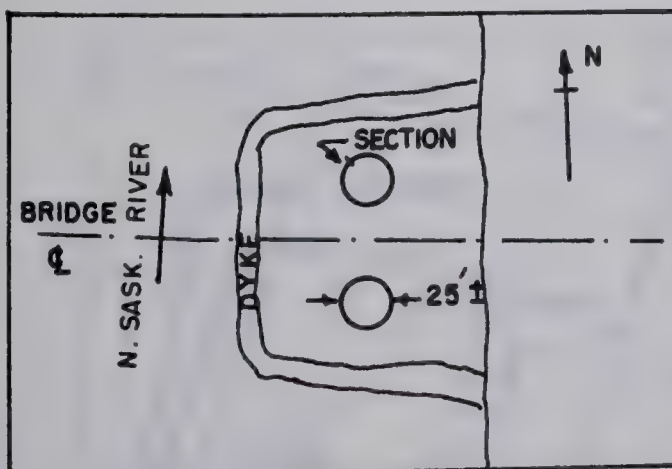
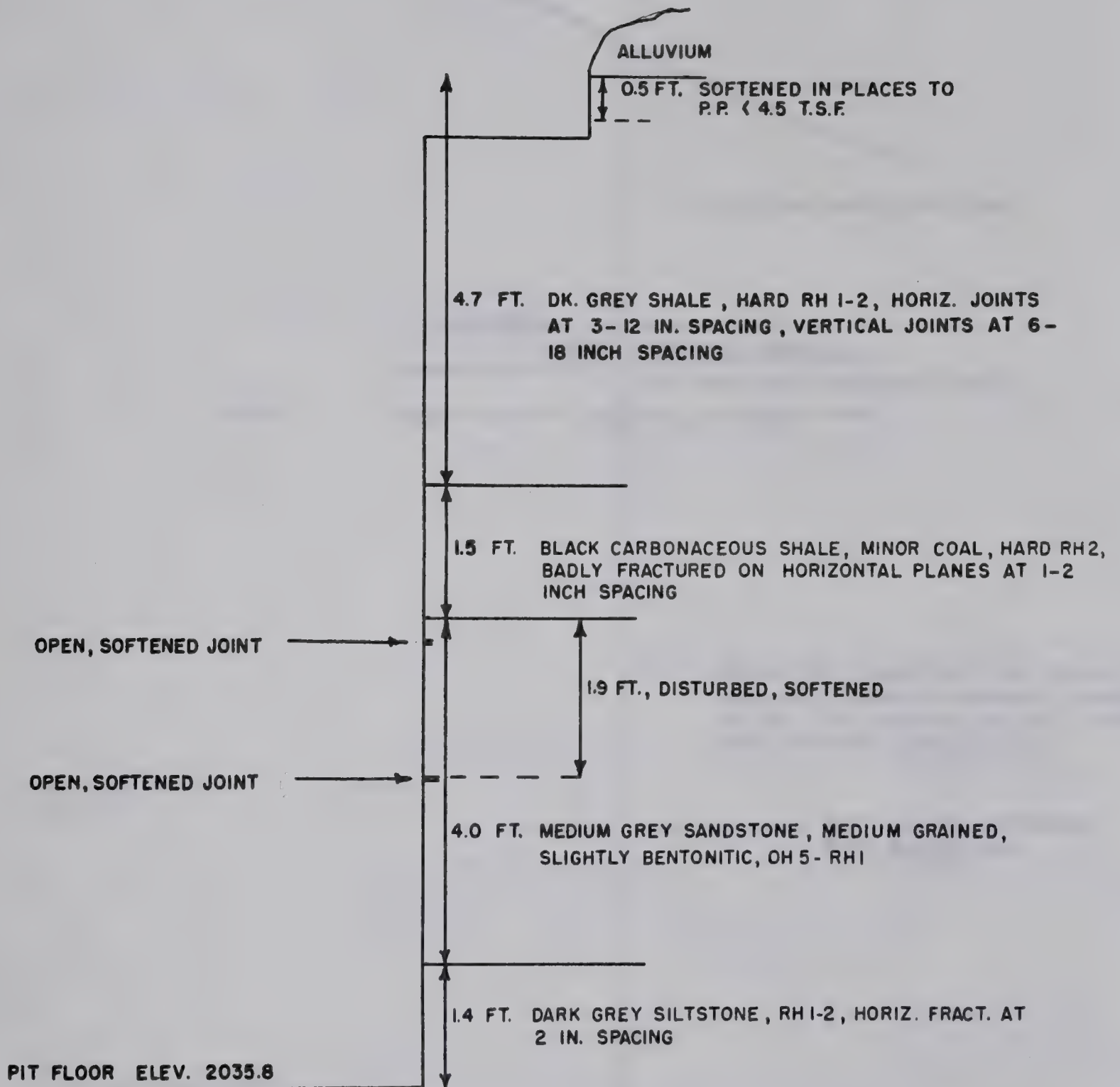


PLAN OF VERTICAL JOINT SET, SOUTH  
EDGE OF PIER 5 EXCAVATION, JAMES  
MACDONALD BRIDGE

FIG. B.2





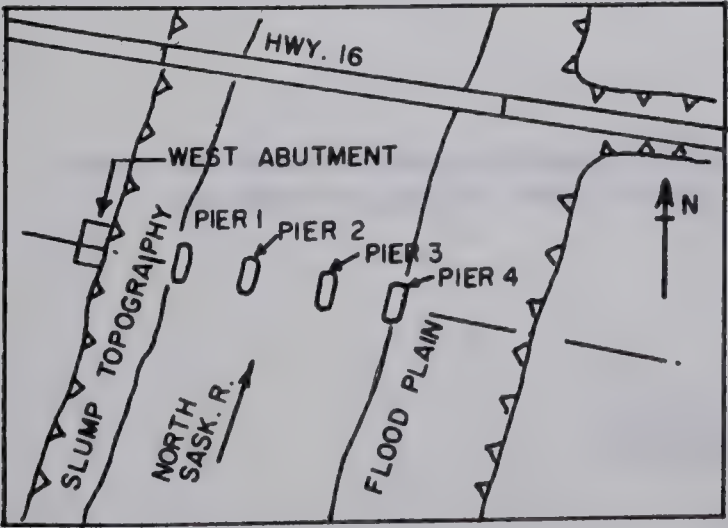
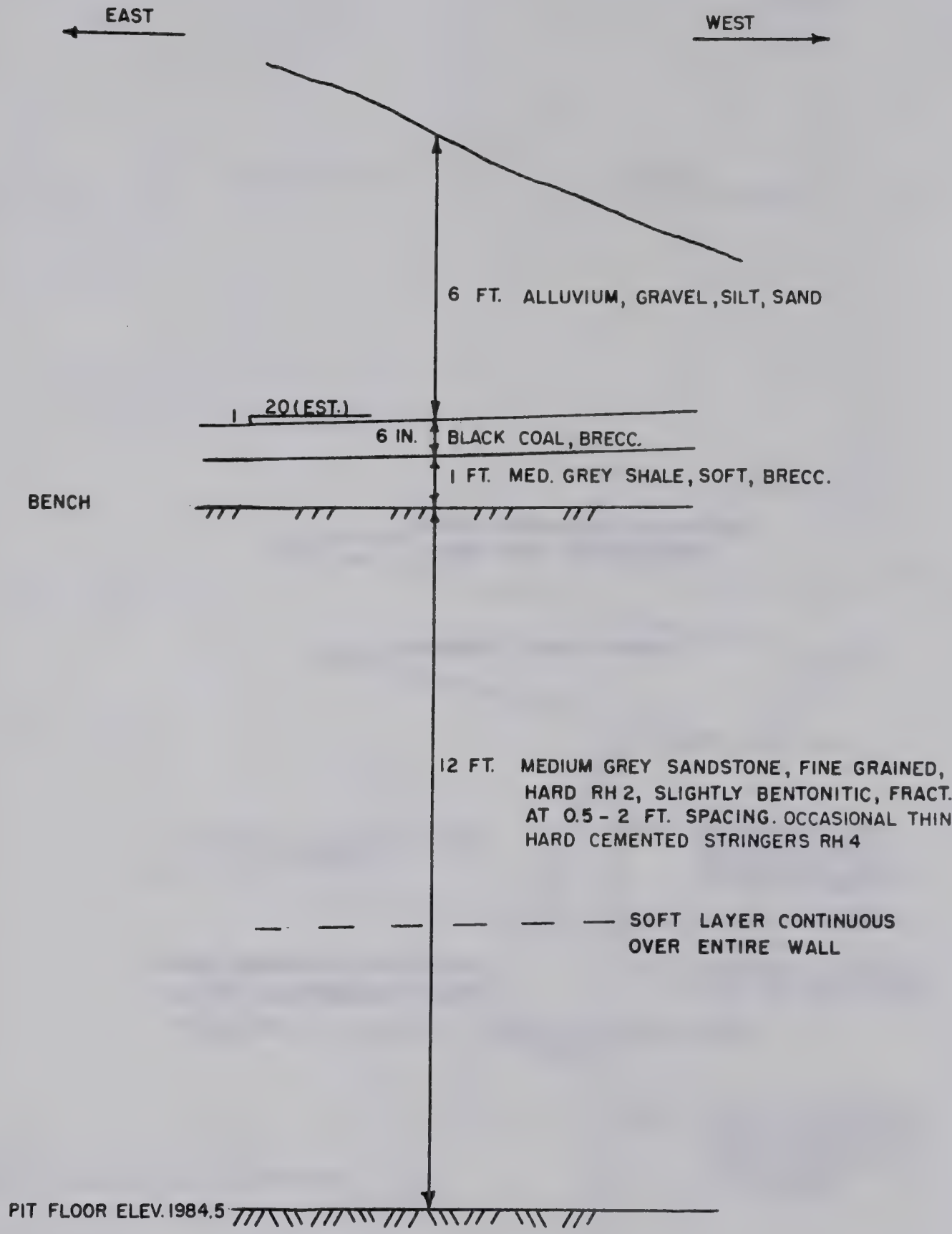


LOCATION SKETCH

STRATIGRAPHIC SECTION, EAST PIER  
EXCAVATION, JAMES MACDONALD BRIDGE

FIG. B.3





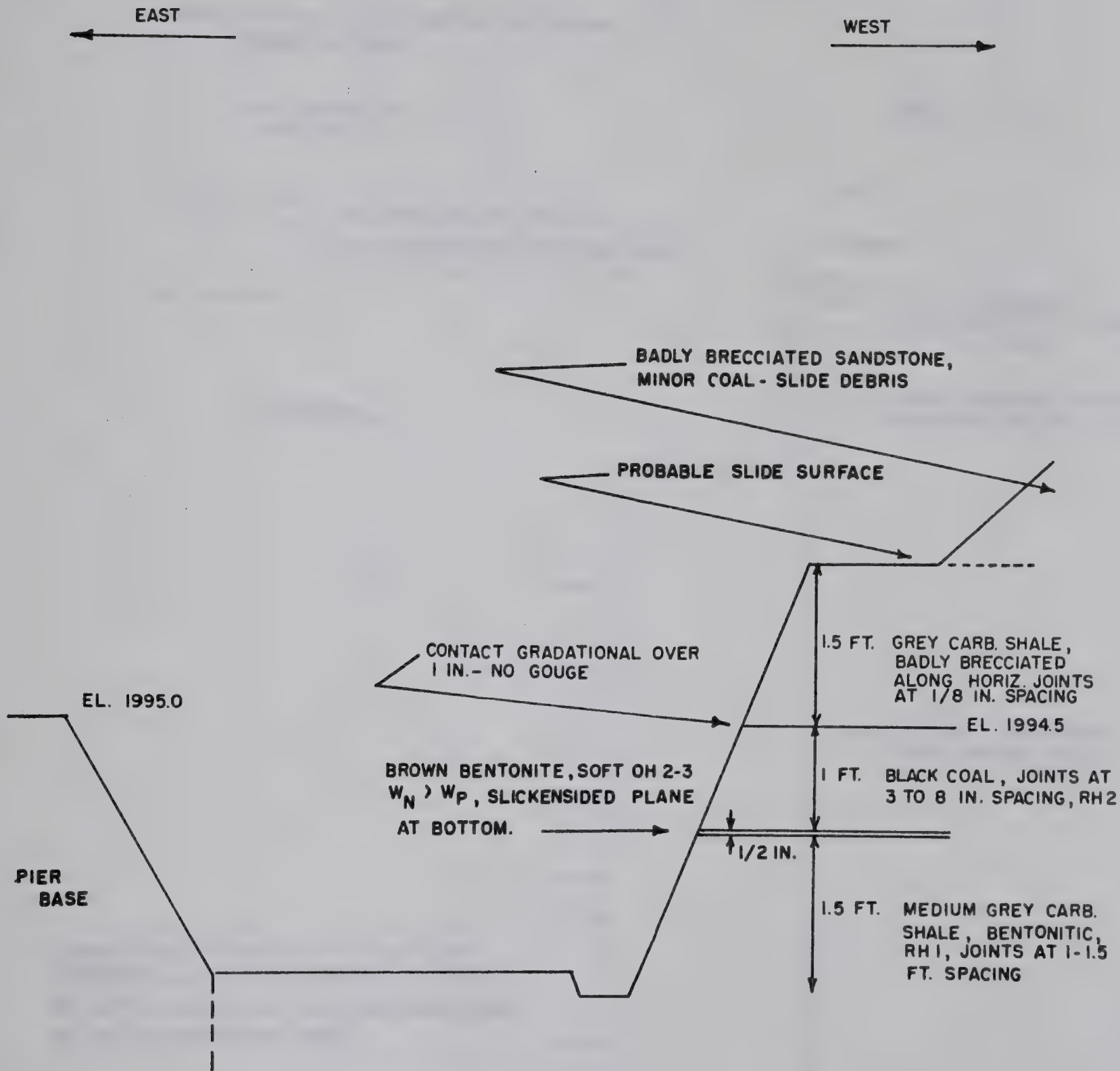
LOCATION SKETCH

STRATIGRAPHIC SECTION, PIER 4  
EXCAVATION, BEVERLY BRIDGE

FIG. B.4





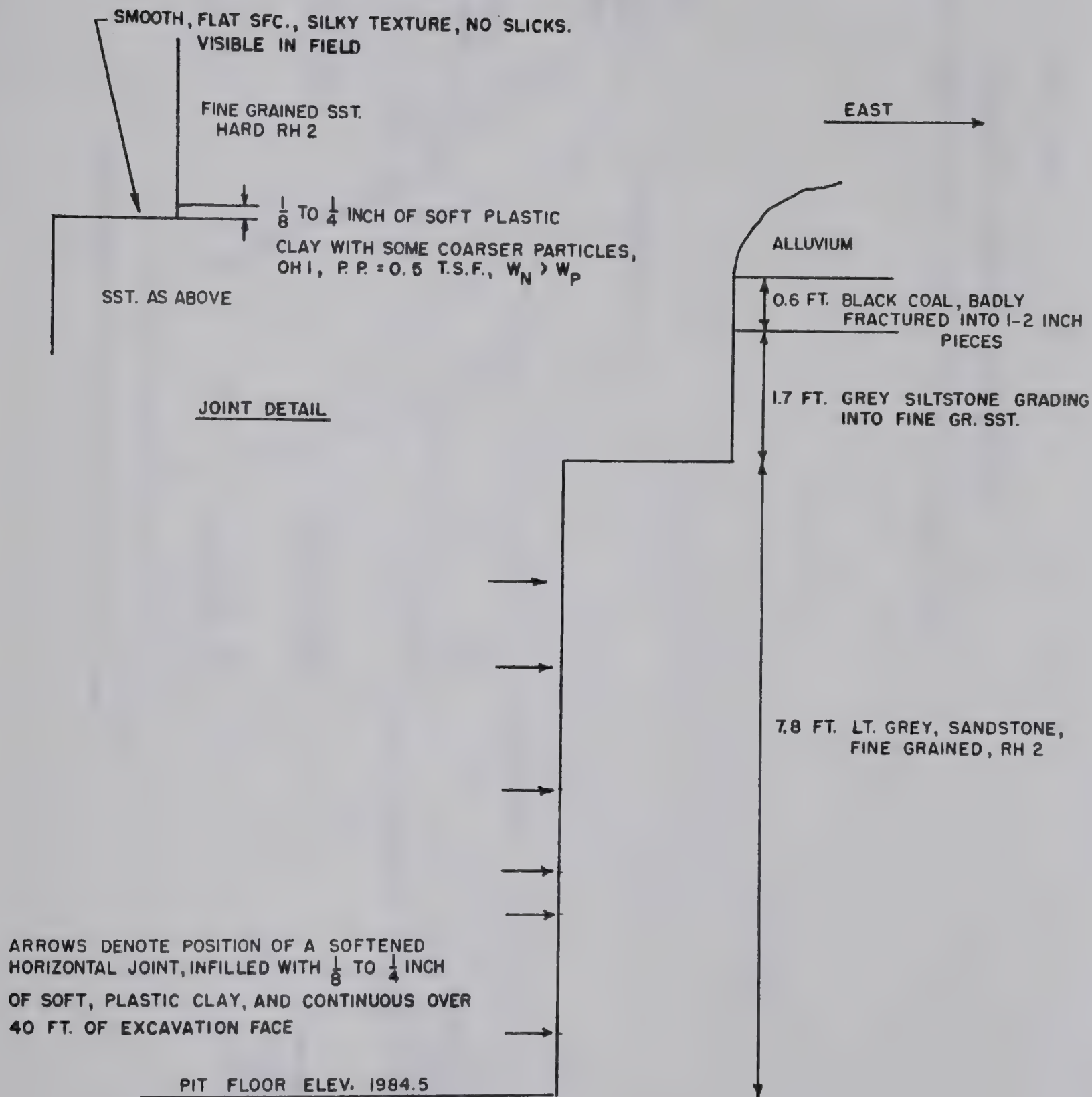


STRATIGRAPHIC SECTION PIER 1

BEVERLY BRIDGE

FIG. B.5





STRATIGRAPHIC SECTION PIER 3  
BEVERLY BRIDGE

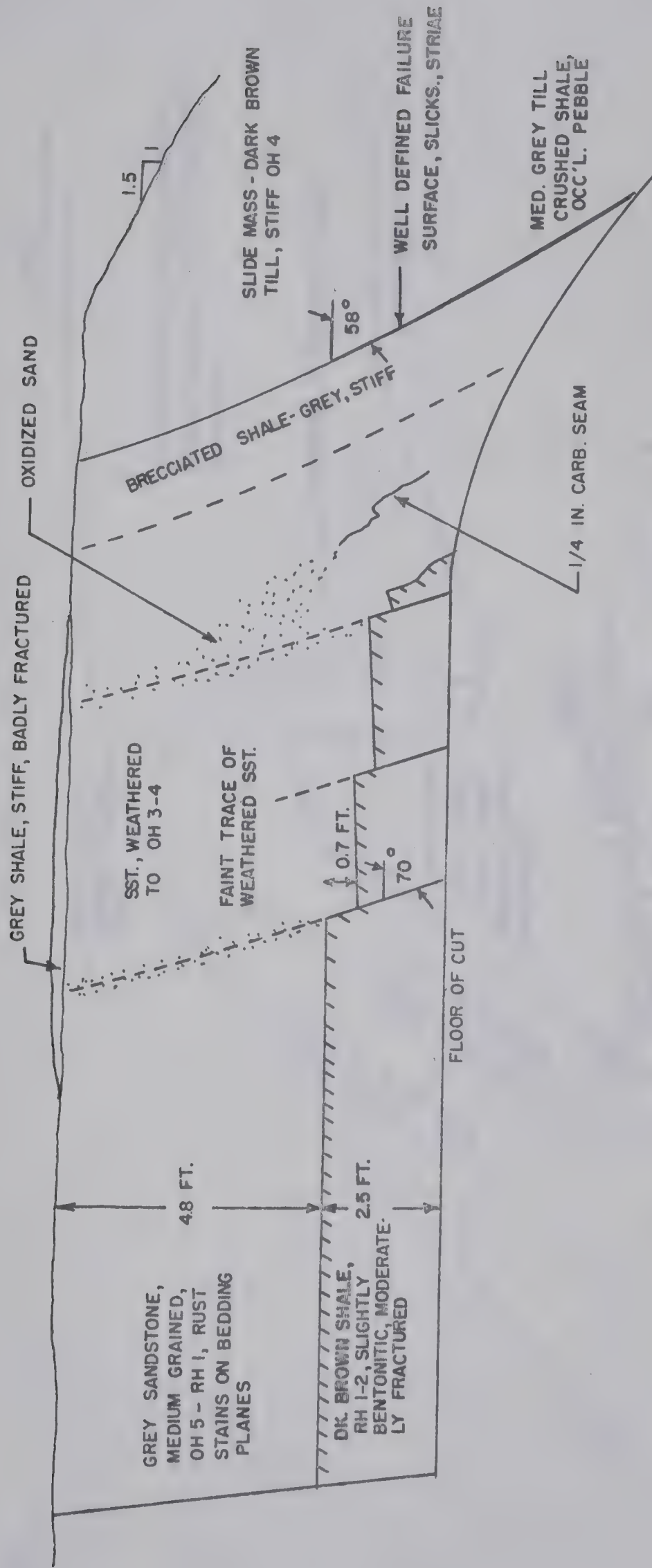
FIG. B.6





WEST

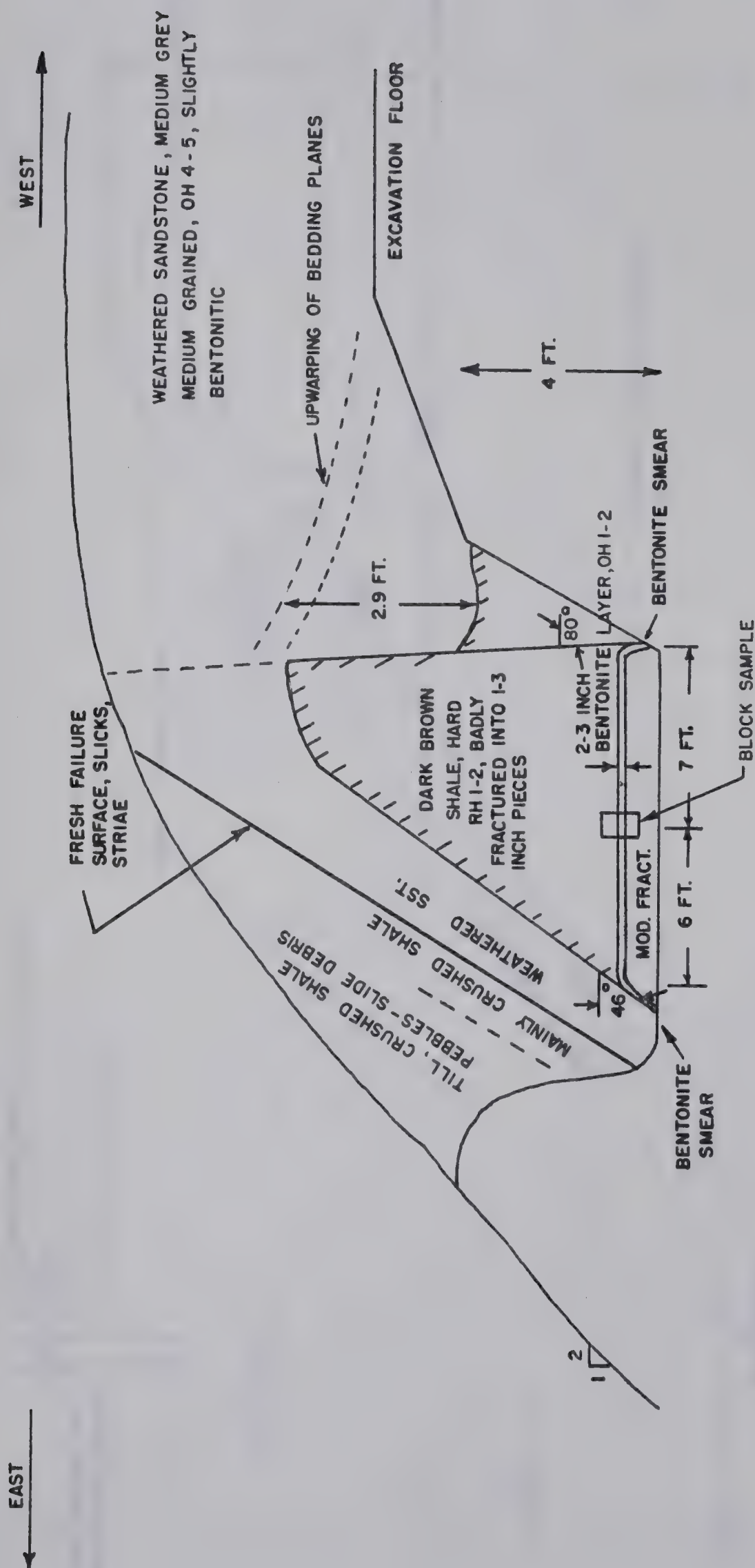
EAST



FIELD SKETCH OF THE NORTH FACE, WEST ABUTMENT  
EXCAVATION BEVERLY BRIDGE

FIG. B.7

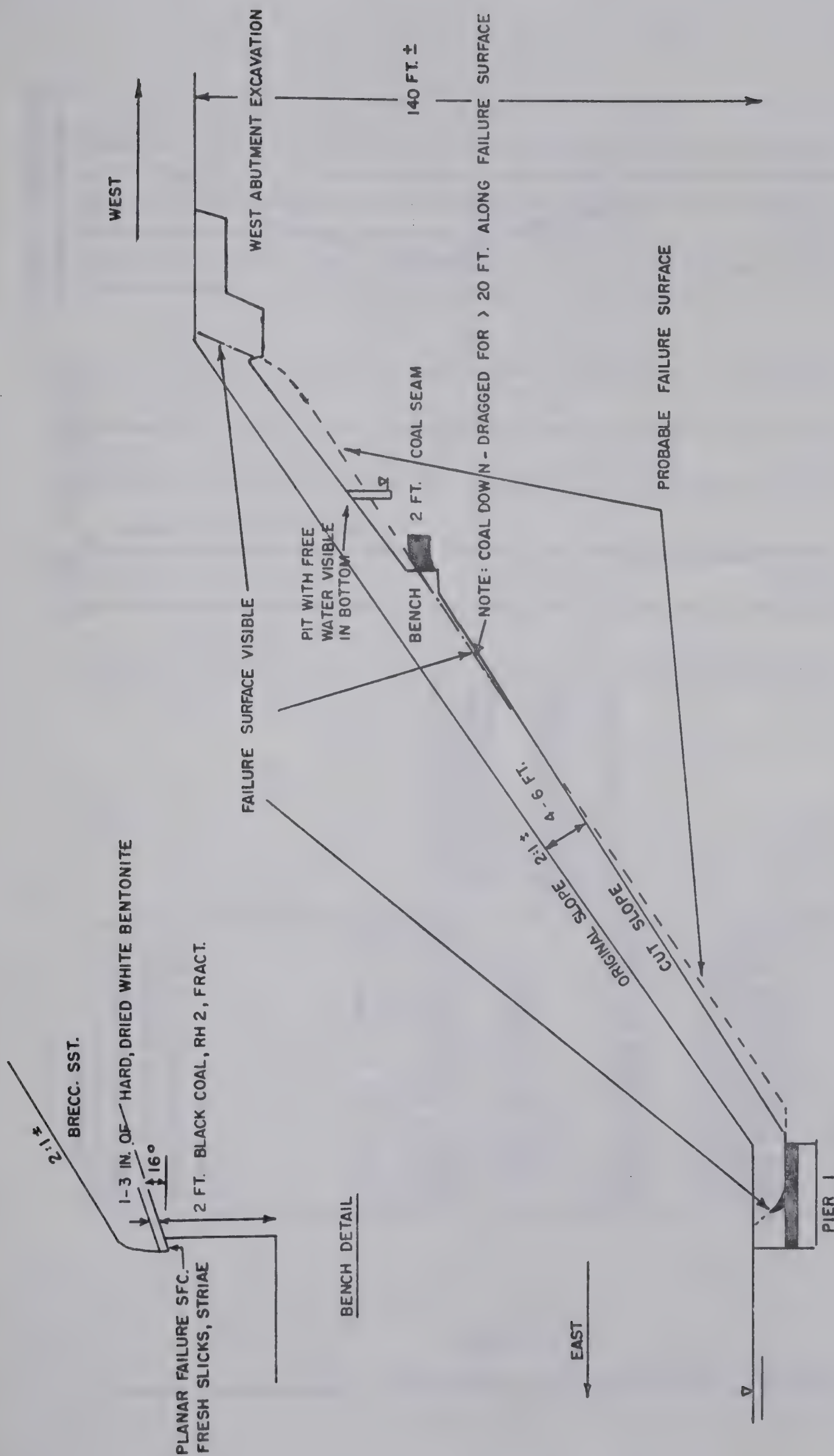




FIELD SKETCH OF THE SOUTH WALL, WEST ABUTMENT  
BEVERLY BRIDGE FIG. B.8







SECTION OF LANDSLIDE WEST ABUTMENT  
BEVERLY BRIDGE FIG. B.9



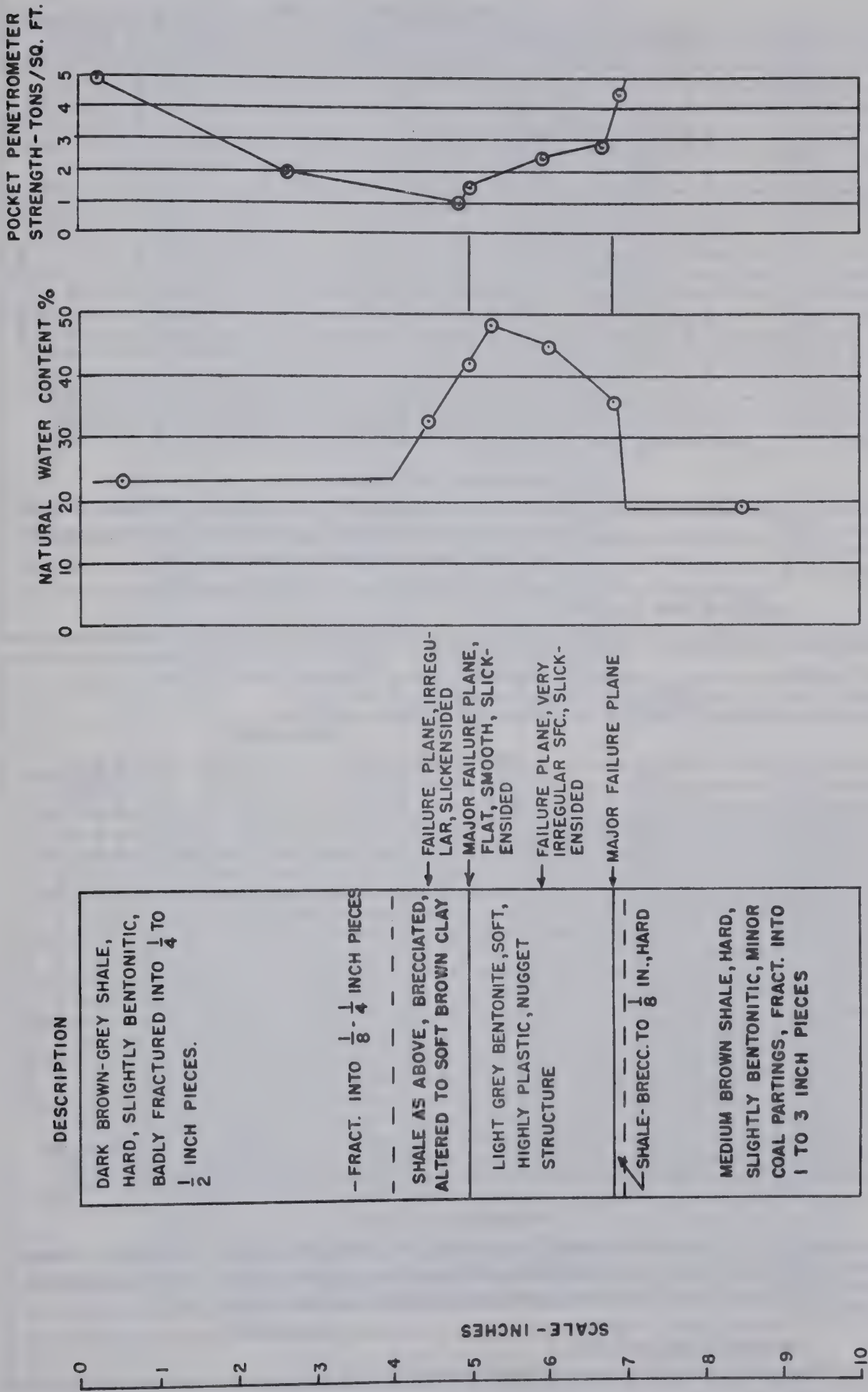


FIGURE B.10 DETAILS OF BENTONITE LAYER FROM WEST ABUTMENT, BEVERLEY BRIDGE





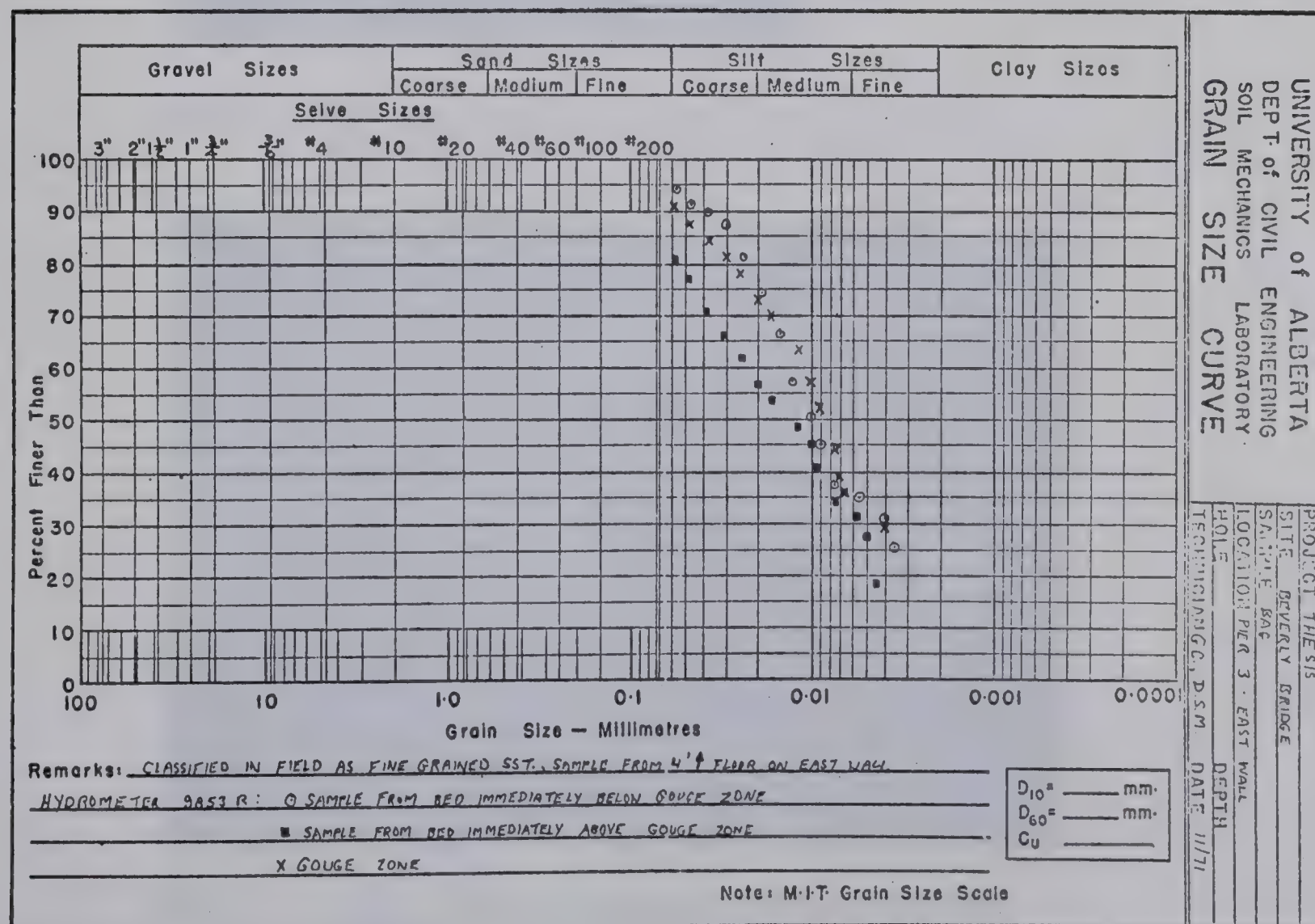
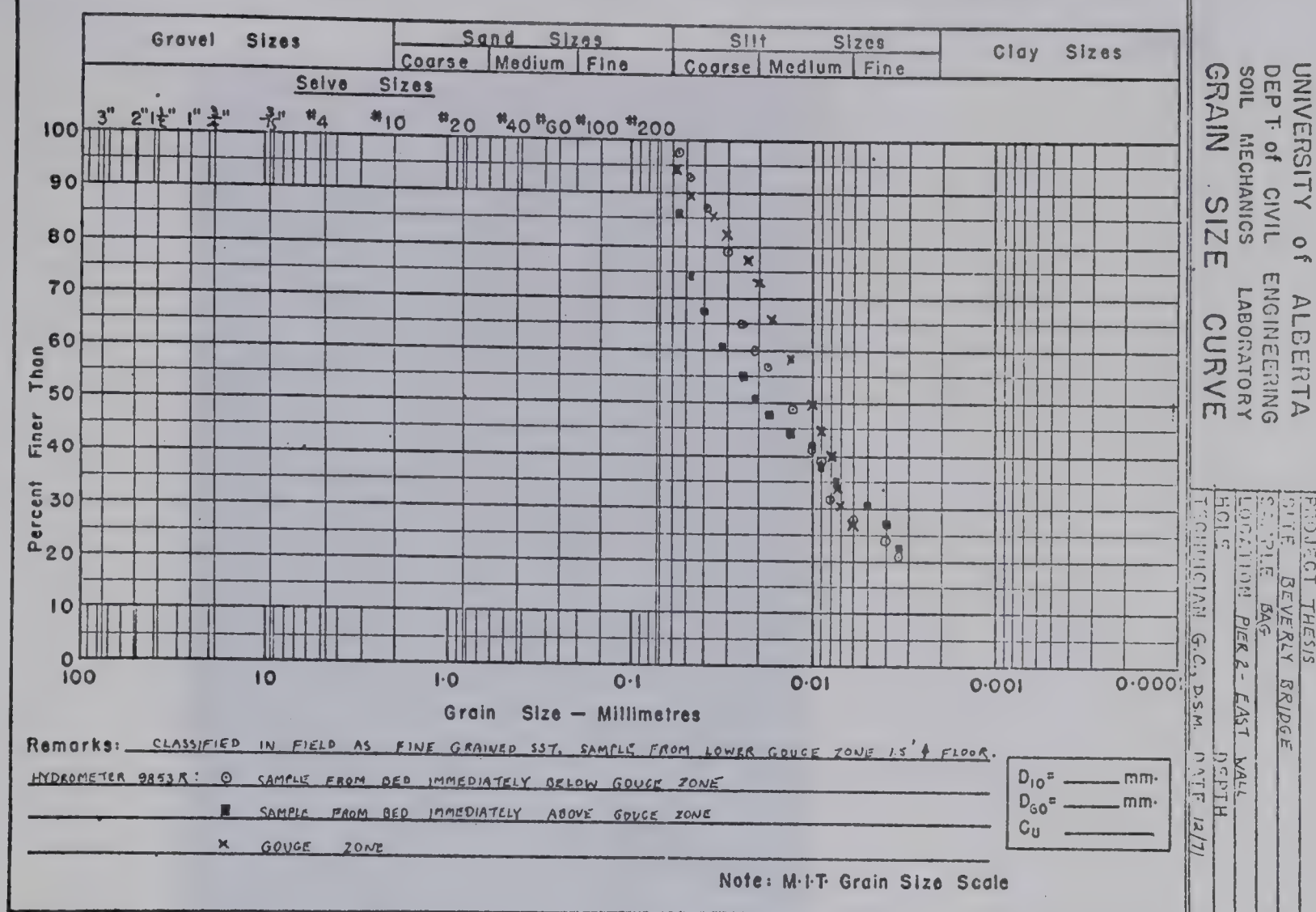


FIGURE B.II GRAIN SIZE CURVES FROM THE BEVERLY BRIDGE







Plate B.1 View of the south face of the south pit, Pier 4 excavation at the James MacDonald bridge.



Plate B.2 View of slickensided surface visible on the south face of the south pit, James MacDonald bridge. Note the pocket knife blade inserted into the gouge zone.







Plate B.3 View of the northeast face of the north pit, Pier 4 James MacDonald bridge. The horizontal softened joint is visible in the sandstone unit 3.5 ft. above the pit floor.



Plate B.4 View looking west along the north wall of the north pit, James MacDonald bridge. Note the softening at the carbonaceous shale - sandstone contact and the softened horizontal joint in the sandstone unit.







Plate B.5 View looking south along the west valley wall at the Beverly bridge. Note the landslide toe on the south wall of the Pier 1 excavation.



Plate B.6 View looking south along the west side of the Pier 1 excavation at the Beverly bridge. Note the brecciated bedrock above the carbonaceous shale in the foreground.







Plate B.7    Closeup of the carbonaceous shale shown in Plate B.6.  
Note evidence of lateral movement towards the excavation  
along horizontal bedding planes.



Plate B.8  
View looking northwest of the  
pier 2 excavation, Beverly bridge.  
Note the dominant horizontal  
bedding planes.







Plate B.9 View of the north wall of the west abutment excavation at the Beverly bridge. Note the near surface failure plane and bedrock disturbance landward of this feature.



Plate B.10 View of the south face of the west abutment excavation looking southwest. Note the rise in the dark-brown shale towards the river.







Plate B.11 View of the south face of the west abutment excavation. Note the recent slide scarp in the upper-left of the photo and the thin bentonite layer near the bottom



Plate B.12 Closeup of the bentonite layer shown in Plate B.11. Note downwarping and smearing of the bentonite by slide activity.



## APPENDIX C

### PROFILES ADJACENT TO RIVER VALLEYS IN ALBERTA





1. Introduction: During the summer of 1970 several weeks were spent surveying profiles of the ground surface back from valley edges in the Province of Alberta. This appendix contains a brief description of the method used and documents the results of these surveys.

2. Procedure:

A preliminary air photo survey of the South Saskatchewan, Red Deer, Pembina, Little Smokey and Peace Rivers in the Province of Alberta showed areas along these rivers where occurrence of a raised valley rim was common. These areas were visited and a number of profiles were surveyed to record the behaviour of the ground surface immediately adjacent to the river valley.

The profiles were generally run at right angles to the valley wall using a Kern precision engineering level. An assumed elevation of 100.0 feet was taken at the start of each profile although in some cases a temporary benchmark was used with an assumed elevation of 100.0 to run several profiles from. No attempt was made to tie these profiles to geodetic benchmarks. Horizontal distances were paced and an error of approximately 3 percent thus exists in the horizontal distances. Errors in elevation are considered insignificant. The profiles were extended far enough back from the valley edge to show any anomalous behaviour of the ground surface immediately adjacent to



the valley as well as the magnitude of local relief in the area.

Most of the profiles were taken near sites where data on the depth of overburden and type and properties of the bedrock are available. At each site the width and depth of valley was scaled from 1:50,000 topographic maps.

### 3. Results:

Five areas of the Province of Alberta were visited and are discussed in the order the work was done.

A. Medicine Hat Area: Surveys were made along the margin of a large clay pit east of Medicine Hat and along the South Saskatchewan River upstream of Medicine Hat. One profile was surveyed along the north edge of the Cypress Hills plateau southeast of Medicine Hat.

The Medicine Hat area is characterized by a number of clay pits (Thomson and Matheson, 1970a) where bedrock has been excavated for the ceramic industry based in Medicine Hat. The term 'clay-pits' is a misnomer as the substance mined is the local bedrock which is competent sedimentary rock of the Oldman formation which is capable of standing vertically for well over one hundred feet.

Clay pit 14 is located in 31-12-4-W4 some 5 miles east of Medicine Hat. The pit has a maximum depth of about 70 feet through 20 feet of till and 50 feet of shale and sandstone of the Oldman formation. The stratigraphy observed in this pit is described by Thomson and Matheson







(1970a, p. 13-14). The pit has been recently abandoned and no evidence of surface erosion was visible around the excavation edge. Seven profiles were run back from the edge of the pit on the two undisturbed sides of the excavation, as shown in Figure C.1. Five of the seven profiles show a rise of the ground surface of about 1 foot beginning some 40 feet back from the pit edge as shown in Figures C.2 to C.5 inclusive. The bedrock visible in the pit is flat-lying and no other cause than rebound of the pit bottom can be the cause of the raised rim around the pit.

Five profiles were surveyed along the South Saskatchewan River upstream of Medicine Hat. The river flows through postglacial valley approximately 3/4 mile wide and 300 feet deep incised through 20 to 30 feet of till and bedrock of the Oldman formation. Profiles 1 and 2 were surveyed on opposite sides of the river at Redcliff some 3 miles upstream of Medicine Hat and are shown in Chapter III. The other profiles were surveyed on the north side of the valley about 4 miles west of Redcliff as shown in Figure C.6. The three profiles, shown in Figure C.7 to C.9 inclusive, show a rise in the ground surface of 10 to 20 feet as the edge of the valley is approached.

The Cypress Hills are an erosional remnant having a maximum elevation of 4800 feet and stand about 2400 feet above the surrounding prairie level. The Pleistocene geology of the area has been mapped by Westgate (1965).



The bedrock geology of the area is given by Crockford (1951). A slight rise along the north edge of the Cypress Hills plateau was observed in many places and Figure C.10 shows a typical profile which reveals a gentle rise of about 1 foot adjacent to the edge of the plateau. At the site some 50 feet of Tertiary gravels cap bedrock of the Ravenscrag formation (Tertiary).

B. Drumheller Area: A number of surveys were made along the Red Deer River upstream of and in the immediate vicinity of Drumheller. Figure C.11 shows a profile surveyed on the east edge of the Red Deer River Valley at Ardley Damsite (discussed in Chapter III) where some 10 to 15 feet of till covers bedrock of the Edmonton formation. A slight rise of about 3 feet occurs towards the valley edge but several feet of local relief occurs in the area and the rise may be due to this factor. The presence of a well developed valley anticline and valley flexure is documented at this site and it appears the absence of a raised valley rim is due to erosion.

A second profile was surveyed on the west side of the Red Deer Valley some 15 miles upstream of Drumheller as shown in Figure C.12. No evidence of a raised rim occurs and it was concluded that erosion along the edge of the main valley has removed practically all evidence of rebound.

A survey of air photos of the Drumheller area showed well developed raised valley rims along a number of the







tributaries to the main valley. Figure C.13 shows the location of surveys made along the east branch of Michichi Creek some 2 miles east of Drumheller. At this site a tributary gully has formed a neck of land forming a plateau or mesa in 18-29-19-4. A raised rim is visible around the entire periphery of this plateau; the valley of Michichi Creek is almost 400 feet deep and the till cover in the area is relatively thin. The raised rim is easily visible along the east edge of the neck of land as shown in Figure C.14 with an average rise in ground surface of about 5 feet occurring over a horizontal distance of 70 to 80 feet. The rise in ground surface along the west side of the neck of land is less pronounced and has been removed by erosion in some places.

Profile M5 was surveyed adjacent to the Red Deer River Valley some 2 miles downstream of Drumheller and a rise in ground elevation of about 18 feet occurs towards the valley. This profile was made in an area of high local relief and may not be a true raised valley rim in view of the absence of this feature in the other sites visited along the Red Deer River Valley.

C. Entwistle Area: Seven profiles were surveyed along the Pembina River near Entwistle some 50 miles west of Edmonton, Alberta. The Pembina River has carved a post-glacial valley about 1300 feet wide and 200 feet deep through a few feet of lacustrine clay, 20 feet of glacial



till, 50 feet of hard well cemented sandstone of the Tertiary Paskapoo formation and about 130 feet of the Edmonton formation (Upper Cretaceous). An air photo survey showed a small raised rim occurring along the outside of meander bends but no evidence of this effect was visible elsewhere along the valley edge. The location of the profiles is shown in Figure C.15 and the profiles are shown in Figures C.16 and C.20 inclusive.

Two of the profiles taken on the outside of meander bends (P2 and P5) show a 6 to 7 foot raised rim while one profile surveyed on the outside of a meander bend (P1) shows little or no evidence of a rise towards the valley edge. Profiles P6 and P7, surveyed opposite the inside of a meander, show no evidence of rebound although the large amount of local relief tends to obscure any rebound effects. Profile P.4 surveyed adjacent to a stretch of valley where little meandering has occurred shows a slight rise in ground surface immediately adjacent to the valley edge.

D. Little Smokey Bridge: A landslide at the Little Smokey River bridge located about 30 miles north of Valleyview, Alberta has been extensively studied by Rennie (1966) and Hayley (1968). The Little Smokey River has re-excavated a preglacial channel infilled with till to a depth of about 320 feet. Bedrock is not exposed in the valley walls but underlies the river at shallow depth and is believed to be the Puskawaskau formation (Upper Cretaceous) of the Upper







Smokey Group. The bedrock is described as a soft, grey, fissile marine shale.

Five profiles were surveyed along the valley edge near the bridge site as shown in Figure C.21. The profiles are shown in Figures C.22 to C.24 inclusive. A poorly defined rise towards the valley of one to three feet occurs in profiles LS 3 and LS 4 as shown in Figure C.23. Local relief of 3 to 4 feet complicates the interpretation of the results and the only well defined raised valley rim occurs in profile LS 2 (Figure C.22) immediately above the scarp of the active landslide on the outside of a meander bend of the river.

E. Peace River: Three profiles were surveyed along the Peace River Valley in the vicinity of the town of Peace River, Alberta as shown in Figure C.25. A 15 to 20 foot rise toward the river valley, which begins about two miles back from the valley edge, occurs in profiles PR 1 and PR 3 as shown in Figures C.26 and C.28. Profile PR 2 (Figure C.27) does not show this feature. The valley of the Peace River in this area is 3 to 4 miles wide and about 700 feet deep. Several hundred feet of glacial and interglacial deposits cover bedrock in this area (Sharma, 1969).

Two additional profiles, PR 4 and PR 5, were surveyed on the north side of the valley some 30 miles upstream of Peace River town as shown in Figure C.29. An airphoto survey, confirmed in the field, showed no raised rim along the



edge of the main valley. However, a minor raised rim was visible on the airphotos in places along the tributary valleys. A distinct raised rim 2 to 3 feet high was observed in profile PR 5 but no such rim occurred in profile PR 4 as shown in Figure C.30. Extensive slumping along the sides of these tributary valleys prevented any observations as to depth of overburden at this location.

#### 4. Discussion:

The raised valley rim was best expressed along the South Saskatchewan River upstream of Medicine Hat where the valley was cut through a relatively shallow veneer of till in a distinctly postglacial valley. Profiles 1, 2 and 4 show a raised rim about 15 feet high starting from 800 to 1800 feet back from the valley edge. Erosion has apparently reduced the raised rim in profile 3 and accentuated it in profile 5 at this site.

The profiles at clay pit 14 cut into the same bedrock, the Oldman formation, show a rise in ground surface of about 1 foot beginning 30 or 40 feet from the excavation edge indicating that both depth and width of excavation affect the height and width of the raised rim.

The poorly defined or non-existent valley rim along the Red Deer River in the vicinity of Drumheller is in marked contrast to the well defined occurrence along Michichi Creek. Erosion has apparently removed the rim along the main valley in places indicating that the tributary







is younger and the intensity of the forces of erosion is much less under present climatic conditions than when the main valley was formed, presumably at the end of the Pleistocene some 15,000 to 20,000 years ago. Evidence to support this concept is present in the profiles from the Pembina river at Entwistle. The absence of a raised rim on the outside of meander bends suggests the removal of this feature by erosion while the occurrence of the raised rim on the inside of meander bends suggests that relatively little time has occurred on a geologic scale for erosion to remove the rim. Airphoto observations on the valley at this point (Matheson, 1970) suggest that the river has widened its channel in bedrock by the process of meandering and the present location of the valley rim on the outside of meander bends should be of recent age and would not date from the original formation of the valley.

A thick depth of glacial deposits can be seen to inhibit the occurrence of the raised rim from the survey results along the Little Smokey and Peace Rivers. A raised rim was only visible on one profile from the Little Smokey bridge area and it is of interest to note its height was only about  $\frac{1}{4}$  of the height of the raised rims observed along the South Saskatchewan river considering that the two valleys of approximately the same depth and width. The fact that this profile occurs above a landslide known to be currently active suggests the present valley rim is recent and little time has elapsed for erosion to suppress it.



The absence or poor expression of a raised rim in the other profiles surveyed at the Little Smokey bridge indicates the relative magnitude of the natural erosion forces which have acted over the 15,000 years or so since deglaciation and formation of the present valley.

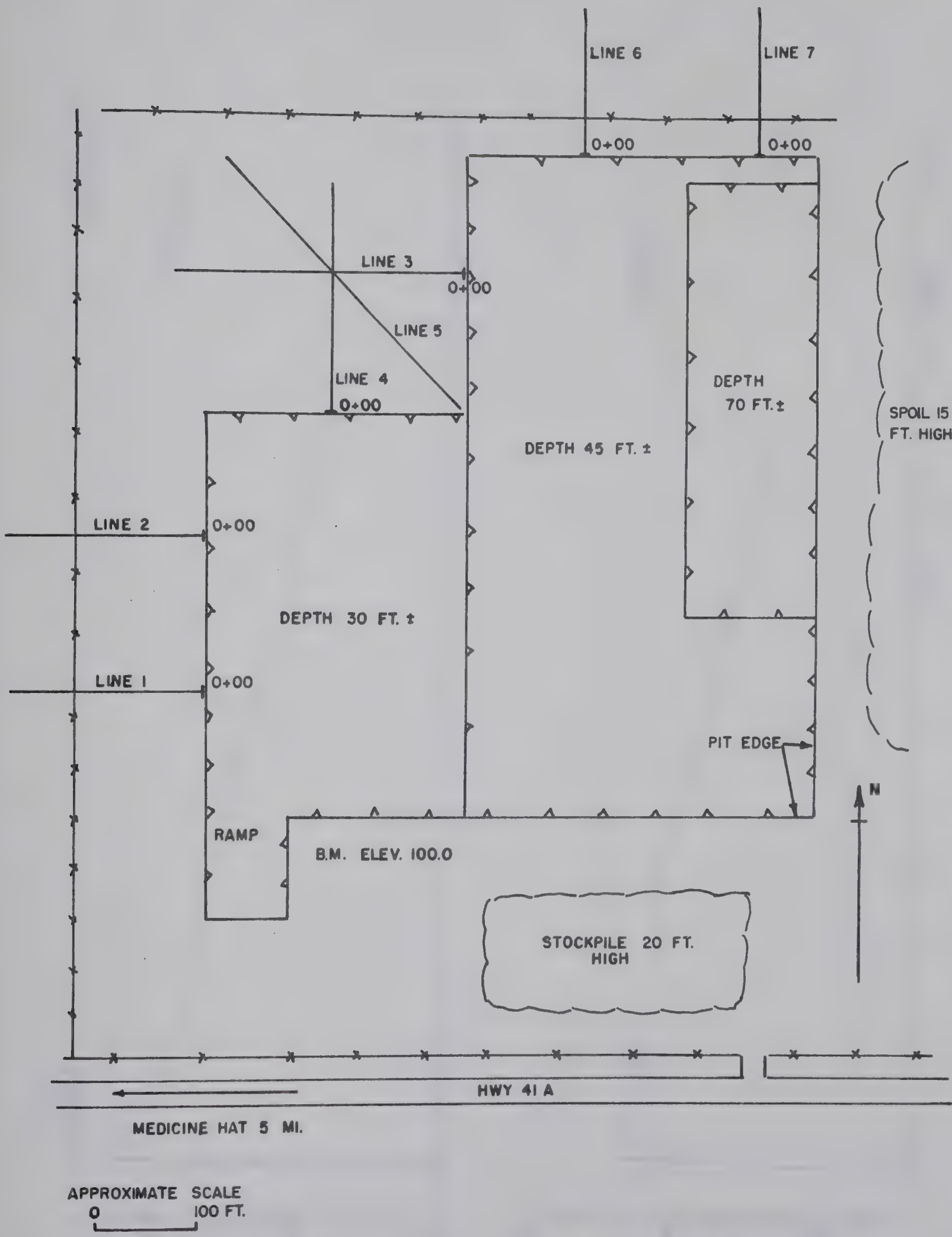
In summary the raised valley rim is best expressed where a wide, deep river valley has downcut through a flat, thin veneer of glacial drift. A raised rim will occur adjacent to a valley cut through till but will be much reduced in height and apparently reflects the relative modulus of elasticity of the two material. The absence or poor expression of the raised rim appears to result from the susceptibility of glacial deposits to weathering, however if a large raised rim is formed it appears resistant to erosion as drainage is then landward and away from the valley. In some cases erosion appears to accentuate the height of the raised rim.

The raised valley rim is best visible along recently formed valley edges. However, extensive landslide actively producing a very flat valley wall appears to subdue to raised rim. An airphoto survey of the South Saskatchewan River downstream of Medicine Hat, in the Bearpaw formation, where extensive landslides have reduced the valley wall to close to 10:1 showed no evidence of the raised rim.





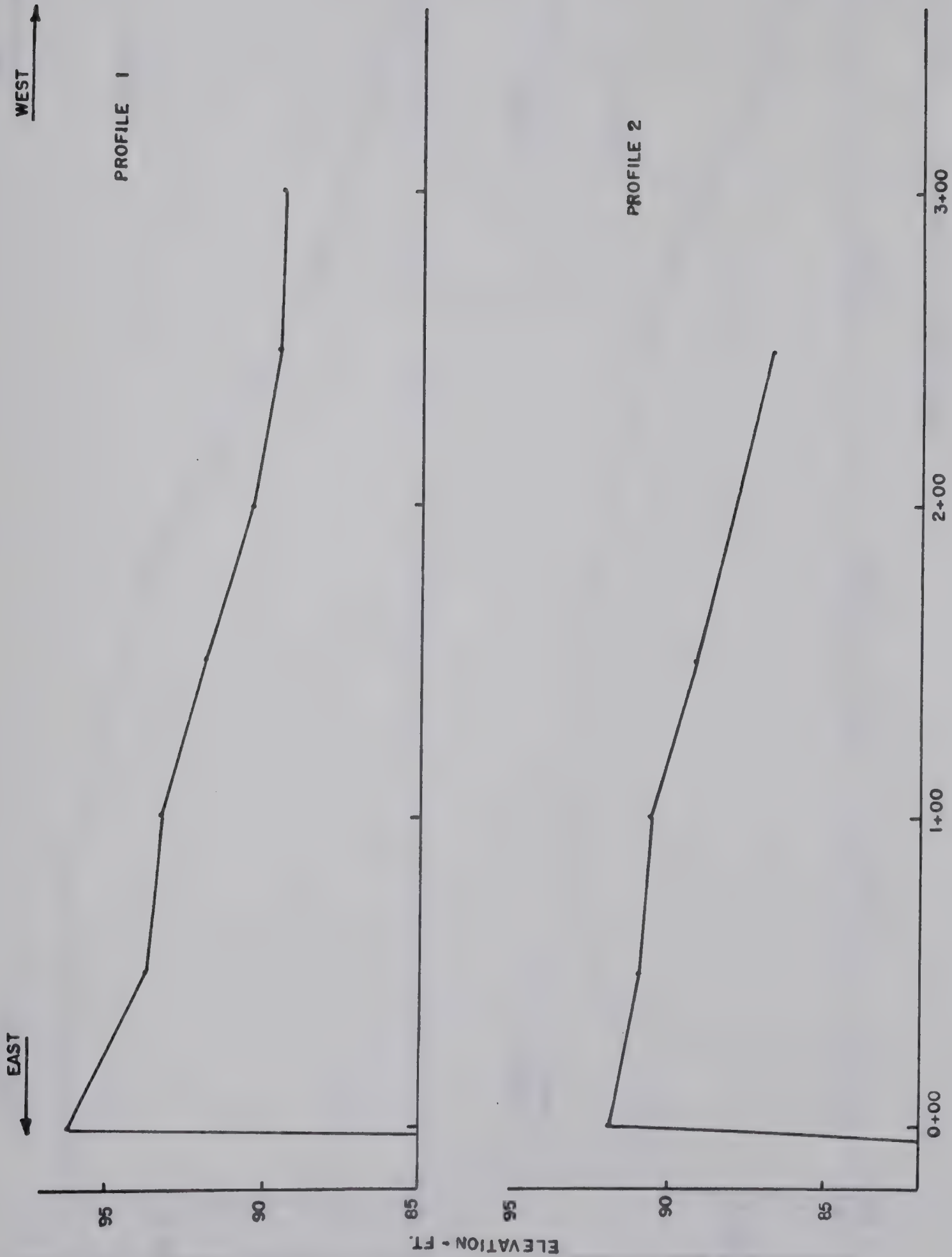




PLAN OF SURVEYS  
CLAY PIT 14, 31-12-4-W4

FIG. C.1



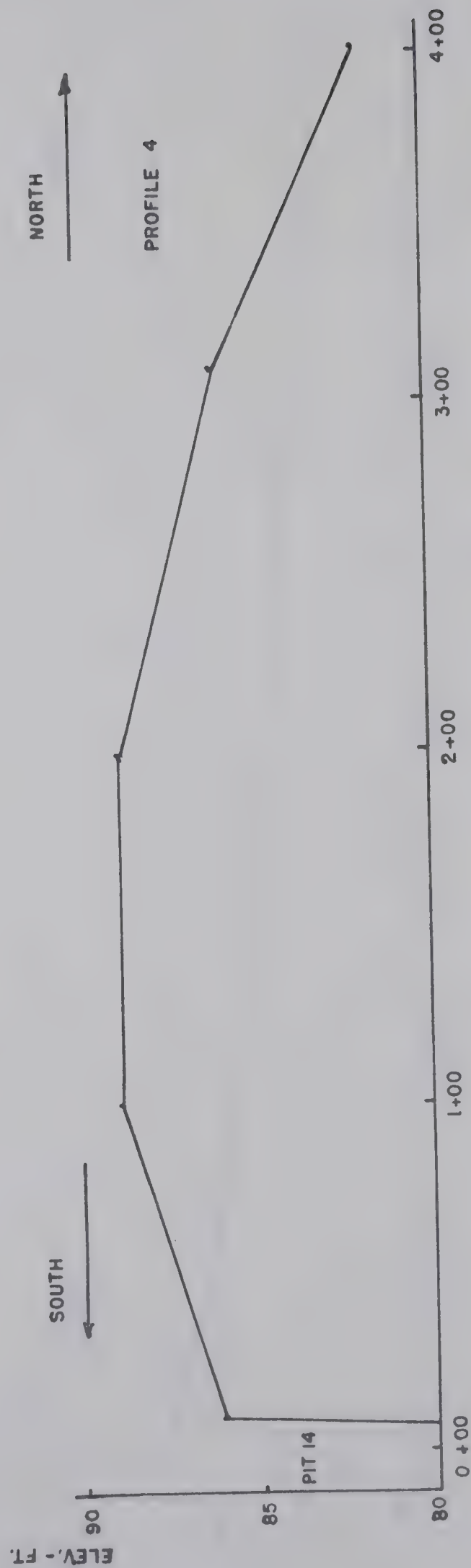
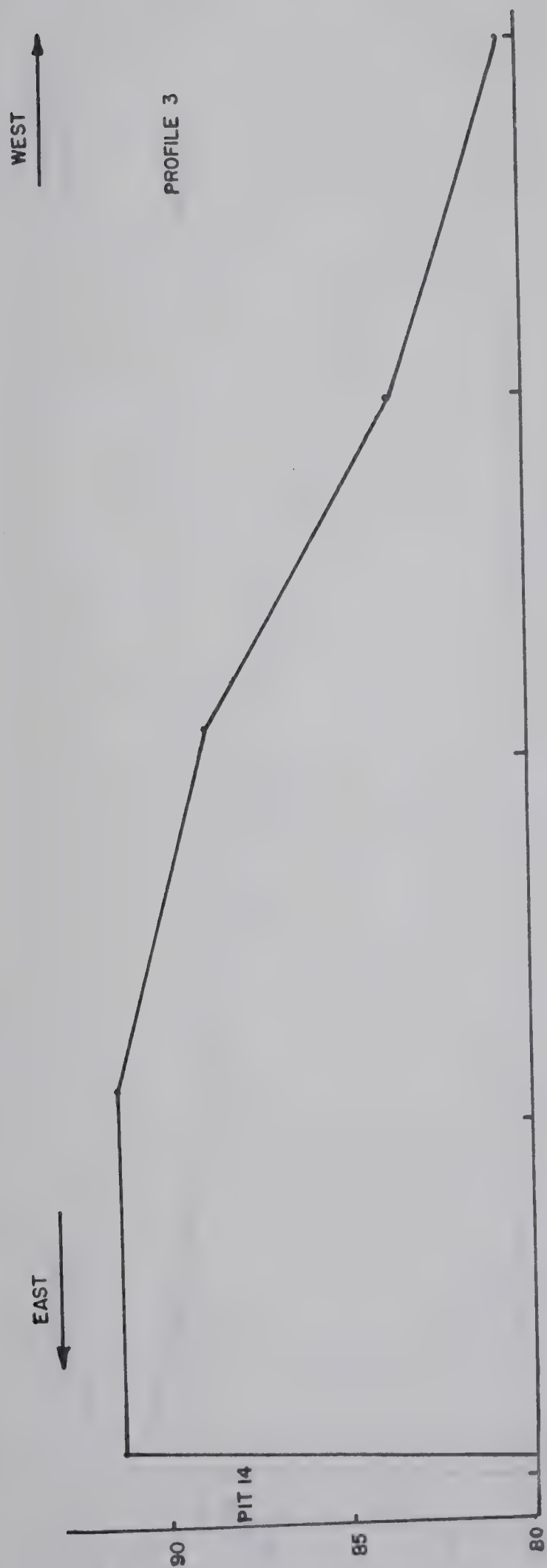


PROFILES CLAY PIT 14

FIG. C.2

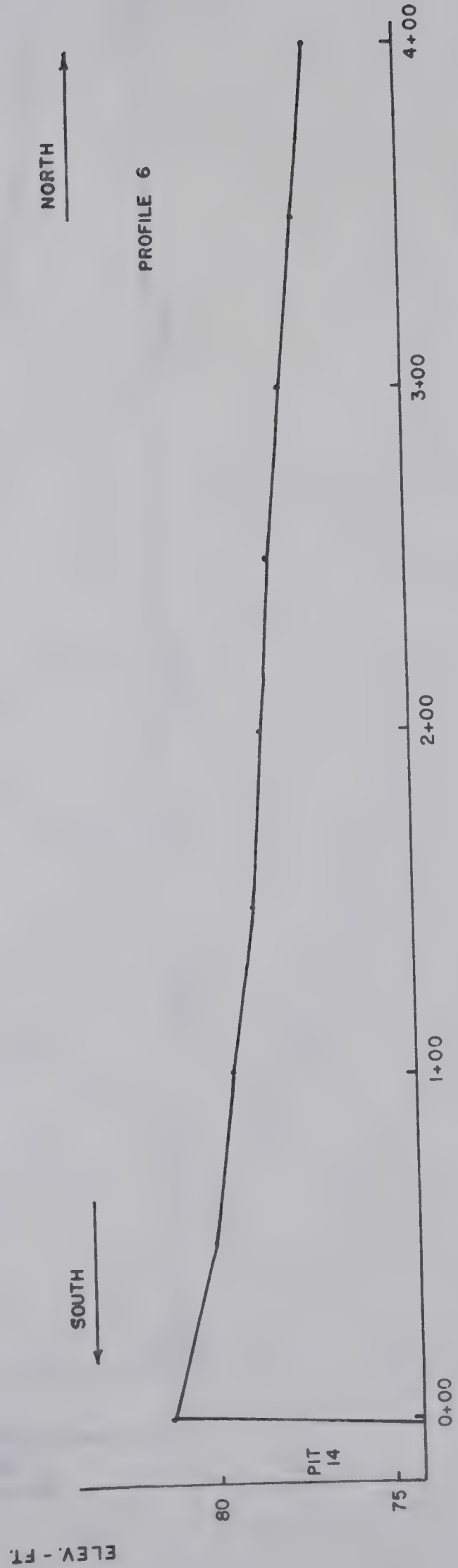






PROFILES CLAY PIT 14 FIG. C.3

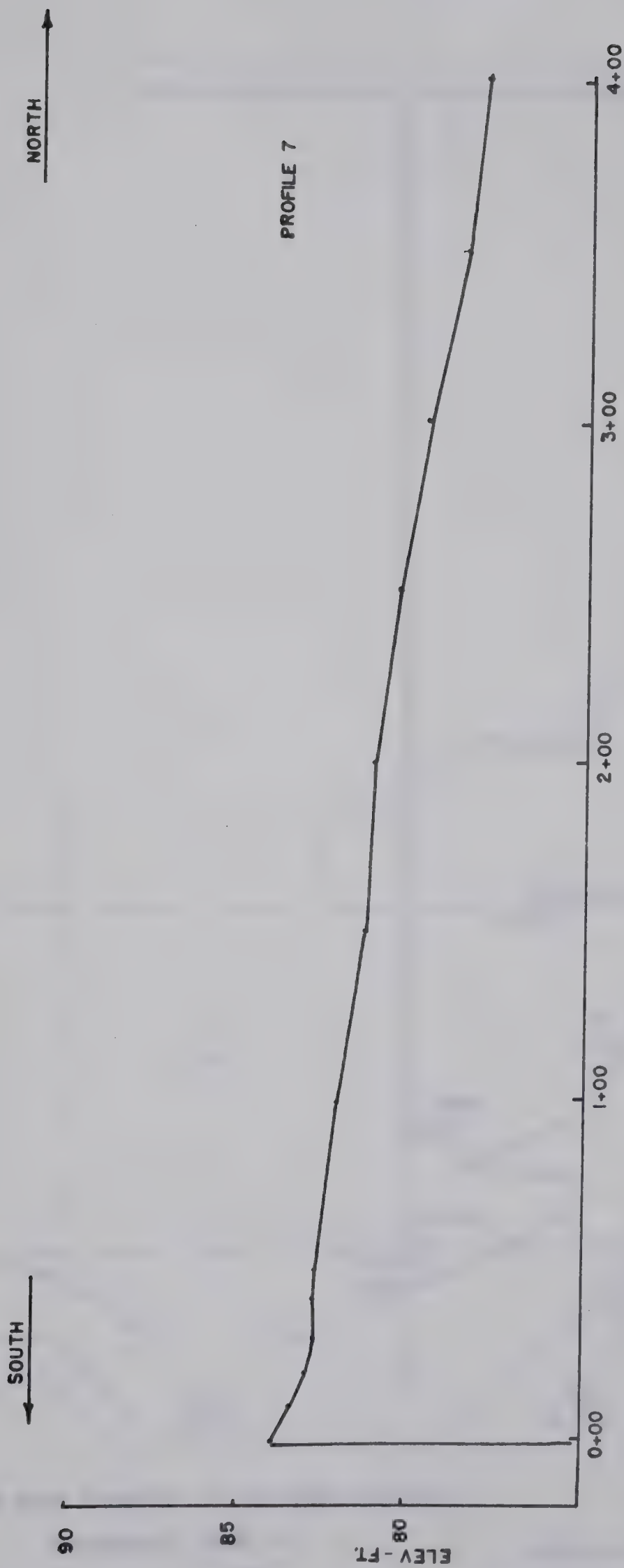




PROFILES CLAY PIT 14 FIG. C.4

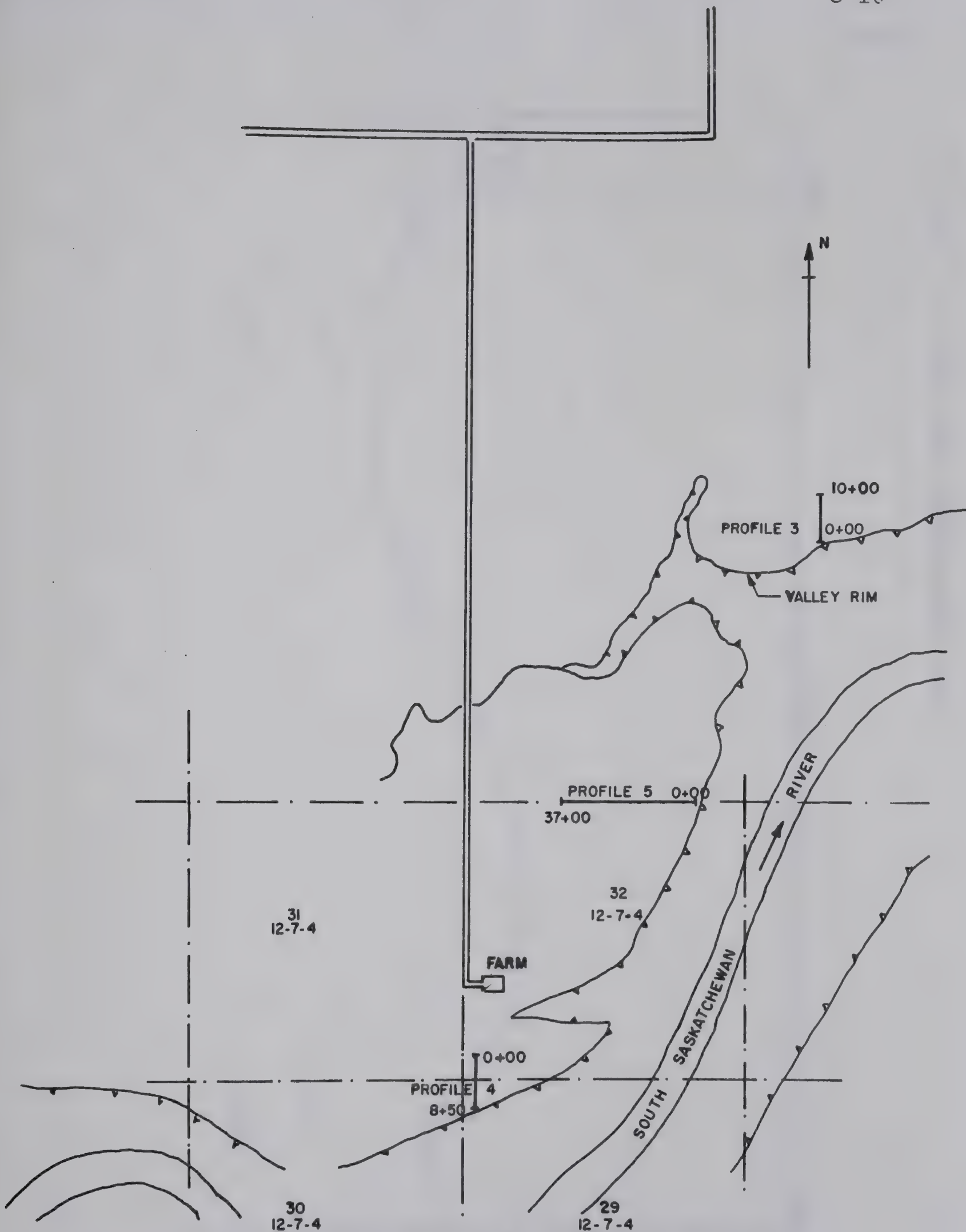






PROFILES CLAY PIT 14      FIG. C.5





TRACED FROM AIRPHOTO C 62.651-5002, YC 529A-74

APPROXIMATE SCALE - FT.

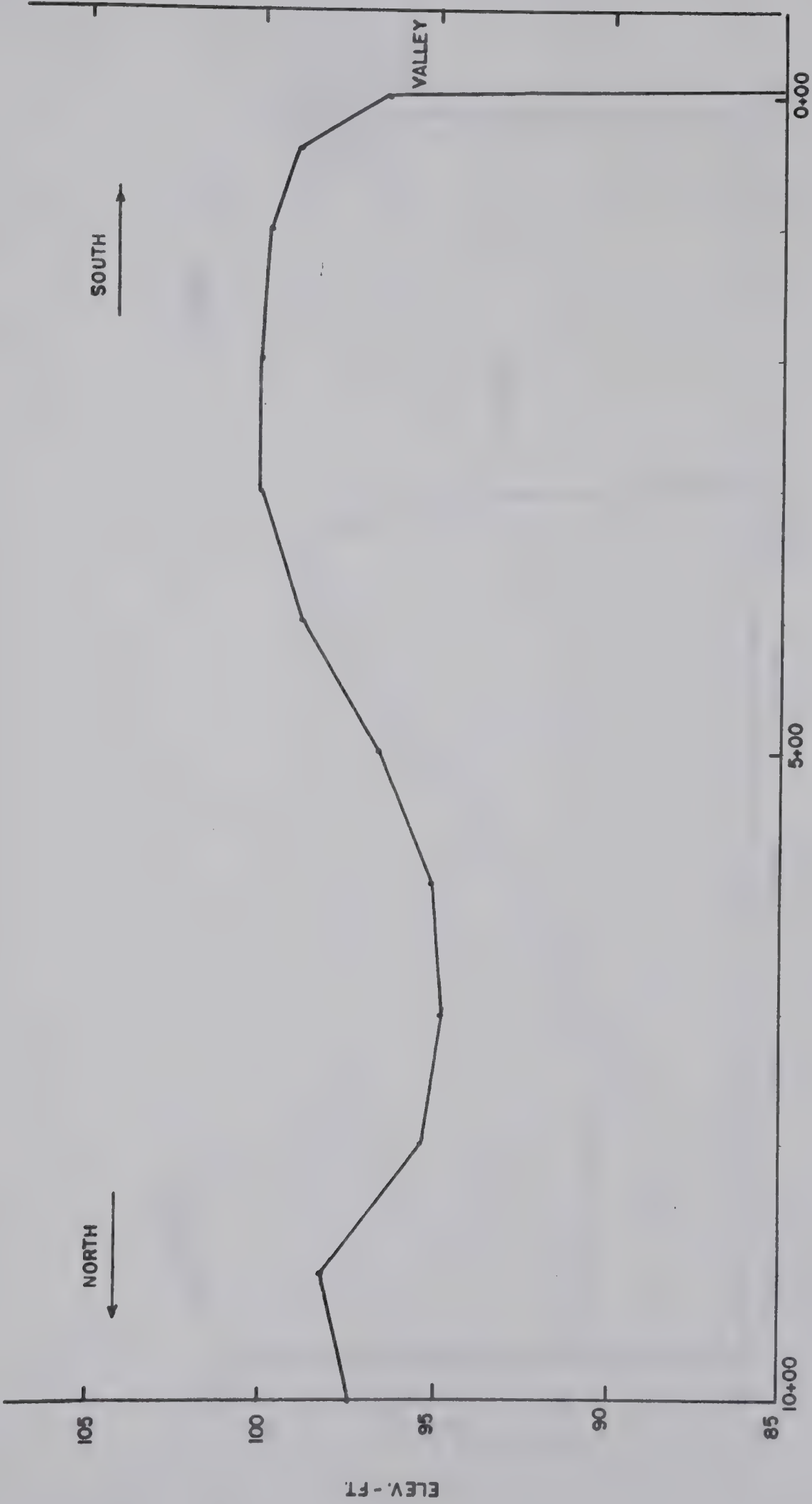
0 2640

PLAN OF SURVEYS  
SOUTH SASKATCHEWAN RIVER

FIG. C.6

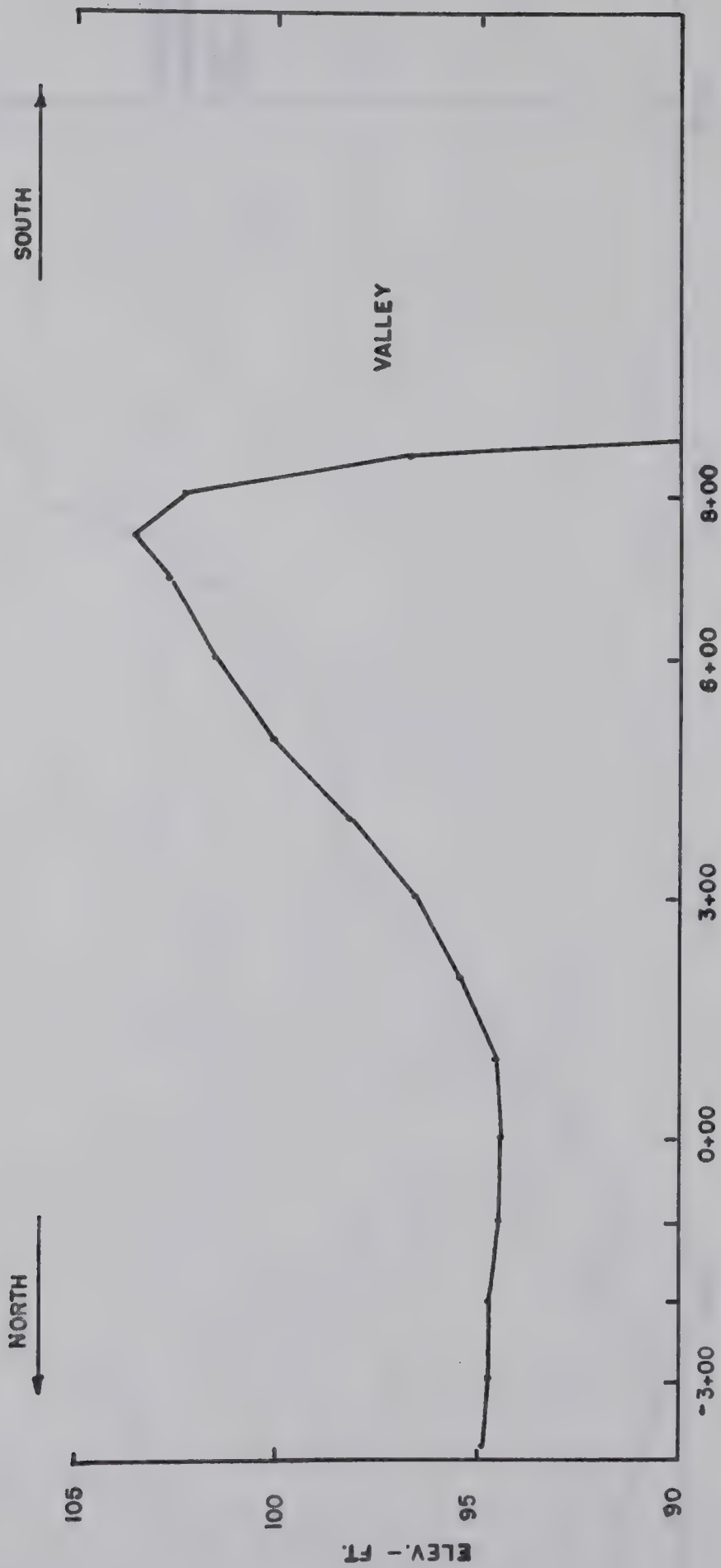






SOUTH SASKATCHEWAN RIVER PROFILE 3 FIG. C.7



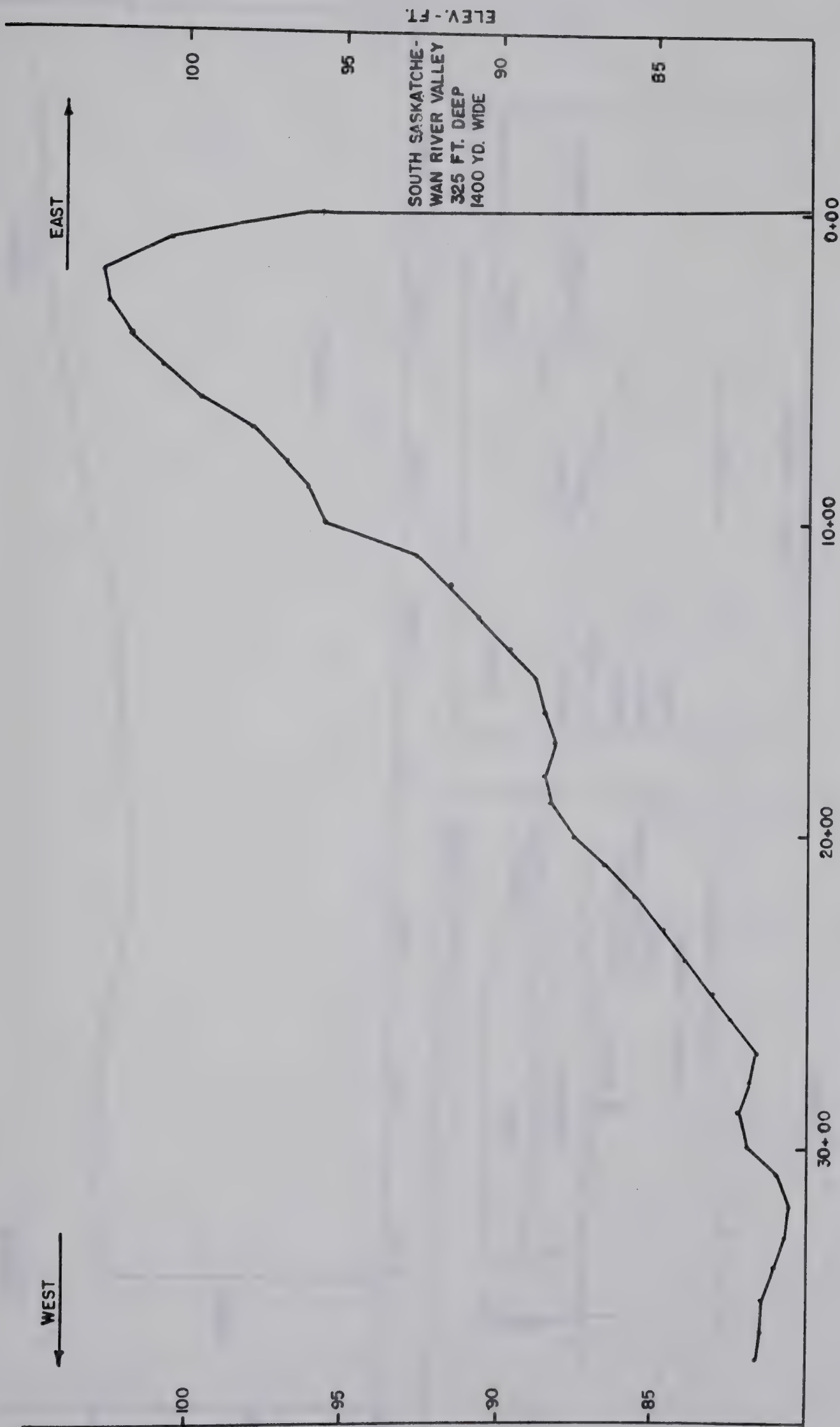


SOUTH SASKATCHEWAN RIVER PROFILE 4

FIG. C.8



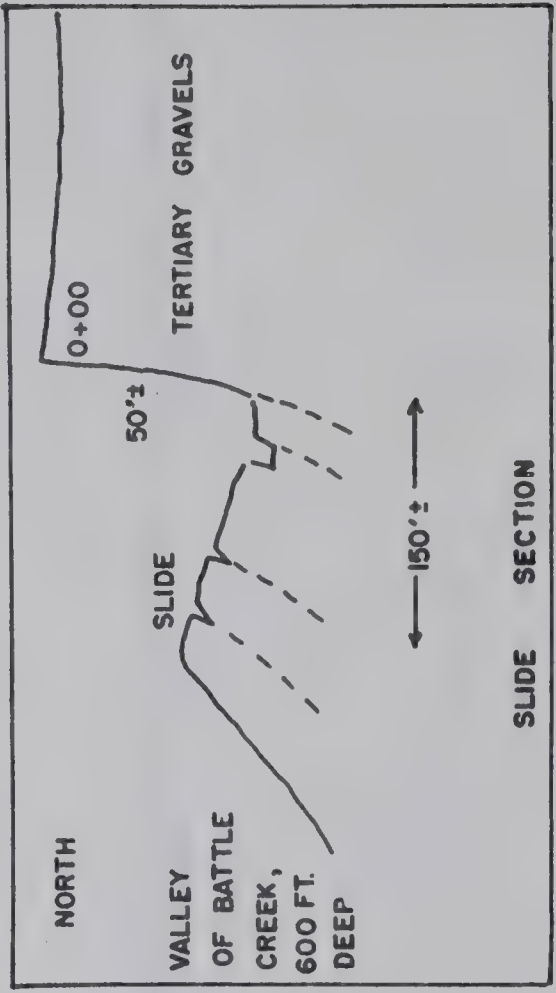
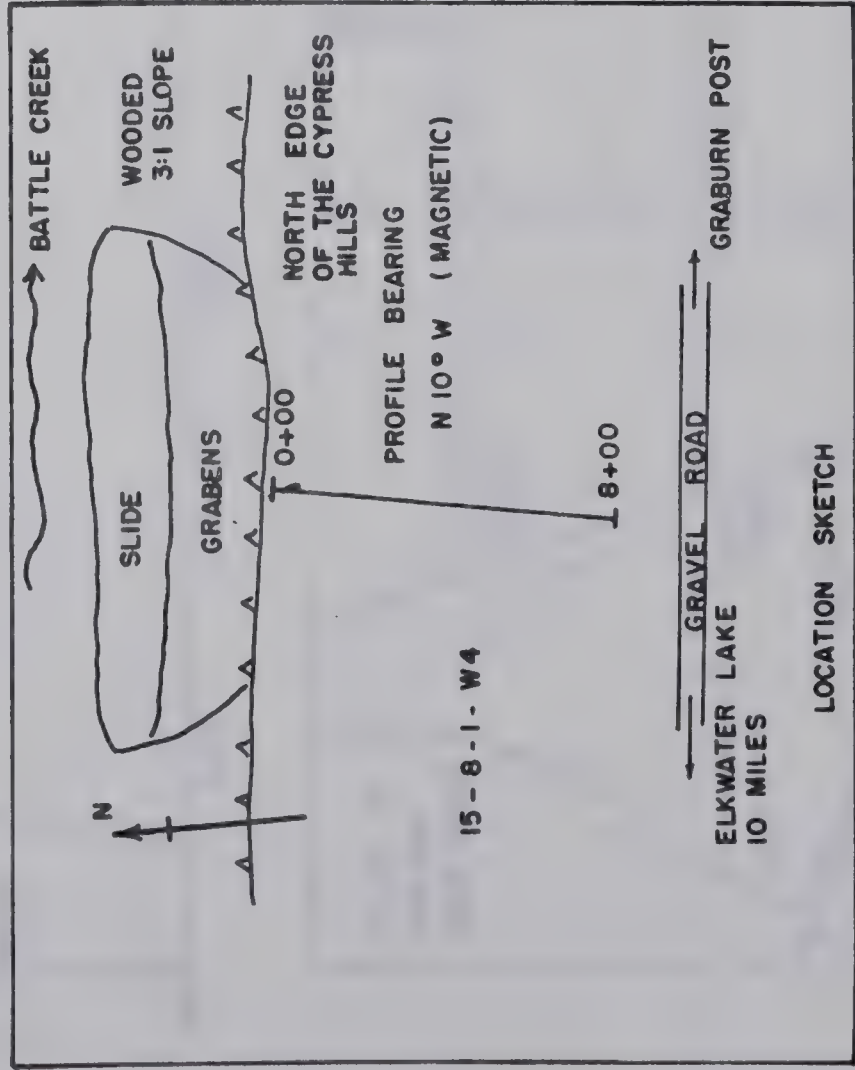
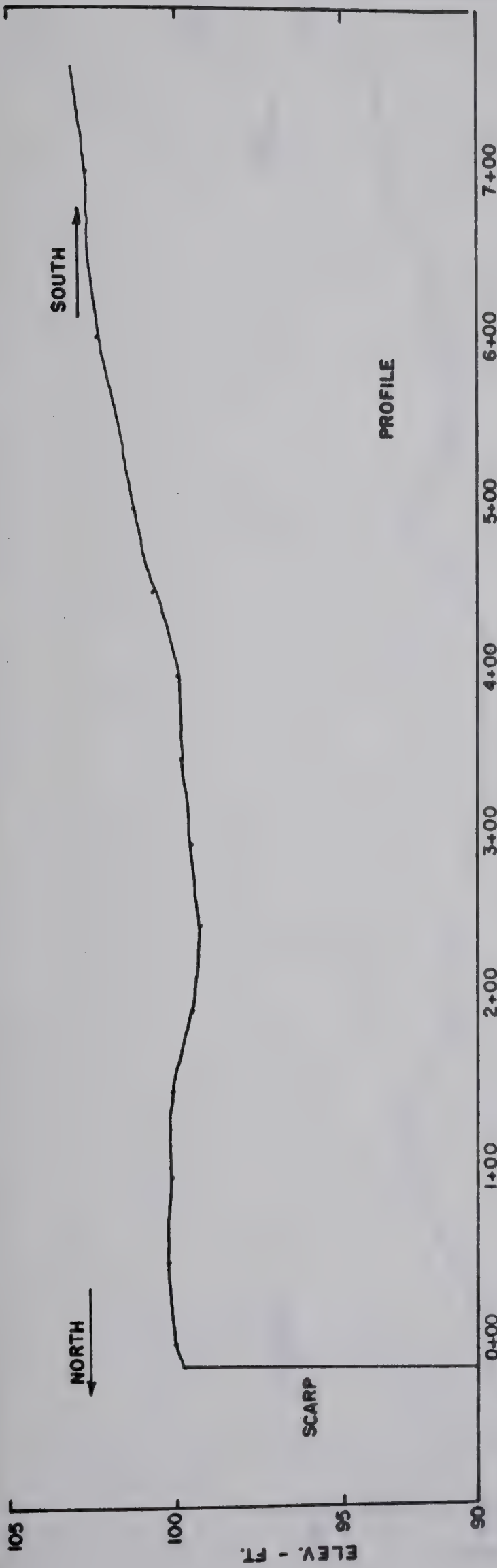




SOUTH SASKATCHEWAN RIVER PROFILE 5

FIG. C.9



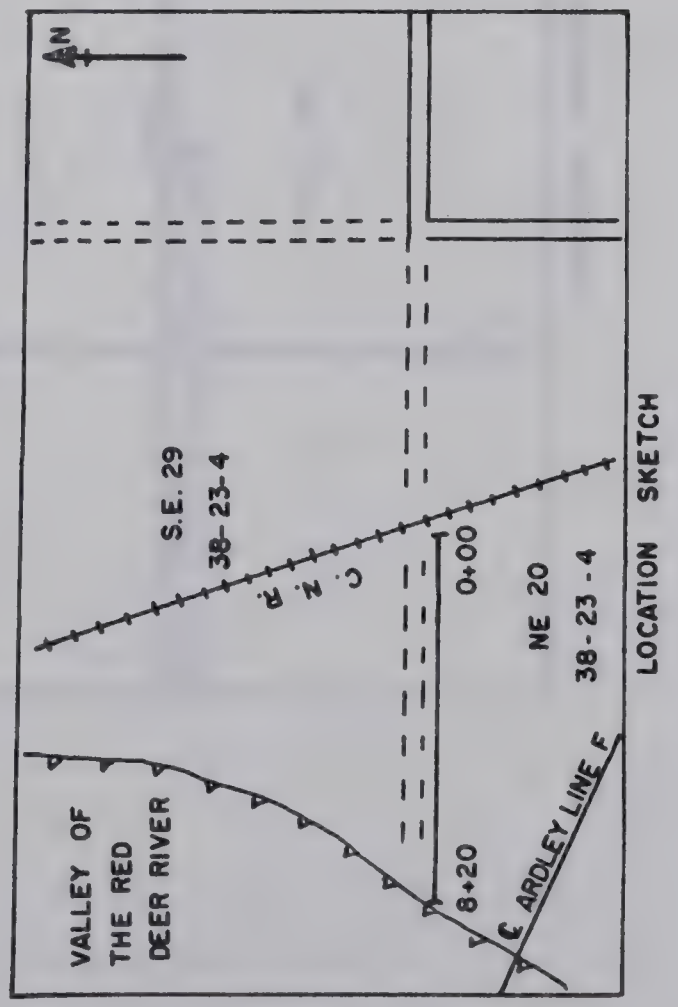
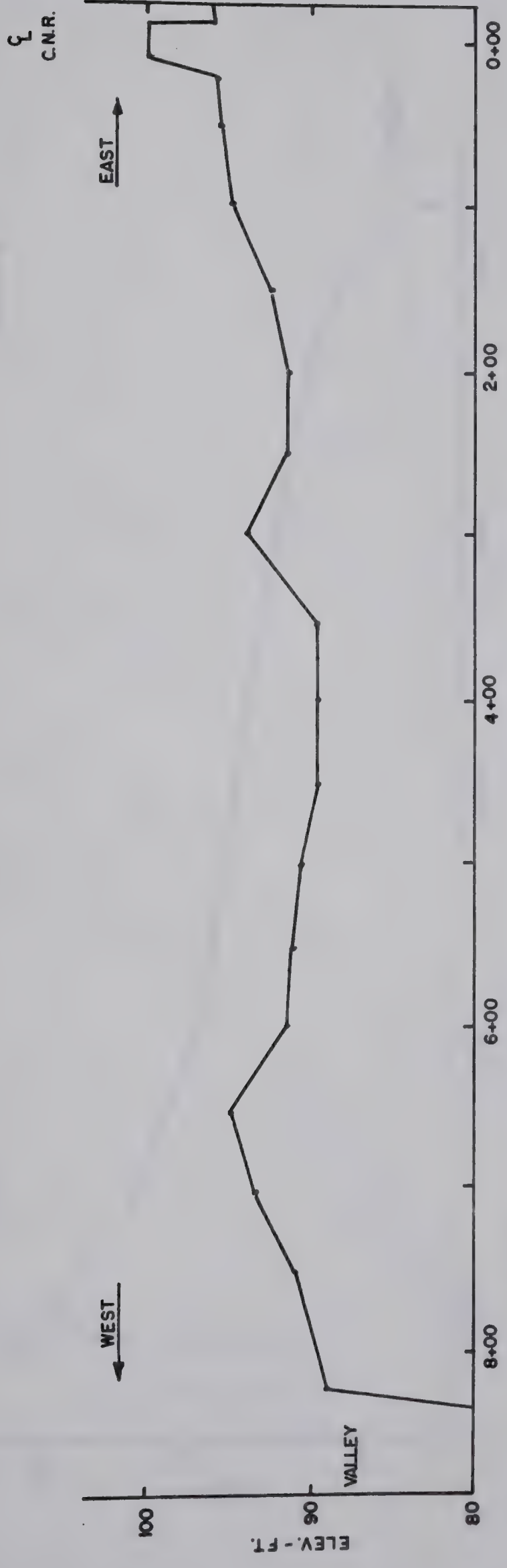


PROFILE OF THE TOP OF THE CYPRESS  
HILLS PLATEAU

FIG. C.10



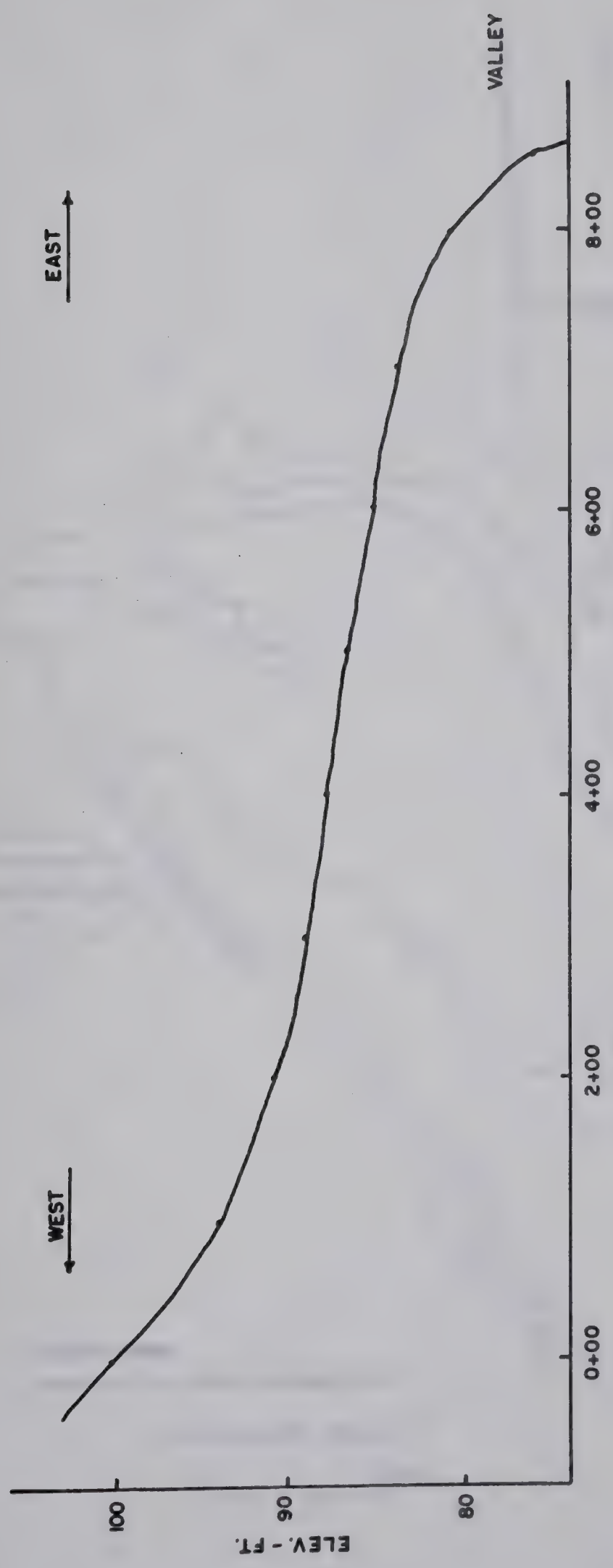




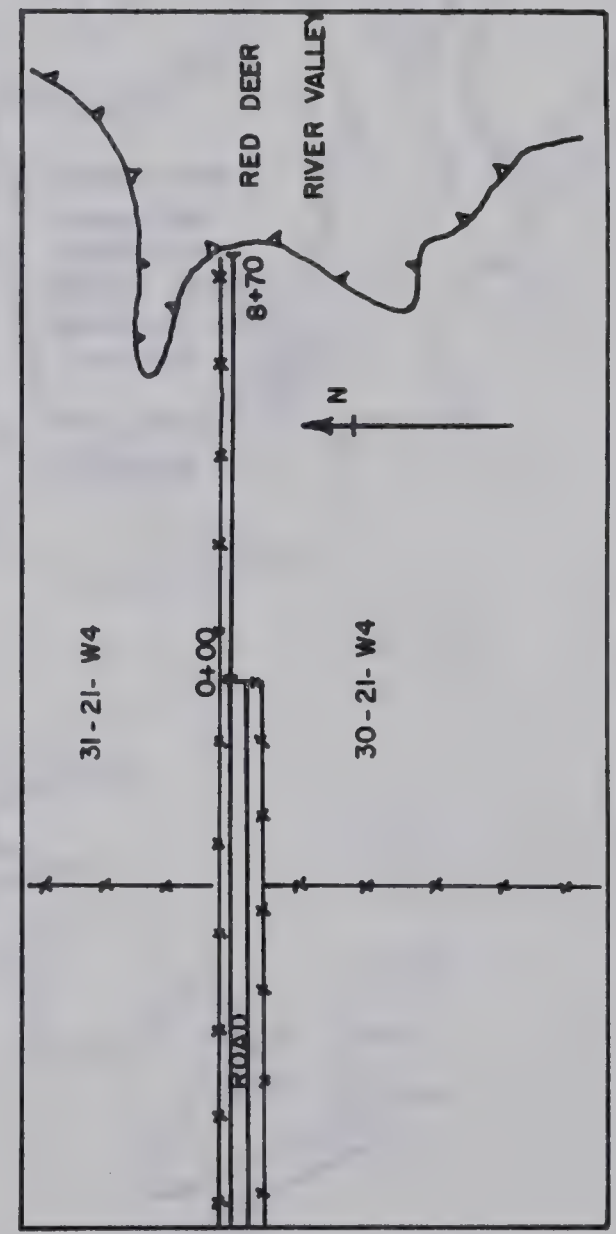
PROFILE ON THE EAST ABUTMENT OF ARDLEY DAMSITE

FIG. C.11





VALLEY



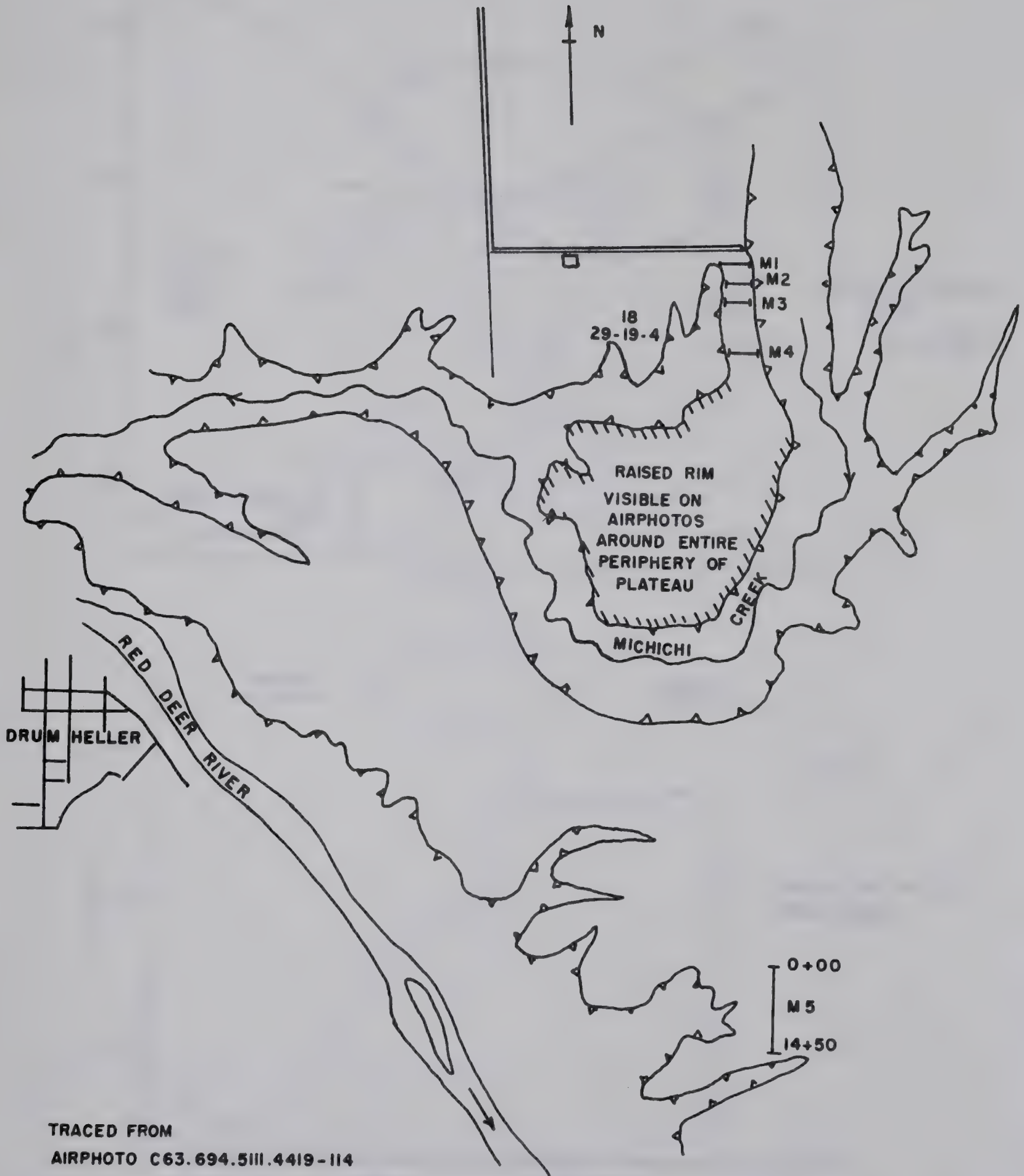
PROFILE WEST SIDE OF RED DEER RIVER

LOCATION SKETCH

FIG. C.12







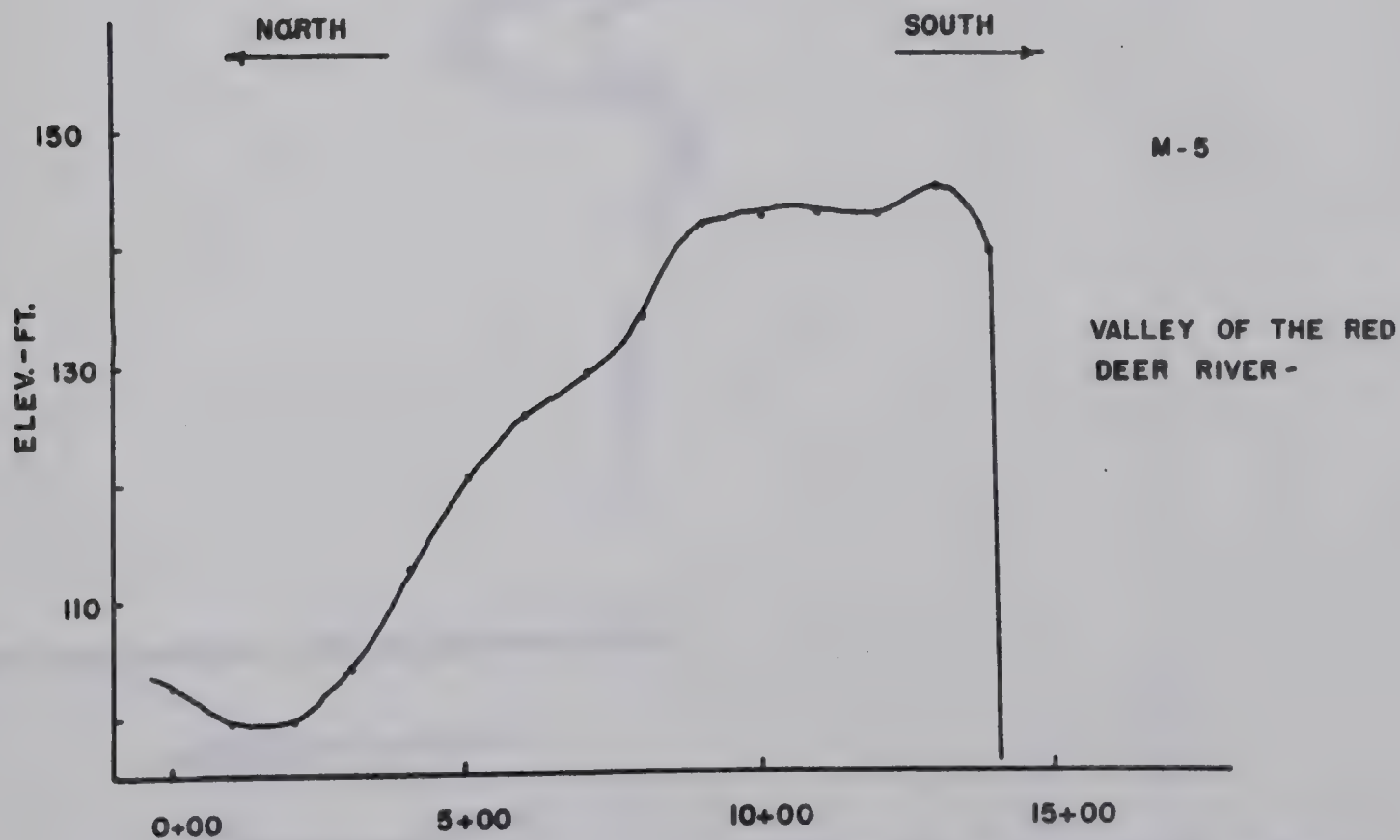
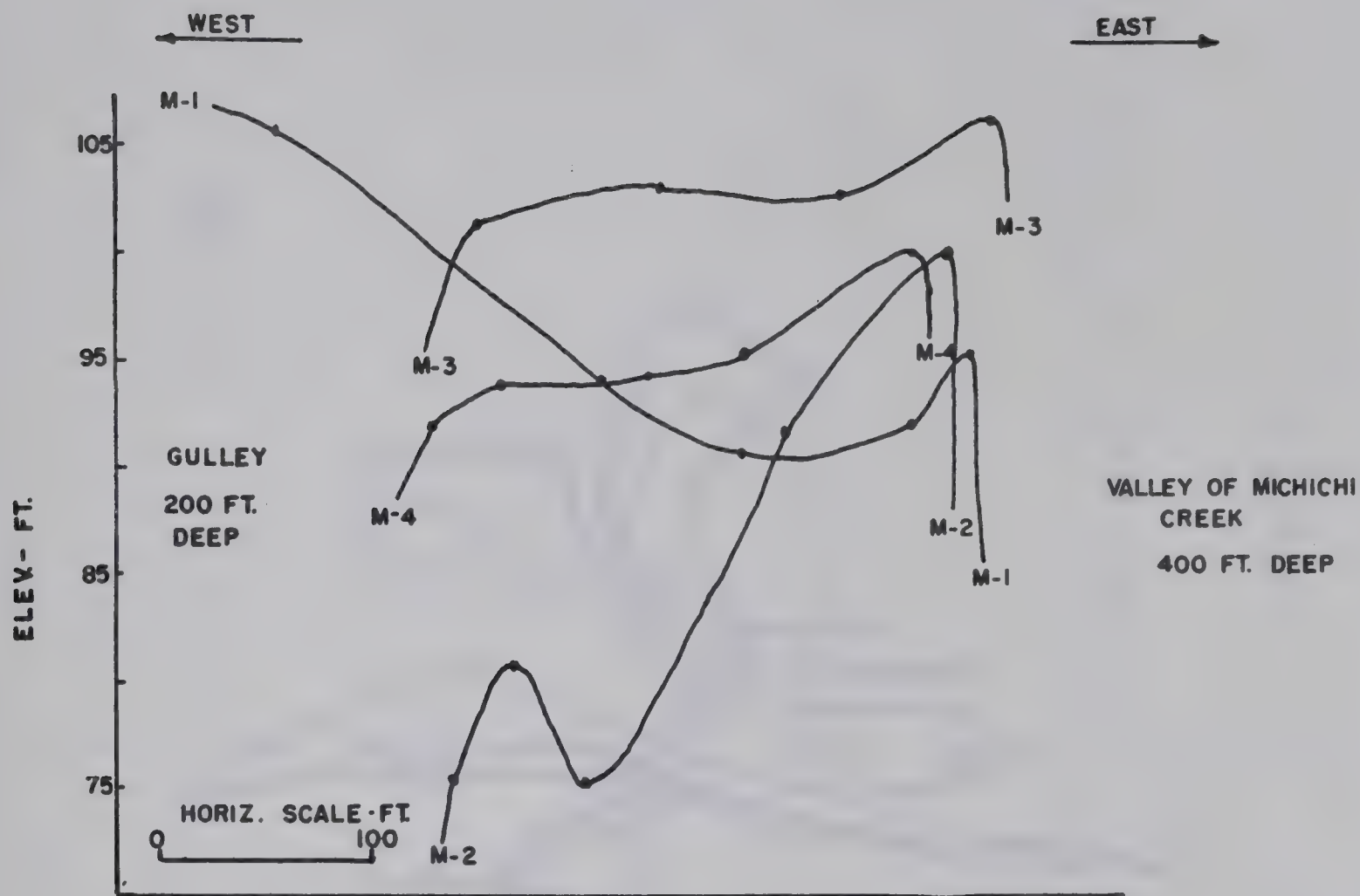
APPROXIMATE SCALE - FT.

0 2640

LOCATION OF PROFILES NEAR  
DRUMHELLER ALBERTA

FIG. C.13



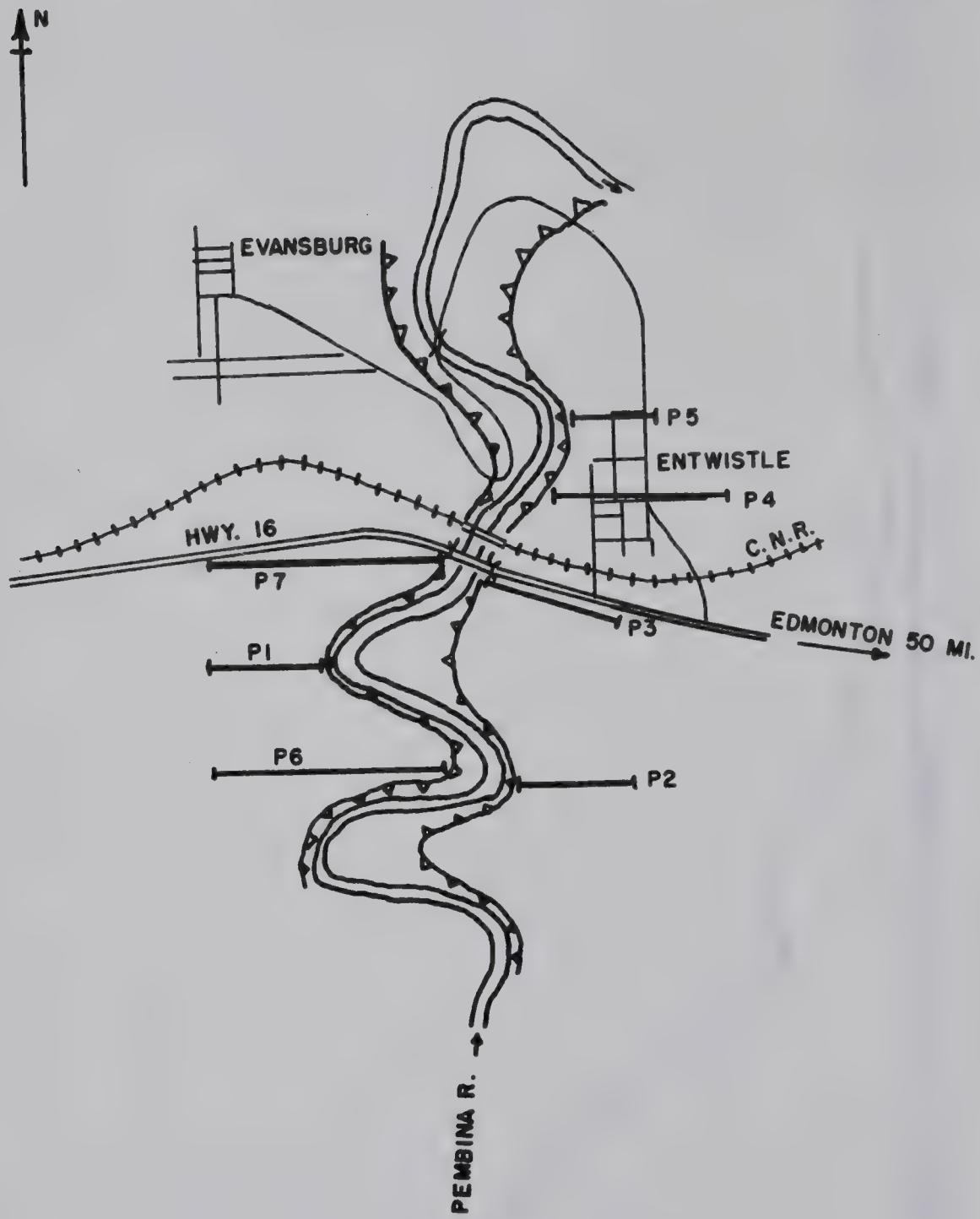


PROFILES NEAR DRUMHELLER

FIG. C.14







TRACED FROM AIRPHOTO 6706.26.867.5314.67131.67

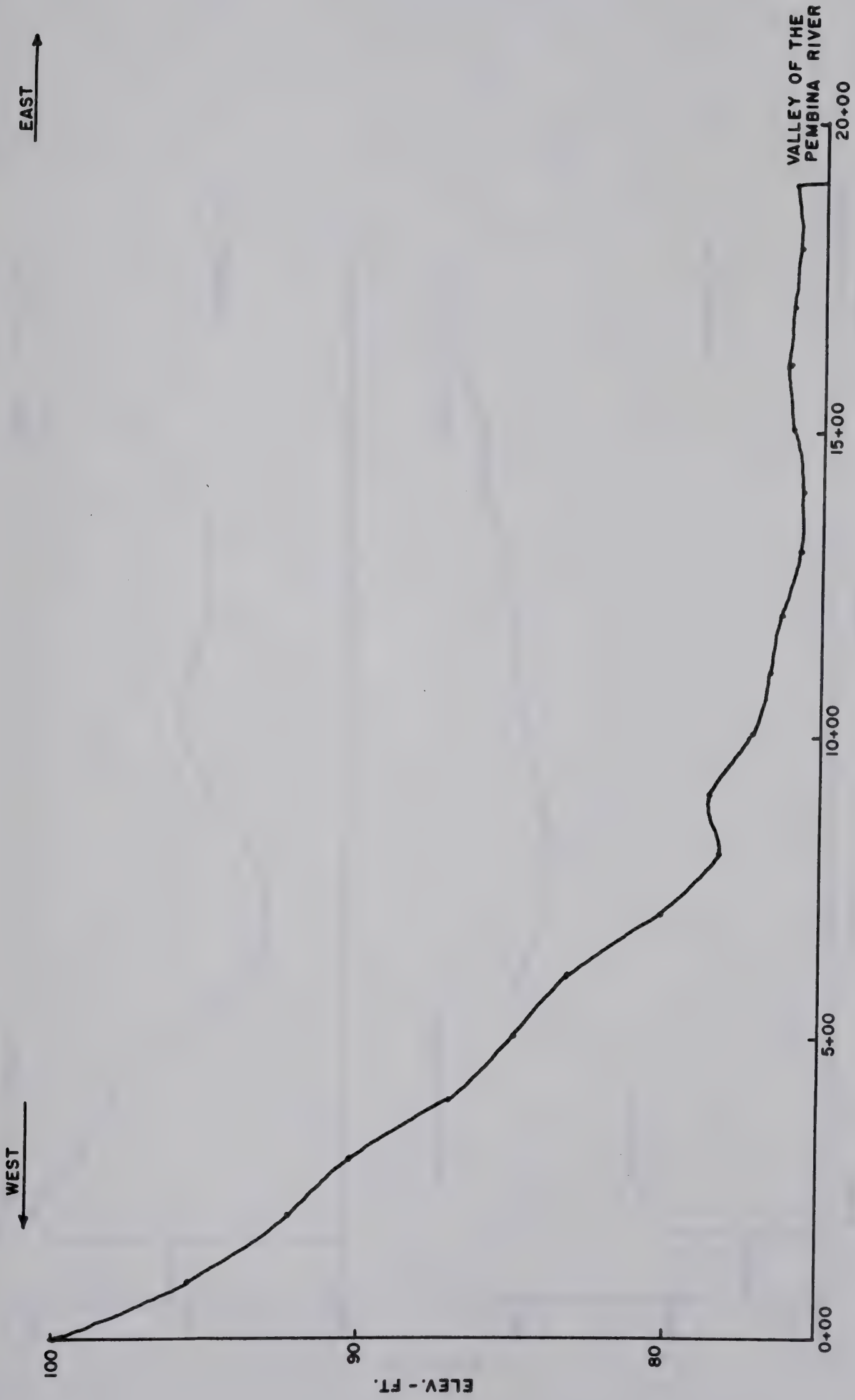
APPROXIMATE SCALE-FT.



LOCATION OF PROFILES NEAR  
ENTWISTLE ALBERTA

FIG. C.15



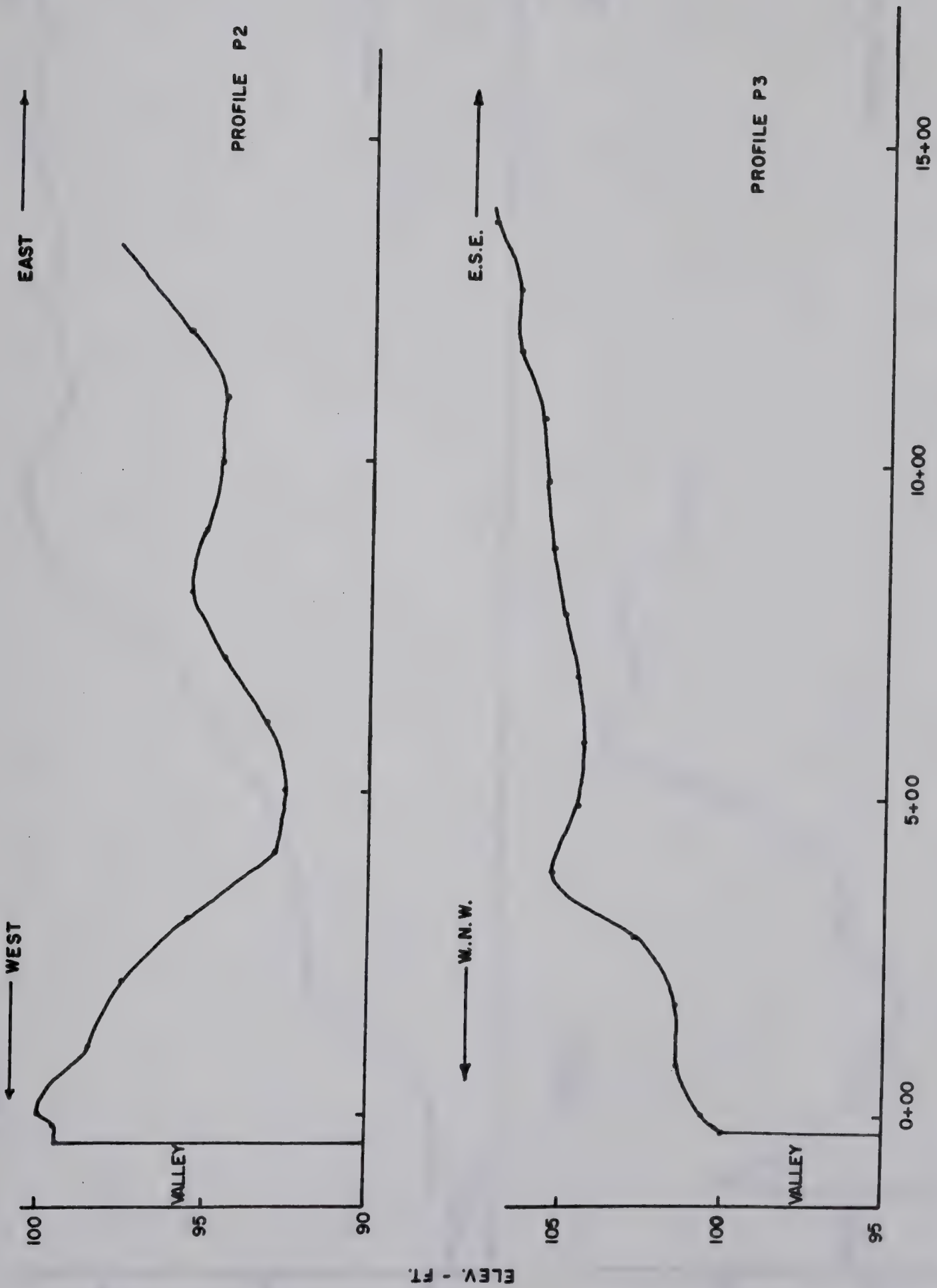


PROFILE PI

FIG. C.16



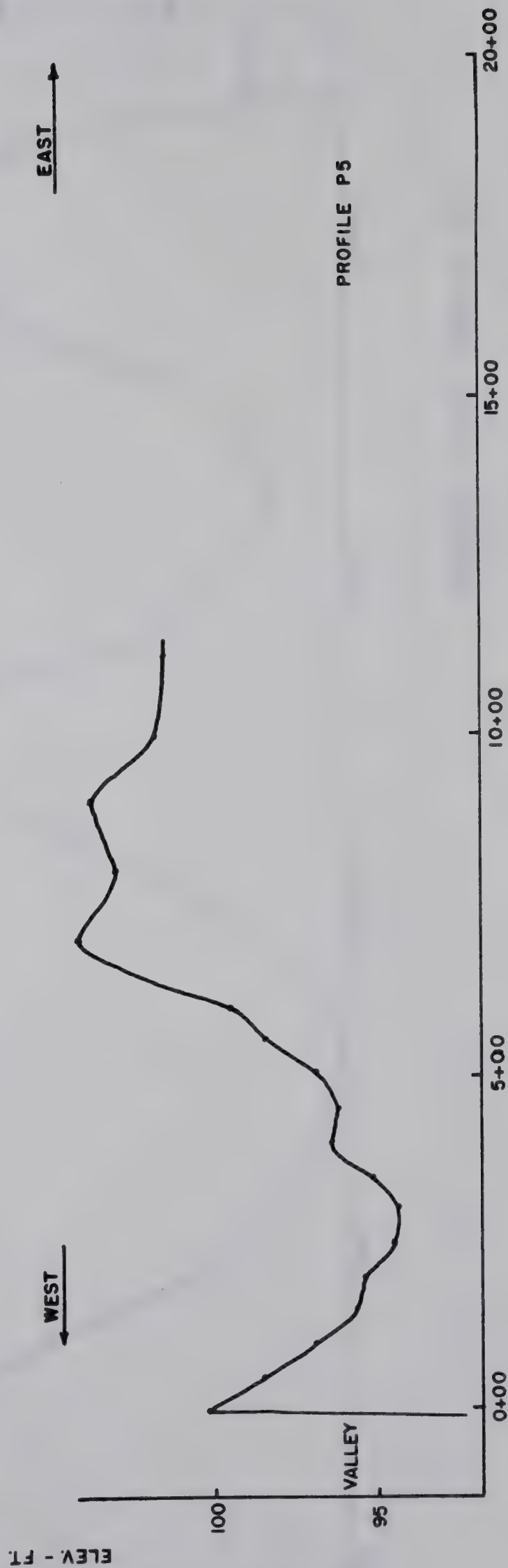
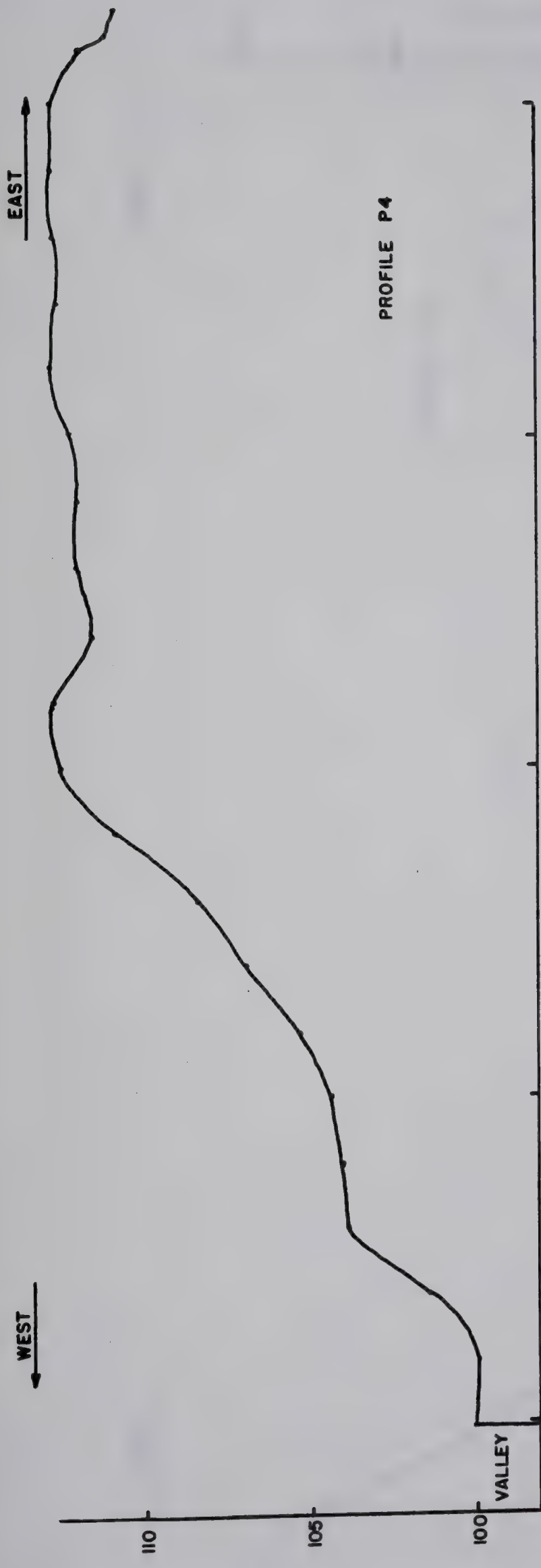




PEMBINA RIVER PROFILES

FIG. C.17



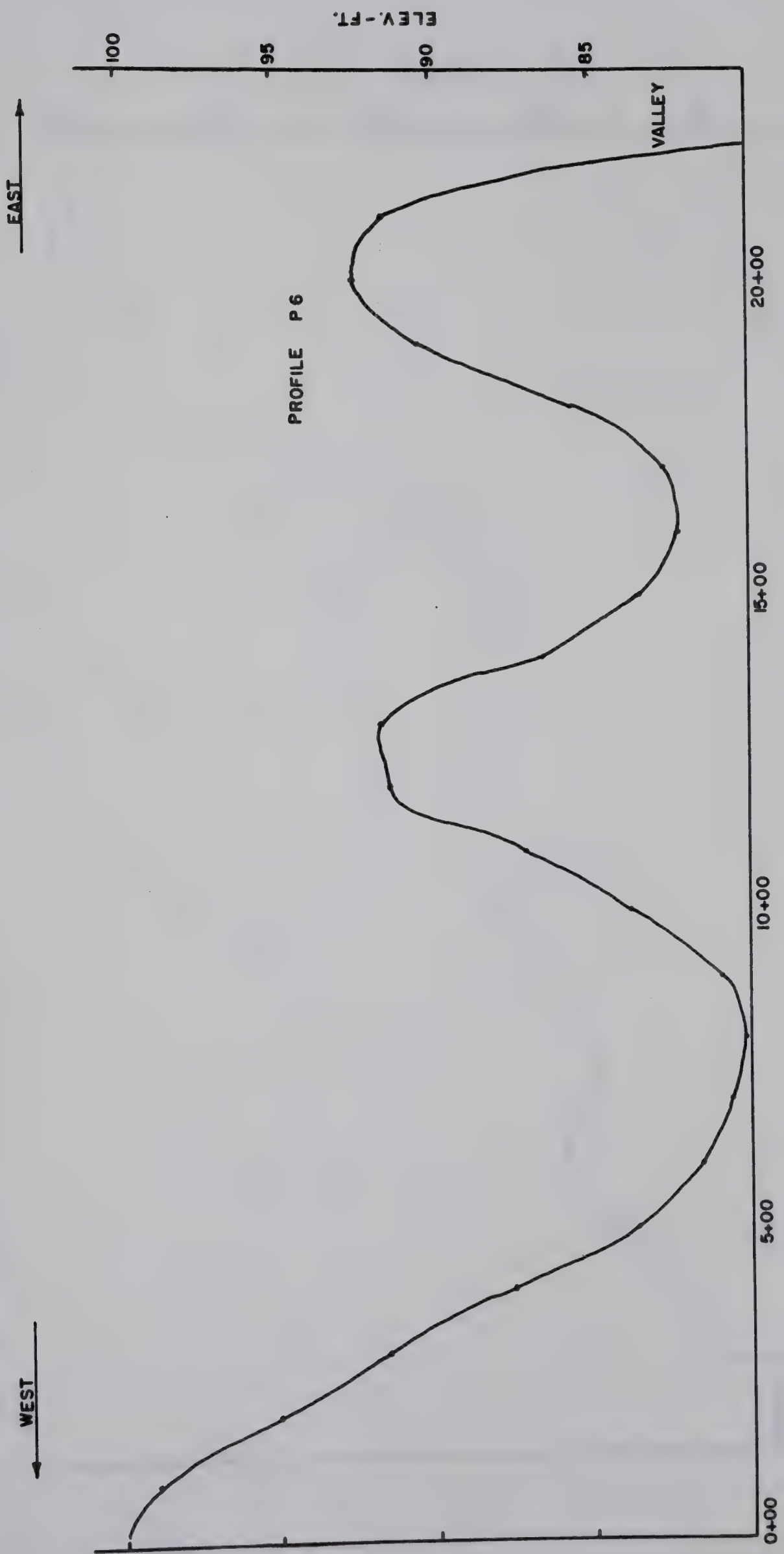


PEMBINA RIVER PROFILES

FIG. C.18







PEMBINA RIVER PROFILE P6

FIG. C.19



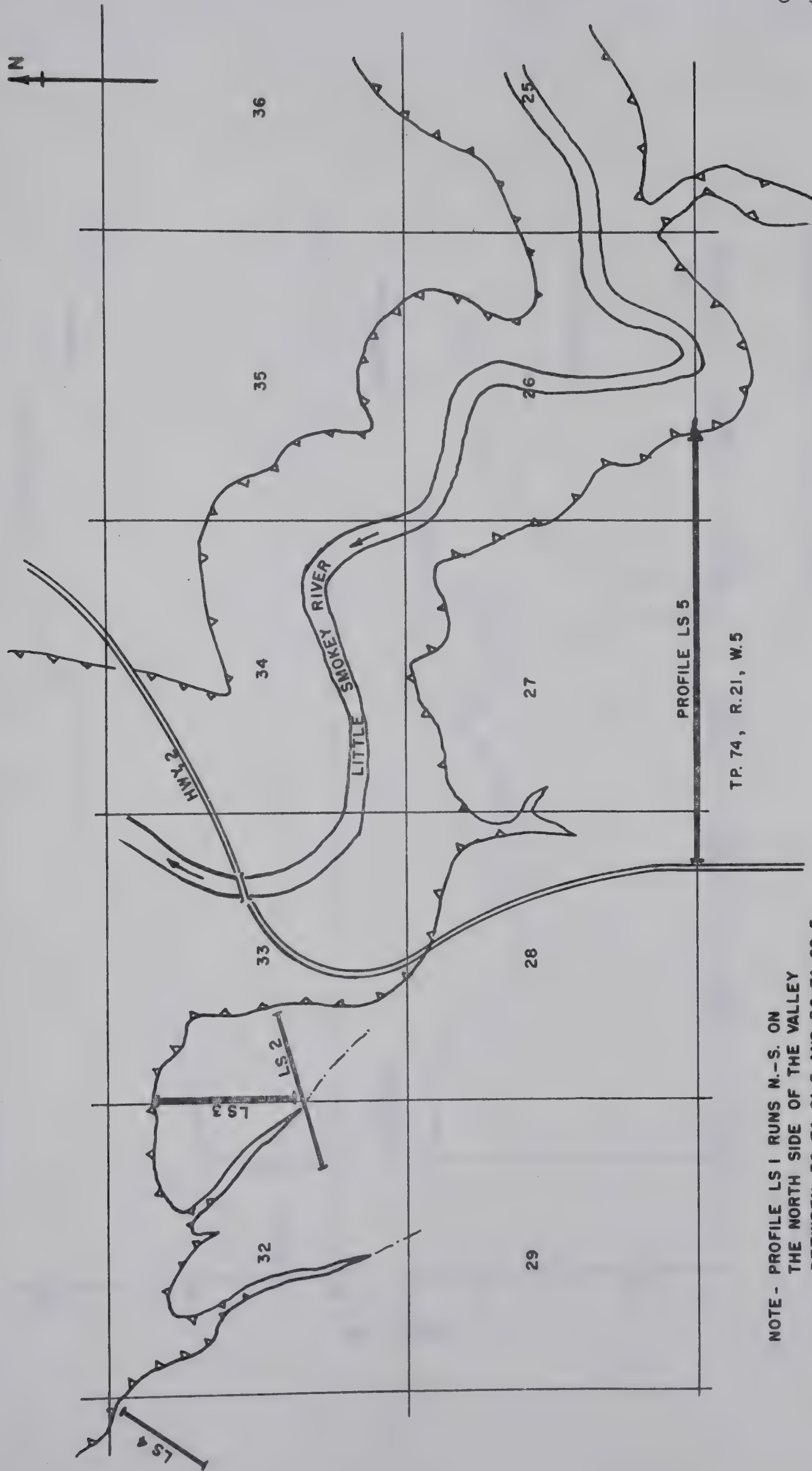


PEMBINA RIVER PROFILE P7

FIG. C.20



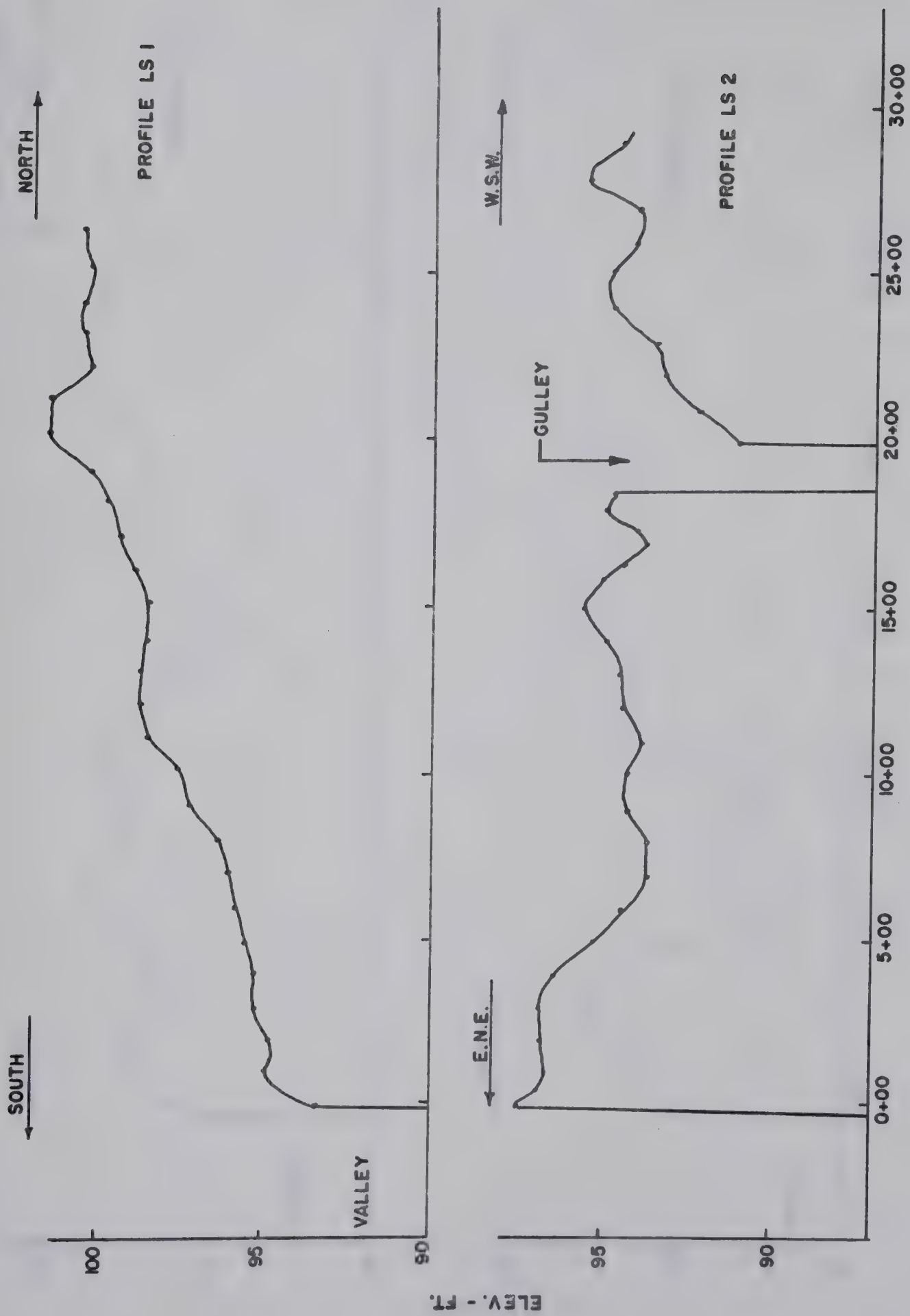




NOTE- PROFILE LS 1 RUNS N.-S. ON THE NORTH SIDE OF THE VALLEY BETWEEN 36-74-21-5 AND 30-74-20-5

LOCATION OF PROFILES NEAR THE LITTLE SMOKEY BRIDGE - FIG. C.21



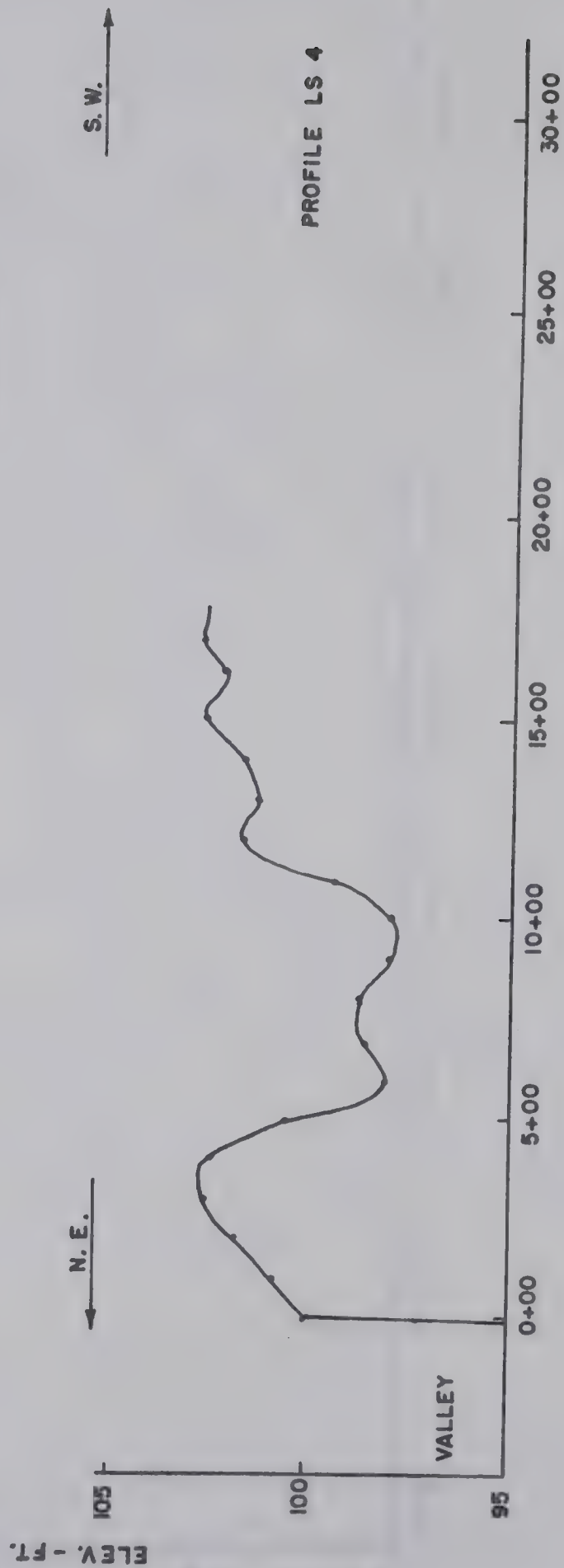
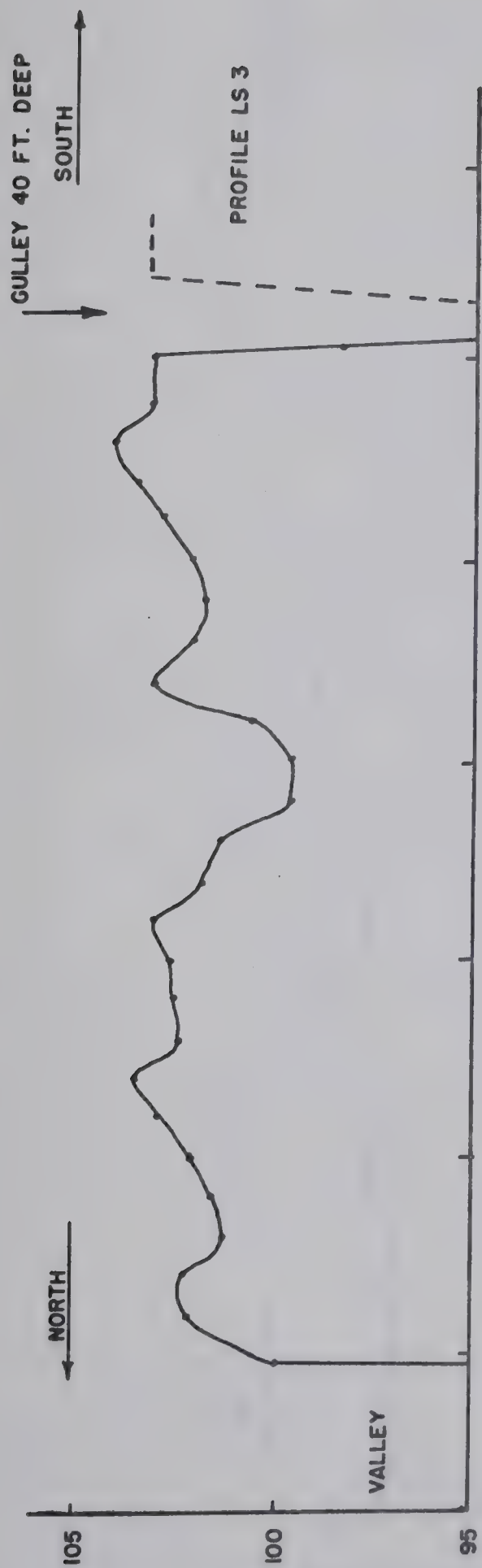


LITTLE SMOKEY RIVER PROFILES

FIG. C.22







LITTLE SMOKEY RIVER PROFILES

FIG. C.23



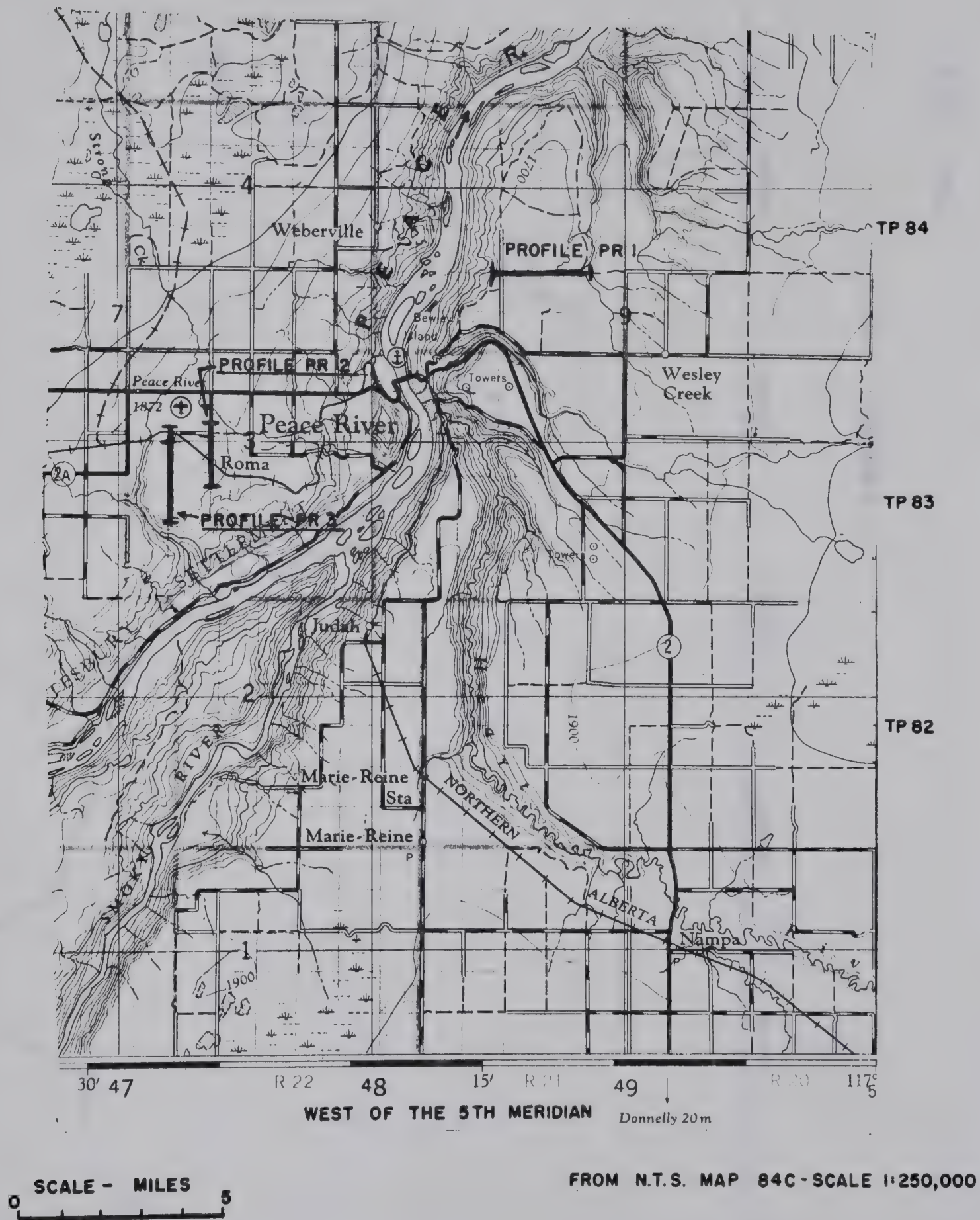


LITTLE SMOKEY RIVER PROFILE 5

FIG. C. 24

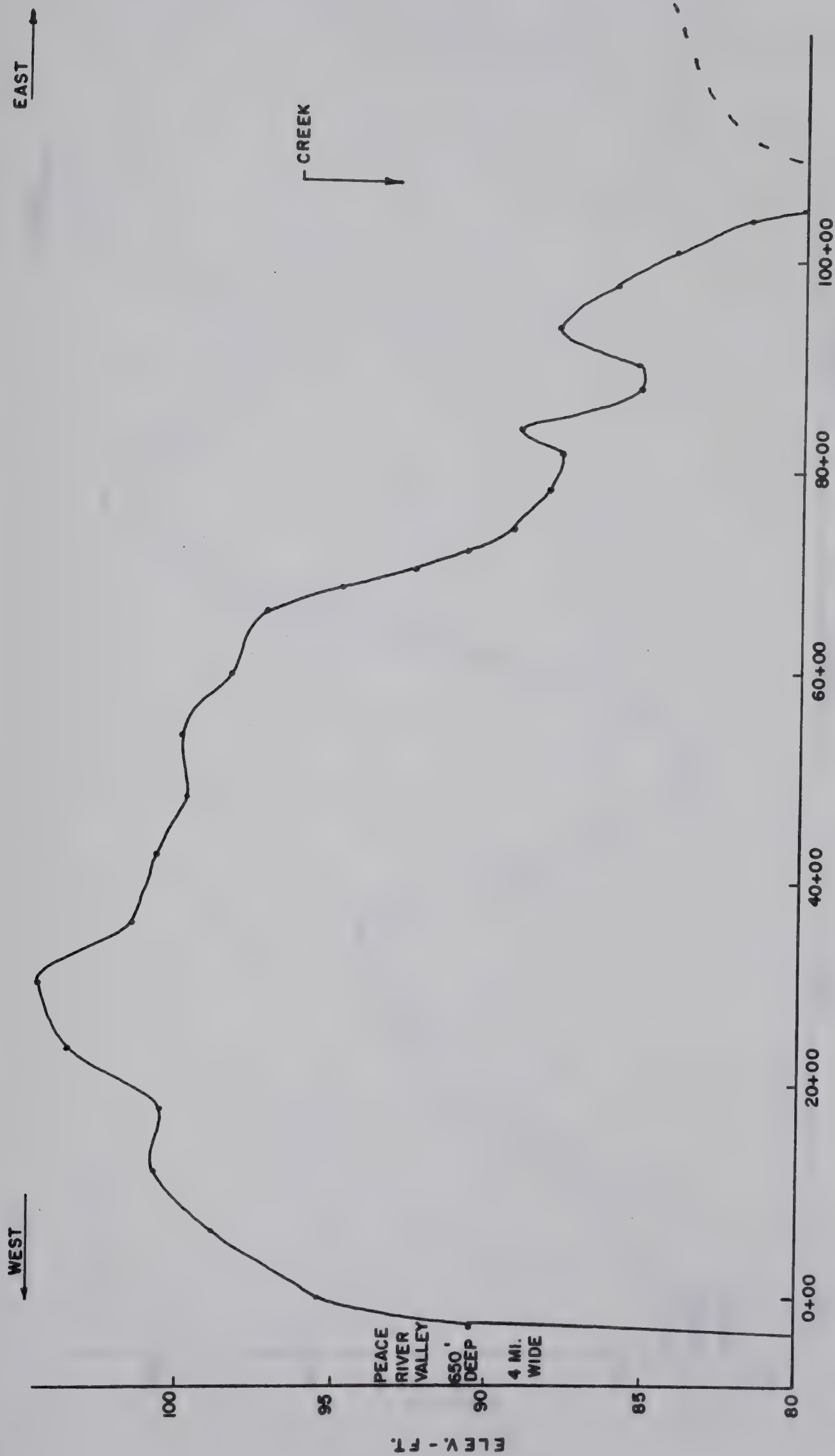






LOCATION OF PROFILES NEAR PEACE  
RIVER ALBERTA



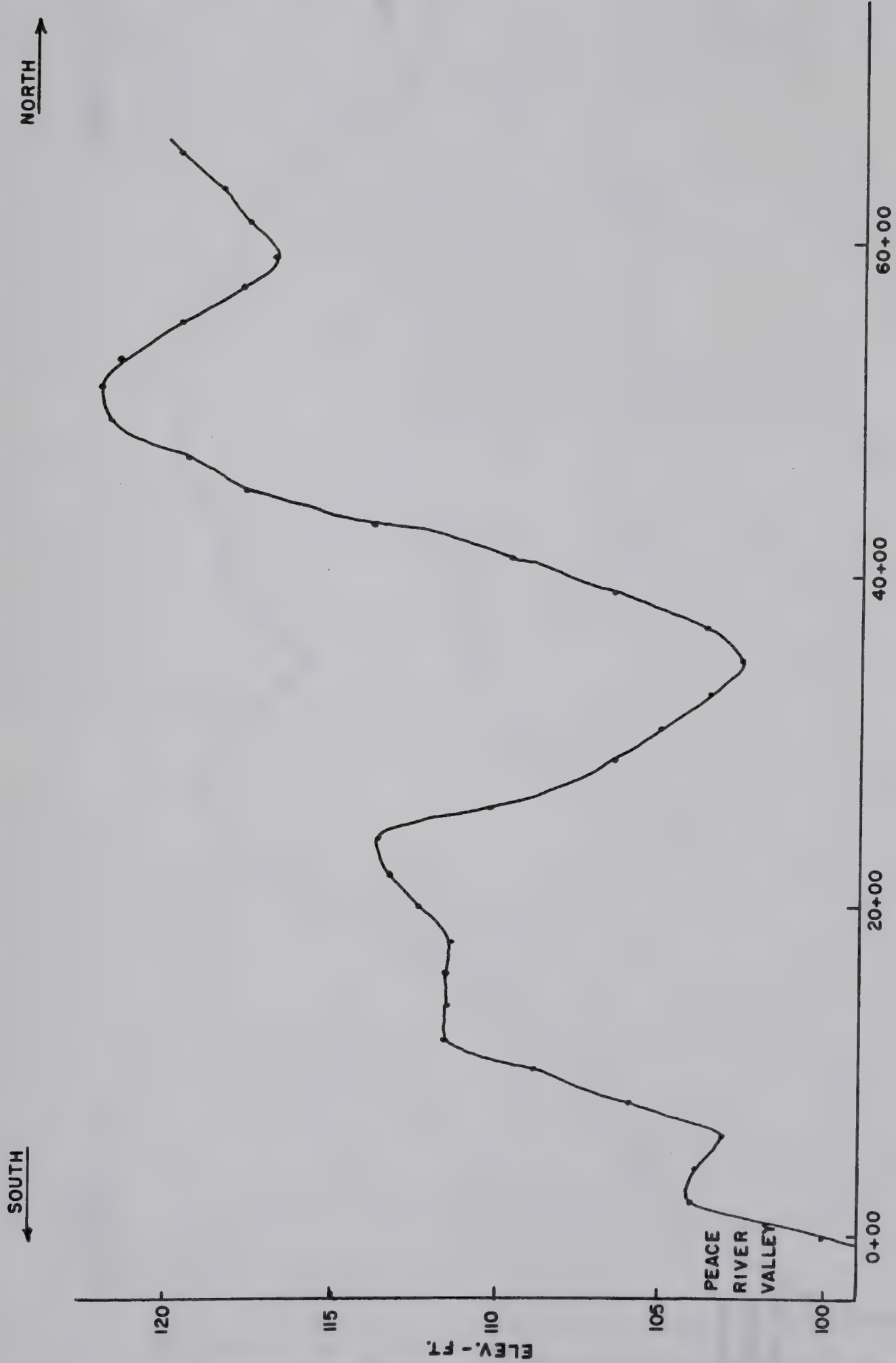


PROFILE PR 1

FIG. C.26



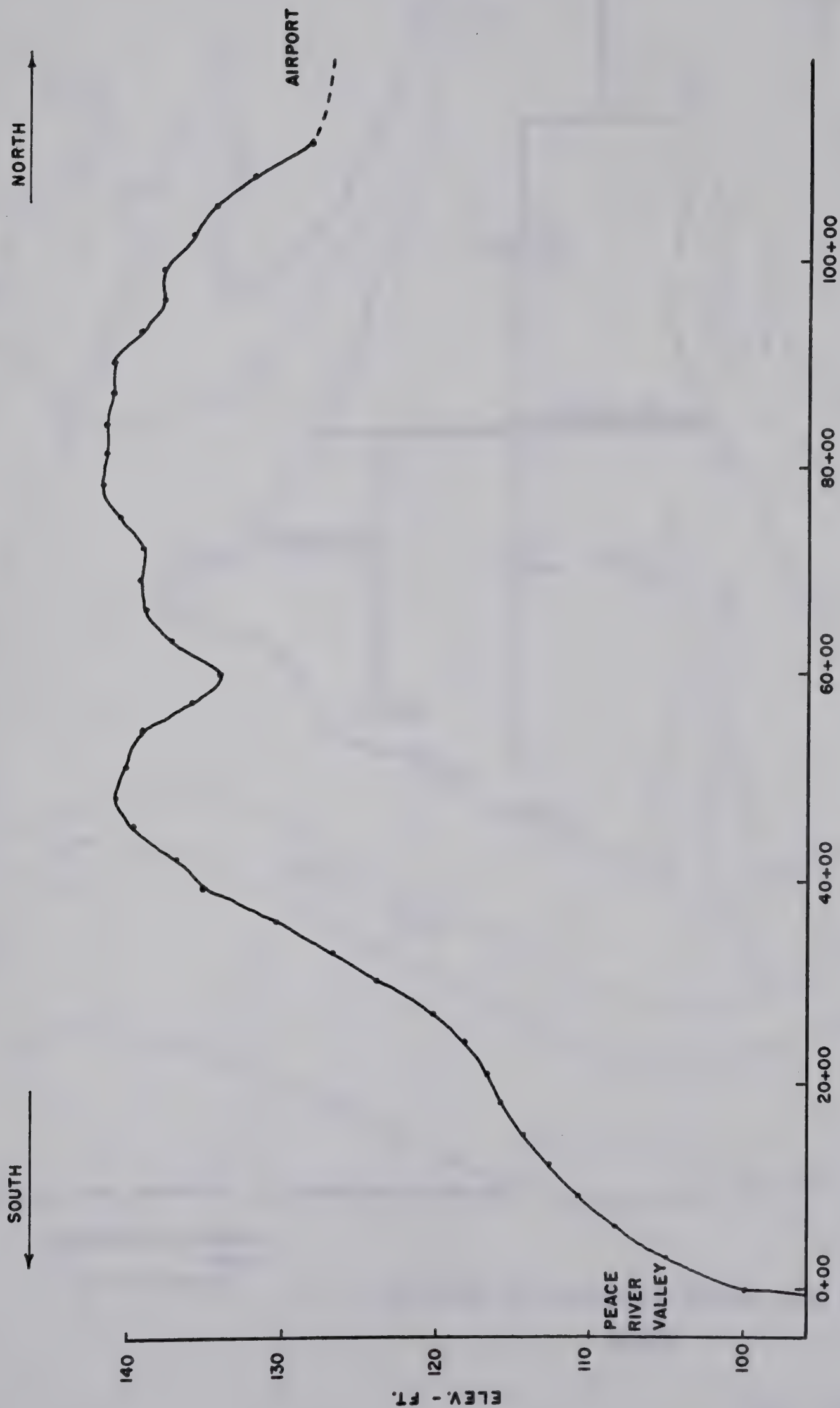




PROFILE PR 2

FIG. C.27



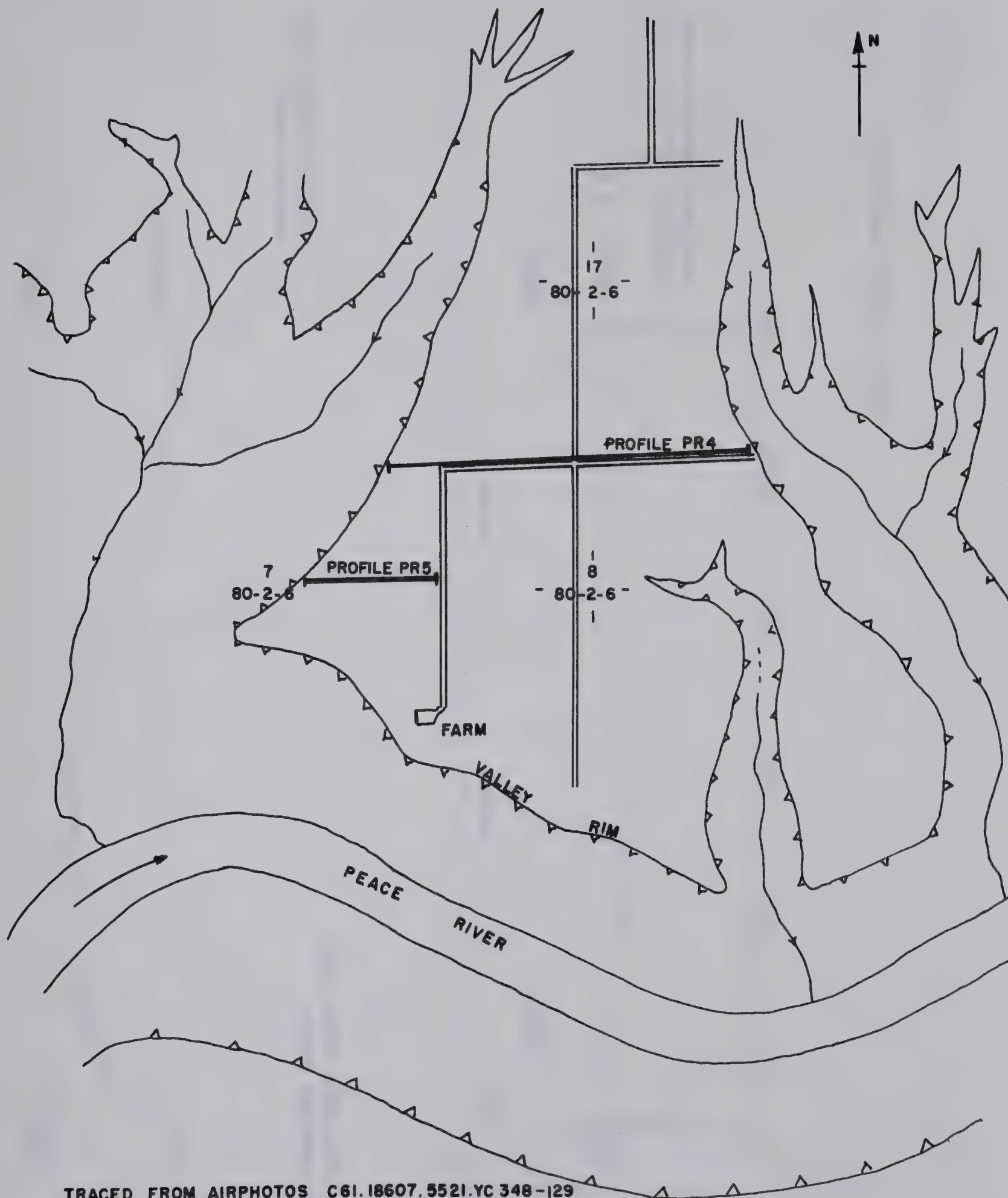


PROFILE PR 3

FIG. C.28



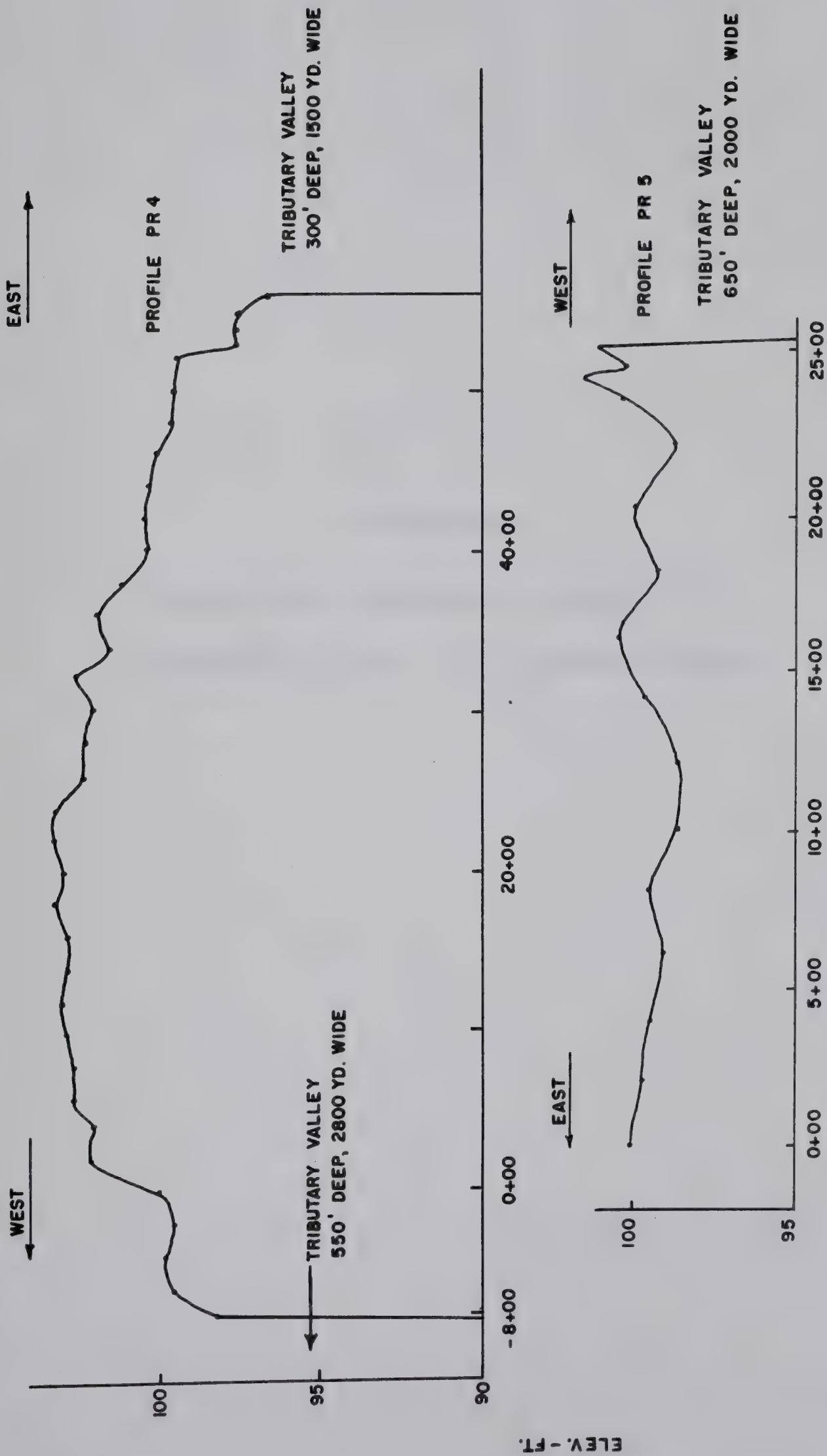




APPROXIMATE SCALE-FT.  
0 2640

LOCATION OF PROFILES ALONG THE PEACE RIVER





PEACE RIVER PROFILES

FIG. C.30





## APPENDIX D

### STRESS AND DEFORMATION ANALYSIS OF EXCAVATION BY THE FINITE ELEMENT METHOD



## 1. Introduction

Excavation by either natural or artificial means into a soil or rock mass causes changes in stress and displacements which are a function of the elastic parameters of the soil/rock mass and the in-situ state of stress which existed before the excavation occurred. This manual describes and illustrates how the final state of stress and the resulting displacements can be found for an excavation made into a homogeneous, elastic soil/rock mass using the finite element technique. The program in this manual is coded in FORTRAN IV for the IBM 360 computer.

## 2. Fundamentals of Finite Element Analysis

The soil/rock mass to be analyzed is idealized by hypothetically dividing it into a series of triangular elements connected at their corners by nodal points as shown in Figure 1. The stiffness characteristics of each element is determined and then assembled into a structural stiffness matrix (K). Stresses acting on the elements are converted to equivalent nodal point forces (P) and the nodal point displacements (u) are found from

$$(P) = (K) \cdot (u) \quad . . . (1)$$

The element stresses are determined from the nodal point displacements by the appropriate constitutive relationship.

The solution of equation (1) is bound with specification of boundary conditions. On the boundary of the finite





element grid either nodal point displacements are specified or nodal point forces are known and are specified.

Details of the method are given by Zienkiewicz and Cheung (1967) and Holand and Bell (1970). Numerous recent examples of the application of the method are found in the literature.

### 3. Initial Stress Conditions

The state of stress in the soil/rock mass before excavation has a marked effect upon the final stress field and displacements. The vertical stress  $\sigma_v$  at some depth  $z$  is taken as

$$\sigma_v = \gamma z \quad . . . (2)$$

where  $\gamma$  is the unit weight of the soil/rock. The horizontal stress is taken as a coefficient  $K_0$ , the coefficient of earth pressure at rest, times the vertical stress

$$\sigma_h = K_0 \gamma z \quad . . . (3)$$

It can be shown that if a soil or rock mass was deposited under conditions of no lateral strain then

$$K_0 = \frac{\nu}{1-\nu} \quad . . . (4)$$

Field evidence shows that the presence of tectonic stresses or 'overconsolidation' of a soil/rock mass will yield values of  $K_0$  considerable in excess of unity.

### 4. Simulation of the Excavation Sequence

Figure 2 shows the state of stress acting along the boundaries of a proposed excavation. The excavation can be



simulated for an elastic material by applying changes in stress  $\Delta\sigma$  to this boundary which are equal to the initial stresses but opposite in sign. This results in a stress free condition along the excavation boundary. Displacements and stress changes occur due to the surface tractions applied to the excavation boundary.

The final state of stress in the soil/rock mass subsequent to excavation is found by adding the stress changes at any given location to the initial state of stress at that location. The initial state of stress can be found at any point using equations (2) and (3) or by the use of the finite element program provided  $K_0 = \nu / (1 - \nu)$ . In this case a grid with a horizontal surface is constructed and the unit weight of the soil/rock input. This is termed a 'gravity switch on' procedure and the initial stresses are output. However, they can easily be found from statics and simple mechanics of materials.

## 5. Program Description

The program used was originally written in 1963 at the University of California, Berkeley for the two dimensional analysis of structures. Full details are given by Wilson (1963). The program was modified at the University of Alberta for plane strain conditions, automatic generation of nodes and elements and superposition of the original pre-excavation stresses upon the stress changes induced by excavation. The program is written in the FORTRAN IV







language and has been run on the University of Alberta's IBM 360/67 using FORTRAN IV, level G.

The program assumes an initial level surface, a constant unit weight  $\gamma$  of the soil/rock material, and a linearly elastic soil/rock mass. Constant strain triangles are used; therefore the strain and hence the stress is constant across each element.

## 6. Sequence of Operations

The program reads the data and then generates not read elements and nodes. Initial node and element stresses are calculated. Data on all elements and nodes along with initial element and nodal stresses are printed. Following this nodal displacements and stress changes due to the excavation are calculated and printed. The stress changes are superimposed upon the initial state of stress and the final state of stress is printed for all nodes and elements. Final stresses are then normalized by dividing by the unit weight  $\gamma$  times the depth of cut. The stresses  $\sigma_x$ ,  $\sigma_y$ ,  $\tau_{xy}$  are printed for all nodes and elements as well as principal stresses  $\sigma_1$  and  $\sigma_2$  and directions  $\theta$ . The maximum shear stress  $\tau_{\max}$  is printed for all nodes and elements.

## 7. Data Cards

A. Title Card (72H): Title to be printed with output.

B. Control Card (8I4, 2E12.5, 1F4.0):

Cols. 1- 4      Number of elements ( $\leq$  1700)



5- 8	Number of read elements ( <u>&lt;</u> 100)
9-12	Number of node points ( <u>&lt;</u> 1100)
13-16	Number of read node points ( <u>&lt;</u> 1100)
17-20	Number of restrained boundary points
21-24	Cycle interval for print of force unbalance
25-28	Cycle interval for print of dis- placements and stresses
29-32	Maximum number of cycles problem may run
33-44	Convergence limit for unbalanced forces ( $\leq .0005 \times$ unbalanced force of 1st cycle)
45-56	Over-relaxation factor (use 1.85)

C. Excavation Data Card (4F10.3)

Cols. 1-10	Unit weight of soil/rock (k.c.f.)
11-20	$K_o$
21-30	Y ordinate of ground surface (ft.)
31-40	Depth of cut (ft.)

D. Element array (4I4, 4E12.4, F8.4): Use one card per element or one card at the ends of a row of uniformly spaced elements.

Cols. 1- 4	Element number
5- 8	Node point i
9-12	Node point j
13-16	Node point k
17-28	Modulus of elasticity in psi
29-40	Unit weight in kips per ft. <sup>3</sup>
	(Note: use only for initial stresses if $K_o = \nu / (1-\nu)$ )
41-52	Poisson's ratio

taken counter-  
clockwise around  
the element





E. Nodal point array (1I4, 2F8.1, 2F12.8) Use one card per node point or one card at the ends of a row of uniformly spaced nodes.

Cols.	1- 4	Node point number	
	5-12	X ordinate in ft.	
	13-20	Y ordinate in ft.	
	21-28	X load in kips	
	29-36	Y load in kips	
	37-48	X displacement	on free nodal points these are initial guesses, on restrained nodal points these are specified displacements
	49-60	Y displacement	

F. Boundary array (2I4, F8.0): One card per point.

Cols.	1- 4	Node point number
	5- 8	0 if node is fixed in X and Y
		1 if node is fixed in X
		2 if node is free to move along a line with slope S
	9-16	Slope S (type 2 only)

## 8. Example Problem

The grid shown in Figure 1 is used to illustrate the use of the finite element program. It is proposed to excavate a 200 ft. deep pit with vertical sides into a rock mass with an initial flat surface. The pit is assumed to be 1200 ft. wide and have a length considerably greater than the width. The rock mass is assumed to have a Young's



modulus (E) of 100,000 psi (100 ksi) and a Poisson's ratio  $\nu$  of 0.20. The initial value of  $K_0$  is assumed to be equal to 1.00.

The slope is idealized by the finite element grid shown in Figure 1. The lateral boundary of the grid is placed at a considerable distance back from the edge of the pit so as to have little effect upon the state of stress around the slope. The nodes on the bottom boundary of the grid are assumed to be fixed in both the x and y direction while the nodes on the lateral boundaries of the grid are assumed to be fixed in the x direction only.

The grid is divided into 600 elements which are connected at 347 nodes. Nodes and elements are numbered from left to right as shown in Figure 1. Nodes are assigned X and Y co-ordinates with node point (NP) 1 as the origin. When devising a grid of this type the aspect ratio of the triangular elements (ratio of length to width) should be less than 5. A closer spacing of elements should be used in zones of interest such as the vicinity of the toe of slope as this program uses an element across which stress, and hence strain, is assumed to be constant. This approximation can lead to considerable errors in zones of high stress gradient such as at the toe of slope. As an automatic node and element generating routine is included in this program, it is often useful to keep the nodes and elements spaced uniformly in the x direction.

The automatic generation of nodes and elements requires





that the element be equally spaced in the x direction. Elements must be constructed as shown in Figure 1 to allow the automatic element generation routine to work.

The first step after laying out the grid is to number the nodes and elements as shown in Figure 1. Following this the initial values of stress before excavation are calculated. As  $K_0 = 1.00$ , Mohr's circle shows the shear stress on each element of rock to be zero. Therefore for the final shear stress field, no initial values will have to be superimposed upon the results of the finite element calculation.

The finite element program is then used to find the displacements and stress changes which occur due to excavation process. The stress on the side and bottom of the excavation are transformed into equivalent nodal forces with a sign opposite to the initial stress. These are tractions rather than compressive forces. Calculation of these nodal forces is illustrated in Figure 3.

## 9. Description of Coding Procedure

The grid illustrated in Figure 1 has 600 elements and 347 nodes. The rock mass is assumed to have a Young's modulus (E) of 100 ksi and Poisson's ratio ( $\nu$ ) of 0.20.

The first card consists of information to be printed with the results. In this case the depth of cut (200 ft.), E(100 ksi),  $\nu$ (0.20), and  $\gamma$ (.150 kcf) are entered.



The control card follows next. The number of elements (600) is entered in card columns (c.c.) 1-4. The number of read elements follows in c.c. 5-8. As the automatic element generation routine is used, only elements at the end of each row are entered. Thus 20 element cards are used and 20 is the number of read elements entered in c.c. 5-8. The total number of node points, 347, is entered in c.c. 9-12. Using the automatic node generation routine, only the nodes at the end of each row of node points need be entered if the nodal force on the interior nodes is zero (i.e., in the body of the grid). If a nodal force is specified, such as on the bottom of the excavation (NP 210-222), each of these node points must be specified by a separate card. Thus the number of read node points is entered in c.c. 13-16 as 34. The nodes are numbered from left to right, as shown in Figure 1, so as to produce a minimum difference in node point members around each element. This will minimize work in the solution process.

Each restricted boundary node point must be entered separately and in sequence. The nodes on the bottom of the grid (N.P. 1-37) are fixed in X and Y (code 0) and the nodes on the sides of the grid (N.P. 38,74,75, 111, 112, 148, etc.) are fixed in X only (code 1). The number of fixed nodes is 52 which is entered in c.c. 17-20.

The remainder of the data on the control card control the Gauss-Siedel iterative procedure and can be changed at the programmer's discretion. Experience has shown that for







most two-dimensional structures, the optimum over-relaxation factor (c.c. 45-56) is between 1.8 and 1.95 (Wilson 1963). A value of 1.85 is used in this example. The convergence limit for unbalanced forces should be  $\leq 0.0005$  of the force unbalance for the first cycle. Use of a larger convergence limit will introduce some error into the output results, use of a smaller limit will increase the running time of the program with little increase in the accuracy of results.

The third card consists of the unit weight of rock (0.150 kcf) in c.c. 1-10. The value of  $K_0$  (1.00) is entered in c.c. 11-20. The Y ordinate of the ground surface (400.0) is entered in c.c. 21-30. The depth of excavation (200.0) is entered in c.c. 31-40.

The element array follows next. One card must be coded for each element read. If an irregular mesh is used, one card must be typed for each element in the mesh. Use of a regular mesh in the X direction allows one to type an element card for only the elements at the end of each row. The input parameters (E and  $\nu$ ) must be the same for each of these two cards and the elements generated between the two end-elements will have the same parameters as specified for the two end elements.

The first element card is for element 1 in the lower left of the grid. The three nodes adjoining the element are designated as I(N.P. 39), J(N.P. 38), and K(N.P. 1) and are coded in c.c. 5-8, 9-12, and 13-16. The value of



E (100,000 psi) and  $\nu$  (0.20) are input in 'E' format. Note no unit weight is input as this would lead to a 'gravity-switch-on' procedure as discussed previously.

The second element card is for element 72 at the right hand side of the bottom row of elements. All elements between are generated automatically with  $E = 100$  ksi and  $\nu = 0.20$ .

In a similar fashion the other rows of elements are specified with a total of 20 element cards used. Hence the number of read elements equals twenty.

The node point array follows next. One card must be coded for each node point read. As a regular mesh in the X-direction allows automatic node generation, two cards are used to generate each row of nodes although each node could be specified sequentially if an irregular mesh is used.

The first node read is N.P. 1 in the lower left of the grid. The X and Y co-ordinate system starts in this corner of the grid so zero is entered for the X and Y ordinates in c.c. 5-12 and c.c. 13-20. The displacement of N.P. 1 is specified as zero (c.c. 37-48 and 49-60) and no boundary loads are specified. Node point 37 is specified next with an X co-ordinate of 1800.0 ft. and a Y co-ordinate of 0.0. All nodes between are generated automatically.

This process continues until the boundaries of the cut are reached. On N.P. 210 both X and Y force are specified (Fig. 3) as 363.25 kips and 750.00 kips respectively. Each node on the bottom of the cut must be specified







separately (N.P. 210-222). Above the base of the cut automatic node generation can be used again with nodal forces specified on the sides of the cut. A total of 34 node cards are prepared.

Following the node cards, the restricted node point array (52 cards) is typed. Starting with N.P. 1, the node points on the bottom of the grid must be coded sequentially (N.P. 1-37). Each of these nodes is fixed in X and Y so code 0 is input in c.c. 8. On the sides of the grid (N.P. 38, 74, 75, 112, 148, 149, 185, 186, 222, 223, 248, 273, 293, and 323) movement is restricted in the X direction only. Thus code 1 is entered in c.c. 8 of these cards.

#### 10. Presentation of Results

The title card is printed followed by the data on the control card. The data for each element and node is then output including the initial state of stress before excavation in ksf. Boundary conditions are output followed by cycle number and force unbalance.

Nodal point displacements are then output in feet with displacements positive upwards and to the right. Thus in the center of the excavation (N.P. 222) an upward displacement (or rebound) of 0.375 ft. is predicted. At the top of slope (N.P. 347) a displacement of 0.184 ft. towards the excavation and 0.0596 ft. upwards is predicted.

Element and nodal stresses are then output in ksf. First the stress changes due to the excavation process are



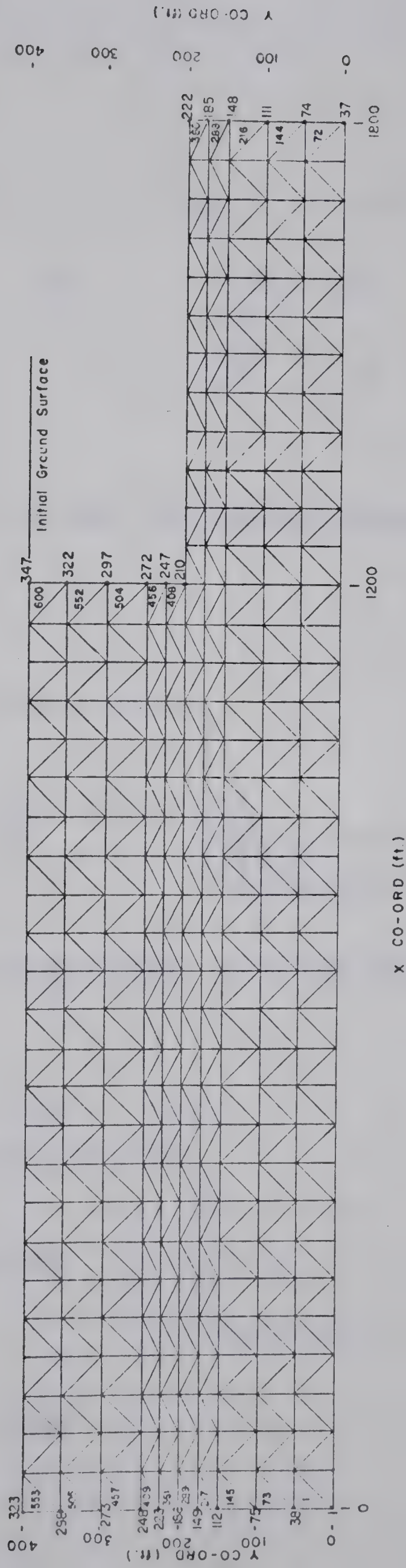
printed with compressive forces taken as negative. These stress changes are superimposed upon the initial state of stress and the final state of stress is printed with compression positive. The final state of stress is normalized by dividing through by  $H$  where  $H$  = depth of cut.

At the toe of slope (N.P. 210) the maximum value of shear stress is 15.782 ksf. Normalized this gives a value of 0.526.

Note when evaluating stresses that nodal point stresses are obtained by averaging element stresses for all elements connected to the nodal point. This produces good results for interior nodal points but will induce some approximation errors on the boundary of the grid. Element stresses will include some approximation errors on the grid boundary due to the type of element used.







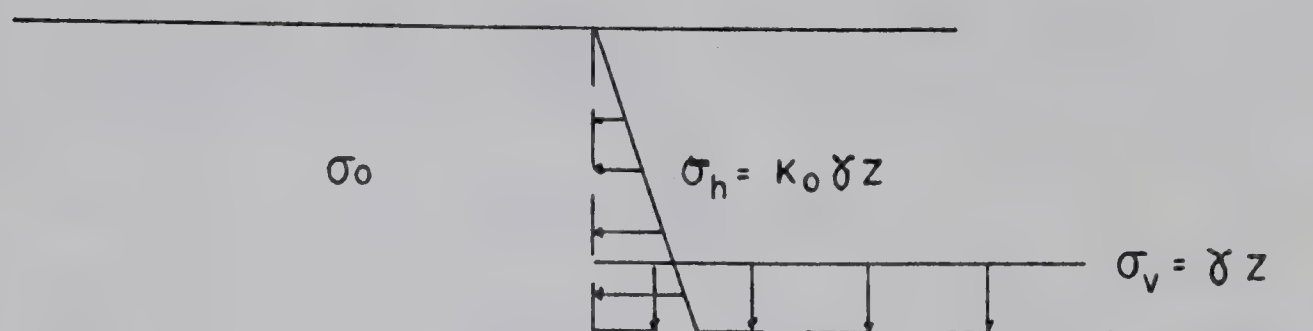
LEGEND  
 ELEMENT 73  
 NODE 75

NUMBER OF ELEMENTS = 600  
 NUMBER OF NODES = 347  
 E=100 KSI,  $\nu = 0.20$ ,  $K_0 = 1.00$

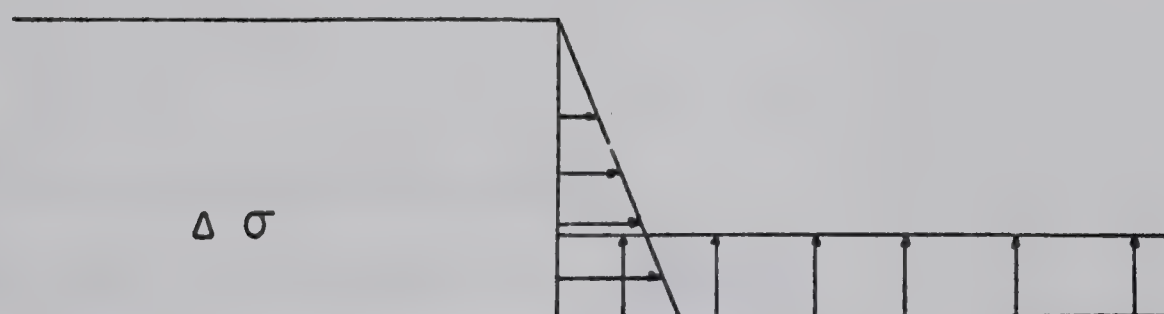
FINITE ELEMENT GRID

FIG. 1

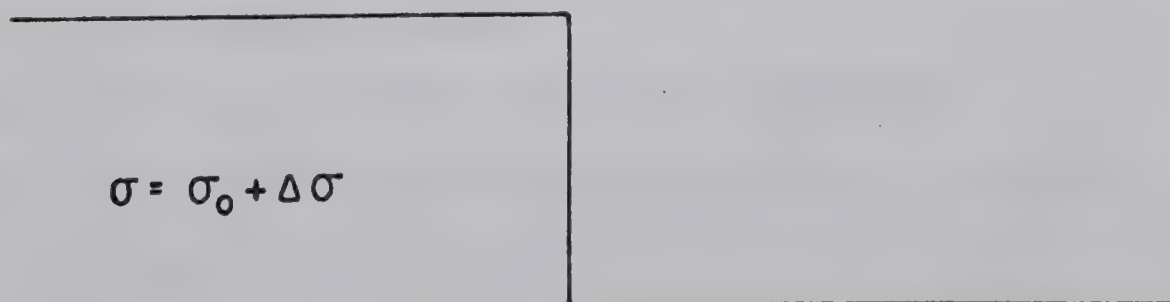




(a) INITIAL STRESS ON BOUNDARY OF PROPOSED EXCAVATION



(b) APPLICATION OF STRESS CHANGE EQUAL AND OPPOSITE TO INITIAL STRESSES

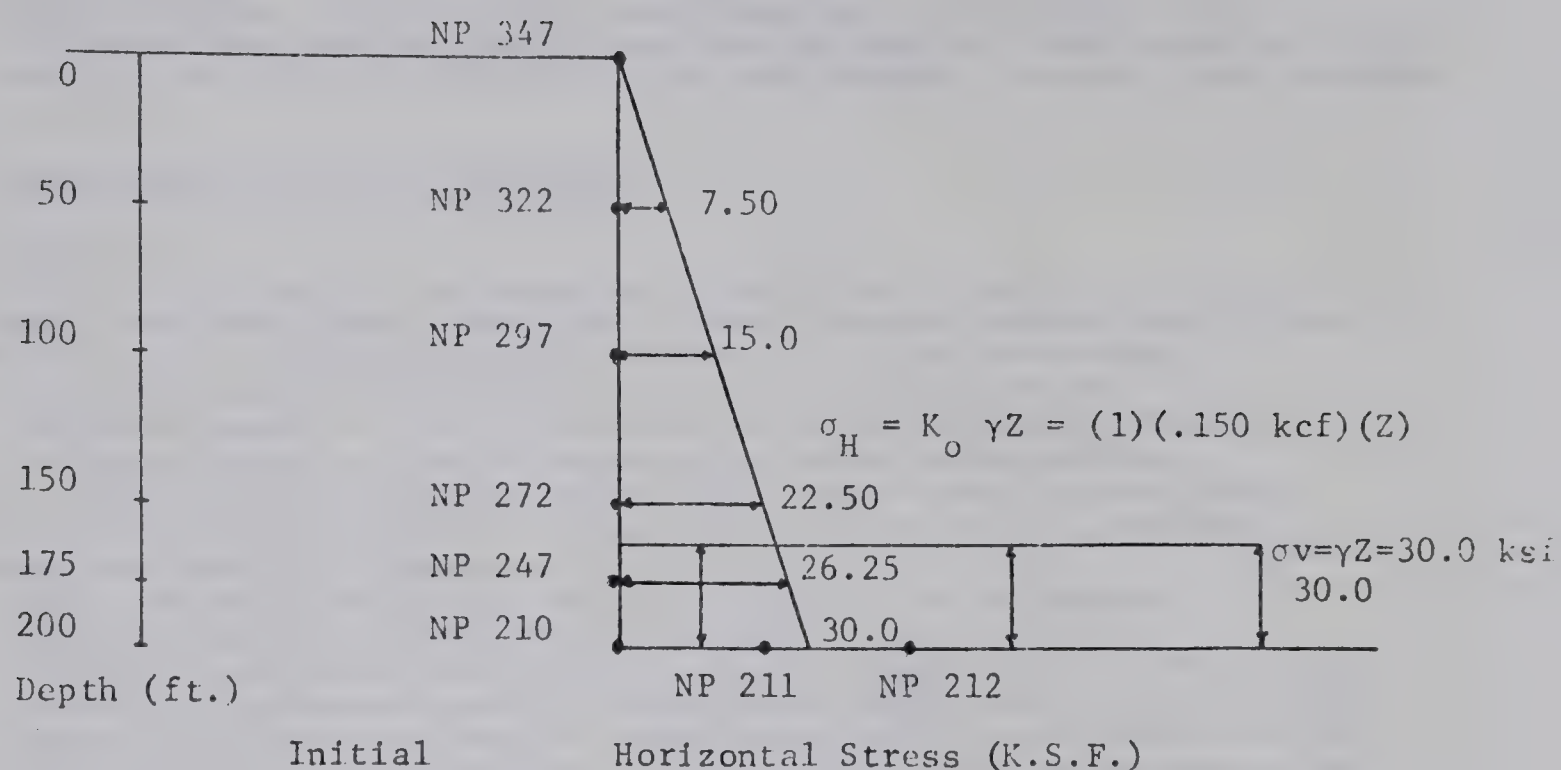


(c) FINAL STATE OF STRESS

FIGURE 2







### 1. Calculation of Vertical Nodal Forces:

$$\sigma_v = \gamma Z = (.150 \text{ kcf})(200 \text{ ft.}) = 30.0 \text{ ksf}$$

for a unit thickness  $\sigma_v = 30.0$  kip/lin. ft.

N.P 210       $P_v = 25 \text{ ft.} \times 30 \text{ kip/lin. ft.} = 750.00 \text{ kip.}$

N.P 211       $P_v = 30.00 \times 50 = 1500.00 \text{ kip}$

etc.

## 2. Calculation of Lateral Nodal Forces:

Lateral stresses are shown above.

$$\text{N.P. 347} \quad P_{LL} = 1/2 \times 25 \text{ ft.} \times 3.75 \text{ ksf} = 46.88 \text{ kip}$$

N.P. 322  $M = 50 \text{ ft.} \times 3.75 \text{ ksf} + 1/2 \times 50 \text{ ft.} \times 7.50 \text{ ksf} = 375.00 \text{ kip}$

etc.

## CALCULATION OF NODAL FORCES

Figure 3



FINITE ELEMENT PROGRAM USING CONSTANT STRAIN TRIANGLES TO FIND THE  
DISPLACEMENTS, STRESS CHANGES AND FINAL STATE OF STRESS DUE TO  
AN EXCAVATION IN A SOIL/ROCK MASS WITH AN INITIAL HORIZONTAL SURFACE.  
THE SOIL/ROCK MASS IS ASSUMED TO BE HOMOGENEOUS, ISOTROPIC AND LINEARLY  
ELASTIC.

# DIMENSION AND COMMON STATEMENTS

REAL KO

DIMENSION NPNUM(1100),XORD(1100),YORD(1100),HEAD(18),  
1DSX(1100),DSY(1100),XLOAD(1100),YLOAD(1100),NP(1100,10),SXX(1100,9  
2),SXY(1100,9),SYX(1100,9),SYY(1100,9),NAP(1100),NPNUM(90),  
3XORDR(90),YORDR(90),XLDR(90),YLDR(90),DSXR(90),DSYR(90)

DIMENSION NUNE(1900),NPI(1900),NPJ(1900),NPK(1900),ET(1900),  
1XU(1900),RO(1900),COED(1900),DT(1900),THERM(1900),AJ(1900),  
2BJ(1900),AK(1900),BK(1900),SIGXX(1900),SIGYY(1900),SIGXY(1900),  
3SLOPE(1100),NUMER(100),NPIR(100),NPJR(100),NPKR(100),ETR(100),  
4RDR(100),XUR(100),COEDR(100),DTR(100)

DIMENSION NPB(1100),NPIX(1100),L4(3),A(6,6),B(6,6),S(6,6)

DIMENSION DEPTH(1700),SIGIY(1100),SIGIX(1100),RAD(1100),  
1TIMAX(1100),SIGMAX(1100),SIGMIN(1100),XF(1100),YF(1100),XYF(1100),  
2XMAXF(1100),XMINF(1100),CF(1100),RF(1100),PAF(1100)

DIMENSION SIGEX(1700),SIGEY(1700),ETMAX(1700),ELSMAX(1700),ELSMIN(1  
1700),XFE(1700),YFE(1700),XYFE(1700),XMAXFE(1700),XMINFE(1700),CFE  
2(1700),RFE(1700),PAFE(1700),RETR(1700),RXUR(1700),YELE(1700),WV(17  
300)

COMMON SXX,SXY,SYX,SYY

EQUIVALENCE (SIGXX(1),RO(1),NPB(1)),(SIGYY(1),COED(1),NPIX(1)),  
1(SIGXY(1),DT(1),SLOPE(1))

# READ AND PRINT DATA

NTRR=0

150 READ(5,100)HEAD

WRITE(6,99)

WRITE(6,100)HEAD

READ(5,1)NUMEL,NUREL,NUMNP,NURNP,NUMBC,NCPIN,NOPIN,NCYCM,TOLER,

1XFAC,T1

READ(5,201)UNTWT,RKD,ZSFC,HCUT

WRITE(6,101)NUMEL

WRITE(6,825)NUREL

WRITE(6,102)NUMNP

WRITE(6,824)NURNP

WRITE(6,103)NUMBC

WRITE(6,104)NCPIN

WRITE(6,105)NOPIN

WRITE(6,106)NCYCM

WRITE(6,107)TOLER

WRITE(6,108)XFAC

WRITE(6,1700) UNTWT

WRITE(6,1701) RKD

WRITE(6,1702) ZSFC

WRITE(6,1703) HCUT

READ(5,553)(NUMER(N),NPIR(N),NPJR(N),NPKR(N),ETR(N),RDR(N),XUR(N),

1COEDR(N),DTR(N),N=1,NUREL)

READ(5,3)(NPNUM(M),XORDR(M),YORDR(M),XLDR(M),YLDR(M),

1DSXR(M),DSYR(M),M=1,NURNP)





```

      RTEMP=ETR(1)
      XTEMP=XUR(1)
C
C      OPTIONAL CONVERSION FOR PLANE STRAIN SOLUTION
C
      DO 550 N=1,NUREL
      ETR(N)=(ETR(N)/(1.-XUR(N)**2))*(144./1000.)
      XUR(N)=XUR(N)/(1.-XUR(N))
550 CONTINUE
C
C      GENERATION OF NOT READ ELEMENTS
C
      DO 161 N=1,NUREL
      M=N+1
      IF(M-NUREL) 162,162,163
162 I=NUMER(M)-NUMER(N)
      IF(I-1)163,163,164
164 L=NUMER(N)
      NUME(L)=NUMER(N)
      NPI(L)=NPIR(N)
      NPJ(L)=NPJR(N)
      NPK(L)=NPKR(N)
      ET(L)=ETR(N)
      RO(L)=ROR(N)
      XU(L)=XUR(N)
      COED(L)=COEDR(N)
      DT(L)=DTR(N)
      NPA=NPIR(N)
      NPC=NPKR(N)
      K=0
      KO=2*K
      KE=2
      IO=I+1
      DO 166 JO=2,IO
      J=JO-1
      LJ=L+J
      NUME(LJ)=NUMER(N)+J
      IF(2-KE)169,168,167
167 NPI(LJ)=NPA+KO
      NPJ(LJ)=NPA-1+KO
      NPK(LJ)=NPC+KO
      GO TO 174
168 NPI(LJ)=NPA+KO
      NPJ(LJ)=NPC+KO
      NPK(LJ)=NPC+1+KO
      GO TO 174
169 IF(3-KE)172,171,166
171 NPI(LJ)=NPA+KO
      NPJ(LJ)=NPC+1+KO
      NPK(LJ)=NPC+2+KO
      GO TO 174
172 NPI(LJ)=NPA+KO
      NPJ(LJ)=NPC+2+KO
      NPK(LJ)=NPA+1+KO
      K=K+1
      KO=2*K
      KE=0
174 ET(LJ)=ETR(N)
      RO(LJ)=ROR(N)
      XU(LJ)=XUR(N)

```



```

      COED(LJ)=COEDR(N)
      DT(LJ)=DTR(N)
      KE=KE+1
166  CONTINUE
      GO TO 161
153  L=NUMER(N)
      NUME(L)=NUMER(N)
      NPI(L)=NPIR(N)
      NPJ(L)=NPJR(N)
      NPK(L)=NPKR(N)
      ET(L)=ETR(N)
      RO(L)=ROR(N)
      XU(L)=XUR(N)
      COED(L)=COEDR(N)
      DT(L)=DTR(N)
161  CONTINUE
C
      DO 3587 N=1,NUMEL
      RETR(N)=RTEMP
      RXUR(N)=XTEMP
      WW(N)=UNTWT
3587 CONTINUE
C
C      GENERATION OF NOT READ NODAL POINTS
C
      DO 151 M=1,NURNP
      N=M+1
      IF(N-NURNP) 152,152,185
152  I=NPNUR(N)-NPNUR(M)
      GO TO 154
186  I=0
154  L=NPNUR(M)
      IO=I+1
      DO 156 JO=1,IO
      J=JO-1
      LJ=L+J
      NPNUM(LJ)=NPNUR(M)+J
      IF(I=0) 188,188,189
188  XORD(LJ)=XORDR(M)
      YORD(LJ)=YORDR(M)
      GO TO 191
189  XORD(LJ)=XORDR(M)+((XORDR(N)-XORDR(M))/I)*J
      YORD(LJ)=YORDR(M)+((YORDR(N)-YORDR(M))/I)*J
191  IF(J=0) 158,158,159
159  IF(J=1) 157,153,156
158  XLOAD(LJ)=XLDR(M)
      YLOAD(LJ)=YLDR(M)
      DSX(LJ)=DSXR(M)
      DSY(LJ)=DSYR(M)
      GO TO 156
153  XLOAD(LJ)=XLDR(N)
      YLOAD(LJ)=YLDR(N)
      DSX(LJ)=DSXR(N)
      DSY(LJ)=DSYR(N)
      GO TO 156
157  XLOAD(LJ)=0
      YLOAD(LJ)=0
      DSX(LJ)=0
      DSY(LJ)=0
156  CONTINUE

```





151 CONTINUE  
862 CONTINUE

C  
C

```

      CALCULATION OF INITIAL ELEMENT STRESSES
      DO 2000 M=1,NUMEL
        I=NP1(M)
        J=NPJ(M)
        K=NPK(M)
        H1=YORD(J)-YORD(I)
        H2=YORD(K)-YORD(I)
        H1A=ABS(H1)
        H2A=ABS(H2)
        IF(H1A.GT.0.0) DY=H1A
        IF(H2A.GT.0.0) DY=H2A
        HMAX=YORD(I)
        IF(YORD(J).GE.HMAX) HMAX=YORD(J)
        IF(YORD(K).GE.HMAX) HMAX=YORD(K)
        YELE(M)=HMAX-(DY/2.)
        DEPTH(M)=ZSFC-YELE(M)
        SIGEY(M)=UNWT*DEPTH(M)
        SIGEX(M)=RKO*SIGEY(M)
        RAD(M)=ABS(SIGEY(M)-SIGEX(M))
        ETMAX(M)=RAD(M)/2.
        IF(SIGEY(M).GE.SIGEX(M)) ELSMAX(M)=SIGEY(M)
        IF(SIGEX(M).GE.SIGEY(M)) ELSMAX(M)=SIGEX(M)
        IF(SIGEY(M).LE.SIGEX(M)) ELSMIN(M)=SIGEY(M)
        IF(SIGEX(M).LE.SIGEY(M)) ELSMIN(M)=SIGEX(M)

```

2000 CONTINUE

C

```

      IF(T1) 551,552,551
552  WRITE(6,110)
      WRITE(6,2)(NUME(N),NP1(N),NPJ(N),NPK(N),RETR(N),WW(N),RXUR(N),
1 SIGEY(N),SIGEX(N),ETMAX(N),N=1,NUMEL)
551 CONTINUE

```

C CALCULATION OF INITIAL NODE STRESSES

C

```

      DO 1001 M=1,NUMNP
        DEPTH(M)=ZSFC-YORD(M)
        SIGIY(M)=UNWT*DEPTH(M)
        SIGIX(M)=RKO*SIGIY(M)
        RAD(M)=ABS(SIGIY(M)-SIGIX(M))
        TIMAX(M)=RAD(M)/2.
        IF(SIGIY(M).GE.SIGIX(M)) SIGMAX(M)=SIGIY(M)
        IF(SIGIX(M).GE.SIGIY(M)) SIGMAX(M)=SIGIX(M)
        IF(SIGIY(M).LE.SIGIX(M)) SIGMIN(M)=SIGIY(M)
        IF(SIGIX(M).LE.SIGIY(M)) SIGMIN(M)=SIGIX(M)

```

1001 CONTINUE

C

```

      IF(T1) 160,155,160
155  WRITE(6,111)
      WRITE(6,109)(NPNUM(M),XORD(M),YORD(M),XLOAD(M),YLOAD(M),
1 DSX(M),DSY(M),SIGIY(M),SIGIX(M),TIMAX(M),M=1,NUMNP)

```

C

C

INITIALIZATION

C

```

160  NCYCLE=0
      NUMPT=NCPIN
      NUMOPT=NOPIN
      DO 175 L=1,NUMNP
        DO 170 M=1,9

```



```

      SXX(L,M)=0.0
      SXY(L,M)=0.0
      SYX(L,M)=0.0
      SYY(L,M)=0.0
170  NP(L,M)=0
      NP(L,10)=0
175  NP(L,1)=L

```

C  
C  
C

#### MODIFICATION OF LOADS AND ELEMENT DIMENSIONS

```

      DO 180 N=1,NUMEL
      ET(N)=ABS(ET(N))
      I=NP1(N)
      J=NPJ(N)
      K=NPK(N)
      AJ(N)=XORD(J)-XORD(I)
      AK(N)=XORD(K)-XORD(I)
      BJ(N)=YORD(J)-YORD(I)
      BK(N)=YORD(K)-YORD(I)
176  AREA=(AJ(N)*BK(N)-BJ(N)*AK(N))/2.
      IF(AREA) 701,701,177
177  THERM(N)=ET(N)*COED(N)*DT(N)/(XU(N)-1.)
      DL=AREA*RD(N)/3.
      XLOAD(I)=THERM(N)*(BK(N)-BJ(N))/2.+XLOAD(I)
      XLOAD(J)=-THERM(N)*BK(N)/2.+XLOAD(J)
      XLOAD(K)=THERM(N)*BJ(N)/2.+XLOAD(K)
      YLOAD(I)=THERM(N)*(AJ(N)-AK(N))/2.+YLOAD(I)-DL
      YLOAD(J)=THERM(N)*AK(N)/2.+YLOAD(J)-DL
180  YLOAD(K)=-THERM(N)*AJ(N)/2.+YLOAD(K)-DL

```

C  
C  
C

#### FORMATION OF STIFFNESS ARRAY

```

      DO 200 N=1,NUMEL
      AREA=(AJ(N)*BK(N)-AK(N)*BJ(N))*0.5
      COMM=.25*ET(N)/((1.-XU(N)**2)*AREA)
      A(1,1)=BJ(N)-BK(N)
      A(1,2)=0.0
      A(1,3)=BK(N)
      A(1,4)=0.0
      A(1,5)=-BJ(N)
      A(1,6)=0.0
      A(2,1)=0.0
      A(2,2)=AK(N)-AJ(N)
      A(2,3)=0.0
      A(2,4)=-AK(N)
      A(2,5)=0.0
      A(2,6)=AJ(N)
      A(3,1)=AK(N)-AJ(N)
      A(3,2)=BJ(N)-BK(N)
      A(3,3)=-AK(N)
      A(3,4)=BK(N)
      A(3,5)=AJ(N)
      A(3,6)=-BJ(N)
      B(1,1)=COMM
      B(1,2)=COMM*XU(N)
      B(1,3)=0.0
      B(2,1)=COMM*XU(N)
      B(2,2)=COMM
      B(2,3)=0.0
      B(3,1)=0.0

```





```

      B(3,2)=0.0
      B(3,3)=COMM*(1.-XU(N))*0.5
C
      DO 182 J=1,6
      DO 182 I=1,3
      S(I,J)=0.0
      DO 182 K=1,3
182  S(I,J)=S(I,J)+B(I,K)*A(K,J)
      DO 183 J=1,6
      DO 183 I=1,3
183  B(J,I)=S(I,J)
      DO 184 J=1,6
      DO 184 I=1,3
      S(I,J)=0.0
      DO 184 K=1,3
184  S(I,J)=S(I,J)+B(I,K)*A(K,J)
C
      LM(1)=NPI(N)
      LM(2)=NPJ(N)
      LM(3)=NPK(N)
      DO 200 L=1,3
      DO 200 M=1,3
      LX=LM(L)
      MX=0
185  MX=MX+1
      IF(NP(LX,MX)-LM(M)) 190,195,190
190  IF(NP(LX,MX)) 185,195,185
195  NP(LX,MX)=LM(M)
      IF(MX-10) 196,702,702
196  SXX(LX,MX)=SXX(LX,MX)+S(2*L-1,2*M-1)
      SXY(LX,MX)=SXY(LX,MX)+S(2*L-1,2*M)
      SYX(LX,MX)=SYX(LX,MX)+S(2*L,2*M-1)
200  SYX(LX,MX)=SYX(LX,MX)+S(2*L,2*M)
C
C      COUNT OF ADJACENT NODAL POINTS
C
      DO 206 M=1,NUMNP
      MX=1
205  MX=MX+1
      IF (NP(M,MX)) 206,206,205
206  NAP(M)=MX-1
C
C      INVERSION OF NODAL POINT STIFFNESS
C
      DO 210 M=1,NUMNP
      COMM=SXX(M,1)*SYY(M,1)-SXY(M,1)*SYX(M,1)
      TEMP=SYY(M,1)/COMM
      SYY(M,1)=SXX(M,1)/COMM
      SXX(M,1)=TEMP
      SXY(M,1)=-SXY(M,1)/COMM
210  SYX(M,1)=-SYX(M,1)/COMM
C
C      MODIFICATION OF BOUNDARY FLEXIBILITIES
C
      WRITE(6,112)
      IF(NTRR-1)871,872,872
871  READ(5,4)(NPB(L),NFI(L),SLOPE(L),L=1,NUMBC)
      WRITE(6,4)(NPB(L),NFI(L),SLOPE(L),L=1,NUMBC)
872  CONTINUE
      DO 240 L=1,NUMBC

```



```

      M=NPB(L)
      NP(M,1)=0
      IF(NFIX(L)-1) 225,220,215
215  C=(SXX(M,1)*SLOPE(L)-SXY(M,1))/(SYX(M,1)*SLOPE(L)-SYY(M,1))
      R=1.-C*SLOPE(L)
      SXX(M,1)=(SXX(M,1)-C*SYX(M,1))/R
      SXY(M,1)=(SXY(M,1)-C*SYY(M,1))/R
      SYX(M,1)=SXX(M,1)*SLOPE(L)
      SYY(M,1)=SXY(M,1)*SLOPE(L)
      GO TO 240
220  SYY(M,1)=SYY(M,1)-SYX(M,1)*SXY(M,1)/SXX(M,1)
      GO TO 230
225  SYY(M,1)=0.0
230  SXX(M,1)=0.0
235  SXY(M,1)=0.0
      SYX(M,1)=0.0
240  CONTINUE
C
C      ITERATION OF NODAL POINT DISPLACEMENTS
C
243  WRITE(6,119)
244  SUM=0.0
      DO 290 M=1,NUMNP
      NUM=NAP(M)
      IF (SXX(M,1)+SYY(M,1)) 275,290,275
275  FRX=XLOAD(M)
      FRY=YLOAD(M)
      DO 280 L=2,NUM
      N=NP(M,L)
      FRX=FRX-SXX(M,L)*DSX(N)-SXY(M,L)*DSY(N)
280  FRY=FRY-SYX(M,L)*DSX(N)-SYY(M,L)*DSY(N)
      DX=SXX(M,1)*FRX+SXY(M,1)*FRY-DSX(M)
      DY=SYX(M,1)*FRX+SYY(M,1)*FRY-DSY(M)
      DSX(M)=DSX(M)+XFAC*DX
      DSY(M)=DSY(M)+XFAC*DY
      IF (NP(M,1)) 285,290,285
285  SUM=SUM+ABS(DX/SXX(M,1))+ABS(DY/SYY(M,1))
290  CONTINUE
C
C      CYCLE COUNT AND PRINT CHECK
C
      NCYCLE=NCYCLE+1
      IF (NCYCLE-NUMPT) 305,300,300
300  NUMPT=NUMPT+NCYPIN
      WRITE(6,120) NCYCLE,SUM
305  IF (SUM-TOLER) 400,400,310
310  IF (NCYCM-NCYCLE) 400,400,315
315  IF (NCYCLE-NUMOPT) 244,320,320
320  NUMOPT=NUMOPT+NCYPIN
C
C      PRINT OF DISPLACEMENTS AND STRESSES
C
400  WRITE(6,99)
      WRITE(6,100)
      WRITE(6,121)
      WRITE(6,122) (NPNUM(M),DSX(M),DSY(M),M=1,NUMNP)
      WRITE(6,7188)
7188  FORMAT(1H1,2X,52HSTRESS CHANGES WITH TENSION POSITIVE,ANSWERS IN K
1SF      //)
      WRITE(6,123)

```





```

DO 420 N=1,NUMEL
  I=NPI(N)
  J=NPJ(N)
  K=NPK(N)
  EPX=(BJ(N)-BK(N))*DSX(I)+BK(N)*DSX(J)-BJ(N)*DSX(K)
  EPY=(AK(N)-AJ(N))*DSY(I)-AK(N)*DSY(J)+AJ(N)*DSY(K)
  GAM=(AK(N)-AJ(N))*DSX(I)-AK(N)*DSX(J)+AJ(N)*DSX(K)
  1+(BJ(N)-BK(N))*DSY(I)+BK(N)*DSY(J)-BJ(N)*DSY(K)
  COMM=ET(N)/(((1.-XU(N)**2)*(AJ(N)*BK(N)-AK(N)*BJ(N)))
  X=COMM*(EPX+XU(N)*EPY)+THERM(N)
  XFE(N)=-X+SIGEX(N)
  Y=COMM*(EPY+XU(N)*EPX)+THERM(N)
  YFE(N)=-Y+SIGEY(N)
  XY=COMM*GAM*(1.-XU(N))*0.5
  XYFE(N)=XY
  SIGXX(N)=X
  SIGYY(N)=Y
  SIGXY(N)=XY
  C=(X+Y)/2.0
  CFE(N)=(XFE(N)+YFE(N))/2.
  R=SQRT(((Y-X)/2.0)**2+XY**2)
  RFE(N)=SQRT(((YFE(N)-XFE(N))/2.0)**2+XYFE(N)**2)
  XMAX=C+R
  XMIN=C-R
  XMAXFE(N)=CFE(N)+RFE(N)
  XMINFE(N)=CFE(N)-RFE(N)
  PAFE(N)=0.5*57.29578*ATAN(2.*XYFE(N)/(YFE(N)-XFE(N)))
  PA=0.5*57.29578*ATAN(2.*XY/(Y-X))
  IF (2.*X-XMAX-XMIN) 405,420,420
405 IF(PA) 410,420,415
410 PA=PA+90.0
  GO TO 420
415 PA=PA-90.0
420 WRITE(6,124)(NUME(N),X,Y,XY,XMAX,XMIN,PA,R)
  WRITE(6,2577)
2577 FORMAT(1H1,10X,98HELEMENT STRESSES WITH INITIAL STRESSES SUPERIMPO
1 SED, COMPRESSIVE STRESSES POSITIVE,ANSWERS IN KSF //)
  WRITE(6,123)
  WRITE(6,124)(N,XFE(N),YFE(N),XYFE(N),XMAXFE(N),XMINFE(N),PAFE(N),R
1 FE(N),N=1,NUMEL)
C  NORMALIZATION OF ELEMENT STRESSES
  CONST=UNTWT*HCUT
  DO 2578 N=1,NUMEL
  XFE(N)=XFE(N)/CONST
  YFE(N)=YFE(N)/CONST
  XYFE(N)=XYFE(N)/CONST
  XMAXFE(N)=XMAXFE(N)/CONST
  XMINFE(N)=XMINFE(N)/CONST
  RFE(N)=RFE(N)/CONST
2578 CONTINUE
  WRITE(6,2579)
2579 FORMAT(1H1,10X,75HELEMENT STRESSES NORMALIZED BY DIVIDING THROUGH
1 BY WT. TIMES HT. OF CUT //)
  WRITE(6,123)
  WRITE(6,124)(N,XFE(N),YFE(N),XYFE(N),XMAXFE(N),XMINFE(N),PAFE(N),
1 RFE(N),N=1,NUMEL)
C
  WRITE(6,7188)
  WRITE(6,823)
  DO 900 M=1,NUMNP

```



```

      X=0.
      Y=0.
      XY=0.
      SRX=0.
      SRY=0.
      R=0.
      DO 860 N=1,NUMEL
        I=NPJ(N)
        J=NPJ(N)
        K=NPK(N)
        IF (M-I) 830,850,830
830    IF (M-J) 835,845,835
835    IF (M-K) 860,840,860
840    I=NPK(N)
        K=NPJ(N)
        GO TO 850
845    I=NPJ(N)
        J=NPJ(N)
850    AA=ABS(XORD(J)+XORD(K)-2.*XORD(I))
        BB=ABS(YORD(J)+YORD(K)-2.*YORD(I))
        RY=BB/(AA+BB)
        SRY=SRY+RY
        Y=Y+SIGYY(N)*RY
        RX=AA/(AA+BB)
        SRX=SRX+RX
        X=X+SIGXX(N)*RX
        R=R+1.
        XY=XY+SIGXY(N)
860    CONTINUE
        X=X/SPX
        XF(M)=-X+SIGIX(M)
        Y=Y/SRY
        YF(M)=-Y+SIGIY(M)
        XY=XY/R
        XYF(M)=XY
        C=(X+Y)/2.
        CF(M)=(XF(M)+YF(M))/2.
        R=SQRT(((Y-X)/2.)**2+XY**2)
        RF(M)=SQRT(((YF(M)-XF(M))/2.)**2+XYF(M)**2)
        XMAX=C+R
        XMIN=C-R
        XMAXF(M)=CF(M)+RF(M)
        XMINF(M)=CF(M)-RF(M)
        PA=0.5*57.29578*ATAN(2.*XY/(Y-X))
        PAF(M)=0.5*57.29578*ATAN(2.*XYF(M)/(YF(M)-XF(M)))
        IF (2.*X-XMAX-XMIN) 805,820,820
805    IF (PA) 810,820,815
810    PA=PA+90.
        GO TO 820
815    PA=PA-90.
820    WRITE(6,124)(M,X,Y,XY,XMAX,XMIN,PA,R)
900    CONTINUE
        WRITE(6,926)
926    FORMAT(1H1,10X,97HNOODAL STRESSES WITH INITIAL STRESSES SUPERIMPOSE
1D,COMPRESSIVE STRESSES POSITIVE,ANSWERS IN KSF //)
        WRITE(6,823)
        WRITE(6,124) (M,XF(M),YF(M),XYF(M),XMAXF(M),XMINF(M),PAF(M),RF(M),
1M=1,NUMNP)
        WRITE(6,927)
        WRITE(6,823)

```





```

927  FORMAT(1H1,10X,57HSTRESSES NORMALIZED BY DIVIDING BY WT. TIMES HT.
1  OF CUT      //)
      CONST=UNTWT*HCUT
      DO 928 M=1,NUMNP
      XF(M)=XF(M)/CONST
      YF(M)=YF(M)/CONST
      XYF(M)=XYF(M)/CONST
      XMAXF(M)=XMAXF(M)/CONST
      XMINF(M)=XMINF(M)/CONST
      RF(M)=PF(M)/CONST
928  CONTINUE
      WRITE(6,124) (M,XF(M),YF(M),XYF(M),XMAXF(M),XMINF(M),PAF(M),RF(M),
1 M=1,NUMNP)
      IF (SUM-TOLER) 440,440,430
430  IF (NCYCM-NCYCLE) 440,440,243
440  WRITE(6,975)SUM,TOLER
975  FORMAT(5H0SUM=1E15.6,6HTOLER=1E15.6)
C
C      PRINT OF ERRORS IN INPUT DATA
C
701  WRITE(6,711)N
      GO TO 925
702  WRITE(6,712)LX
C
C      FORMAT STATEMENTS
C
1  FORMAT(8I4,2E12.5,1F4.0)
2  FORMAT(1X,4I4,3E12.4,3F12.2)
553 FORMAT(4I4,4E12.4,F8.4)
3  FORMAT(114,2F8.1,1F8.2,1F8.2,2F12.8)
4  FORMAT (2I4,1F8.3)
5  FORMAT (3E15.8)
99  FORMAT (1H1)
100 FORMAT(18A4)
101 FORMAT (30H0NUMBER OF ELEMENTS           =1I4/)
102 FORMAT (30H NUMBER OF NODAL POINTS       =1I4/)
103 FORMAT (30H NUMBER OF BOUNDARY POINTS     =1I4/)
104 FORMAT (30H CYCLE PRINT INTERVAL          =1I4/)
105 FORMAT (30H OUTPUT INTERVAL OF RESULTS   =1I4/)
106 FORMAT (30H CYCLE LIMIT                   =1I4/)
107 FORMAT (30H TOLERANCE LIMIT               =1E12.4/)
108 FORMAT (30H OVER RELAXATION FACTOR        =1F6.3)
109 FORMAT (118,2F12.1,2F12.2,2F12.8,3F12.2)
110 FORMAT (99H1EL.   I   J   K           E(PSI)   DENSITY(KCF) POISSON
1 SIG-Y-INIT SIG-X-INIT TAU-MAX-INIT
)
111 FORMAT(118H1      NP      X-ORD      Y-ORD      X-LOAD      Y-LOAD
1      X-DISP      Y-DISP      SIG-Y-INIT SIG-X-INIT TAU-MAX-INIT )
112 FORMAT(20H BOUNDARY CONDITIONS)
119 FORMAT(34H0      CYCLE      FORCE UNBALANCE)
120 FORMAT (11I12,1E20.6)
121 FORMAT(42H0NODAL POINT X-DISPLACEMENT Y-DISPLACEMENT)
122 FORMAT (11I12,2E15.6)
123 FORMAT(2X,4HELNO 2X,8HX-STRESS 4X,8HY-STRESS 3X,9HXY-STRESS 3X,10H
1 MAX-STRESS 3X,10HMIN-STRESS 4X,9HDIRECTION 2X,16HMAX SHEAR STRESS
2 )
124 FORMAT(115,3E12.5,4E13.5)
711 FORMAT(32H0ZERO OR NEGATIVE AREA. EL.NO. =1I4)
712 FORMAT(33H0OVER 8 N.P. ADJACENT TO N.P. NO.1I4)
823  FORMAT(2X,4HNODE 2X,8HX-STRESS 4X,8HY-STRESS 3X,9HXY-STRESS 3X,10H

```



```

1 MAX-STRESS 3X,10HMIN-STRESS 4X,9HDIRECTION 2X,16HMAX SHEAR STRESS
2 //)
824 FORMAT (30H NUMBER OF READ NODAL POINTS =114/)
825 FORMAT (30H NUMBER OF READ ELEMENTS =114/)
201 FORMAT(4F10.3)
1700 FORMAT(30HUNIT WEIGHT IN K.C.F.= F10.3/)
1701 FORMAT(30HKO= F10.3/)
1702 FORMAT(30HELEVATION OF GROUND SURFACE= F10.3/)
1703 FORMAT(30HDEPTH OF CUT (FT.) = F10.3/)
925 STOP
END
C ***** DATA CARDS FOR A TYPICAL PROBLEM *****
WILSON 1963,GRID F,E=10 KSI,U=0.30,KO=2.00 EL/E=0.10
800 28 455 46 59 5 3003000 1.E01 1.85E00
0.150 2.000 400.000 200.000
1 43 42 1 .1E05 .03E01
80 81 41 82 .1E05 .03E01
81 84 83 42 .1E05 .03E01
160 122 82 123 .1E05 .03E01
161 125 124 83 .1E04 .03E01
240 163 123 164 .1E04 .03E01
241 166 165 124 .1E05 .03E01
320 204 164 205 .1E05 .03E01
321 207 206 165 .1E05 .03E01
368 229 189 230 .1E05 .03E01
369 232 231 206 .1E05 .03E01
416 254 230 255 .1E05 .03E01
417 257 256 231 .1E05 .03E01
464 279 255 280 .1E05 .03E01
465 282 281 256 .1E05 .03E01
512 304 280 305 .1E05 .03E01
513 307 306 281 .1E05 .03E01
560 329 305 330 .1E05 .03E01
561 332 331 306 .1E05 .03E01
608 354 330 355 .1E05 .03E01
609 357 356 331 .1E05 .03E01
656 379 355 380 .1E05 .03E01
657 382 381 356 .1E05 .03E01
704 404 380 405 .1E05 .03E01
705 407 406 381 .1E05 .03E01
752 429 405 430 .1E05 .03E01
753 432 431 406 .1E05 .03E01
800 454 430 455 .1E05 .03E01
1
41 1600.0
42 80.0
82 1600.0 80.0
83 140.0
123 1600.0 140.0
124 150.0
164 1600.0 150.0
165 200.0
189 960.0 200.0 585.00 600.00
190 1000.0 200.0 1200.00
191 1040.0 200.0 1200.00
192 1080.0 200.0 1200.00
193 1120.0 200.0 1200.00
194 1160.0 200.0 1200.00
195 1200.0 200.0 1200.00
196 1240.0 200.0 1200.00

```





197	1280.0	200.0	1200.00
198	1320.0	200.0	1200.00
199	1360.0	200.0	1200.00
200	1400.0	200.0	1200.00
201	1440.0	200.0	1200.00
202	1480.0	200.0	1200.00
203	1520.0	200.0	1200.00
204	1560.0	200.0	1200.00
205	1600.0	200.0	600.00
206		220.0	
230	960.0	220.0	1080.00
231		240.0	
255	960.0	240.0	960.00
256		260.0	
280	960.0	260.0	840.00
281		280.0	
305	960.0	280.0	720.00
306		300.0	
330	960.0	300.0	600.00
331		320.0	
355	960.0	320.0	480.00
356		340.0	
380	960.0	340.0	360.00
381		360.0	
405	960.0	360.0	240.00
406		380.0	
430	960.0	380.0	120.00
431		400.0	
455	960.0	400.0	15.00
1	0		
2	0		
3	0		
4	0		
5	0		
6	0		
7	0		
8	0		
9	0		
10	0		
11	0		
12	0		
13	0		
14	0		
15	0		
16	0		
17	0		
18	0		
19	0		
20	0		
21	0		
22	0		
23	0		
24	0		
25	0		
26	0		
27	0		
28	0		
29	0		
30	0		
31	0		



32	0
33	0
34	0
35	0
36	0
37	0
38	0
39	0
40	0
41	0
42	1
82	1
83	1
123	1
124	1
164	1
165	1
205	1
206	1
231	1
256	1
281	1
306	1
331	1
356	1
381	1
406	1
431	1









**B30021**